2

CRANFIELD UNIVERSITY

DAVID OLUSINA ROWLANDS

TECHNO-ECONOMIC RESEARCH ANALYSIS FOR EFFECTIVE POWER GENERATION FROM AERO-ENGINES

School of Aerospace Transport and Management (SATM)

PhD in Aerospace (Full Time)
Academic Year: 2015-2018

Supervisors:
Prof. Mark Savill
Dr. Timoleon Kipouros
January 2019

CRANFIELD UNIVERSITY

School of Aerospace Transport and Management (SATM)

PhD in Aerospace (Full Time)
Academic Year: 2015-2018

DAVID OLUSINA ROWLANDS

Techno-Economic Research Analysis for Effective Power Generation from Aero-Engines

Supervisors:
Prof. Mark Savill
Dr. Timoleon Kipouros
January 2019

This thesis is submitted in partial fulfilment of the requirements for the degree of Doctor of Philosophy in Aerospace.

ABSTRACT

This research focuses on the techno-economic assessment of Brayton cycles and provides a platform through which the evaluation and optimization of gas turbine engine performance and economics may be achieved in an economical and cost effective way. In this study, a techno-economic analysis model has been developed which takes into account technical, environmental and economic variables during analysis in order to arrive at reasonable solutions for gas turbine system optimization from a technical and economic perspective, and in a viable and cost effective way. The model integrates elements of machine learning, regression analysis, economics, thermodynamic and optimization analysis into a cohesive whole to enable robust techno-economic investigation.

In order to provide a baseline for the research analysis and investigation, a case study engine model similar to the Tumansky-R25-300 turbojet engine is created. This engine choice seeks to provide an alternative, profitable civil use for the grounded jet engines owned by the Nigerian Air force. A study is conducted using the developed techno-economic methodology to determine the feasibility, from a performance and economic perspective, of repurposing the selected case study engine into an aero-derivative engine for electrical power generation application. At ISA conditions, burning natural gas, the repurposed engine model (REM) delivers 18.52MW of power at 33.5% thermal efficiency. With respect to the case, study environment, Nigeria (Tropical region), at an average altitude of 700m, the repurposed engine model delivers 17.66MW of Power at 31.6% thermal efficiency. Repurposing the power plants of the considered grounded aircrafts has the potential to consolidate electrical generating capacity in Nigeria by about 8% in simple cycle and 10% in combined cycle applications

Techno-economic analysis conducted on the repurposed engine model reveals that investment in the REM over a 15years planning horizon would break even at 5years with 22% return on investment (ROI) in simple cycle and 19% ROI in combined cycle application. In simple cycle, the REM deliver a NPV of $24.21 million at a levelized cost of energy, LCOE, of 0.155$/MWh and investment base of $18.24 million. In combined cycle investigations, the REM delivers a NPV of $23.98 million at an LCOE of 0.121$/MWh and investment base of $20.85 million in combined cycle. Performance and economic optimization analysis conducted on the repurposed engine model achieved a 39% reduction in fuel flow, 39% reduction in NOx emission generated and about 30% decrease in LCOE from baseline values while maintaining positive profitability.

Based on the techno-economic analysis conducted, assumptions made and results obtained from this study, it is feasible, from a performance and economic perspective, to apply the repurposed engine model (REM) for electrical power generation, both within and outside the considered case study region with minimal loss in performance output and economic profitability. Further investigations reveal that the repurposed engine model (REM) can favorably compete, from a performance and economic perspective, with some of the competitor units considered in this study.

A techno-economic cost modelling and analysis tool based on the developed techno-economic analysis methodology has been developed and integrated with TURBOMATCH performance simulation software. The integration of the tool with TURBOMATCH has extended its potential application scope to cover numerous areas including preliminary

design investigation, technology comparison, power cycling analysis, project selection from alternatives, capital budgeting problems, novel cycle investigations, life cycle cost analysis and sensitivity analysis.

ACKNOWLEDGMENTS

I will like to sincerely acknowledge the almighty God for his grace, mercy and favour over my life throughout the course of this research. His wisdom, guidance and faithfulness have kept me from being overwhelmed by the abundant demands of this Research. I will like to appreciate my sponsors, the Commonwealth Scholarship Commission for their consistent support in cash and kind over the course of my research effort. I specifically acknowledge, my programme officer, Irene Costello for her patience with me through my demands, requests and inquires to the commission over the course of my research.

Further acknowledgement goes to my incredible supervisors Prof. Mark Savill and Dr. Timoleon Kipouros for their unparalleled guidance, encouragement and support throughout the course of my research.

Honour goes to a deserving parent; I will like to specially acknowledge my parents Mr and Mrs Henry Rowlands, for their unrelenting prayers, encouragement, patience and support prior to and all the way through my research. My profound gratitude will forever be expressed.

Special thanks also goes to all my friends and family whom I am unable to acknowledge directly in this report. Thank you for your patience and understanding. Finally, I will like to acknowledge and appreciate my special partner, friend and mate, Chidinma Chuckwu for her incredible patience and unfading love over the course of my research. I pray the almighty reward you abundantly for your faithfulness.

TABLE OF CONTENTS

ABSTRACT iii
ACKNOWLEDGMENTS v
TABLE OF CONTENTS vi
LIST OF FIGURES ix
LIST OF TABLES xv
LIST OF EQUATIONS xv
NOMENCLATURES xix
1 INTRODUCTION 24
1.1 Relevance of Research to Nigeria 25
1.2 Likely Developmental Impact of Research Project to Nigeria 26
1.3 Background 28
1.3.1 Techno-economic Investigations 28
1.3.2 Artificial Neural Network (ANN) Investigations 29
1.4 Report Summary 31
2 STATEMENT OF AIM AND OBJECTIVES 32
2.1 Research Aim 32
2.2 Objectives 32
2.3 Research Contributions and Impact 32
2.3.1 Research Contribution 32
2.3.2 Research Impact 33
3 BACKGROUND LITERATURE 34
3.1 Gas turbine engine operation 34
3.1.1 Gas turbine Emissions 34
3.1.2 Gas Turbine Categorization 41
3.2 Engine Conversion 42
3.3 Performance Simulation 44
3.3.1 Gas Turbine Performance Simulation 44
3.4 Gas Turbine Performance Optimization 51
3.4.1 Optimization Goal 51
3.4.2 Optimization Objective 51
3.4.3 Optimization Problem 52
3.4.4 Performance optimization approach 52
3.5 Regression Analysis (RA) 57
3.6 Artificial Neural Network (ANN) 59

3.6.1 Feed-forward and Back-Propagation Network 60
3.7 Economic Analysis 61
3.7.1 Economic analysis Overview 61
3.7.2 Project selection 64
3.7.3 Economic Model 65
4 METHODOLOGY 66
4.1 Overall Research Approach 66
4.1.1 Research Development Phase 66
4.1.2 System Analysis Phase 66
4.1.3 System Optimization Phase 66
4.1.4 Result Analysis and interpretation Phase 66
4.2 Techno-Economic Analysis Approach 68
4.2.1 Price Estimating Model 68
4.2.2 Life Approximating Model 82
4.2.3 Emissions Model 86
4.2.4 Performance Model 90
4.2.5 Cost Model 92
4.2.6 Levelized Cost of Energy (LCOE) 97
4.2.7 Selection Model 98
4.2.8 Optimization Model 101
5 RESEARCH TECHNIQUES 104
5.1 Engine Selection 104
5.2 Feasibility Study 105
5.2.1 Feasibility Study - Approach 106
5.3 Performance Simulation - Considered Scenarios 112
5.3.1 Aero-derivative engine baseline 113
5.4 Price Estimation 118
5.4.1 Acquisition cost estimation using regression analysis (RA) 118
5.4.2 Acquisition cost estimation using Artificial Neural Network (ANN) 125
5.4.3 Adopted Price estimating model 127
5.5 Economic Analysis 127
5.5.1 Operating Assumptions 127
5.5.2 Economic Assumptions 128
5.5.3 Analysis Approach 128
5.6 Optimization Analysis 129

5.6.1 Modifications to basic thermodynamic cycle. 130
5.6.2 Performance optimization using optimization solver 131
5.6.3 Economic optimization using optimization solver 132
5.6.4 Techno-Economic Cost Modelling Tool – ECM Tool 133
6 RESULTS AND DISCUSSION 136
6.1 Performance Simulation Results 136
6.1.1 Design Point Engine Performance at ISA and Tropical Condition 136
6.1.2 Varied Ambient Temperature Assessment 137
6.1.3 Varied Firing Temperature Assessment ISA Vs Tropical Condition (*at varying ambient temperature and fixed relative humidity*) 139
6.1.4 Fixed Firing Temperature Assessment ISA Vs Tropical Condition (*at varying ambient temperature and relative humidity*) 141
6.1.5 Deterioration Effects on engine performance 142
6.1.6 Transient Performance analysis at ISA Condition 150
6.1.7 Effects of degradation on transient engine operation 154
6.2 Acquisition Cost Estimate - Results 157
6.2.1 Regression Analysis estimating results 157
6.2.2 Artificial Neural Network estimating results 158
6.2.3 Acquisition Cost Estimate Comparison 160
6.3 Economic Analysis Results 161
6.3.1 Baseline Techno-Economic analysis Results 161
6.3.2 Effect of engine degradation on Techno-economic analysis 170
6.3.3 Influence of Transient Operation on gas turbine Techno-economics 174
6.3.4 Effects of power cycling on engine economics 178
6.3.5 Techno-economic analysis results for REM operating in Tropical Environment. 183
6.3.6 Effect of Emissions control technology on engine techno-economics 187
6.3.7 Effect of Acquisition Cost on engine techno-economics 192
6.4 Optimization Analysis Results 197
6.4.1 Performance optimization 197
6.4.2 Economic Optimization 202
6.4.3 Techno-economic Analysis Results for the Optimized Engine model 204
7 DISCUSSION OF RESULTS 209
7.1 Thermodynamic Performance Analysis Results 209
7.1.1 Performance Modelling and Simulation 209
7.1.2 Performance Deterioration Analysis 209

7.2 Techno-economic Modelling and Analysis Results 210
7.2.1 Baseline Techno-economic analysis 210
7.2.2 Factors Influencing Baseline Techno-economic Analysis 211
7.3 Techno-economic optimization analysis Results 212
8 CONCLUSION 213
8.1 Selection of Case Study Engine 213
8.2 Thermodynamic Performance Analysis 213
8.3 Development of Cost and Economic analysis model 213
8.3.1 Price estimating model component 213
8.3.2 Life approximating model component 214
8.3.3 Emissions model component 214
8.3.4 Performance-modelling and simulation component 214
8.3.5 Cost model component 214
8.3.6 Optimization model component 214
8.3.7 Selection model component 215
8.4 Baseline Techno-economic Analysis 215
8.4.1 Performance Analysis of repurposed engine model 215
8.4.2 Economic Analysis of repurposed engine model 215
8.5 Techno-economic Optimization Analysis 217
8.6 Techno-economic Cost Modelling and Analysis Tool 217
8.7 Summary 217
9 FUTURE WORK 219
10 BIBLIOGRAPHY 220
APPENDIX A 227
APPENDIX B 254
APPENDIX C 257
APPENDIX D 263
APPENDIX E 267

LIST OF FIGURES

Figure 1: Required Generating Capacity versus Current Generating Capacity in Nigeria 27
Figure 2: Ideal Brayton Cycle 34
Figure 3: Aero engine image (Turbojet) 41
Figure 4: 7HA heavy-duty Gas Turbines (bpress, 2014) 41
Figure 5: LM1800e aero-derivative engine (Gas and Steam Turbines, 2012) 42
Figure 6: Aerodynamically coupled power turbine (Emad, 2013) 42
Figure 7: Hot End Drive (Aft of Gas turbine) (MHPS Gas Turbine Generator Set , 2015) 43

Figure 8: Cold end drive (Integrated output shaft; fore of Gas turbine) (MHPS Gas Turbine Generator Set , 2015).....43
Figure 9: Roll Royce Avon Turbo jet engine (Advanced Animations UK, 2016).....43
Figure 10: Pratt and Whitney GG4 Aero-derivative Gas Turbine (WGPW, 2016).....44
Figure 11: Performance Simulation process for a simple gas turbine power plant (Rahman, et al., 2011). 46
Figure 12: Cycling Cost with increased wind and solar penetration from Fossil-Fuelled Generator Perspective (Kumar, et al., 2012).....47
Figure 13: Performance Parameter Vs Engine Runtime.....48
Figure 14: Performance loss due to Gas Turbine deterioration over time 49
Figure 15: CO emissions from an industrial gas turbine. Abstracted from GE Power Systems – GER-4311-03/01 ('Layi Fagbenle, 2014) 51
Figure 16: Simple Cycle with reheat 52
Figure 17: T-S Diagram for reheated gas turbine 53
Figure 18: Simple cycle with heat exchanger (Regenerator).....53
Figure 19: T-S diagram for a regenerated gas turbine.....54
Figure 20: Simple Cycle with intercooler 55
Figure 21: T-S Diagram for intercooled gas turbine.....55
Figure 22: The Steam Injected gas turbine (STIG) cycle 56
Figure 23: Graphical Representation of Regression Analysis 58
Figure 24: Artificial Neural Network Schematic 59
Figure 25: Illustration of a simple ANN System 60
Figure 26: Feed-Forward Back Propagation Network 61
Figure 27: Project Selection Steps 64
Figure 28: Research Approach/Methodology.....67
Figure 29: Techno-economic Model Overview.....68
Figure 30: Neural Network Estimating Methodology and Code Structure 69
Figure 31: Complex-Underlying Process of the ANN 71
Figure 32: Neural Network Overfitting 74
Figure 33: Estimates from an over-fitted network 74
Figure 34: Neural Network Overfitting Regularized 74
Figure 35: Estimates from a regularized network 75
Figure 36: Regression Analysis Methodology for Estimating Acquisition Cost 75
Figure 37: Illustration of Temperature Rise and drop in life Factor 83
Figure 38: Change in Engine Life Vs Operating point TET.....86
Figure 39: Emissions Model component of overall economic model 87
Figure 40: Emissions Model Vs SYCOM Estimates (Conrolled NOx).....89
Figure 41: Emissions Model Vs SYCOM Estimates (Uncontrolled NOx) 89
Figure 42: Emissions Model Vs CTG Estimates 90
Figure 43: Performance Model Integration flowchart 91
Figure 44: Typical modular engine model schematic 92
Figure 45: Cost model component of overall economic model 93
Figure 46: Selection Model component of Techno-economic Model.....98
Figure 47: Optimization Methodology.....102
Figure 48: Mikoyan Gurevich MiG-21 fighter jet Aircraft (Mikoyan Gurevich, 2011; leatherneck, 2014).....104

Figure 49: Tumansky- R25-300 turbojet engine on an engine mount (mm330046, 2007)...104
Figure 50: Schematic of the Tumansky-R-25-300 Turbojet Engine 106
Figure 51: TURBOMATCH Schematic of Simulated turbojet engine model 106
Figure 52: Schematic of Aero-derivative Engine model 106
Figure 53: TURBOMATCH Schematic of Simulated Aero-derivative Engine....106
Figure 54: Plot of Performance against pressure ratio....107
Figure 55: Schematic Illustration of Engine Model Modification 109
Figure 56: REM Fuel Type - Power Output and Thermal Efficiency Comparison 110
Figure 57: REM Fuel Type - Fuel Flow and Specific Fuel Consumption Comparison....111
Figure 58: Scatter Plot of Power Output Vs Acquisition Cost....118
Figure 59: Scatter Plot of Engine RPM Vs Acquisition Cost 118
Figure 60: Scatter Plot of Engine Heat rate Vs Acquisition Cost....119
Figure 61: Scatter Plot of Power Output against RPM 120
Figure 62: Scatter Plot of Power Output against Heat Rate 120
Figure 63: Scatter Plot of RPM against Heat Rate 120
Figure 64: Scatter Plot of Power Output Vs Acquisition Cost Showing Regression Line....121
Figure 65: Graphical Residual Analysis with respect to Power output....122
Figure 66: Scatter Plot of Transformed Dataset 122
Figure 67: Graphical Residual Analysis of Transformed Dataset....123
Figure 68: Acquisition Cost Prediction Interval 125
Figure 69: Comparison of training and testing error cost (overfitting observed) 126
Figure 70: Comparison of training and testing error cost (overfitting minimized) 126
Figure 71: Modified Engine Model Schematic....130
Figure 72: Modified Engine Model T-S Diagram....130
Figure 73: ECM Code Interaction/ Structure 133
Figure 74: ECM General Layout (performance tab)....134
Figure 75: Design Point Performance Map Low pressure compressor - LPC 136
Figure 76: Design Point Performance Map High pressure compressor - HPC....136
Figure 77: Varied Ambient Temperature Assessment TE and SFC Vs Ambient Temperature at constant TET....137
Figure 78: Varied Ambient Temperature Assessment SHP and FF Vs Ambient Temperature at Constant TET 137
Figure 79: Comparison of engine operation at ISA and Tropical....138
Figure 80: Varied Firing temperature assessment ISA condition (SFC/TE Vs TIT) 139
Figure 81: Varied Firing temperature assessment Tropical condition (SFC/TE Vs TIT) 139
Figure 82: Varied Firing temperature assessment ISA condition (SHP/FF Vs TIT)....140
Figure 83: Varied Firing temperature assessment Tropical condition (SHP/FF Vs TIT)....140
Figure 84: Fixed Firing temperature assessment ISA Vs Tropical condition (SFC and TE Vs Ambient Temperature) 141
Figure 85: Fixed Firing temperature assessment ISA Vs Tropical condition (SHP and FF Vs Ambient Temperature) 141
Figure 86: Effect of Deterioration on LPC 142
Figure 87: Effect of Deterioration on HPC 143
Figure 88: Effect of deterioration on repurposed engine model performance 144
Figure 89: Deterioration effect on TE and SFC with varied TET....145
Figure 90: Deterioration effect on SHP and FF at varied TET 145

Figure 91: Unwashed Engine Deterioration (Fuel Flow & Shaft Power Vs operating hours) 146
Figure 92: Unwashed Engine Deterioration (Thermal Efficiency & SFC Vs Operating Hours) 146
Figure 93: Unwashed Engine Deterioration (Mass Flow & TET Vs Operating Hours) 146
Figure 94: Washed Engine deterioration (FF & SHP Vs operating hours) 147
Figure 95: Washed Engine deterioration (TE & SFC Vs Operating hours) 148
Figure 96: Washed Engine deterioration (Mass Flow & TET Vs operating hours) 148
Figure 97: Percentage Power drop over operating hours 149
Figure 98: Percentage SFC rise over operating hours.....149
Figure 99: Transient Working Line of HPC 150
Figure 100: Power Variation with engine runtime 150
Figure 101: Fuel Flow to combustor through transient acceleration and deceleration 151
Figure 102: COT pattern through the engine runtime.....151
Figure 103: Rotational speed pattern during engine transient acceleration 151
Figure 104: SFC Variation with runtime.....152
Figure 105: Exhaust Temperature Variation.....152
Figure 106: Fuel flow against rotational speed variation 153
Figure 107: Fuel flow against SFC variation 153
Figure 108: Transient Working Line of HPC 154
Figure 109: Power Variation with runtime 154
Figure 110: Fuel Flow to combustor through transient acceleration and deceleration 155
Figure 111: COT pattern through the engine runtime.....155
Figure 112: Rotational speed pattern during engine transient acceleration 155
Figure 113: SFC Variation.....156
Figure 114: Exhaust Temperature Variation.....156
Figure 115: Acquisition Cost Prediction Interval 158
Figure 116: Error Cost Vs Number of Iterations - Post Regularisation 159
Figure 117: Neural Network Confusion Matrix.....160
Figure 118: Acquisition Cost Estimate Comparison.....160
Figure 119: Estimating Accuracy Comparison 161
Figure 120: Baseline Economic Analysis (MARR 2.5%) - Simple Cycle 162
Figure 121: Baseline Economic Analysis (MARR 2.5%) - Combined Cycle.....162
Figure 122: Baseline Economic Analysis - NOx Removed.....163
Figure 123: Baseline Economic Analysis - Cost Effectiveness and Electricity Cost Impact....163
Figure 124: Baseline Economic Analysis - Fuel Penalty and Running Cost.....164
Figure 125: Return on Investment and Break Even Point - Simple Cycle 165
Figure 126: Return on Investment and Break Even Point - Combined Cycle 165
Figure 127: NPV Sensitivity to fuel price at constant LCOE 166
Figure 128: NPV Sensitivity to MARR in Simple Cycle Operation 167
Figure 129: NPV Sensitivity to MARR in Combined Cycle Operation 167
Figure 130: Sensitivity to Emissions Tax - Simple Cycle Operation 168
Figure 131: Sensitivity to Emissions Tax - Combined Cycle Operation.....168
Figure 132: Desirability Score - Baseline Analysis.....169
Figure 133: Effects of Engine Degradation on Economic Analysis - Simple cycle Application 170

Figure 134: Effects of Engine Degradation on Economic Analysis - Combined Cycle Application 171
Figure 135: Effects of Engine Degradation on Emissions Generated 171
Figure 136: Effects of Engine Degradation on Cost Effectiveness and Electricity Cost Impact 172
Figure 137: Effect of Engine Degradation on Running Cost 172
Figure 138: Effect of Degradation on Annual Operation and Maintenance Cost 173
Figure 139: Effects of Degradation on Return on Investment and Break Even Point - Simple Cycle 173
Figure 140: Effects of Degradation on Return on Investment and Break Even Point - Combined Cycle 174
Figure 141: Effect of Transient Operation on Economic Analysis - Simple Cycle 175
Figure 142: Effects of Transient Operation on Economic Analysis - Combined Cycle 175
Figure 143: Effects of Transient Operation on Emissions Generated 176
Figure 144: Effects of Transient Operation on Cost Effectiveness and Electricity Cost Impact 176
Figure 145: Effects of Transient Operation on Annual Running Cost 177
Figure 146: Effects of Transient Operation on Operation and Maintenance Cost 177
Figure 147: Effects of Transient Operation on Return on Investment and Break Even Point - Simple Cycle 178
Figure 148: Effects of Transient Operation on Return on Investment and Break Even Point - Combined Cycle 178
Figure 149: Effects of Power Cycling on Economic Analysis - Simple Cycle 179
Figure 150: Effects of Power Cycling on Economic Analysis - Combined Cycle 180
Figure 151: Effect of Engine Power Cycling on Emissions Generated 180
Figure 152: Effect of Engine Power Cycling on Cost Effectiveness and Electricity Cost Impact 181
Figure 153: Effect of Engine Power Cycling on Running Cost 181
Figure 154: Effect of Power Cycling on Operation and Maintenance Cost 182
Figure 155: Effects of Power Cycling on Return on Investment and Break Even Point - Simple Cycle 182
Figure 156: Effects of Power Cycling on Return on Investment and Break Even Point - Combined Cycle 183
Figure 157: Effect of Tropical Region on Economic Analysis - Simple Cycle 184
Figure 158: Effect of Tropical Region on Economic Analysis - Combined Cycle 184
Figure 159: Effects of Tropical Region on Emissions Generation 185
Figure 160: Effects of Tropical Region on Cost Effectiveness and Electricity Cost Impact 185
Figure 161: Effects of Tropical Region on Running Cost 186
Figure 162: Effects of Tropical Region on Operation and Maintenance Cost 186
Figure 163: Effects of Tropical Region on Return on Investment and Break Even Point - Simple Cycle 187
Figure 164: Effects of Tropical Region on Return on Investment and Break Even Point - Combined Cycle 187
Figure 165: NOx Technology Comparison in Simple Cycle 188
Figure 166: NOx Technology Comparison in Combined Cycle 189
Figure 167: NOx Technology Comparison w.r.t. NOx Removed 189

Figure 168: NOx Technology Comparison w.r.t. Effectiveness and Impact.....190
Figure 169: Effect of Emissions Control Technology on Running Cost.....190
Figure 170: Effect of Emissions Control Technology on Operation and Maintenance Cost .191
Figure 171: Effects of Control Technology on Return on Investment and Break Even Point - Simple Cycle.....191
Figure 172: Effects of Control Technology on Return on Investment and Break Even Point - Combined Cycle.....192
Figure 173: Effect of Acquisition Cost on Economic Analysis - Simple Cycle.....193
Figure 174: Effect of Acquisition Cost on Economic Analysis - Combined Cycle.....194
Figure 175: Effect of Acquisition Cost on NOx Emissions Removed.....194
Figure 176: Effect of Acquisition Cost on Technology Cost effectiveness and impact.....195
Figure 177: Effect of Acquisition Cost on Annual Running Cost.....195
Figure 178: Effect of Acquisition Cost on Operation and Maintenance Cost.....196
Figure 179: Effect of Acquisition Cost on Return on Investment and Break Even Point - Simple Cycle.....196
Figure 180: Effect of Acquisition Cost on Return on Investment and Break Even Point - Combined Cycle.....197
Figure 181: Intercooled Engine Power and Compressor Work Vs Intercooler effectiveness198
Figure 182: Intercooled Engine Thermal Eff. and Exhaust Temp. Vs Intercooler Effectiveness 198
Figure 183: Intercooled Engine SFC and Fuel Flow against Intercooler Effectiveness.....199
Figure 184: NOx Emissions Rate Vs Intercooler Effectiveness.....199
Figure 185: Annual Running Cost Vs Intercooler Effectiveness.....199
Figure 186: LCOE Vs Intercooler Effectiveness.....200
Figure 187: Effect of Performance Optimization on Fuel Flow.....201
Figure 188: Effect of Performance Optimization on TET and EGT.....201
Figure 189: Effect of Economic Optimization on LCOE in Simple Cycle.....202
Figure 190: Effect of Economic Optimization on Annual Benefits - Simple Cycle.....203
Figure 191: Effect of Economic Optimization on LCOE in Combined Cycle.....203
Figure 192: Effect of Economic Optimization on Annual Benefits in Combined Cycle.....204
Figure 193: Effect of Optimization on Economic Analysis – Simple Cycle.....204
Figure 194: Effect of Optimization on Economic Analysis – Combined Cycle.....205
Figure 195: Effect of REM Optimization on NOx Emissions Removed.....205
Figure 196: Effect of REM Optimization on Cost Effectiveness and Electricity Cost Impact.206
Figure 197: Effect of REM Optimization on Running Cost.....206
Figure 198: Effect of REM Optimization on Operation and Maintenance Cost.....207
Figure 199: Effects of REM Optimization on Return on Investment and Break Even Point - Simple Cycle.....207
Figure 200: Effects of REM Optimization on Return on Investment and Break Even Point - Combined Cycle.....208
Figure 201: Water/ Steam Injection Power Output Comparison.....255
Figure 202: Water/Steam Injection Fuel Flow Comparison.....255
Figure 203: Water/Steam Injection Thermal Efficiency Comparison.....256

LIST OF TABLES

Table 1: Showing general turbojet engine components, specification and performance rating at ISA 105
Table 2: Comparison between Simulated and Actual turbojet engine performance results at ISA 108
Table 3: Aeroderivative engine simulation results at ISA (Kerosene) 111
Table 4: Aero-derivative engine simulation results at ISA (Natural Gas) 112
Table 5: Aero-derivative Engine Simulation Results @ 0% Relative Humidity (Kerosene) ... 112
Table 6: Aero-derivative Engine Simulation Results @ 60% Relative Humidity (Kerosene) . 112
Table 7: Baseline Aero-derivative Engine Parameters (Natural Gas) 113
Table 8: Investigated Deterioration Cases and implanted faults 113
Table 9 : Required Transient Performance Input Data 114
Table 10: Power generated on each shaft 116
Table 11: Evaluated Torque and Moment of Inertia 116
Table 12: Effective component volumes 117
Table 13: Hypothesis/t-test results 124
Table 14: Engine Operating Parameters 127
Table 15: Showing Comparison of performance between ISA and Tropical Conditions for varied ambient Temperature 138
Table 16: Ambient Temperature Categorisation 138
Table 17: Comparison of Power to Weight Ratio 142
Table 18: Effect of deterioration on engine performance 144
Table 19: Engine Performance Parameters 157
Table 20: Accuracy of Regression Analysis Estimate (2017 dollars) 158
Table 21: Accuracy of ANN Estimate (2017 dollars) 159
Table 22: Desirability Grading Matrix 169
Table 23: Engine Washing Parameters 170
Table 24: Additional Transient Input Parameters 174
Table 25: Power Cycling Input Parameters 179
Table 26: Emissions Technology Comparison Input data 188
Table 27: Performance Optimization Results 201
Table 28: Economic Optimization Results - Simple Cycle 202
Table 29: Economic Optimization Results - Combined Cycle 203

LIST OF EQUATIONS

Equation 1: Air Emissions Calculation 40
Equation 2: Regenerator Effectiveness 53
Equation 3: Intercooler Effectiveness 54
Equation 4: Objective function 56
Equation 5: Linear inequality constraints 57
Equation 6: Linear equality constraint 57
Equation 7: Non Linear Inequality constraints 57
Equation 8: Linear equality constraints 57
Equation 9: Objective bounds 57
Equation 10: Regression Model Relationship 58
Equation 11: Synapse Output 60

Equation 12: Sigmoid Activation Function 60
Equation 13: Calculated Error 61
Equation 14: Change in Weights 61
Equation 15: Net Present Value (Present Worth) 62
Equation 16: Overall Rate of Return 63
Equation 17: Scale Adjusted ORR 63
Equation 18: ORR of One-time expenditure projects with different project lives 63
Equation 19: Inflation rate 69
Equation 20: Price in current year due to inflation 69
Equation 21: Normalized data 69
Equation 22: Activity in layer two 70
Equation 23: Activation function 70
Equation 24: Activity in layer three 70
Equation 25: Cost Function 70
Equation 26: Output Estimate 70
Equation 27: Overall Cost Equation 71
Equation 28: Gradient of cost function or Partial derivative of error cost between the hidden and output layer 71
Equation 29: Change in weights between the hidden and output layer 71
Equation 30: Gradient of cost function or Partial derivative of error cost between the input and hidden layer 72
Equation 31: Change in weights between the input and hidden layer 72
Equation 32: Numerical Gradient 72
Equation 33: Numerical Gradient Checking 72
Equation 34: Error Cost with overfitting considered 73
Equation 35: Pearson's Correlation Formula 76
Equation 36: Simple Linear Regression Model 77
Equation 37: Simple Linear Regression Model for a sample 78
Equation 38: Slope of the regression line 78
Equation 39: Intercept of the regression line 78
Equation 40: Price Estimating Relationship 78
Equation 41: Coefficient of Determination 79
Equation 42: Coefficient of Correlation 79
Equation 43: Standard Error of Estimate 79
Equation 44: Coefficient of Variation 80
Equation 45: Standard Error of the slope 80
Equation 46: Variable t_p 81
Equation 47: Variable t_c 81
Equation 48: Non-linear Regression Model in fit space 81
Equation 49: Non-linear regression model in unit space 81
Equation 50: Estimated Slope of the non-linear regression line 82
Equation 51: Estimated Intercept of the non-linear regression line 82
Equation 52: Unit Space Equivalent of $\ln A$ 82
Equation 53: Prediction Interval 82
Equation 54: Gas Turbine Life Approximation Model 83
Equation 55: Lifing Factor (Current) 83

Equation 56: Lifing Factor (Initial) 83
Equation 57: Gas Turbine Life Approximation Model (Representation 2) 83
Equation 58: Gas Turbine Life Approximation Model (Representation 3) 84
Equation 59: Reduction Factor, RF evaluation 84
Equation 60: Operating Point Life at DP_{TET} equals OP_{TET} 84
Equation 61: Operating point life at higher DP_{TET} 84
Equation 62: Operating point life at Lower DP_{TET} 84
Equation 63: Operating point life at higher sensitivity to creep 85
Equation 64: Life approximating model component of overall economic model 85
Equation 65: Emissions Rate Calculation 86
Equation 66: Emissions Factor Calculation $_a$ 87
Equation 67: Matching Factor 87
Equation 68: Emissions Tax Estimation 88
Equation 69: Emissions Factor Calculation $_b$ 88
Equation 70: Cost Effectiveness of Emissions Technology (ONSITE SYCOM Energy Corporation , 1999) 88
Equation 71: Total productive life cost Equation 92
Equation 72: Total Capital Cost Equation 93
Equation 73: Total Operation and Maintenance Cost (TOM) 93
Equation 74: Total Direct Operating Cost Equation 94
Equation 75: Total Standing Charge Equation 94
Equation 76: Depreciation Cost 94
Equation 77: Insurance Cost 94
Equation 78: Interest Charge 94
Equation 79: Total Maintenance Cost 94
Equation 80: Maintenance Burden 94
Equation 81: Downtime Cost 95
Equation 82: Cost due to engine Washing 95
Equation 83: Maintenance Cost of Steam unit 95
Equation 84: Total maintenance cost per kilogram of steam 95
Equation 85: Total Running Cost 95
Equation 86: Total Fuel Cost 95
Equation 87: Fuel Volume 95
Equation 88: Transient Fuel Cost 96
Equation 89: Transient Operating Hours 96
Equation 90: Total Transient Duration 96
Equation 91: Total un-incurred Fuel Cost 96
Equation 92: Un-incurred Fuel Cost during engine washing 96
Equation 93: Personnel Cost 96
Equation 94: Emissions TAX 96
Equation 95: Transient Emissions TAX 97
Equation 96: Total Indirect Operating Cost 97
Equation 97: Levelized Cost of Energy (LCOE) 97
Equation 98: Power generated over unit life 98
Equation 99: Total power generated per year 98
Equation 100: Total Annual Cost 99

Equation 101: Total Annual Benefits 99
Equation 102: Benefits on energy 99
Equation 103: Additional Annual Benefits and Savings 99
Equation 104: Power Loss per year due to washing 99
Equation 105: Total benefits Less Cost 99
Equation 106: Net Present Value after tax 100
Equation 107: Net Cash flow after Tax 100
Equation 108: Before tax cash flow 100
Equation 109: Annual Depreciation Allowance 100
Equation 110 : Maximum Specific Work 107
Equation 111: Mach number, M (Walsh & Fletcher, 2004) 108
Equation 112: Moment of inertia (hyperphysics, 2016) 115
Equation 113: Torque Calculation (hyperphysics, 2016) 115
Equation 114: Angular Velocity (hyperphysics, 2016) 115
Equation 115: Angular Velocity when $\omega 0 = 0$ 116
Equation 116: Angular acceleration in rad/s 116
Equation 117: Referred Fuel Flow (Cranfield Department Of Power and Propulsion, 1999) 117
Equation 118: Referred Fuel Flow (Cranfield Department Of Power and Propulsion, 1999) 117
Equation 119: Developed Linear Estimating Relationship 121
Equation 120: Residual Calculation 121
Equation 121: Implemented nonlinear regression model 122
Equation 122: Implemented nonlinear regression model in unit space 123
Equation 123: Equation for minimum useful work 131
Equation 124: Implemented Objective Function 131
Equation 125: Exit Gas Temperature Constraint 131
Equation 126: Turbine Entry Temperature Constraint 131
Equation 127: Gas Mass flow Constraint 131
Equation 128: Useful Work Constraint 131
Equation 129: Performance Optimization Boundaries 132
Equation 130: Initial Point of optimization 132
Equation 131: Implemented Economic Objective Function 132
Equation 132: Useful Work Constraint 132
Equation 133: Performance Optimization Boundaries 132
Equation 134: Initial Point of optimization 132

NOMENCLATURES

Symbol	*Meaning*	*Unit*	*Page*
M	Mach number		18
a	Speed of Sound	m/s	108
A	Net cash flow		62
$A_{(t,x)}$	Before tax Net cash flow without inflation		100
a	Applied activation Function		60
$A'_{(t,x)}$	Before tax Net cash flow with Inflation considered		100
atm	Atmospheres		110
CW	Compressor work	MW	131
cpcold	Specific heat capacity for cold section		131
cphot	Specific heat capacity for hot section		131
Ceq	Non-linear equality constraint		131
C	Non-linear inequality constraints		131
D	Depreciation allowance		100
$D_{(t,x)}$	Annual Depreciation rate		100
DPwgas	Design point gas mass flow	Kg/s	131
e	error in estimated output		60
egt	Exit gas temperature	K	131
epsilon	Perturbation vector		72
Echarge	Emissions Charge	$/ton	96
Erate	Emissions rate	Tons/yr	96
ETax	Emissions Tax	$/ton	96
EPgen	Total power generated per year	MW	98
EPlife	Total power generated per life	MW	98
EPsc	Engine power in simple cycle	MW	98
ExitArea	Exhaust exit area	m^2	131
f	function		56
ff	Fuel flow	Kg/s	131
Fminunc	MATLAB unconstrained minimization function		73
GradCheck	Gradient Checking		72
I	Moment of Inertia	$Kg.m^2$	115
$i_{premium}$	Insurance premium		94
i_{rate}	Interest rate		94
Inf_{rate}	Inflation rate		69
J	cost function		70
k	Number of independent variables		80
K	Degree Kelvin		83
max	maximum		142
MaxEGT	Maximum exit gas temperature	K	131
MaxTET	Maximum turbine entry temperature	K	131
MaxWair	Maximum air mass flow	Kg/s	131
MinUSFWK	Minimum useful work	MW	131
N	Number of samples		57
ln	Natural log		81

n	Length of analysis period		62
η	Efficiency	%	53
norm	Normal		69
η_t	Turbine Efficiency	%	107
η_{th}	Thermal Efficiency	%	111
Num	Numerical		72
PL_{NW}	Power Benefit loss due to engine washing		99
PPIcyear	Producer price index for current year		69
PPIpyear	Producer price index for previous year		69
PT	Power Turbine		110
r	Pearson's Correlation Coefficient		76
R^2	Coefficient of determination		79
rpm	revolutions per minute		68
rps	revolutions per second		68
S_1	Standard Error of the slope		80
t	time	s	116
τ	Torque	Nm	115
TETval	Turbine entry temperature	K	131
t	Current analysis period		116
T_1	Inlet Temperature	K	54
T_4	Turbine Entry Temperature	K	54
TW	Turbine work	MW	131
t_c	Calculated Statistical Test		124
t_p	Tabulated Statistical Test		124
Tamb	Ambient temperature	κ	131
Ttwo	Compressor outlet temperature	κ	131
$V_{T/O}$	Take Off Velocity	m/s	108
Vegt	Exit gas velocity	m/s	131
W	Mass Flow	kg/s	131
W	Weight		59
wair	Mass flow of air	Kg/s	131
X	Marginal income tax rate		100
x	Investment or project designation		100
$\boldsymbol{X}$	Network Input		69
Xnorm	Normalised Data		69
$Y_{(t,x)}$	Net cash flow after tax		100
$\boldsymbol{Y}$	Target Output		71
$\hat{y}$	Network Output Estimate		70
z	Additional analysis period		63
Z	Activity in layer		63
α	Angular acceleration	rad/s^2	116
β_0	*y* intercept		77
β_1	Slope		77
δ	Partial derivative		71
λ	Regularization term		73
ω	Angular velocity	rad/s	115

ω_0	Initial Angular velocity	rad/s	115
!=	Not equal to		124
≠	Not equal to		81
=	Equal to		80

Abbreviations

ANN	Artificial Neural Network		29
BCR	Benefit-cost ratio		61
BEP	Break even period		164
BFGS	Broyden–Fletcher–Goldfarb–Shanno algorithm		102
BOE	Benefits on energy		99
CC	Combined cycle		33
COT	Combustor Outlet Temperature	K	117
CV	Coefficient of variation		79
DLE	Dry low emission		38
DLN	Dry low NOx		128
DP	Design Point		84
ECM	Economic Cost Model		90
ECV	Effective Component Volume	m^3	114
EGT	Exit Gas Temperature	K	131
E	Emission		86
EMH	Engine maintenance hours		94
EOH	Engine operating hours		88
EPL	Engine productive life		94
F_{flow}	Fuel Flow	kg/s	95
FPT	Free Power Turbine		108
HPC	High Pressure Compressor		114
HPT	High Pressure Turbine		114
IB	Investment base		63
IPH	Investigated planning horizon		164
IRR	Internal Rate of Return		62
ISA	International Standard Atmosphere		78
LCOE	Levelized cost of energy		65
LIA	Life Approximation Analysis		83
LPC	Low Pressure Compressor		114
LPT	Low Pressure Turbine		114
LF	Lifing Factor		83
MARR	Minimum acceptable rate of return		63
MF	Matching Factor		87
NAF	Nigerian Air Force		26
NAN	News Agency of Nigeria		27
NDMF	Non-dimensional Mass flow		113
NPV	Net present value		29
OP	Operating point		84
ORR	Overall Rate of Return		62
ORRs	Scaled overall rate of return		63

PCN	Rotational Speed		136
PL	Power Loss due to engine washing		99
PPI	Producer price index		68
PR	Pressure ratio		107
PT	Power Turbine		110
RA	Regression Analysis		118
REM	Repurposed engine model		iii
$REM_{(Unoptimized)}$	non-intercooled and un-optimized engine model		200
REMOptim	non-intercooled but optimized engine model		200
$REMINT_{(Unoptimized)}$	Intercooled but un-optimized engine model		200
REMOptimINT	Intercooled and optimized engine model		200
RF	Reduction Factor		83
ROI	Return on investment		164
RPM	Revolutions per minute		118
rpm	Revolutions per minute		116
RPS	Revolutions per second		114
SE4ALL	Sustainable Energy for All		24
SC	Simple cycle		33
SE	Standard error of estimate		79
SFC	Specific Fuel Consumption	mg/J	105
SHP	Shaft Power	MW	137
SP	Spare Cost		93
SW	Specific Work		107
TBLC	Total benefits less costs		99
TCC	Total capital cost		92
TDOC	Total direct operating cost		93
TERA	Techno-Economic and Environmental Risk Assessment		28
TET	Turbine Entry Temperature	K	83
TIDOC	Total indirect operating cost		93
TIT	Turbine Inlet Temperature	K	105
TOM	Total Operation and Maintenance Cost		92
TPLC	Total productive life cost		92
UN	United Nations		24
UR	Upgrade/retrofitting cost		92

Subscript

%increase		138
AQC	acquisition cost	121
benefit		98
c	Compressor	107
charge		88
cost		93
cyear	current year	69
density		95
Engine Life		83

exhaust	Exhaust	144
flow		95
gen		98
life		83
premium		94
PWR	power	99
pyear	previous year	69
rate		69
Steam		95
t	Turbine	107
T/O	Take off	108
Tax		87
th	Thermal	111
volume		95
x	independent variable	76
y	dependent variable	76

Superscript

T	Transpose	70
(1)	layer one designation	69
(2)	layer two designation	69
(3)	layer three designation	69

1 INTRODUCTION

According to records from the World Bank Sustainable Energy for All (SE4ALL) database and reports from the United Nations (UN), about 13% of the worlds population does not have access to electricity (The World Bank Group, 2019). This number suggests that a vast expanse of the world's population is not connected to the electricity grid. This worldwide challenge is particularly evident in developing and least developed countries and notably increases as considerations extend to countries without stable access to electricity.

The world's least developed countries desperately need much more reliable power sources this is because inadequate access to power suppresses economic growth and inhibits the proliferation of a digital revolution in such regions. In developing countries where power is somewhat available, it is not reliable and often leads to recurring blackouts. As such, organisations and companies are relegated to the use of generators, which adds to their already high operation and maintenance cost. Unfortunately, the energy sector, for developing and least developed countries, gets very little attention when it comes to global development projects. According to a 2015 report by the UN, only about 1.8% of official development assistance aid is allocated to support expansion or integration of power generation in developing and least developed countries. This suggests that the UN is a long way from hitting one of its 17 Sustainable Development Goals to "ensure access to affordable, reliable, sustainable and modern energy for all" by 2030 (United Nations, 2015). Although electricity production between 1990 and 2014 quadrupled in the least developed countries, due to population growth, the overall impact was only a factor of 2.5 (Rooks, 2017).

One solution with potential to consolidate power-generating efforts across the globe is technology adaptation. This effort considers repurposing certain existing technologies and systems for electrical power generation. An instance considered in this study involves repurposing the power plants of obsolete or grounded aircraft engines (gas turbines) for electrical power generation. Such adaptations are popular in the aerospace industry with aircraft engines being converted to aero-derivative engines. Repurposing an aircraft's gas turbine for electrical power generation demands a lot of technical modifications and financial investment, which may or may not be worthwhile. In order to identify the potential costs and benefits of such an endeavour from concept, through implementation to decommissioning, techno economic analysis is necessary.

Gas turbine engines are one of the major prime movers used in industry and aviation to produce energy and power. However, a major limitation of gas turbines in relation to climate change is that they are powered by fossil fuels, which generate certain emissions, in varying amounts, into the environment. Studies suggest that some of these emissions favour an increase in the rate of climate change, which is currently of worldwide concern. Numerous governments, organizations and industries have allocated substantial resources to the investigation, research and assessment of traditional as well as novel cycles and systems to optimise gas turbine performance and potentially address the broad scope of this emissions challenge. As such, techno-economic analysis is necessary to evaluate, quantify and assess the implications of these emerging potential solutions from a technical and economic perspective and in the most viable and cost effective way.

Techno-economic analysis is one of the major tools used by organisations to gauge the benefit-cost ratio (BCR) of an investment over the life of that investment even before any resource or capital is allocated to the project. Without proper investigation into the elements of a proposed project or investment, an organisation runs the risk of miss management and allocation of resources or even failure over the life of the investment. This will mean loss of the scarce resources that could have been invested elsewhere to generate profit for the organisation. As such, every organisation places very high importance on conducting a robust and concise economic analysis to enable informed decision-making and minimise the risk of failure.

Organisations planning to invest in gas turbine engines require tailored and relevant information on the potential costs and benefits obtainable when certain investment is made on one unit over other alternatives. The investment choice must be justified as being beneficial, in the medium to long term, to the organisations profit and sustainability. Depending on the type and nature of a project, the elements and forces that determine the effective distribution of scare resources may vary. For instance, the techno-economic analysis required for the choice of a gas turbine unit, for power generation, may vary depending on factors like; Engine Application, Performance requirement, Geographical location, Government policies, Unit Acquisition cost e. t. c. Despite the variability in the influence of these factors on an economic analysis, the resultant gauging criteria is usually the same and is referred to as the project selection criteria

In light of this, this research aims at providing an approach for assessing potentially significant solutions for gas turbine engine performance optimization from a technical and economic perspective by investigating Brayton cycles. Brayton cycles are used in the aviation and power generation industry due to their benefits of small weight-to-power ratio, capability to accommodate large volumes of gases and variability in fuel type. The outcome and focus of this research is made sufficiently generic to provide a potential read across to existing and future power generating platforms and engine systems.

1.1 Relevance of Research to Nigeria

In 1975, the Nigerian government procured 25 MiG-21 MFs and 6 MIG-21 UM. But by the 1990s, due to lack of spares and finance, the aircrafts were grounded (GlobalSecurity, 2015). In 2004 attempt was made to refurbish the fleet of MIG-21s but this effort was suspended due to the purchase of an alternative aircraft at the time. This purchase was deemed more economical than the refurbishment of the MiG-21s (GlobalSecurity, 2015). The fleet of MIG-21 aircraft has remained grounded ever since.

For several years now, Nigeria has had to deal with the challenge of effective generation and distribution of adequate and consistent power supply to its citizens. According to reports from NAN, Nigeria needs an estimated 140,000MW of power to handle, adequately, the power demand in the country. However, current national generating capacity is a little above 4000MW. A number of people argue that the primary challenge facing the power sector in Nigeria is power distribution and not generation. While the challenge of power distribution is undeniably true, there lies the fundamental challenge of power generation. “You can only distribute what has been generated”. As at yet, Nigeria has not been able to achieve an acceptable quota of generated power. This needs to be addressed before improvements and

upgrades of available distribution networks can be effectively implemented. The rationing of light across the country is more a function of the insufficiency in the generated electricity than it is of the distribution.

As a support to the national generating capacity, the conversion of the power plants for the currently grounded, Nigerian Air Force (NAF), MIG-21 fighter jets to aero-derivative gas turbines, for electrical power generating applications, can supplement the current generating capacity in the country by a predicted estimate of about 10-12%. This proposed conversion will provide benefits in the following areas:

- Enhanced national generating capacity
  Converting the grounded NAF MIG-21 power plants to aero-derivative will supplement the current national power generating capacity by about 10%.
- Revenue generation for NAF
  In addition to supplementing electrical power generation, the power plant conversion will provide an alternate profitable use for the engines of the grounded NAF MIG-21 aircrafts.
- Addition of value and prestige to the NAF
  The unique contribution to economic growth obtainable by supplementing the current national power generating capacity in Nigeria will enhance widespread respect and admiration for the NAF.
- Reduction in emissions foot print
  Nigeria has a heavy record of fossil fuel emissions via piston engine generators. Availability of an improved power generating capacity will enhance the potential of attaining consistency in electricity supply. This will minimize the use of piston engine generators and thus minimize the annual atmospheric emissions generated across the country from the use of generators. Furthermore, a reduction in emission generated will also contribute to the realization of the vision 202020 goal of 10% emissions reduction in the country and extend support towards the achievement of the goals of the recently signed global emissions consensus.

The challenges briefly outlined above have fuelled the execution of a study to determine the feasibility, from a performance and economic perspective, of converting the power plant of the MIG-21 fighter jet to an aero-derivative for electrical power generation. The initial objective of the study is to develop a generic model/ approach for techno economic analysis and performance optimization with sufficient flexibility for extended application in investigating and simulating various gas turbine performance scenarios and their economic implications. The developed method will then be implemented in simulating and investigating, the power plant model, for the MIG-21 fighter jet, repurposed for electrical power generation.

1.2 Likely Developmental Impact of Research Project to Nigeria

In Nigeria today, the demand for electricity far outweighs the current supply from power generation platforms. Estimates from the Centre for Global Development in 2010 revealed that less than 10% of electricity demand in Nigeria was being met. According to an article posted on the Nigerian tribune website on 6 September 2014, written by Sani Adamu, Nigeria would need an estimated 140,000MW to guarantee stable supply of power for an estimated

population of 170 million but at present, generating only about 5,000 MW (Figure 1). Nigeria therefore needs to sustain and optimize existing power generation platforms and build new ones if the country is to attain the vision 2020 goal of being among the twenty largest economies in the world.

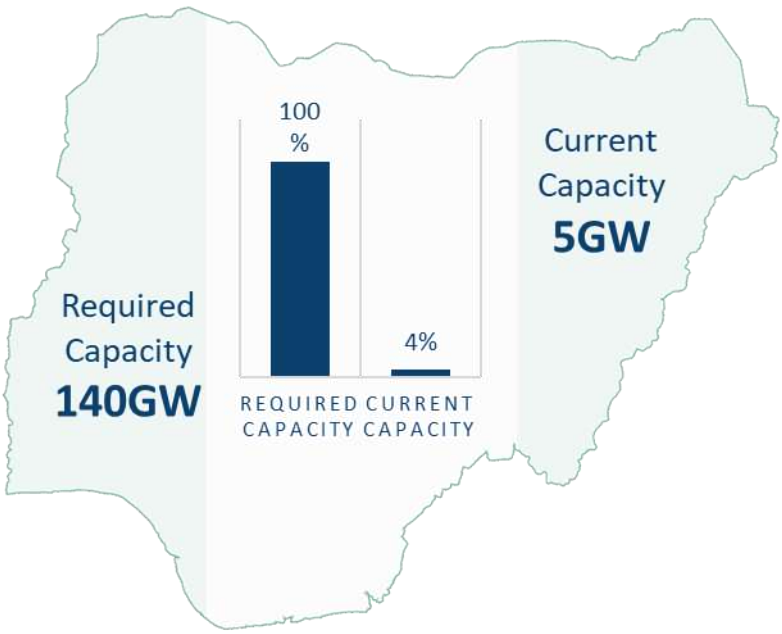

Figure 1: Required Generating Capacity versus Current Generating Capacity in Nigeria

Certain measures are already being implemented to develop the power sector in Nigeria, which involves both government and private sector initiatives. Sani Adamu of NAN outlines that four projects expected to generate about 4,774 MW have been completed while six others are at 80 to 90 percent completion. However, the developments of power generating platforms are not without costs. Most power generating platforms in Nigeria burn fossil fuel to produce thermal energy, which is converted to electricity. The resulting products of the combustion process are released in differing amounts into the atmosphere. These products are more generally referred to as emissions. Growing evidence around the world reveals that many of these emissions like, Carbon dioxide, Sulphur dioxide and oxides of nitrogen may be part of the causes of climate change. Another cost that cannot be overlooked in the establishment and sustenance of power generating platforms is the cost of installation, operation and maintenance, which may be categorized as life cycle cost. It encompasses all costs ranging from establishing a new plant, retrofitting an existing plant to maintenance and eventual decommissioning of the platform.

This research project assess how modifications to the basic thermodynamic cycle of a gas turbine may be used to minimize operation and maintenance cost and maintain profitability for industrial and aero-derivative gas turbine engine applications. The study, conducted from a technical and economic perspective pivots on performance optimization, cost modelling, economic modelling and emissions evaluation based on present and projected cycles for the future. This is with the view of accommodating the ever-changing technological and economic climate in the world and contributing towards the achievement of a vibrant and sustained power infrastructure service that supports the mobilization of the economic sector in Nigeria.

This research also presents an approach for estimating the emissions generated by gas turbine cycles. This is necessary for effective evaluation of the techno-economic implication

of a considered system. Furthermore, outcomes of this research provide sufficient leeway for the development of eco-friendly engine systems technology, in event of future interests of countries like Nigeria in gas turbine engine technology design and development. The research approach adopted is sufficiently generic in its focus and outcomes to ensure a potential read across to conventional power generating platforms both within and outside the country.

Numerous research activities have already been conducted in the area of Brayton cycle performance investigation and optimization. This research however, aims at complimenting as well as building upon previous and current research efforts from a performance and economic optimization perspective, with the view of providing conservative answers to typical technical, environmental and economic questions such as:

- Is the considered system viable and cost effective?
- Does the proposed option accommodate present and projected future cycles?
- What are the cost and environmental implications of this option?
- Is the effectiveness of this option independent of geographical location?
- What other potential options are identifiable?

1.3 Background

Diverse scholars have addressed the investigated research domain.

1.3.1 Techno-economic Investigations

(Wanis, 2013), effectively simulated the engine operations of a fleet of gas turbine engines and their attendant costs under different scenarios based on TERA (Techno economic, environment, Risk analysis) philosophy. He documented that the approach was capable of determining the appropriate engine parameters necessary to optimize a fleet of engines, to meet current power requirements. He also presented a novel means for meeting market growth demands while minimizing cost and environmental impact (Wanis, 2013).

A limitation of this in-depth study is the reliance on escalation factors in the economic analysis. The use of escalation factors can lead to cost overrun due to the potential for cost underestimation. This can happen because, determination of escalation rates are specific to an item or class of items and not as a general nature. Furthermore, escalations are driven by changes and imbalances (often uncontrollable and time based) which are specific to certain goods or services in the economy. This makes them less sustainable (Hollmann & Dysert, 2007).

(Khan, 2012), in his study on "*TERA for Rotating Equipment Selection*" developed a multidisciplinary simulation tool. This was to aid in decision making relating to plant selection, operation and maintenance planning (Khan, 2012).

The application scope of this study can potentially widen by implementing a multi-objective optimization analysis model, to enable the optimization (maximization or minimization) of factors and elements that can influence plant performance, operation and maintenance which in turn could influence critical organizational decisions relating to a plant or unit.

(Christina, 2011), in an industry wide review documented that it is technically feasible to burn ethanol in a retrofitted Brayton cycle system. She reported that such a system would

potentially provide comparable system efficiencies and significant greenhouse gas emissions reduction to natural gas. Furthermore, she pointed out the existence of economic uncertainties in relation to the net present value (NPV) and levelized cost analysis of ethanol in relation to natural gas (Christina, 2011).
This study is limited in its consideration of certain performance and economic elements likely to occur in service. For instance, the effects of unit deterioration and power cycling on unit performance, emissions, operation and maintenance are not considered. These can have a potent effect on the overall analysis and investigation of a potentially adoptable Brayton cycle system.

(Evangelos, 2008), presented a novel generic techno-economic, environmental risk analysis method for the investigation of the life cycle economic feasibility of existing novel marine gas turbine power plants (Evangelos, 2008).
The study gives a concise insight into the analysis of Brayton cycles from a technical and economic perspective. However, the study does not consider the effects of gas turbine components performance degradation, which can have dynamic consequences on engine performance as well as environmental and economic implications.

(Zhang & Lior, 2006), proposed a novel power cycle with the integration of LH2 Cryogenix exergy. Their analysis revealed that nearly 50% of the LH2 cryogenic exergy could be converted into power with negligible release of pollutants to the environment, high reliability and low operating cost due to the simple design of the system (Zhang & Lior, 2006).
This investigation although highly insightful and innovative, does not consider the economic implications of implementing the proposed cycle particularly against similar power cycles in operation. The economics in addition to the performance and environmental implications of the system is important (from an operator or investors perspective) in determining the feasibility of any potential investment in the proposed cycle.

1.3.2 Artificial Neural Network (ANN) Investigations

(Ilbas & Mahmut, 2012), employ Artificial Neural Network, ANN, to estimate the exhaust gas temperature at maximum continuous and take-off power settings for a turbofan engine. The study uses certain engine operational parameters to perform estimates (Ilbas & Mahmut, 2012). Their comparison of ANN model predictions with engine ground measurements and estimates from regression analysis reveal that ANNs are capable of accurately predicting Exit gas temperature, EGT, in turbofan engines (Ilbas & Mahmut, 2012). They concluded that application of ANN, as a tool for predicting gas turbine engine parameters is feasible.
A similar approach, implemented in this research, estimates gas turbine engine price from rated engine performance parameters.

(Hans & Douglas, 1999), apply ANN in the detection and classification of gas turbine faults by observing changes in gas turbine performance parameters against a benchmark performance (Hans & Douglas, 1999). A robust dual approach combines the attributes of neural networks, Kalman filters, statistical analysis, Bayesian/Evidence based decision-

making, and rule based analysis. An expert system integrates the analysis and conducts value analysis, used in making recommendations. With this approach, the higher accuracy realized in the determination and classification of faults for improved decision-making translates to cost saving. This is directly attributable to the reduced down time, improved planning and asset management obtainable from improved decision-making accuracy (Hans & Douglas, 1999).
This study only adopts the elements of Hans and Douglas study associated with ANN technology and extends it to techno-economic cost analysis.

(Orlando, et al., 1994), employ ANN in the development of a system for the diagnosis and prognosis of gas turbine engine fuel faults. The study delivers a system called "TEDANN" (Turbine Engine Diagnostic Artificial Neural Networks), which applies artificial neural network to real-time automated diagnosis and prognosis of fuel faults in the AGT-1500 gas turbine engine used on the M1A1 Abrams tank (Orlando, et al., 1994). They concluded that the application of ANN technology holds great promise for enhancing the effectiveness of Army maintenance practices.
This study applies ANN technology in the estimation of gas turbine acquisition cost which is a critical variable in accurate economic analysis.

(Stephen & Riti, 2006), present a technique, which applies multiple neural networks to gas path analysis. They propose that the described methodology combined with inference tools, such as expert systems like fuzzy logic, is extendable to engine health monitoring applications.
The study presented in this report applies artificial neural network to retrieve quantitative information on gas turbine price and uses the output as input data for further analysis in a techno-economic analysis model.

This thesis documents the outcomes of a study, focused on the development of an approach for investigating cost effective solutions, for effective power generation, from Brayton cycles. The study attempts to minimize inaccuracies in economic analysis by eliminating the use of escalation factors and adopting a near first principle approach to estimating economic variables.

In this study, a techno-economic analysis methodology, developed with sufficient generality, permits flexible and adaptable applications, of the method, in the analysis of different Brayton cycle systems for power generation. The approach encompasses multiple disciplines including artificial neural network (ANN), economics, thermodynamics and mathematical optimization. The developed techno-economic model implements *ANN* technology to provide accurate estimates of unit acquisition cost, which is a major driver of accurate techno-economic analysis. The implementation of a multi-objective optimization model has extended the applicability of the techno-economic methodology to different areas, including sensitivity analysis, feasibility studies, project assurance, project selection from alternatives and capital budgeting problems. Furthermore, the methodology takes into account technical, environmental and economic variables (policies included) in the evaluation of an optimum solution, based on an investigated system, scenario or cycle option.

This study applies the developed methodology to investigate the technical and economic implications of adopting a repurposed turbojet engine for electrical power generation, against similar competitor units. The investigations in this report, conducted from a technical and economic perspective, focus on performance optimization, cost minimization, emissions evaluation and profit maximization.

1.4 Report Summary

This report describes and presents the outcomes and results obtained throughout the research effort. Chapter 1 gives an introduction into the relevance of the research and its likely developmental impact on the economy, environment and technology. Also briefly presented in this chapter, are the research efforts by various scholars who have previously investigated the research domain considered in this report.

In chapter 2, a statement of the research aim, the research objectives as well as the potential impact and contributions of this research are outlined. Chapter 3 gives an overview of the features and general mode of operation of gas turbines. It describes the types of gas turbines with a focus on aero-derivative gas turbine engines. The requirements and mode of aero-engine conversion to aero-derivative for industrial application is described in this chapter. Chapter 3 also provides an overview of the techniques, theories and approach employed in this study. Explanations describing various models, concepts, challenges and philosophies are also presented.

Chapter 4 outlines and describes the developed and adopted research methodologies. In chapter 5, the contextual implementation of the research methodologies, models and techniques described in chapter 4 are presented. Chapter 6 presents the results obtained from the research with relevant discussion on the research outcomes.

Chapter 7 presents an overall discussion of results and highlights identified research findings from the results obtain in chapter 6. Chapter 8 outlines the research conclusions in relation to the research aim and objectives and highlights some of the observation and outcomes of the research effort. Chapter 9. Identifies limitations of the study and outlines some recommendations for future work.

Chapter 10 contains a list references and bibliography.

2 STATEMENT OF AIM AND OBJECTIVES

2.1 Research Aim

The aim of this research is to develop a method for assessing potentially significant solutions for gas turbine engine performance and system optimization from a technical and economic perspective and in a viable and cost effective way through the investigation of Brayton cycles.

2.2 Objectives

Undertaking the following objectives deliver the research aim.

- Select case study engine for research analysis.
- Conduct thermodynamic performance analysis for steady state and transient engine operation using TURBOMATCH.
- Develop and implement new cost and economic analysis model.
- Perform Baseline Techno-economic analysis on a case study engine, taking into account steady state and transient engine performance.
- Implement optimization analysis into the economic model.
- Develop robust decision-making tool and integrate with TURBOMATCH.
- Analyse and interpret results obtained from the study.

2.3 Research Contributions and Impact

Outlined below are the contributions and impact of this research

2.3.1 Research Contribution

- Development of a price estimating approach, using artificial neural network (ANN) for estimating gas turbine acquisition cost based on engine performance parameters.
- Development of a price estimating approach, using regression analysis for estimating gas turbine acquisition cost based on engine performance parameters.
- Development of an emissions model capable of estimating gas turbine emissions rate, emissions tax and quantity of emissions controlled.
- Performance modelling and simulation of an engine similar to the TUMANSKY-R25-300 turbojet engine. The developed engine model performance closes matches the real engine performance with 4.5% difference in specific fuel consumption and less than 1% difference in maximum dry thrust.
- Performance modelling and simulation of the aero-derivative variant of an engine similar to the TUMANSKY-R25-300 turbojet repurposed for electrical power generation.
- Development of a multidisciplinary techno-economic modelling and analysis approach applicable in techno-economic analysis and optimization of gas turbines systems in both simple and combined cycle applications.
- Development of a techno-economic modelling and analysis tool, which combines elements of performance modelling and simulation, price estimation, emission evaluation, life approximation and techno-economic optimization into a cohesive whole for robust techno-economic analysis. The tool has been integrated with TURBOMATCH to widen its scope of application for techno-economic analysis.
- Techno-economic modelling, analysis and optimization of a turbojet engine repurposed for electrical power generation.

2.3.2 Research Impact

- **Revenue generation for the Nigerian Air force (NAF)**
  This study identifies an alternative profitable use in electrical power generation for the power plants of a fleet of grounded fighter jets owned by the Nigeria Air force. Research investigations reveal that the repurposed engine model is economically feasible and can compete favourable with potential competitor units. This implies that investment in repurposing the power plant of the fleet of grounded aircrafts for electrical power generation has the potential to generate revenue for the Nigerian Air force. Therefore, it is possible to regain a certain percentage (equivalent cost of the power plant) on the amount spent on purchasing the now grounded MiG-21 aircraft while generating revenue for the Nigerian Air force and contributing to national growth and progress in the area of power generation and emissions mitigation.
- **Enhanced national generating capacity**
  Repurposing the power plants of the considered grounded aircrafts has the potential to supplement and consolidate the current national generating capacity in Nigeria by about 8% in simple cycle (SC) and 10% in combined cycle (CC) applications.
- **Tools and information for enlightened decision-making**
  The research investigation delivers the tools and quantitative information, needed for informed decision making, on the potential to repurpose the considered engine for electrical power generation. For example, results from investigations reveal that application of the repurposed engine model in combined cycle is most beneficial to the potential investors (The Nigerian Air force) and their potential customers (Nigeria).
- **Reduction in emissions footprint**
  The potential contribution, identified in this study, of investing to repurpose the power plant of the grounded aircrafts will enhance national power generating capacity in Nigeria. Nigeria has a heavy record of fossil fuel emissions via privately owned piston engine generators. Availability of an improved power generating capacity will enhance the potential of attaining consistency in electricity supply. This will minimize the use of piston engine generators and thus minimize the annual atmospheric emissions generated across the country from the use of generators. Furthermore, a reduction in emission generated will also contribute towards the realization of the vision 202020 goal of 10% emissions reduction in the country and extend support towards the achievement of the goals of the recently signed global emissions consensus.
- **Addition of value and prestige to the Nigerian Air force (NAF)**
  The unique contribution to economic growth obtainable by supplementing the current national power generating capacity in Nigeria (via the proposed investment) will enhance widespread respect and admiration for the NAF.

3 BACKGROUND LITERATURE

3.1 Gas turbine engine operation

Gas turbine engines are one of the major prime movers used in industry and aviation to produce energy and power. However, a major limitation of gas turbines in relation to climate change is that they are powered by fossil fuels, which generate emissions into the environment. This favours climate change, which is currently a worldwide challenge. Gas turbines operate based on the Brayton Cycle principle (Figure 2).

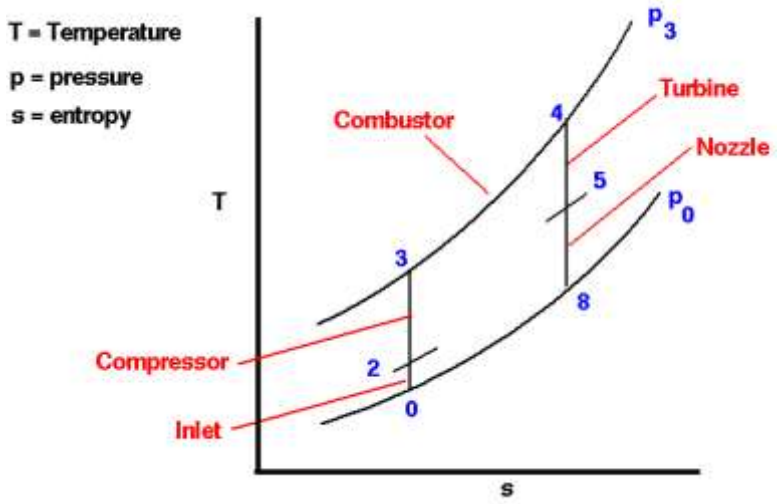

Figure 2: Ideal Brayton Cycle

The Brayton Cycle is a thermodynamic cycle that undergoes a series of thermodynamic processes to produce energy for work. Essentially, the temperature of compressed air is increased by the addition of heat. This is achieved by burning a mixture of the compressed air with fuel thus raising the internal energy of the compressed mass of air. The heated compressed air (gas) is then expanded through a turbine. The expansion process extracts some of the heat and energy from the gas and uses it to do work. Finally, the expanded gas is released into the atmosphere as exhaust, which usually contains oxides of carbon, oxides of sulphur, oxides of nitrogen, particulate matter and un-burnt hydrocarbons (Badr, 2013). These products are referred to as atmospheric emissions.

3.1.1 Gas turbine Emissions

Gas turbine engines primarily emit nitrogen oxides (NO_x), carbon monoxide (CO), volatile organic compounds (VOC) and particulate matter (PM). PM emissions are much more predominant in gas turbines burning liquid fuels (United States Environmental Protection Agency, 1995). Gas turbines emit trace to low amounts of and hazardous air pollutants (HAP) and sulphur dioxide (SO_2). The amount of sulphur emissions generated by a gas turbine is directly influenced by the sulphur content in its fuel. The formation of nitrogen oxide in a gas turbine is strongly dependent on high temperatures generated in the combustion chamber. On the other hand, emissions of CO, VOC, HAP and PM are the results of incomplete combustion. Ash and metallic additives in fuel may also contribute to PM in the exhaust (ONSITE SYCOM Energy Corporation , 1999; Pavri & Moore, 2001).

3.1.1.1 Nitrogen Oxides

NOx formation in the combustion chamber of a gas turbine is driven by two fundamental mechanisms. These include:

- Oxidation of atmospheric nitrogen found in combustion air, resulting in thermal NOx and prompt NOx.
- Reaction of nitrogen chemically bound in fuel, resulting in Fuel NOx.

3.1.1.1.1 Thermal NOx

Thermal NOx is formed when oxygen and nitrogen present in combustion air chemically react at, high temperatures, to form NOx. This reaction is known as the Zeldovich mechanism, which occurs at the high temperature region of the combustion chamber (ONSITE SYCOM Energy Corporation , 1999). According to the Zeldovich reaction, thermal NOx increases exponentially with increasing temperature and linearly with increasing residence time.

3.1.1.1.2 Prompt NOx

Prompt NOx is formed when intermediate combustion products such as HCN, N and NH undergo oxidation resulting in NOx. Prompt NOx is created around the flame front in both fuel-rich and dry low NOx (DLN) combustion zones. For combustors burning near stoichiometric conditions, the contribution of prompt NOx to the overall NOx emissions generated by a gas turbine is relatively small (United States Environmental Protection Agency, 1995). However, in DLN combustors, the quantity of prompt NOx generated accounts for a significant amount of the overall thermal NOx. As a result, prompt NOx becomes a significant consideration during DLN combustor design as it establishes a minimum attainable NOx level in lean mixtures (Pavri & Moore, 2001).

3.1.1.1.3 Fuel NOx

Fuel NOx is formed from the combustion of fuel containing nitrogen. During combustion, nitrogen bonds in the fuel break and some of the nitrogen undergoes oxidation to form fuel NOx (Pavri & Moore, 2001). The degree of NOx formation is usually a function of the nitrogen content of the gas turbine fuel. The fraction of fuel-bound nitrogen (FBN) converted to fuel NOx decreases with increasing nitrogen content, although the absolute magnitude of fuel NOx increases. For stationary gas turbines firing natural gas, fuel NOx does not significantly contribute to overall NOx emissions (ONSITE SYCOM Energy Corporation , 1999).

3.1.1.1.4 Factors Influencing NOx Formation

NOx formation is unique from one gas turbine to another. This is due to difference in gas turbine specifications, performance and operating conditions (Pavri & Moore, 2001). The major factors that influence the quantity of NOx generated by a gas turbine include:

- Ambient Conditions
- Combustor design
- Power Output
- Operating Cycle
- Fuel Type

3.1.1.1.4.1 Ambient Conditions

The ambient conditions that influence NOx formation are humidity, temperature and pressure (United States Environmental Protection Agency, 1995). Humidity has the most significant effect on NOx formation due to the water vapour content. However, this effect varies depending on ambient temperature levels. At high humidity levels and high ambient temperatures (typically above 50°F (10°C)), NOx emissions decrease with increasing

temperature. At high humidity and low ambient temperature levels, NOx emissions increases with temperature. At low humidity level, NOx emissions increase with ambient temperature. In relation to pressure, as ambient pressure increases, NOx formation tends to increase. This is because higher ambient pressures results in elevated temperature in the combustor (ONSITE SYCOM Energy Corporation , 1999).

3.1.1.1.4.2 Combustor design

Combustor design parameters such as cooling airflow, flame temperature, residence time, pre-combustion mixing, operating load and air/fuel ratio control, influence NOx formation in a gas turbine (ONSITE SYCOM Energy Corporation , 1999). These parameters govern the characteristics of gas turbine combustors as pertaining emissions generation and control. Combustor design is the most important factor influencing NOx formation.

3.1.1.1.4.3 Power Output

The firing temperatures of gas turbines are govern by the required/demanded power output. Firing temperatures are directly associated with combustor flame temperatures. A high load demand will require high firing temperatures leading to higher NOx formation and vice versa. At high load, the flame front reaches its maximum size and length, with a greater percentage of fuel undergoing combustion and less air available to quench combustion products. This results in the formation of greater amounts of NOx emissions than at lower loads.

3.1.1.1.4.4 Operating Cycle

For turbines used in combined cycle or cogeneration cycle applications involving the use of duct burners, there have been observation where net NOx emissions reduction have been observed in flows across a duct burner. The reason for this reduction has not been firmly established. However, it is believed that the reduction in NOx is the result of chemical reaction, in the duct burner, between the intermediate combustion products and already present NOx in the gas turbine exhaust (ONSITE SYCOM Energy Corporation , 1999).

3.1.1.1.4.5 Fuel Type

The quantity of NOx emissions generated by gas turbines varies with fuel type and composition. Fuel mixtures containing higher molecular weight hydrocarbons burn at higher flame temperatures and can result in higher NOx emission levels. This characteristic is primarily concerned with gaseous fuel mixtures. In contrast to the characteristic described above, gaseous fuels containing a significant amount of inert gases typically emit lesser NOx emissions. This is because during combustion, the inert gases absorb heat and lower the flame temperature of such gaseous fuels. Liquid fuels like distillate oil burn at higher flame temperatures that natural gas and result in higher NOx emissions. Low Btu fuels burn at lower flame temperature and result in lower NOx emissions. An example of such low Btu flame is Coal gas (ONSITE SYCOM Energy Corporation , 1999).

3.1.1.2 Carbon Monoxide (CO)

CO formation is the result of incomplete combustion in gas turbine combustors. Incomplete combustion occurs when there is insufficient residence time, quenching by dilution air or incomplete mixing in a combustion chamber to permit the complete oxidation of fuel carbon. At gas turbine temperatures, oxidation of CO to CO_2 is a slow process in comparison to similar reaction in most hydrocarbons. In liquid fuels, the carryover of larger fuel droplets from the

atomizer may aggravate CO formation (United States Environmental Protection Agency, 1995).

Gas turbine loading also influences the rate of CO formation. Gas turbines operating under full load reduce the formation of carbon monoxide. This is because at full load, the turbine experiences greater fuel efficiencies. Conversely, Gas turbines operating at medium or light load increase the formation of carbon monoxide. This is because of the lesser fuel efficiencies experienced at these loads due to incomplete combustion (Pavri & Moore, 2001).

3.1.1.3 Volatile Organic Compounds (VOC)

VOC are the results of incomplete combustion in a gas turbine. VOCs are emitted when some fuel remains completely or partially unburnt during a combustion process. With gaseous fuels, some organics emerge as unreacted trace elements of the gas while in liquid fuels, large fuel droplets emerging in the quenching zone account for majority of unreacted organic emission. Similar to CO emissions, VOC emissions are influenced by gas turbine operating load. Gas turbines operating a high loads emit higher concentrations of volatile organic compounds when compared to similar units operating at low loads (United States Environmental Protection Agency, 1995).

3.1.1.4 Particulate Matter (PM)

Particulate matters (PM) emissions are the result of non-combustible trace constituents in gas turbine fuels. Due to low ash content, PM emissions are negligible in natural gas fired gas turbines and only minimal considerable in liquid fuel fired units. PM can be classified as either “filterable” or “condensable”. The portion of total PM, in liquid or solid form, found in a stack is the filterable PM while condensable PM is the portion of total PM, in gaseous state, found in a stack but condenses in ambient air to form particulate matter. Condensable PM is generally considered, to be less than 1.0 micrometre in aerodynamic diameter (United States Environmental Protection Agency, 1995; Pavri & Moore, 2001).

3.1.1.5 Hazardous air pollutants (HAP) Emissions

Due to the high operating temperatures of gas turbines, HAP emission levels are lower in gas turbines compared to other combustion sources. Formaldehyde is the most significant HAP emission from gas turbines. In natural gas fired turbines, two-thirds of total HAP emissions are formaldehyde compounds. Other compounds like benzene and toluene e. t. c. account for the remaining HAP emissions generated. In distillate oil fired turbines, trace amounts of metallic HAP can be identified in the exhaust, in addition to the gaseous HAP emissions already described. Similar to CO emissions, HAP emissions are influenced by gas turbine operating loads. Higher loads generate greater HAP emissions and vice versa. Most turbines operate at full loads in other to achieve higher fuel efficiency. This minimizes the amount of HAP emissions generated during normal operation (United States Environmental Protection Agency, 1995).

3.1.1.6 Control Technologies

Emission control technology refers to a device, system and/or approach that monitors and limits emissions generated by gas turbines. Emission control in gas turbines can be categorized as wet controls, dry controls and post combustion controls.

3.1.1.6.1 Wet Controls

These reduce combustion temperatures for emissions control. Wet control technologies include steam or water injection and are pre-formation control technologies.

3.1.1.6.1.1 Water/Steam Injection

This emissions control technology suppresses NOx emissions from gas turbines. Water or steam injection reduce peak temperatures in the combustor flame zone. This is achieved when water or steam is injected into the flow stream or directly into the combustion chamber, resulting in an increase in thermal mass. Water or steam injection can reduce NOX emissions by 60% or higher. This is because NOx emission levels exponentially increases with temperature. Therefore, reducing peak temperatures generally lowers the NOx generated during combustion (Bender, 2006). However, the reduction in temperature enhances the potential for generation of CO and VOC emissions. In general, the degree of steam or water injection in gas turbine directly influences CO and VOC emission levels (United States Environmental Protection Agency, 1995).

In addition to NOx emission reduction, water or steam injection can deliver an increase in power output of up to 6 percent. This is directly attributable to the increase in mass flow resulting from injection. There is usually an efficiency penalty incurred with water or steam injection. This penalty is often between 2 to 3 percent. Water or steam injection is usually in ratios of water to air (water-air-ratio) or fuel (water-fuel-ratio) less than 1 (United States Environmental Protection Agency, 1995).

3.1.1.6.2 Dry Controls

These controls suppress NOx emission formation and promote CO burnout in combustors through advanced combustor designs. Some common example of these advanced combustor designs include Lean combustors, Two-stage lean/lean combustors and Two-staged rich/lean combustors. Dry controls are pre-formation control technologies and are identified by a variety of names, including Dry-Low NOx (DLN), Dry-Low Emissions (DLE), or SoLoNOx (Bender, 2006).

3.1.1.6.2.1 Lean combustors

This involves the introduction of excess air into the combustion mixture resulting in a leaner combustion than at stoichiometric conditions. When excess air is introduced, the peak and average temperatures in the combustor reduce, thus suppressing the formation of thermal NOx. Furthermore, the residence time at peak temperature also reduces due to the increase in air-fuel-ratio.

3.1.1.6.2.2 Two-stage lean/lean combustors

Two-stage lean/lean combustors are fuel-staged, premixed combustors, which burn an extremely lean air-fuel-mixture while ensuring a stable flame. The combustion process in this combustor design occurs in two stages in which each stage burns lean. An initial pilot flame burning at stoichiometric condition ignites the premixed gas and provides flame stability (United States Environmental Protection Agency, 1995). This high temperature pilot flame is very small and emits an insignificant level of NOx. There are two primary reasons responsible for the low NOx emission level of this type of combustor (Bender, 2006).

- Air and fuel premixing which prevents the formation of localized “hotspots” within the combustion chamber.

- Lean combustion resulting in cooler flame temperatures

3.1.1.6.2.3 Two-staged rich/lean combustors

Two-stage rich/lean combustors are air-staged, premixed combustors, which burn a rich air-fuel-mixture in the primary zone and a lean air-fuel mixture in the secondary zone. Due to incomplete combustion in the primary zone, lower temperatures (below stoichiometric) and higher concentrations of CO and H_2 are produced. There is also a reduction in oxygen available for NOx formation due to the rich fuel-mixture in the primary zone. On entry to the secondary zone, excess air is introduced to quench the exhaust from the primary zone. This creates a lean air-fuel mixture in the secondary zone. The lean mixture is pre-ignited and the combustion completed in the secondary zone. Combustion in a fuel lean, low temperature environment minimizes NOx formation in the secondary zone (Bender, 2006).

3.1.1.6.3 Post - Combustion Controls (Catalytic Reduction Systems)

These are post-formation control technologies, which apply catalysts to reduce NOx and oxidize CO emissions from gas turbines. Selective catalytic reduction (SCR) is one of the primary post-combustion control technologies currently in use. In the SCR system, ammonia injected into the post- combustion flow stream (exhaust path) reacts with NOx, in the presence of a catalyst (e.g. Vanadium Pentoxide), to produce molecular nitrogen N_2 and water H_2O (Schorr & Chalfin, 1999). The SCR system is located within the "heat recovery steam generator" (HRSG) usually in the region where the temperature of the exhaust stream accommodates the operating temperature of the catalyst. This temperature is typically between 400°F (204°C) - 800°F (427°C) for a conventional SCR system.

SCR systems can be of a conventional, low temperature or high temperature Variant. The low temperature SCR system operates between a range of 300°F (149°C) - 400°F (204°C). This is ideal for retrofit application because the low operating temperature of the catalyst avoids potentially expensive retrofit of the HRSG to locate the catalyst within the HRSG as with the conventional SCR. High temperature SCR systems operate between a temperature range of 800°F (427°C) - 1100°F (593°C). The high operating temperature of the catalysts permits it to be located directly downstream of the exhaust without the need to alter the exhaust system with a HRSG (ONSITE SYCOM Energy Corporation , 1999). There are certain issues associated with SCR systems. Some of these include Ammonia slip (accidental release of stored ammonia into the atmosphere), use with sulphur bearing fuels (possess significant risk to equipment damage) and the cost of disposing spent catalyst (Schorr & Chalfin, 1999).

Another post-combustion control is SCONO$_x$™. SCONO$_x$™ is a post-combustion catalytic control system that removes NOx and CO from gas turbine exhausts without the injection of ammonia. SCONO$_x$™ uses platinum as catalyst and potassium carbonate as the active NOx removal agent. CO undergoes oxidation to CO_2 by the platinum catalyst and NO undergoes oxidation to NO_2. NO_2 then react with the removal agent to form potassium nitrites and nitrates on the catalyst surface (Schorr & Chalfin, 1999). The SCONO$_x$™ system can suppress NOx emissions levels to less than 1ppm and deliver 100% removal of CO from exhaust emissions (ONSITE SYCOM Energy Corporation , 1999).

3.1.1.7 Air Emission – Emissions Rate

Air emission occurs when harmful or excessive quantities of substances (including chemicals, compounds and biological molecules) are introduced into the atmosphere. In relation to air

emissions, emissions rate refers to the amount of a given pollutant generated and emitted into the atmosphere, by a system, over a period. The emission rate of any system is a measure of the activity rate of the system, the emissions factor of the system and the efficiency of any emissions control associated with the system.

$$Emissions\ Rate = \text{Activity Rate} \times \text{Emissions Factor} \times \text{Emissions Control}$$

Equation 1: Air Emissions Calculation

3.1.1.7.1 Emissions Rate

Emissions rate gives information relating to a single system or unit. This is because the type and quantity of pollutant emitted defers from one system to another. Even when identical systems are considered, emissions rate may defer due to differences in operating conditions, operating environment and the considered emissions. Emissions rate is typically expressed in mass per period (mass/period).

3.1.1.7.2 Activity Rate

The activity rate is a measure of how active a system is. The activity rate of a system can be measured in various ways including quantity processed per period, quantity consumed per period, elapsed time per period e. t. c. In general, units of activity rate are in "activity units" per period.

3.1.1.7.3 Emissions Factor

The emissions factor relates the activity of a process or system to the type and amount of pollutants emitted by the system. Determining the emissions factor for a system can be quite a challenging and complex process. In general, there are four ways to determine the emissions factor of a system.

1. Use of emissions data sheet (for example, the environmental protection agency's AP 42 data sheet)
2. Engineering Calculation (conduct complex mathematical and scientific analysis and calculations)
3. Mass Balance (apply the principles of conservation of mass to analyse the physical system)
4. Measurement and testing (source testing, stack sampling or stack monitoring)

The measurement unit for air emissions factor is in mass per activity.

3.1.1.7.4 Emissions Control

This is the ability of a device or mechanism to suppress the emissions generated by a system. Measuring the levels of pollutant flow into and out of a control device defines the emissions control efficiency of that device or system. The actual efficiency of a control is dependent on the implemented technology in that control device or system.

When a control factor **of one** is used, this mean the emissions factor adopted is controlled. Thus, the investigated system may or may not have an external emissions control technology implemented (e.g. water/steam injection, SCR) but may have some form of emissions control built into the system (e.g. DLN technology). In either case, the specifics and history of the adopted emissions factor must be known, for accurate estimation of the emissions rate. A control factor **greater than zero** captures the amount by which one or more adopted emission control technologies suppress emissions generated in a system.

In this study, a model for estimating the emissions rate of gas turbines is presented. Integration of this model with a techno-economic analysis model is presented in subsequent chapters.

3.1.2 Gas Turbine Categorization

Gas turbines can be broadly categorized as aero-engines, industrial engines or aero-derivative engines.

Aero-engines are Brayton cycles that release hot gasses at high velocity through a nozzle to generate the thrust required to propel an aircraft through the air (Figure 3). Some aero-engines (known as turboprop) extract nearly all the energy from the hot gases through a turbine, which convert the energy into shaft power. This shaft power is used to drive an aircraft propeller and other accessory units on the aircraft.

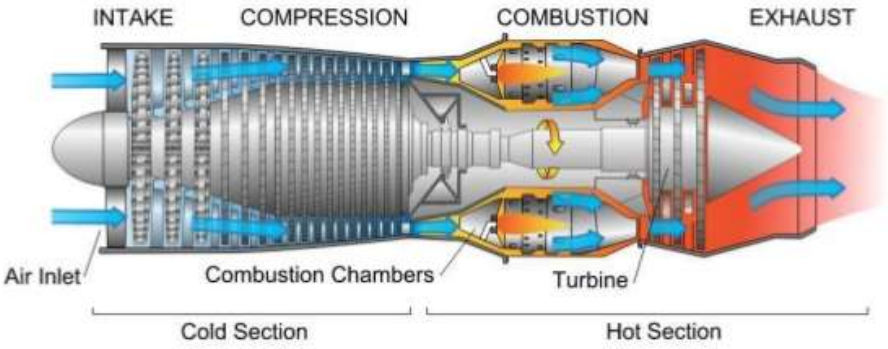

Figure 3: Aero engine image (Turbojet)

Industrial engines are similar to aero-engines; they operate based on the principle of the Brayton cycle and generate shaft power, which is used to drive an electric generator for power generation. Industrial gas turbine engines can be heavy or light frame engines (Figure 4). They generally have slow start up times (ranging up to an hour), low thermal efficiency, and are heavier than aero-engines. Industrial engines are also used for combined cycle, combined heat and power applications, and can reach high efficiencies (up to 60%) in such applications.

Figure 4: 7HA heavy-duty Gas Turbines (bpress, 2014)

Aero-derivative engines (Figure 5) are aero-engines (originally designed for aviation industry) which have been repurposed for industrial applications like power generation, mechanical drive applications, combined cycle or combined heat and power applications (Paul, 2012). Because they are derivatives of aero-engines, they are lighter as their components are made from the lighter aircraft engine design materials. They have much faster start up and shut down times (in minutes) than industrial frame engines. Due to their small size compared to industrial frame engines, they can be used for emergency power, or peaking demand. They also find suitable applications where space availability is a challenge such as marine and offshore platforms.

Figure 5: LM1800e aero-derivative engine (Gas and Steam Turbines, 2012)

3.2 Engine Conversion

Aero-derivative engines are engines originally designed for aviation applications, but repurposed for industrial applications. They are a hybrid of aero and industrial engines. In an aero-derivative gas turbine, the intake and exhaust nozzle of the originally designed aero-engine (turbojet, turboshaft or turboprop) are replaced with the appropriate systems that support industrial applications. The nozzle of the aero-engine is replaced with a power turbine to drive an electrical generator or for mechanical drive applications. Essentially, the core components of the aero-engine are maintained in an aero-derivative variant. In some cases, modifications to certain aspects of the core components like the combustor, compressor, and Turbine inlet guide vanes are made to optimize the engine performance for industrial application.

A major concern in aero-engine conversion for industrial application is the location of the Power turbines. The power turbine can be aerodynamically coupled (liquid coupling), Figure 6. In this configuration, the gas generator exhaust provides the energy to drive the power turbine aerodynamically. Another configuration involves connecting the power turbine, aft of the gas generator (where temperatures are high), with a shaft. This configuration is known as hot end drive (Figure 7).

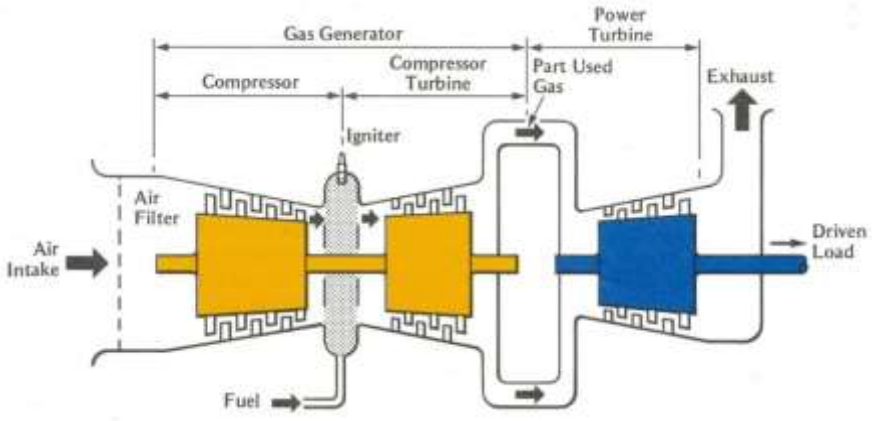

Figure 6: Aerodynamically coupled power turbine (Emad, 2013)

Figure 7: Hot End Drive (Aft of Gas turbine) (MHPS Gas Turbine Generator Set , 2015)

An alternative configuration to the hot end drive is the cold end drive. The power turbine is located upstream of the gas generator (Gas turbine) and is connected with a shaft extension (Figure 8).

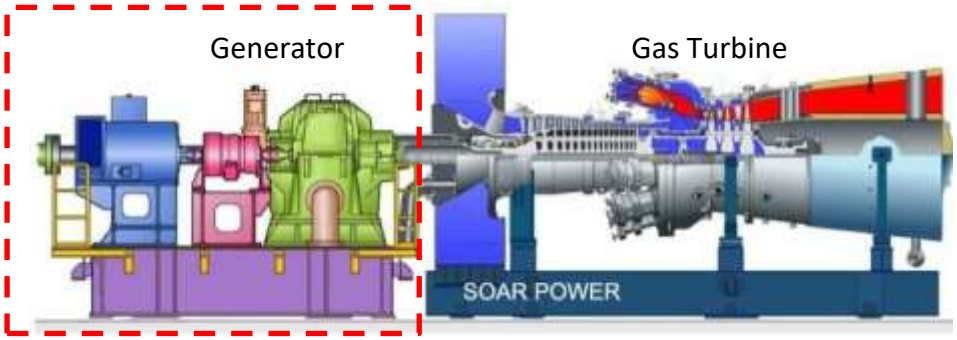

Figure 8: Cold end drive (Integrated output shaft; fore of Gas turbine) (MHPS Gas Turbine Generator Set , 2015)

The choice of power turbine to engine configuration is usually dependent on several factors such as, maintainability, flexibility required, engine application, cost effectiveness, reliability and performance requirement.

Conversion of aero-engines for aero-derivative applications have been performed over the years and have had great success in various industries. For example, the Rolls Royce Avon, a turbojet engine, was originally designed (in 1964) for use on Fighter jets (Paul, 2012). It was later adapted for use as a turbo generator and due to its impressive power to weight ratio, it became very popular on offshore applications. Some Roll Royce Avon aero-derivative engines are still in service today. Typical output for the RR Avon in simple cycle operation ranges between 16 to 22MW (Paul, 2012).

Figure 9: Roll Royce Avon Turbo jet engine (Advanced Animations UK, 2016)

Another aero-derivative engine that has found successful application is the Pratt and Whitney GG4/FT4 gas turbine. It was developed from the Pratt & Whitney J75/JT4 turbojet engine. Typical output of the GG4 in simple cycle operation ranges between 16 to 30MW. This is usually dependent on the engine configuration and operating conditions. The GG4/FT4 aero-derivative gas turbine is still in operation today finding application in power generation and mechanical drive applications.

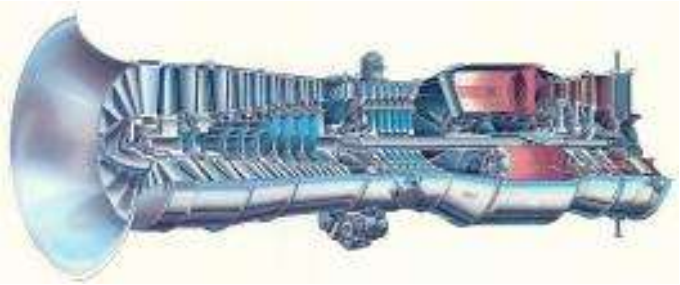

Figure 10: Pratt and Whitney GG4 Aero-derivative Gas Turbine (WGPW, 2016)

3.3 Performance Simulation

In general, performance simulation is the process of imitating a situation or a real-world process or system through the aid of computational modelling, especially for the purpose of study (Banks, et al., 2001). The venture of simulation requires that a model be developed; this model often constitutes the fundamental characteristics, behaviours and functions of the considered physical or abstract system or process. The model describes the considered system itself, whereas the simulation represents the operation of the system over time.

Simulation is applied in many areas, some of which include:

- Simulation of technology for performance analysis and optimization (e.g. Piston engine simulation)
- Safety engineering (e.g. failure/crash testing)
- System testing (e.g. Software application testing)
- System training (e.g. Pilot training)
- Education and Learning
- Video games (e.g. Flight simulator)

Often, computer based experiments are used to study simulation models. Simulation is also used with scientific and mathematical models of natural or human systems to acquire a deeper understanding of their functioning (Smith, 2000); examples of such application can be found in economics. Simulation can be used to show the eventual real effects of alternative conditions and courses of action. Simulation is also used when the real system cannot be engaged, because it may not be accessible, may be dangerous or unacceptable to engage, it is being designed but not built, or it may simply not exist (Sokolowski & Banks, 2009).

3.3.1 Gas Turbine Performance Simulation

Gas turbine performance simulation is a process of simulating the characteristics, behaviour and operation of a gas turbine with the aid of computational models. It is an effective approach for supporting the design, testing and operation of gas turbine systems. Gas turbine performance simulation combines several disciplines including computational modelling, heat and mass transfer, thermodynamics, fluid dynamics and environmental science to model

the behaviour and characteristics of Brayton cycles. This provides a platform for simulating both current and projected future systems cycles and encourages innovation, in operation, design, development and analysis for better performing systems, capable of delivering the required output, with low environmental and economic implications. Rahman et al applied performance simulation to study the effect of cycle parameters on thermodynamic performance of a gas turbine. They developed and simulated the gas turbine performance model in MATLAB. They concluded that, for the investigated scenario, the effect on cycle parameters on the engine's thermodynamic performance was economically feasible and potentially beneficial to the gas turbine operation (Rahman, et al., 2011).

Figure 11 presents a performance simulation methodology applicable in the simulation of a simple gas turbine power plant (Rahman, et al., 2011). The model simulates the performance of a gas turbine based on a set of operating conditions and performance requirement supplied into the model. Air fuel ratio is varied, and associated output conditions calculated until an initially specified power demand is achieved. The calculated output variables at the instance where the performance requirement is met represent the gas turbine output performance variables at that investigated condition or scenario of operation. Energy balance simulates the occurrence in the combustion chamber and with a predicted air fuel ratio, estimates the turbine inlet temperature, which is a key variable in determining the power output delivered by the simulated gas turbine unit.

Gas turbine performance simulation can be applied to simulate and investigate the behaviour of a gas turbine unit in real-world applications. Described in the following sections are some gas turbine conditions that can be investigated with the aid of performance simulation models.

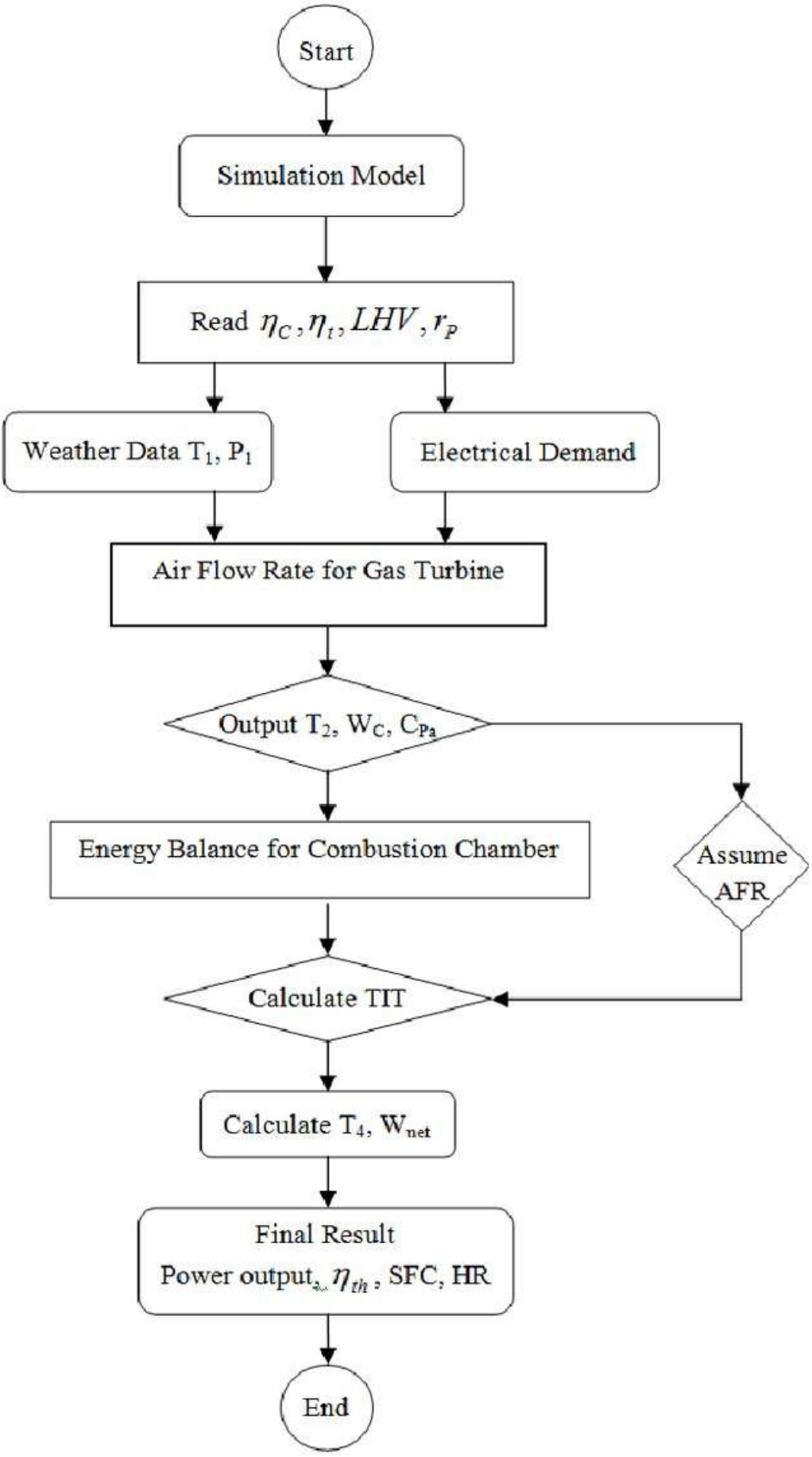

Figure 11: Performance Simulation process for a simple gas turbine power plant (Rahman, et al., 2011).

3.3.1.1 Power Plant Cycling Analysis

In electrical or electronic equipment, power cycling is the action of switching a device or equipment off and then back on again to rectify a fault or failure. The interval between switching off and switching on could range from 5 seconds to 30 seconds depending on the equipment and the manufacturer. Power cycling in electronics is done, mostly, to correct a malfunction in an equipment or device (Techopedia, 2017).

Conversely, in gas turbine operation, power cycling also called power plant cycling involves the intermittent operation of gas turbine units at different power settings over a period. This cycling could be seasonal, daily or even at different times within a particular day. The action of power plant cycling induces stress on gas turbines components, which could potentially influence the health and life of a unit. Power cycling costs have significant effect on plant operation and maintenance. In Figure 12 the effect of increased wind and solar penetration on cycling cost is shown.

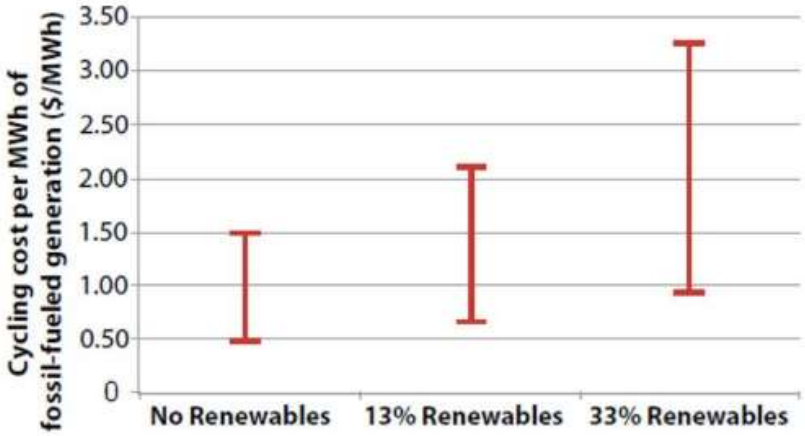

Figure 12: Cycling Cost with increased wind and solar penetration from Fossil-Fuelled Generator Perspective (Kumar, et al., 2012)

Factors such as the increased use of intermittent power generation sources (e.g. renewables) creates challenges for power plants, particularly those in baseload applications. These challenges result from flexible operations (frequent start and stop cycles, varying power settings) of the power plants in order to accommodate the power generated from intermittent sources (ASME Power & Energy Conference, 2018). Due to increasing demand for the adoption and implementation of renewable energy sources for power generation, minimizing equipment damage and assessing the true cost of power plant cycling is more important than ever. Furthermore, there is increasing argument that cycling of units' results in so much carbon emissions that it completely negates the carbon saved by the renewable sources of electricity (Moothart, 2016).

Performance simulation is a tool that provides a means for investigating the effects of power plant cycling on gas turbines. It enables designers, manufacturers and operators to investigate the potential effects of taking certain design, manufacturing and operational decisions and guides trade-offs made between options in order to arrive at the most cost effective and best performance possible in power plant cycling scenarios.

The effect of power cycling on gas turbine power plants is less when cycling occurs over wider interval (e.g. seasonal power plant cycling) but increases as the cycling interval reduces (e.g. daily power plant cycling). Aero-derivative engines are better suited to accommodate the

effects of power plant cycling due to their aero-engine based design as opposed to heavy frame units.

3.3.1.2 Transient Performance Analysis

The future development of gas turbines and associated systems depends on an increasingly detailed understanding of the phenomena and processes taking place within the engine. This fact is also relevant in relation to the economics of gas turbine operation and maintenance. Consideration of the transient operation of gas turbines particularly as standby units and in service units undergoing power cycling can provide better insight into the economic and environmental implications of the transient phase of power plant operation.

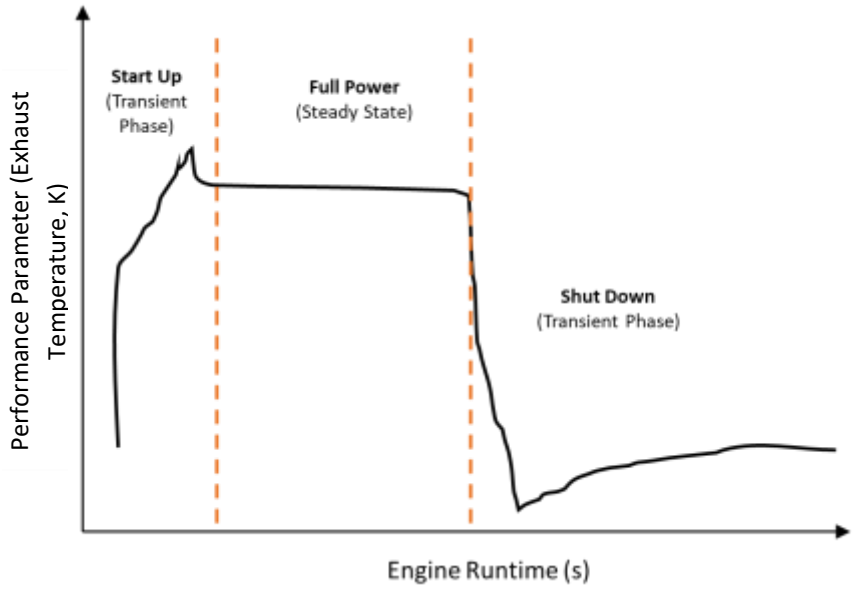

Figure 13: Performance Parameter Vs Engine Runtime

The transient phase (illustrated in Figure 13) is the brief period of time in which a power plant adjusts to a new power setting. During this phase, many components operate close to their performance limits, such as surge in the compressors, high temperatures in the turbines, and in some cases rotor over speeding. Performance simulation enables the modelling and simulation of this phenomenon and provides the platform for understanding the transient characteristics of a particular unit and its influence on the environment (emissions) and economics of operation and maintenance. In 1990, Torella studied the transient performance and behaviour of gas turbine engines. Using both the volume and iterative methods, he developed a code for simulating the behaviour of gas turbine engines during transient operation. He concluded that the iterative approach to transient simulation is fast, reliable and flexible (Torella, 1990).

3.3.1.3 Performance Degradation Analysis

Gas turbine degradation refers to the deterioration or disintegration of gas turbine components. This results in decay in power plant performance over time. Figure 14 illustrates decay in gas turbine performance over time. Deterioration of gas turbine component induces changes in unit thermodynamic performance observable by irregularities in unit efficiencies and flow capacities. These irregularities produce changes in observable engine parameters such as temperatures, pressure, rotational speeds and fuel flow rate. The degradation in performance reflected from these observations can be used to detect, isolate and accommodate component faults (Li, 2002).

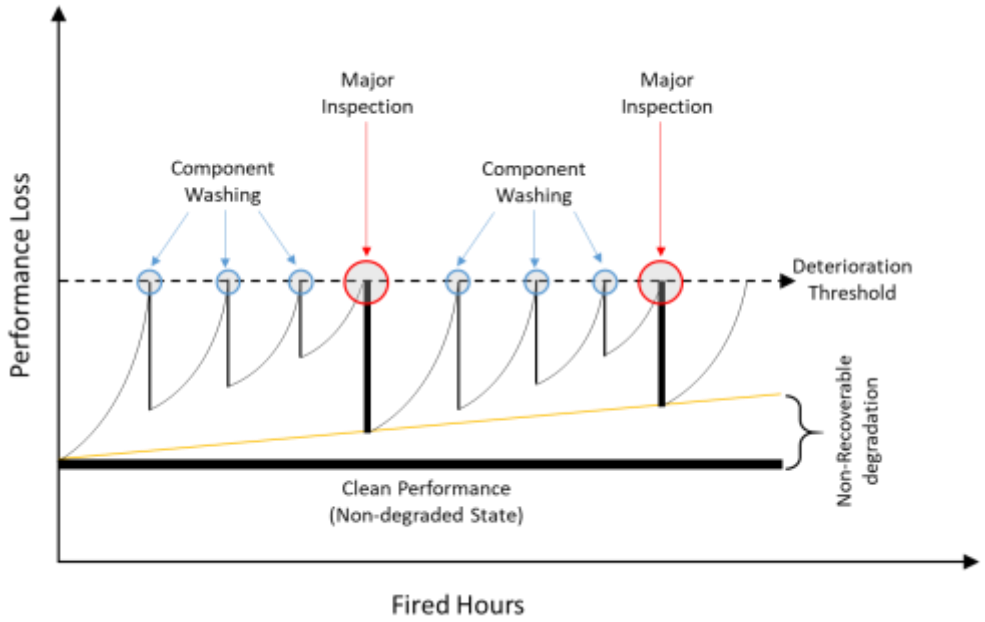

Figure 14: Performance loss due to Gas Turbine deterioration over time

The rate and type of deterioration in a power plant is dependent on numerous factors. These can be modelled to simulate the deterioration of a gas turbine engine. Introduction of degradation element into gas turbine performance simulation model can enable the analysis of certain degradation factors and effects on gas turbines performance as well as investigate the influence, of external factors (environmental and economic factors) on the operation of a degraded unit. In 2014, Rowlands investigated the effect of degradation on two single spool gas turbines. He applied results from the investigation to estimate the remaining useful life of the case study units by implementing a "Gas path diagnostic and prognostic" technique (Rowlands, 2014).

Several mechanism characterize gas turbine degradation. These include:

- Fouling
- Corrosion, hot corrosion, and oxidation
- Erosion and Abrasion
- Particle Fusing
- Mechanical Degradation

3.3.1.3.1 Fouling

Fouling is the adherence of tiny particles to gas turbine component aerofoil and annulus surfaces. Overtime, this build-up of material results in increased surface roughness and alters the shape of the aerofoil. If not adequately addressed, fouling could result in blade stall and engine surge. The gas turbine component most prone to Fouling is the compressor. However, other components also experience some level of surface deposition (Kurz, et al., 2014).

Cold section component fouling can usually be removed by component washing and cleaning. However, hot section component fouling, due to the baking of deposits on hot section component surfaces, require more drastic deposit removal measures. Examples of particles that cause fouling are Smoke, oil, mists, carbon, and sea salt e. t. c. these particles are typically smaller than 2 to 10µm. In gas turbines, the rate of component fouling can be controlled by an appropriate air filtration system and can, to some degree, be reversed by component washing (Kurz, et al., 2014).

3.3.1.3.2 Corrosion, hot corrosion, and oxidation

Corrosion is the wearing of surface metals due to chemical reaction of the metal with the environment. Corrosion mainly involves the reaction of metal with oxygen in the air. How be it, there are other chemical reactions, which participate in the corrosion mechanisms. Gas turbine corrosion can be categorized into hot section corrosion and cold section corrosion. The former comprises oxidation, sulfidation, and hot corrosion and the latter crevice corrosion and pitting (Kurz, et al., 2014).

Corrosion can significantly influence the life and performance of gas turbine engines. The effect of corrosion can be minimized by the use of high quality filtration systems and the application of corrosion resistant coatings.

3.3.1.3.3 Erosion and Abrasion

Erosion is the abrasive removal of material from the surfaces of components in the flow path of a gas turbine. This is usually caused by hard or incompressible particles, typically larger than 10µm, impinging on the flow surface. Foreign objects striking flow path components may also cause damage (Kurz, et al., 2014).

Similar to erosion, abrasion occurs when a rotating surface rubs on a stationary surface. Some engines use abradable surfaces where a certain amount of rubbing is allowed during engine run, in order to establish proper clearances. To rectify the effects of erosion or abrasion, a gas turbine engine component may require adjustment, repair or even replacement.

3.3.1.3.4 Particle Fusing

This is a phenomenon synonymous to fouling but predominant in newer generation gas turbine units. When particles enter the hot section component path, if the fusion temperature of these particles is lower than the turbine operating temperature, the particles melt and stick to the component hot metal surface. This can cause blockage of cooling passages, alter the shape of component surface and interfere with heat transfer. This eventually leads to thermal fatigue. Affected surfaces are permanently damaged and will need replacement (Kurz, et al., 2014).

3.3.1.3.5 Mechanical degradation

This comprises all degradation effects due to mechanical loses, vibration, mechanical wear and tear, faults in lubrication system, component creep and thermal ratcheting, improper maintenance e. t. c.

Performance simulation enables the modelling, simulation and subsequent analysis of the unique characteristics peculiar to a gas turbine in relation to varying influencing factors (Kurz, et al., 2014).

3.3.1.4 Emissions Analysis

Gas turbine engines burn a mixture of fossil fuel and air to generate energy. The products of the combustion generate emissions in deferring amounts into the atmosphere. The amount of emissions generated by a gas turbine varies with firing temperature, fuel type, operating conditions among other influences. Figure 15 shows the CO emissions from an industrial gas turbine. Performance simulation models can be developed to imitate the operation and associated emissions generated from a gas turbine engine. Such a model can investigate the

influence of factors such as ambient conditions, geographical location, economic and environmental policies on gas turbine performance, emissions, operation and maintenance.

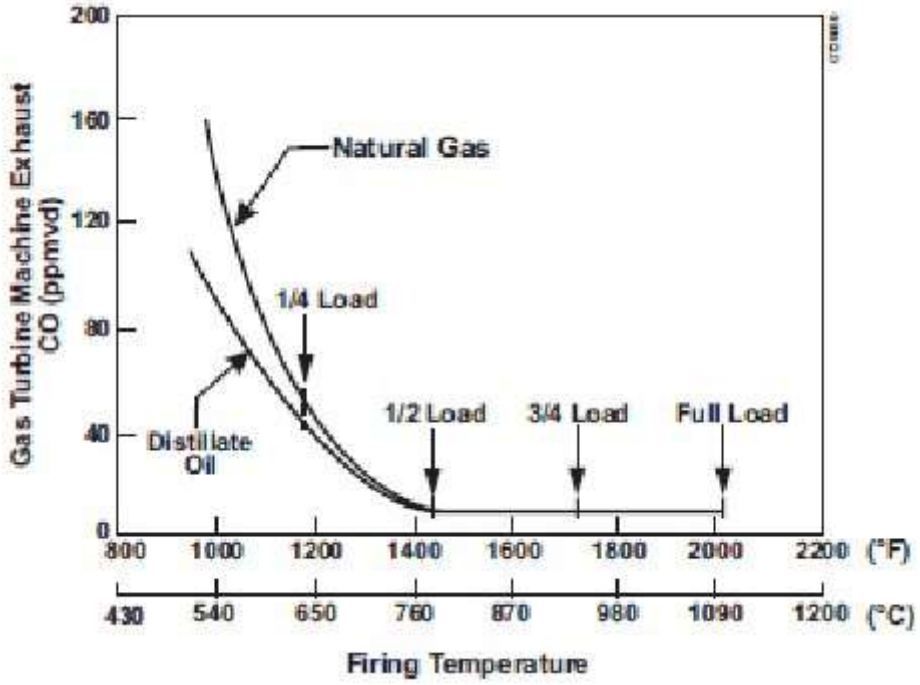

Figure 15: CO emissions from an industrial gas turbine. Abstracted from GE Power Systems – GER-4311-03/01 ('Layi Fagbenle, 2014)

3.4 Gas Turbine Performance Optimization

This is the action of making the best or most effective use of gas turbines, operating under certain condition, to meet specific application demands. Gas turbine performance optimization entails one or a combination of the following (Silva, et al., 2005):

- Minimization of fuel consumption
- Maximization of Power output
- Maximization of engine life
- Minimization of engine Emissions

3.4.1 Optimization Goal

The first step in executing a successful performance optimization involves clearly outlining the optimization goal. This is an important step in enabling a focused investment of resources towards achieving a common goal. The optimization goal is a general overview of the expected results post performance optimization. For example, an optimization goal could be to minimize operating cost.

3.4.2 Optimization Objective

A clearly setup optimization goal narrows all considerations to one or more optimization objectives. An optimization problem addressing more than one objective is called a multi-objective optimization problem. Fuel flow minimization at fixed power output is an example of a gas turbine performance optimization objective, potentially, capable of achieving an optimization goal of operating cost minimization.

3.4.3 Optimization Problem

To address optimization objectives, an optimization problem, which captures all elements of a considered system, must me formulated. An optimization problem is a model of a design or decision problem and consists of the following elements:

3.4.3.1 Optimization variables

All design or decision parameters associated with an optimization problem are modeled as variables.

3.4.3.2 Objective function

The objective function calculates the desired quantity to be minimized or maximized (optimized). It is the model set up to capture and address the optimization objective.

3.4.3.3 Constraints

Constraints are conditions of an optimization problem that a solution must satisfy. Constraints limit the possible values of optimization variables and can be linear or nonlinear.

3.4.4 Performance optimization approach

In general, gas turbine performance optimization involves any of the following:

1. Modifications to the basic thermodynamic cycle
2. Modifications to gas turbine component design
3. Applying optimization algorithms to solve optimization problems

3.4.4.1 Modifications to the basic thermodynamic cycle

This consists of modifications, which influence the gas turbine thermodynamic cycle in order to enhance performance output. Some of these modifications including reheat, regeneration, intercooling, water/steam injection e. t. c., are described below.

3.4.4.1.1 Reheat

Reheating is applied in gas turbines to increase work output without increasing compressor work. A re-heater is essentially another combustor introduced between the high-pressure and low-pressure turbine to reheat the gas flow and extract additional energy (work), from the gas, as it flows through subsequent turbine stages, before it is exhausted as waste. In a plain, reheat cycle, work output increases and gas turbine thermal efficiency decreases (Saravanamuttoo, et al., 2001). Figure 16 and Figure 17 illustrate the reheat cycle.

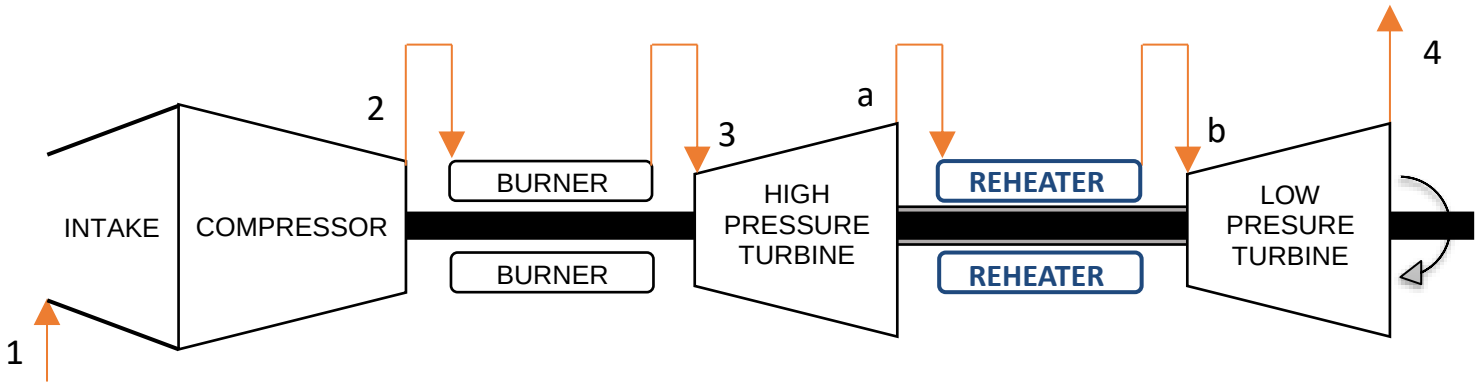

Figure 16: Simple Cycle with reheat

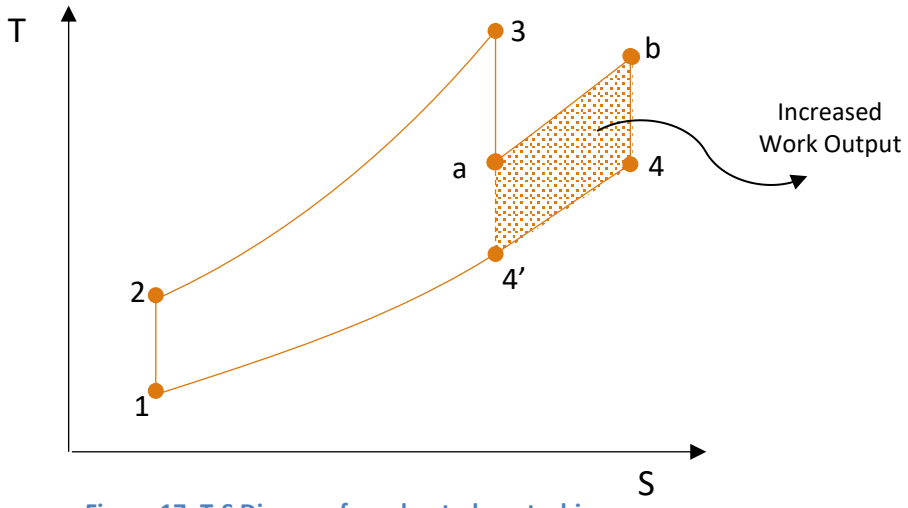

Figure 17: T-S Diagram for reheated gas turbine

3.4.4.1.2 Regeneration

This process involves the use of a heat exchanger to extract heat from gas turbine exhaust. The turbine exhaust gas, via a heat exchanger, raises the temperature of already compressed air flow prior to combustion. In a regenerated gas turbine cycle, thermal efficiency increases. Heat input into the cycle increases without increasing fuel flow. For the same work output, less fuel is consumed. Figure 18 and Figure 19 illustrate a regenerated gas turbine cycle.

The effectiveness of a Regenerator is the ratio of the heat transfer to the compressor exit gas (enthalpy change) to the maximum possible heat transfer to the compressor exit gas (Maximum available enthalpy). Equation 2 describes regenerator effectiveness. An ideal heat exchanger (with no pressure drops during heat addition or rejection) has a regenerator effectiveness of one (Saravanamuttoo, et al., 2001; Senanayake, 2016). Typical regenerator effectiveness is about 0.75.

$$\eta_{reg} = \frac{Change\ in\ enthalpy}{Max.avalable\ enthalpy\ change} = \frac{h_x - h_2}{h_4 - h_2}$$

Equation 2: Regenerator Effectiveness

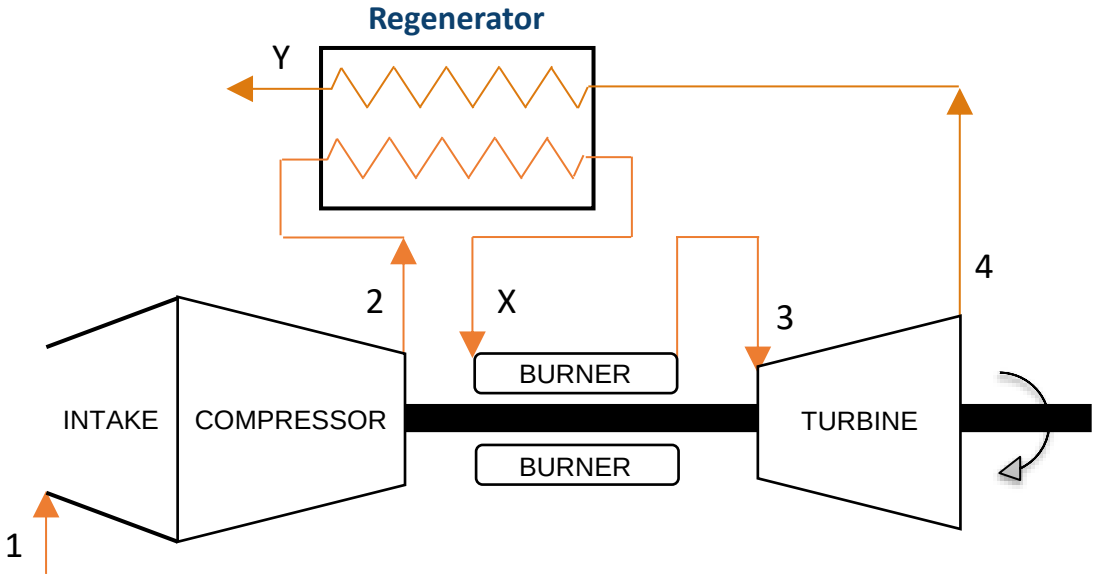

Figure 18: Simple cycle with heat exchanger (Regenerator)

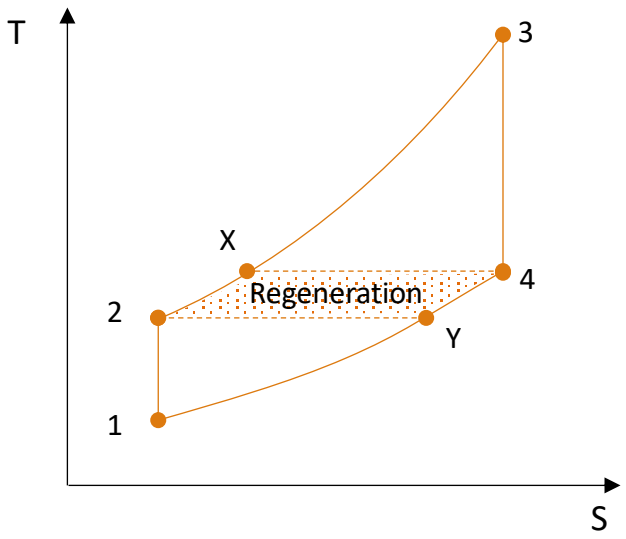

Figure 19: T-S diagram for a regenerated gas turbine

Equation 2 assumes that maximum enthalpy change occurs when $h_x = h_4$. This means T_x can only be heated as high as T_4.

Regenerated gas turbines can result in an efficiency increase of up to 5%. Application of regeneration for gas turbine performance optimization is only recommended when gas turbine exhaust temperature is higher than compressor exit temperature.

3.4.4.1.3 Intercooling

This involves the use of heat exchangers to cool compressed air, flowing between low pressure and high-pressure compression units. The heat exchanger cooling fluid can be air or water. Figure 20 and Figure 21 illustrates the intercooled gas turbine cycle. Intercooling reduces the amount of work (energy) input required for compression. In general, about two thirds of the power generated by a gas turbine drives compression. Thus, any reduction in required compressor work will increases power output. In certain circumstances, (e.g. when an engine is operating at fixed firing temperature), intercooling may result in higher fuel flow. Intercooling also results in a slight drop in compressed air pressure. A well-implemented intercooling system can enhance gas turbine output.

Intercooler effectiveness is the ratio of actual inlet-air temperature drop to the maximum achievable inlet-air temperature drop in an intercooler. It is a measure of how effective an intercooler is in reducing the temperature of compressed air flowing through it. An ideal intercooler has an intercooling effectiveness of one. This is however, not achievable in real situations. Equation 3 describes intercooler effectiveness.

$$\eta_{intercooler} = \frac{Actual\ Temperature\ Drop}{Max.acheivable\ Temperature\ drop} = \frac{T_C - T_d}{T_C - T_1}$$

Equation 3: Intercooler Effectiveness

Equation 3 assumes that maximum temperature drop occurs when $T_d = T_1$.

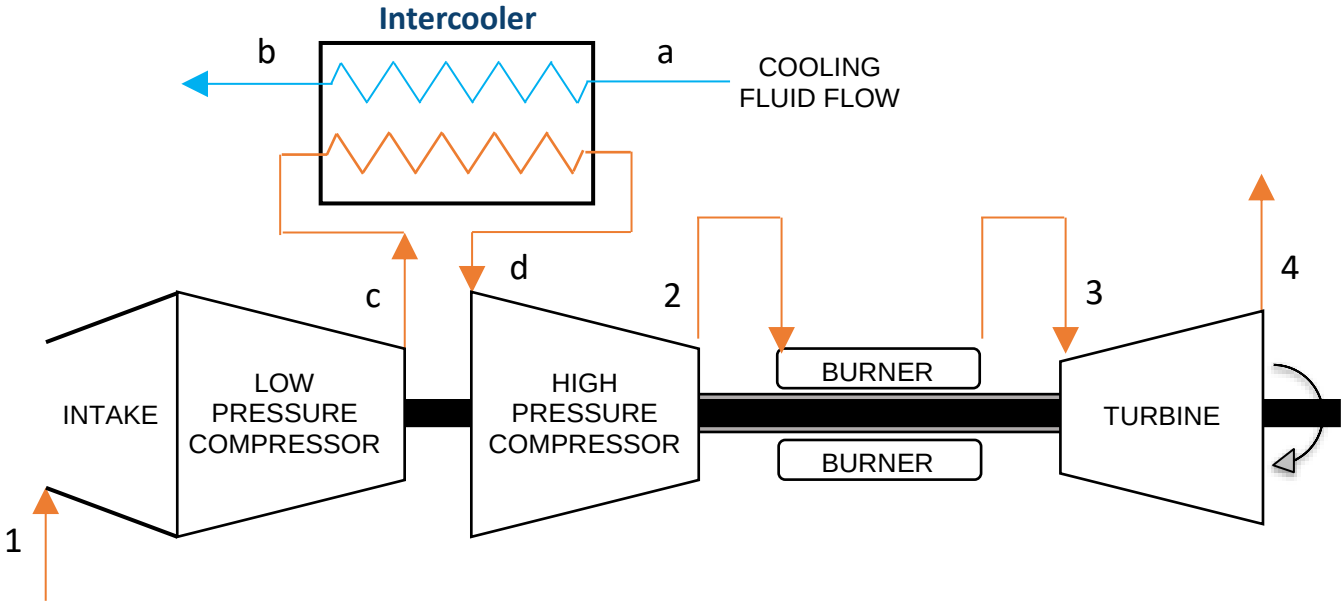

Figure 20: Simple Cycle with intercooler

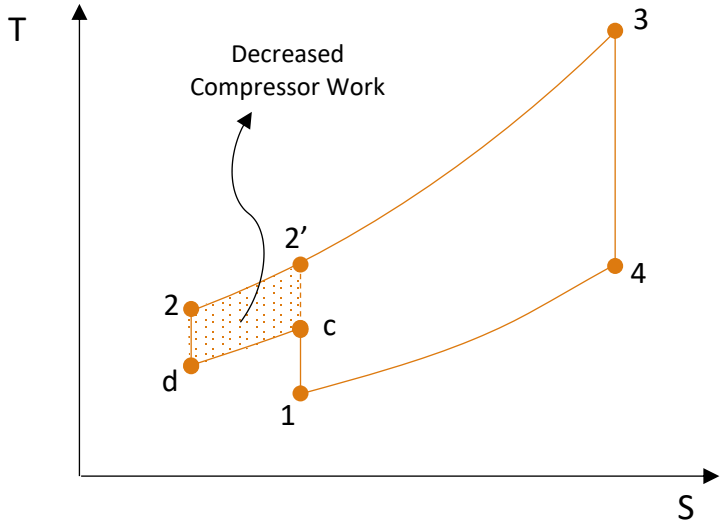

Figure 21: T-S Diagram for intercooled gas turbine

3.4.4.1.4 Water/steam injection

This modification involves the injection of water or steam into the gas turbine flow stream or directly into the gas turbine combustion chamber resulting in a reduction in the combustor flame-zone peak temperatures and an increase in thermal mass. Reducing peak temperatures can lowers NOx emission levels by 60% or more. Due to the increase in mass flow from water/steam injection, the power output of a gas turbine can be increase by up to 6%. While Water/steam injection has, the benefit of lowering NOx level, it enhances the potential for generation of CO and VOC emissions in gas turbines and incurs an efficiency drop penalty between 2 to 3 percent. Figure 22 illustrates a steam injected gas turbine (STIG) cycle.

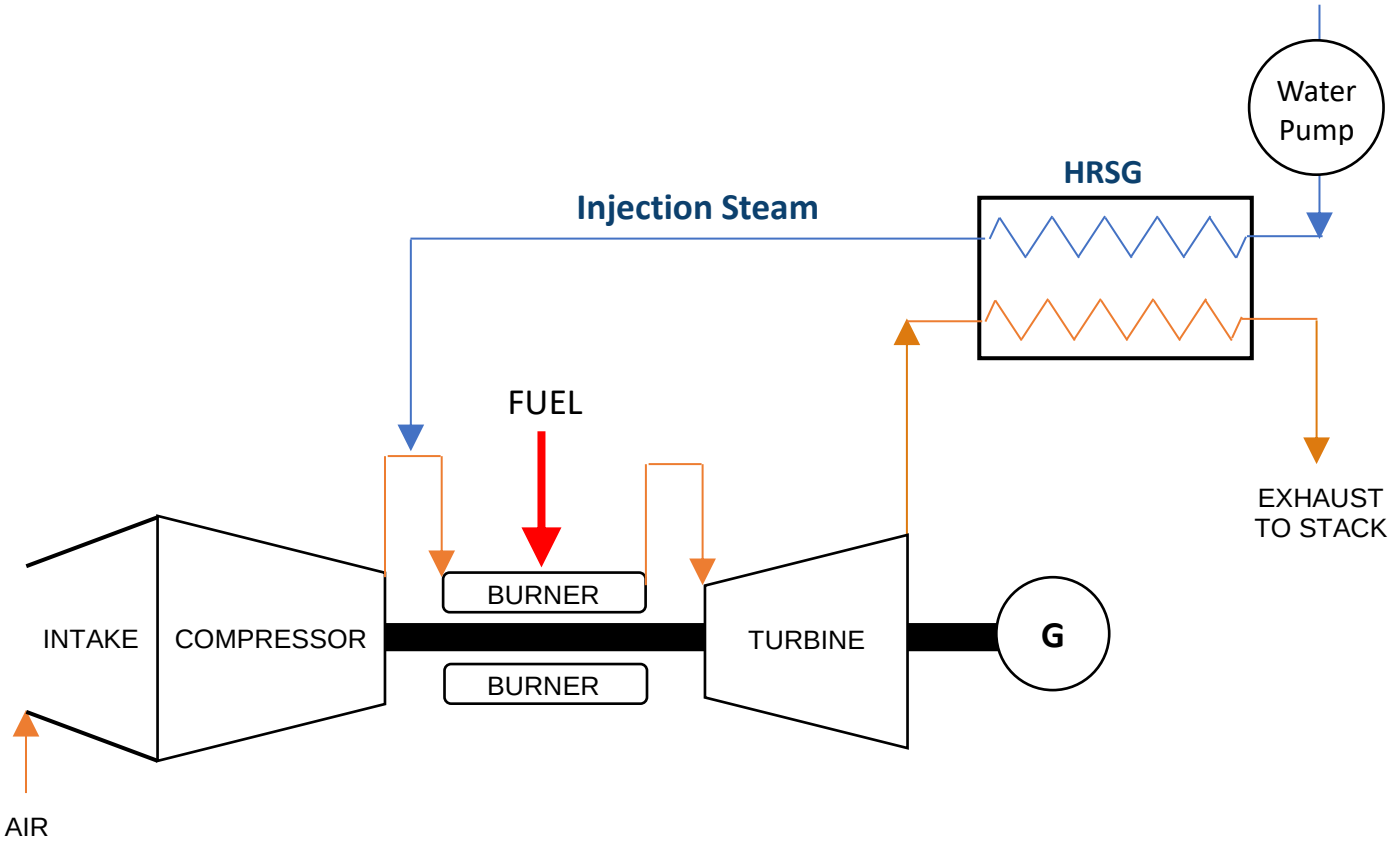

Figure 22: The Steam Injected gas turbine (STIG) cycle

3.4.4.2 Modifications to gas turbine component design

The modification or complete redesign of gas turbine components to improve reliability, aerodynamic performance, thermal properties, operating life e. t. c. is referred to as design optimization. The successful optimization of a gas turbine component design will have varying effects on the overall performance of a gas turbine unit. Trade-offs are often made between the potential outcomes of component design optimization and effect on the overall performance of a gas turbine. For example, turbine blade cooling design optimization may influence temperatures and pressures in the flow stream, which may lead to a drop in power output and efficiency.

3.4.4.3 Applying optimization algorithms to solve optimization problems

Linear and nonlinear programming solve optimization problems through the implementation of appropriate optimization algorithms. Linear programming works to deliver the best outcome in a mathematical model (optimization problem) whose requirements (constraints) are represented by a linear relationship. Nonlinear programming on the other hands solves optimization problems where some or all of the constraints associated with an objective function are nonlinear. Equation 4 to Equation 9 present the variables and parameters associated with optimization using linear and nonlinear programing.

3.4.4.3.1 Function

$$Objective\ function \approx \min or\ max\ f(x)@\ x_0$$

Equation 4: Objective function

Where x is the objective and x_0 is the initial value of x.

3.4.4.3.2 Constraints

$$A_x \leq B$$

Equation 5: Linear inequality constraints

$$A_{eq} \leq B_{eq}$$

Equation 6: Linear equality constraint

$$C(x) < 0$$

Equation 7: Non Linear Inequality constraints

$$C_{eq}(x) = 0$$

Equation 8: Non Linear equality constraints

Where A, B and C are matrices or vectors.

3.4.4.3.3 Bounds

$$LB \leq x \leq UB$$

Equation 9: Objective bounds

Where LB and UB represent the lower and upper limit of the objective.

This study only implements two of the described performance optimization strategies. The implemented strategies include modifications to the basic thermodynamic cycle and application of optimization algorithms to solve optimization problems. The methodology adopted to implement these strategies in the context of the research area and results obtained from the implementation are presented in subsequent chapters.

3.5 Regression Analysis (RA)

Regression analysis consists of a collection of statistical methods for determining the association between variables. These include several techniques for modelling and analysing the relationship between a dependent variable and one or more independent variables. Dependent variables refer to predicted values in a regression model while independent variables are the factors, which influence the predicted variable. Regression models consists of parameters and variables. The interaction of these variables and parameters describe the regression model (Akinyemi, 2008). Outlined below are the parameters and variables associated with a regression model.

- Dependent Variables ***Y***
- Independent Variables ***X***
- Unknown Variables **β**
- Number of unknown variables ***K***
- Number of Samples or data points ***N***

Regression models relate a dependent variable **Y** to a function of independent variables **X** and unknown variables **β** as described by Equation 10. This relationship is implemented for each sample point in a dataset set of **N** sample points.

$$Y \approx f(X, \beta)$$

Equation 10: Regression Model Relationship

The unknown variable **β** represents a scalar or vector quantity.

When the number of samples points **N** is less than the number of unknown variables **K**, the system of equations defining the regression model is **underdetermined**.

$$(N < K)\ underdetermined\ regression\ model$$

When the number of samples points **N** is equal to the number of unknown variables **K**, the function ***f*** is linear and Equation 10 can be solved exactly rather than approximately.

$$(N = K)\ linear\ function$$

When the number of samples points **N** is greater than the number of unknown variables **K**, there is enough information in the data to estimate the unknown variable **β** in Equation 10. The system of equations defining the regression model is **overdetermined**.

$$(N > K)\ overdetermined\ regression\ model$$

In an overdetermined regression model, the values of the unknown parameters **β** that minimizes the difference between measured and predicted values of the dependent variables **Y** can be evaluated. This implementation is the method of least squares. Furthermore, in an overdetermined regression model, regression analysis utilizes the excess information available to give statistical information about the unknown parameter **β** and the estimates of the dependent variable **Y** (Saint-Germain, 2001).

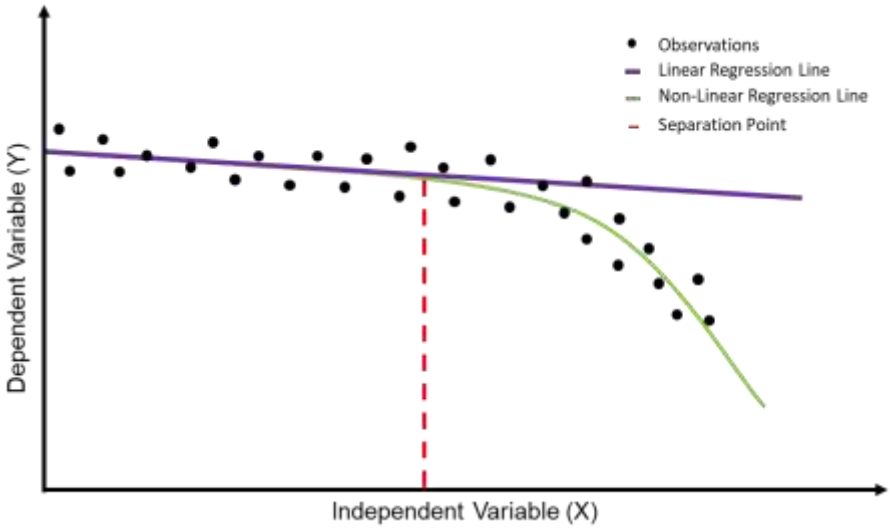

Figure 23: Graphical Representation of Regression Analysis

In Figure 23, the observations (data samples) are the results of random deviations from an underlying relationship represented by the linear and no-linear regression lines. The separation point also called the transition point is the point at which the random observations becomes non-linear. In such a situation, a non-linear regression model should characterize the underlying relationship between the dependent (Y) and independent variables (X) (Li & Nilkitsaranont, 2009).

Regression analysis helps to identify the interaction between the dependent and independent variables and provides insight into the degree of influence that changes in various dependent variables, associated with an investigated system or scenario, have on a dependent variable. For example, regression analysis can estimate the effect that factors like weather, competitor influence and population density have on an organizations current and future sale. In such an investigation, **the dependent variable (criterion variable) is organizational sales** and **all other variables that can influence organizational sales are the independent variables (Predictor variables).** (Rowlands, 2014), applied regression analysis to predict the remaining useful life of two single spool gas turbine engines. He concluded that the quality and quantity of data available for the regression analysis as well as the prediction interval influences the accuracy of the prediction (Rowlands, 2014).

This study applies regression analysis to estimate the acquisition cost of gas turbine engines based upon engine performance parameters from a dataset of engine historical records.

3.6 Artificial Neural Network (ANN)

Artificial neural networks (ANN) are computational systems modelled after the operation of the human brain and nervous system. (Shiffman, 2012), in his book, "The Nature of Code" describes the artificial neural network as a "connectionist" computational system. Connectionist referring to the interconnected networks of simple units (Shiffman, 2012). Typically, ANNs consist of layers, neurons and synapses. Figure 24 illustrates the schematic of an ANN.

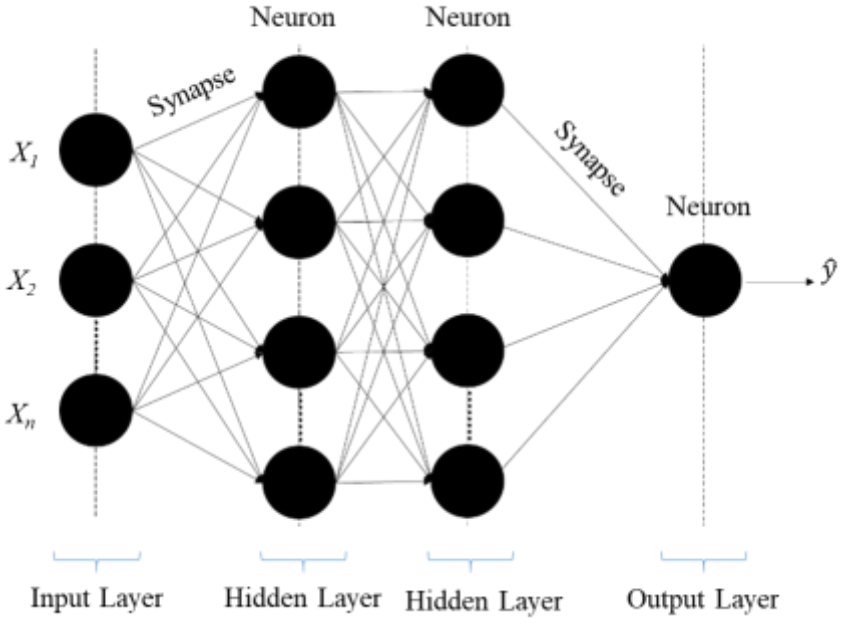

Figure 24: Artificial Neural Network Schematic

Neurons in ANNs are series of nodes consisting of input variables (X_i) and associated weights (W_i), organized into layers. These layers are interconnected by links known as synapses. Synapses take the values from their respective inputs, multiply them by specific weights and output the result. Neurons add together the output from all their synapses, as presented in Equation 11, and apply an activation function Equation 12. Certain activation functions allow neural networks to model complex non-linear patterns that simpler models may miss. In this study, the sigmoid activation function is applied. Figure 25 shows a diagrammatic illustration of simple ANN system

$$Z = \sum_{i=1}^{i=n} (X_i \times W_i)$$

Equation 11: Synapse Output

$$a = \frac{1}{1 + e^{-z}}$$

Equation 12: Sigmoid Activation Function

Where 'Z' is the sum of the output from the synapse or the sum of weighted inputs to each neuron and 'a' is the activation function.

3.6.1 Feed-forward and Back-Propagation Network

A Neural Networks exhibits the ability to learn and adapt its computational system and internal structure with respect to the information provided to the system. This adaptation is accomplished by adjusting the weights (W_i) realised from an initial forward propagating step. The weights are adjusted by multiplying the error (e_i) in the estimated output ($\hat{y}$) of the initial processing step by the input (X_i). This process is iteratively repeated until the network output estimates matches the already known desired output ($\hat{y}$).

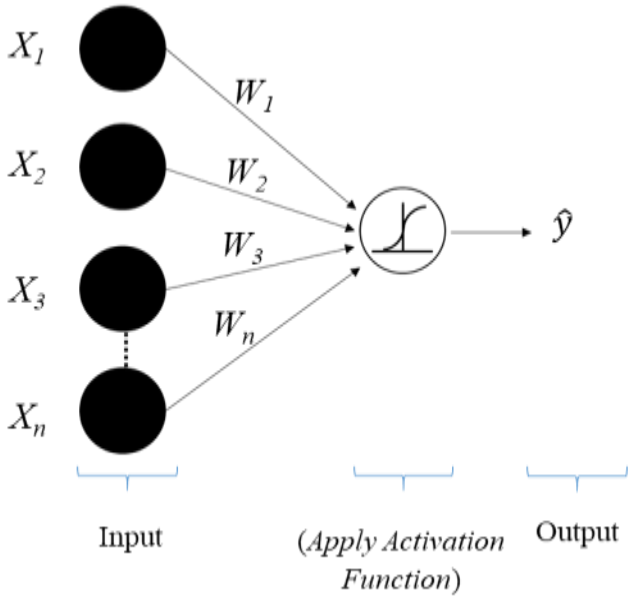

Figure 25: Illustration of a simple ANN System

The process of iteratively adjusting the weights in a network, to estimate accurately the known desired output, is referred to as network training. This described method of training a neural network is the feed-forward Back-propagation approach (Nielsen, 2015). Another name used to describe the adopted method is the supervised learning strategy or the supervised regression/ classification problem (Shiffman, 2012). The adjective regression in the description of the approach indicates that the generated output is continuous. For a classification problem, the generated output is fixed with respect to certain classifying criteria. Figure 26 illustrates the feed- forward Back Propagation approach.

The neural network makes an initial guess of weights, (W_i). At initial guess (W_i) is a random value. The output estimate, ($\hat{y}$), based on this initial guess, is compared with the known

desired output (y) and necessary adjustments are made in accordance with the calculated error as described in Equation 13 and Equation 14. This process is repeated with $W_i = \Delta W_i$ (*Where* ΔW_i *is the adjusted weight*) until the output estimate, $(\hat{y})$ equals the desired output(y).

$$e_i = y_i - \hat{y}_i$$

Equation 13: Calculated Error

$$\Delta W_i = W_i + (e_i \times X_i)$$

Equation 14: Change in Weights

The feed-forward Back-propagation network is the network strategy adopted for this study.

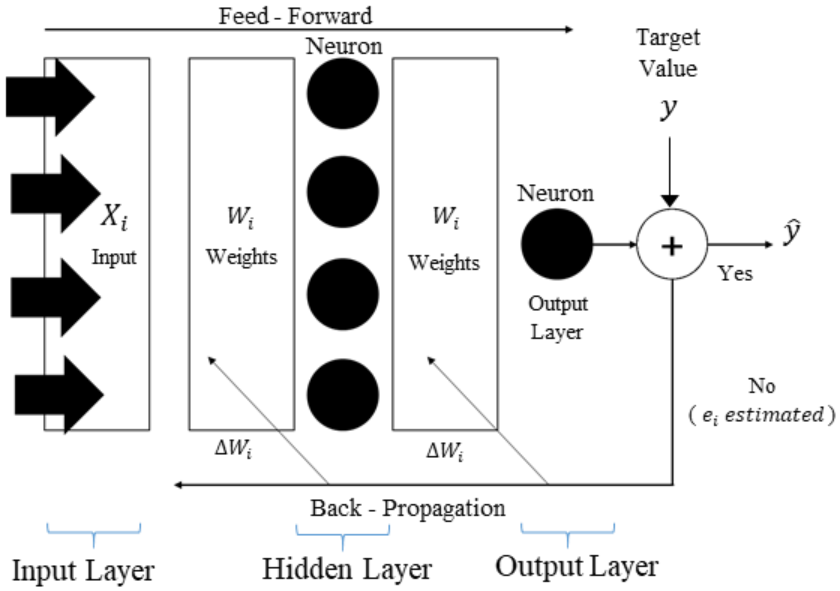

Figure 26: Feed-Forward Back Propagation Network

Several scholar in the gas turbine field have applied artificial Neural Networks to gas turbine investigations. Presented in Chapter 1 are some of these studies. An example of such study is the application of ANN in the detection and classification of gas turbine faults, by observing changes in gas turbine performance parameters, against a benchmark performance (Hans & Douglas, 1999).

In this study, a feed-forward back propagation neural network has been applied to predict gas turbine engine price from inputted engine performance parameters.

3.7 Economic Analysis

3.7.1 Economic analysis Overview

Economic analysis is one of the major tools used by organizations to gauge the benefit-cost ratio (BCR) of an investment over the life of that investment even before any resource or capital allocation to the project. Without proper investigation into the elements of a proposed project or investment, an organization runs the risk of miss management and allocation of resources or even failure over the life of the investment. This will mean loss of the scarce resources that could be invested elsewhere to generate profit for the organization. As such,

every organization places very high importance on conducting a robust and concise economic analysis to enable informed decision-making and minimize the risk of failure.

Organizations planning to invest in gas turbine engines require tailored and relevant information on the potential costs and benefits obtainable when investment is made on one unit over other alternatives. The investment choice must be justified as being beneficial, in medium to long term, to the organizations profit and sustainability. Depending on the type and nature of a project, the elements and forces that determine the effective distribution of scare resources may vary. For instance, the economic analysis required for the choice of a gas turbine unit, for power generation, may vary depending on factors like:

- Engine Application
- Performance requirement
- Geographical location
- Government policies
- Unit Acquisition cost e. t. c.

Despite the variability in the influence of these factors on an economic analysis, the resultant gauging criteria is usually the same and referred to as the project selection criteria. Described below are the project selection criteria evaluated in this study.

3.7.1.1 Net Present Value (Present Worth)

This is the most widely used criterion for investment evaluation and selection from alternatives (Hendrickson & Sue, 1996). The net present value (NPV) is an output of present worth analysis, which reduces all cash flows over the life of an investment into a single equivalent cash flow (Palm & Qayum, 1985). Due to the time value of money, investors, place a critical importance on the timing of cash flows. This is because, future cash flows may not be as valuable as the same cash flow today (Short, 1996). Equation 15 describes the NPV estimation.

$$\mathrm{NPV}_x = \sum_{t=0}^{n} \frac{A_{(t,x)}}{(1 + MARR)^t}$$

Equation 15: Net Present Value (Present Worth)

Where; $\boldsymbol{n}$ is the length of the analysis period, $\boldsymbol{t}$ is the present (the beginning of the analysis period), $\boldsymbol{A}$ is the net cash flow, $\boldsymbol{x}$ is the investment or project being analysed and $\boldsymbol{MARR}$ (Minimum acceptable rate of return) is the discount rate expressed in percentage change per year. From an economic standpoint, a positive NPV indicates that an investment is worthwhile while a negative NPV indicates that the investment will not yield the desired return as represented by the minimum acceptable rate of return employed in the analysis (Short, 1996).

3.7.1.2 Rate-of-return

There are two rate of return criteria adopted in this study. This include the internal rate of return (IRR) and the overall rate of return (ORR) [4]. The “rate-of-return” investment criteria is often described as being more intuitive, easy to understand and interpret than net present value.

Internal rate of return, IRR, can be described as the minimum acceptable rate of return for which a projects NPV is zero. The IRR is independent of an investments actual minimum acceptable rate of return (hurdle rate) (Beaves, 1996). Typically, a potential investment with IRR less than the MARR is rejected. Some investments may have multiple IRRs and other may have none at all. This makes ranking of projects solely based on IRRs risky (Beaves, 1996).

Overall rate of return, ORR, is the average periodic rate earned on a fixed investment amount, over the expected life of an investment (Beaves, 1996). This fixed investment amount is known as the projects investment base, IB. Equation (2) defines the ORR.

$$\mathrm{ORR} = \left[\frac{(IB + NPV) \times (1 + MARR)^n}{IB}\right]^{1/n} - 1$$

Equation 16: Overall Rate of Return

The project investment base represents all external funds, not provided by the investment itself, but needed to finance the project. It is the minimum cumulative present value, associated with a projects cash flow, multiplied by -1 (Beaves, 1996). Equation 16 above for calculating ORR is only appropriate when the investments being compared have the same IBs. For investments, which do not have the same IB (mutually exclusive investments), the IBs, must be adjusted to a common value. This is preferably the largest IB among competing projects. Equation 17 is used to calculate the adjusted ORR. This is termed scale adjusted ORRs where S is the common investment base between competing projects.

$$\mathrm{ORR_s} = \left[\frac{(S + NPV) \times (1 + MARR)^n}{S}\right]^{1/n} - 1$$

Equation 17: Scale Adjusted ORR

Certain challenges arise when comparing investments that have different project lives. In such situations, assumptions must be made as to what occurs at the end of the project life. For analysis involving on time expenditure projects, NPVs can be directly compared even if the projects have different lives. This is based on the assumption that funds released by any of the projects generate the organizations opportunity cost until the end of the longest-lived period (Beaves, 1996).

However, ORR of one-time expenditure projects with different project lives cannot be compared. The ORR of such competing projects must be calculated over a common analysis period. This is based on the assumption that funds can be invested, at the organizations opportunity cost, throughout the additional analysis periods. Equation 18 describes this.

$$\mathrm{ORR_{s,n+z}} = \left[\frac{(S + NPV) \times (1 + MARR)^{(n+z)}}{S}\right]^{1/(n+z)} - 1$$

Equation 18: ORR of One-time expenditure projects with different project lives

z is the difference between the shortest and longest analysis period or the additional analysis period required to bring all projects to a common base year. For situations involving competing project where the projects are replaced after their initial project lives, and all projects have varying project lives, project comparison cannot be based solely on NPVs of

respective projects. In such cases, revised projects, should be generated for each competing project by extending cash flow streams to a common terminal point (Beaves, 1996). Therefore, calculating NPVs and ORRs for such revised projects should deliver consistency in project ranking for a reliable investment comparison.

3.7.2 Project selection

The selection of an appropriate investment option from potential alternatives describes the overall objective of an economic analysis. Decision is made based on a meticulous evaluation of potential costs and revenues over an expected period for each investment option. Hendrickson and Sue categories the project selection challenge into 3 general classes (Hendrickson & Sue, 1996).

- Accept-reject problems. This is also known as the feasibility determination problem; to determine if an investment is beneficial.
- Project selection from a collection of mutually exclusive projects. Termed mutually exclusive project selection problems.
- Project selection with respect to budget constraints. Also described as Capital budgeting problems.

Figure 27 describes the steps involved in project selection. A collection of investment options with established planning horizons is generated. The planning horizon is the length of the analysis period used in the economic analysis for each investment option. The cash flow profile for each investment alternative is estimated. For each alternative, the investment ranking criteria are computed using the specified discount rate (MARR) (Hendrickson & Sue, 1996).

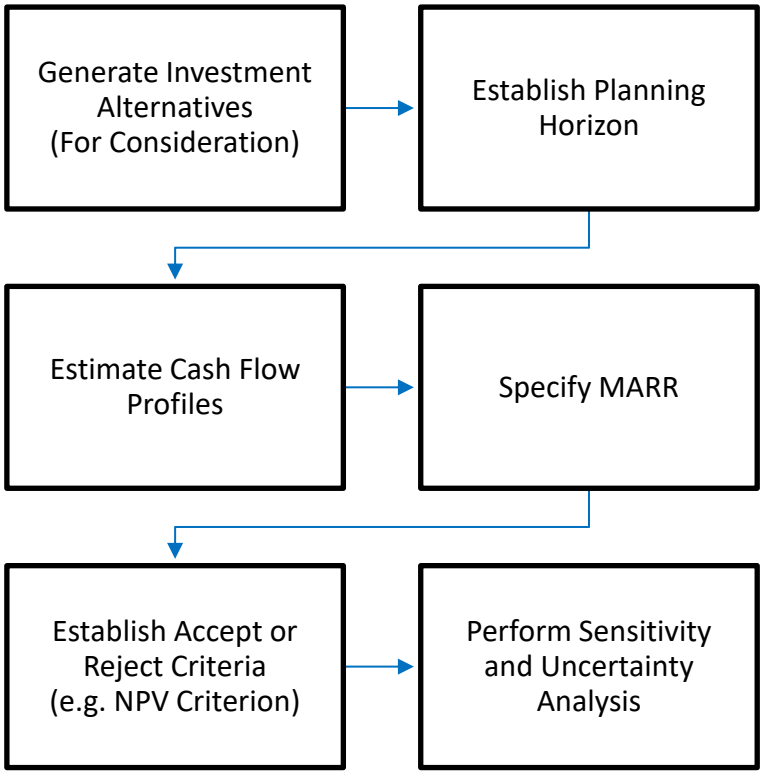

Figure 27: Project Selection Steps

Following the computation of the selection criteria, an additional measure is establish for selecting the best option from among a collection of mutually exclusive alternatives. Uncertainty analysis is performed to measure the effect of certain crucial input values on the favoured investment option.

3.7.2.1 Acceptance criteria

Investment options with a positive NPV are accepted. In a collection of accepted alternatives, the investment option delivering the highest NPV should be selected. For economic analysis where the rate-of-return criteria is used as benchmark for project selection, only investments with IRR greater than MARR should be accepted. Similarly, ORR must be greater than or equal to MARR for a project to be accepted. From a collection of acceptable alternatives, the investment option with the highest IRR and ORR should be selected (Beaves, 1996).

3.7.3 Economic Model

A techno-economic model has been developed which evaluates the productive life costs and benefits of gas turbine engine units, in simple cycle and combined cycle applications, over an established planning horizon. The output of the evaluation provides a basis for smart and informed decision making to address challenges of economic feasibility determination, project selection from mutually exclusive options and project selection with respect to capital budgeting constraints. The developed economic model takes into account a broad range of elements categorized into components. These components are:

- Price Estimating model Component
- Life approximating model component
- Emissions model component
- Performance model component
- Cost model component
- Optimization model component
- Selection model component.

Chapter 4 describes, in detail, each component of the economic model.

In this study, the NPV, IRR and ORR are used as criteria for project selection. A desirability grading system is implemented to grade investigated scenarios, based on grading criteria of cost effectiveness, present worth, electricity cost impact, fuel penalty, Investment Base, Levelized cost of electricity (LCOE), running cost, emissions removed and Return on investment (ROI).

A study conducted in 2012, implemented a methodology called TERA (Techno-economic Risk Assessment) in the development of a multidisciplinary simulation tool for rotating equipment selection. This was to aid in decision making relating to plant selection, operation and maintenance planning (Khan, 2012). Diverse scholars have addressed the investigated research domain. A review of some of these investigations is presented in chapter 1.

4 METHODOLOGY

This aspect of the research is presented from two perspectives; The Overall research approach and the Techno-economic analysis approach.

4.1 Overall Research Approach

This methodology is divided into four phases; the research development phase, the system analysis phase, the system optimization phase and results interpretation/implication phase.

4.1.1 Research Development Phase

The research development phase involves the proper identification and validation of the conceived research idea and area of focus. The research idea was repeatedly evaluated and scrutinized for its usefulness and application with respect to the identified area of research (*Brayton cycle emissions reduction and system optimization*). This was followed by an initial scoping and planning of the entire research strategy, required resources and time scale for delivery. The choice of a case study engine was made at this stage and feasibility study was conducted to determine its validity for use in this research. This phase also encompassed initial data gathering and literature review to aid in adequate contextual mapping of the research idea and focus.

4.1.2 System Analysis Phase

In this phase, the development and application of a techno-economic analysis methodology commences. Assumption based analyses, from a technical and economic perspective, are conducted. The implications of these analyses on system performance, the economy and environment are investigated. In this phase, no system optimization technique is implemented. Thus, a series of baseline results are obtained, which provide a platform for subsequent analysis and investigation.

4.1.3 System Optimization Phase

The system optimization phase involves the implementation of emission mitigating and performance optimization techniques into the techno-economic analysis. This is with the aim of enhancing system performance while optimizing economic benefits. In this phase, baseline system limitations are identified and appropriate optimization solutions are adopted and implemented to mitigate the system limitations and optimize system performance.

4.1.4 Result Analysis and interpretation Phase

This phase involves the comparison, assessment and interpretation of the results obtained from investigations carried out in previous phases. The qualitative and quantitative implications of implemented optimization and emissions mitigation strategies are analysed, results are consolidated and conclusions are reached. Observations from this phase can potentially provide useful information to guide organizations, operators and policy makers in decision making concerning system performance, environmental, economic, design, manufacture, operation and maintenance issues.

Figure 28 illustrates the Overall Research Approach described above.

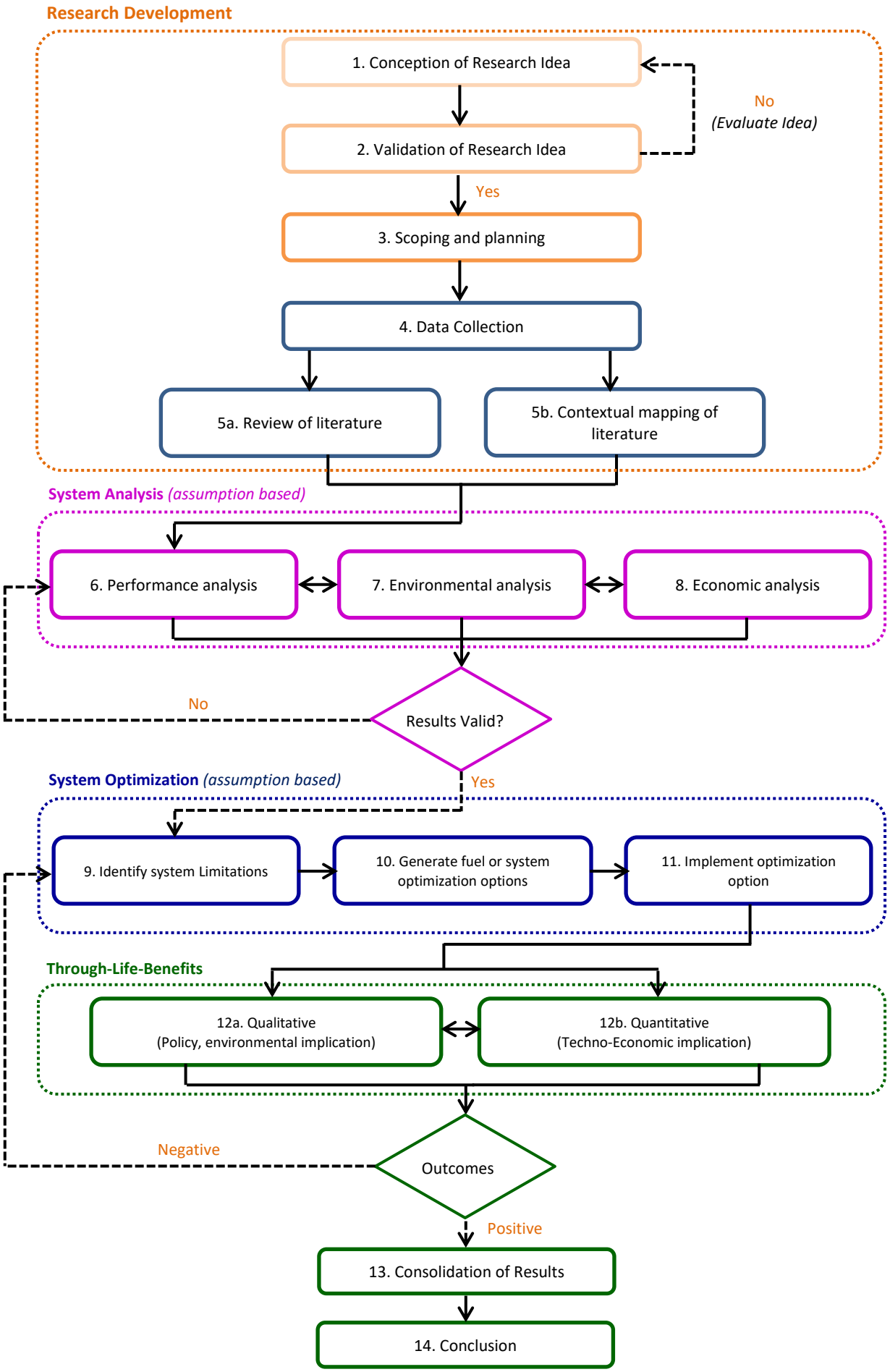

Figure 28: Research Approach/Methodology

4.2 Techno-Economic Analysis Approach

This analysis approach comprises of six models, also identified, in this study, as components of the overall economic model Figure 29. The following sections in this chapter describe each component in detail.

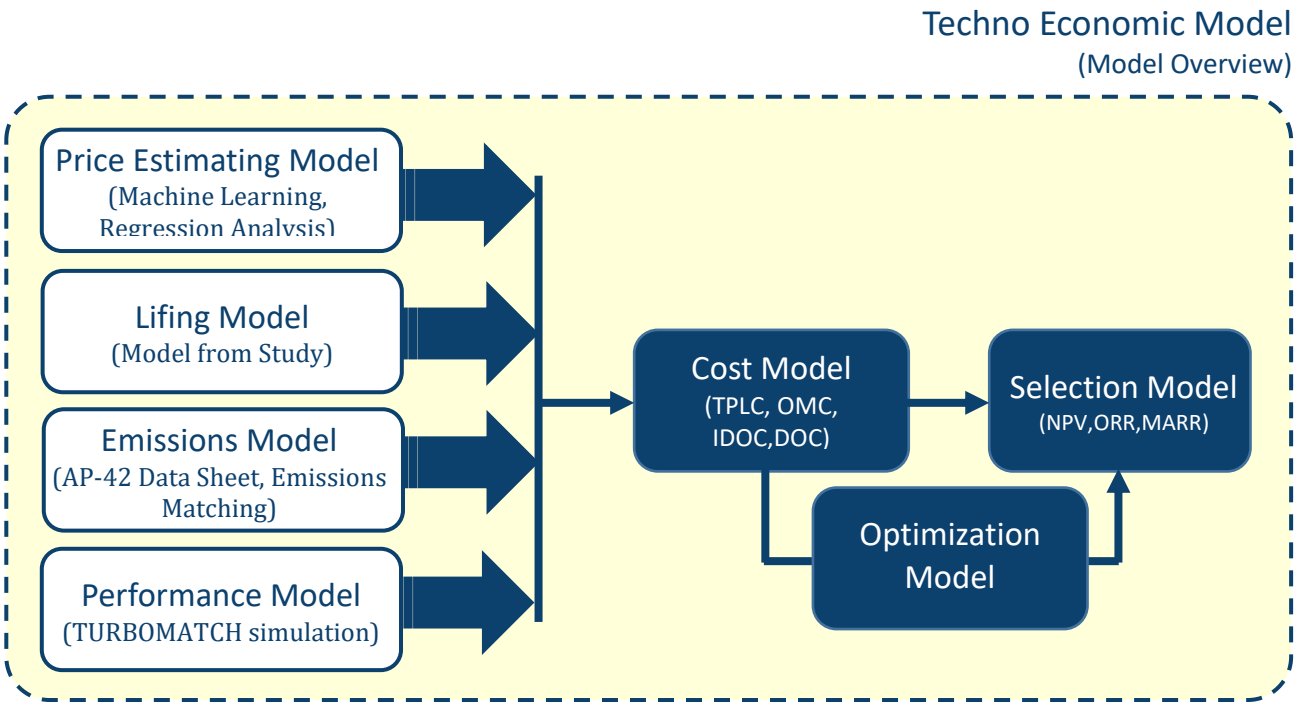

Figure 29: Techno-economic Model Overview

4.2.1 Price Estimating Model

This is the component of the overall economic model associated with the estimation of gas turbine acquisition cost. This component adopts a modular approach to price estimation using artificial neural network and regressions analysis. Each engine price estimating approach will be described separately.

4.2.1.1 Gas Turbine Price Estimation Using Artificial Neural Network (ANN)

The neural network estimating methodology adopted in this study is presented in Figure 30. The method consists of a network prompter, network trainer, network optimizer and an estimator. This section describes each element of the implemented ANN methodology and how it is applied to estimate gas turbine acquisition cost.

4.2.1.1.1 Network Prompter

This element of the ANN methodology comprises two steps.

4.2.1.1.1.1 Data Gathering, Normalization and Standardization

Relevant data compiled from historical records create a dataset of engine power output, engine heat rate, PT rpm and engine price. This dataset is used as input and output data for training the network. The historical pricing information used in this study have been retrieved from various sources including the Gas Turbine World Handbook, Turbomachinery International and the Nye Corporation Database. To ensure the consistency and relevance of the compiled dataset as input and output into the network, the dataset is standardized by normalizing and scaling the values. The data is normalized by accounting for inflation in engine price using the producer price index (PPI) industry data provided by the U.S. Bureau of Labour Statistics (U.S. Bureau of Labor, 2017; Thompson, 2009). Equation 19 and Equation 20 describe the process.

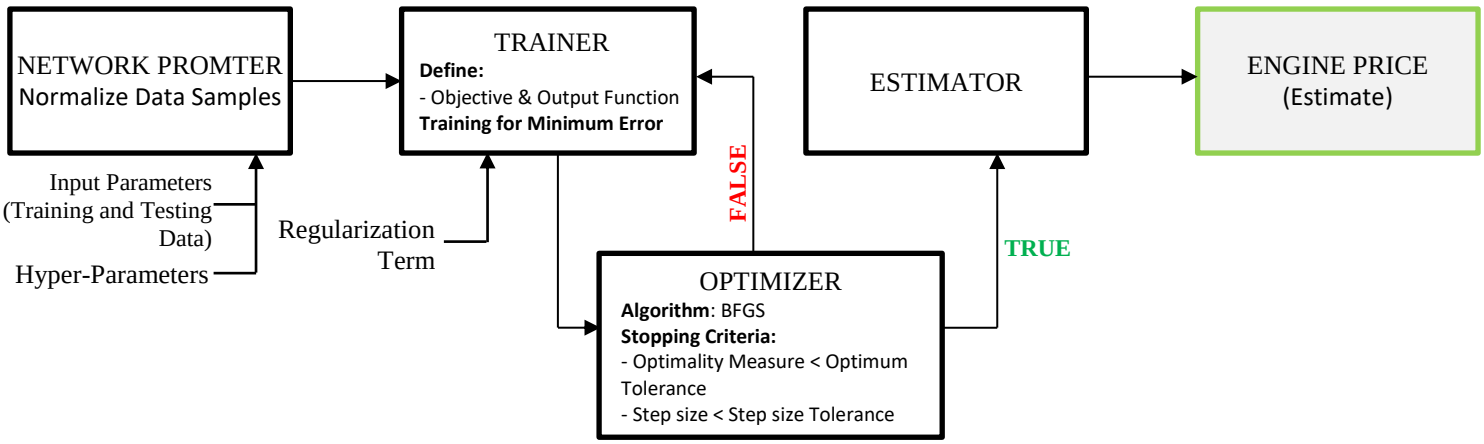

Figure 30: Neural Network Estimating Methodology and Code Structure

Further normalization is performed by verifying and ensuring consistency in parameter units and currency of records. Data scaling is performed using Equation 21.

$$inflation\ rate, inf_{rate} = \frac{PPI_{cyear}}{PPI_{pyear}}$$

Equation 19: Inflation rate

$$Price_{cyear} = \text{Price}_{pyear} \times (1 + inf_{rate})$$

Equation 20: Price in current year due to inflation

$$X_{norm} = \frac{X}{max(X)}$$

Equation 21: Normalized data

Where PPI_{cyear} is the PPI in the current year and PPI_{pyear} is the PPI in the previous year. X is the input before scaling and X_{norm} is the scaled input.

4.2.1.1.1.2 Neural Network Construction

The Neural Network built consists of one input layer, one hidden layer and one output layer Figure 31. In building the network structure and behaviour, certain constants, called hyper-parameters have been set. Hyper-parameters establish the structure, behaviour and size of the network. In this study, the input layer contains three neurons representing the three inputs of power output, rpm and heat rate. The output layer contains one neurons for the network output of engine price and the hidden layer contains four neurons. The choice of number of neurons for the hidden layer is made based on the study conducted by (Karsoliya, 2012). It was proposed that the total number of neurons in the hidden layer should be less than twice the number of neurons in the input layer (Karsoliya, 2012).

4.2.1.1.2 Network Trainer

4.2.1.1.2.1 Forward propagation through Network

The dataset is passed along the network using matrices. This saves computation time and enables large computational speed-ups particularly when propagating very large datasets. The input data *X* represented in matrix form is of dimension (86×3). Indicating there are 86 data samples for each of the inputs considered. Similarly, the corresponding output data in

matrix form is of dimension (86×1) indicating 86 data samples for the target output value (engine price). For each neuron, each input value, *X*, is multiplied with a corresponding weight $W^{(1)}$ (Equation 22). The result for each neuron, added together, gives the activity $Z^{(2)}$ in layer two.

$$Z^{(2)} = XW^{(1)}$$

Equation 22: Activity in layer two

X and $W^{(1)}$ are matrices. *X* is the matrix of inputs and $W^{(1)}$ is the matrix of weights between the input and hidden layer. Next, an activation function $a^{(2)}$ is applied to $Z^{(2)}$, as described in Equation 23. Propagating $a^{(2)}$ to the output layer completes the forward propagating step, Equation 24.

$$a^{(2)} = f(Z^{(2)})$$

Equation 23: Activation function

$$Z^{(3)} = a^{(2)}W^{(2)}$$

Equation 24: Activity in layer three

Where $W^{(2)}$ is the matrix of weights between the hidden and output layer. $Z^{(3)}$ is the activity in layer 3. The final step in estimating the output with respect to input X is to apply the activation function to $Z^{(3)}$ as represented in Equation 26.

4.2.1.1.2.2 Error Quantification, Gradient Calculation and Back-Propagation

The process of back propagation is initiated by computing the error cost in the feed-forward network estimate. The computed error cost is used to adjust the weight in the network to minimize error in subsequent iterative estimates. A cost function J is developed to express the error in the network estimates. This is achieved by summing the square of the error for each output value estimated. Equation 25 describes J.

$$J = \sum \frac{1}{2} e^2$$

Equation 25: Cost Function

Where J is the error cost (cost function) of the estimates and e is the error for each estimate calculated as described by Equation 13. In general, the smaller the error cost, the more accurate the estimate.

$$\hat{y} = f(Z^{(3)})$$

Equation 26: Output Estimate

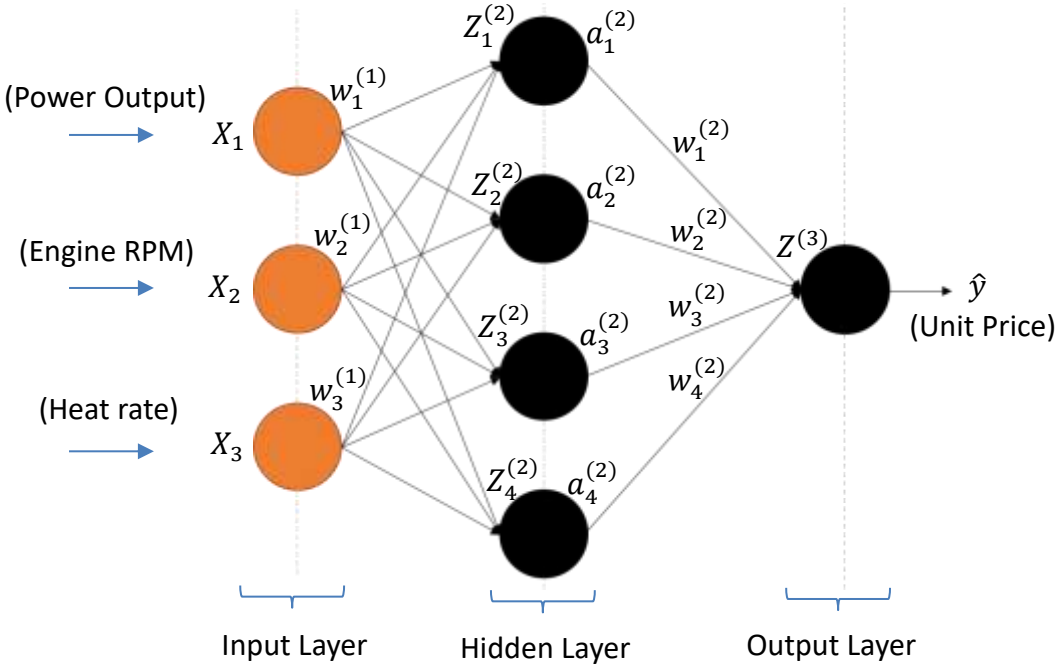

Figure 31: Complex-Underlying Process of the ANN

Neural Network training entails minimizing the Cost function (Nielsen, 2015; Welch, 2015). The cost function is minimized by adjusting the weights appropriately until the best combination of weights, which estimates the target values accurately, is obtained. This is, the combination of weights that give the lowest cost. To minimize computation time and overcome the problem of dimensionality and premature optimization, batch gradient decent approach is used to optimize the network for minimum error cost. Combining Equation 22Equation 26), a single cost equation is developed as described in Equation 27.

$$J = \sum \frac{1}{2}(y - f(f(XW^{(1)})W^{(2)}))^2$$

Equation 27: Overall Cost Equation

Taking the partial derivative, $\frac{\delta J}{\delta W}$of Equation 27, the rate of change of J with respect to W for each value of W is evaluated. This is the gradient of the cost function as described by Equation 28-Equation 31). A positive gradient indicates an increasing cost function and a negative gradient indicates a decreasing cost function.

$$\frac{\delta J}{\delta W^{(2)}} = (a^{(2)})^T \cdot \delta^{(3)}$$

Equation 28: Gradient of cost function or Partial derivative of error cost between the hidden and output layer

Where

$$\delta^{(3)} = -(y - \hat{y}) * f'(Z^{(3)})$$

Equation 29: Change in weights between the hidden and output layer

And

$$\frac{\delta J}{\delta W^{(1)}} = X^T \cdot \delta^{(2)}$$

Equation 30: Gradient of cost function or Partial derivative of error cost between the input and hidden layer

Where

$$\delta^{(2)} = \delta^{(3)}(W^{(2)})^T f'\left(Z^{(2)}\right)$$

Equation 31: Change in weights between the input and hidden layer

Summing all the gradients using batch gradient decent approach gives an approximate direction in which the cost function is travelling (Welch, 2015). Adopting the batch gradient decent approach for gradient calculation, reduces the probability of the Network getting stock at a local minimum, during training (Ng, 2012; Ng, et al., 2013). Hence, subtracting the resultant gradients from the weights, results in a reduction in the error cost for subsequent feed forward steps. This is the process of back-propagation.

4.2.1.1.2.3 Gradient Validation

To validate the gradient computed by the neural network, numerical gradient checking is implemented. A perturbation vector, epsilon, is added to each weight W in the network and the cost function is computed as (Loss A). The process is repeated with epsilon subtracted from the weights and another cost function (Loss B) is computed. The numerical gradient is then evaluated as described by Equation 32.

$$Num_{grad} = \frac{Loss\ A - Loss\ B}{2 * epsilon}$$

Equation 32: Numerical Gradient

Where

Num_{grad} is the evaluated numerical gradient.

Comparison is made between the evaluated numerical gradient and the gradients computed by the network. This is achieved by dividing the norm of the difference by the norm of the sum as described by Equation 33. The results for gradient checking should typically be in the order of 10^{-8} or less (Welch, 2015).

$$GradCheck = \frac{norm(ANN_{grad} - Num_{grad})}{norm(ANN_{grad} + Num_{grad})}$$

Equation 33: Numerical Gradient Checking

4.2.1.1.2.4 Neural Network Training

The Quasi-Newton BFGS numerical optimization algorithm is used to optimize the neural network for minimum cost (LeCun & Bottou, 1998). This algorithm overcomes some of the limitation of plain gradient decent by estimating the second derivative of the Cost Function. The information generated by implementing the BFGS algorithm enables the model to make

informed decisions downhill. It also enhances the potential for faster and more frequent solutions by the network.

The 'Fminunc' function in MATLAB applies the BFGS algorithm to train the network with the following stopping criteria.

- Optimality Measure < Optimality Tolerance
- Step size < Step Tolerance

The optimality and step tolerance values have been set to the order of 10^{-13} (Ng, et al., 2013). With the network trained, the random weight values at the initial forward propagating step are replaced with the output weights, post training.

4.2.1.1.2.5 Neural Network Testing

The dataset compiled to train the network only reflects an observation of the underlying process involved in pricing an engine. As such, gas turbine engines with similar operating parameters may not cost the same, due various reasons. There is always an element of uncertainty in estimation, which cannot be adequately represented by a model (Welch, 2015; Ng, 2012). The neural network model needs to reflect this.

A portion of the dataset compiled is trained separately and used for testing. The testing dataset in matrix form is of dimension (26×3) for the input data and (26×1) for the output data. Testing is conducted by comparing the training and testing error cost. This reveals the points where overfitting occurs, that is, points where the error costs are further apart as illustrated in Figure 32.

Overfitting has been tackled by implementing a regularization technique. With the implemented technique, a regularization term λ is introduced into the cost function, which penalizes overly complex models (Nielsen, 2015; Welch, 2015; Ng, et al., 2013). This is achieved by adding the product of λ and the square of the weights to the cost function and then normalizing the cost function with respect to the number of data samples. Equation 34 describes this step. Higher values of λ impose a bigger penalty for high model complexity.

$$J = \frac{\left(\frac{1}{2}e^2\right)}{length(X)} + \left(\left(\lambda/2\right) * \left(\left(\sum W^{(1)^2}\right) + \left(\sum W^{(2)^2}\right)\right)\right)$$

Equation 34: Error Cost with overfitting considered

In Figure 32, at about 320 iterations, the effects of overfitting is evident. This is represented by the notable separation been the plots of the training and testing error cost. Fig 26 illustrates estimates from a network with overfitting. The network is unable to, adequately, capture elements of uncertainties in the estimates. However, in Figure 34, with the regularization technique implemented, the plotted network training and testing error costs are much closer. This is because the effect of overfitting is minimized. Fig 28 illustrates estimates from a regularized network. The network better reflects elements of uncertainty in the estimates.

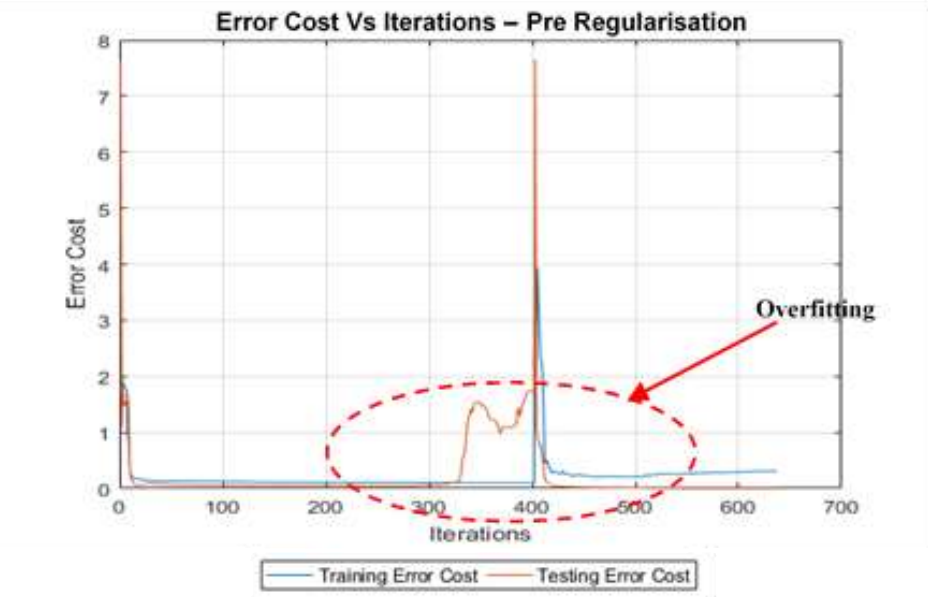

Figure 32: Neural Network Overfitting

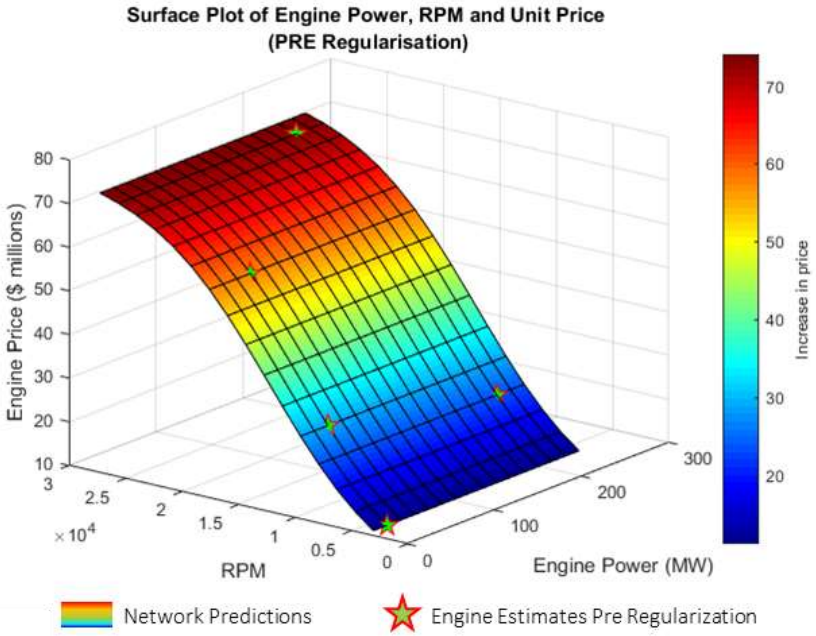

Figure 33: Estimates from an over-fitted network

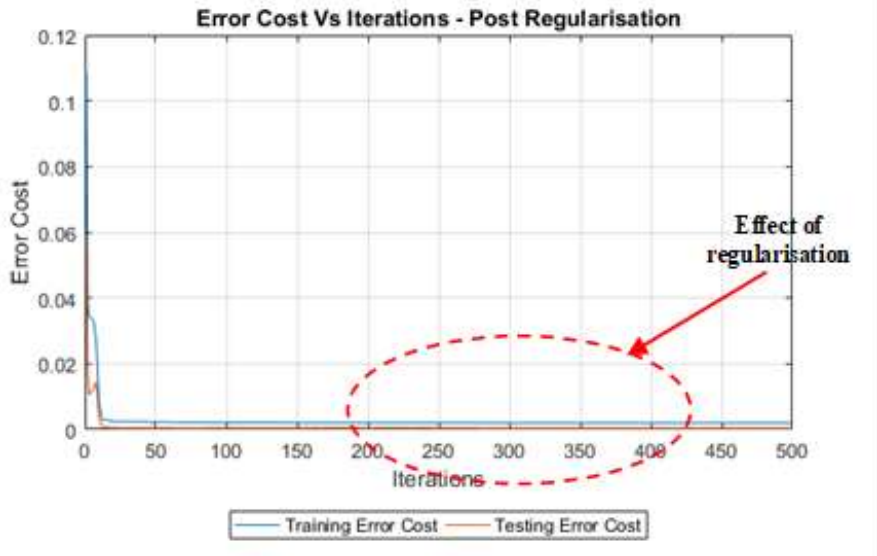

Figure 34: Neural Network Overfitting Regularized

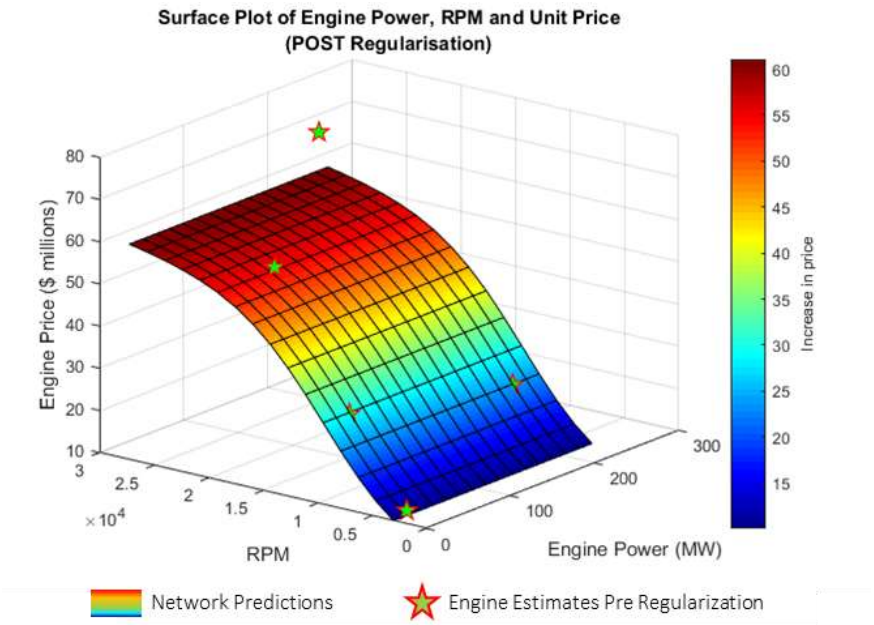

Figure 35: Estimates from a regularized network

4.2.1.1.3 Estimator

With the network trained, the output weights from the trained network are used to estimate the acquisition cost of various gas turbines units. Input values of engine power output, PT rpm and heat rate are provided to the trained network and estimates are generated in one forward processing step based on the supplied input. The result and analysis section of this study presents the results obtained from the application of the artificial neural network to predict gas turbine engine price.

4.2.1.2 Gas turbine Price estimation using regression analysis (RA)

The implemented regression analysis methodology is presented in Figure 36. The methodology involves the compilation of relevant data, the development and validation of an estimating relationship relevant to the compiled data and application of the validated relationship for estimating the price of any gas turbine unit within an established estimating circle. This section describes the elements of the implemented RA methodology and how it is applied to estimate gas turbine acquisition cost.

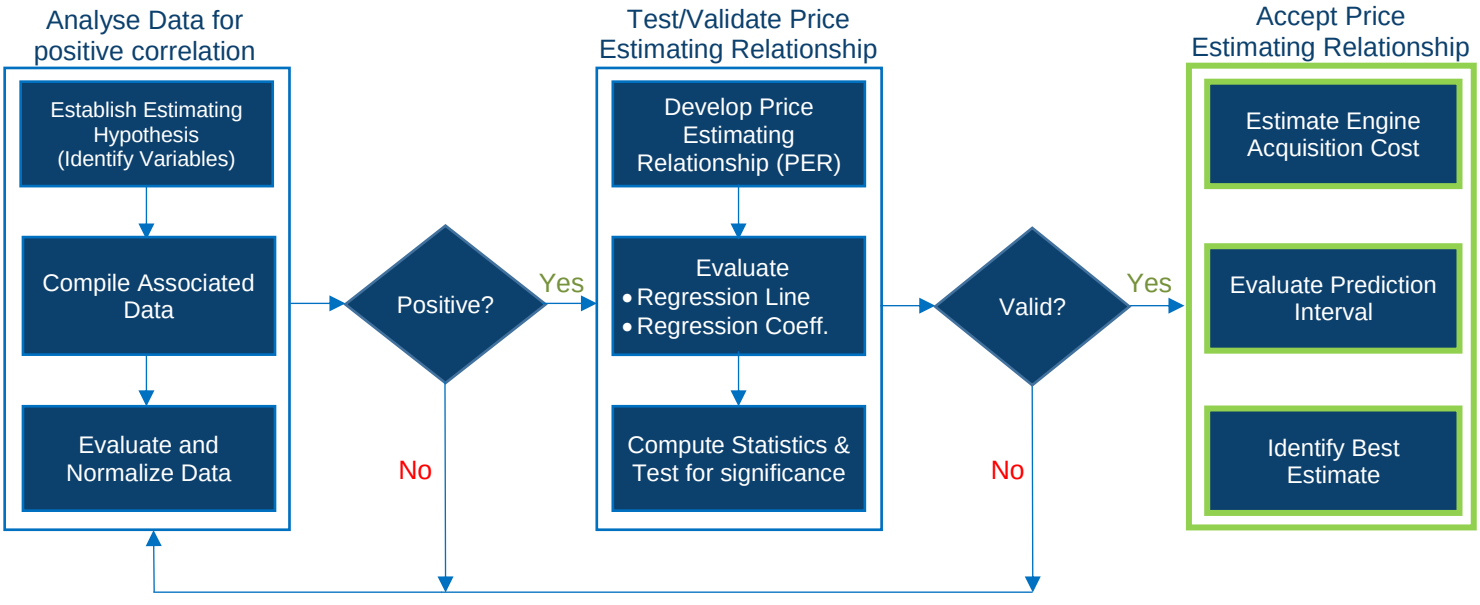

Figure 36: Regression Analysis Methodology for Estimating Acquisition Cost

4.2.1.2.1 Compilation and Analysis of data for positive correlation

This section of the methodology identifies the correlation between the variables and parameters of a dataset to be used for regression analysis. The correlation could be positive or negative. A positive correlation indicates a positive relationship between variables and favours the application of a dataset for analysis. A negative correlation indicates a negative relationship between variables and favours the application of a dataset for analysis. A correlation of zero indicates there is no correlation between variables and discourages application of a dataset for further analysis unless the dataset is reviewed.

4.2.1.2.1.1 Establish estimating Supposition

The first step in identifying correlation, which is also the first step in implementing the RA estimating methodology, involves developing an estimating supposition from which appropriate estimating variables are identified. Defining a supposition is important in guiding the nature and type of data to compile. In this study, gas turbine acquisition cost is estimated based on an underlying relationship between engine rated performance and associated acquisition cost.

4.2.1.2.1.2 Compile Associated Data

With a supposition, defined, appropriate data is compiled from historical records of engine acquisition costs and performance parameters retrieved from various sources including the Gas Turbine World Handbook, Turbomachinery International and the Nye Corporation Database. The compiled dataset consists of engine price, engine power output, engine rpm and engine heat rate. Appendix D presents the compiled Dataset.

4.2.1.2.1.3 Normalize and Evaluate Data

The compiled data is normalized to ensure consistency and homogeneity. Normalization of the data in this study involves standardization of data units and data scaling by accounting for inflation in engine price using Equation 19Equation 21. The producer price index (PPI) industry data provided by the U.S. Bureau of Labour Statistics is used to evaluate inflation (U.S. Bureau of Labor, 2017; Thompson, 2009).

The normalized dataset is evaluated using a scatter plot and the Pearson's Correlation Coefficient (also called Pearson's r) to identify correlation between variables. The correlation coefficient is a single summary number that gives a good idea about how closely a variable relates to another variable (Higgins, 2005). Equation 35 describes the Pearson's correlation coefficient.

$$r_{XY} = \frac{\sum XY - \frac{(\sum X)(\sum Y)}{n}}{\sqrt{(SS_X)(SS_Y)}}$$

Or

$$r_{XY} = \frac{\sum XY - \frac{(\sum X)(\sum Y)}{n}}{\sqrt{\left[\left(\sum X^2 - \frac{(\sum X)^2}{n_X}\right)\left(\sum Y^2 - \frac{(\sum Y)^2}{n_Y}\right)\right]}}$$

Equation 35: Pearson's Correlation Formula

Where **X** and **Y** are the variables in a dataset and n is the number of samples for each variable in the dataset. A positive relationship means that an increase in the value of one variable initiates a predictable increase in the value of another variable. A negative relationship implies that an increase in the value of a variable results in a predictable decrease in the value of another. No correlation indicates that a change in the value of a variable does not influence any change in the value of another variable. The degree of influence which one variable has over another is quantified by Pearson's correlation coefficient, which always falls between -1.00 and +1.00 (Higgins, 2005). A value of -1.00 indicates a perfect negative correlation and +1.00 indicates a perfect positive correlation. The closer the value of the correlation coefficient is to -1.00 or +1.00 the stronger the relationships between variables and the greater the predictability of the influence of on variable over the other. The correlation coefficients for the dataset compiled in this study are presented in Section 5.4.1. Furthermore, the assumptions made to validate the application of the Pearson's Correlation Coefficient in this study are outlined below.

- Variables are measured on an interval or ratio scale
- The dependent variable (acquisition cost) is normally distributed in the population.
- The relationship between the variables are characterized by a linear relationship.
- The values of the dependent variable are normally distributed across each value of the independent variable (Assumption of Homoscedasticity).

4.2.1.2.2 Development and Validation of Price Estimating Relationship

After establishing correlation between variables, regression analysis is conducted. This involves developing a price estimating relationship (PER), testing and validating the PER using analysis of variance (ANOVA) techniques and other statistical methods. The sections below describe these steps.

4.2.1.2.2.1 Develop price-estimating relationship (PER)

A price estimating relationship PER is developed with acquisition cost as the dependent variable, **Y** and Power output as the independent variable, **X**. Engine Power output parameter is the only independent variable implemented in this analysis due to the strong positive correlation observed between power output and engine acquisition cost. The evaluation of other variables revealed a very weak correlation with acquisition cost (Section 5.4.1).

Since analysis of the dataset reveals a linear functional form represented by the strong positive correlation between power output and acquisition cost, a simple linear regression (SLR) model is initially applied, Equation 36.

$$Y = \beta_0 + \beta_1 X + E$$

Equation 36: Simple Linear Regression Model

Where $\boldsymbol{\beta_0}(Yintercept)$, $\boldsymbol{\beta_1}(the\ slope)$ are the population regression coefficients and $\boldsymbol{E}$ is the random error or residual disturbance term. $\boldsymbol{Y}$ is the dependent variable and $\boldsymbol{X}$ is the independent variable.

Data samples are generated from the compiled dataset using the simple linear regression model for a sample.

$$\hat{Y} = \hat{b}_0 + \hat{b}_1 X$$

Equation 37: Simple Linear Regression Model for a sample

Where $\boldsymbol{\hat{b}_0}(Yintercept)$, $\boldsymbol{\hat{b}_1}(the\ slope)$ are the population regression coefficients, $\boldsymbol{\hat{Y}}$ (acquisition cost) is the dependent variable and $\boldsymbol{X}$ is the independent variable (power output).

4.2.1.2.2.2 Evaluate regression line and regression coefficient

The regression coefficients are evaluated from Equation 38 and Equation 39. Figure 64 and Figure 66 (in section 5.4.1.1) show plots of the calculated sample data points (regression line) superimposed with the actual data from the compiled data set.

$$\hat{b}_1 = \frac{n\sum XY - (\sum X)(\sum Y)}{n\sum X^2 - (\sum X)^2}$$

Equation 38: Slope of the regression line

$$\hat{b}_0 = \frac{n\sum Y - \hat{b}_1(\sum X)}{n}$$

Equation 39: Intercept of the regression line

With the regression coefficients evaluated, a simple linear regression model for price estimation is defined as shown in Equation 40. Thus, a predicted average value for the dependent variable $\hat{Y}_{AQC}$ can be determined for any value of the independent variable X_{PWR}.

$$\hat{Y}_{AQC} = \hat{b}_0 + \hat{b}_1 X_{PWR}$$

Equation 40: Price Estimating Relationship

To ensure the validity of the implemented price estimating approach and the analysed database, the following assumptions are made:

- The database obtained for analysis is homogeneous. This implies that the items in the database are of the same category. All engines are used for similar applications and are operated under similar conditions (at ISA SLS).
- A linear relationship exists between power output (independent variable, X) and engine acquisition cost (dependent variable, Y).
- The independent variables (power output, X) have been measured without error. Thus, any deviation in the data analysis is restricted to the dependent variables (cost, Y).
- Residuals, E, are normally distributed about the regression line.
- The residuals, E, come from an identically and independently distributed random distribution with mean zero and constant variance. Thus, residuals cannot be predicted from knowledge of the independent variable (power output, X).
- All acquisition costs have been adjusted for inflation to a common base year (2017).
- Engine acquisition costs include the cost of installation and accessories.

4.2.1.2.2.3 Compute statistics and test of significance.

Tests are conducted to measure the validity of the regression line. This is essentially to determine how well the developed price estimating relationship (PER) predicts the dependent variable and whether or not a trend exists. Ultimately, these tests provide a basis for selecting or discarding the developed regression equation.

Four techniques are used to assess the regression analysis performed. These include:

- Calculation for the Coefficient of determination (R^2 or r^2)
- Calculation for the Coefficient of correlation (R or r)
- Calculation for the standard error of estimate(SE)
- Calculation for the Coefficient of variation (CV)
- Graphical Residual Analysis
- Hypothesis test

4.2.1.2.2.3.1 Calculation for the Coefficient of determination (R^2)

Coefficient of determination (R^2) measures the accuracy of the regression line fit to the sample data points. R^2 ranges from 0 to 1 (0 to 100 percent). An R^2 equal to or greater than 90 percent is typically desired. An R^2 of 97 percent means that the regression model explains 97 percent of deviation leaving only 3 percent to chance. An R2 of 100 means the regression model perfectly explains the deviations in considered variables. Equation 41 describes the coefficient of determination.

$$R^2 = \frac{[\sum XY - n(\bar{x})(\bar{Y})]^2}{[\sum X^2 - n(\bar{X})^2][\sum Y^2 - n(\bar{Y})^2]}$$

Equation 41: Coefficient of Determination

4.2.1.2.2.3.2 Calculation for the Coefficient of correlation (R or r)

The coefficient of correlation (R) is similar to R^2 but yields one piece of information not provided by R^2. This is the direction of the slope, whether negative or positive. In additions, it is a singular value, which gives information on how closely a considered variable relates to another. The coefficient of correlation is the square root of R^2 as described in equation below. It can also be evaluated from Equation 35. Typically a value of R closer to -1.00 or +1.00 is desired. A value of R closer to or equal to zero indicates a weak or non-existent correlation. This is not desired.

$$R = \sqrt{R^2}$$

Equation 42: Coefficient of Correlation

4.2.1.2.2.3.3 Calculation for the standard error of estimate (SE)

Standard error of the estimate (SE) is an absolute measure of the deviation of sample point from the regression line. It is calculated for each estimate using Equation 43.

$$SE = \sqrt{\frac{\sum\left(Y - \hat{Y}\right)^2}{n - k - 1}}$$

Equation 43: Standard Error of Estimate

Where n is the sample size, k is the number of independent variables in the PER. SE should be as small as possible.

4.2.1.2.2.3.4 Calculation for the Coefficient of variation (CV)

The Coefficient of variation (CV) is a statistic that employs the standard error of estimate (SE) to evaluate the validity a regression line. It is desirable that CV be less than 20 percent. CV is calculated from Equation 44.

$$CV = \frac{SE}{\bar{Y}}$$

Equation 44: Coefficient of Variation

4.2.1.2.2.3.5 Graphical Residual Analysis

With respect to the assumption that the Residuals, E, are independent, normally distributed, random variables, with a mean of zero and constant variance, another examination is required to determine the appropriateness of the developed PER for the regression analysis. This is to check whether the computed errors satisfy the assumption.

A random scatter plot of residuals against the independent variable is generated for each estimate. Visually analysing the plots should reveal that all points fall approximately within an equal band above and below a zero line. This would indicate that the errors are independent and normal as earlier assumed. If this is not observed, an alternative PER is considered.

4.2.1.2.2.3.6 Hypothesis test

A hypothesis test is conducted to determine if the slope (the coefficient of the independent variable) is significantly different from zero.

- A slope of zero would indicate that the regression relationship is purely by chance
- A slope that is not zero **but also not** significantly different from zero means, knowing the independent variable is of no use in estimating (predicting) the dependent variable.
- A slope significantly different from zero indicates that a knowledge of the independent variable is significant in estimating the dependent variable. Thus, the developed regression relationship (Equation 40) is regarded as significant and can thus be retained.

To conduct the test, it is necessary to calculate the standard error of the slope (S_1) given by:

$$S_1 = \frac{SE}{\sqrt{\sum X^2 - n\sum \bar{X}^2}}$$

Equation 45: Standard Error of the slope

A null and an alternative hypothesis is defined. The hypotheses considered in this study are as follows:

a) Null hypothesis

$$H_0: b_1 = 0$$

b) Alternative hypothesis

$$H_1: b_1 \neq 0$$

A significance level of 0.05 is chosen for the test. The considered significance level is the probability of an analyst committing a type 1 error. A type 1 error occurs when an analyst rejects a null hypothesis when it is true.

Due to the composition of the alternate hypothesis, the test is defined as a two-tailed test. Variable t_p (from t-table) and t_c (Equation 47) are computed and a comparison of the values of t_c and t_p either accept or reject the established hypothesis.

$$t_p = t_{1-\alpha/2,n-2}$$

Equation 46: Variable t_p

$$t_c = \frac{\hat{b}_1}{S_1}$$

Equation 47: Variable t_c

If $|t_c| > |t_p|$, null hypothesis rejected (NASA, 2015)

If $|t_c| \leq |t_p|$, null hypothesis is NOT rejected (NASA, 2015)

If the hypothesis is accepted, the coefficients are statistically insignificant and the regression equation discarded. Alternatively, a rejected hypothesis indicates that the coefficients are statistically significant and the initial regression equation retained.

If the statistical tests and analysis conducted, reveal that developed price, estimating relationship, PER, adequately predicts the dependent variable Y, then the adopted regression model and computed regression line are identified as valid. Alternatively, if the results are unfavourable, an alternative regression model (e.g. Simple nonlinear regression) is considered. Equation 48 - Equation 52 describe the simple nonlinear regression model. It is worth mentioning that even though a regression analysis provides valid outcomes from a statistical perspective, the causality of the equation is still analysed for a logical relationship.

4.2.1.2.2.4 Simple Nonlinear Regression Models

When applying nonlinear regression analysis, the non-linear functional form of the dataset is expressed in linear form (transformed) by taking the natural log of the considered variables (dependent and independent variables). This yields the equation for a straight line in fit space where the transformed variables exist with slope *B* and intercept $ln\, A$ (NASA, 2015).

$$ln\, \hat{Y} = ln\, \hat{A} + \hat{B}\, ln\, X$$

Equation 48: Non-linear Regression Model in fit space

$$\hat{Y} = \hat{A}X^{\hat{B}}$$

Equation 49: Non-linear regression model in unit space

The method of least squares is then applied to calculate the predictive values of slope B and intercept $ln\, A$ from Equation 50 and Equation 51.

$$\hat{B} = \frac{n\sum(ln\,X\,ln\,Y) - (\sum ln\,X)(\sum ln\,Y)}{n\sum(ln\,X)^2 - (\sum ln\,X)^2}$$

Equation 50: Estimated Slope of the non-linear regression line

$$ln\,\hat{A} = \frac{\sum ln\,Y - \hat{B}\sum ln\,X}{n}$$

Equation 51: Estimated Intercept of the non-linear regression line

$$\hat{A} = e^{ln\,\hat{A}}$$

Equation 52: Unit Space Equivalent of $ln\,A$

Computing the statistics and tests of significance, to measure the validity of the nonlinear regression curve, is done using similar approach as described in section 4.2.1.2.2.2. However, calculations for the coefficient of determination R^2 are performed using the transformed dependent and independent variables.

4.2.1.2.3 Estimation of Acquisition Cost

With the price estimating relationship, PER, accepted, the adopted regression model can be applied to estimate the acquisition cost for any gas turbine, at 95% confidence level, based on the engine's rated power output. The interval within which the estimates are expected to fall is computed using Equation 53.

$$PI = \hat{Y}_0 \pm t_p\,SE\sqrt{\frac{n+1}{n} + \frac{(X_0 - \bar{X})^2}{\sum X^2 - n\bar{X}^2}}$$

Equation 53: Prediction Interval

Where PI is the prediction interval, SE is the standard error or standard deviation of the estimate, $\hat{Y}_0$ is the target or best estimate and t_p is obtained from the t table.

4.2.2 Life Approximating Model

This is the component of the overall economic model associated with estimating the life of a gas turbine. A gas turbine typically consists of an air intake system, compressor, combustor, turbine and Nozzle or Power turbine. Each of these components have different life(s), which are influenced by numerous variables that occur randomly over time.

The Life of a gas turbine can be approximated as the life of the component with the highest potential to experience failure due to creep over an operating period. Thus, the life of a gas turbine is tantamount to the life of the component with shortest creep life. This is usually the combustor or the High Pressure (HP) turbine blade.

The life of a gas turbine is typically about 3-5years before an overhaul/replacement of major gas path components is required. Multiple factors occurring simultaneously influence gas turbine component life. These factors could be due to mechanical, environmental or operational influences. However, there is great complexity in attempting to capture all these

potential factors in a model. As such, approximations can be used to estimate the life of a gas turbine, among other methods.

Presented in this section is an approach for approximating the life of gas turbine units based on the effect of TET increase on the blade life. An approximation is implemented that for every 20K rise in temperature, the turbine blade life is halved (Gad-Briggs, et al., 2013). It is worth mentioning that this approximation is not directly linear but signifies an exponential decrease by a factor of half for every 20K rise in TET. Figure 37 illustrates this approximation.

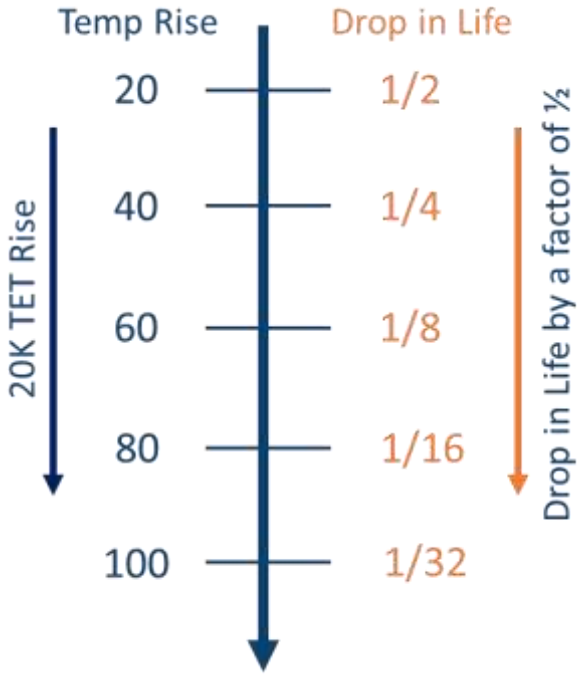

Figure 37: Illustration of Temperature Rise and drop in life Factor

4.2.2.1 Model approach for life approximation

A mathematical model has been developed and applied to approximate the life of gas turbine units. This model is presented below.

$$OP_{Engine\ Life} = DP_{Engine\ Life} \pm LF_{current}$$

Equation 54: Gas Turbine Life Approximation (LIA) Model

Where

$$LF_{current} = ((0.5 \times RF) + LF_{intial})$$

Equation 55: Lifing Factor (Current)

$$LF_{intial} = (1 - RF)$$

Equation 56: Lifing Factor (Initial)

Thus

$$OP_{Engine\ Life} = DP_{Engine\ Life} \pm \left((0.5 \times RF) + LF_{initial}\right)$$

Equation 57: Gas Turbine Life Approximation Model (Representation 2)

$$OP_{Engine\ Life} = DP_{Engine\ Life} \pm \left((0.5 \times RF) + (1 - RF)\right)$$

Equation 58: Gas Turbine Life Approximation Model (Representation 3)

Where

$$RF = abs\left(\frac{OP_{TET} - DP_{TET}}{20_{Temp.\ rise}}\right)^{-1}$$

Equation 59: Reduction Factor, RF evaluation

$OP_{Engine\ Life}$ and $DP_{Engine\ Life}$ are the design point and operating point engine life respectively. LF_{intial} and $LF_{current}$ are initial and current lifing factors. RF is the reduction factor.

The application of the approximation model (Equation 54-Equation 59) depends on the value of the turbine entry temperature at operating point (OP_{TET}) with respect to the turbine entry temperature at design point (DP_{TET}).

- At $\boldsymbol{DP_{TET} = OP_{TET}}$; $\boldsymbol{RF}$ **and** $\boldsymbol{LF_{initial}}$ **are zero**. This mean that when the turbine entry temperature at design point is equal to the turbine entry temperature at operating point, the reduction factor is zero. **Therefore:**

$$OP_{Engine\ Life} = DP_{Engine\ Life}$$

Equation 60: Operating Point Life at DP_{TET} equals OP_{TET}

- At $\boldsymbol{DP_{TET} > OP_{TET}}$; $\boldsymbol{RF}$ **is less than one**. When turbine entry temperature at design point is higher than the turbine entry temperature at operating point, the reduction factor is less than one. **Therefore, operating point life is evaluated as**:

$$OP_{Engine\ Life} = DP_{Engine\ Life} + LF_{current}$$

Equation 61: Operating point life at higher DP_{TET}

- At $\boldsymbol{DP_{TET} < OP_{TET}}$; $\boldsymbol{RF}$ **is also less than one**. When turbine entry temperature at design point is lower than the turbine entry temperature at operating point, the reduction factor is less than one. **Therefore, operating point life is evaluated as**:

$$OP_{Engine\ Life} = DP_{Engine\ Life} - LF_{current}$$

Equation 62: Operating point life at Lower DP_{TET}

NOTE:
The Design point life $DP_{Engine\ Life}$ of a gas turbine can be obtained from the OEM (original Engine Manufacturer) or by inquiry from an experienced operator. Typically, gas turbine design point life is between 3 - 5 years.

The developed gas turbine Life approximation model is an iterative estimating model. Thus, at the initial point of estimation, initial lifing factor (LF_{intial}) is zero. To simulate higher sensitivity to creep, initial lifing factor (LF_{intial}) can be permanently set to zero, irrespective of the value of RF. In such a scenario, Operating point life is evaluated as:

$$OP_{Engine\ Life} = DP_{Engine\ Life} \pm (0.5 \times RF)$$

Equation 63: Operating point life at higher sensitivity to creep

4.2.2.2 Life Approximating Model Flowchart

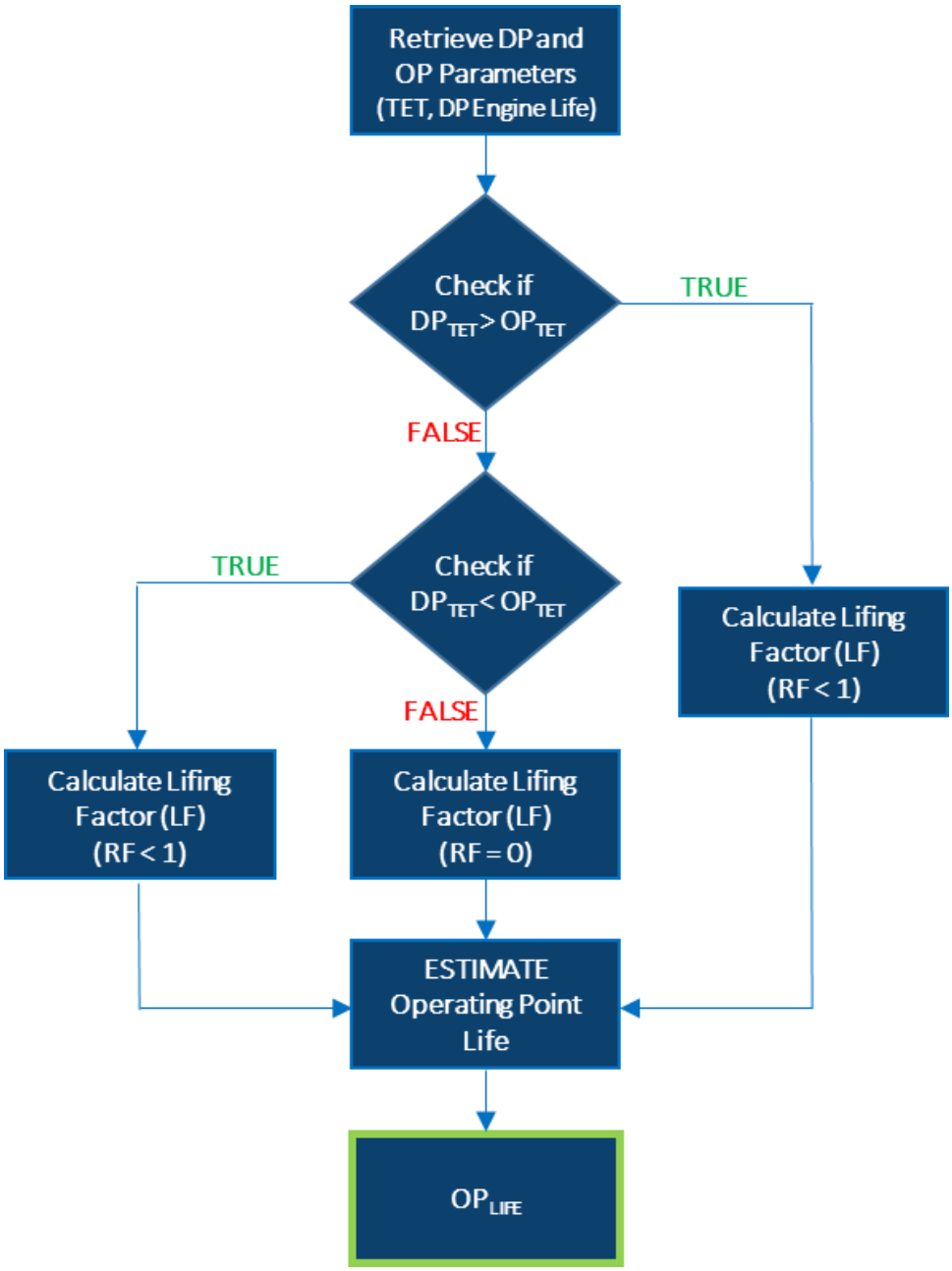

Equation 64: Life approximating model component of overall economic model

Design point and operating point parameters retrieved from a performance simulation model or retrieved as direct input values are supplied as input into the approximation model. Appropriate checks are performed to identify if the Design point TET (DP_{TET}) is equal to, greater than or less than the Operating point TET (OP_{TET}). Once identified, an appropriate algorithm is applied to estimate the operating point life of considered gas turbine units. Figure 38 illustrates change in engine life with respect to engine operating point TET.

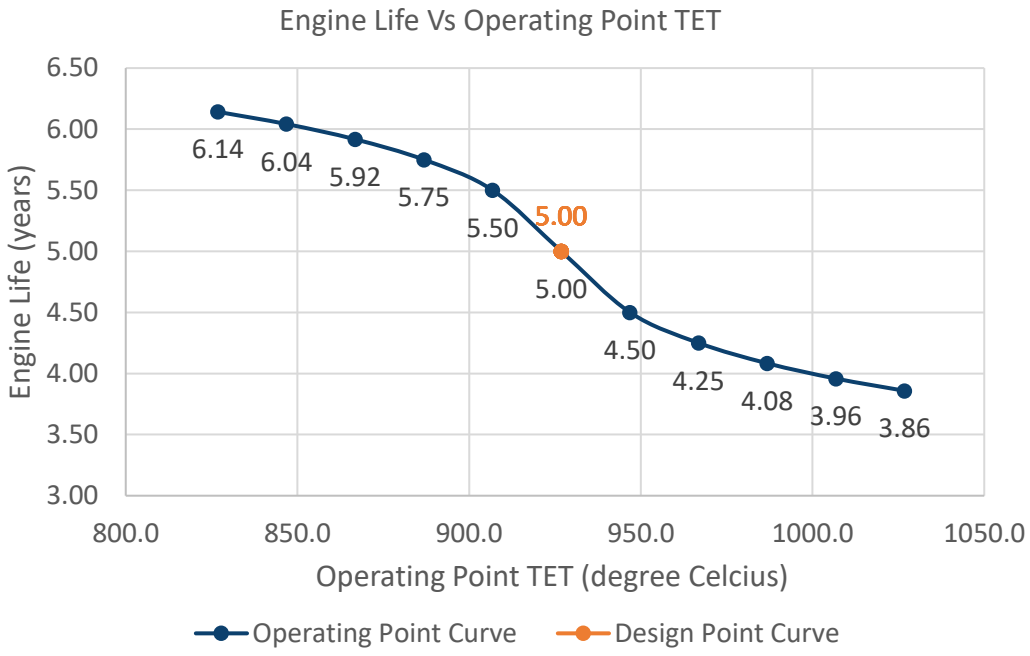

Figure 38: Change in Engine Life Vs Operating point TET

4.2.3 Emissions Model

This is the component of the overall economic model associated with estimating the emissions generated and any potential emissions tax payable on emissions generated by a gas turbine.

The developed emissions model applies gas turbine information on fuel type, emissions type and adopted emissions control to estimate the emissions generated by a gas turbine (Figure 39). Equation 65 - Equation 68 characterize the emissions estimating model.

4.2.3.1 Emissions Rate

The emissions rate of any system is characterized by the emissions activity, the emissions factor and the emissions control associated with the system. The emissions activity quantifies how active the system is. The emissions factor relates the activity of the system to the type and amount of pollutant generated and the emissions control quantifies the efficiency of pollutant control. Equation 65 describes the emissions rate.

$$EMR = E_{Activity} \times E_{Factor} \times E_{control}$$

Equation 65: Emissions Rate Calculation

EMR is the Emissions rate per period, $E_{Activity}$ is the emissions activity per period, E_{Factor} is the emissions factor per activity and $E_{control}$ is the emissions control factor. In this study, a control factor of 1 indicates that the emission control factor is built into the considered system and no external control technology is implemented. A control factor less than 1 quantifies the efficiency of emissions control for an adopted external emissions control technology.

4.2.3.2 Emissions Factor

The emission factor is evaluated from Equation 66 using data from the U.S. Environmental Protection Agency's emissions factor documentation (AP-42 data sheet) for gas turbines. In this documentation, pollutant concentrations provided are based on average values from multiple tests conducted on various turbines, and are categorized based on fuel type and

control technology for all pollutants generated from gas turbines. A matching factor is used to map the evaluated emissions factor to a particular engine unit as described in Equation 66 and Equation 67.

$$E_{Factor} = \left(P_{conc.} \times 10^{-6} \times \left(\frac{1}{Molar\ Volume}\right) \times Molar\ Weight \times F_d \times \left(\frac{20.9}{20.9 - \%O_2}\right)\right) \times MF$$

Equation 66: Emissions Factor Calculation [a]

Where

$$MF = \frac{E_{Factor}}{E_{FactorE}}$$

Equation 67: Matching Factor

MF is the matching factor. The matching factor compensates for differences in fuel type, gas composition and engine operating conditions. E_{Factor} is the actual emissions factor and $E_{FactorE}$ is the estimated emissions factor. When $MF = 1$, $E_{Factor} = E_{FactorE}$ this implies that no matching is required. F_d represents the dry oxygen factor of the considered fuel type and $\%O_2$ represents the corrected oxygen concentration. F_d, Molar Volume and $\%O_2$ are the gas properties associated with the considered fuel type. Molar Weight describes the considered pollutant properties.

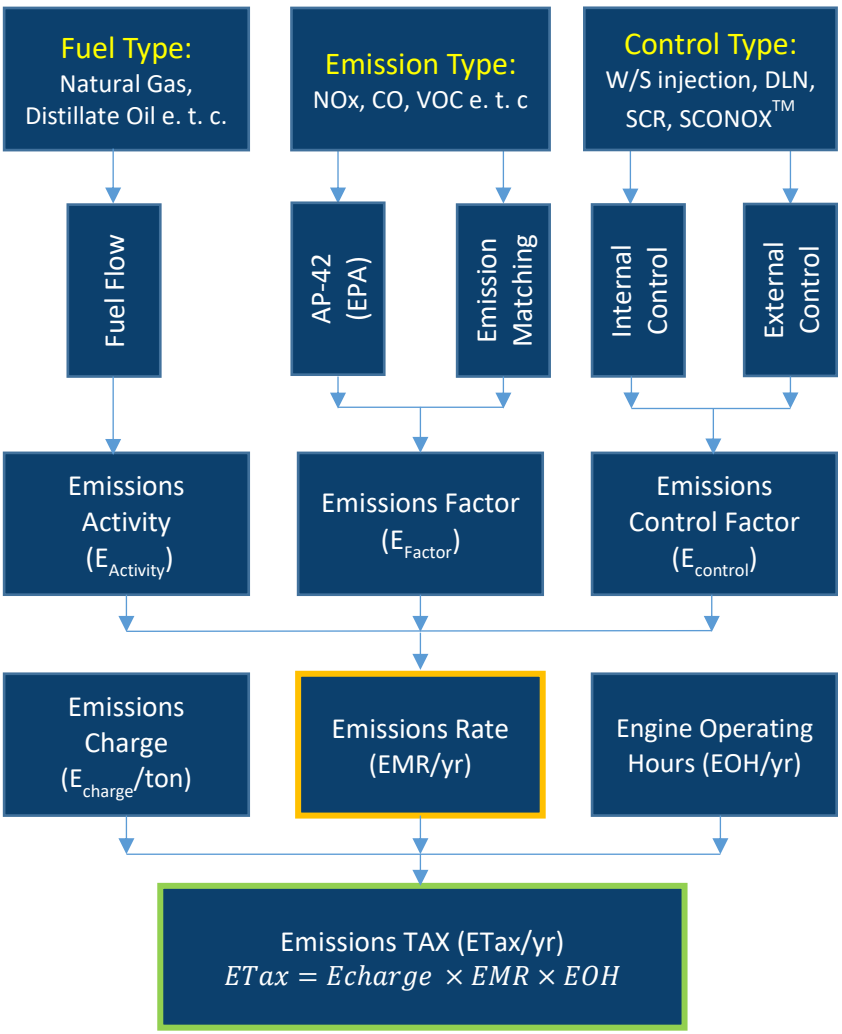

Figure 39: Emissions Model component of overall economic model

4.2.3.3 Emissions Tax

The implemented emissions methodology provides for the estimation of emissions tax per period, with respect to a set emissions charge, an evaluated emissions rate and engine operating hours of a considered unit. Equation 68 describes this aspect of the emissions model.

$$ETax = E_{charge} \times EMR \times EOH$$

Equation 68: Emissions Tax Estimation

ETax is the emissions tax per period considered. E_{charge} is the charge per tons of emissions generated. EMR is the emissions rate per period descried in Equation 65 and EOH is the engine operating hours per considered period.

4.2.3.4 Emissions evaluation methodology

Input information relating to fuel type (obtained from unit performance and operating point data), emission type and emission control are retrieved for a considered gas turbine unit. The fuel flow rate of the gas turbine is the emissions activity. This is converted to MMBTU/yr.

Based on the considered emissions and emissions control technology, the EPA's AP-42 data sheet is consulted to retrieve the appropriate emissions factor. The emissions factor retrieved from the AP-42 documentation is classed as the estimated emissions factor $E_{FactorE}$. Equation 69 is then applied to evaluated the actual emissions factor E_{Factor} in lb/MMBTU. As opposed to using the AP-42 data sheet, the engine's pollutant concentration can be provided in PPMV (parts per million by volume) and Equation 66 applied to evaluate E_{Factor} in lb/MMBTU.

$$E_{Factor} = E_{FactorE} \times MF$$

Equation 69: Emissions Factor Calculation [b]

After obtaining the actual emissions factor E_{Factor}, the emission rate, EMR in lb/yr. is evaluated from Equation 65. Further conversion expresses the calculated emissions rate in tons/yr. The expression of emissions generated in tons per year enables the easier evaluation of the cost effectiveness of an adopted emissions mitigation technology as described in Equation 70.

$$Cost\ Effectiveness = \frac{Owning\ Cost\ of\ Emissions\ Technology}{Amount\ of\ Emissions\ Removed}$$

Equation 70: Cost Effectiveness of Emissions Technology (ONSITE SYCOM Energy Corporation , 1999)

Finally, an annual emission tax is calculated from Equation 68 based on the evaluated emission rate, retrieved annual engine operating hours and emissions charge in dollars per ton of emissions generated.

4.2.3.5 Model Validation

As a validation to the implemented methodology, the developed emissions model has been applied to estimate the emissions rate for some gas turbines. Results from the estimates are compared with records from investigations, conducted for the U.S. department of energy, by ONSITE SYCOM Energy Corporation (ONSITE SYCOM Energy Corporation , 1999) and

Investigations conducted by the California energy commission for the EL Segundo Power Redevelopment Project (ESPR) (California Energy Commission, 2007). Figure 40Figure 42 compare results obtained from model estimates with those documented from investigations conducted.

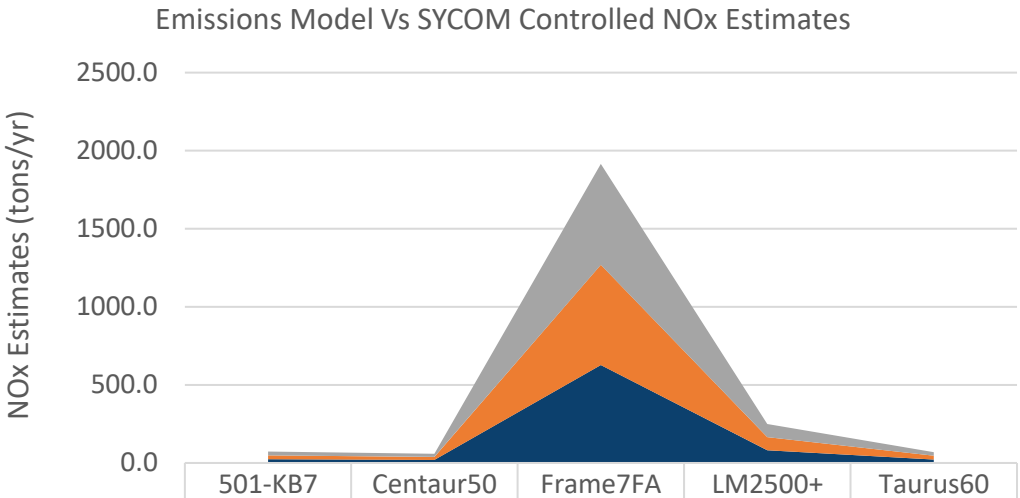

	501-KB7	Centaur50	Frame7FA	LM2500+	Taurus60
SYCOM	24.9	19.9	645.9	83.9	23.4
Matched	24.8	19.8	642.0	83.4	23.3
Unmatched	24.2	19.3	627.5	81.5	22.8

Figure 40: Emissions Model Vs SYCOM Estimates (Conrolled NOx)

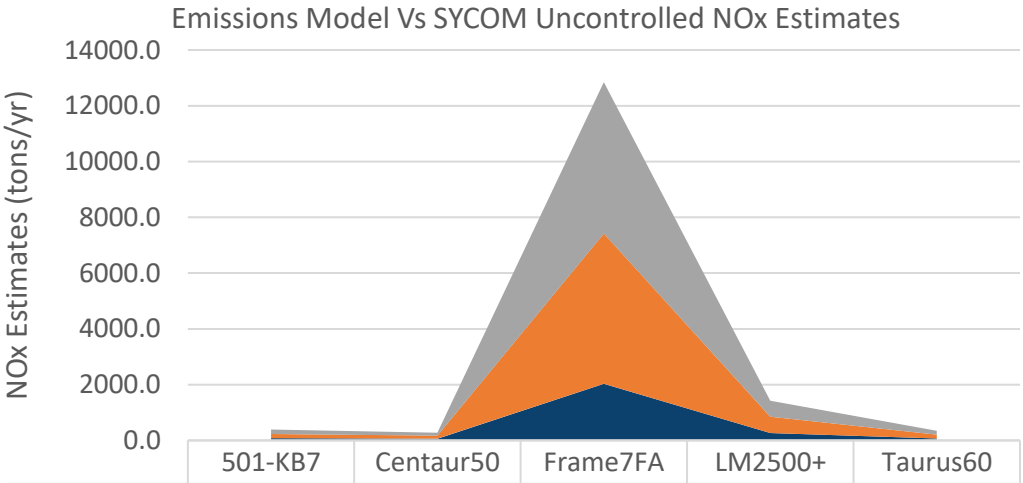

	501-KB7	Centaur50	Frame7FA	LM2500+	Taurus60
SYCOM	154.4	106.6	5426.0	584.1	134.1
Matched	153.5	106.0	5392.6	580.5	133.2
Unmatched	78.2	62.5	2028.4	263.6	73.6

Figure 41: Emissions Model Vs SYCOM Estimates (Uncontrolled NOx)

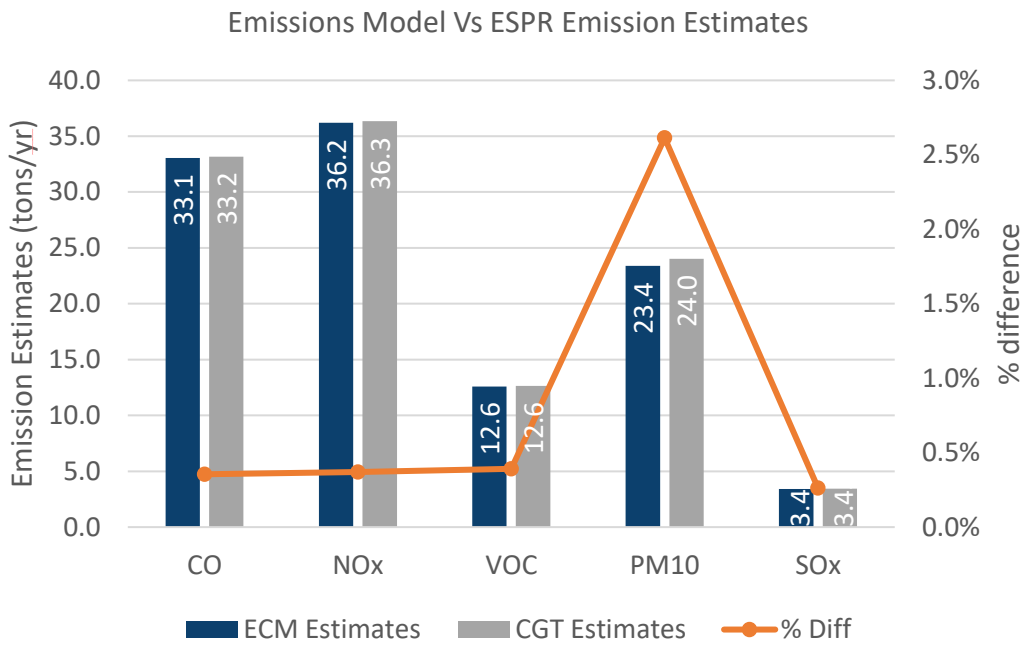

Figure 42: Emissions Model Vs CTG Estimates

Outlined below, are the assumptions made for model validation.

- All engines are running at 80% capacity (ONSITE SYCOM Energy Corporation , 1999).
- All engines operate 8000 full load hours per year (ONSITE SYCOM Energy Corporation , 1999).
- All engines operate on Natural Gas with Identical fuel composition (California Energy Commission, 2007).

In Figure 40 and Figure 41, the 'Matched' model estimates for NOx emissions rate are very similar to actual estimates from SYCOM investigations with percentage difference less than 1% for the considered gas turbine with and without emissions control. In the 'Unmatched' case, model estimates for the gas turbine, with emissions control, were close to SYCOM estimates (percentage difference less than 3%). There was large variations between model estimates and SYCOM estimate for the gas turbine without emissions control. This is due to the unaccounted variation in fuel composition and operating conditions in the 'Unmatched' model estimates.

In Figure 42, ECM refers to economic cost model. The model estimates for emission rate in tons per year are very close to the actual estimates from ESPR investigations with percentage difference less than 3% for all pollutants considered.

The emission estimating approach presented in this section has been integrated into the cost model component of the overall economic model.

4.2.4 Performance Model

This is the component of the overall techno-economic model associated with performance modelling and simulation of Brayton cycle systems necessary for techno-economic analysis. Performance modelling and simulation is conducted with TURBOMATCH. TURBOMATCH is a modular performance modelling and simulation tool, built at Cranfield University, for gas turbine thermodynamic performance modelling and simulation. It is built to simulate both steady state and transient engine performance for both aero and industrial gas turbines. The

tool is also capable of simulating engine component degradation and enables novel cycle performance modelling. Figure 43 shows the schematic of the TURBOMATCH performance simulation model and its integration with components of the economic model.

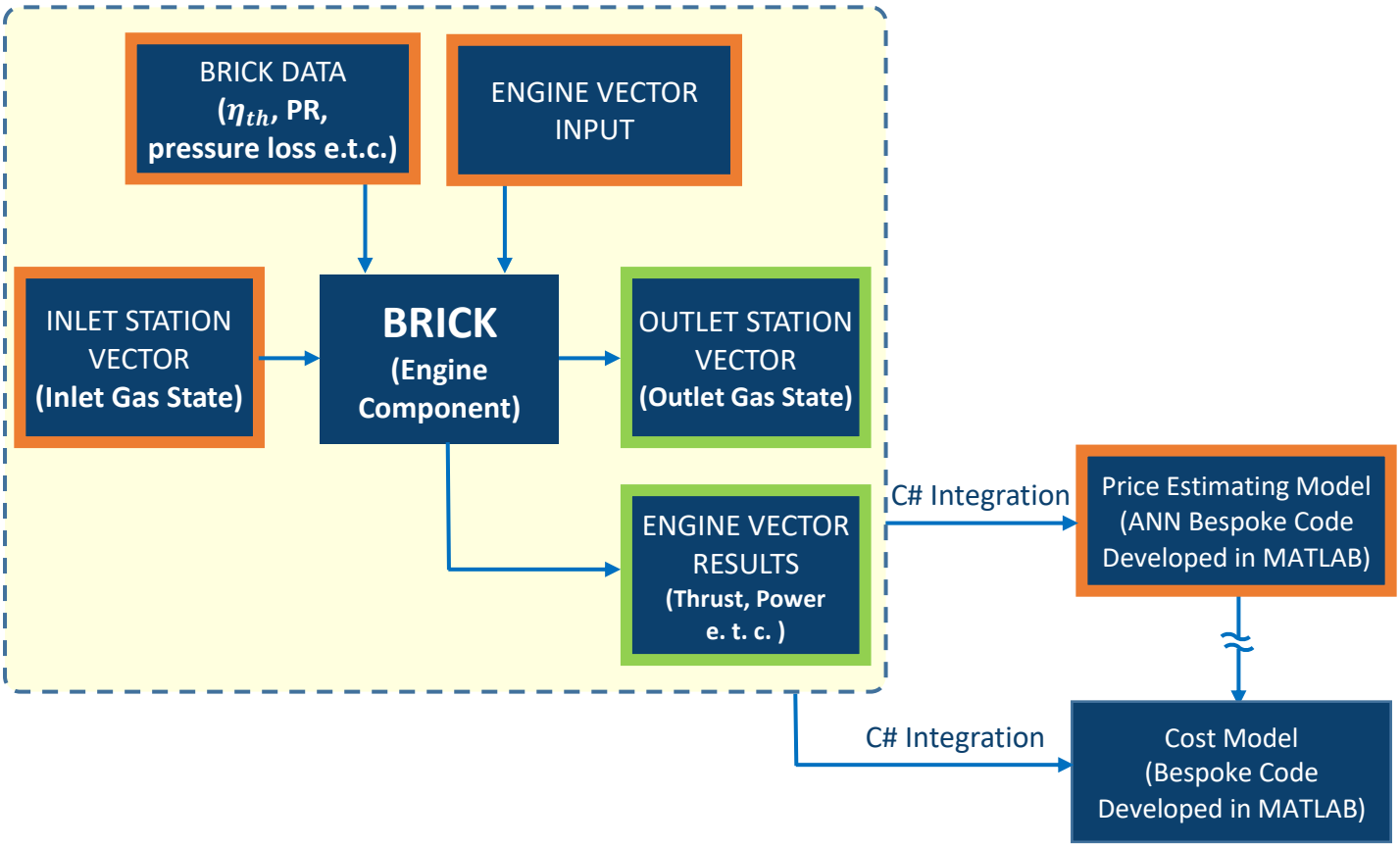

Figure 43: Performance Model Integration flowchart

The TURBOMATCH model framework consists of bricks, station vectors and engine vectors.

4.2.4.1 Brick

A brick corresponds an engine component and accommodates input parameters associated with characterizing that component. These input parameters are called brick data. For example, a compressor brick is characterized by inputs of pressure ratio, component efficiency, compressor characteristic map, rotational speed, pressure loss e. t. c.

4.2.4.2 Station vectors

Station vectors specify the flow stream (air/gas) state and thermodynamic properties at the inlet and outlet of a brick. These properties include temperature, pressure and velocity e. t. c.

4.2.4.3 Engine vectors

Engine vectors are bricks, different in kind from station vectors, which generate outputs or inputs. Engine vectors can be identified as either engine vector results or engine vector data. Engine vector results describe the output generated from a brick (for example, thrust, power output, fuel flow, compressor work e. t. c.) and Engine vector data describe vector results (for example compressor work), which are required as input into certain bricks.

4.2.4.4 Performance simulation in TURBOMATCH

The process of performance simulation in TURBOMATCH involves building a modular engine model by using pre-programmed controls called bricks. Each brick corresponds to a particular engine component. The entire engine model is divided into stations with the inlet and outlet of each brick corresponding to a station number as shown in Figure 44. Additional bricks for arithmetical operations and for, both intermittent and final performance simulation output are also included in the model. Station Vector and brick data values appropriately specify the performance simulation handles. Once the engine performance model is prepared, the simulation is run and simulation results are stored in appropriate formats, suitable for post processing. Output of engine power output, heat input, fuel flow, turbine entry temperature e. t. c., from the performance simulation results are supplied to the price and cost estimating model component of the overall techno-economic model through integration using C# and MATLAB code.

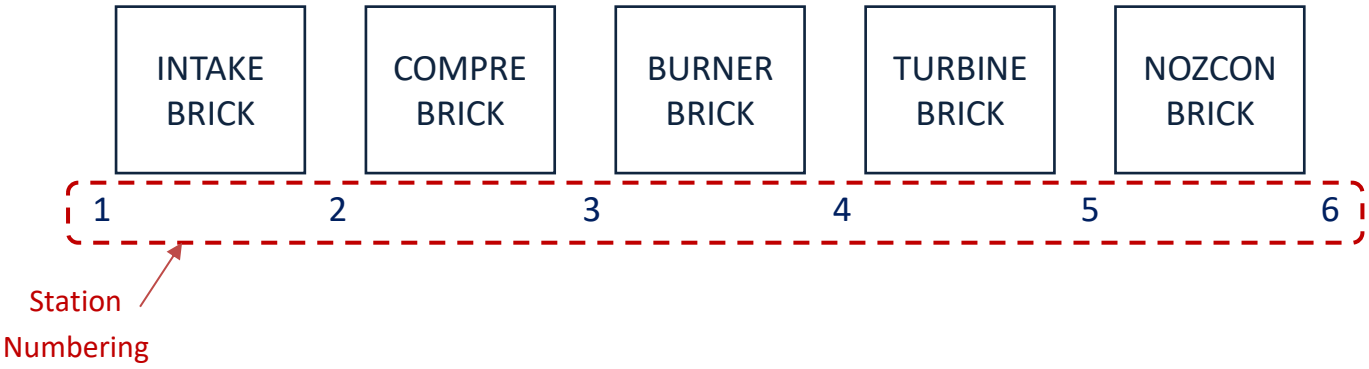

Figure 44: Typical modular engine model schematic

The described performance simulation approach has been applied to simulate gas turbine engine performance in both steady and transient state with and without engine degradation considered. Details of this implementation, including results, are presented in the Section 6.1.

4.2.5 Cost Model

This is the component of the overall techno-economic model associated with cost analysis. The model utilizes output from the gas turbine engine performance, price estimating, emissions and life approximation models to provide quantitative information on the economic implications of an investigated cycle, system or investment option. Essentially, the cost model evaluates gas turbine total productive life cost and profitability.

The cost model estimates the total productive life cost (TPLC) of a unit in simple and combined cycle applications as defined by Equation 71. Figure 45 illustrates the cost model.

$$\mathrm{TPLC} = \mathrm{TCC} + \mathrm{TOM}$$

Equation 71: Total productive life cost Equation

Where TCC is the total capital cost and TOM is total operation and maintenance cost.

4.2.5.1 Total Capital Cost (TCC)

The total capital cost is the sum of all initial costs required for investment (Jenkinson, et al., 1999). It is sometimes the same as the project investment base (Beaves, 1996). In this study, TCC includes the cost of unit spares (SP_{cost}), Upgrade/retrofit cost (UR_{cost}), Refurbishment cost (RF_{cost}), the unit acquisition cost of steam (AQS_{cost}) and gas turbine (AQ_{cost}) as described

in Equation 72. The unit acquisition cost is estimated using artificial neural network (Jenkinson, et al., 1999).

$$\mathrm{TCC} = \mathrm{AQ}_{cost} + \mathrm{AQS}_{cost} + \mathrm{SP}_{cost} + \mathrm{UR}_{cost} + \mathrm{RF}_{cost}$$

Equation 72: Total Capital Cost Equation

In simple cycle application, turbine (AQS_{cost}) is zero.

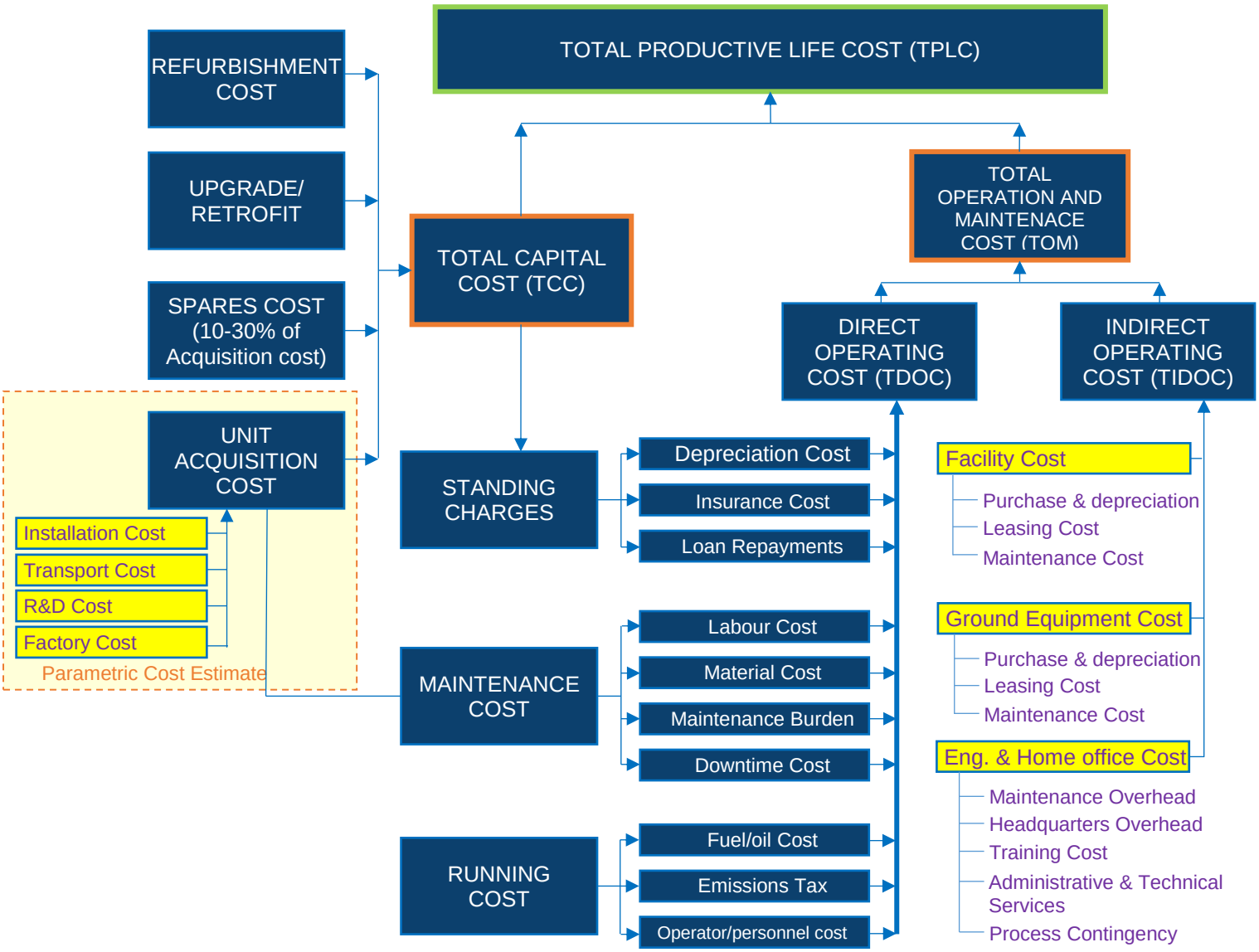

Figure 45: Cost model component of overall economic model

4.2.5.2 Total operation and Maintenance Cost (TOM)

This represents the sum of all direct operating costs (DOC) and indirect operating costs (IDOC) as described in Equation 73 (Jenkinson, et al., 1999).

$$\mathrm{TOM} = \mathrm{TDOC} + \mathrm{TIDOC}$$

Equation 73: Total Operation and Maintenance Cost (TOM)

4.2.5.2.1 Total Direct Operating Cost (TDOC)

The direct operating cost, DOC consists of all the costs directly attributed to running and maintaining an engine unit, Equation 74. These costs are described below.

$$\mathrm{TDOC} = \mathrm{TS}_{charge} + \mathrm{TMT}_{cost} + \mathrm{TRN}_{cost}$$

Equation 74: Total Direct Operating Cost Equation

4.2.5.2.1.1 Total Standing Charge (TS charge)

The Standing charges refers to costs that are not directly associated with gas turbine operation but are regarded as overhead on operations. These costs include depreciation cost (DEP cost), insurance cost (INS cost) and loan repayments (INT charge) (Jenkinson, et al., 1999). Equation 75 describes the standing charge.

$$\mathrm{TS}_{charge} = \mathrm{DEP}_{cost} + \mathrm{INS}_{cost} + \mathrm{INT}_{charge}$$

Equation 75: Total Standing Charge Equation

Where

$$\mathrm{DEP}_{cost} = \frac{TCC - Salvage\ Value}{EPL}$$

Equation 76: Depreciation Cost

$$\mathrm{INS}_{cost} = i_{premium} \times \mathrm{AQ}_{cost}$$

Equation 77: Insurance Cost

$$\mathrm{INT}_{charge} = \mathrm{i}_{rate} \times \mathrm{TCC}$$

Equation 78: Interest Charge

Where EPL is engine productive life, $i_{premium}$ is annual insurance premium and $\mathrm{i}_{\mathrm{rate}}$ is the interest rate on loans.

4.2.5.2.1.2 Total Maintenance cost ($\mathrm{TMT}_{\mathrm{cost}}$)

The total maintenance cost is the sum of all labour costs ($\mathrm{L}_{\mathrm{cost}}$), material costs ($\mathrm{M}_{\mathrm{cost}}$), maintenance burden ($\mathrm{MB}_{\mathrm{cost}}$), downtime costs ($\mathrm{DT}_{\mathrm{cost}}$), engine washing Costs ($\mathrm{MC}_{\mathrm{DEW}}$) and Steam Turbine Maintenance cost ($\mathrm{MS}_{\mathrm{cost}}$) incurred per year as described by Equation 79.

$$\mathrm{TMT}_{cost} = \mathrm{L}_{cost} + \mathrm{M}_{cost} + \mathrm{MB}_{cost} + \mathrm{DT}_{cost} + \mathrm{MC}_{\mathrm{DOW}} + \mathrm{MS}_{cost}$$

Equation 79: Total Maintenance Cost

In this study, the maintenance burden captures the costs incurred due to unit maintenance outages (planned or unplanned). Equation 80 describes the estimation for maintenance burden adopted in this study.

$$\mathrm{MB}_{cost} = \mathrm{Overhead}_{rate} \times \mathrm{EMH}$$

Equation 80: Maintenance Burden

Where EMH refers to unit maintenance hours per year. Downtime cost captures the costs incurred, when the unit is not generating any profit, due to unit outages unrelated to

maintenance. This includes planned and unplanned outages. Equation 81 describes downtime cost.

$$\mathrm{DT}_{cost} = abs((\mathrm{Overhead}_{rate} \times \mathrm{DTH}) - \mathrm{MB}_{cost})$$

Equation 81: Downtime Cost

Where DTH refers to downtime hours. DT $_{cost}$ will be zero when the EMH is the same as the DTH. Maintenance cost incurred due to engine washing, MC_{DEW}, is described in Equation 82.

$$\mathrm{MC}_{DEW} = \mathrm{WPY} \times \mathrm{CPW}$$

Equation 82: Cost due to engine Washing

Where WPY refers to the number of engine washes per year and CPW is the cost incurred per engine wash. The Maintenance cost of the steam unit is calculated as described in Equation 83.

$$\mathrm{MS}_{cost} = \mathrm{MT}_{steam} \times \mathrm{EMH}$$

Equation 83: Maintenance Cost of Steam unit

Where MT $_{steam}$ is the total maintenance cost per kilogram of steam given by Equation 84. PW $_{steam}$ is the power generated by the steam turbine and OMS $_{cost}$ is the operation and maintenance cost of steam per kilowatt-hour. OMS cost is usually less than o.4$c/KWh.

$$\mathrm{MT}_{steam} = \mathrm{PW}_{steam} \times \mathrm{OMS}_{cost}$$

Equation 84: Total maintenance cost per kilogram of steam

4.2.5.2.1.3 Total Running Cost (TR cost)

This is the total cost of running a unit. It comprises the sum of the fuel cost, F $_{cost}$, Personnel Cost, P $_{cost}$, operation and maintenance cost of Emissions control technology, CTOM, and any emissions tax E $_{tax}$ incurred by the unit (Jenkinson, et al., 1999). Equation 85 describes the total running cost.

$$\mathrm{TRN}_{cost} = \mathrm{F}_{cost} + \mathrm{P}_{cost} + \mathrm{E}_{Tax} + \mathrm{CTOM}$$

Equation 85: Total Running Cost

The major driving factor of TDOC is the total running cost, which is largely influenced by fuel price (F $_{price}$). Equation 86 describes the total fuel cost.

$$\mathrm{F}_{cost} = \left(\mathrm{F}_{volume} \times \mathrm{F}_{price} \times \mathrm{EOH}\right) + \mathrm{FC}_{Transient} - \mathrm{FC}_{UNDEWtotal}$$

Equation 86: Total Fuel Cost

Where F $_{price}$ is fuel price and F $_{volume}$ is fuel volume given by Equation 87. EOH is the engine operating hours per year. FC $_{Transient}$ is the fuel cost during transient operation given by Equation 88 and FC $_{UNDEW\ total}$ is the total un-incurred fuel cost during engine washing given by Equation 91.

$$\mathrm{F}_{volume} = \frac{\mathrm{F}_{flow}}{\mathrm{F}_{density}}$$

Equation 87: Fuel Volume

In Equation 87, F_{flow} refers to the engine fuel flow and $F_{density}$ is the engine fuel density.

$$\mathrm{FC}_{Transient} = \mathrm{FV}_{Transient} \times \mathrm{F}_{price} \times \mathrm{TOH}$$

Equation 88: Transient Fuel Cost

Where $FV_{Transient}$ is the total transients fuel volume in transient regime. TOH is transient hours per year, described in Equation 89.

$$TOH = \mathrm{T}_{Cycles} \times \mathrm{TD}_{total}$$

Equation 89: Transient Operating Hours

T_{cycles} is the number of transient cycles per year and TD_{total} refers to the total transient duration described in Equation 90.

$$\mathrm{TD}_{total} = Startup\ Duration + Shutdown\ Duration$$

Equation 90: Total Transient Duration

$$\mathrm{FC}_{UNDEWtotal} = \mathrm{FC}_{UNDEW} \times \mathrm{WPY}$$

Equation 91: Total un-incurred Fuel Cost

Where FC_{UNDEW} is un-incurred fuel cost during engine washing described in Equation 92 and WPY is the number of washes per year.

$$\mathrm{FC}_{UNDEW} = (\mathrm{F}_{volume} - (\mathrm{F}_{volume} - (\mathrm{F}_{volume} \times \%DFV_{EW}))) \times \mathrm{F}_{price} \times \mathrm{DOW}$$

Equation 92: Un-incurred Fuel Cost during engine washing

Where $\%\mathrm{DFV}_{\mathrm{EW}}$ refers to percentage drop in fuel volume during engine washing. DOW is the duration of wash.

In relation to Equation 85, the total Personnel cost (P_{cost}) is described by Equation 93. The Personnel cost is the total cost attributed to the number of operators assigned to operate a unit per year.

$$\mathrm{P}_{cost} = \mathrm{avg.\,hourly\ rate} \times \mathrm{EOH} \times Operators\ Per\ shift$$

Equation 93: Personnel Cost

Where EOH is the engine operating hours per year. The emissions tax (E_{tax}) is total charge paid per annum on emissions generated by a unit. Equation 94 describes the emissions tax. The unit emissions rate (E_{rate}), expressed in tons/hour, is used to calculate emissions tax based on a set emissions charge (E_{charge}).

$$\mathrm{E}_{Tax} = \left(\mathrm{E}_{charge} \times \mathrm{E}_{rate} \times EOH\right) + \mathrm{ETax}_{Transient}$$

Equation 94: Emissions TAX

The emissions rate is estimated using the approach described in Chapter 4.2.3. Similarly, the transient emissions Tax, $ETax_{Transient}$ is estimated using Equation 95.

$$\mathrm{ETax}_{Transient} = (\mathrm{E}_{rate} \times \mathrm{E}_{index} \times TOH)$$

Equation 95: Transient Emissions TAX

TOH is the transient engine operating hours per year.

In summary, the total direct operating cost, TDOC is the sum of the total standing charge (TS $_{charge}$), the total Maintenance Cost (TMT $_{cost}$) and the total running cost (TRN $_{cost}$) as described in Equation 74.

4.2.5.2.2 Total Indirect Operating Cost (TIDOC)

The total indirect operating cost comprises those costs not directly attributable to running and maintaining an engine unit (Jenkinson, et al., 1999). For this study, the elements of TIDOC have been categorized into three aspects.

- Facility cost, FA $_{cost}$
- Ground Equipment Cost, GE $_{cost}$
- Engineering and Home Office Cost, HM $_{cost}$

The sum of all categories of the indirect operating cost, gives the total indirect operating cost, TIDOC, described in Equation 96.

$$\mathrm{TIDOC} = \mathrm{FA}_{cost} + \mathrm{GE}_{cost} + \mathrm{HM}_{cost}$$

Equation 96: Total Indirect Operating Cost

As defined in Equation 73, the sum of TDOC and TIDOC gives the total operation and maintenance cost, TOM, per annum.

The output of the cost model component of the overall techno-economic model is the total productive life cost, TPLC, obtained by summing the total unit capital cost, TCC, with the total operation and maintenance cost, TOM, defined in Equation 71.

4.2.6 Levelized Cost of Energy (LCOE)

The levelized cost of energy is the price at which electricity must be generated to break even over the life of a unit. It is an economic assessment of the cost of an energy-generating system including all the costs over its lifetime: initial investment, operations and maintenance, cost of fuel, and cost of capital (U.S. Department of Energy | Office of Indian Energy, 2015; U. S. Energy Information Administration | Annual Energy Outlook, 2017).

In this study, the LCOE is calculated with respect to the useful life of the considered unit. While LCOE can be extended to compare different technology options, this study applies LCOE to the comparison of engine units, with similar technologies, operating in simple or combined cycle application. The levelized cost of energy is calculated from the TPLC as described in Equation 97.

$$\mathrm{LCOE} = \frac{TPLC}{EP_{life}}$$

Equation 97: Levelized Cost of Energy (LCOE)

Where

$$EP_{life} = EP_{gen} \times (\mathrm{EOH} \times \mathrm{EPL})$$

Equation 98: Power generated over unit life

$$EP_{gen} = ((EP_{sc} \times EP_{\%increase}) + EP_{sc})$$

Equation 99: Total power generated per year

EP_{life} is power generated over unit life, EP_{gen} is total power generated per year. EP_{SC} is power generated by unit in simple cycle operation. $EP_{\%\ increase}$ is the percentage increase in power generated in combined cycle application and EPL is the engine productive life.

4.2.7 Selection Model

This component of the overall economic model utilizes output from the cost model to estimate total annual cost (TA_{cost}) and benefit ($TA_{benefit}$) and applies these estimates to perform present worth analysis. Figure 3 illustrates the selection model.

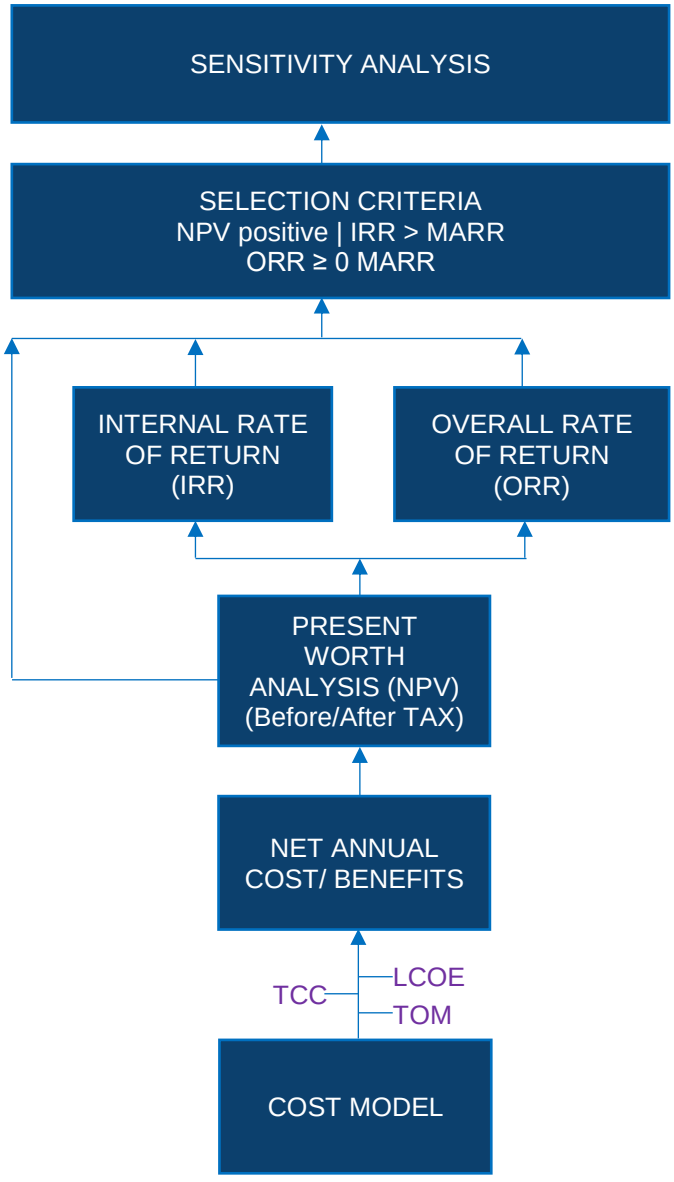

Figure 46: Selection Model component of Techno-economic Model

4.2.7.1 Total Annual Cost (TA $_{cost}$)

The total annual cost is the sum of the total operation and maintenance cost per year and any additional annual cost (AD $_{cost}$) incurred, not captured by the cost model. This is described by Equation 100.

$$TA_{cost} = \mathrm{TOM} + AD_{cost}$$

Equation 100: Total Annual Cost

4.2.7.2 Total Annual Benefits (TA $_{Benefit}$)

The total annual benefits is the sum of Benefits on energy generated (BOE) and any quantifiable annual saving or benefits (AD $_{benefit}$) less power loss due to engine washing (PL_{NW}). Equation 101 describes this.

$$TA_{benefit} = \mathrm{BOE} + AD_{benefit} - PL_{NW}$$

Equation 101: Total Annual Benefits

Where

$$BOE = EP_{gen} \times \mathrm{EOH} \times \mathrm{LCOE}$$

Equation 102: Benefits on energy

$$AD_{benefit} = Additional\ Annual\ Benefits + Additional\ Annual\ Savings$$

Equation 103: Additional Annual Benefits and Savings

$$PL_{NW} = (\mathrm{PWR} - (\mathrm{PWR} - (PWR \times \%DP_{EW}))) \times LCOE \times \mathrm{DOW} \times WPY$$

Equation 104: Power Loss per year due to washing

Where PWR is the engine power output. %DP $_{EW}$ is the percentage drop in power during engine washing. DOW is the duration of wash and WPY is the number of engine washes per year.

4.2.7.3 Total Benefit less Cost (TBLC)

This is the revenue generated per annum after all expenses, excluding income tax, have been deducted. Equation 105 defines TBLC.

$$TBLC = TA_{benefit} - TA_{cost}$$

Equation 105: Total benefits Less Cost

TBLC is the cash flow before tax without considering inflation, also identified as $A_{(t,x)}$

4.2.7.4 Present Worth and Rate-of-return Analysis

The present worth analysis is considered from two perspectives; before tax consideration and after tax consideration.

4.2.7.4.1 Before Tax Consideration

This consideration calculates the NPV, IRR, and ORR without considering the effect of tax liability on the net cash flows, across the project-planning horizon (Au, 1996). The project selection criteria, for the before tax consideration, are calculated using Equation 15 - Equation 18 as appropriate.

4.2.7.4.2 After Tax Consideration

This consideration takes into account the effect of tax liability on net cash flows across the project-planning horizon. It also takes into account the impact of inflation on the tax liability of an investment. Tax planning with inflation considered is an important determinant of the economic feasibility of a project as future tax liabilities will be based on then current dollars (Au, 1996). Equation 106 defines the NPV for this consideration.

$$\text{NPV}_x = \sum_{t=0}^{n} \frac{Y_{(t,x)}}{(1 + MARR)^t}$$

Equation 106: Net Present Value after tax

Where $Y_{(t,x)}$ the net cash flow after tax is given by Equation 107.

$$Y_{(t,x)} = A'_{(t,x)} - (X_{(t,x)} \times (A'_{(t,x)} - D_{(t,x)}))$$

Equation 107: Net Cash flow after Tax

$$A'_{(t,x)} = A_{(t,x)} * (1 + inflation\ rate)^t$$

Equation 108: Before tax cash flow with inflation considered

$X_{(t,x)}$ is the marginal income tax rate, $A'_{(t,x)}$ is the before tax cash flow with inflation considered, $A_{(t,x)}$ is the before tax cash flow without inflation. $D_{(t,x)}$ is the annual depreciation allowance estimated from Equation 109.

$$D_{(t,x)} = \frac{TCC - Salvage\ Value}{Facility\ life}$$

Equation 109: Annual Depreciation Allowance

When inflation is not considered, inflation rate is zero and $A'_{(t,x)} = A_{(t,x)}$. With the after tax, cash flow consideration, the rate-of-return criteria are calculated using Equation 16Equation 18 as appropriate.

Output from the present worth and rate-of-return analysis are used as criteria to judge if an investment is worthwhile or not. A project is accepted as profitable if

- The NPV is positive.
- ORR is greater than or equal to MARR
- IRR is greater than MARR.

Performing economic analysis with multiple considerations provides deeper insight into the potential benefits an investment option will deliver and enlightens investors on the elements

that will have greater impact on the investment. This is particularly important for investments faced with capital budgeting challenges.

4.2.7.5 Sensitivity Analysis

Sensitivity analysis is conducted using any of the economic model element as handle. For the chosen element, a pessimistic, optimistic and target value is prepared and used to analyse the sensitivity of an investment to changes (due to uncertainty) in the values of the handle. In this study, the engine fuel flow and emissions tax rate are used as handle for sensitivity analysis.

4.2.8 Optimization Model

This component of the overall techno-economic model deals with optimization analysis. In this study, optimization analysis consists of both performance and economic optimization. Details of each aspect of the implemented optimization analysis approach are presented below.

4.2.8.1 Performance Optimization

In this study, performance optimization analysis is conducted from two perspectives. This include modifications to the basic thermodynamic cycle of a considered unit and implementation of an optimization algorithm to solve a performance optimization problem.

4.2.8.1.1 Modifications to basic thermodynamic cycle

This involves altering the basic thermodynamic structure/configuration of a considered gas turbine in order to optimize unit performance or enhance performance output. Some modifications that can be implemented to optimize gas turbine performance include application of intercooler, reheat, regeneration, steam/water injection e. t. c. These modifications, implemented individually or combined, provide potential solutions to optimization problems. Detailed description of some modification to basic thermodynamic cycle are presented in chapter 3.4.4

4.2.8.1.2 Implementation of optimization algorithm to solve optimization problems

This is the second approach to solving performance optimization problems adopted in this study. An optimization algorithm is applied to minimize an objective function with respect to certain outlined constraints and boundaries.

4.2.8.2 Economic optimization

This study applies an optimization algorithm to solve economic optimization problems. The algorithm is applied to minimize an objective function based on outlined constraints and within specified objective boundaries.

4.2.8.3 Implemented algorithm

An interior point algorithm is implemented for both performance and economic optimization. The interior point algorithm, for function minimization, has the characteristics of high efficiency (Hessian calculated from 'bfgs' algorithm), low memory usage (may be high for larger problems) and ability to solve large problems quickly. Implementation of the interior point optimization algorithm in the optimization model is presented in section 5.6.2 and section 5.6.3.

4.2.8.4 *Optimization analysis methodology*

Prior to implement the optimization methodology, a clear understanding and definition of the optimization goal and objectives is necessary. Figure illustrates the implemented optimization methodology.

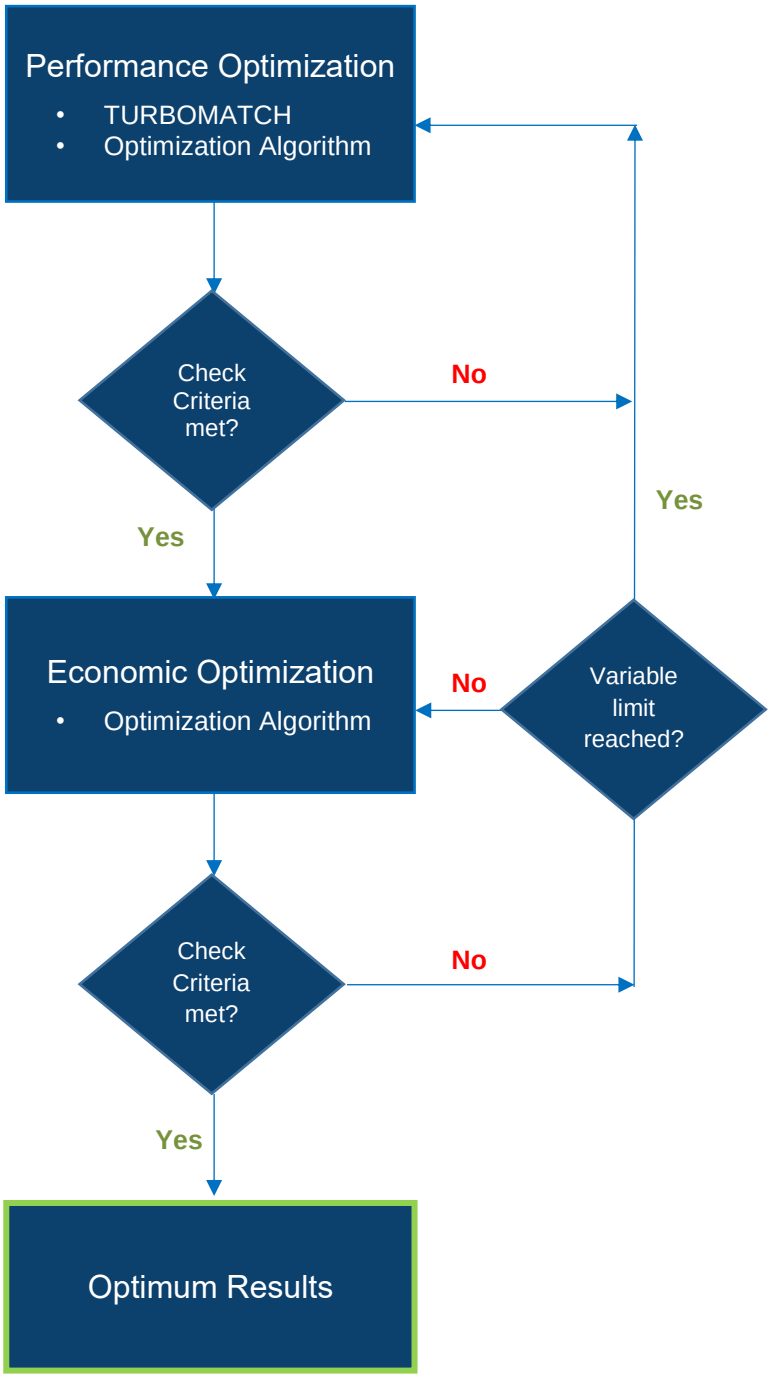

Figure 47: Optimization Methodology

Performance optimization is undertaking in two steps. First appropriate modifications, capable of achieving some or all of the desired performance objectives, are made to the basic thermodynamic cycle of a considered unit. These modifications are modelled and simulated in TURBOAMTCH. Once an optimum solution is achieved from cycle modification, further performance optimization is performed using an optimization algorithm. Output from the performance simulation are supplied as variables into an optimization solver and a performance objective function is optimized based on certain predefined constraints and

boundaries. After an optimum performance solution is obtained, a check is performed to see if the performance objectives have been met. If results are not satisfactory, adjustments are made to the performance optimization variables and implemented cycle modifications. However, satisfactory performance optimization results permit the advancement of the optimization methodology to economic optimization.

During economic optimization, output from the performance optimization model, as well as those from the cost model component of the economic model are supplied as variables into an optimization solver and the economic objective function is optimized with respect to predefined constraints and boundaries. A check is performed to identify if the economic optimization objectives have been met. If results are satisfactory, the overall optimum results comprising both performance and economic values are collated. If results are unsatisfactory, adjustments are made to the economic optimization variables and optimization analysis is repeated until satisfactory results are obtained or a variable limit is reached. Reaching a variable limit without achieving satisfactory economic optimization results will require a re-evaluation of the performance optimization analysis. Usually, trade-offs between conflicting requirements to satisfy certain objectives will have to be made.

5 RESEARCH TECHNIQUES

This chapter presents the contextual implementation of the research methodologies and models described in chapter 4.

5.1 Engine Selection

In order to provide a baseline for the overall research analysis and investigation, a case study engine has been selected. The engine is the Tumansky-R25-300 turbojet engine presented in Figure 48 and Figure 49. This engine choice seeks to investigate an alternative, civil profitable use for grounded jet engines. The selection also enables investigation into the feasibility of applying the power plants of grounded fighter jets (specifically the grounded MiG-21 fighter jets of the Nigerian Air force) for electrical power generation in Nigeria.

A study was conducted to determine the feasibility (from a performance perspective) of converting the selected case study engine into an aero-derivative engine for civil power generation application. Results are presented in Chapter 6.1. Table 1 shows the general engine components, characteristics and performance rating of the Tumansky-R25-300 turbojet engine.

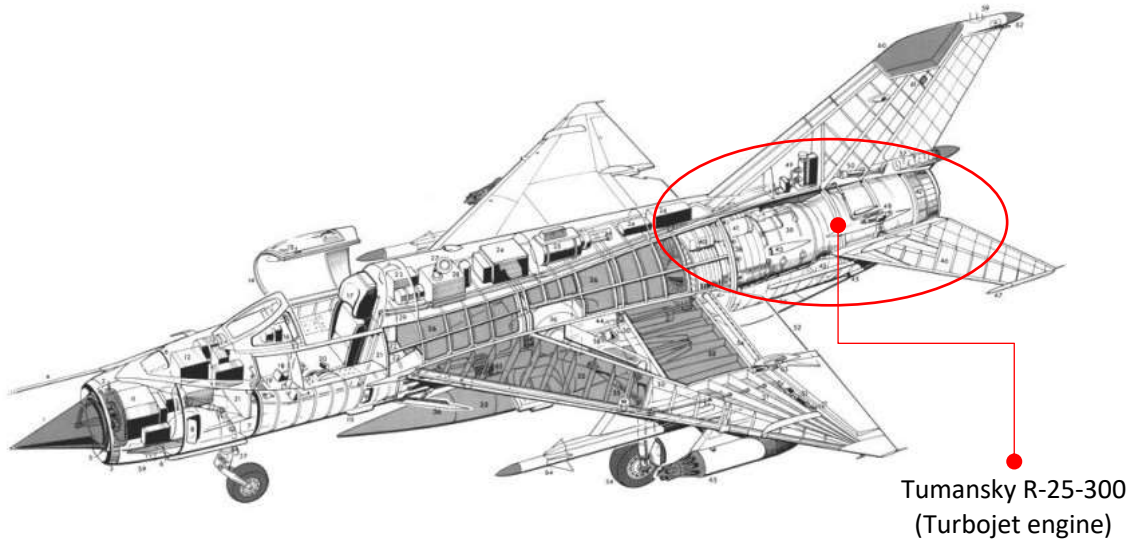

Figure 48: Mikoyan Gurevich MiG-21 fighter jet Aircraft (Mikoyan Gurevich, 2011; leatherneck, 2014)

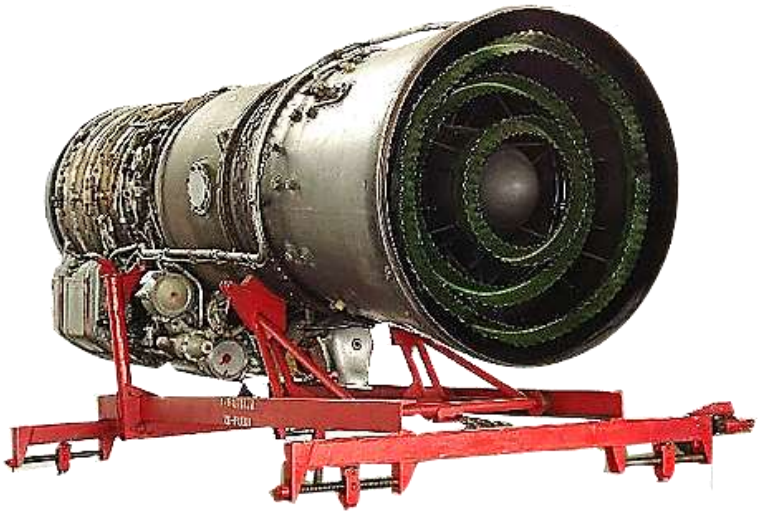

Figure 49: Tumansky- R25-300 turbojet engine on an engine mount (mm330046, 2007)

Table 1: Showing general turbojet engine components, specification and performance rating at ISA

General Characteristics			Components	Performance Parameters		
Two - spool turbo jet with afterburner			LP Compressor (3-stage no IGVs or VS)	Mass flow	68.50	kg
				Pressure Ratio	9.55	---
No Separate intake structure			HP Compressor (5-stage)	TIT	1.037	^{o}C
				THRUST		
DIMENSIONS			Combustor (Can annular)	Max dry (at 11,150rpm)	40.26	KN
				Normal (Cruise)	33.35	KN
Overall Length	4,615	mm	LP Turbine (Single Stage)	1F(with after burner at 11,500 rpm)	66.03	KN
Overall height	1, 191	mm		ChR (after burner at 11,150 rpm)	68.47	KN
Maximum diameter	907	mm	HP Turbine (Single Stage)	ChR (Mach1)	95.47	KN
WEIGHT				SFC		
Dry	1,215	kg	Afterburner (with step-less augmentation)	Max dry	27.20	mg/Ns
				Normal	25.78	mg/Ns
			Control System (Hydro mechanical) Accessories	Regime 1F	63.67	mg/Ns
			Nozzle	Regime ChR (Static)	70.74	mg/Ns

5.2 Feasibility Study

A study has been conducted to determine the feasibility of converting the selected case study engine into an aero-derivative engine for civil power generation application. In the course of the study, an engine performance model similar to the Tumansky-R25-300 turbojet was developed and simulated using TURBOMATCH. The engine model design point operation was matched with that of the Tumansky-R25-300 at ISA conditions. Figure 50 and Figure 51 show the Schematic of the developed turbojet engine model.

Modifications were made to the matched turbojet engine model in order to convert it into an aero-derivative variant capable of civil power generation. Figure 52 and Figure 53 illustrate the schematic of the aero-derivative engine model. Performance results obtained from the simulation of the aero-derivative engine variant gave suitable results, which favour the application and conversion of the Tumansky-R25-300 turbojet engine model into aero-derivative engine for civil power generation applications. Further study has been conducted on the aero-derivative variant to determine its performance under varying operating

conditions. Results are presented in Chapter 6.1. The following sections present the details of the feasibility study.

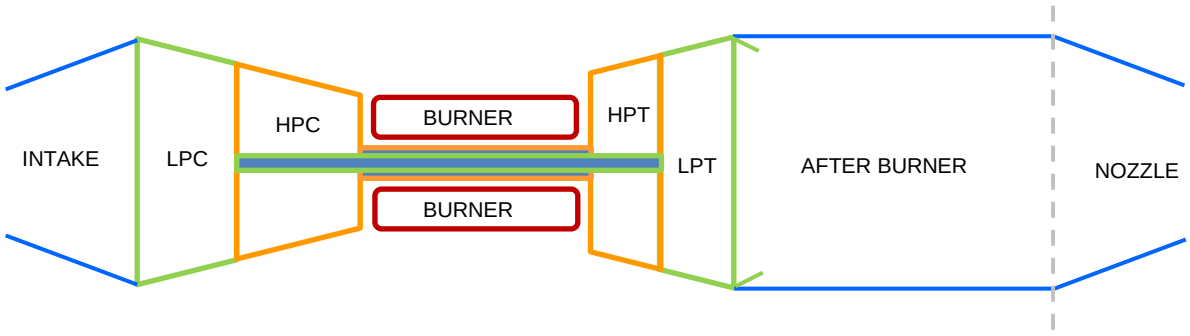

Figure 50: Schematic of the Tumansky-R-25-300 Turbojet Engine

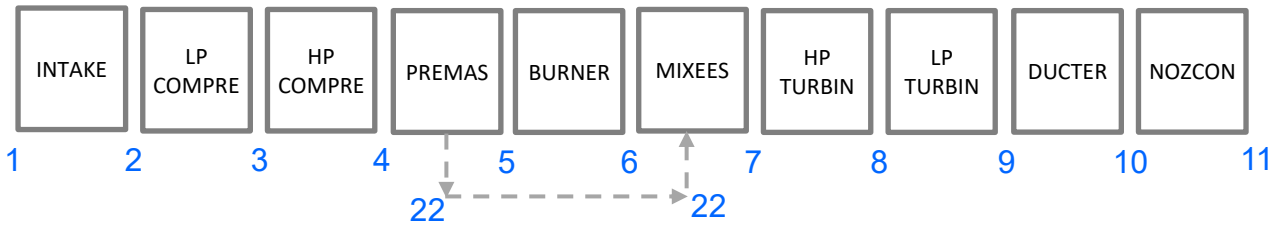

Figure 51: TURBOMATCH Schematic of Simulated turbojet engine model

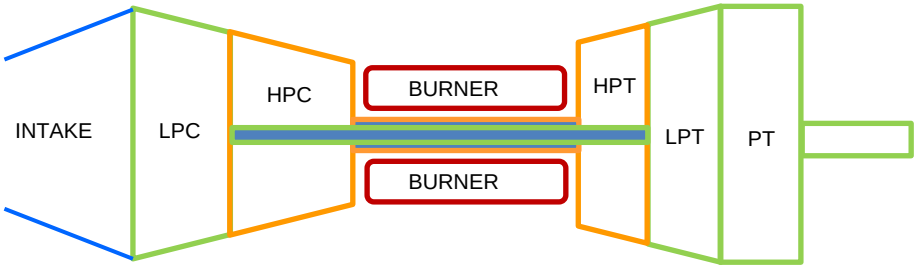

Figure 52: Schematic of Aero-derivative Engine model

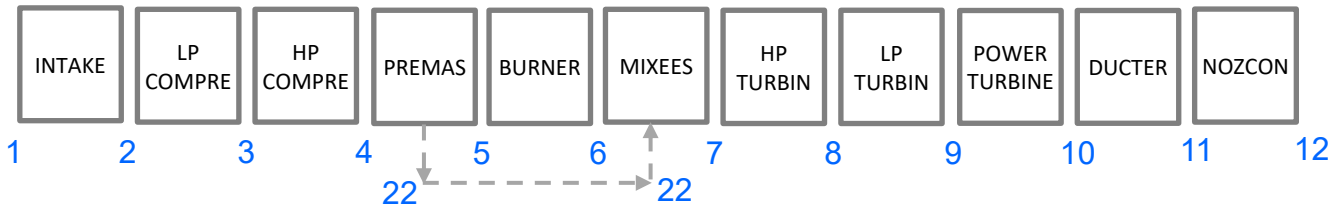

Figure 53: TURBOMATCH Schematic of Simulated Aero-derivative Engine

5.2.1 Feasibility Study - Approach

The feasibility study was conducted from a technical (thermodynamic) performance perspective. The scope of the study was to determine the feasibility of converting an engine similar to the Tumansky-R25-300 turbojet engine to an aero-derivative engine for civil power generation application. This is to serve as a prerequisite for subsequent performance,

environmental and economic analysis, on the converted engine, aimed at providing viable information for decision making on an organizational and executive level. The feasibility study conducted is based on the development and modification of performance simulation models and not actual engine prototypes. Performance models are adapted to simulate the considered engines and scenarios due to certain restrictions and limitations inhibiting the development of physical prototypes.

5.2.1.1 Turbojet engine model development and matching

The first step in the study involved developing a turbo jet engine model similar to the Tumansky-R25-300 in TURBOMATCH. Data for the development of the engine model was obtained from Janes's Aero-engines (Gunston, 2001) and is shown in Table 1. The next step was to match the engine model's design point to that of the Tumansky-R25-300 at ISA condition. To achieve this, the component efficiencies for the compressor and turbine were estimated using the equation for maximum specific work.

For maximum specific work

$$PR = \left(\eta_c \times \eta_t \frac{T_4}{T_1}\right)^{\frac{\gamma}{2(\gamma-1)}}$$

Equation 110 : Maximum Specific Work

Since the overall pressure ratio (PR) for the engine is given as 9.55 (Table 1), the component efficiencies at maximum specific work can be evaluated. This calculation was iteratively conducted using spreadsheet for different values of component efficiencies (ranging from 0-1) and pressure ratios (ranging from 0-35). A curve of pressure ratio against component performance was created (Figure 54) from which component efficiencies were obtained. The component efficiencies at the point of maximum specific work, where pressure ratio (PR) coincided with that obtained from literature was chosen. This gave values of 88.7% compressor efficiency and 90% turbine efficiency.

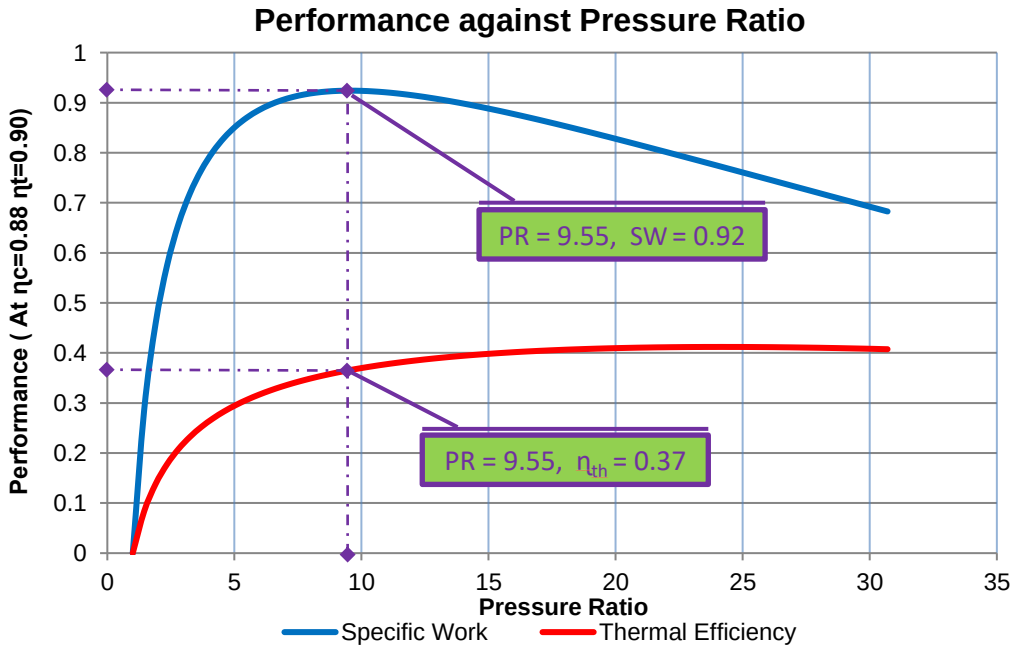

Figure 54: Plot of Performance against pressure ratio

After obtaining component efficiencies, the turbojet engine model's take off Mach number was estimated using Equation 111. This was to ensure that matching of the engine performance model with the real turbojet engine was as close as possible.

$$M = \frac{V}{a}$$

Equation 111: Mach number, M (Walsh & Fletcher, 2004)

Where

$V_{T/O} = 370km/h\ \ (102.78m/s\ )$; Take off speed (leatherneck, 2014)

$a = 340.29m/s\ (speed\ of\ sound)$

$Thus,$

$$M = 0.30$$

The engine simulation was matched in TURBOMATCH by varying the following parameters.

- Cooling bypass (0.90)
- Combustor pressure loss (0.05)
- Duct pressure loss between turbine and nozzle (0.2363)

The Mach number was not varied because it was obtained via calculation as shown above. Table 2 compares the model simulation results with those obtained from literature in Table 1.

Table 2: Comparison between Simulated and Actual turbojet engine performance results at ISA

PARAMETER	DATA FROM LITERATURE	TURBOJET ENGINE MODEL SIMULATION	% DIFFERENCE
Max dry Thrust (N)	40260.00	40259.54	0.0011%
SFC_{dry}(mg/Ns)	27.20	30.6633	-12.73%

The percentage difference between the simulated engine model results and those obtained from literature are reasonably small. This suggests that the engine model simulation closely matches the real turbojet engine operation at ISA conditions. The larger percentage difference in SFC is reflective of differences in the calorific value of Kerosene fuel.

5.2.1.2 Aero-derivative engine model development

Certain modifications and assumptions were required to simulate the conversion of the turbojet engine model into an aero-derivative engine model. One major modification made to the performance model was the replacement of the turbojet exhaust nozzle and afterburner with a free power turbine (FPT) to extract energy from the hot exhaust gas and produce power, which can be used to drive an electric generator. This resulted in a configuration known as the dual spool split output shaft configuration (Giampaolo, 2003). A free power turbine (FPT) indicates that the power turbine is aerodynamically coupled as illustrated in Figure 55.

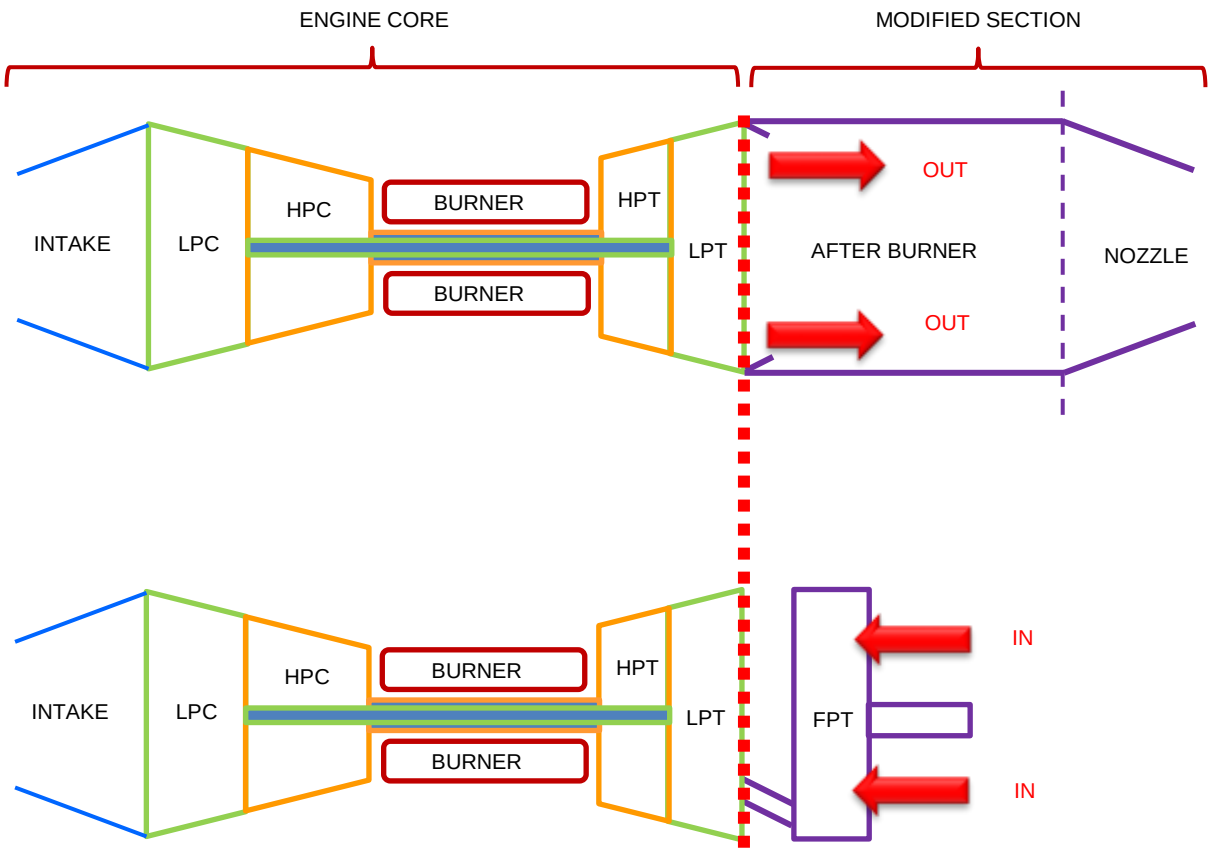

Figure 55: Schematic Illustration of Engine Model Modification

5.2.1.2.1 Benefits of free power turbine

Outlined below are some of the benefits of adopting a free power turbine for the turbojet modification.

- Flexibility

  A free power turbine enables easier, faster and cooler gas generator start-up. Thus, the gas turbine can obtain adequate self-sustaining speed before picking up the free power turbine load. This means less work is demanded by the system and less fuel is burnt. Additionally, this configuration permits the adoption of power turbines operating at the same or similar speeds to the electric generator. Thus with the gas generator component fixed, the power turbine can be varied to suit the required electric power generating cycle.

- Cost effectiveness

  This configuration eliminates the need for a complex and expensive gearbox system. Thus, significantly reducing potential capital and maintenance costs. The maintenance cost is reduced because no resource will be allocated for gearbox maintenance.

- Reliability

  The absence of a complex gearbox means system reliability and availability increases.

- Performance

  The flexibility of the free power turbine configuration means that the gas generator can be operator at optimum performance rating without influencing the output of the power turbine and electric generator. This capability improves the overall unit efficiency.

5.2.1.2.2 Potential drawbacks and counter measures

- Maintenance accessibility

The adopted configuration may present servicing difficulty as the assembly must be dismantled and reassembled via the exhaust duct.

- Performance

Pressure drop is experienced across the thermodynamic coupling between the gas generator and the free power turbine. This pressure loss can be minimized by good coupling design. There is also the constraint of power turbine output shaft length due to the high temperatures experienced by the free power turbine. This means bearing life and operation may be affected. High temperature bearings may be used to counter this with some penalties on cost throughout the operating life of the unit.

5.2.1.3 Aero-derivative engine model simulation

It was ensured that all performance parameters required for the simulation of the aero-derivative engine model were kept similar to that of the turbojet performance model. This was to ensure a consistent and valid performance simulation of an engine core similar to the Tumansky-R-25-300 engine.

The engine model simulation Mach number is zero (0) because the aero-derivative engine is stationary. Intake conditions are at ISA (Similar to the turbojet engine model). The parameters listed below were varied in TURBOMATCH to achieve convergence with the aero-derivative engine model.

- Duct total pressure-loss between Power turbine (PT) and Exhaust (0.01).
- Since the PT output power was unknown, the power turbine (PT) exit-pressure was inputted into the model as tending towards ambient (1.013 atm). TURBOMATCH automatically calculates the PT output power in this case.
- PT efficiency was set as 90% (Giampaolo, 2003).

5.2.1.4 Engine Fuel Type Selection

Investigation was conducted to identify the benefits and draw backs of implementing different types of fuel on the repurposed engine model. Performance simulation was conducted for engine model operation using kerosene, diesel or natural gas at ISA conditions. Figure 56 and Figure 57 summaries the effect of fuel type on the repurposed engine model (REM) performance.

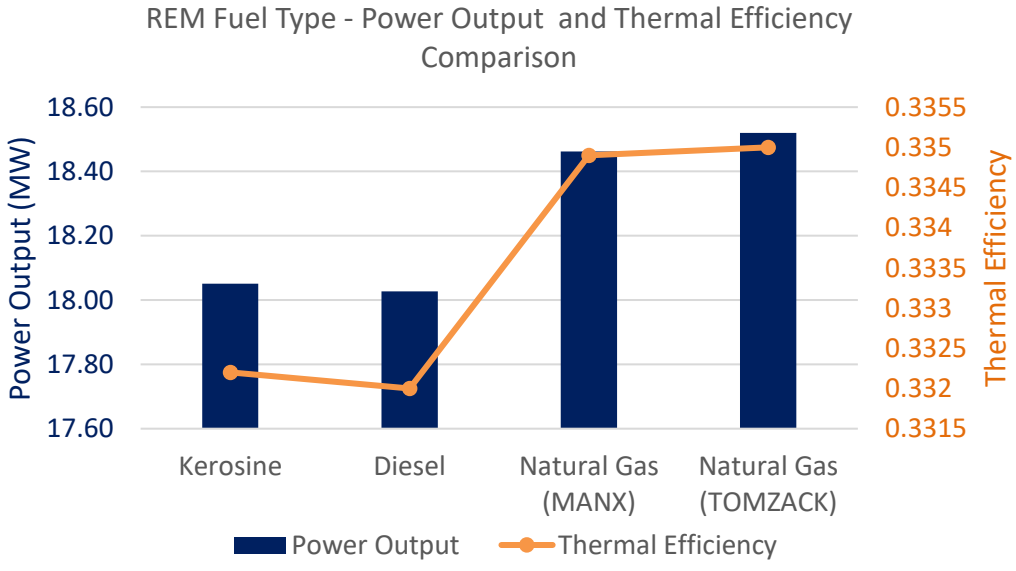

Figure 56: REM Fuel Type - Power Output and Thermal Efficiency Comparison

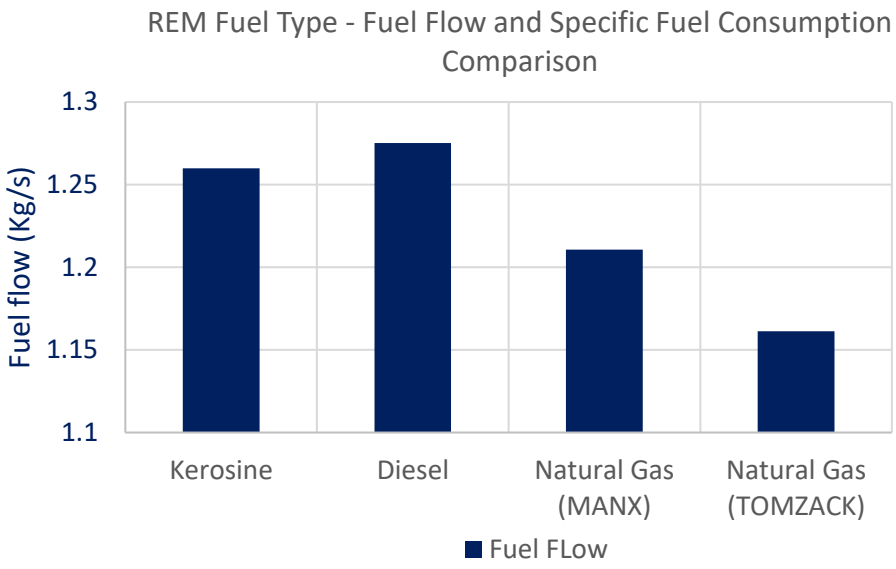

Figure 57: REM Fuel Type - Fuel Flow Comparison

Overall, the natural gas delivered the highest power output and thermal efficiency, in comparison to kerosene or diesel. In terms of fuel flow, natural gas has the lowest fuel flow at ISA conditions, in comparison to kerosene or diesel fired engine model. Two variants of natural gas (MANX and TOMZACK) were applied in the simulation. Of these fuel types, natural gas (TOMZACK) gave the most desirable performance. Being the cleanest burning fossil fuel, natural gas fired units generate lesser emissions in comparison to other fossil fuels.

Natural gas is abundantly available in Nigeria (the case study region). Nigeria has the largest natural gas reserve in Africa and the ninth largest in the world (Shell Nigeria, 2018). This suggests that natural gas can be readily supplied to meet any potential demand within the country. Subsequent economic analysis in this study is based on a natural gas fired engine model.

Table 3 and Table 4 show the performance results obtained from the Aero-derivative engine model simulation at design point (DP) using Kerosene and natural gas as fuel.

Table 3: Aeroderivative engine simulation results at ISA (Kerosene)

Parameter	Data	Unit
Shaft Power (MW)	18.05	(MW)
Fuel Flow	1.2598	(kg/s)
Thermal Efficiency, η_{th}	33.22	(%)
Exhaust Temperature	769.86	(K)
Mass Flow	68.50	(Kg/s)

Table 4: Aero-derivative engine simulation results at ISA (Natural Gas)

Parameter	Data	Unit
Shaft Power (MW)	18.52	(MW)
Fuel Flow	1.1612	(kg/s)
Thermal Efficiency, η_{th}	33.51	(%)
Exhaust Temperature	770.47	(K)
Mass Flow	68.50	(Kg/s)

5.3 Performance Simulation - Considered Scenarios

Performance simulation for the aero-derivative engine was conducted for two operating scenarios, ISA condition and tropical condition. The tropical simulation case was set at an altitude of 700m (average altitude above sea level in Nigeria). Relative humidity effects were investigated at design point for ISA and tropical conditions. Results are shown in Table 5 and Table 6. Further investigations have been conducted with respect to the cases outlined, for ISA and Tropical conditions. Results are presented in the Chapter 6.1.

Table 5: Aero-derivative Engine Simulation Results @ 0% Relative Humidity (Kerosene)

SIMULATION INPUT PARAMETERS				
OPERATING CONDITION	MASS FLOW (kg/s)	TET (K)	RELATIVE HUMIDITY (%)	ALTITUDE (m)
DP @ ISA	68.50	1310.15	0	0
DP_TROPICAL	68.50	1310.15	0	700
SIMULATION OUTPUT				
PARAMETER	SHAFT POWER OUTPUT (MW)	SFC (mg/J)	THERMAL EFFICIENCY (%)	FUEL FLOW (Kg/s)
DP @ ISA	17.94	0.070	33.26	1.2508
DP_TROPICAL	17.11	0.074	31.37	1.2651
	% drop	**% rise**	**% drop**	**% rise**
	-4.9%	5.4%	-6.0%	1.1%

Table 6: Aero-derivative Engine Simulation Results @ 60% Relative Humidity (Kerosene)

SIMULATION INPUT PARAMETERS				
OPERATING CONDITION	MASS FLOW (kg/s)	TET (K)	RELATIVE HUMIDITY (%)	ALTITUDE (m)
DP @ ISA	68.5	1310.15	60	0
DP_TROPICAL	68.5	1310.15	60	700
SIMULATION OUTPUT				
PARAMETER	SHAFT POWER OUTPUT (MW)	SFC (mg/J)	THERMAL EFFICIENCY (%)	FUEL FLOW (Kg/s)
DP @ ISA	18.05	0.070	33.22	1.2598

DP_TROPICAL	17.20	0.074	31.34	1.2725
	% drop	% rise	% drop	% rise
	-4.9%	5.4%	-6.0%	1.0%

5.3.1 Aero-derivative engine baseline

A performance baseline for the aero-derivative engine has been set at ISA condition with a relative humidity of 60% and fuel type natural gas (TOMZACK). Table 7 contains the baseline model performance parameters. This baseline engine model has been used for additional performance analysis needed for subsequent techno-economic investigations. Detailed simulation results are presented in Chapter 6.1.

Table 7: Baseline Aero-derivative Engine Parameters (Natural Gas)

SIMULATION INPUT PARAMETERS				
OPERATING CONDITION	MASS FLOW (kg/s)	TET (K)	RELATIVE HUMIDITY (%)	ALTITUDE (m)
DP @ ISA	68.50	1310.15	60	0
SIMULATION OUTPUT				
PARAMETER	SHAFT POWER OUTPUT (MW)	SFC (mg/J)	THERMAL EFFICIENCY (%)	FUEL FLOW (Kg/s)
DP @ ISA	18.52	0.063	33.51	1.1612

5.3.1.1 Aero-derivative engine deterioration

Faults were implanted into the baseline aero-derivative engine model to simulate engine deterioration due to recoverable and non-recoverable losses. These losses are represented as deterioration in engine component performance. Outlined in Table 8 are the investigated deterioration cases and implanted faults.

Table 8: Investigated Deterioration Cases and implanted faults

S/N	Component	Parameter	Deterioration (%)
1	LP Compressor	Non-Dimensional Mass Flow (NDMF)	2.0
		Pressure Ratio (PR)	6.0
		Component Efficiency (η_c)	4.0
2	HP Compressor	Non-Dimensional Mass Flow (NDMF)	2.0
		Pressure Ratio (PR)	6.0
		Component Efficiency (η_c)	4.0
3	LP Turbine	Non-Dimensional Mass Flow (NDMF)	2.0
		Enthalpy Drop (DH/T)	1.5
		Component Efficiency (η_t)	2.5
4	HP Turbine	Non-Dimensional Mass Flow	2.0
		Enthalpy Drop (DH/T)	1.5
		Component Efficiency (η_t)	2.5
5	Burner	Component Efficiency (η_c)	4.0

There is great difficulty associated with adequately quantifying deterioration. This is due to variables such as operating environment, maintenance policy, engine function, engine type,

mode of operation e. t. c. (Brooks, 2006) Therefore, certain assumptions are required for the investigated conditions to be valid.

5.3.1.1.1 Engine deterioration Assumptions 1st Case

- Engine component deterioration is linear and constant.
- Deterioration effects in HPC and LPC are similar.
- Deterioration effects in HPT and LPT are similar.
- Engine degradation is measured every 4,800 hours of operation.
- Implanted component degradation is maximum at 24,000 hours.
- No measure for rectifying recoverable or non-recoverable loss has been implemented.
- Degraded components are not been replaced.

Further deterioration analysis has been conducted to investigate engine deterioration over 24,000 hours of operation, with and without engine washing. For this investigation to be valid, modifications have been made to the assumptions above.

5.3.1.1.2 Engine deterioration Assumptions 2nd Case

- Engine component deterioration is linear and constant.
- Deterioration effects in HPC and LPC are similar.
- Deterioration effects in HPT and LPT are similar.
- Degraded components have not been replaced.
- Engine deterioration level is measured every 4800 hours of operation.
- For the washed case, engine washing occurs when PR, η_c and NDMF fall below 1.5%, 0.8% and 0.4% and this occurs every 4800 hours of operation.
- Deterioration in engine performance is quantified by a drop in component efficiency.
- When engine is washed, all engine component parameters return to design point performance except component efficiency. This accounts for the fact that engine washing does not give 100% restoration in performance.

The simulation of a partial restoration in engine performance is to accounts for the fact that engine washing does not give a 100% restoration of engine performance. It only delays the need for component replacement and prolongs engine component life.

5.3.1.2 Aero-derivative engine transient simulation

The transient simulation analysis was conducted using TURBOMATCH. Table 9 outlines the data input required for the transient simulation.

Table 9 : Required Transient Performance Input Data

Component	Requirement	Source
Compressor 1	• Effective component volume ECV (m^3)	• Calculated
Compressor 2	• Effective component volume ECV (m^3)	• Calculated
Turbine 1	• Effective component volume ECV (m^3) • Rotor rotational speed in rps	• Calculated • Literature • Calculated

	• Rotor moment of inertia (kg.M^2)	
Turbine 2	• Effective component volume ECV (m^3) • Rotor rotational speed in rps • Rotor moment of inertia (kg.M^2)	• Calculated • Literature • Calculated
Turbine 3	• Effective component volume ECV (m^3) • Rotor rotational speed in rps • Rotor moment of inertia (kg.M^2)	• Calculated • Literature • Calculated

The rotational speed for each component was obtained from literature (Gunston, 2001) and is presented in Table 10. Calculations used to obtain the moment of inertia (*I*) and the effective component volumes are presented below.

5.3.1.3 Moment of inertia calculation

The moment of inertia *I* is given by

$$I = \frac{\tau}{\alpha}$$

Equation 112: Moment of inertia (hyperphysics, 2016)

Where

$I = Moment\ of\ Inertia$

$\alpha = Angular\ acceleration\ in\ rads/s^2$

$\tau = Torque\ (Nm)$

Torque τ is given by

$$\tau = \frac{P}{2\pi(n/60)}$$

Equation 113: Torque Calculation (hyperphysics, 2016)

Where

$P = Power\ (Watts\ or\ Nm/s)$

$n = rotational\ speed\ (rpm)$

It is known that angular velocity ω is given by

$$\omega = \omega_0 + \alpha t$$

Equation 114: Angular Velocity (hyperphysics, 2016)

Where

$\omega = angular\ velocity\ in\ rads/s$

$\omega_0 = Initial\ angular\ velocity\ in\ rads/s$

Assuming a constant angular acceleration, it is assumed that the angle of rotation is zero at t=0. Therefore at time = 0, initial angular velocity ω_0 = 0.

Thus, when ω_0 = 0,

$$\omega = \alpha t$$

Equation 115: Angular Velocity when ω_0 = 0

Rearranging the equation

$$\alpha = \frac{\omega}{t}$$

Equation 116: Angular acceleration in rad/s

Substituting the values of torque and angular acceleration into Equation 112 and Equation 113 gives the movement of inertia *I*. Equation 112 is used to evaluate the moment of inertia of each component based on the power generated on the HP shaft, LP shaft and the power turbine respectively. Table 10 presents the power generated on each shaft.

Table 10: Power generated on each shaft

Component	Power (Watts)	rpm	rps
HPT to HPC	22443000	11150	185.83
LPT to LPC	10035000	11150	185.83
Power Turbine	16754000	3000	50

Moment of inertia is calculated for each shaft using Equation 112 and Equation 113. The results are presented in Table 11.

Table 11: Evaluated Torque and Moment of Inertia

Component	Torque (Nm)	Moment of Inertia (kgm^2)
HP Shaft	19221.10	16.50
LP Shaft	8594.40	7.40
Power Turbine	53329.60	45.70

5.3.1.4 Effective component volume (ECV) evaluation

The effective component volume (ECV) is evaluated from the engine dimension obtained from literature (Gunston, 2001). Table 12 presents the evaluated ECV for each component.

Table 12: Effective component volumes

	LPC	HPC	BURNER	HPT	LPT
ECV (m)	0.355	0.160	0.716	0.120	0.136

The evaluated transient simulation parameters are imputed into TURBOMATCH and a fuel schedule is prepared. TURBOMATCH can perform transient simulation using a fuel increment with time schedule or a fuel schedule calculated from referred fuel flow and referred rotational speed approach. Using a fuel increment with time schedule limits the available control of the transient simulation over the combustor outlet temperature (COT). However, a referred fuel flow vs rotational speed approach employs the TURBOMATCH algorithm, which enables the maximum COT to be controlled.

A fuel schedule table calculated from referred fuel flow and referred rotational speed was prepared and used to feed the fuel flow into the engine simulation from start up to maximum power. APPENDIX A contains a sample of the fuel scheduled used. Equation 117 and Equation 118 where used to calculate the referred fuel flow and referred rotational speed.

$$Ref.Rotational\ Speed = \frac{N_{shaft}}{\sqrt{\frac{T_tHPCin}{T_{ISA\ SLS}}}}$$

Equation 117: Referred Fuel Flow (Cranfield Department Of Power and Propulsion, 1999)

$$Ref.Fuel\ Flow = \frac{W_{ff}}{\frac{P_tBURNERin}{P_{ISA\ SLS}}\sqrt{\frac{T_tBURNERin}{T_{ISA\ SLS}}}}$$

Equation 118: Referred Fuel Flow (Cranfield Department Of Power and Propulsion, 1999)

Where

$N_{shaft} = PCN.N_{DP}(rps)$
$P_{ISA\ SLS} = 101325Pa$
$T_{ISA\ SLS} = 288.15K$

Fuel schedules were prepared for both engine acceleration (from start up to maximum power) and engine deceleration (from maximum power to engine cut off) this was to simulate the transient operating cycle of the engine.

The transient simulation is run from an initial performance simulation time of 0 seconds through 60 seconds. The acceleration fuel schedule (called FS1) was initiated from 0 to 30secs with a maximum permissible COT of 1350K. The deceleration fuel schedule (FS2) was initiated from 30 to 60 seconds with a limiting COT of 750K. Results of the simulation are presented in Chapter 6.1.6.

5.4 Price Estimation

Performance simulation output of engine power, engine rpm and engine heat rate are supplied as input into the cost-estimating model. Estimates of acquisition costs are performed using two parametric cost-estimating techniques as described in this section.

5.4.1 Acquisition cost estimation using regression analysis (RA)

The compiled performance dataset (described in Chapter 4.2.1.2.1) is normalized and associated engine parameters are evaluated for correlation by means of scatter plots. Figure 58Figure 60 show the scatter plots of power output, engine rpm and heat rate (independent variables) against acquisition cost (the dependent variable). The Pearson's Correlation formula (Equation 35) is used to identify and quantify the correlation between the considered variables.

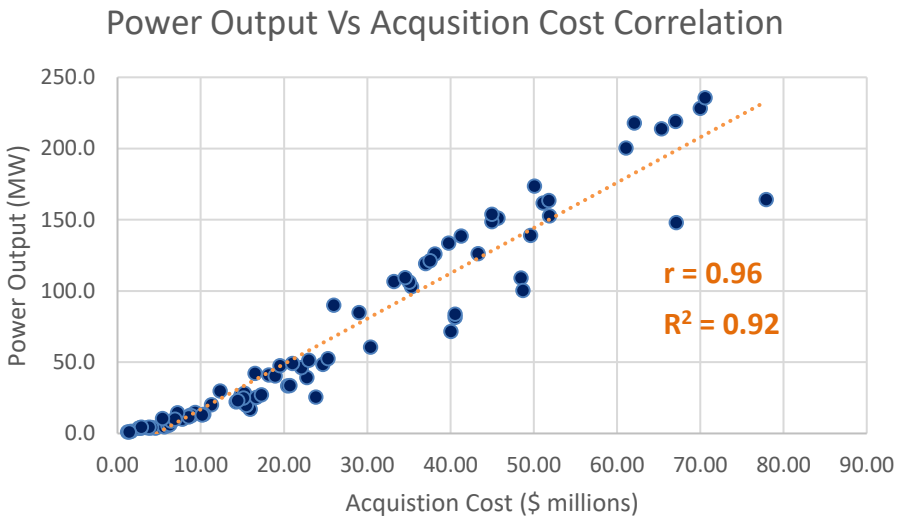

Figure 58: Scatter Plot of Power Output Vs Acquisition Cost

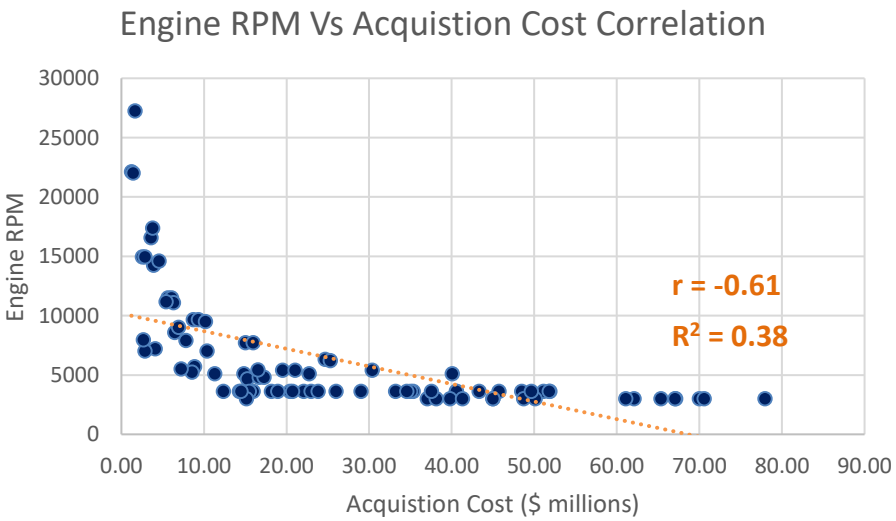

Figure 59: Scatter Plot of Engine RPM Vs Acquisition Cost

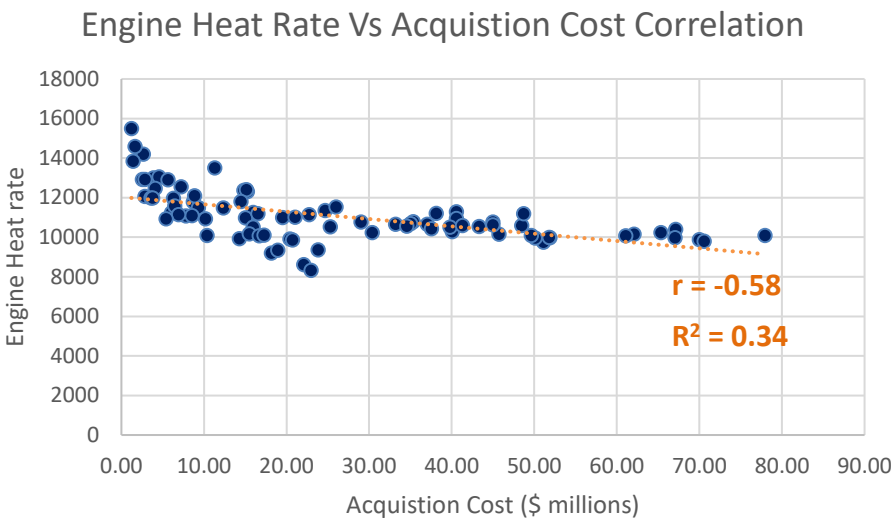

Figure 60: Scatter Plot of Engine Heat rate Vs Acquisition Cost

Evaluation of the dataset for each variable reveals the following:

- Power output has a strong positive correlation with acquisition cost (r=0.96). This means a strong relationship exists between power output and acquisition costs. The high R^2 value of 0.92 indicates that more variance is accounted for in estimates and thus more accurate predictions of gas turbine acquisition costs are possible with accurate knowledge of gas turbine power output. Furthermore, a positive correlation suggests that an increase in gas turbine rated power output can influence an increase in gas turbine acquisition cost.
- RPM has a weak negative correlation with acquisition cost(r=-0.61). This means a weak relationship exists between engine rpm and acquisition costs. The very low R^2 value of 0.38 indicates lesser accuracy in the prediction of gas turbine acquisition cost from the knowledge of engine rpm. A negative correlation suggests that engines with lower values of rated rpm are likely to have higher acquisition costs.
- Heat rate has a weak negative correlation with acquisition cost(r=-0.58). This means a weak relationship exists between engine Heat rate and acquisition costs. The very low R^2 value of 0.34 implies lesser accuracy in the prediction of gas turbine acquisition cost from knowledge of engine heat rate. A negative correlation suggests that engines with lower values of heat rate are likely to have higher acquisition costs.

Figure 61 - Figure 63 show scatter plots evaluating the coefficient of correlation and determination between the dataset of the independent variables.

Figure 61 and Figure 62 reveal that power output has a weak negative correlation with engine rpm and heat rate. This means a weak relationship exists between them. The low values of R^2 suggest that any predictions made, based solely on the identified relationships, may not be accurate.

Figure 63 shows a moderately strong positive relationship between rpm and heat rate. This suggests that there is some relationship between rpm and heat rate with the potential to make moderately accurate predictions. It also suggests that engines with higher rpm may have higher heat rates.

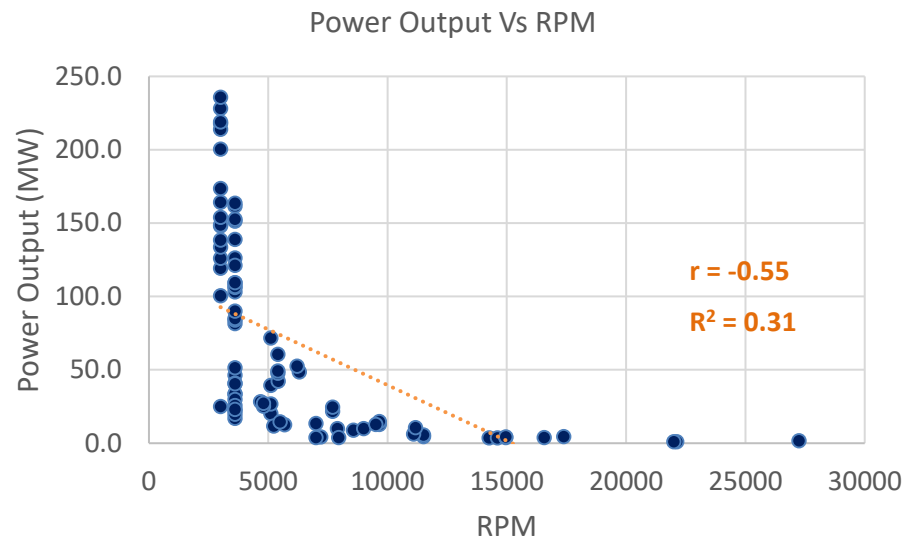

Figure 61: Scatter Plot of Power Output against RPM

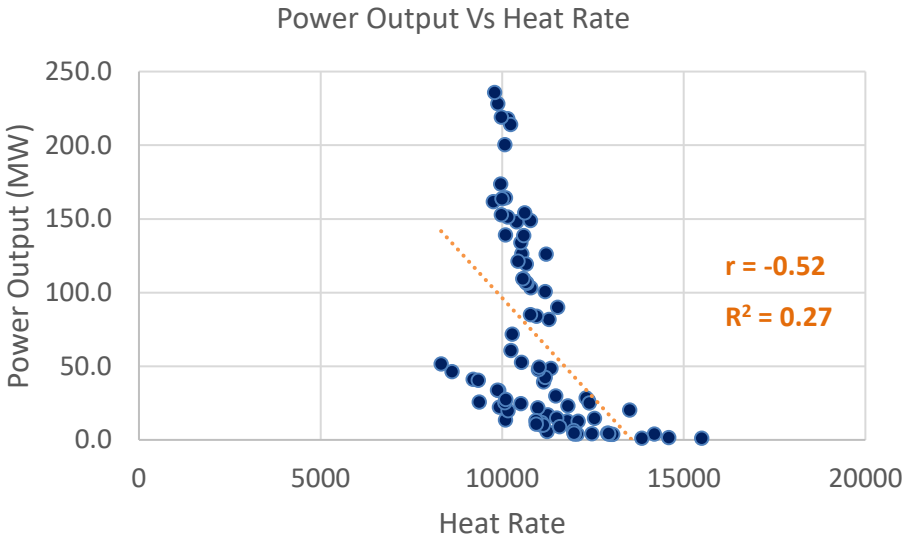

Figure 62: Scatter Plot of Power Output against Heat Rate

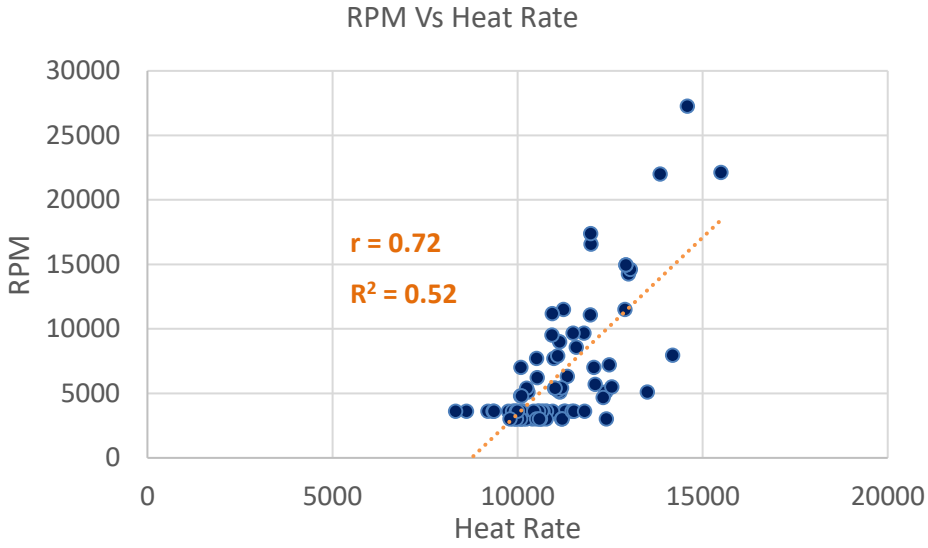

Figure 63: Scatter Plot of RPM against Heat Rate

The evaluation of the compiled dataset identified a very strong relationship between engine power output and acquisition cost and a weak relationship between other variables. Furthermore, due to the very low values of the coefficient of determination, R^2 (presented in Figure 58 - Figure 63) the application of engine rpm and heat rate dataset in the development of a regression model for estimating acquisition cost was discouraged. Therefore, only power output dataset is utilized for the regression analysis in this study.

5.4.1.1 Regression model

Upon evaluating and establishing correlation, a linear estimating relationship (Equation 119) is developed based on Equation 36 and Equation 37. The estimating relationship is used to evaluate a regression line. Figure 64 presents the regression.

$$\hat{Y}_{AQC\ estimate} = \hat{b}_0 + \hat{b}_1 X_{Power}$$

Equation 119: Developed Linear Estimating Relationship

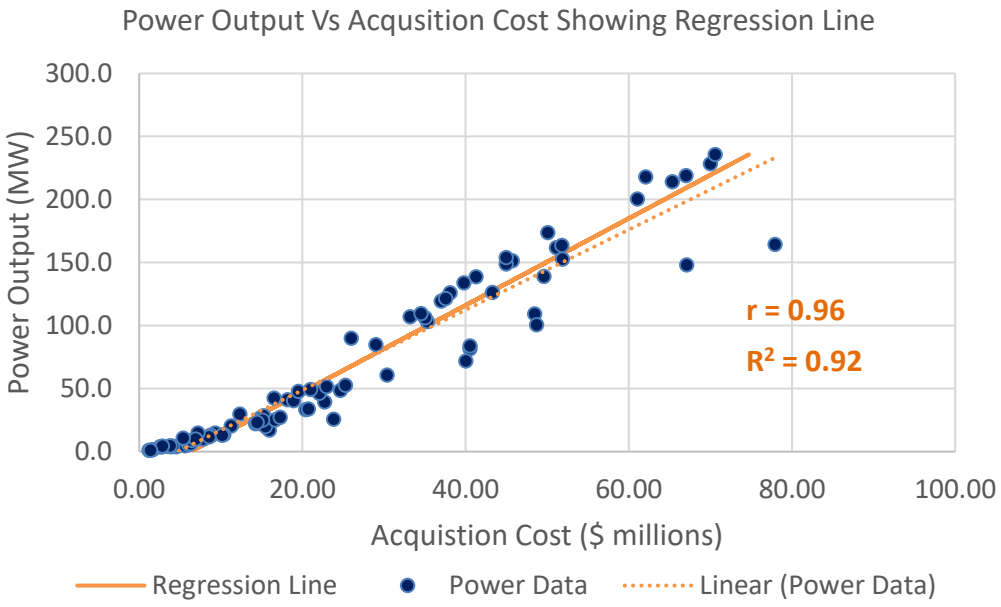

Figure 64: Scatter Plot of Power Output Vs Acquisition Cost Showing Regression Line

Analysis of the plot in Figure 64 reveals an increasing spread in data samples from left to right. It also reveals that the data samples are not normally distributed, equally, around the regression line. Even though a strong positive correlation has been identified in the dataset between power output and acquisition cost, the offset in the regression line suggests that residuals may not be normally distributed as previously assumed (in Section 4.2.1.2.2.2). This could mean that the applied regression model is not appropriate for the analysis. Therefore, in order to validate the developed regression model, graphical residual analysis is performed to identify if the previous assumption (*residuals are independently and normally distributed, random variables, with a mean of zero and constant variance*) is valid. The residuals are evaluated using Equation 120 and a plot of residuals against power output is analysed.

$$E = Y_{AQC} - \hat{Y}_{AQC\ estimate}$$

Equation 120: Residual Calculation

Where *E* is the residual; the error between each data samples and regression estimate.

Observation of the plot in Figure 65 shows that the residuals are not normally distributed. Therefore, the implemented linear regression model is discarded and a simple non-linear regression model applied.

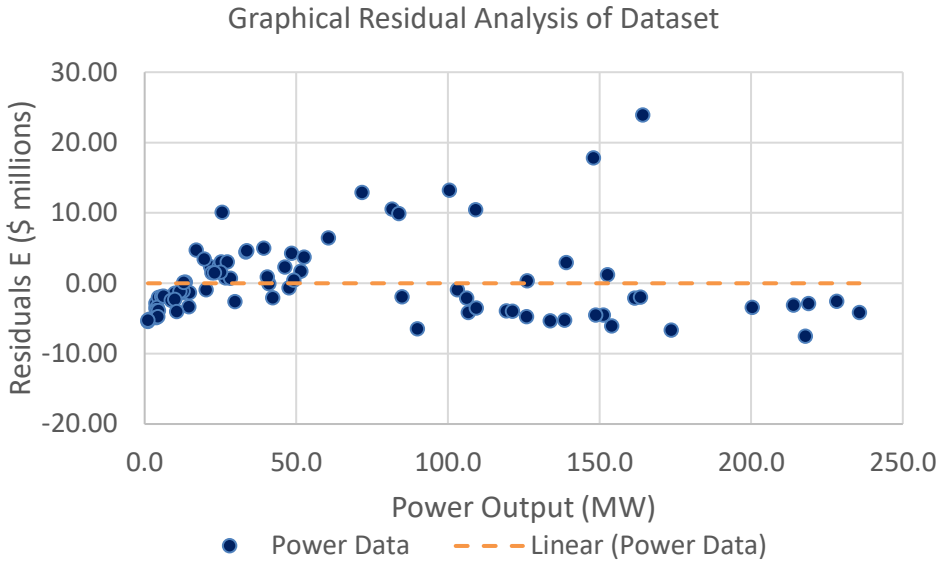

Figure 65: Graphical Residual Analysis with respect to Power output

A simple non-linear regression model (described in section 4.2.1.2.2.4) is implemented. Since the dataset has been identified as not having a linear functional form, the dataset set is transformed (expressed in linear form) by taking the natural log of the dependent and independent variables. This yields a nonlinear regression model of the form described in Equation 121. The transformed dataset is used to evaluate a new regression line. Figure 66 shows the non-linear regression line superimposed over the transformed dataset.

$$ln\,\hat{Y}_{estimate} = ln\,\hat{A} + \hat{B}\,ln\,X_{Power}$$

Equation 121: Implemented nonlinear regression model

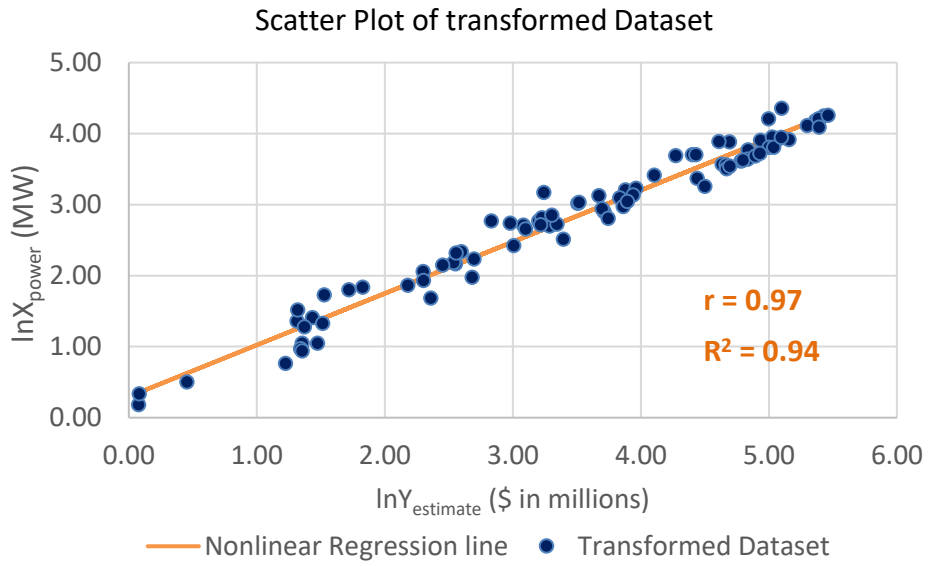

Figure 66: Scatter Plot of Transformed Dataset

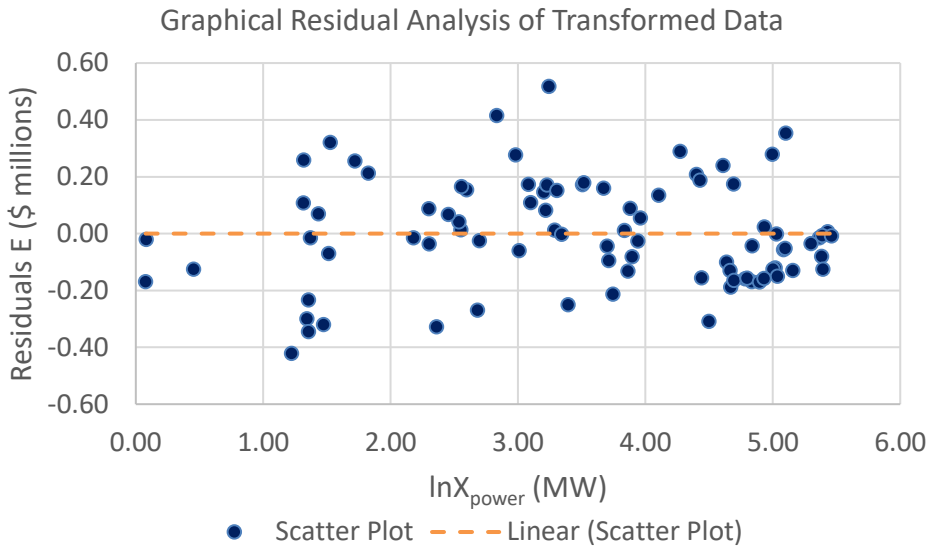

Figure 67: Graphical Residual Analysis of Transformed Dataset

Already, a much more evenly distributed dataset is observed from the scatter plot and graphical residual analysis, of the transformed data, shown in Figure 66 and Figure 67. For the evaluation of actual values in unit space, the nonlinear regression model expressed in unit space form is used to evaluate the dependent variable (acquisition cost) from Equation 122.

$$\hat{Y}_{estimate} = \hat{A}X_{power}{}^{\hat{B}}$$

Equation 122: Implemented nonlinear regression model in unit space

Where $\hat{A}$ and $\hat{B}$ are evaluated using Equation 50Equation 52.

5.4.1.2 Statistics and significance Tests

In order to validate the implemented non-linear regression model, several statistical tests, as described in section 4.2.1.2.2.3, are computed. Graphical residual analysis is performed to identify if the assumption of normality and independence of residuals is valid. This assumption has been validated in Figure 67 by an even distribution of residuals about a mean zero line.

5.4.1.2.1 The coefficient of determination, R^2

The coefficient of determination, R^2 is calculated from Equation 41 to measure the accuracy of the evaluated regression line fit to the transformed sample data points. An R^2 of 0.94 (94 percent) was obtained. This means that the implemented nonlinear regression model adequately explains 94 percent of deviations leaving only 6 percent to chance.

5.4.1.2.2 The coefficient of Correlation, r

The coefficient of Correlation, r is evaluated using Equation 42. Evaluation of r gives information on the type and direction of the relationship between the dependent and independent variable. The coefficient of determination was evaluated as 0.97 this implies a very strong positive correlation between the transformed dependent and transformed independent variables. Identification of correlation between the variables supports the application of a regression model for estimation of acquisition cost.

5.4.1.2.3 Standard error of estimate, SE

Evaluation of the standard error of estimate, SE, gives an absolute measure of the deviation of sample points from the nonlinear regression line (i.e. a measure of unexplained error). SE

was evaluated using Equation 43 and gave a value of $5.1 million. The standard error of estimate on its own cannot be used to evaluate a regression line but can only be used for comparison between regression lines (NASA, 2015).

5.4.1.2.4 Coefficient of variation, CV

The calculated standard error of estimate, SE, is used to compute a coefficient of variation, CV, from Equation 44. The coefficient of variation is a relative standard error computed in order to validate a regression line based on a desired limit, less than or equal to 20 percent (NASA, 2015). The CV has been evaluated as 0.196 (19.6 percent). This suggests that the adopted nonlinear regression model is valid since its CV falls below 20 percent.

5.4.1.2.5 Hypothesis Test

Hypothesis test was conducted to identify if the coefficient of the independent variable (slope) is significantly different from zero. The test was conducted using the approach described in section 4.2.1.2.2.3.6. A significance level of 0.05 is adopted for the test. Outcomes from the test (Table 13) reveal that the slope coefficient is statistically significant. This means that a knowledge of the independent variable (Power output) is significant in estimating the dependent variable (acquisition cost). Therefore, the developed nonlinear regression relationship is significant and thus retained.

Table 13: Hypothesis/t-test results

α	t_p	t_c	Hypothesis status	Description
0.05	1.99	36.78	Rejected	Slope Coefficient is Statistically Significant (H1:b1 !=0)

5.4.1.3 Prediction Interval

With the nonlinear regression model validated and accepted, a prediction interval (PI), within which estimates may fall, is computed with respect to the evaluated regression line. Equation 53 is applied to evaluate the prediction interval. Figure 68 shows the upper and lower prediction intervals for the considered data set.

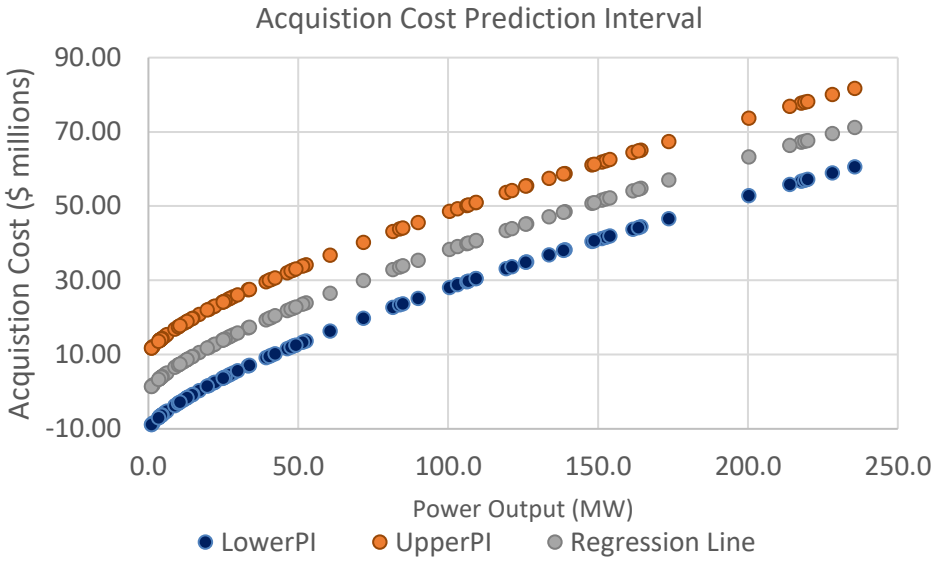

Figure 68: Acquisition Cost Prediction Interval

5.4.1.4 Regression Model Estimate Validation

The developed price-estimating regression model has been applied to predict the price of known gas turbine engines based on performance input of engine power output. Comparison is made the between regression model estimates and actual engine acquisition costs obtained from literature. Results are presented in Chapter 6.

5.4.1.5 Engine model Acquisition cost estimation using regression model

The power output of the repurposed engine model is supplied as input from the performance simulation model to the regression model and an estimate of the engine's acquisition cost is evaluated. Regression estimates for the REM are presented in Chapter 6.

5.4.2 Acquisition cost estimation using Artificial Neural Network (ANN)

Similar to the approach adopted for regression analysis in section 5.4.1, the compiled performance dataset is normalized and associated engine performance parameters are evaluated for correlation by means of the Pearson correlation formula and scatter plots.

5.4.2.1 Neural Network Model

Upon establishing, some form of correlation between the variables of the compiled dataset, the developed artificial neural network (described in section 4.2.1.1), is trained and tested. Although not all correlations identified between the variables are strong, all parameters in the dataset are applied to train and test the artificial neural network. This is because artificial neural networks have a proven reputation of being excellent methods for identifying association and regularities within patterns (section 1.3.2). They have proven to be effective in identifying relationships between variables that are difficult, complex or too ambiguous to describe. Hence, since some level of correlation has been identified between all variables considered, the entire dataset has been applied for the neural network analysis in order to enhance estimating accuracy.

5.4.2.1.1 Network training

Network training involves supplying the independent variables of power output, engine rpm and heat rate into the neural network for an initial estimate of (known) associated values of the dependent variable (acquisition cost) using the method described in section 4.2.1.1.2. The difference between the network estimates of acquisition cost and values from the dataset is

evaluated as the error in the estimate. The smaller the error, the more accurate the estimate. The computed error is used to adjust subsequent network estimations through a process known as back propagation until the error becomes as small as possible or non-existent at all. When the computed error is satisfactorily minimized, the network is identified as trained.

5.4.2.1.2 Network Testing

A portion of the compiled dataset has been separately trained and identified as the testing dataset. The testing data is usually about 30 percent of the overall dataset. The process of network testing involves comparing the error cost (evaluated from Equation 34) between the training and testing dataset to check for overfitting. Overfitting is the term used to characterize a neural network the does not adequately account for uncertainties in estimates. This comparison is done by plotting the evaluated error costs as shown in Figure 69: Comparison of training and testing error cost (overfitting observed). For an over-fitted network, separation can be observed between the plotted error costs (Figure 69). After introducing, a regularization term to capture the effects of overfitting, lesser separation is observed between the plotted error costs. Figure 70 shows the regularized neural network. Details of the adopted methodology for network testing are presented in section 4.2.1.1.2.5.

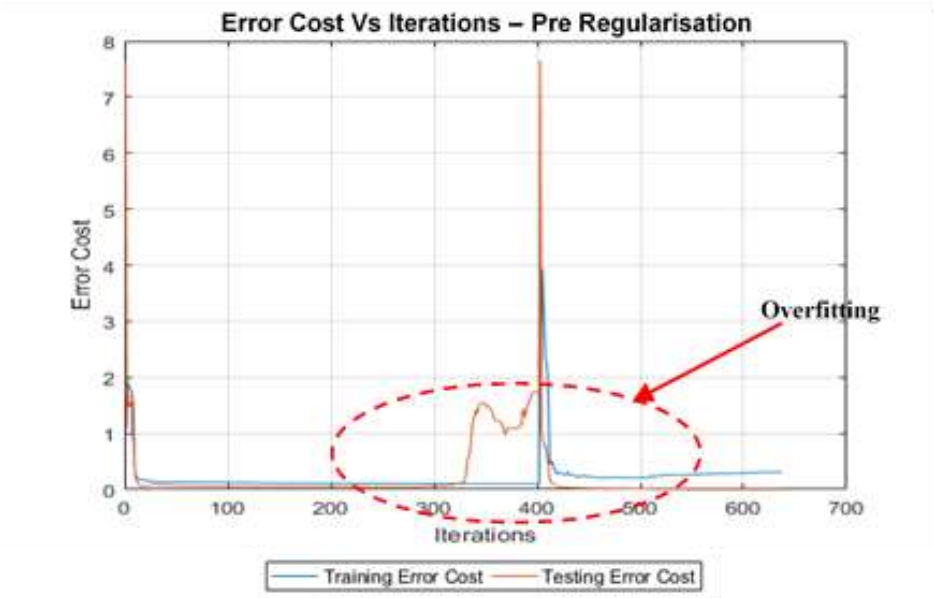

Figure 69: Comparison of training and testing error cost (overfitting observed)

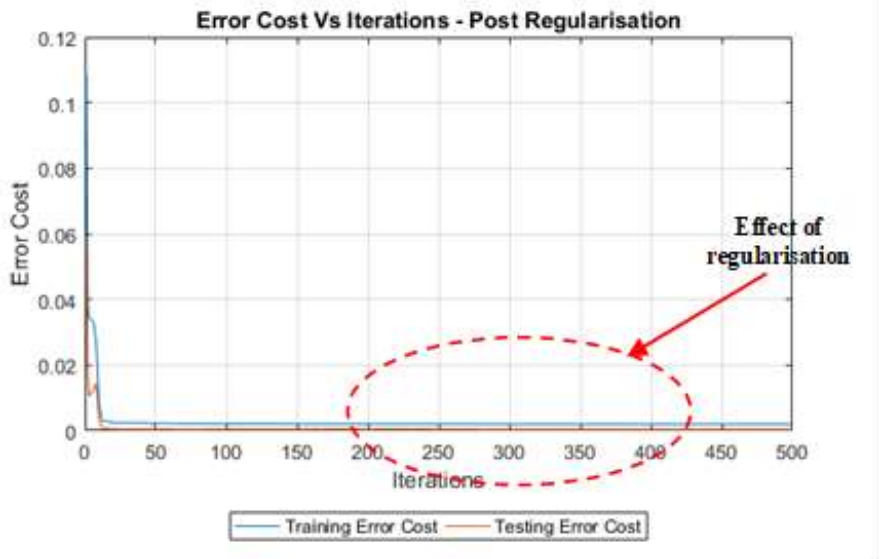

Figure 70: Comparison of training and testing error cost (overfitting minimized)

5.4.2.1.3 ANN model estimate validation

The developed artificial neural network (ANN) model has been applied to predict the price of known gas turbine engines based on performance input of engine power output, PT rpm and heat rate. Comparison is made the between ANN model estimates and actual engine acquisition costs obtained from literature. Results are presented in Chapter 6.

5.4.2.2 Engine model acquisition cost estimation using artificial neural network

The power output, power turbine rpm and heat rate of the repurposed engine model are supplied as input from the performance simulation model to the artificial neural network and an estimate of the engine's acquisition cost is evaluated. The ANN estimate for the repurposed engine model is presented in Chapter 6.

5.4.3 Adopted Price estimating model

Comparison made between acquisition cost estimates from the developed artificial neural network (ANN) model with those from the regression analysis (RA) model reveal that the ANN model made better predictions than the regression model estimates. As a result, the ANN price estimating methodology has been adopted for subsequent implementation in the techno-economic analysis model. Comparison results are presented in Chapter 6.

5.5 Economic Analysis

Economic analysis is conducted on the engine performance model of a repurposed gas turbine engine to be used for electrical power generation. It is assumed that the engine model has been repurposed, for electrical power generation, from a turbojet engine similar to the TUMANSKY R-25-300 engine. The analysis is necessary to determine the economic feasibility of the repurposed engine model for power generation and also to compare its profitability against other competitor engines.

The required engine performance and operating parameters have been retrieved for each engine unit (as contained in Table 14) and supplied as input into the cost component of the economic model. Performance parameters for the repurposed engine model (REM), have been retrieved as input from the performance simulation analysis described in section 5.2.1.2

Table 14: Engine Operating Parameters

Engine	Power Output (MW)	rpm	Heat rate (kJ/kWh)	Fuel Flow (kg/s)	Fuel Density (kg/m^3)	Emissions Index (ppm)
REM	18.52	11150	9749	1.1612	0.712	25
GG4/FT4	17.00	3000	12397	1.1034	804.0	15
LM2500	22.20	3600	9922	1.5925	0.712	25
LM1600	13.00	7000	10086	1.5925	0.712	15

To ensure the relevance of the investigation to the scenario considered, the following assumptions have been made.

5.5.1 Operating Assumptions

All units are operating in similar environments and under similar conditions.

- Unit productive life is 5years.
- All main engine components are completely replaced after 24,000 hours of operation.

- Each engine unit operates for 6000 hours each year at 80% capacity.
- All engines except the GG4/FT4 burn natural gas and are fitted with a DLN combustor.
- The GG4/FT4 burns fuel oil and uses water/steam injection for emissions control.
- Unit facility remains operational for 15 years.
- In combined cycle application, all units power identical steam turbines.
- The percentage increase in power output for all units are the same in combined cycle application.

5.5.2 Economic Assumptions

The economic parameters as contained in Table 2 are consistent for all units.

Parameter	Values
MARR	2.50%
Percentage Spare costs in Acquisition cost	30.0%
Depreciation rate $\{Salvage\ value = TCC \times (1 - Depreciation\ rate)\}$	35.0%
Insurance Premium, $i_{premium}$	5.00%
Interest rate, i_{rate}	0.00%
Inflation rate *(2016-2017 inflation rates)*	0.23%
Emissions tax rate, E_{rate} ($/ton)	$0.00
Marginal Income Tax rate, $X_{(t,x)}$	38.0%

5.5.2.1 Additional assumptions

- A major overhaul cost of 174$/kW (w.r.t. REM power output) is incurred, on each unit, every 24,000 hours of operation.
- DLN emissions control systems incurs an owning cost of 19.2$/kW w.r.t. REM output.
- Water/steam injection systems incurs an owning cost of 37$/kW w.r.t. REM output.
- The repurposed engine model (REM) incurs a onetime refurbishment cost of 145$/kW and delivers an annual savings of 22.3$/kW w.r.t. REM power output.
- In combined cycle application, the installed capital cost of the steam turbine is 400$/kW with an operation and maintenance cost of 0.1$c/kWh (The World Alliance for Decentralized Energy, 2006).
- Since the REM has already been purchased and will only undergo refurbishment during repurposing, interest on loan repayment (i_{rate}) will be zero percent.

5.5.3 Analysis Approach

Unit acquisition costs have been estimated using artificial neural network as described in section 5.4.2.1. For each unit, the total productive life cost (TPLC), total capital cost (TCC) and the total operation and maintenance cost (TOM) are estimated using Equation 71-Equation73 as described in section 4.2.5. Similarly, the levelized cost of energy (LCOE) is estimated for each unit as described in Equation 97. The cost analysis is performed for engine units operating in both simple and combined cycle applications.

Output from the cost model is applied in the selection model to compute the total annual cost (TA cost) and benefits (TA benefit) for each unit. Evaluation of the total benefits less cost (TBLC) gives the net cash flow before tax as described in Equation 105.

Present worth analysis is conducted, using the net cash flows, to evaluate respective unit NPVs. For each unit, the before tax and after tax evaluations are considered. The results of the present worth analysis are presented in Chapter 6.

The evaluated NPVs are applied, as described in Equation 16 - Equation 18, to determine the rate-of-return criteria for each engine unit. Output from the present worth and rate-of-return evaluations are analysed to determine the economic feasibility of each unit. Further ranking is performed to identify the engine unit and system cycle, which delivers the highest economic profitability.

Sensitivity analysis is conducted on favoured investment options to determine vulnerability to uncertainty in fuel price and emissions tax rate. Results have been generated and are presented in Chapter 6.

Further investigation is conducted into the effect of various environmental and operating conditions on the techno-economics of the considered repurposed engine model. Some of these investigations include:

- Effect of engine degradation on unit operating cost.
- Effect of power cycling on engine techno-economic performance.
- Effect of Emissions control Technology on operation and maintenance cost.

The analysis and results for these considerations are presented in Chapter 6.1.

5.6 Optimization Analysis

After completing a baseline techno-economic analysis on the repurposed engine model (REM), further techno-economic analysis is conducted on an optimized variant of the REM, The following sections describe the optimization approach implemented on the REM.

The goal is to optimize the performance and economics of the repurposed engine model (REM). In order to deliver this goal, an overall objective, involving the minimization of cost and emissions while maintaining profitability is identified. To achieve the overall objective, certain performance and economic optimization sub-objectives must be met. These objectives are outlined below.

Sub Objective 1: Performance Optimization Objectives

- Minimize fuel consumption and emissions generated without loss of power output.

Deliverables:

- Minimized operation and maintenance cost
- Reduced Emissions generated
- Consistent/Increased Power output
- Minimized LCOE

Sub Objective 2: Economic Optimization Objectives

- Minimize LCOE at Maximum Total annual Benefits and Minimum engine operating hours.

Deliverables:

- Reduced Levelized cost of energy
- Maximized Total Annual Benefits

Optimization analysis was conducted using the methodology described in section 4.2.8.4. The first step in the multi-objective optimization analysis involved performance optimization, which is conducted from two perspectives; modifications to the basic thermodynamic cycle of the REM and implementation of an optimization algorithm to minimize a variable.

5.6.1 Modifications to basic thermodynamic cycle.

The adopted modification to the thermodynamic cycle of the REM was the implementation of an intercooler between the low-pressure and high-pressure compressor. Figure 71 and Figure 72 illustrate the schematic of the modified engine model.

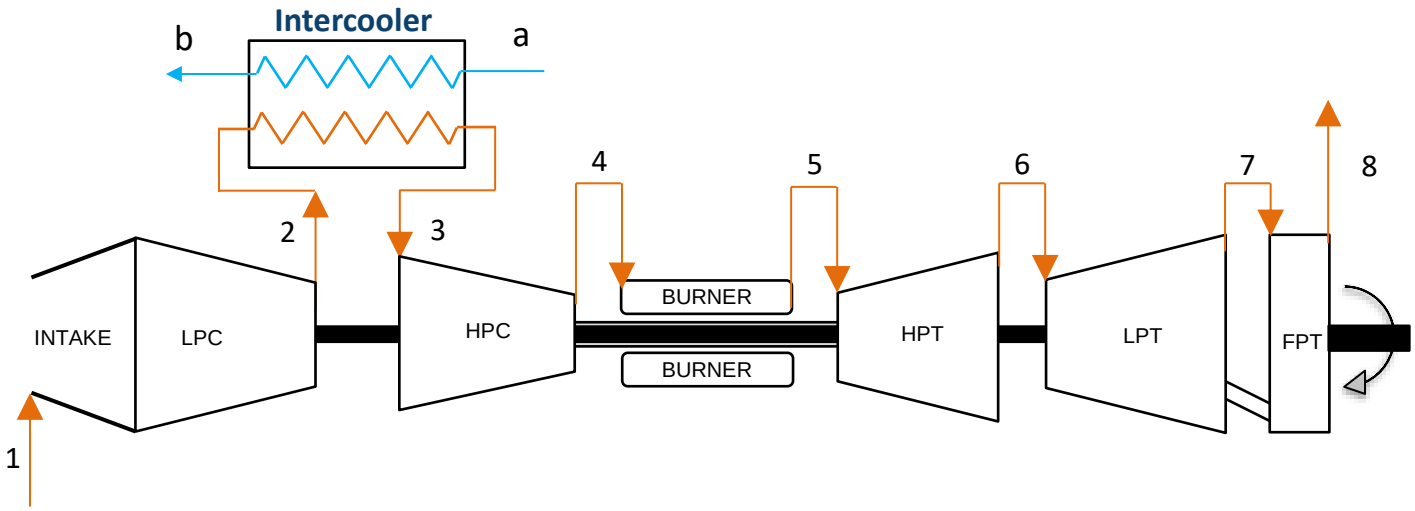

Figure 71: Modified Engine Model Schematic

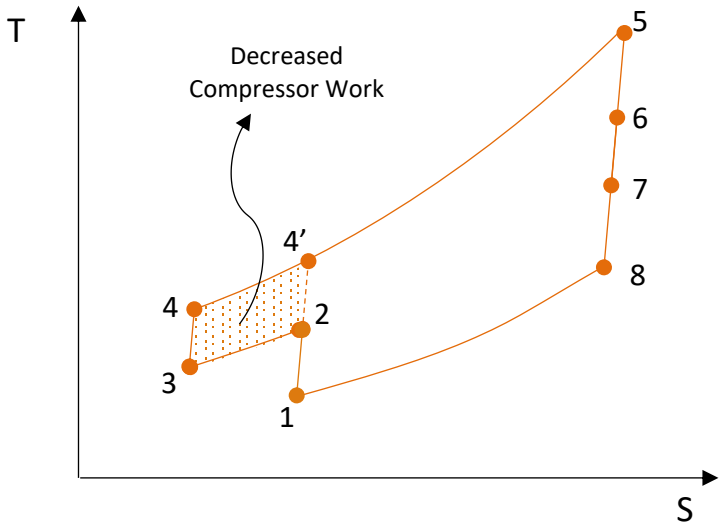

Figure 72: Modified Engine Model T-S Diagram

The modification was modelled in TURBOMATCH with performance simulation variables assigned as intercooling effectiveness, rotational speed and fuel flow. Other parameters include fuel type (defined as natural gas - TOMZACK) and emissions control technology (DLN combustor). Simulation was conducted for different values of intercooling effectiveness ranging from 0.65 -1. Outcome of the investigation is presented in Chapter 6.

5.6.2 Performance optimization using optimization solver

Upon achieving a satisfactory performance solution from the performance modification, further performance optimization was performed using an interior-point optimization algorithm to minimize fuel flow. Output from the satisfactory performance simulation of the modified engine model were provided as input into the optimization solver.

The objective function implemented in the solver is an expression of the equation for useful work and is described by Equation 123 and Equation 124.

$$MinUSFWK = TW - CW$$

Equation 123: Equation for minimum useful work

Where $MinUSFWK$ is minimum useful work, TW is the Turbine Work and CW is Compressor Work.

Objective Function @(ff) :

$$MinUSFWK - ((((ff + (MaxWair)).*(cphot.*MaxTET.*(1 - (MaxEGT/MaxTET)))) - cw))$$

Equation 124: Implemented Objective Function

The implemented constraints are described by Equation 125 - Equation 128

Inequality Constraints - $\mathbf{c(x) \leq 0}$:

Constraint 1 - EGT

$$c(1) = (((ff * (Vegt)) + ExitArea) - MaxEGT)$$

Equation 125: Exit Gas Temperature Constraint

Constraint 2 - TET

$$c(2) = (((MinUSFWK + (wair * cpcold * (Ttwo - Tamb))) + ((ff + wair) * cphot * egt))/((ff + wair) * cphot)) - MaxTET$$

Equation 126: Turbine Entry Temperature Constraint

Constraint 3 – W_{gas}

$$c(3) = (ff + MaxWair) - DPwgas$$

Equation 127: Gas Mass flow Constraint

Equality Constraints - $\mathbf{ceq(x) = 0}$:

Constraint 1 - USFWK

$$ceq(1) = (((ff + MaxWair) * (cphot * TETval * (1 - (egt/TETval)))) - cw) - MinUSFWK$$

Equation 128: Useful Work Constraint

Boundaries - $lb \leq x \leq ub$:

$$x = ub = ff\ at\ design\ point$$

$$x = lb < ff\ at\ design\ point$$

Equation 129: Performance Optimization Boundaries

Initial Point - x_0 :

$$x_0 = ff\ at\ design\ point$$

Equation 130: Initial Point of optimization

Outcome from performance optimization are presented in Chapter 6.4.

5.6.3 Economic optimization using optimization solver

Satisfactory optimization results from both performance optimization perspectives permit the advancement of the optimization analysis into economic optimization aspect. Output data from the performance optimization analysis were supplied as input into an economic optimization solver.

The objective function implemented in the solver is an adaptation of the equation for Total Annual Benefits (Equation 101) adopted in this study and is described by Equation 131.

Objective Function @(EOH) :

$$TA_{benefit} - ((EP_{gen} * EOH * LCOE_{baseline}) + AnnualBenefits + AnnualSavings - PL_{NW})$$

Equation 131: Implemented Economic Objective Function

The implemented constraint is described in Equation 125 - Equation 128

Equality Constraints - $\mathbf{ceq(x) = 0}$:

Constraint 1 – LCOE

$$ceq(1) = LCOE_{optim} - (TPLC/(EP_{gen} * EOH * EOPL))$$

Equation 132: Useful Work Constraint

Boundaries - $lb \leq x \leq ub$:

$$x = ub = 8760\ (maximum\ hours\ in\ a\ year)$$

Equation 133: Performance Optimization Boundaries

Initial Point - x_0 :

$$x_0 = EOH\ at\ design\ point$$

Equation 134: Initial Point of optimization

Outcomes from economic optimization are presented in Chapter 6.4.

5.6.4 Techno-Economic Cost Modelling Tool – ECM Tool

A techno-economic analysis tool, which integrates gas turbine performance modelling and simulation with economic analysis has been developed using Visual Studios C# and MATLAB. The tool employs the programing capabilities of the C# and MATLAB platform to develop a robust decision making tool capable of techno-economic modelling and optimization analysis. Figure 73 illustrates the ECM code structure.

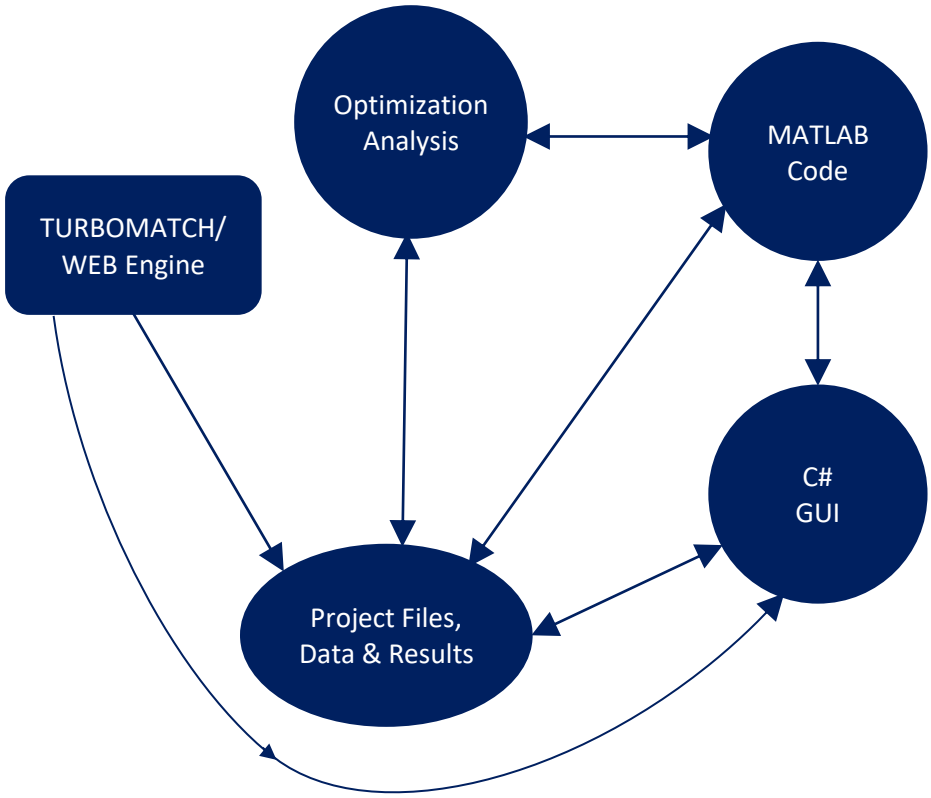

Figure 73: ECM Code Interaction/ Structure

MATLAB is used to develop and run various component of the techno-economic model described in Chapter 4. The C# platform is used to create a graphical user interface to make implementation of the ECM tool easier.

5.6.4.1 Application and Capability

The ECM tool is integrated with TURBOMATCH, a gas turbine performance simulation software developed at Cranfield University. This integration has widen the scope of potential application of the ECM tool for various investigation. Some of the potential benefits of integrating the tool with TURBOMATCH, have been exploited in this study to conduct investigations into the effects of power cycling on engine economics, influence of operating conditions on engine techno-economics, effect of implemented emission technology on operation and maintenance cost, effect of Gas turbine degradation on productive life cost e. t. c. The scope of potential application of this tool for gas turbine studies varies from preliminary design investigations and feasibility studies to project selection from alternatives, capital budgeting problems, scenario investigations, technology comparisons, power cycling analysis, emissions analysis, cost analysis, sensitivity analysis among other things.

One of the features of the developed tool is the ability to, simultaneously, conduct techno-economic analysis and optimization for multiple engines (both similar and dissimilar). This

enables a flexible and coordinated evaluation of multiple considerations in an investigation while minimizing complexity.

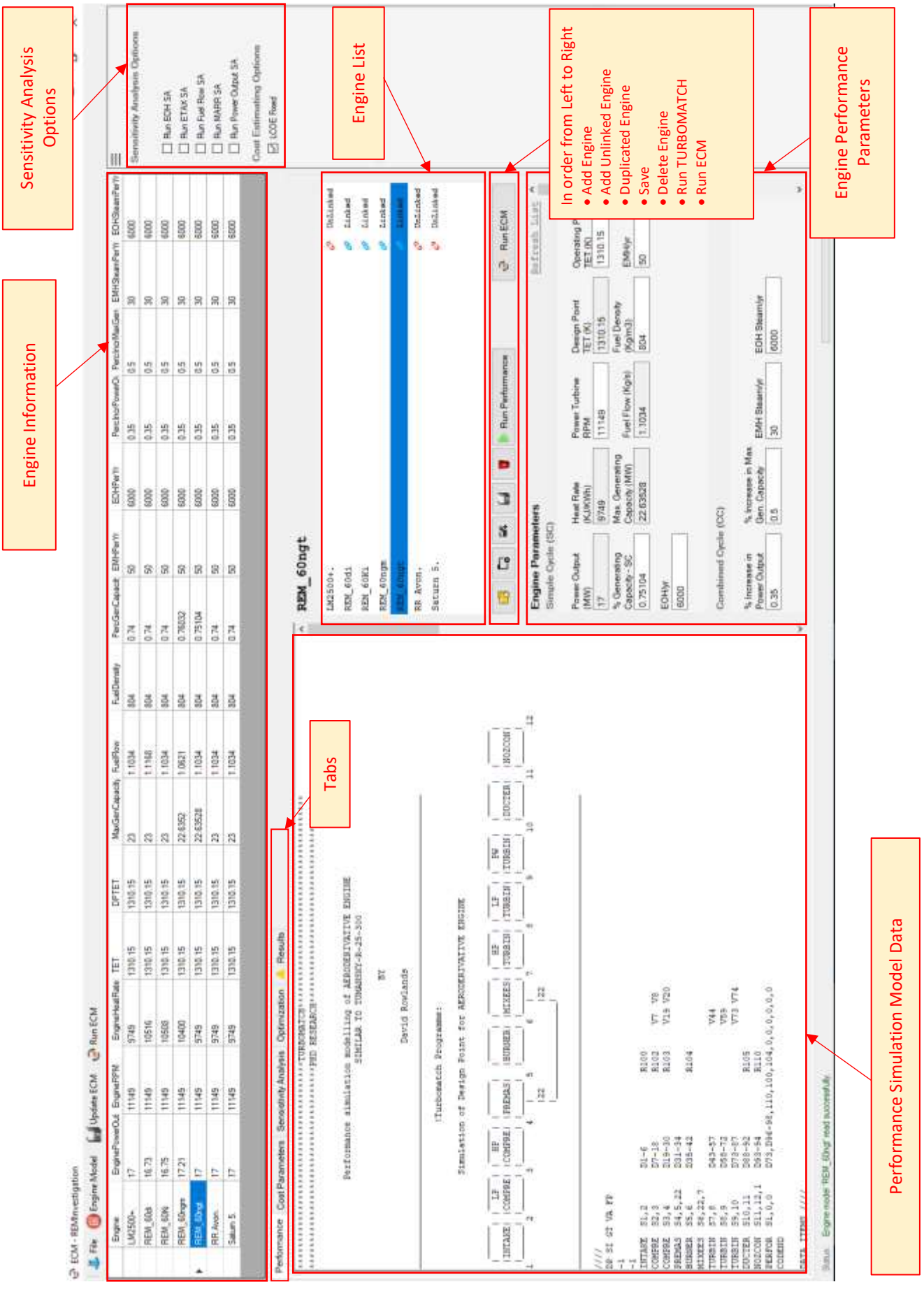

Figure 74: ECM General Layout (performance tab)

5.6.4.2 General Layout

The general layout for the ECM tool is presented in Figure 74. It consist of five tabs. These include:

- **The performance tab:** Retrieves and displays engine model performance-data, information and parameters.
- **Cost Parameters Tab:** Retrieves and displays all cost and economic modelling information and parameters including Capital cost parameters, standing charge parameters, Running cost parameters, operation and maintenance parameters and any additional cash flow information. Appendix C presents an image of the cost parameters tab.
- **Sensitivity Analysis Tab:** Retrieves information relating to boundaries associated with sensitivity analysis to be conducted post baseline investigation.
- **Optimization Tab:** Optimization Tab retrieves and displays optimization analysis information such as constraint and optimization variable information, optimization boundary conditions, initial optimization point, e. t. c. Appendix C presents an image of the optimization tab.
- **Results Tab:** Displays baseline analysis results as well as sensitivity analysis plots and charts for easy and quick evaluations of investigated scenarios.

The ECM tool stores all analysis results in spreadsheet formats and provides capability for post processing some of the results into plots and chart which are displayed in the results tab of the user interface. Future versions of the ECM tool may include integration with TURBOMATCH Web engine, which is currently under development. Additional Illustrations of the ECM Tool are presented in Appendix C.

6 RESULTS AND DISCUSSION

6.1 Performance Simulation Results

Presented in this section are results from the performance feasibility study and deterioration analysis conducted on the repurposed engine model (REM). Performance simulation was undertaking in the following areas:

6.1.1 Design Point Engine Performance at ISA and Tropical Condition

6.1.1.1 Performance map –LPC

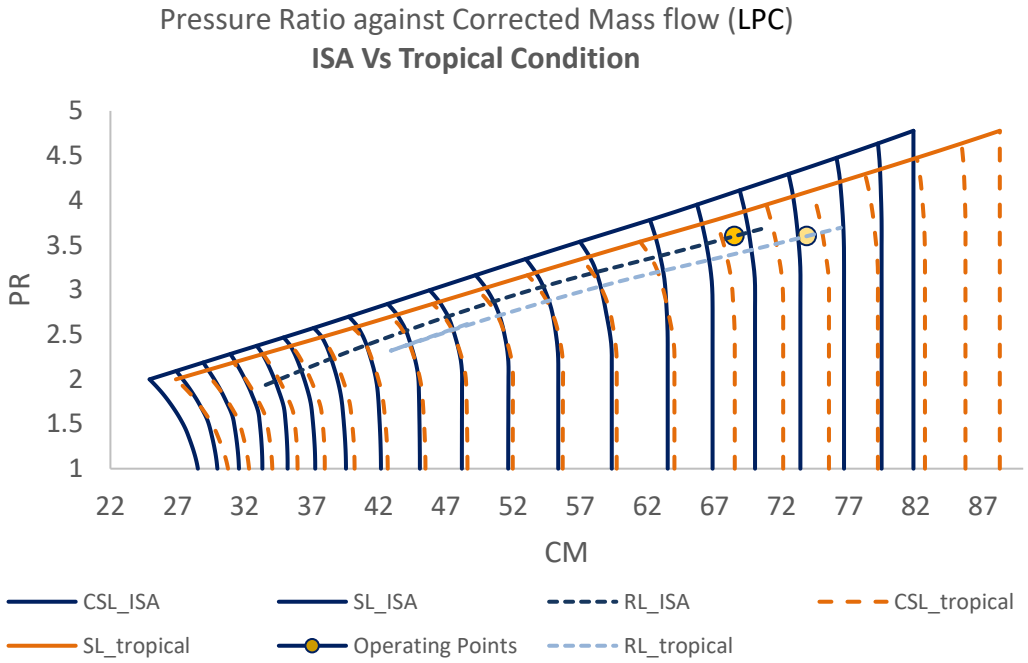

Figure 75: Design Point Performance Map Low pressure compressor - LPC

6.1.1.2 Performance map –HPC

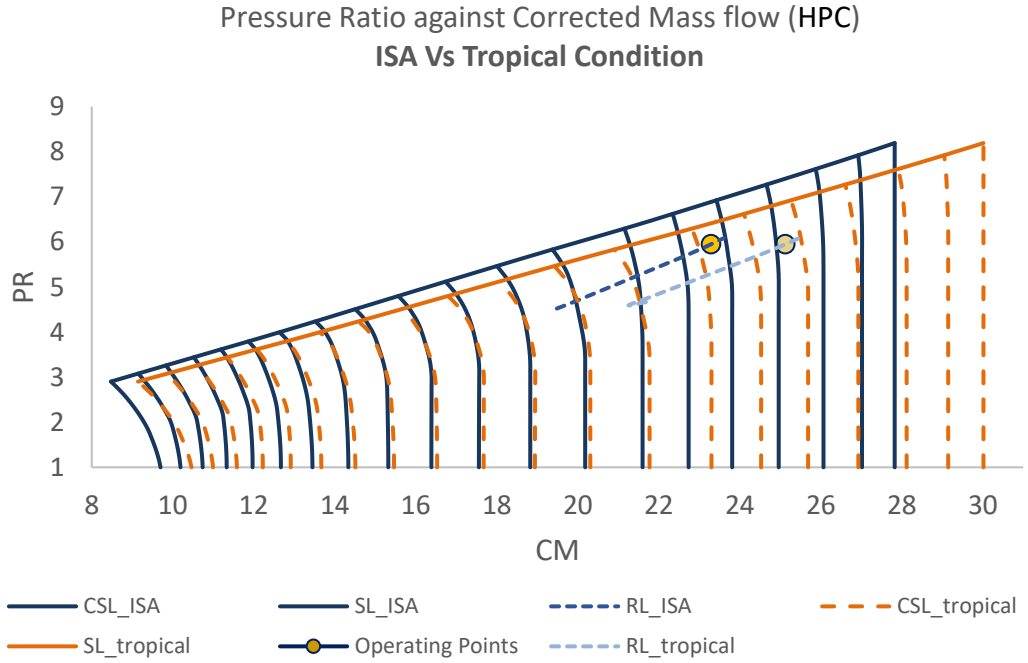

Figure 76: Design Point Performance Map High pressure compressor - HPC

The performance map provides information about the characteristics of the engine model at the investigated conditions. Figure 75 and Figure 76, reveal that the minimum LPC and HPC operating range at ISA condition is about 62% and 90% of PCN (rotational speed) respectively.

In tropical conditions, the operating range is shortened by 10.1% for the LPC and increases by 2.2% for the HPC. Furthermore, the maps reveal that due to the drop in total ambient temperature and pressure at 700m altitude (case study tropical altitude) there is a 7.9% increase in mass flow. This is indicated by the slight shift, to the right, in the performance Map for the tropical simulation case.

6.1.2 Varied Ambient Temperature Assessment

Investigation into the REM performance under varying ambient temperatures in both ISA and tropical conditions gave the following results:

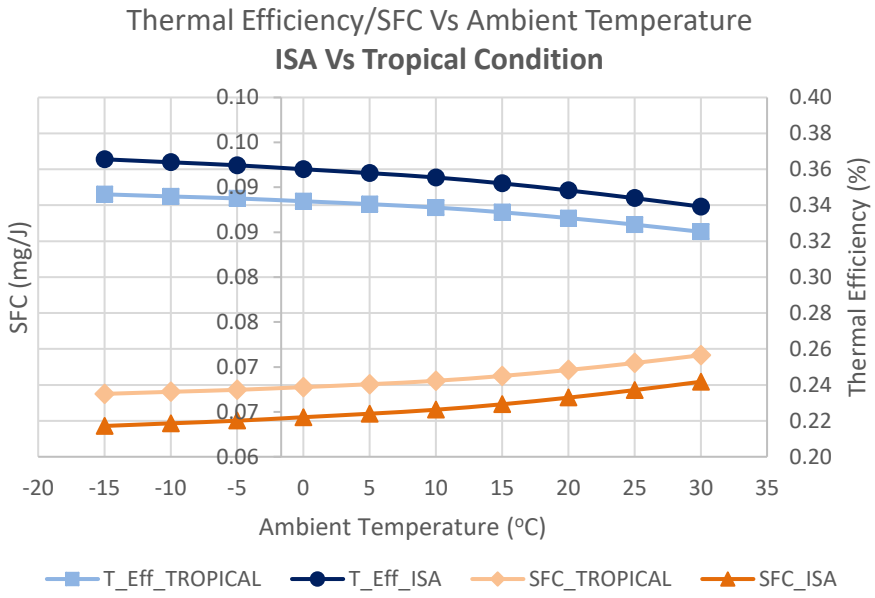

Figure 77: Varied Ambient Temperature Assessment TE and SFC Vs Ambient Temperature at constant TET

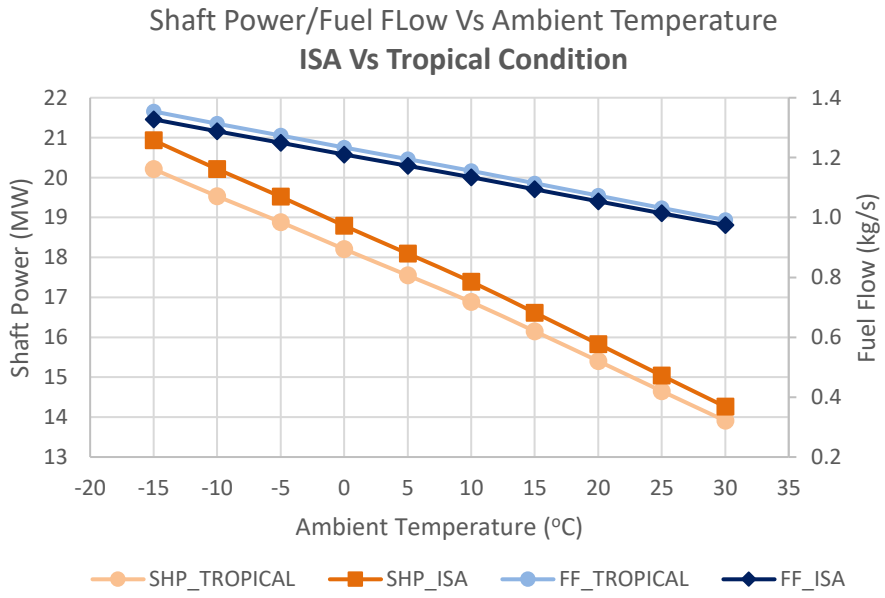

Figure 78: Varied Ambient Temperature Assessment SHP and FF Vs Ambient Temperature at Constant TET

In Figure 77 and Figure 78, SFC increases with increasing ambient temperature while Thermal efficiency (TE), shaft power (SHP) and fuel flow (FF) decreases with increasing ambient temperature. This result is consistent with typical expectations since the performance simulation is conducted at constant Turbine entry temperature (TET). Table 15 shows the comparison between ISA and Tropical performance simulation results at varied ambient

temperature and fixed TET. It is evident that there is an overall increase in SFC and FF for the tropical condition while SHP and TE decrease.

Table 15: Showing Comparison of performance between ISA and Tropical Conditions for varied ambient Temperature

	SFC (mg/J)	FF (Kg/s)	SHP (MW)	TE
ISA Average	0.065	1.1519	18	0.35
Tropical Average	0.069	1.1736	17	0.34
% difference	5.0	1.9	3.0	4.8
	% Increase	% Increase	% decrease	% decrease

Investigation into REM performance on cold, standard and hot days revealed a notable drop in REM performance output when the engine operates in tropical conditions versus operation at ISA condition. This observation is presented in Figure 77 and Figure 78. However, at fixed power setting, the penalties incurred in running the engine on days with vastly varying ambient temperatures (e.g. cold & hot, cold & standard or standard & hot days) is lesser in tropical conditions than at ISA conditions. This is probably due to the lower ambient conditions of total temperature, total pressure and density at the higher altitude of 700m for the investigated tropical region. Figure 79 presents the evaluated penalties (*in percentage*) associated with the varied ambient temperature assessment of the REM.

The implications of this observation is that the REM will potentially experience lesser stress (both mechanical and thermal), during operation, resulting from ambient temperature variation across an operating period within the considered tropical region.

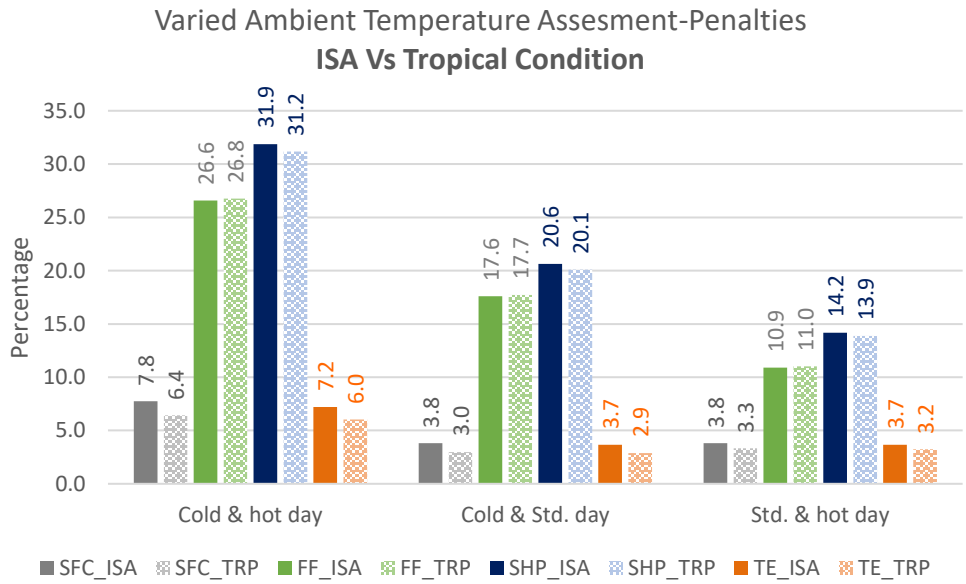

* Chequered columns indicate tropical condition.

Figure 79: Comparison of engine operation at ISA and Tropical

Table 16 shows the categorisation of cold, standard and hot day temperatures adopted in this study.

Table 16: Ambient Temperature Categorisation

Day	Cold	Standard	Hot
Temperature	(-15°C) – (+10°C)	(+11°C) – (+20°C)	(+21°C) – (+30°C)

6.1.3 Varied Firing Temperature Assessment ISA Vs Tropical Condition (*at varying ambient temperature and fixed relative humidity*)

Results obtained as shown in Figure 80 -Figure 83 are consistent with typical expectations and are similar for both ISA and tropical conditions. As anticipated, hotter days deliver higher penalty on performance output. SFC increases by an amount in the range 1-6% while thermal efficiency (TE) decreases by an amount in the range 1-6% from low to high firing temperatures. Shaft power (SHP) decreases by an amount in the range 1-7% from low to high firing temperatures. This Investigation is conducted for different firing temperatures across an ambient temperature range of -30°C to 40°C with a fixed relative humidity of 60%.

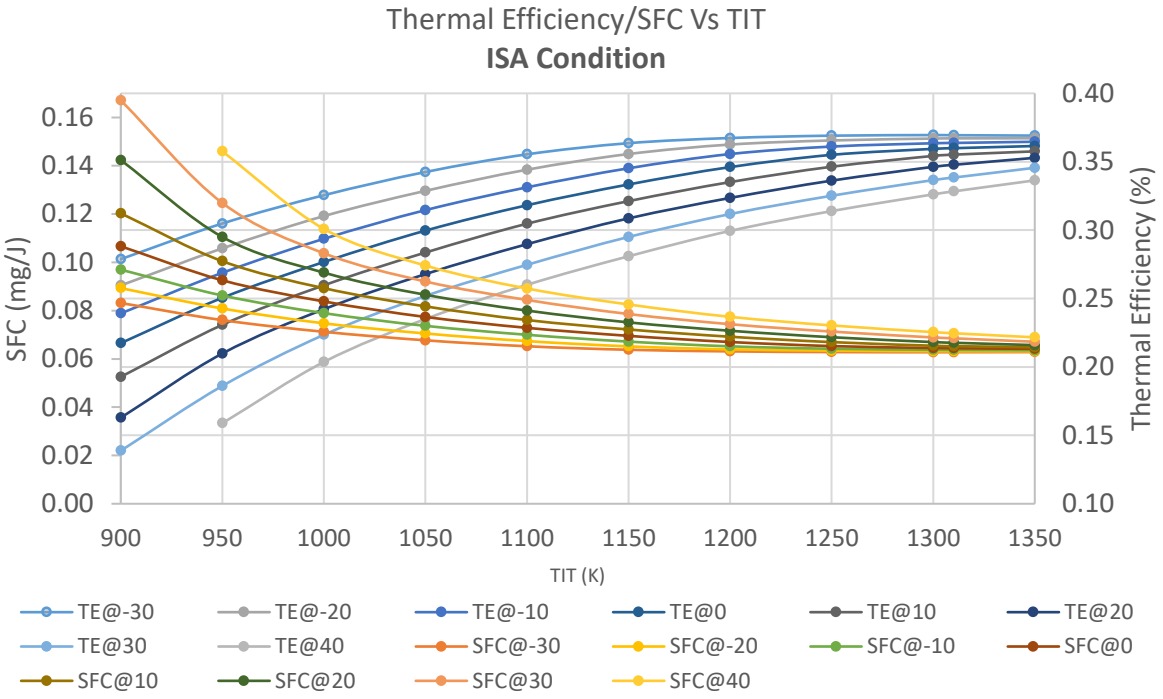

Figure 80: Varied Firing temperature assessment ISA condition (SFC/TE Vs TIT)

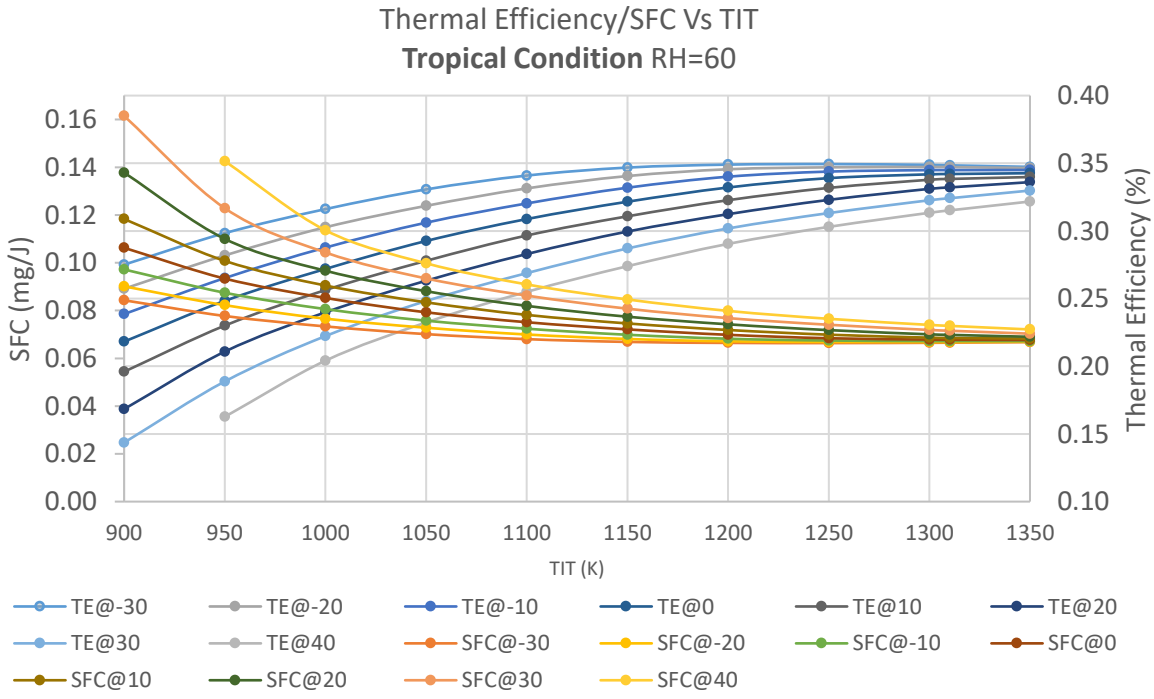

Figure 81: Varied Firing temperature assessment Tropical condition (SFC/TE Vs TIT)

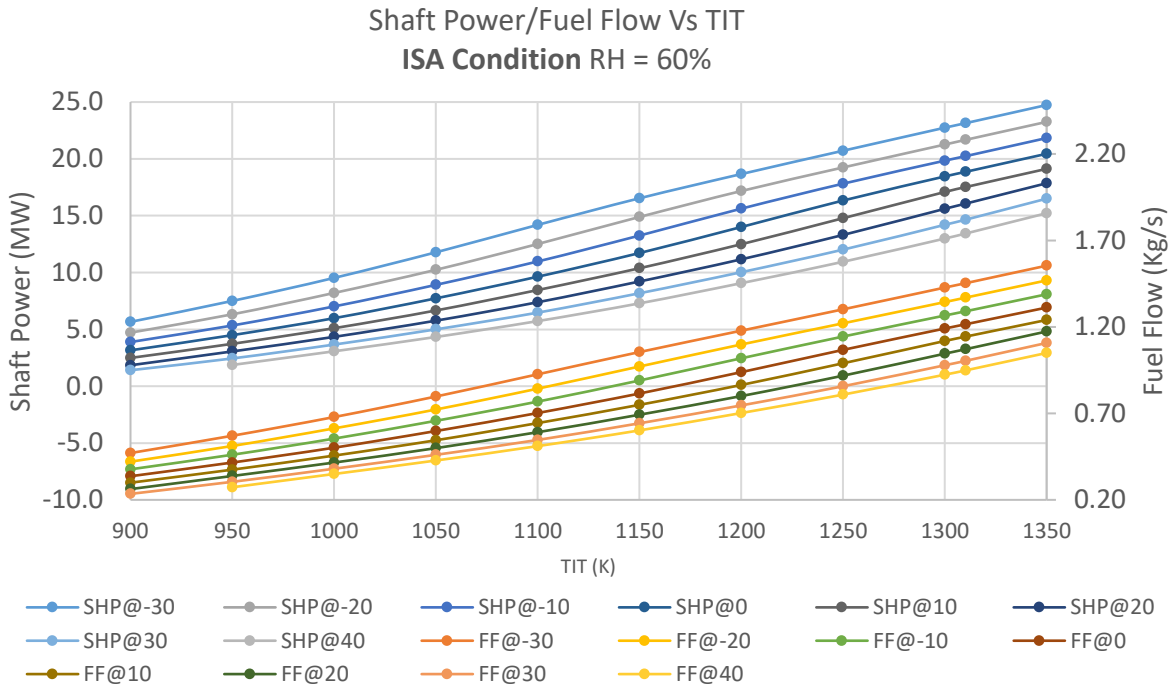

Figure 82: Varied Firing temperature assessment ISA condition (SHP/FF Vs TIT)

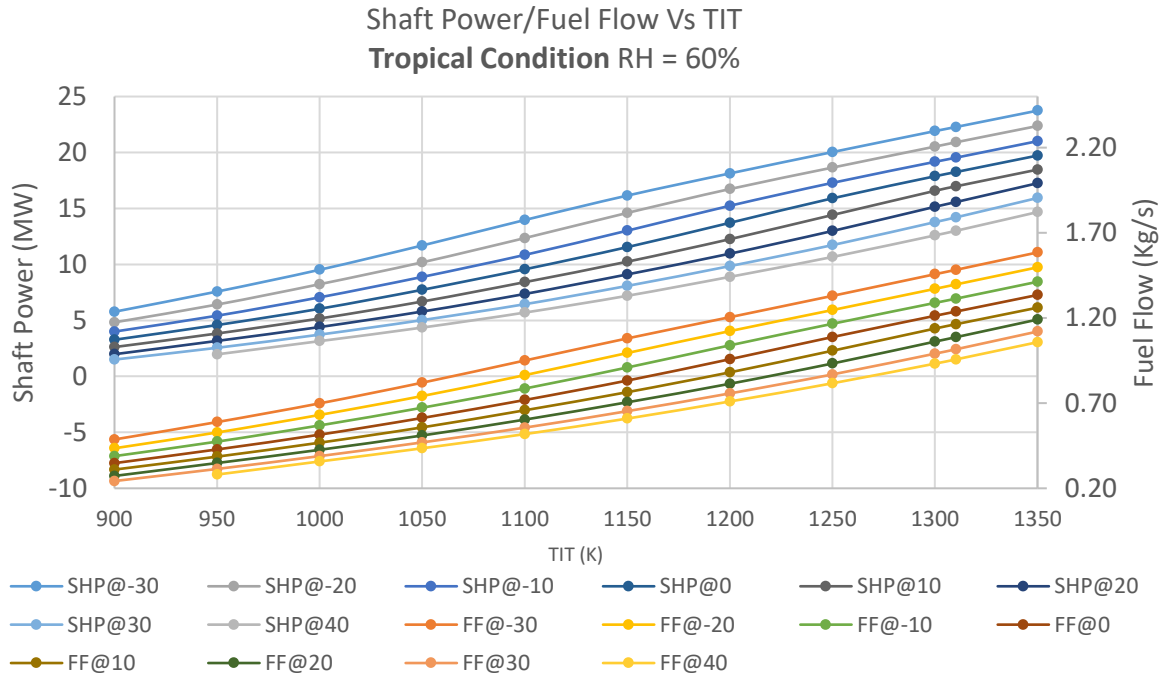

Figure 83: Varied Firing temperature assessment Tropical condition (SHP/FF

Observation of fuel flow (FF) results reveals that fuel flow is higher at lower ambient temperatures and lower at higher ambient temperatures. This is the case because for each consideration of ambient temperature during the simulation, power output is not fixed but variable. Therefore, at higher ambient temperatures, inlet mass flow and engine power output will be lesser than at lower ambient temperatures. Therefore, since the required power output is not fixed, lesser fuel flow will deliver an associated lower power output.

6.1.4 Fixed Firing Temperature Assessment ISA Vs Tropical Condition (*at varying ambient temperature and relative humidity*)

At a fixed firing temperature, the REM's thermal efficiency, fuel flow and shaft power decrease with increase in ambient temperature. Because of the decreasing fuel flow and power output, the engines specific fuel consumption increases with increasing ambient temperatures. Therefore, at a fixed firing temperature, the engines performance will decrease on hotter days. In order to maintain a given power output on such days, fuel flow or mass flow will have to increase. Increase in mass flow can be achieved through water injection. With the implementation of a water injection system, engine performance on hot days can be consolidated. This however will have an influence on the capital, operation and maintenance cost of the unit.

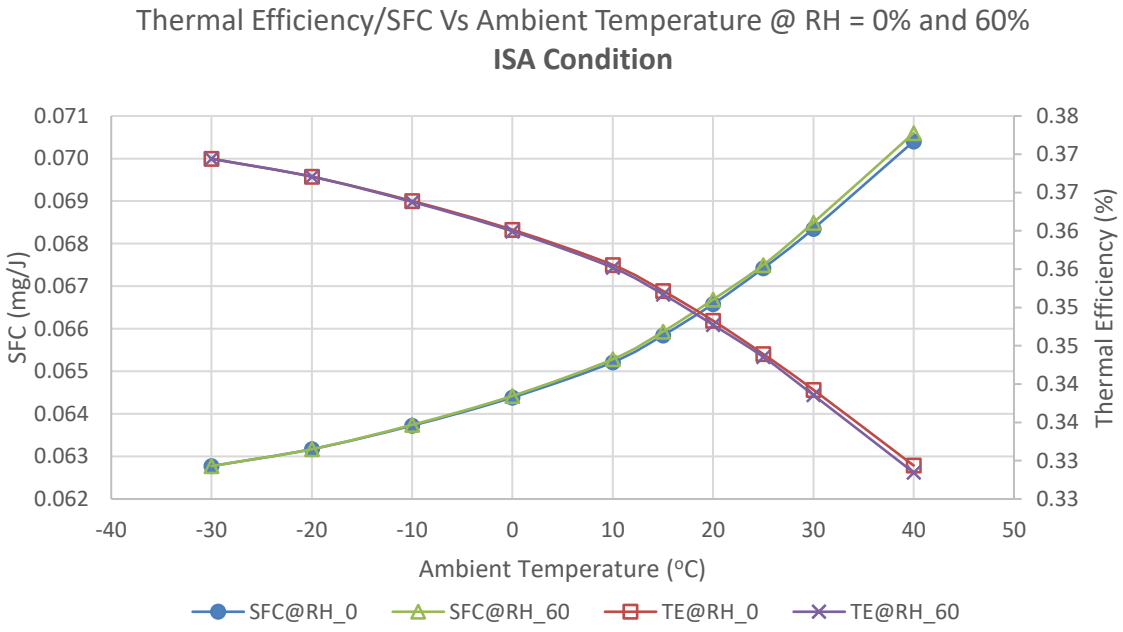

Figure 84: Fixed Firing temperature assessment ISA Vs Tropical condition (SFC and TE Vs Ambient Temperature)

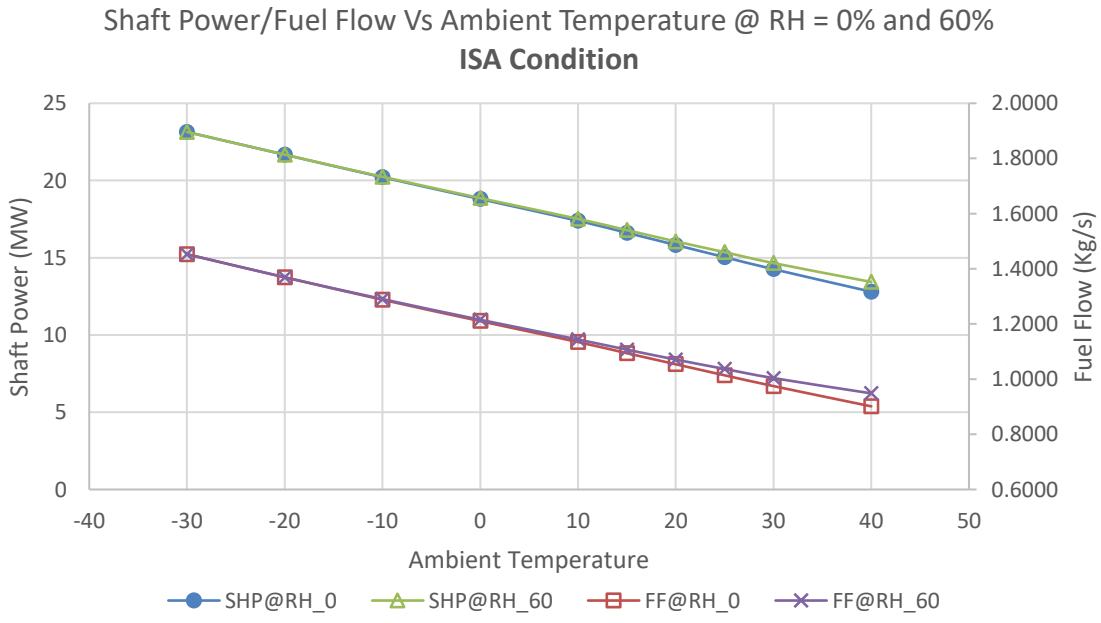

Figure 85: Fixed Firing temperature assessment ISA Vs Tropical condition (SHP and FF Vs Ambient Temperature)

Observation of the influence of relative humidity on the engine performance at fixed firing temperatures reveals that on standard to hot days, relative humidity has a greater effect on the engine's performance output. On colder days, the effect of relative humidity on the engine performance is very small.

6.1.4.1 Power to weight Ratio

Comparison of the repurposed engine model's power to weight ratio with that of larger engines like the LM2500 and GG4/FT4 reveal a higher power to weight ratio for the engine model (Table 17). This evaluation is based on the assumption that the repurposed engine model is 40% heavier than the dry weight of its turbojet variant.

Table 17: Comparison of Power to Weight Ratio

Engine	Power$_{(MW)}$	Weight$_{(kg)}$	Power/weight ratio		Thermal Efficiency
			Min	Max	
LM2500	24-30	4672	0.005	0.006	37
GG4/FT4	16-30	2277	0.007	0.013	---
REM	17-23	1700	0.010	0.014	36

6.1.5 Deterioration Effects on engine performance

Deterioration analysis has been conducted on the REM using the approach described in section 5.3.1.1. The first observation is the effect of engine deterioration on the engine performance maps.

6.1.5.1 Performance Map-LPC

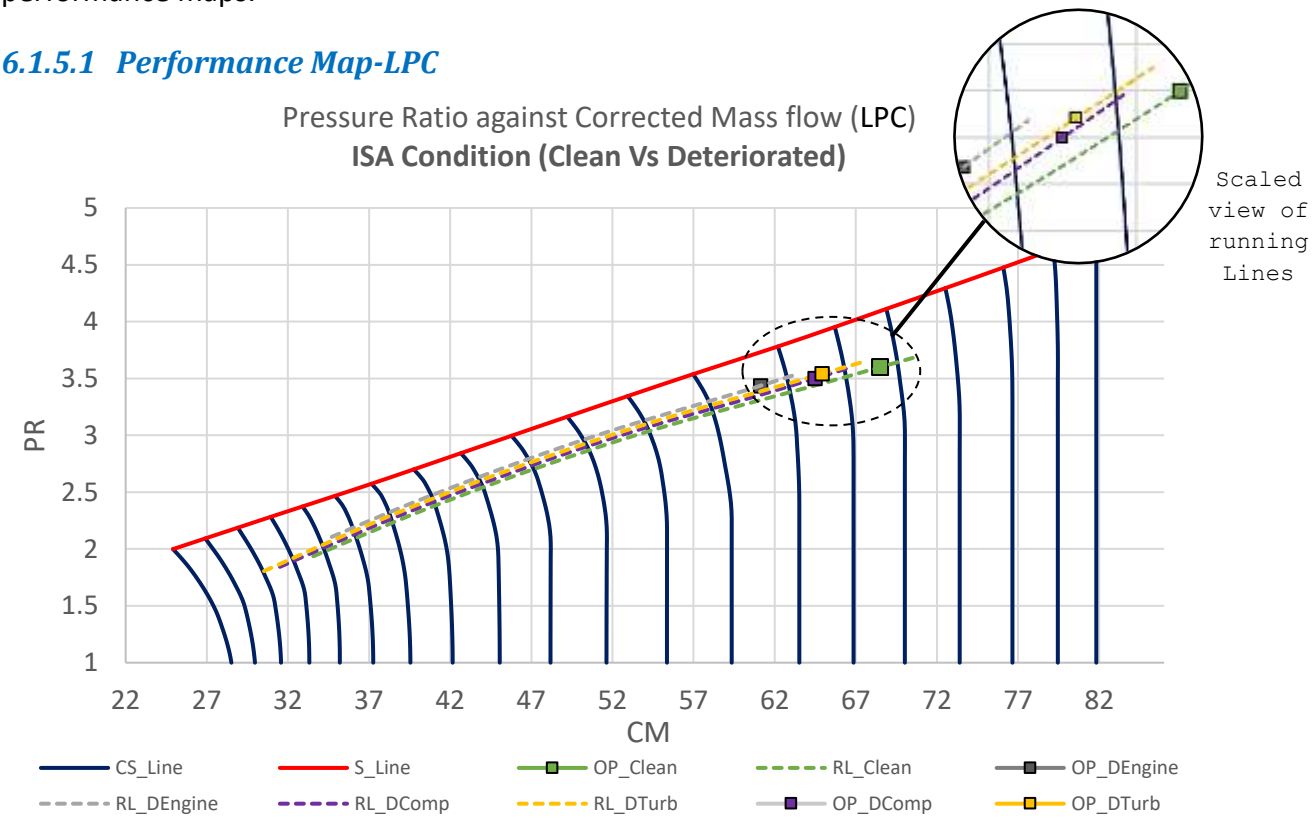

Figure 86: Effect of Deterioration on LPC

With respect to the investigated deterioration cases, the effect of deterioration on the LPC map is outlined below.

- **Combined Deterioration Effect**
  - Engine operating range is reduced
  - Engine design point and operating line move towards surge
  - Design point PR and CM drop by about 5% and 11% respectively
- **Compressor Deterioration Effect**
  - Engine design point and operating line move towards surge
  - Design point PR and CM drop by about 2.7% and 5.9% respectively
- **Turbine Deterioration Effect**
  - Engine design point and operating line move towards surge
  - Design point PR and CM drop by about 1.6% and 5.2% respectively

6.1.5.2 Performance Map-HPC

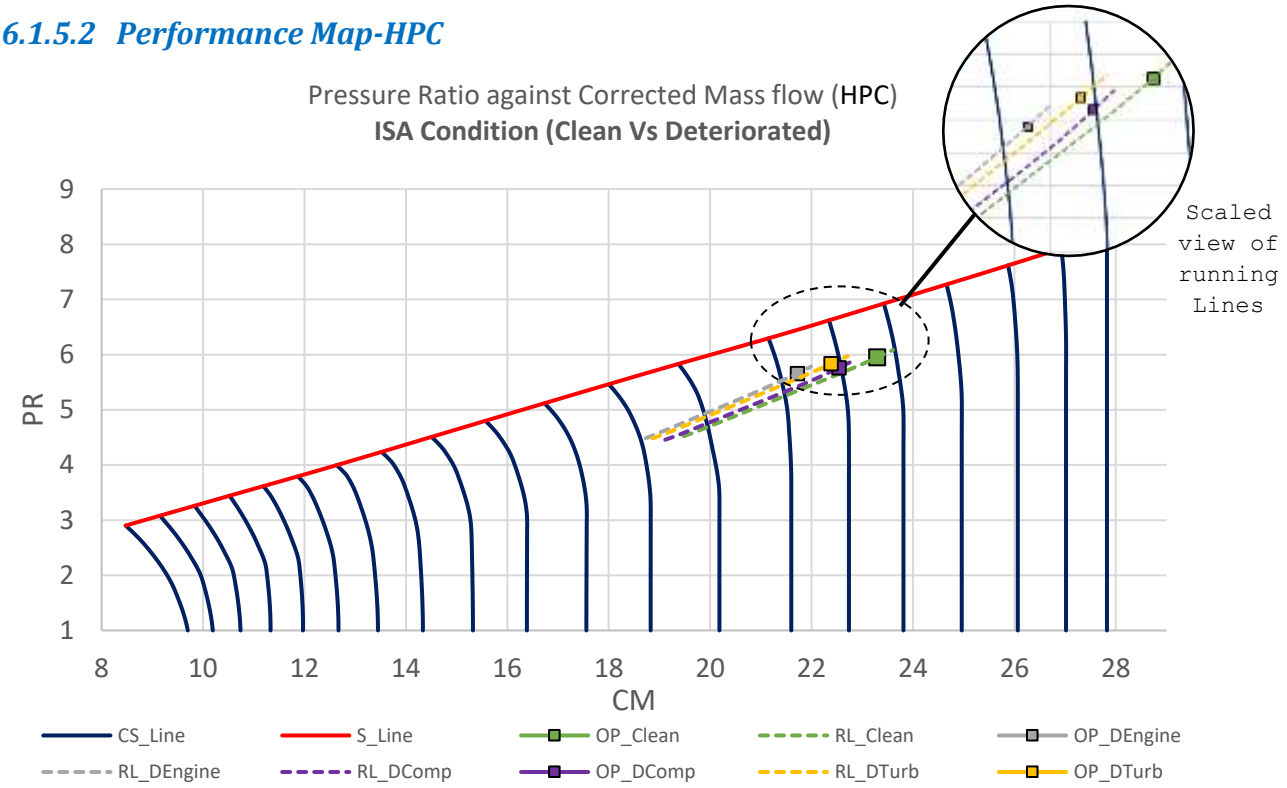

Figure 87: Effect of Deterioration on HPC

The effect of deterioration on the HPC map is outlined below.

- **Combined Deterioration Effect**
  - Engine operating range is reduced
  - Engine design point and operating line move towards surge
  - Design point PR and CM drop by about 5% and 6.8% respectively
- **Compressor Deterioration Effect**
  - Engine design point and operating line move towards surge
  - Design point PR and CM drop by about 3.2% and 3.3% respectively
- **Turbine Deterioration Effect**
  - Engine design point and operating line move towards surge
  - Design point PR and CM drop by about 2% and 4% respectively

Table 18 shows the effect of deterioration on the REM performance at constant firing temperature.

Table 18: Effect of deterioration on engine performance

	SFC (mg/J)	FF (Kg/s)	SHP (MW)	TE	W_{MFlow} (Kg/s)	PR	$T_{exhaust}$ (K)	TET(K)
Clean	0.066	1.103	17	0.35	68.5	21.4	648	1310.2
Det.(Combined)	0.071	0.998	14.0	0.32	61.1	19.5	670	1310.2
Det. Comp	0.068	1.039	15.1	0.34	64.5	20.2	672	1310.2
Det. Turbine	0.069	1.060	15.5	0.34	64.9	20.7	661	1310.2

Results obtained from the degradation analysis revealed the combined deterioration case to have the worst deterioration effect on the engine. Figure 88 presents this observation graphically.

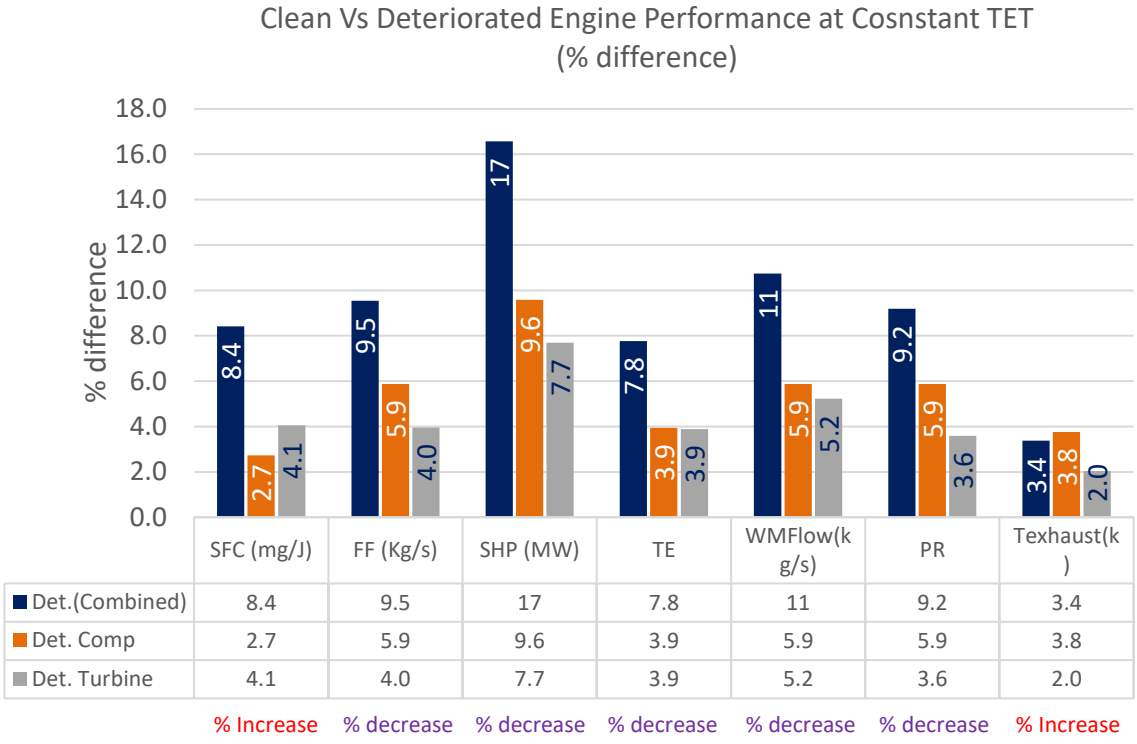

Figure 88: Effect of deterioration on repurposed engine model performance

The lower fuel flow observed in each deteriorated case is due to reduced power output and reduced mass flow resulting from the deterioration in component performance.

The Compressor deterioration case gives the highest exhaust temperature of 672K. This may be favourable result for combined cycle applications. However, the penalties incurred from the increased SFC, reduced output power and reduced Thermal efficiency may have a notable effect on the engine's operation and maintenance cost.

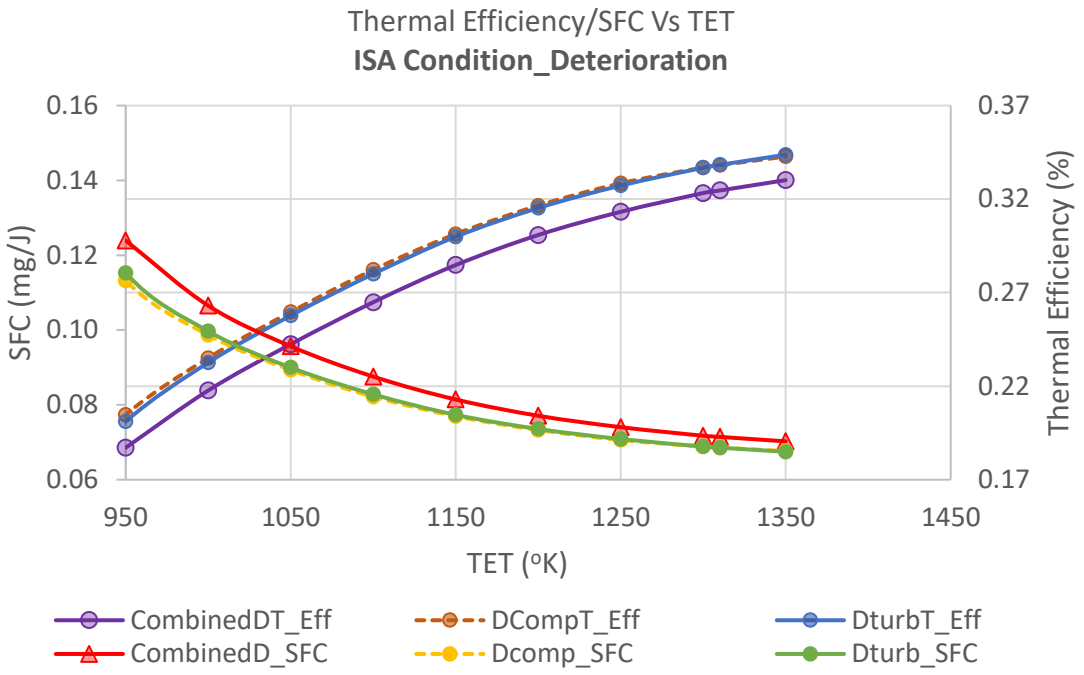

Figure 89: Deterioration effect on TE and SFC with varied TET

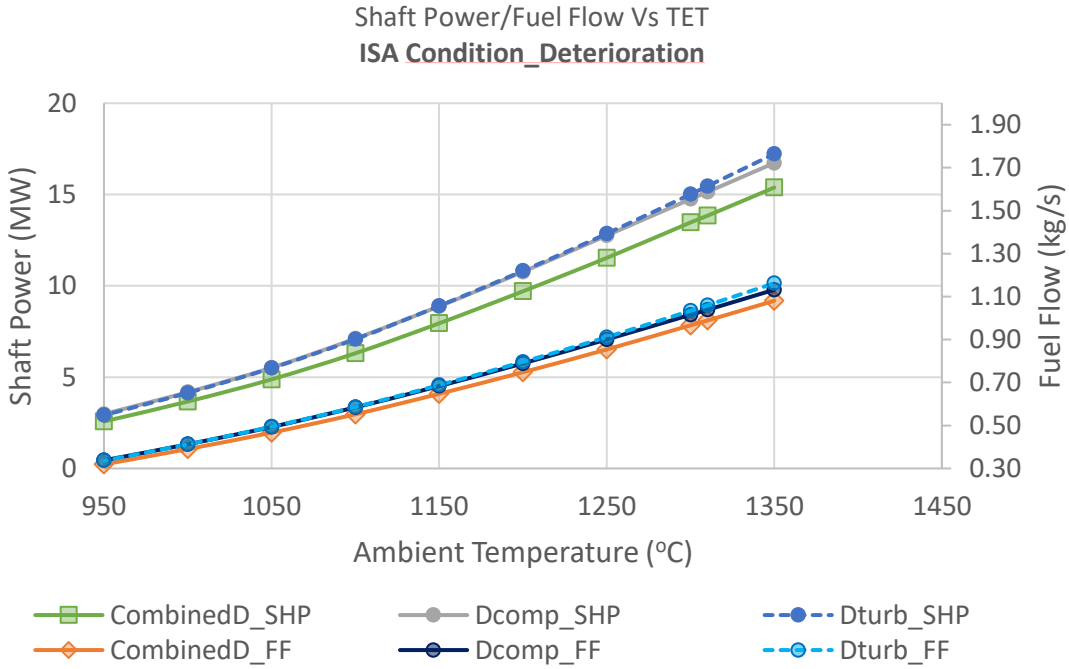

Figure 90: Deterioration effect on SHP and FF at varied TET

The deterioration analysis results obtained are consistent and typical as expected. The combined deterioration case shows a wider deviation in performance output (Figure 89 and Figure 90). This demonstrates the greater effect of combined deterioration on the repurposed engine model's performance. Deterioration analysis has been conducted to provide instances for subsequent economic analysis, on the repurposed engine model.

6.1.5.3 Deterioration analysis Washed and Unwashed Engine

Presented below are results from deterioration analysis conducted for the engine model, operating over 24,000 hour (3 years). These results are presented under two cases, the unwashed engine case and the washed engine case.

6.1.5.3.1 Unwashed Engine case

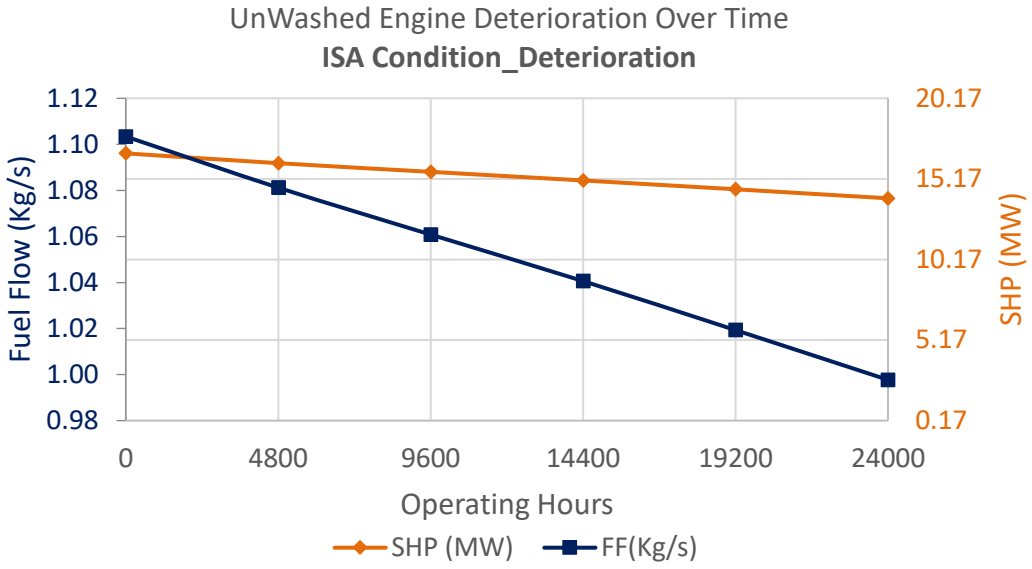

Figure 91: Unwashed Engine Deterioration (Fuel Flow & Shaft Power Vs operating hours)

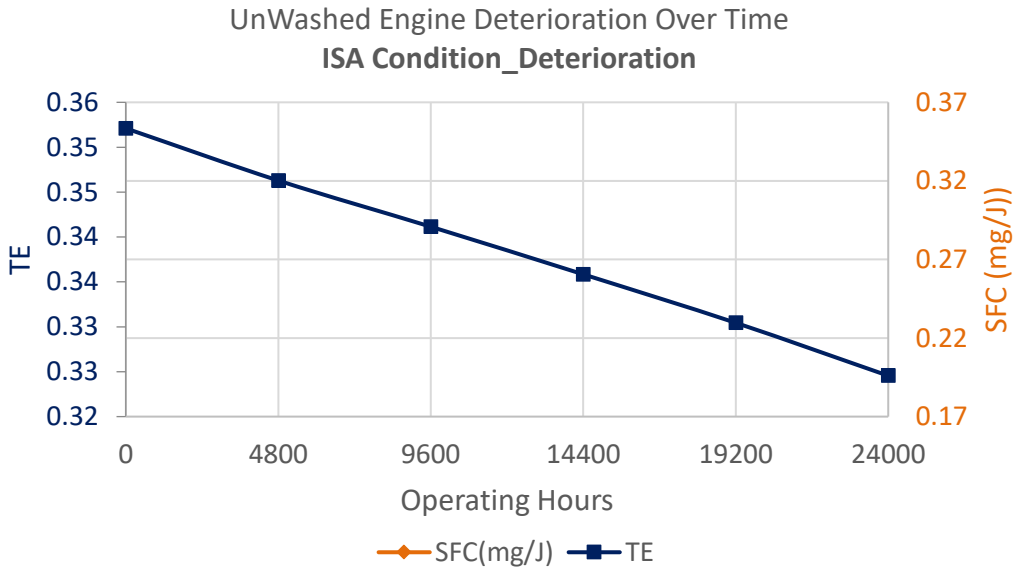

Figure 92: Unwashed Engine Deterioration (Thermal Efficiency & SFC Vs Operating Hours)

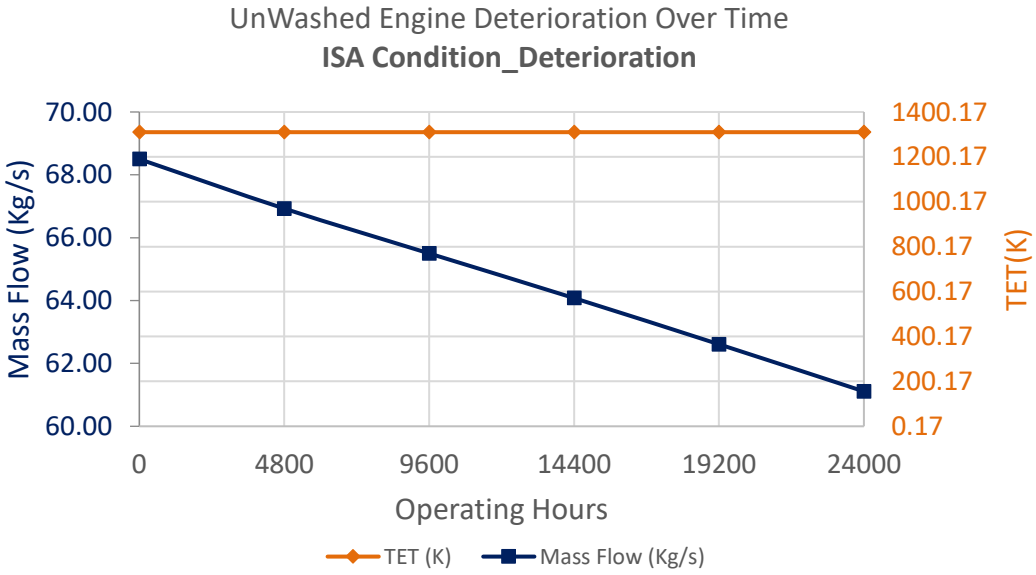

Figure 93: Unwashed Engine Deterioration (Mass Flow & TET Vs Operating Hours)

Figure 91, Figure 92 and Figure 93 show results for the deterioration in the repurposed engine model's performance over time, for an unwashed case, at a constant firing temperature of 1310.2K. Fuel flow, power output, thermal efficiency and mass flow decrease steadily over 24,000 hours. This is because the effect of degradation on the engine continues to increase with time and since no measure for recovering losses due to degradation (like engine washing) has been implemented, there is a steady fall in the engine performance over time. Figure 92 shows an increase in SFC due to the implanted degradation, resulting in a continuous fall in mass flow and power output over time.
At 24,000 hours, there is a 17% drop in power output, 11% drop in Mass flow, 8% drop in Thermal efficiency and an 8% rise in SFC. The results obtained for this investigation are based on implanted deterioration rates, described in section 5.3.1.1, to simulate the engine deterioration over 24,000 hours of operation.

The following section compares the repurposed engine model's performance in a washed and unwashed scenario over a 24000 hours period.

6.1.5.3.2 Washed Case

Presented below are the results for the repurposed engine model deterioration over time with engine washing. It is assumed that HP and LP compressors experiecnes an incremetal deterioration in efficiency of about 0.8% every 4800 hours of operation and the HP and LP turbine experience an incremental deterioration in efficiency of 0.5% every 4800hours.

The results obtained indicate that at constant firing temperature, after 24,000 hours of operation, power output for the washed case drops by 6.7% to a value of 15.63 MW (Figure 94) while that for the unwashed case drops by 17% to 13.9MW. Even after 48,000 hours of operation, the power output for the washed case only drops by 11% to about 14.97MW. This implies that after 48,000hour of operation, the washed case still delivers higher performance than the unwashed after 24000hour of operation. This translates to a prolonged engine model productive life for the washed case in comparison to the unwashed case.

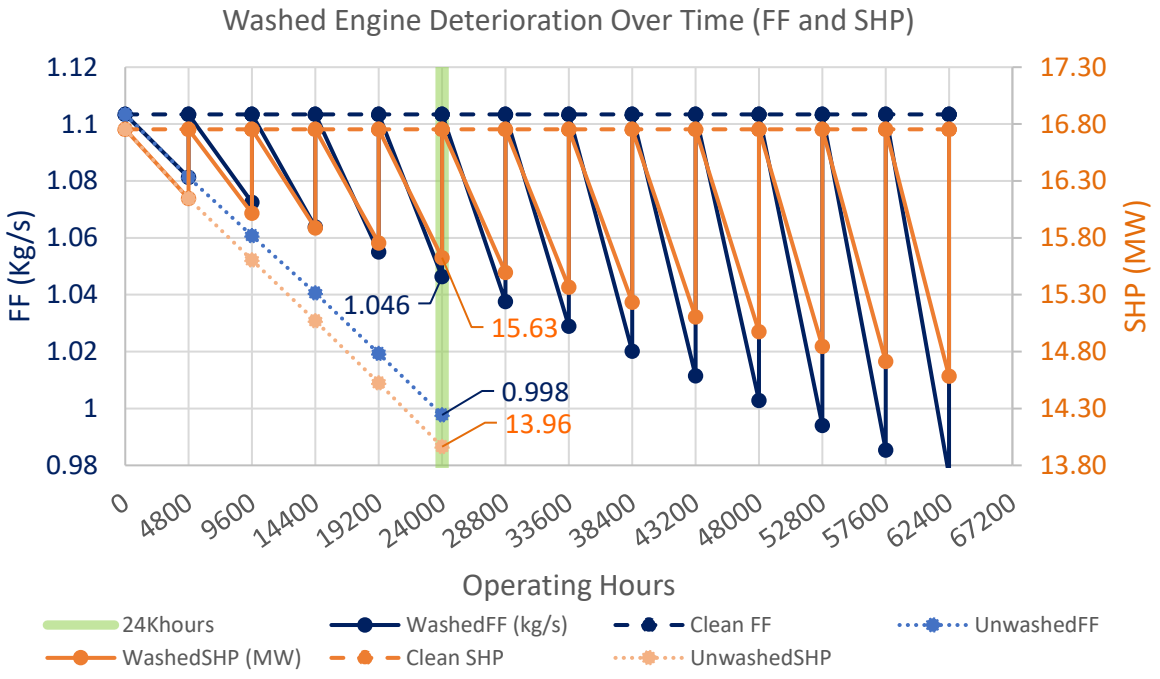

Figure 94: Washed Engine deterioration (FF & SHP Vs operating hours)

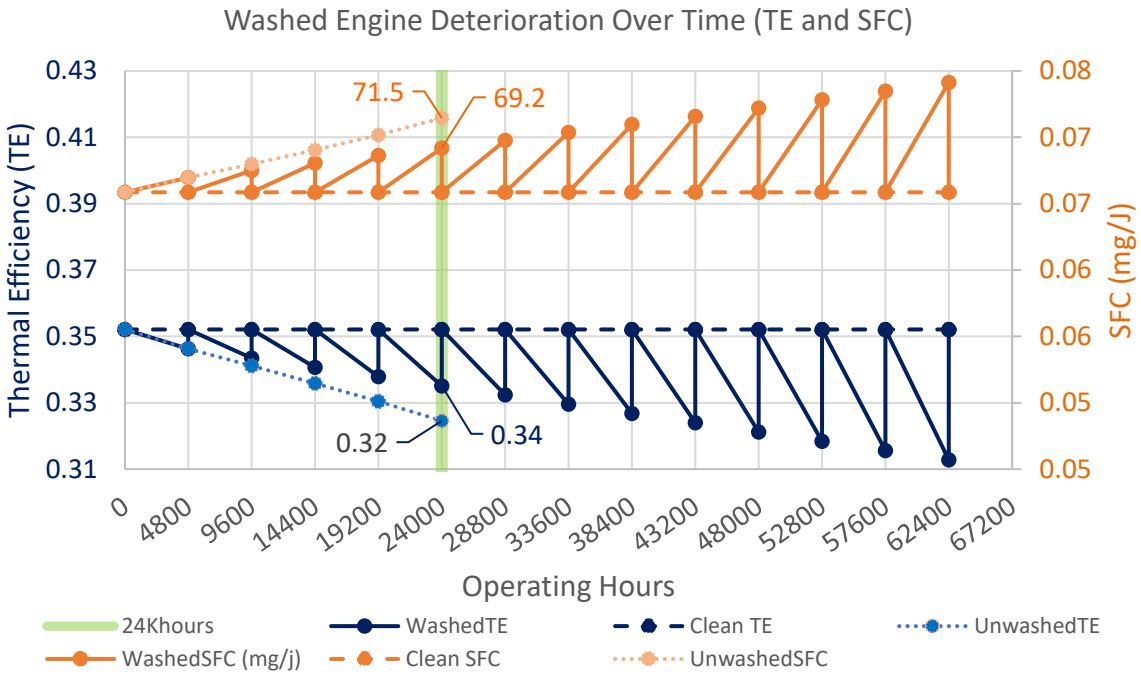

Figure 95: Washed Engine deterioration (TE & SFC Vs Operating hours)

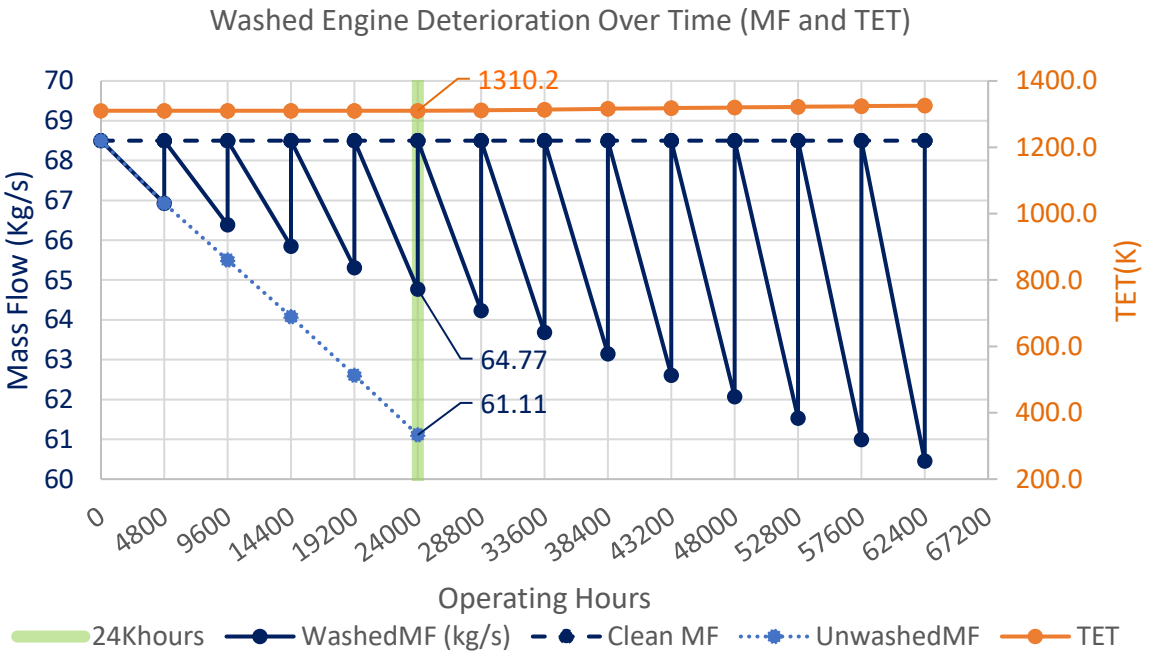

Figure 96: Washed Engine deterioration (Mass Flow & TET Vs operating hours)

In Figure 95, after 24,000 hours of operation, there is a 4.8% drop in thermal efficiency and a 5.1% rise in specific fuel consumption for the washed engine case. The unwashed case experiences a much more severe drop of about 8.5% in thermal efficiency and 7.8% rise in specific fuel consumption.

In Figure 96, TET remains constant throughout the considered operating period because the engine is operating at a constant firing temperature. After 24,000hours of operation, result reveal a 5.4% drop in mass flow for the washed case and a much more severe drop in mass flow of about 10.8% for the unwashed case.

6.1.5.3.3 Comparison of Washed and Unwashed Case

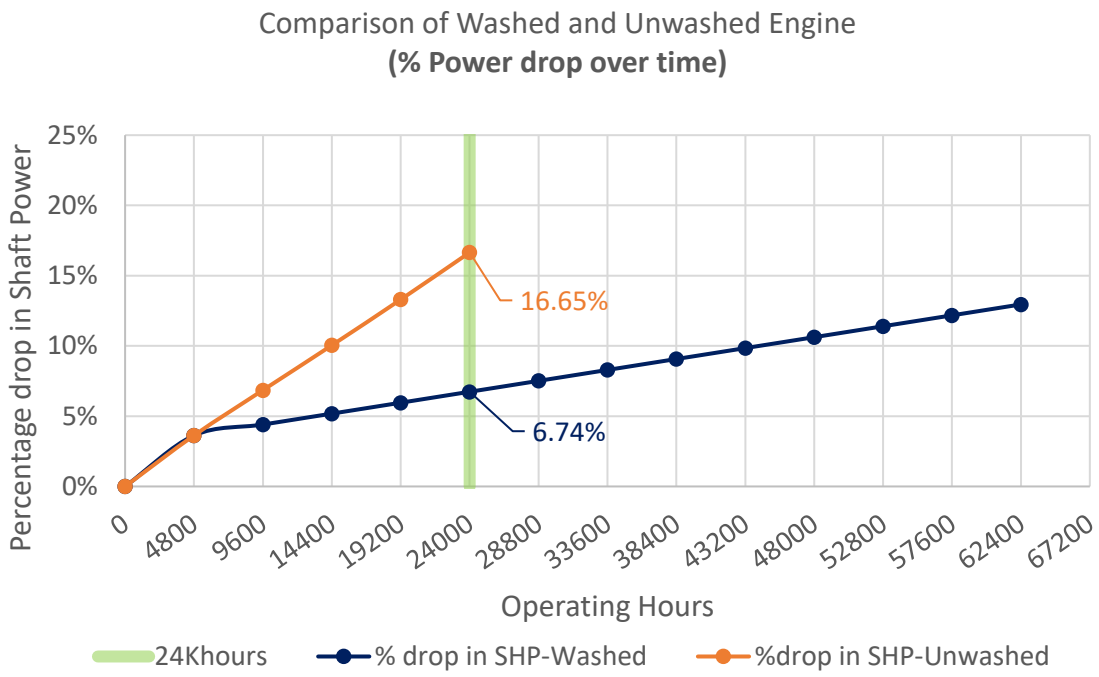

Figure 97: Percentage Power drop over operating hours

At 24,000 hours of operation, there is a 16.7% drop in power output for the unwashed engine case while the washed case reveals a 6.74% drop (Figure 97). Similarly, the Thermal efficiency drop for the unwashed case is more severe than for the washed case. The unwashed case reveals a 7.8% drop in thermal efficiency at 24,000 hours of operation while the washed case reveals a 5% drop as plotted in Figure 98.

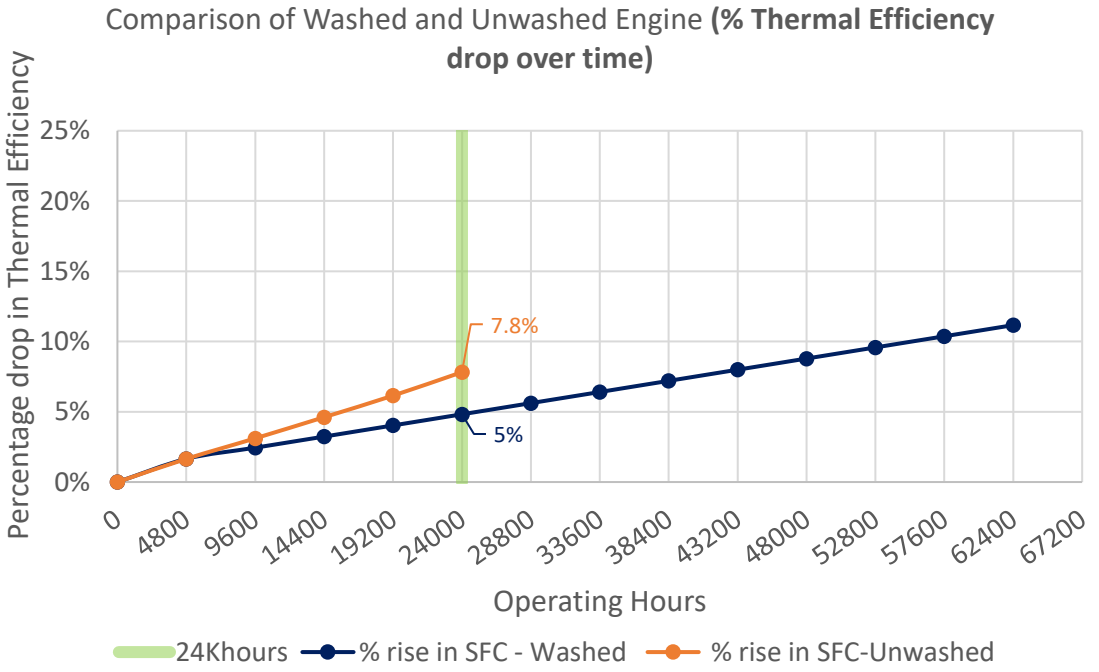

Figure 98: Percentage drop in thermal efficiency over operating hours

In general, the washed engine scenario experienced less severe deterioration in engine performance over time. The implementation of engine washing, though beneficial to the performance of a gas turbine, are not without economic implications. The economic implications of implementing engine washing on the REM have been investigated and results are presented in section 6.3.2.

6.1.6 Transient Performance analysis at ISA Condition

Presented below in Figure 99 Figure 107 are results obtained from the transient performance analysis of the repurposed engine model.

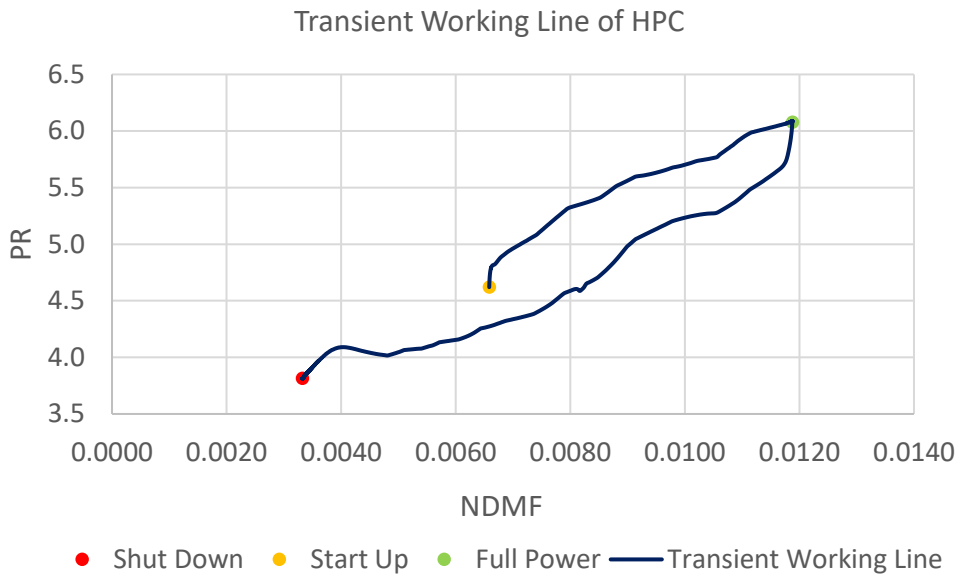

Figure 99: Transient Working Line of HPC

Figure 99 shows engine model transient running line for the HPC from start up, through full power to shut down. The transient performance simulation is conducted for 60 seconds of engine runtime. The engine accelerates from zero (at start up) to 30 secs (at full power). Deceleration then begins from 30 seconds of engine runtime to engine cut-off and shut down.

The transient simulation plots show that engine power, fuel flow, combustor outlet temperature (COT) and engine rotational speed (PCN) continue to rise steadily on start up before peaking at full power. The SFC falls steadily until the engine attains full power where it stabilizes. The reverse occurs at deceleration.

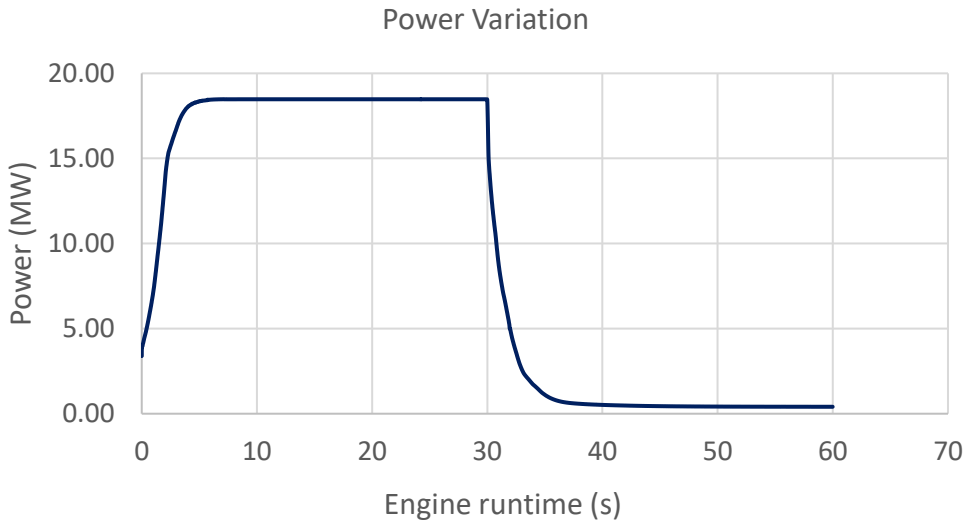

Figure 100: Power Variation with engine runtime

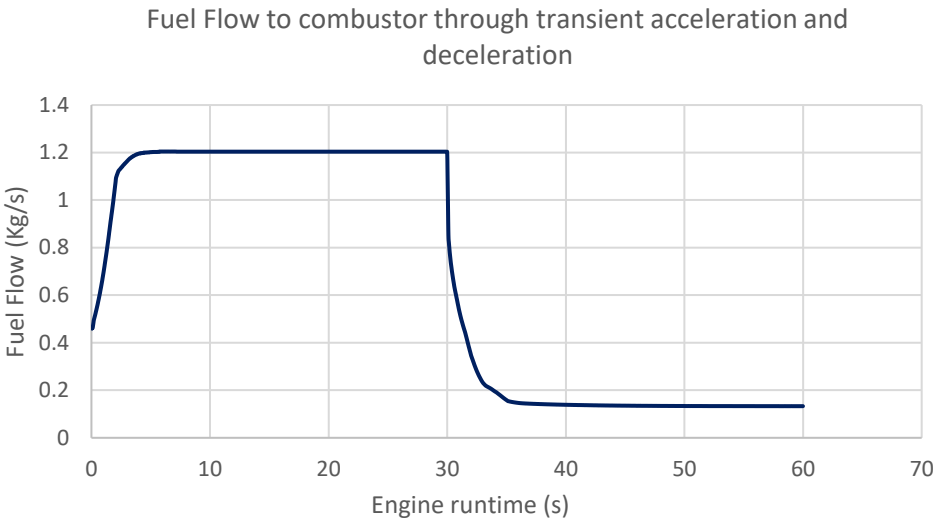

Figure 101: Fuel Flow to combustor through transient acceleration and deceleration

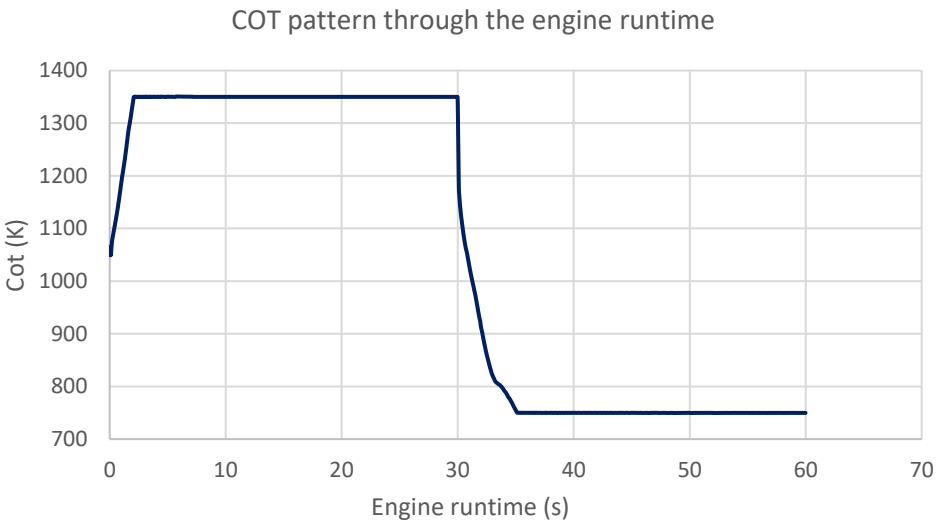

Figure 102: COT pattern through the engine runtime

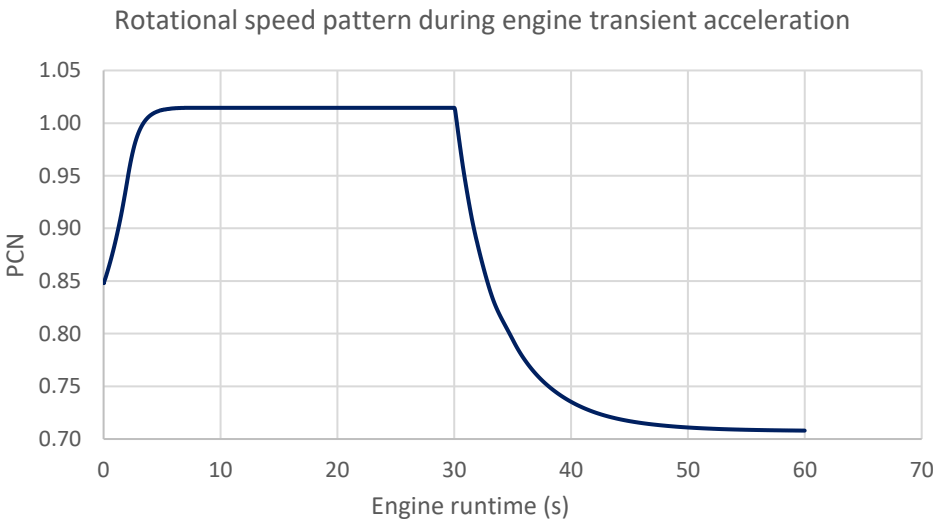

Figure 103: Rotational speed pattern during engine transient acceleration

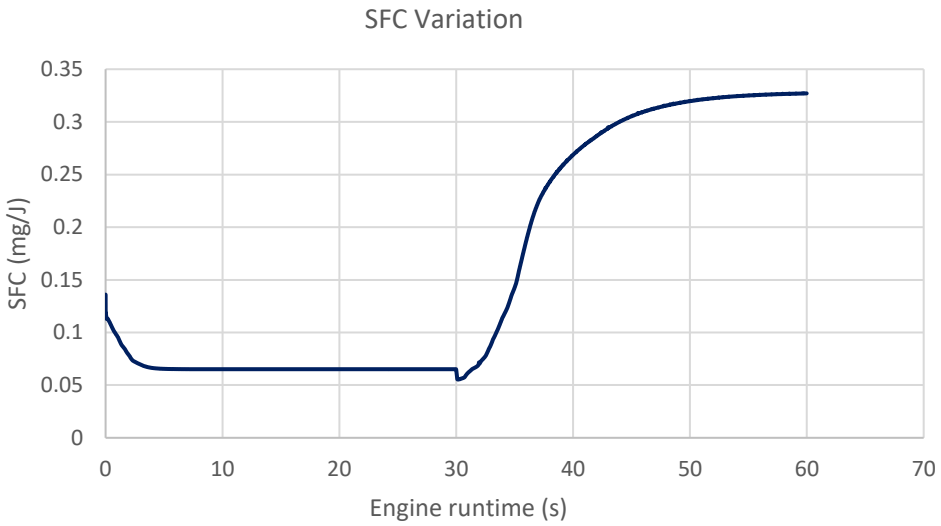

Figure 104: SFC Variation with runtime

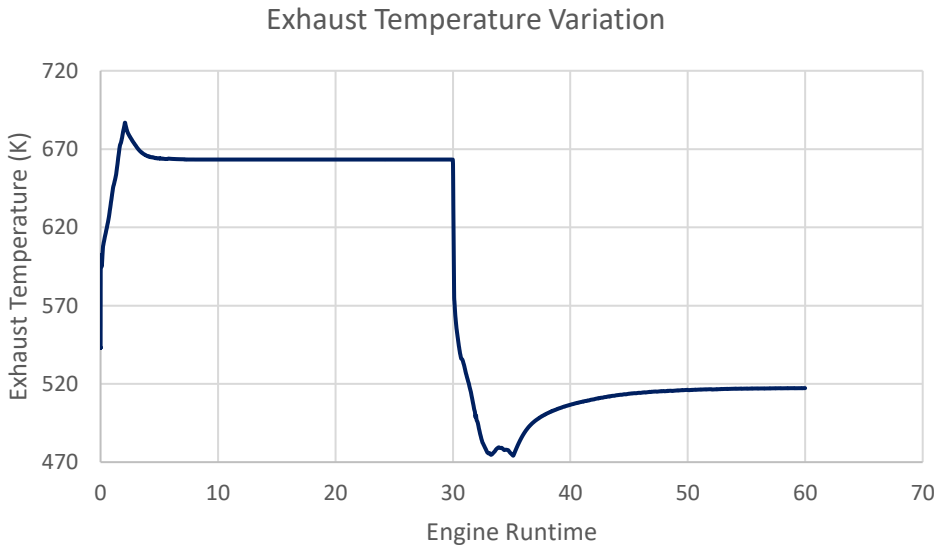

Figure 105: Exhaust Temperature Variation

During deceleration, due to the lag in the engines response to change in power setting, there is a slight delay in the drop in the rotational speed even when fuel flow reduces (Figure 106). This account's for the slight drop in the SFC (Figure 107), during deceleration, just before SFC begins to rise as engine power and fuel flow continue to drop.

In Figure 105, the exhaust temperature during the engine acceleration overshoots the simulated design-point exhaust temperature at full power. This brief period of overshoot in the exhaust temperature is attributed to an estimated over-fuelling factor of 30%. Also at about 33seconds of engine runtime the effect of under-fuelling on the engine exhaust temperature is also observed. A 30% increase (acceleration) and decrease (deceleration) has been implemented in the transient simulation fuel schedule.

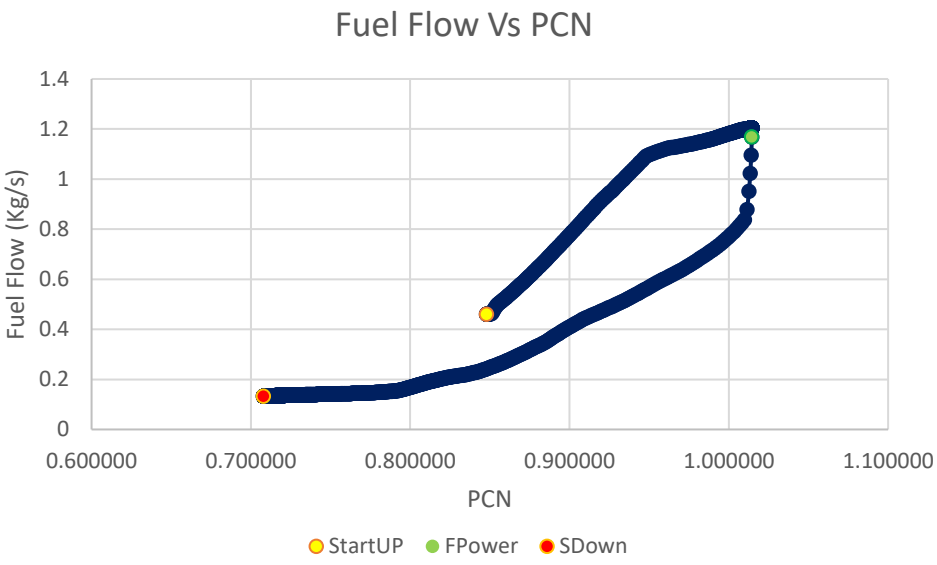

Figure 106: Fuel flow against rotational speed variation

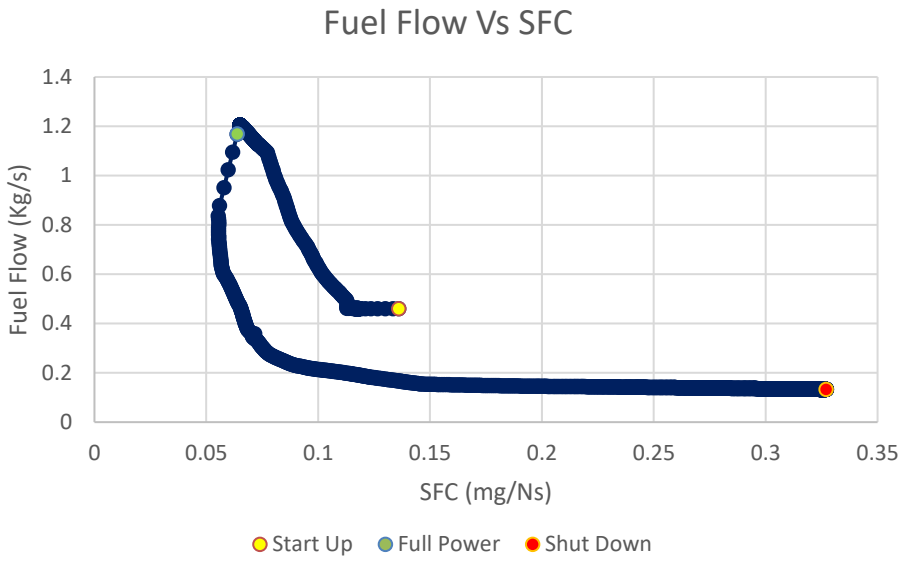

Figure 107: Fuel flow against SFC variation

6.1.7 Effects of degradation on transient engine operation

Investigation into the effect of degradation on the transient performance of the engine model are presented below.

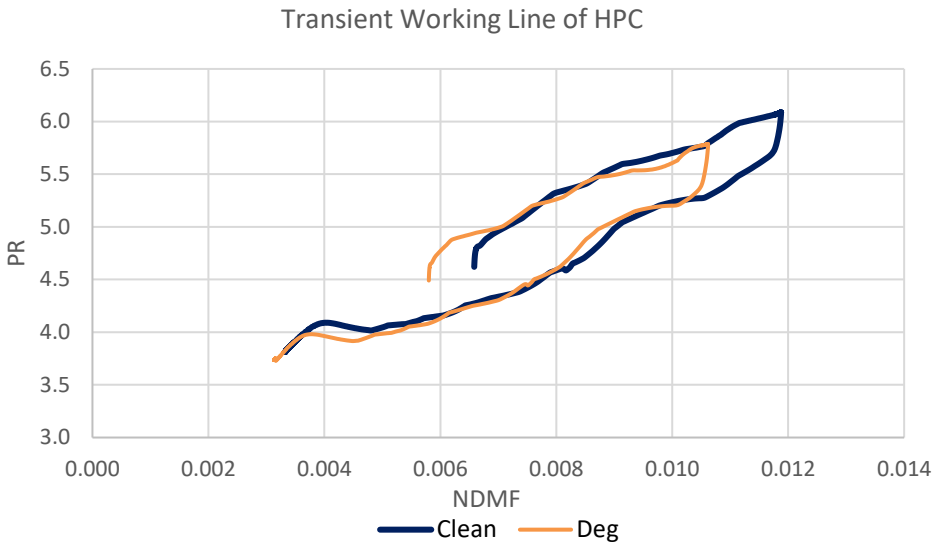

Figure 108: Transient Working Line of HPC

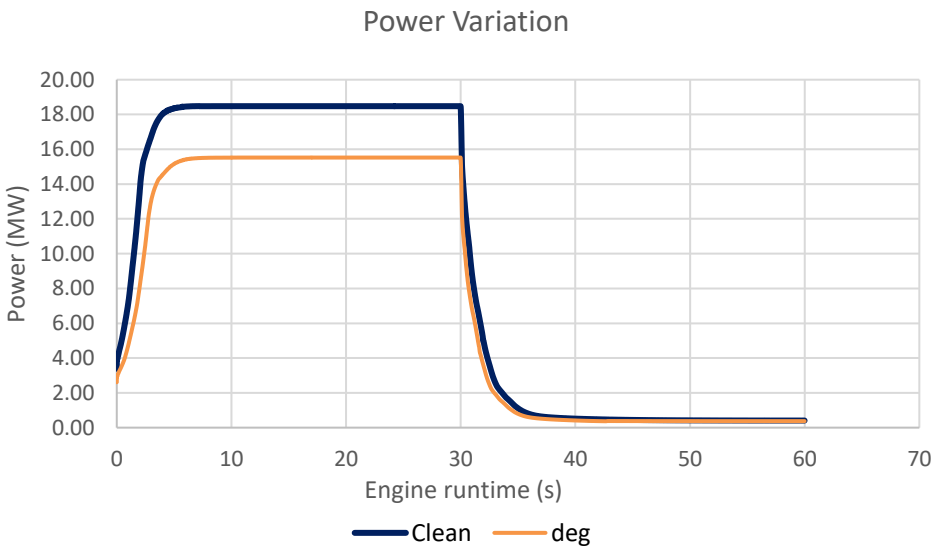

Figure 109: Power Variation with runtime

The plots in Figure 109 - Figure 112 indicate a drop in PCN, fuel flow and power output during engine acceleration for the degraded case. The average percentage drop in Power output is about 18%. Both the clean and degraded case present similar trends for SFC during acceleration. However, Figure 113 indicates a more severe rise in SFC for the degraded case as the engine decelerates. It is also observable that the exhaust temperature variation for the degraded case (Figure 114) is higher than the clean case for both acceleration and deceleration.

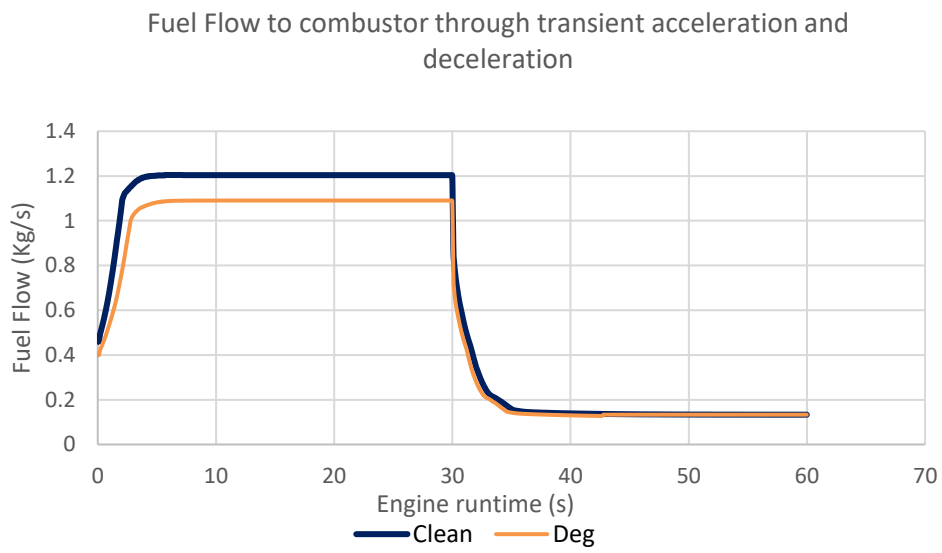

Figure 110: Fuel Flow to combustor through transient acceleration and deceleration

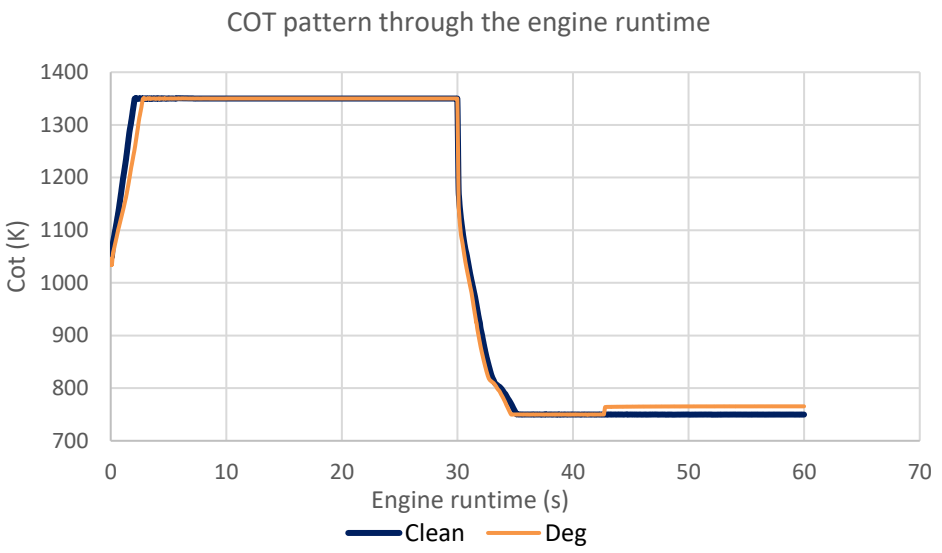

Figure 111: COT pattern through the engine runtime

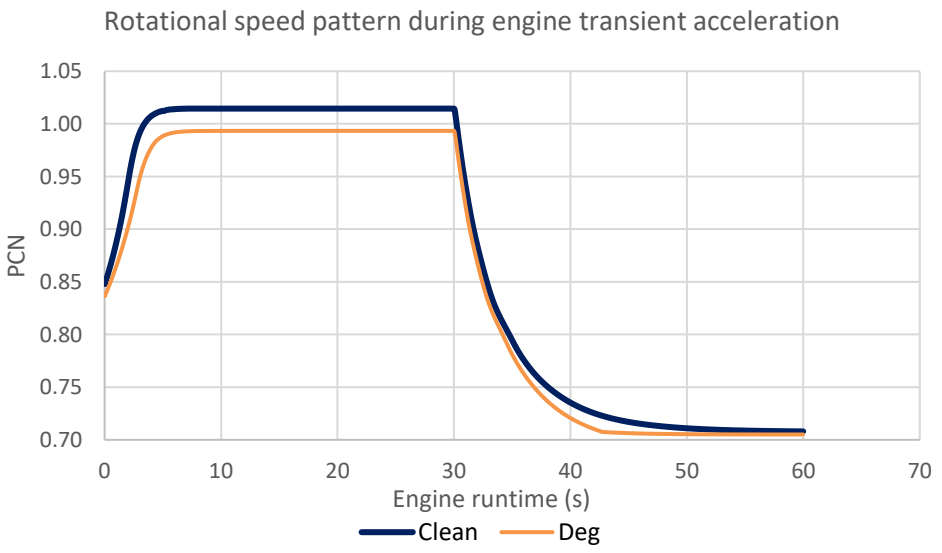

Figure 112: Rotational speed pattern during engine transient acceleration

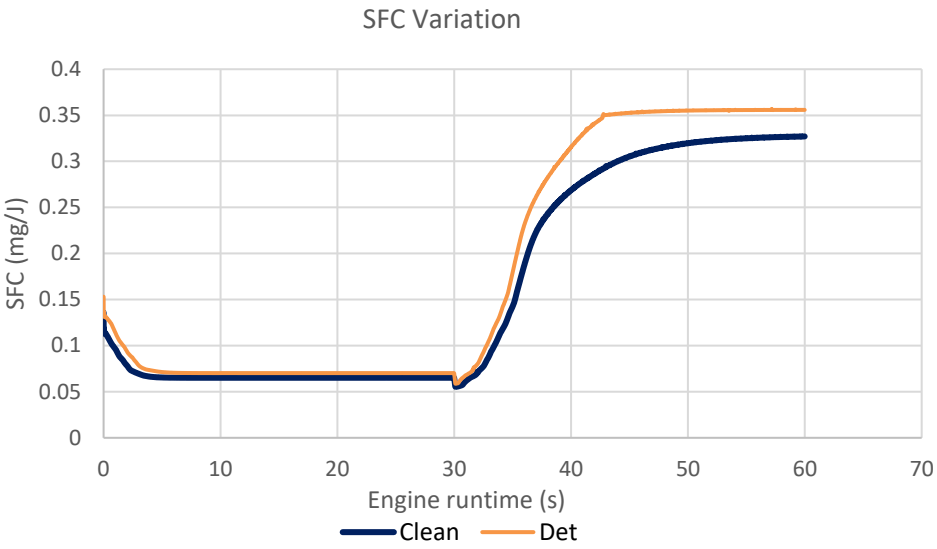

Figure 113: SFC Variation

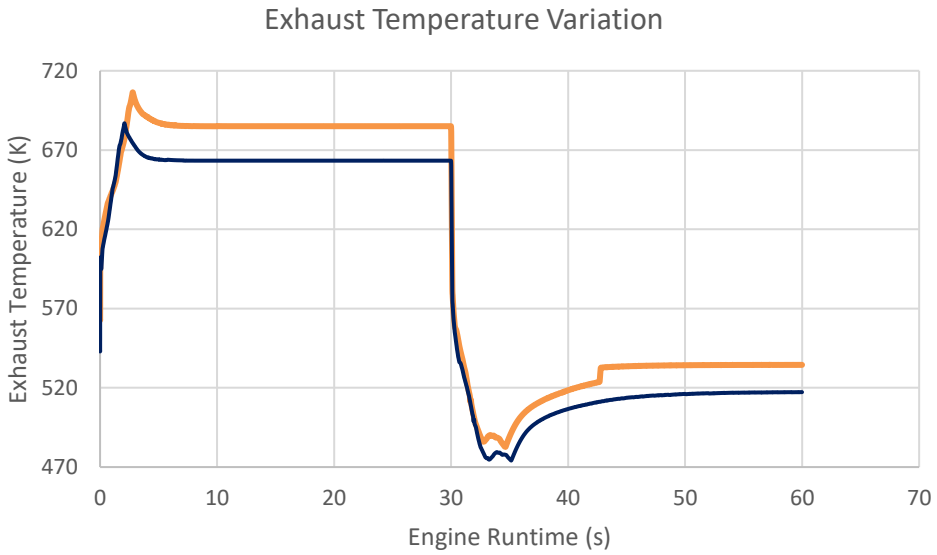

Figure 114: Exhaust Temperature Variation

At about 43 seconds, due to the deterioration in the component efficiencies, the PCN rapidly flattens out (Figure 112). This result in lesser energy being extracted from the hot gases flowing out of the combustor, hence the rise in the COT at that point (Figure 111). Also, due to lesser energy being extracted in relation to the fuel flow rate which remains fairly constant, there is a stepper rise in the engine specific fuel consumption (SFC) and exhaust temperature for the degraded engine model case in comparison to the clean engine model case.

For the same COT, even though fuel flow is lower during engine acceleration for the degraded engine case, power output is also lower from acceleration through to full power for the same case. This means to achieve design point power output, fuel flow will need to increase for the degraded engine case and this will increase the SFC during acceleration. This increase in SFC can translate into an increase in operation and maintenance cost, as more fuel will be required to produce a specific amount of power. There would also be an increase in the frequency of maintenance for the hot gas path components, which may lead to an increase in maintenance cost. Furthermore, an increase in fuel burnt, due to engine deterioration, may result into an increase in emissions generated by the engine model.

Results obtained from the investigation indicate that engine degradation has a significant effect on the engine model transient performance. Even though the engine will spend very little time in transient operation, the economic implication of this operating regime may have significant effect on operational logistics and costs, particularly if the engine is required to operate under severe power cycling schedules. Subsequent economic analysis investigates the effect of transient operation on engine operation and maintenance cost.

6.2 Acquisition Cost Estimate - Results

The estimates for acquisition cost, from the price estimating techniques implemented in this study are presented below. Table 19 present the performance simulation parameters supplied as input into the price estimating models.

Table 19: Engine Performance Parameters

Engine	Power Output (MW)	rpm	Heat Rate (KJ/KWh)	PR	Exhaust Temp. (K)	NOx (ppm)
Engine Model (REM)	18.52	11149	9749	9.6	770.5	N/A
GG4/FT4C-1D	26.00	3600	12397	N/A	N/A	N/A
LM 2500+G4 DLE	32.50	3600	9867	24.2	825.2	25.0
Siemens SGT-800	47.50	6608	9547	20.1	814.2	15.0
RR Trent 60DLE	58.29	3600	8798	36.0	702.2	25.0

The RR Trent 60 engine specification and pricing is referenced from an order made by Qatar in 2006 (Forecast International, 2018). The engines were ordered to complement gas boost duty. In 1977, the West German Navy ordered six LM2500 engines at $4.2million ($17million in 2017 dollars) each. This was to power six new frigates (Gas Turbine International, 1977). An advert in 2013 placed a 26MW GG4/FT4C-1D gas turbine for sale at $14million ($14.7million in 2017 dollars) (General Equipment, 2013). A Siemens SGT-800 was priced in 2016 at $17million ($17.3million in 2017 dollars) (Forecast International, 2018).

For the price estimations conducted in this study, all engine acquisition costs are adjusted, for inflation, to 2017 dollars.

6.2.1 Regression Analysis estimating results

The developed regression analysis model (4.2.1.2) has been applied to estimate the price of an aero-derivative engine model. This engine model is derived from a turbojet engine similar to the TUMANSKY R-25-300 Turbo Jet engine and has been repurposed for power generation. To determine the economic feasibility of selecting the engine model for power generation, an economic analysis is necessary for which the acquisition cost of the engine model is required.

As a validation to the accuracy of the regression model predictions, the acquisition price for four known engine models have also been estimated using the regression model. Table 19 contains the engine performance parameters, used as input into the trained neural network, for each of the engines considered. Table 20 contains results obtained from the regression analysis estimate.

Table 20: Accuracy of Regression Analysis Estimate (2017 dollars)

Engine	Target Value ($ in millions)	RA Estimate ($ in millions)	Accuracy (%)
Engine Model (REM)	N/A	11.00	N/A
GG4/FT4C-1D	14.71	14.30	97.21
LM 2500+G4DLE	17.04	16.86	98.94
Siemens SGT-800	17.34	22.22	71.84
RR Trent 60DLE	23.25	25.70	89.46

Comparing the price estimates computed by the neural network with known actual engine acquisition costs, obtained from literature (Pequot Publishing Inc, 1973-2017); it is observable that the regression analysis predictions are close to the actual engine costs. This indicates that the developed regression model estimates are reasonably accurate and can be applied to estimate gas turbine engine acquisition costs for preliminary economic analysis and planning. Figure 118 presents the results on a chart.

The prediction interval within which acquisition cost estimate for the repurposed engine model (REM) may fall is shown in Figure 115.

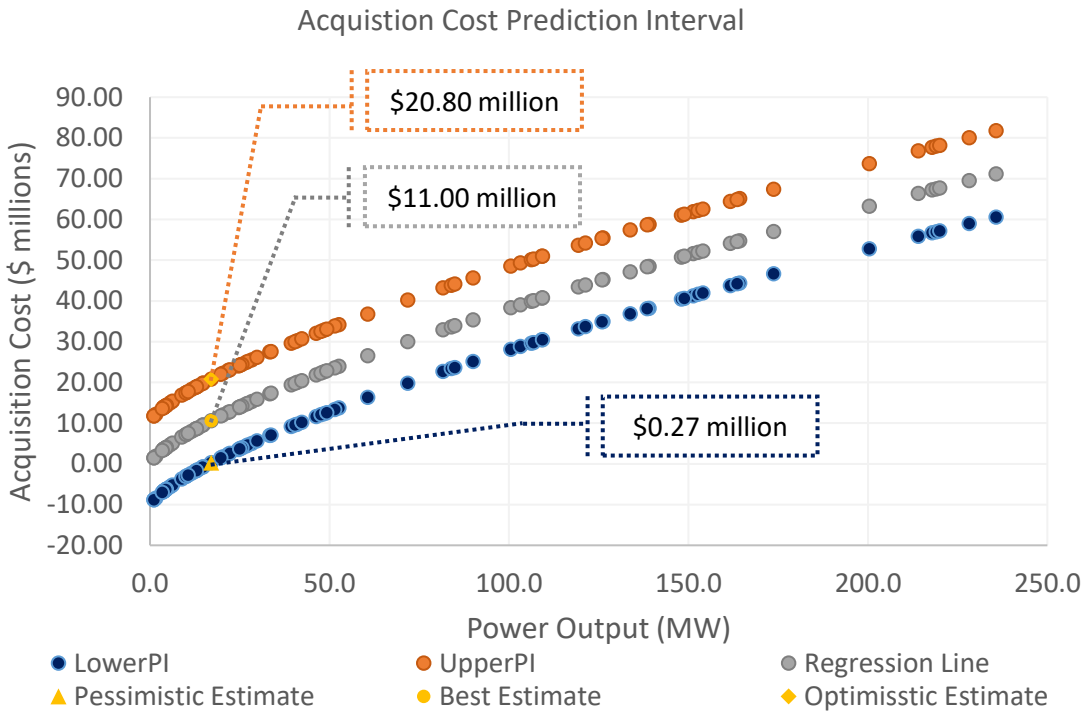

Figure 115: Acquisition Cost Prediction Interval

6.2.2 Artificial Neural Network estimating results

The developed artificial neural network (section 4.2.1.1) has been applied to estimate the price of an aero-derivative engine model. This engine model is derived from a turbojet engine similar to the TUMANSKY R-25-300 Turbo Jet engine and has been repurposed for power generation. To determine the economic feasibility of selecting the engine model for power generation, an economic analysis is necessary for which the acquisition cost of the engine model is required.

As a validation to the accuracy of the neural network prediction, the acquisition price for four known engine models have also been estimated using the neural network. Table 19 contains

the engine performance parameters, used as input into the trained neural network, for each of the engines considered. Table 21 contains results obtained from the ANN estimate.

Table 21: Accuracy of ANN Estimate (2017 dollars)

Engine	Target Value ($ in millions)	ANN Estimate ($ in millions)	Accuracy (%)
Engine Model (REM)	N/A	11.20	N/A
GG4/FT4C-1D	14.71	14.72	99.94
LM 2500+G4DLE	17.04	17.15	99.34
Siemens SGT-800	17.34	17.92	96.62
RR Trent 60DLE	23.25	24.41	95.02

Comparing the price estimates computed by the neural network with the known actual engine acquisition costs, obtained from literature (Pequot Publishing Inc, 1973-2017); it is evident that the neural network predictions are very close to the actual engine costs. This indicates that the developed neural network estimates are accurate and can be applied to estimate gas turbine engine acquisition costs for preliminary economic analysis and planning. Figure 118 presents the results on a chart.

Figure 116 shows the neural network error plot, post regularisation. It is evident that the effect of overfitting is minimized. The value of the applied regularisation term (λ) is set at 10^{-05}. Figure 117 shows the confusion matrix for the neural network. The chosen network architecture got 100% of predictions correct as shown in cell E. This indicates that the chosen architecture is sufficient to make accurate estimates of engine acquisition costs.

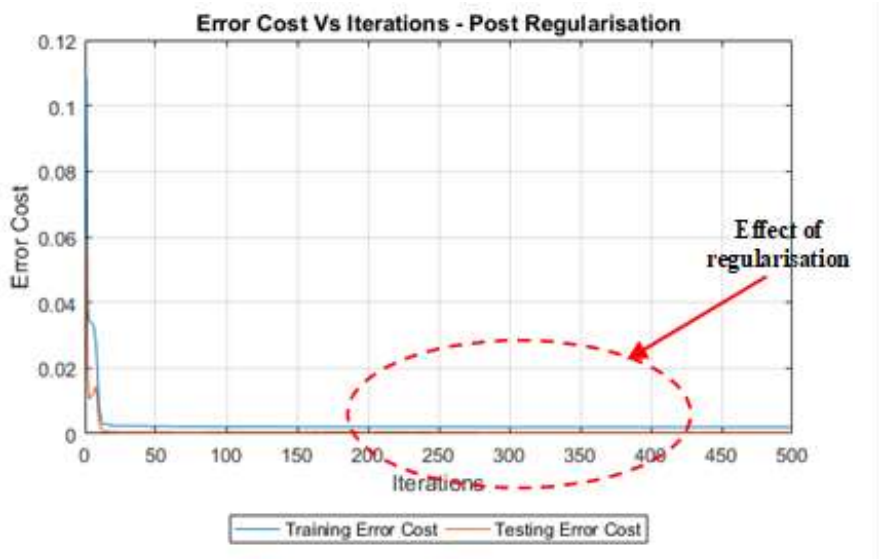

Figure 116: Error Cost Vs Number of Iterations - Post Regularisation

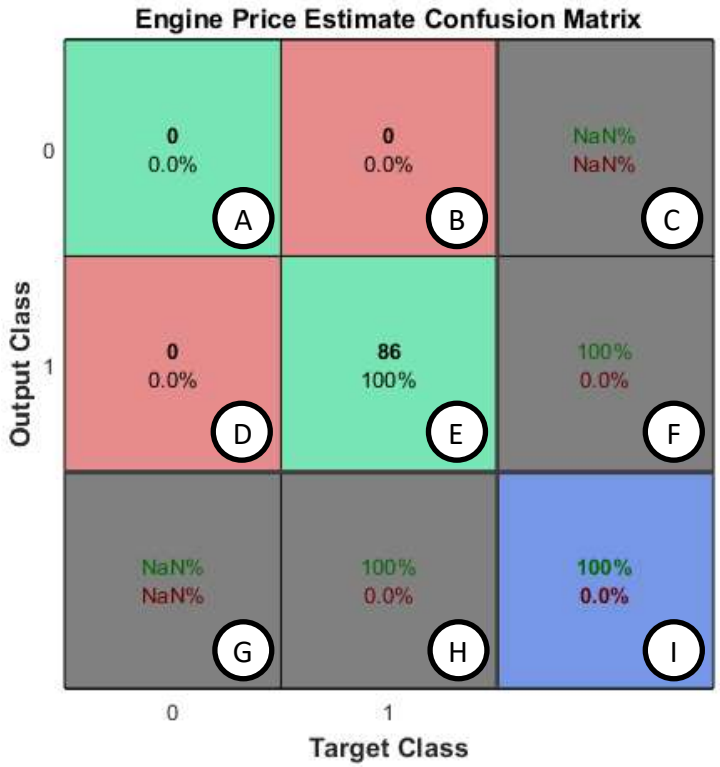

Figure 117: Neural Network Confusion Matrix

6.2.3 Acquisition Cost Estimate Comparison

Further investigation has been conducted to compare the estimates made by the neural network with those made from regression analysis, RA (Rowlands & Savill, 2018). Results reveal that the artificial neural network makes a much more accurate prediction of the engine acquisition costs. Therefore, subsequent economic analysis in this study apply the artificial neural network for estimating engine acquisition costs. Table 20 and Table 21 show the accuracy of the estimates in relation to the target costs. Figure 118 and Figure 119 show the graphical comparison of model estimates.

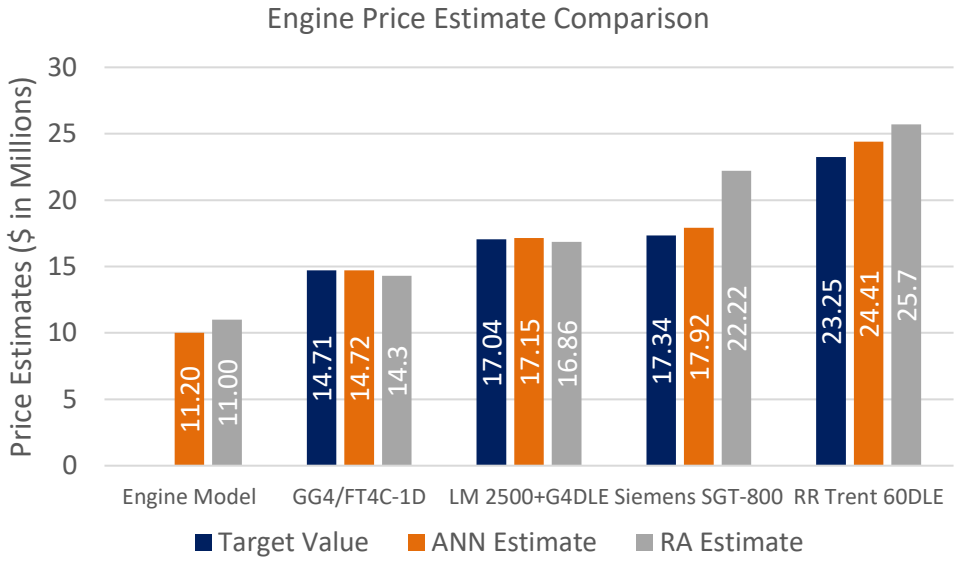

Figure 118: Acquisition Cost Estimate Comparison

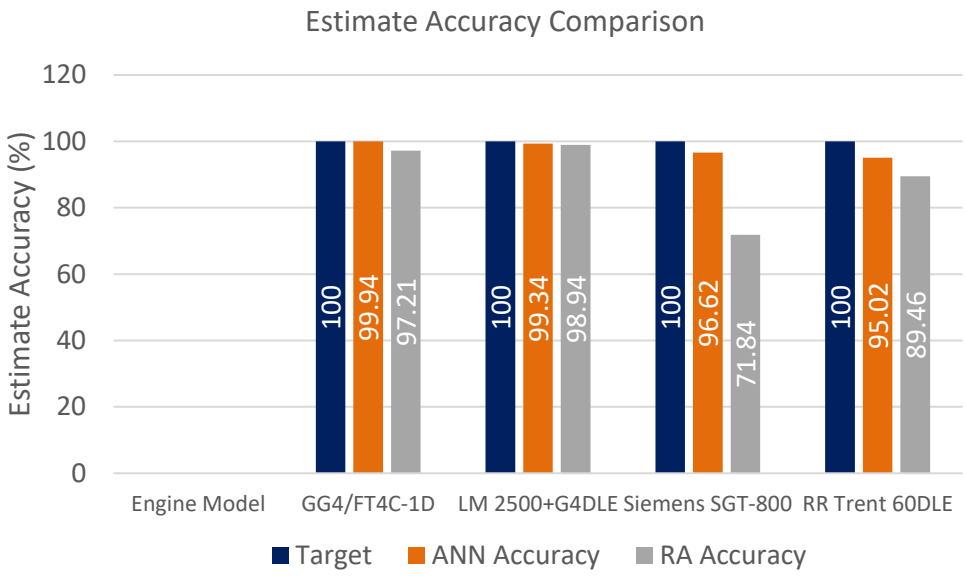

Figure 119: Estimating Accuracy Comparison

6.3 Economic Analysis Results

The methodology described in this study (Chapter 4 and Chapter 5) has been applied to conduct techno-economic analysis on a repurposed engine model (REM). The analysis is necessary to determine the economic feasibility of the repurposed engine model for electrical power generation and to compare its profitability against other potential competitor engines. The results obtained have been compared with results from similar analysis conducted on, competitor units and are presented below.

The required engine performance and operating parameters have been retrieved for each considered engine unit (as contained in Table 14), and supplied as input into the cost component of the economic model.

6.3.1 Baseline Techno-Economic analysis Results

Baseline analysis is conducted for the repurposed engine model in simple and combined cycle application; with and without emissions control.

6.3.1.1 Present Worth analysis Results

Results obtained reveal that all units deliver a positive NPV over the investigated horizon. In Figure 120 and Figure 121, the LM2500 engine unit delivers the highest NPV for all considerations, in both simple and combined cycle applications. The repurposed engine model (REM) delivers the second highest NPV, which is, 12% lower than the LM2500 and 3% higher than the GG4/FT4 in both simple and combined cycle application. It is evident from the NPV results that the two main competitors to the REM are the LM2500 and the GG4/FT4. ***The term REM_UC (REM Uncontrolled) refers to the repurposed engine model without any emissions control implemented***.

A closer look at the investment base, IB in Figure 120 and Figure 121 reveals that a higher capital investment will be required for the LM2500 investment option in comparison to the other units. The LM2500 investment option requires an investment base, which is 14% higher than the REM, in both simple and combined cycle applications. The GG4/FT4 option requires an investment base 3.6% and 4% less than the REM in both simple and combined cycle applications. Furthermore, comparison of the LCOE results as shown in Figure 120 and Figure

121 reveal a 7% decrease in LCOE for investment in the LM2500 and a 52% increase in LCOE for investment in the GG4/FT4 option, when compared with the REM, in simple and combined cycle applications.

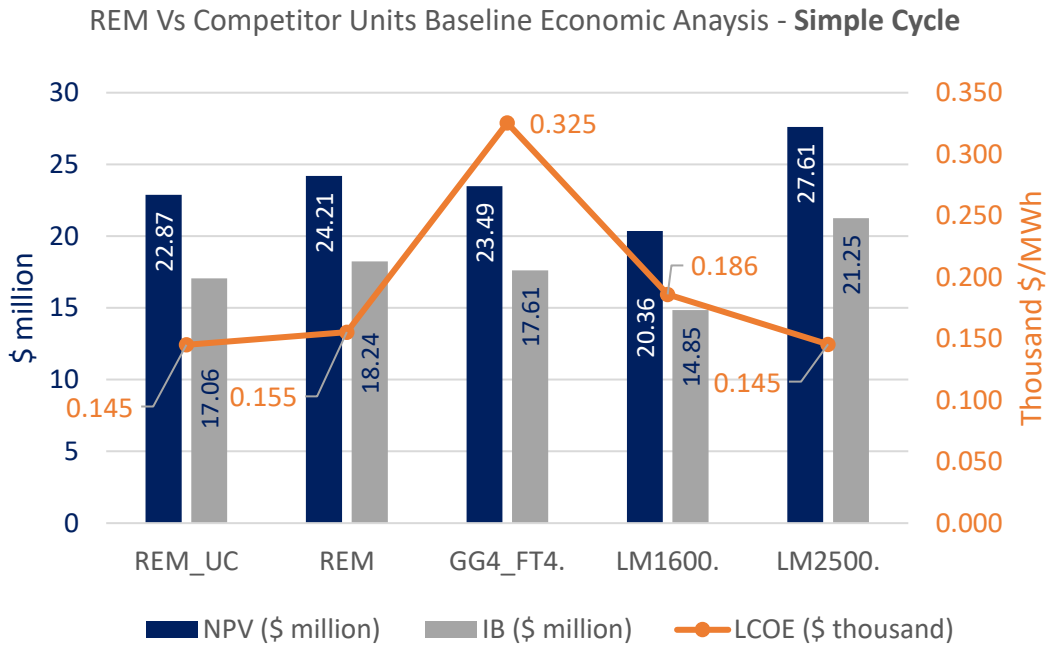

Figure 120: Baseline Economic Analysis (MARR 2.5%) - Simple Cycle

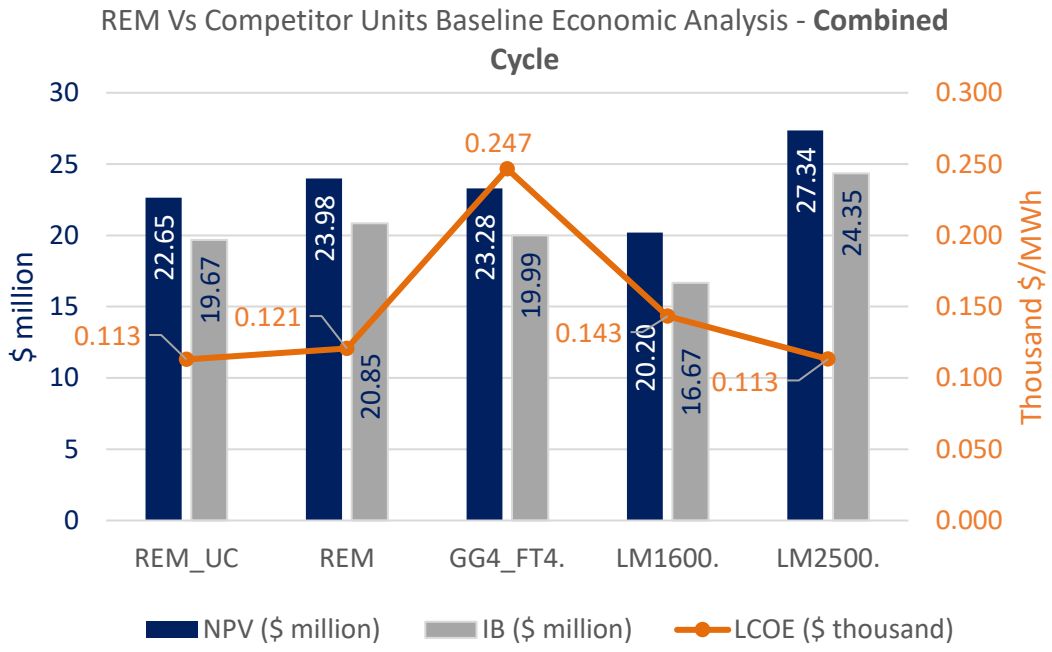

Figure 121: Baseline Economic Analysis (MARR 2.5%) - Combined Cycle

Investment in the LM1600 unit requires the lowest investment base (about 23% less than is required for the REM and 30% less than is required for the LM2500 unit). Though positive, investment in the LM1600 delivers the lowest NPV (about 19% less than the REM) in both simple and combined cycle applications. The investment also results in an LCOE 16% higher than the REM. Higher LCOE means that, electricity will be sold at higher prices to consumers in order to break even at the end of the planning horizon.

6.3.1.2 Emission Control Analysis

In Figure 122, the evaluated amount (in tons per year) and percentage of NOx removed annually is presented. The result reveal that the GG4/FT4 records the highest amount of NOx removed in tons per year. The LM1600 records the lowest amount of NOx removed in tons per year.

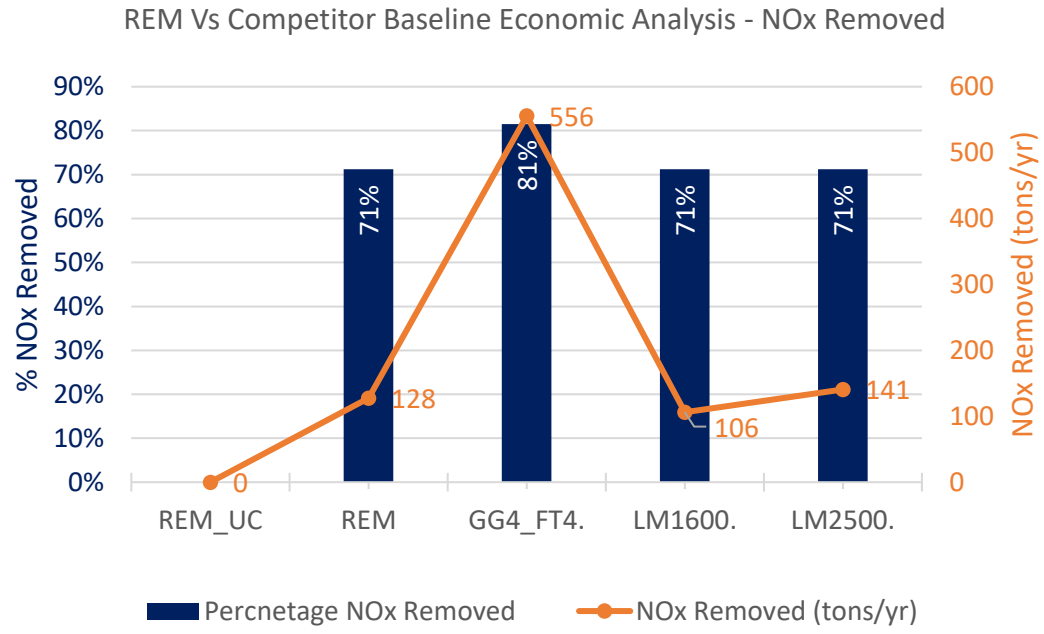

Figure 122: Baseline Economic Analysis - NOx Removed

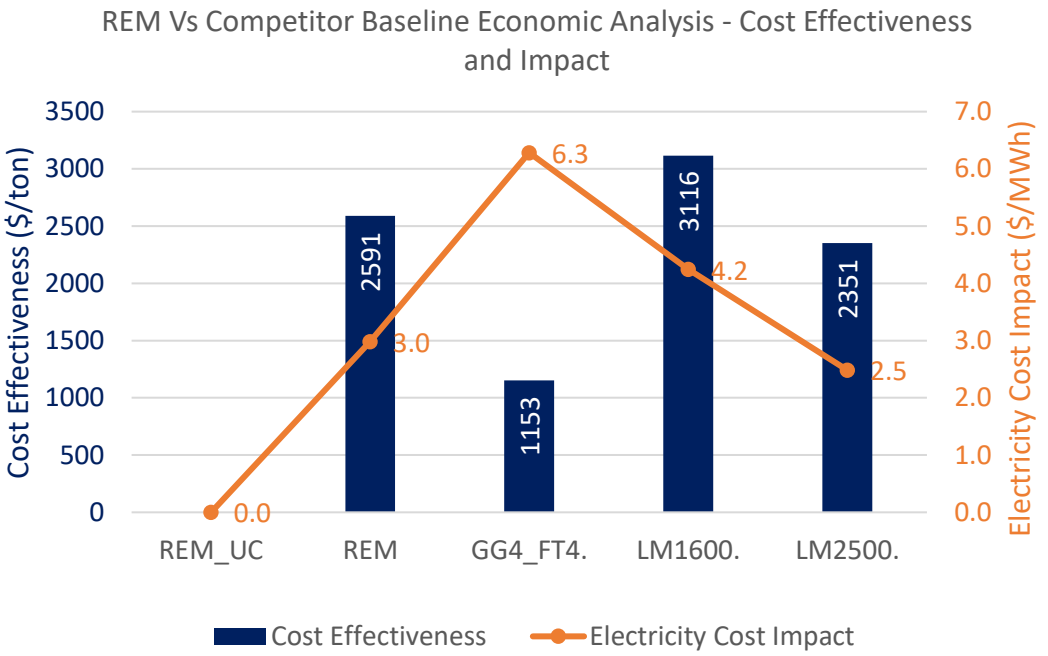

Figure 123: Baseline Economic Analysis - Cost Effectiveness and Electricity Cost Impact

Figure 123 relates the cost of owning the implemented emissions control technology with the amount of emissions removed. This evaluates to the cost effectiveness of the emission control technology. In general, the higher the cost effectiveness the less desirable the investment option. The cost effectiveness has been evaluated from Equation 70. In Figure 123, the cost effectiveness of the REM is 9% higher than that for the LM2500 and 55% higher than the GG/FT4. This is so because in relation to the owning cost, the amount of NOx removed annually is higher on the GG4/FT4 and the LM2500 than the REM. Figure 123 also provides information on the electricity cost impact of the emissions control for all considered engines.

This is the impact the cost of owning the implemented emissions control technology has over the electricity generated annually. The results show that the REM has an electricity cost impact 17% higher than the LM2500 and 53% lower than the GG4/FT4. In general, the higher the electricity cost impact of an option, the less desirable the option.

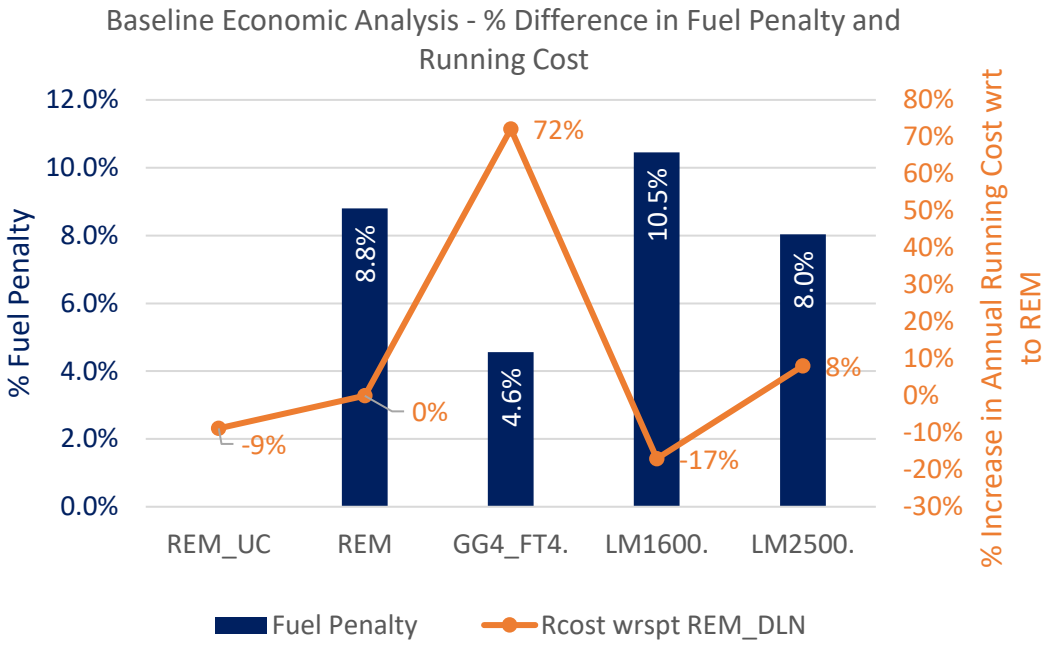

Figure 124: Baseline Economic Analysis - Fuel Penalty and Running Cost

Figure 124 presents the fuel penalty incurred due to the adopted emissions control on each unit considered. The REM incurs a 8.8% fuel penalty while the GG4/FT4 and LM2500 respectively incur a 4.6% and 8.0% fuel penalty. Although the REM incurs a higher penalty compared to the identified major competitor units, it incurs an annual running cost 72% lower than the GG4/FT4 and 8% lower than the LM2500 options. This suggests that even though there is a potential 8.8% increase in the REMs running cost due to fuel penalty, it is still cheaper to operate the REM than the main competitor units.

6.3.1.3 Return on Investment (ROI) and Break Even Point (BEP)

The return on investment quantifies the profitability of investing in any of the considered unit based on invested capital. Results plotted in Figure 125 and Figure 126 present the break-even point (BEP), the return on investment at break-even point and return on investment over the investigated planning Horizon for each engine investigated.

Results in Figure 125 reveal that in simple cycle application, the REM will break-even at 5year with a 22% ROI at break-even point and a 232% ROI over the investigated planning horizon (IPH). The LM2500 will break-even at 5years with 18% ROI at break-even point and a 227% ROI over the investigated planning horizon (IPH). The GG4/FT4 will break-even at 5years with a 22% ROI at break-even point and a 233% ROI over the investigated planning horizon (IPH).

Results in Figure 126 reveal that in combine cycle application, the REM will break-even at 5year with a 19% ROI at break-even point and a 228% ROI over the investigated planning horizon (IPH). The LM2500 will break-even at 5years with a 16% ROI at break-even point and a 224% ROI over the investigated planning horizon (IPH). The GG4/FT4 will break-even at 5years with a 20% ROI at break-even point and a 229% ROI over the investigated planning horizon (IPH).

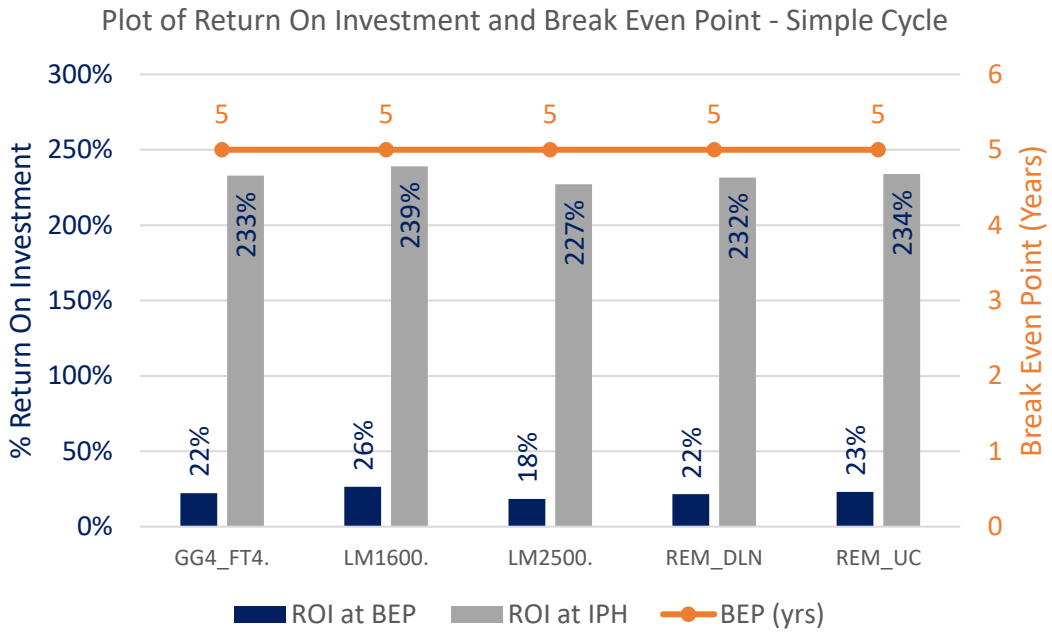

Figure 125: Return on Investment and Break Even Point - Simple Cycle

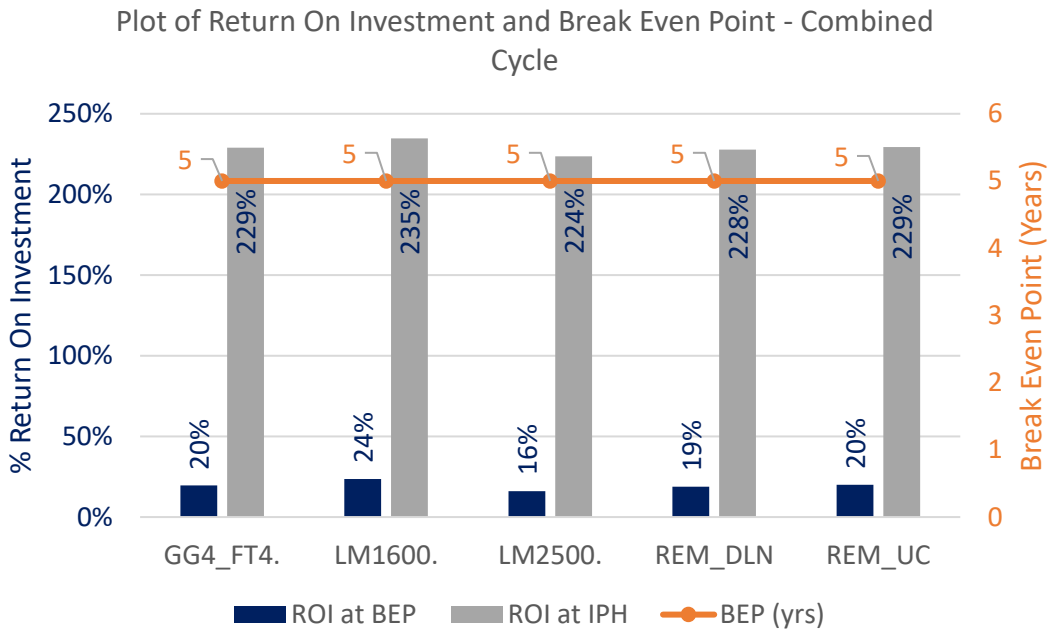

Figure 126: Return on Investment and Break Even Point - Combined Cycle

Observing that all considered options break-even within the same period with varying return on investments, the choice of most applicable investment option will have to include considerations of other factors like present worth, Investment base, running cost, emissions policy, sensitivity analysis e. t. c.

6.3.1.4 Sensitivity Analysis Results

Sensitivity analysis has been conducted on the REM to determine its sensitivity to changes in fuel price, Emission Tax rate and minimum acceptable rate of return (MARR). The After tax cash flow with inflation considered is used for the sensitivity analysis as this captures the effect of inflation over the planning horizon. The sensitivity analysis results are present below.

6.3.1.4.1 Sensitivity to Changes in Fuel Price

Since the GG4/FT4 model burns on fuel oil, its associated fuel price per litre is higher than for the other engine models, which run on natural gas. As such, the interpretation of sensitivity results obtained will be slightly different for the GG4/FT4 engine model.

In Figure 127, at fixed LCOE, as fuel price increases, NPV decreases. This reveals that for fuel prices approaching 0.37$/litre, LCOE will have to increase to maintain a positive NPV for the GG4/FT4 engine model. In relation to the engine models running on natural gas, for fuel prices approaching 1.50E-04$/litre, LCOE will have to increase to maintain a positive NPV. At higher fuel prices where NPV is negative, the required increase in LCOE to obtain a positive NPV is lower for the REM investment option than competitor units. The LM2500 and GG4/FT4 engine model show a higher sensitivity to changes in fuel price than the REM. These observations are consistent in both simple and combined cycle applications.

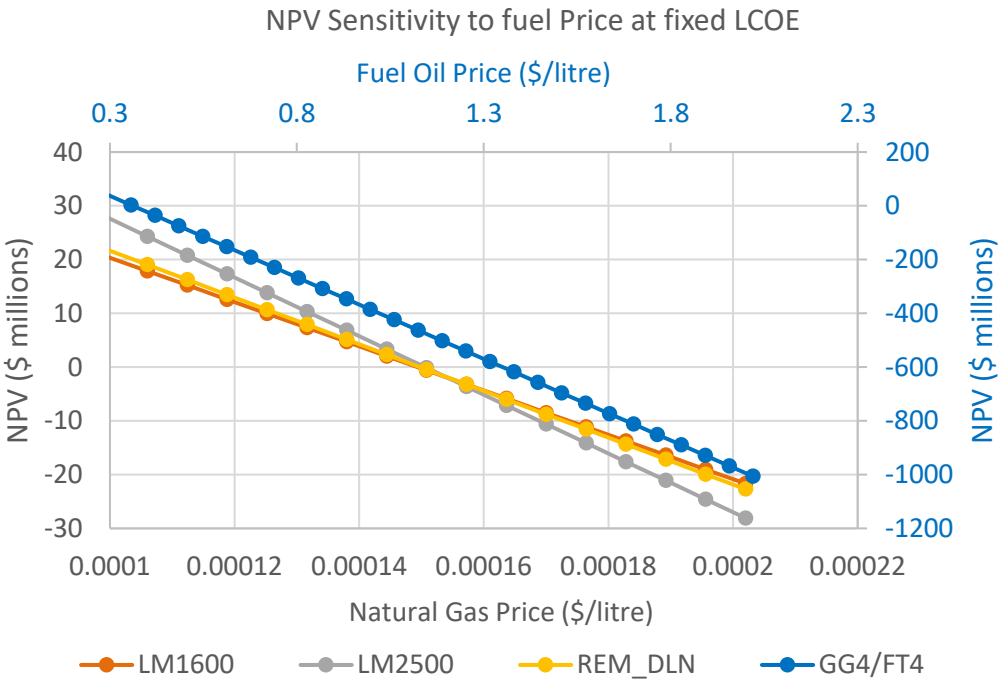

Figure 127: NPV Sensitivity to fuel price at constant LCOE

6.3.1.4.2 Sensitivity to Changes in MARR

Results obtained in Figure 128 and Figure 129 show the sensitivity of the REM investment option to changes in MARR. Increasing the minimum acceptable rate of return, MARR, reduces the NPV. However, the REM option remains profitable up to a MARR of 14% in simple cycle operation and 13% in combined cycle operation. Furthermore, results reveal that at MARR values higher than 13.8%, the REM investment option delivers higher NPVs than the LM2500 and GG4/FT4 engine models, in simple cycle application. In combined cycle, at MARR values higher than 12.5%, the REM delivers higher NPV than the LM2500. The NPV of the GG4/FT4 model remains slightly higher than the REM in this case. Results in both investigations indicate that the NPV of LM2500 and the GG4/FT4 engine models are more sensitive to changes in MARR.

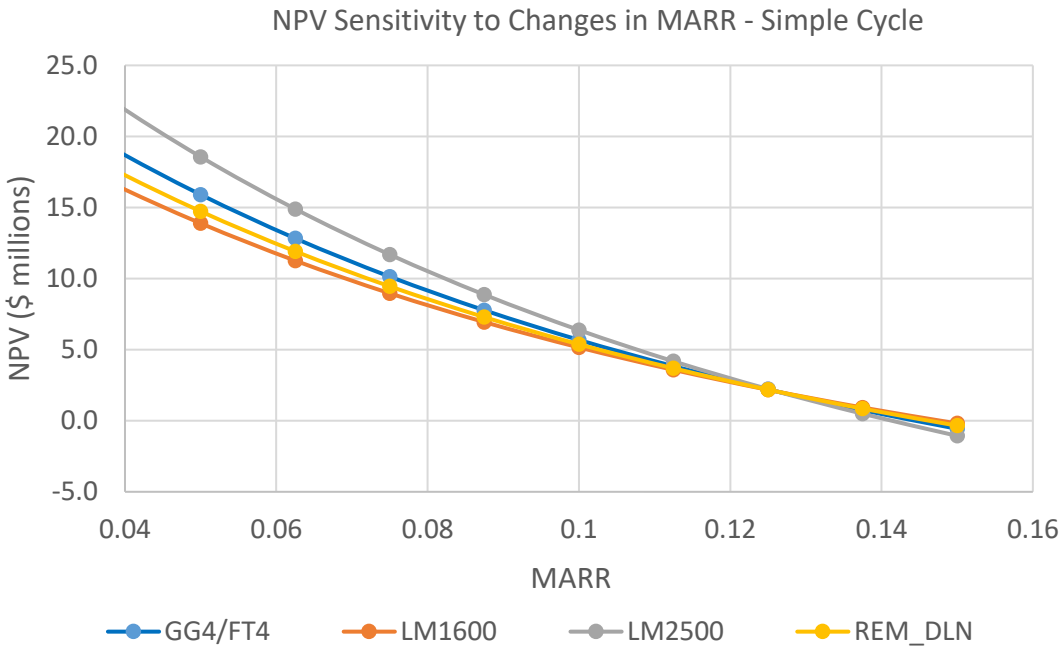

Figure 128: NPV Sensitivity to MARR in Simple Cycle Operation

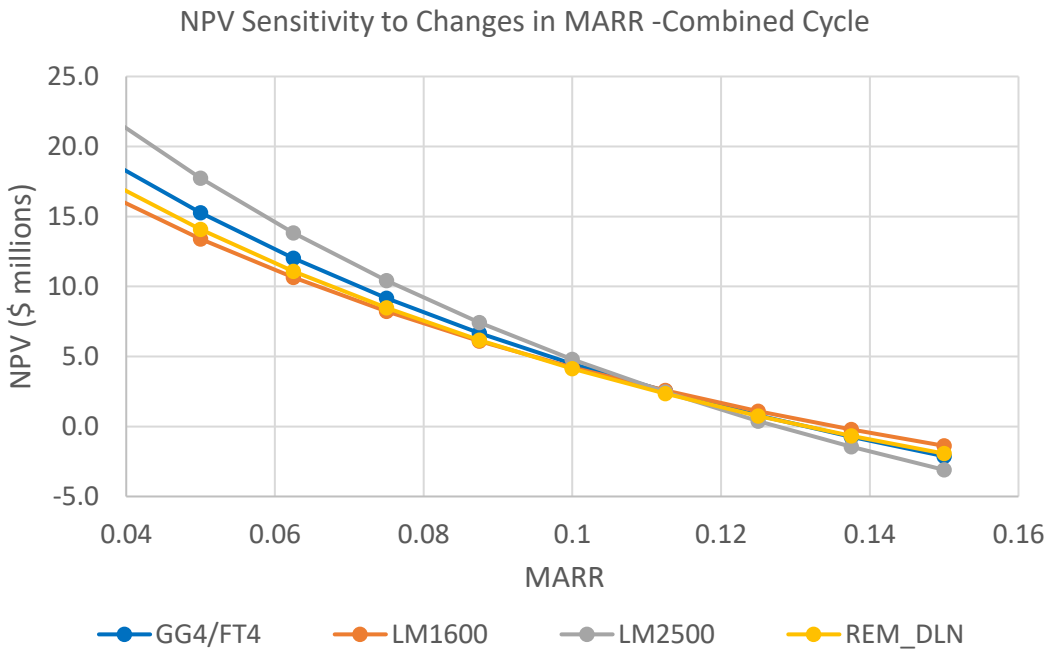

Figure 129: NPV Sensitivity to MARR in Combined Cycle Operation

6.3.1.4.3 Sensitivity to Changes in Emissions Tax rate

In order to investigate the sensitivity of the REM to any potential future changes in policy requiring the taxation of NOx emissions, sensitivity analysis has been conducted. Results obtained in Figure 130 and Figure 131 reveal that as emissions tax increase, NPV of the engine models decrease. The NPV of the GG4/FT4 engine model shows a very high sensitivity to emissions tax rate at a rate of 2% for every 10$ rise or fall in emissions tax. All other engine model show lower sensitivity at a rate of 1% for every 10$ rise or fall in emissions tax. At emission tax rates above 72$/ton, the NPV of the GG4/FT4 investment option falls below that of the REM.

Upon observing the steep nature of the slopes in Figure 130 and Figure 131, it can be deduced that the REM investment option is less sensitive to changes in emissions tax rate in

comparison to the GG4/FT4 investment option but shares identical sensitivity, with the other engine models, to changes in emissions tax rates. This observation is consistent in both simple and combined cycle applications.

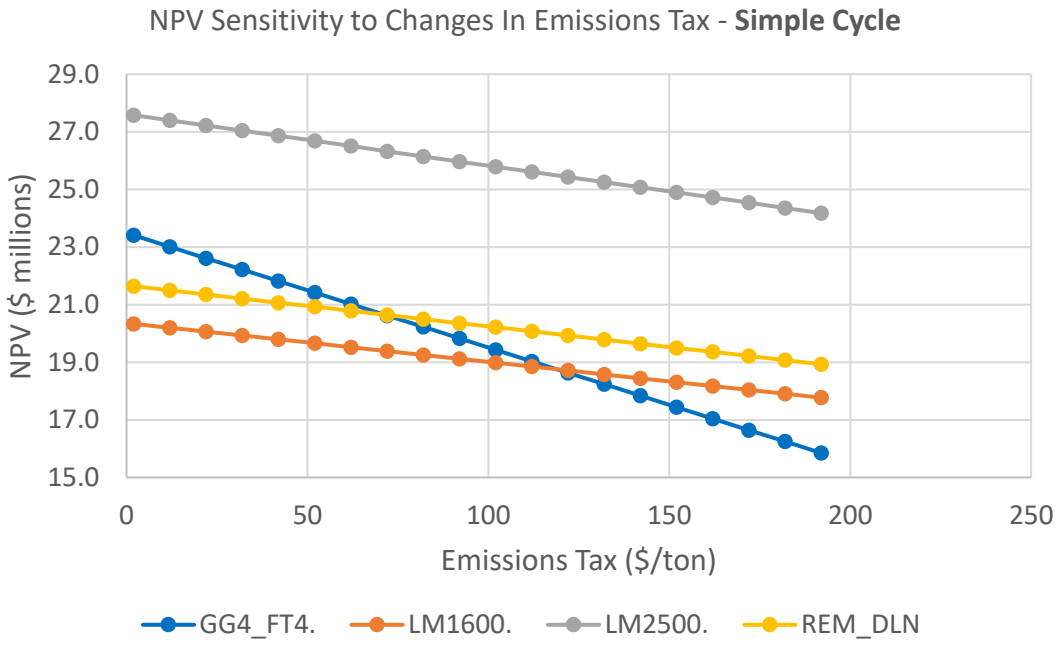

Figure 130: Sensitivity to Emissions Tax - Simple Cycle Operation

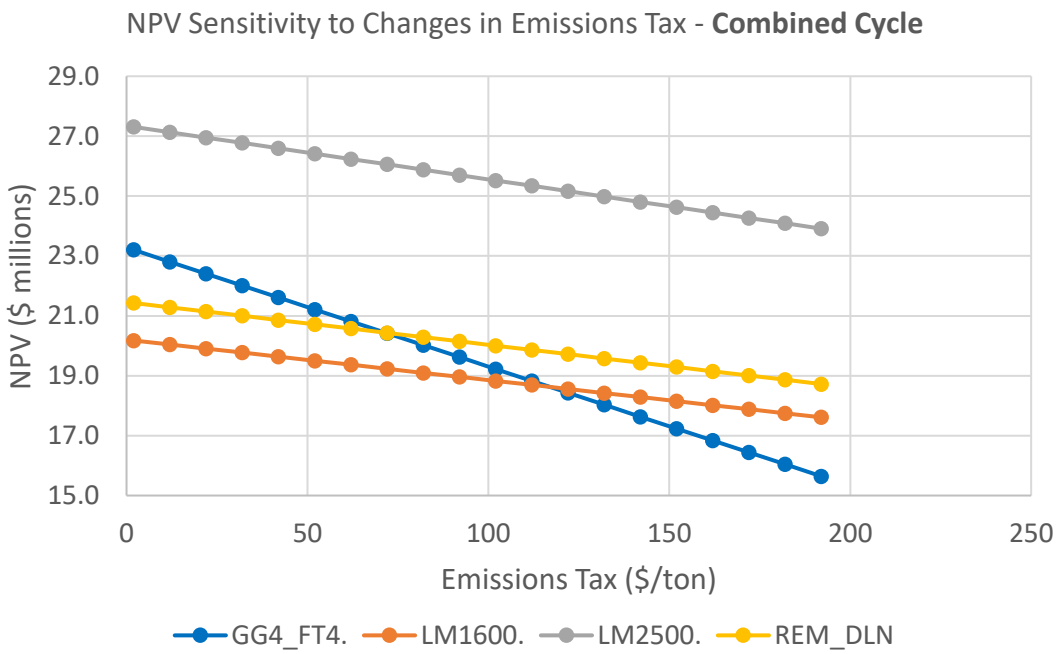

Figure 131: Sensitivity to Emissions Tax - Combined Cycle Operation

6.3.1.5 Desirability Matrix/ Grading System

A desirability grading system has been developed and applied to score each engine unit considered based on a set of desirable criteria. This system guides engine selection from a range of graded desirable characteristic. It also provides a quick summary of the most favourable results obtained from the techno-economic analysis of all engines considered.

Table 22 shows the grading matrix. Each considered engine criteria is assigned a value between zero and three. Zero being the least desired and three the most desired. The total

for each engine model is expressed as a percentage score. Figure 132 presents the desirability scores for the considered units.

Results reveal that the LM2500 is the most desirable option from the techno-economic analysis conducted with a desirability score of 59%. The desirability of the repurposed engine model (REM) and the GG4/FT4 engine model evaluate to a score of 52%, making them the second most desirable option from the investigation. The LM1600 is the least desirable option with a desirability score of 48%. The grading system and grading criteria is in no way the ultimate evaluation of desirability or feasibility of an investment option. It only functions as a guide for informed decision making, which is influenced by a number of technical, environmental, economic, social and even cultural variables.

Table 22: Desirability Grading Matrix

DESIRABILITY GRADING SYSTEM											
			Least Desired						Most Desired		
			0	1	2	3					
ENGINE	COST EFF.	COST IMPACT	RUNNING COST	FUEL PENALTY	NPV	IB	LCOE	% NOx Removed	ROI	TOTAL	SCORE
REM	1	2	2	1	2	1	2	2	1	14	52%
GG4/FT4	3	0	0	3	1	2	0	3	2	14	52%
LM1600	0	1	3	0	0	3	1	2	3	13	48%
LM2500	2	3	1	2	3	0	3	2	0	16	59%

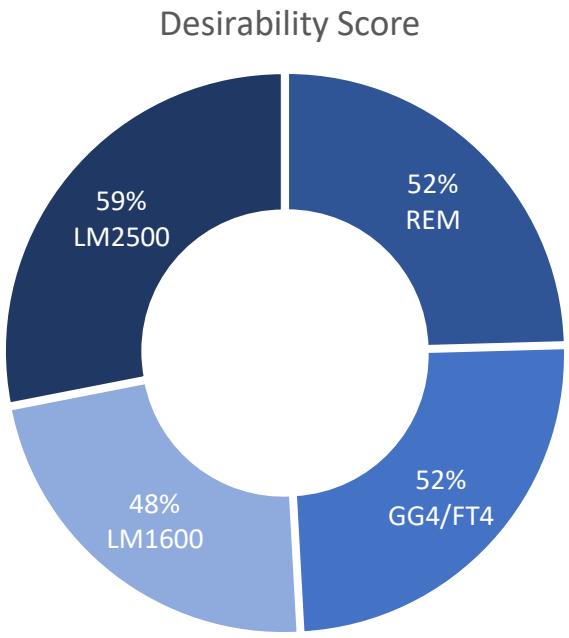

Figure 132: Desirability Score - Baseline Analysis

Based on the techno-economic analysis conducted, assumptions made and results obtained from this investigation, it is feasible to apply the repurposed engine model for electrical power generation from a performance and economic perspective. Although with some shortcomings and limitations, results obtained have revealed that the repurposed engine model (REM) can favourably compete, from an economical and performance perspective, with the considered competitor units.

6.3.2 Effect of engine degradation on Techno-economic analysis

This section presents the results from investigations on the influence of engine component deterioration on techno-economic analysis. The repurposed engine model has been used as the case study unit for this investigation. The assumptions made in relation to the conducted investigation are outlined in section 5.3.1.1.1 and 5.3.1.1.2.

6.3.2.1 Effect of Engine Degradation on Present Worth and LCOE

Figure 133 and Figure 134 present the result obtained from analysis conducted to investigate the effects of degradation on engine Techno-economics. In comparison to the clean engine, degradation results in an increase in NPV and LCOE. This rise in NPV is the result of a 13% increase in LCOE required to sustain the profitability of the investment when running a degraded unit. The LCOE increase eventually results in a 26% rise in NPV at the end of the unit productive life.

In comparison to the clean case, the introduction of engine washing to maintain unit performance output over longer operating period reveals a 0.48% drop in NPV and a 0.62% rise in LCOE. This suggests that it will cost less to implement engine washing (both online and offline washing) than to run the engine in a degraded state over the engines productive life. Figure 137 and Figure 138 further emphasise the effects of the implanted degradation on the engines operation and maintenance cost. This observation is consistent in both simple and combined cycle investigations. Table 23 shows the implemented engine washing parameters.

Table 23: Engine Washing Parameters

	Cost per Wash ($/kW)	Washing Interval (hours)	Duration of Wash (hours)	Drop in Fuel flow (%)	Drop in Power (%)
Online	1.140	4000	8	30	60
Offline	4.570	12000	24	100	100

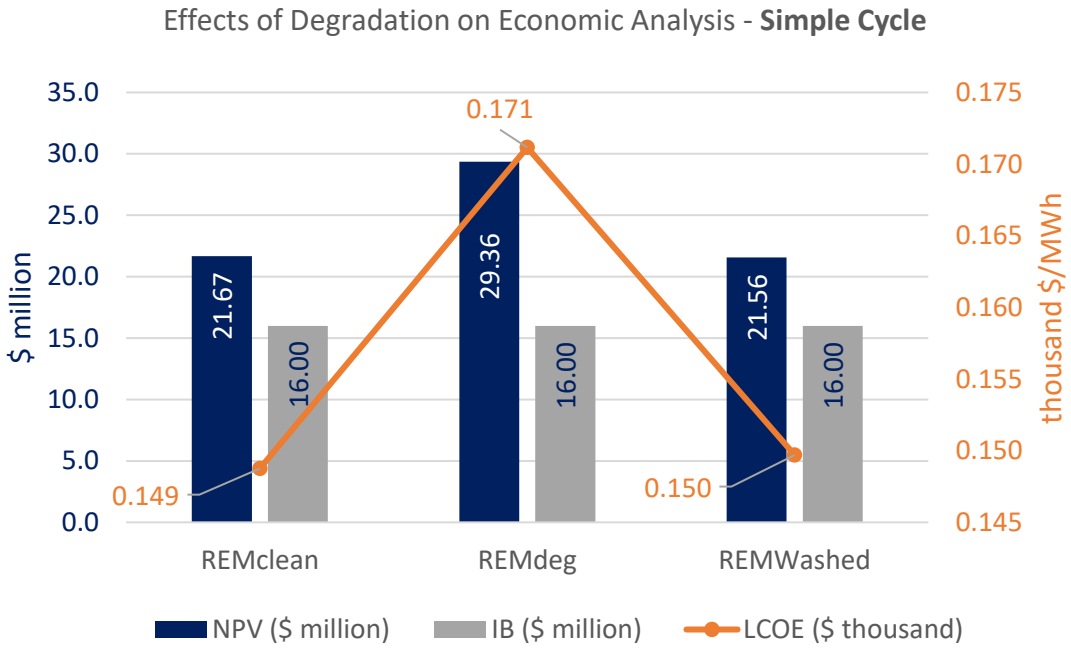

Figure 133: Effects of Engine Degradation on Economic Analysis - Simple cycle Application

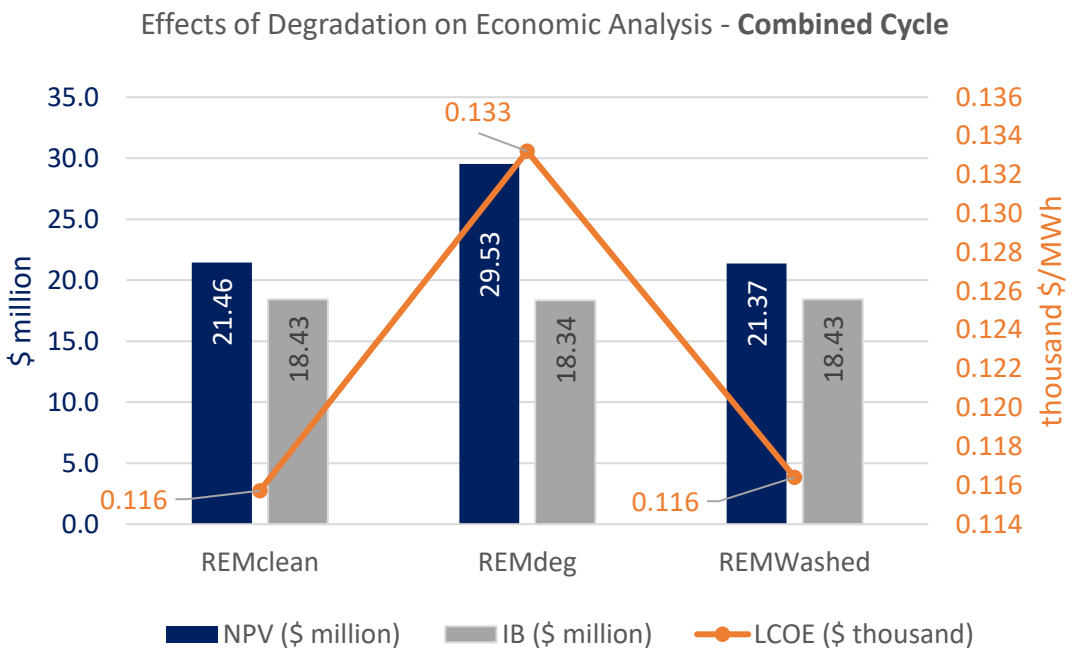

Figure 134: Effects of Engine Degradation on Economic Analysis - Combined Cycle Application

6.3.2.2 *Effect of Degradation on Emissions*

Figure 135 and Figure 136 present results on the effects of engine model deterioration on emissions. With the degraded engine model, less NOx is removed in comparison to the amount of NOx generated. This is because of the increased fuel flow into the combustor required to compensate for the fall in mass flow due to compressor degradation. Furthermore, the rise in engine exhaust temperature, due to turbine degradation or the overall effect of component deterioration, suggests that more NOx is released into the atmosphere than is controlled.

With the washed case, the level of NOx removal is identical to the clean case. This implies that engine washing contributes positively to the effort in minimising NOx emissions on the repurposed engine model.

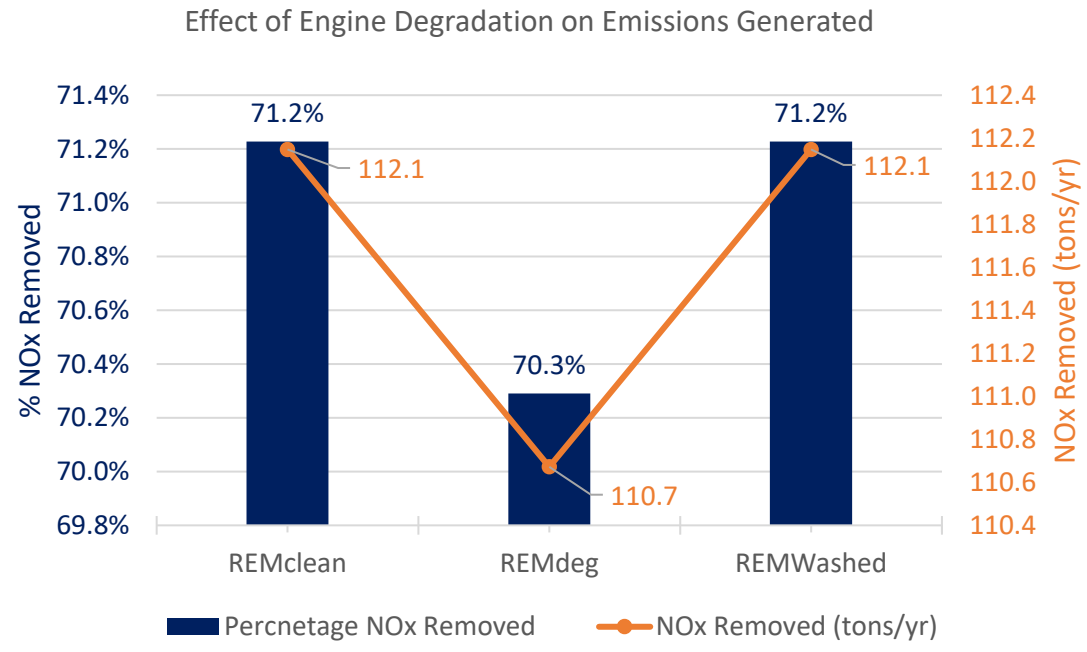

Figure 135: Effects of Engine Degradation on Emissions Generated

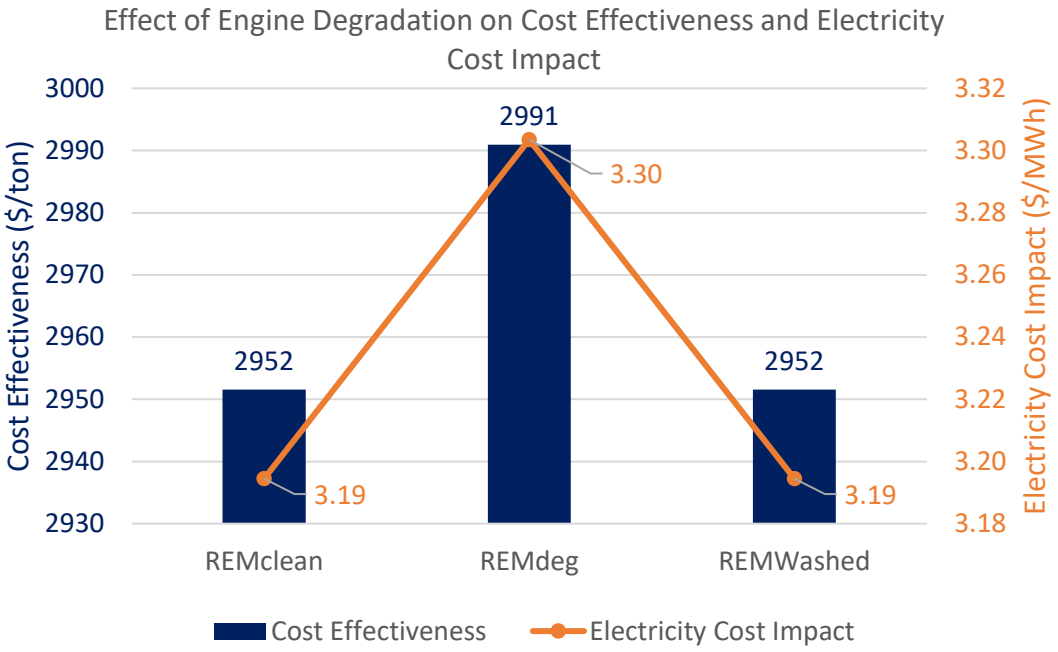

Figure 136: Effects of Engine Degradation on Cost Effectiveness and Electricity Cost Impact

In Figure 136, the degraded case has a higher cost effectiveness, which implies that with respected to the implemented emissions control technology, it is more expensive to control emissions in the degraded case than in the clean or washed case. Furthermore, due to the fall in power generated, the degraded case has a greater impact on the cost of electricity.

6.3.2.3 Effect of Degradation on Cost

In Figure 137 and Figure 138, engine degradation result in a 2.7% increase in annual running cost and a 7.4% increase in annual operation and maintenance (O&M) cost. With engine washing, annual running cost and O&M cost increase respectively by 01% and 0.5% in both simple and combined cycle investigations. This suggests that the implementation of engine washing to sustain unit performance will only increase operating costs by less than 1%. This observation is consistent for both simple and combined cycle investigations.

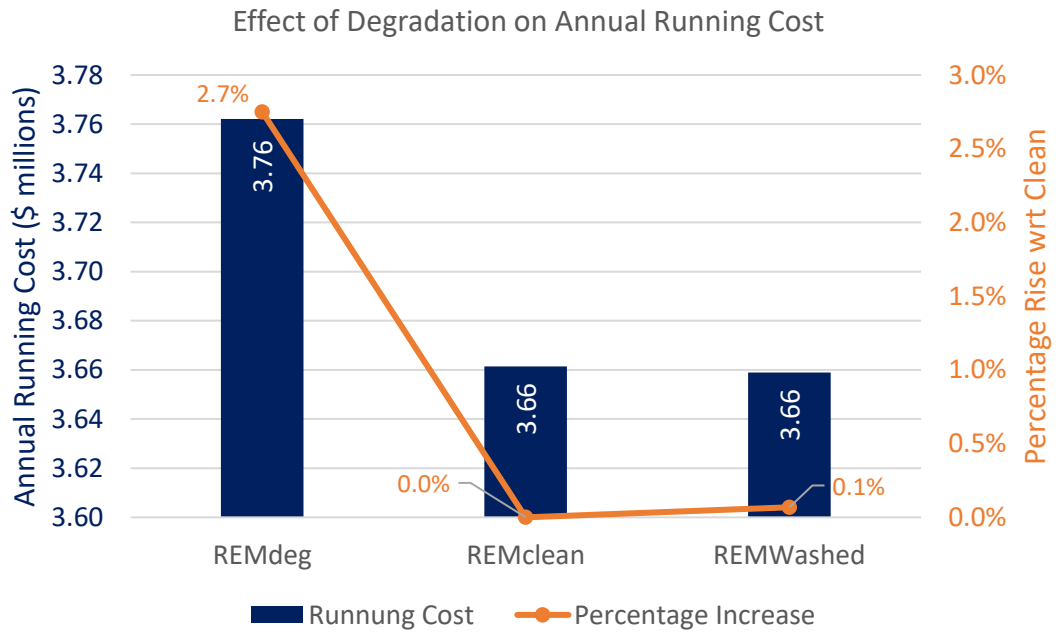

Figure 137: Effect of Engine Degradation on Running Cost

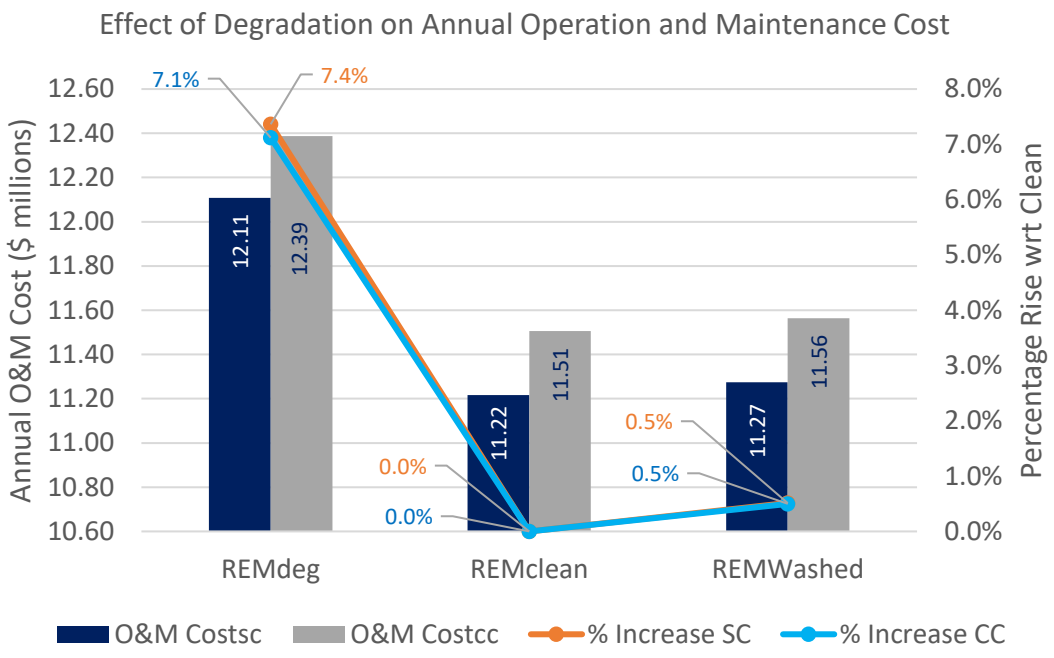

Figure 138: Effect of Degradation on Annual Operation and Maintenance Cost

6.3.2.4 *Effect of Degradation on Return on Investment (ROI) and Break Even Point (BEP)*

In comparison to the clean case, the degraded engine scenario will break even at 4years with 17% return on investment at break-even period and 315% return on investment over the investigated planning Horizon. This seemingly beneficial result is realised because of the increased LCOE in the deteriorated case. The LCOE increases in order to ensure and sustain profitability over the investigated planning Horizon. However, the increase translates into higher cost of electricity for consumers.

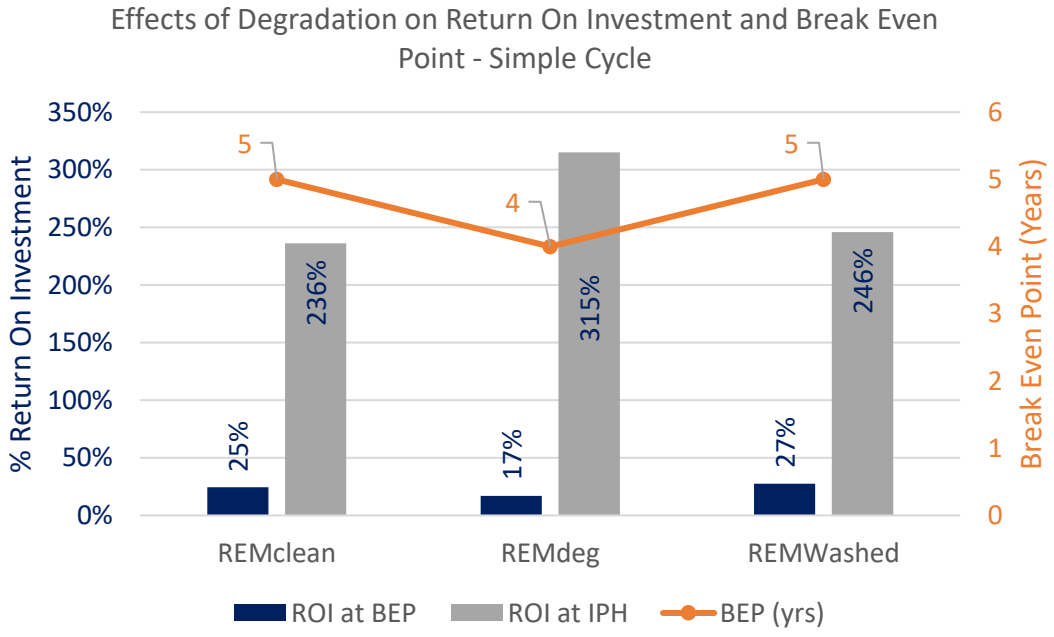

Figure 139: Effects of Degradation on Return on Investment and Break Even Point - Simple Cycle

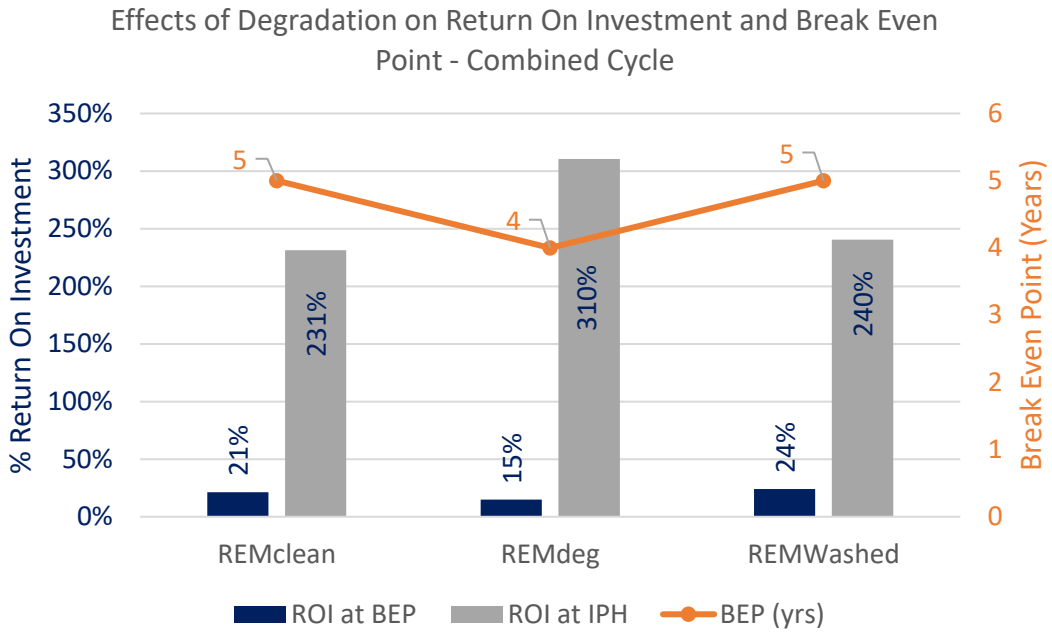

Figure 140: Effects of Degradation on Return on Investment and Break Even Point - Combined Cycle

The clean and washed case break-even at 5years with 25% and 27% ROI at break-even period, and 236% and 246% ROI at the investigated planning Horizon, in simple cycle investigations. Though the clean and washed case deliver lesser ROI over a longer period, they provide the benefit of lower LCOE and operating costs in comparison to the deteriorated case. This is consistent with outcomes from the combined cycle investigation.

6.3.3 Influence of Transient Operation on gas turbine Techno-economics

Results from investigation into the effect of engine transient operation on techno-economics are presented in this section. The repurposed engine model transient simulation results (presented in section 6.1.6) have been used for this investigation. The engine model variant burning fuel oil has been used for this investigation to amplify the effects of fuel consumption and transient operation, which are greater in this variant. Additional input parameters used for the investigation are shown in Table 24.

Table 24: Additional Transient Input Parameters

Regime	Duration (s)	Cycles
Start Up	600 (10mins)	30
Shut Down	600 (10mins)	30

It is assumed that the engine in this scenario undergoes frequent start and stop cycles up to 30 cycles per year. The total engine transient duration for each cycle lasts 20mins.

6.3.3.1 Effect of transient operating regime on Present worth and LCOE

Figure 141 and Figure 142 reveal that there is no significant change in the NPV and LCOE between the engine model analysis with and without transient operation considered. This is so because of the little effect that transient operation has on the cost of operating a gas turbine engine and hence is often ignored in economic analysis. However, the economic model developed in this study enables transient evaluation for economic analysis involving

standby engines or other class of engines operating in extremely unusual circumstances where the effect of transient duration is magnified. The inclusion of transient evaluation in this study also envisions future extension of the model to aero engine techno-economic analysis, which may experience greater transient operating regimes.

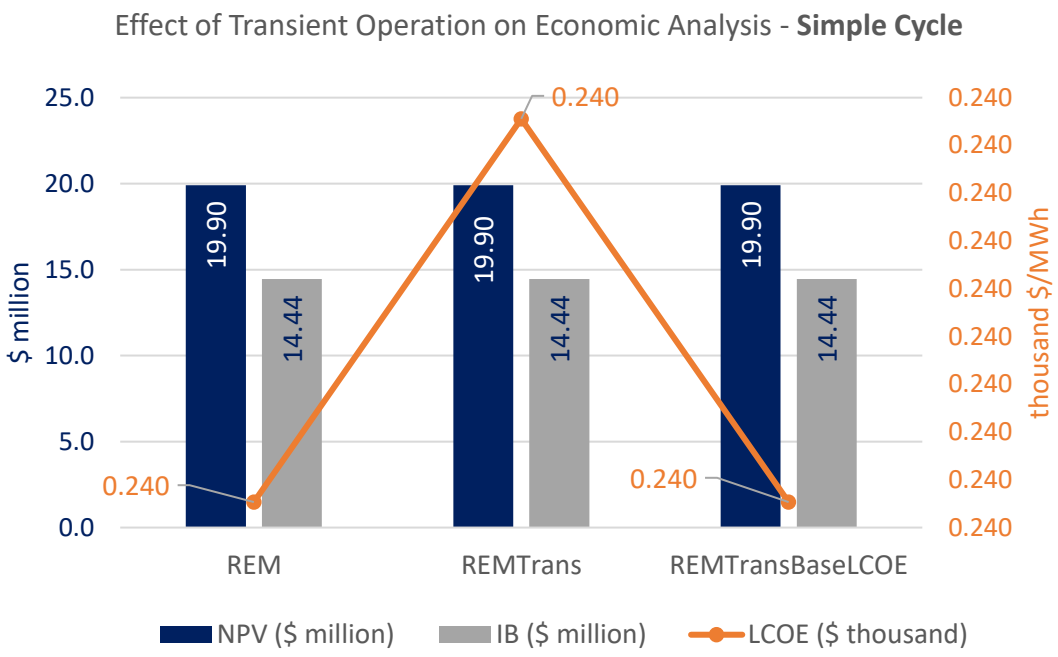

Figure 141: Effect of Transient Operation on Economic Analysis - Simple Cycle

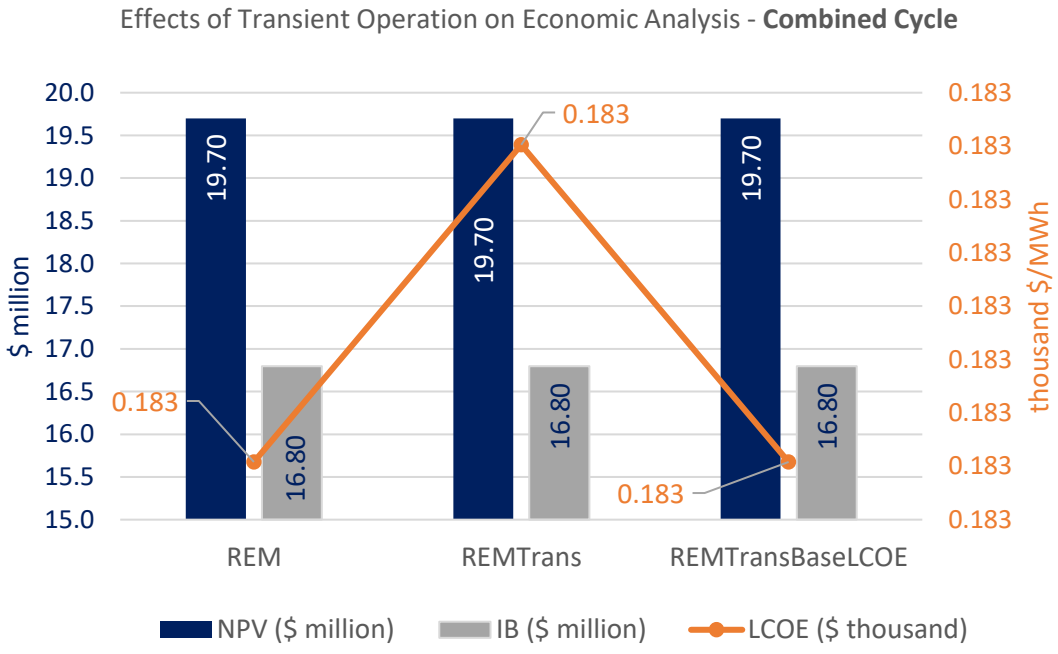

Figure 142: Effects of Transient Operation on Economic Analysis - Combined Cycle

6.3.3.2 *Effect of transient operating regime on Emission*

Similar to its effect on present worth and LCOE, the repurposed engine models transient operating regime has an insignificant effect on the amount of emissions generated and removed (Figure 143). One reason attributable to this is that in relation to the considered 6000 hours of normal engine operation per year, the transient operating regime, for the considered scenario only last for 600 minutes (10 hours) per year. This is less than 1 percent (about 0.2%) of normal engine-operating period per year. Hence, the quantity of fuel burnt

during the few hours of the transient operating regime is very small. Figure 143 and Figure 144 show the effects of transient operation on emissions. The cost effectiveness and electricity cost impact remain the same with or without considering the effects of the engines transient operation regime.

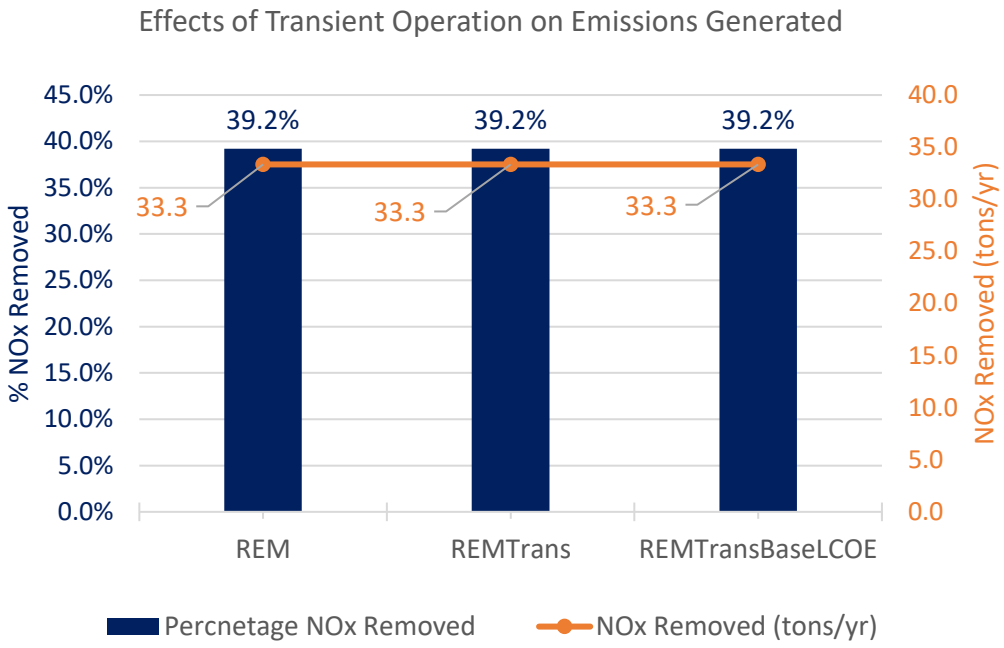

Figure 143: Effects of Transient Operation on Emissions Generated

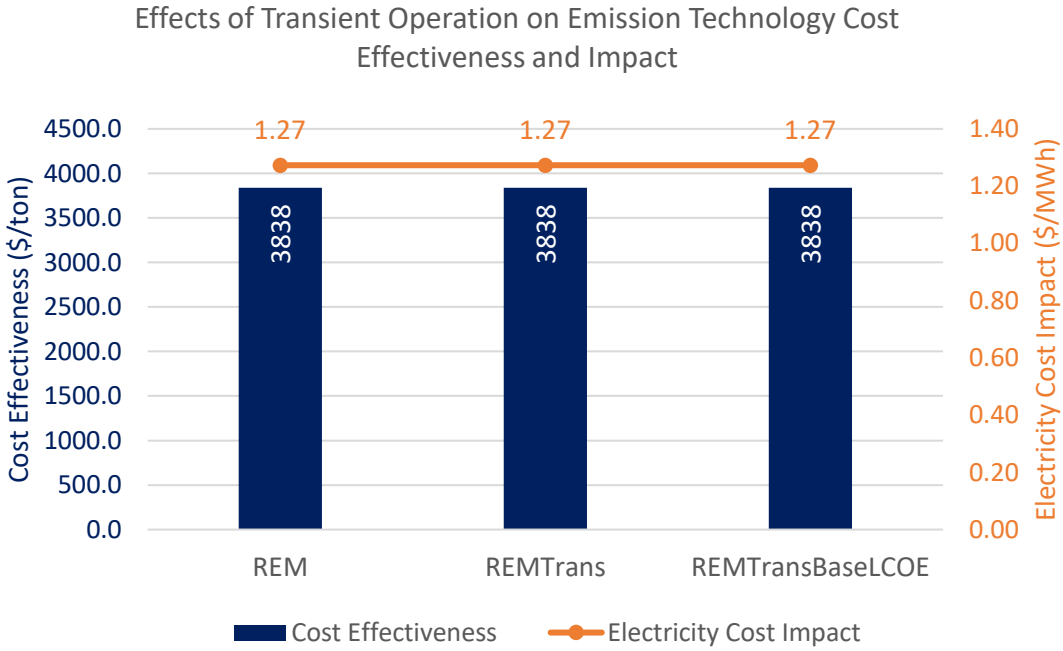

Figure 144: Effects of Transient Operation on Cost Effectiveness and Electricity Cost Impact

6.3.3.3 Effect of transient operating regime on Cost

Figure 145 and Figure 146 reflect the effects of the transient operating regime on running and operating cost. Though very little, transient operation results in a 0.03% increase in running cost and a 0.02% increase in operation and maintenance cost in both simple and combined cycle investigations.

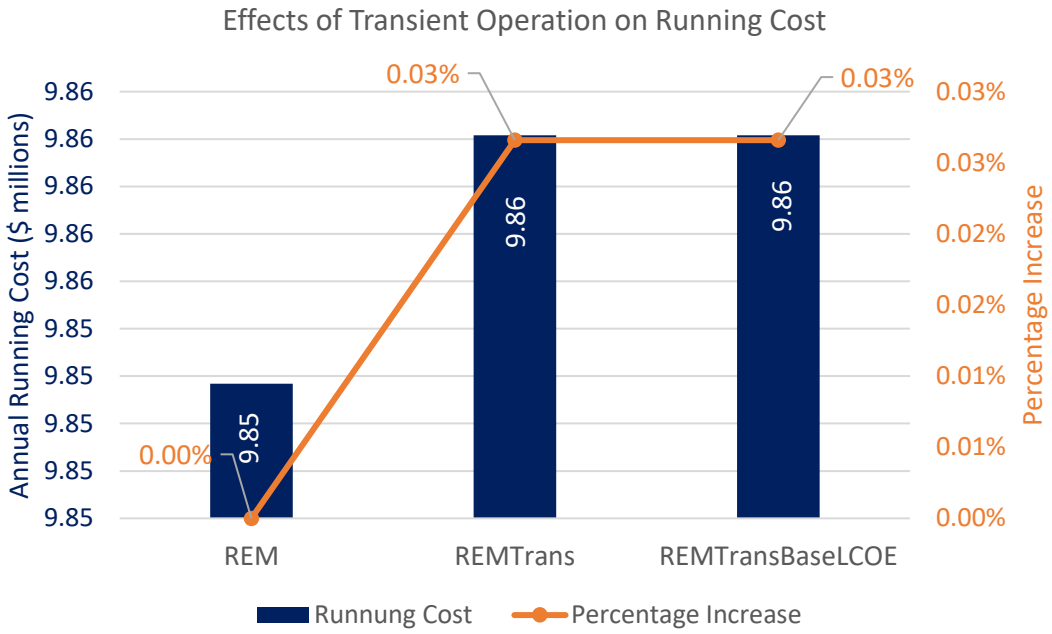

Figure 145: Effects of Transient Operation on Annual Running Cost

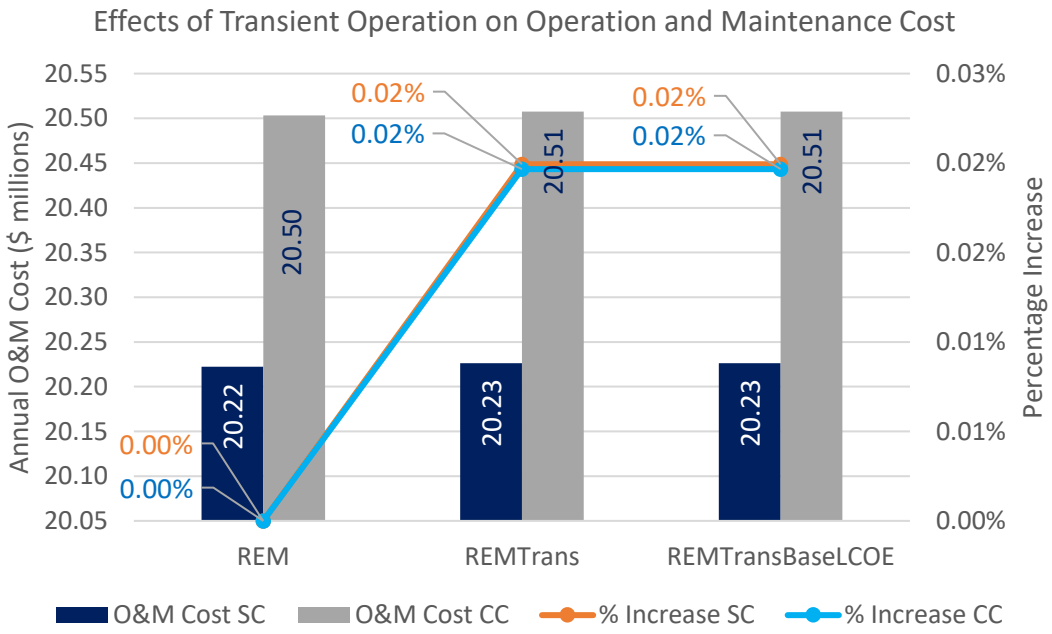

Figure 146: Effects of Transient Operation on Operation and Maintenance Cost

6.3.3.4 *Effect of transient operating regime on Return on Investment (ROI) and Break Even Point (BEP)*

The repurposed engine models transient operating has no significant effect on return on investment and break-even point over the investigated horizon. This is due to similar reasons described in section 6.3.3.1 and section 6.3.3.2.

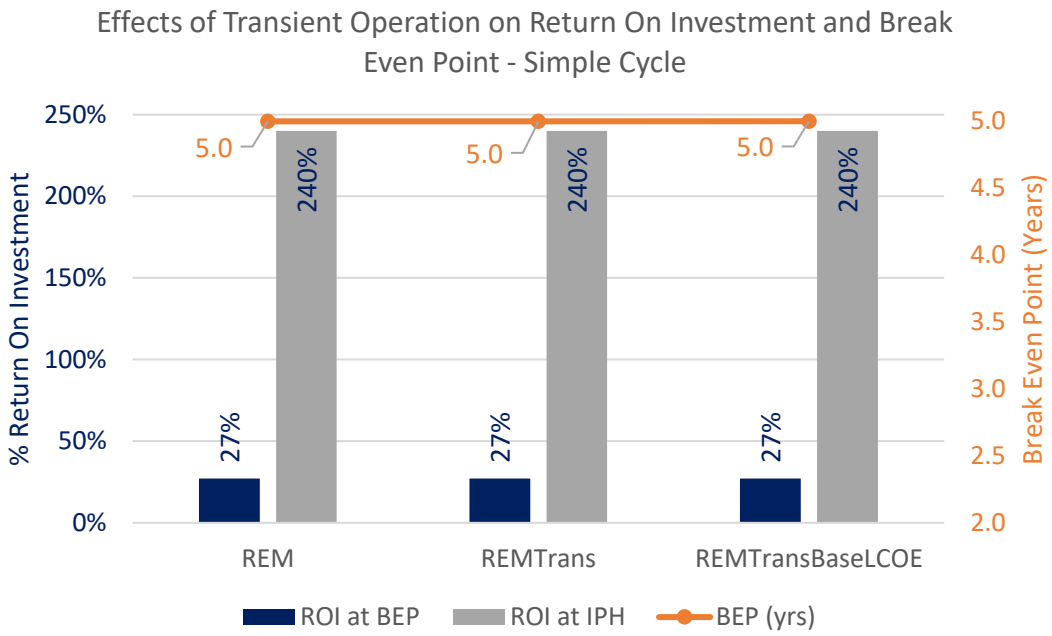

Figure 147: Effects of Transient Operation on Return on Investment and Break Even Point - Simple Cycle

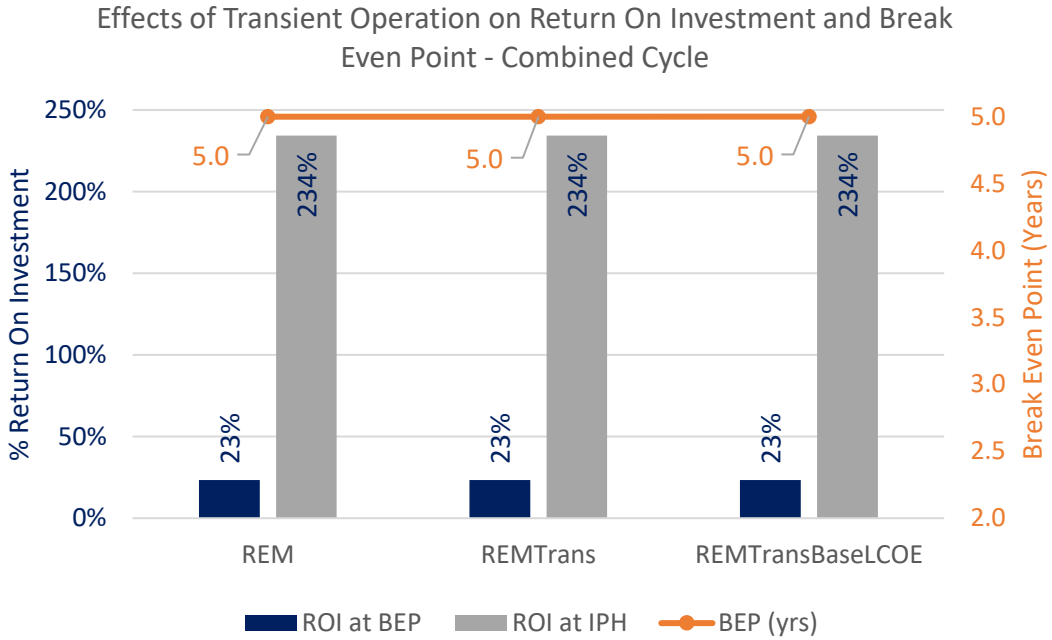

Figure 148: Effects of Transient Operation on Return on Investment and Break Even Point - Combined Cycle

In summary, the investigated transient operating regime has no significant effect on the techno-economics of the considered repurposed engine model.

6.3.4 Effects of power cycling on engine economics

Investigation into the effects of power cycling on gas turbine economics has been conducted. The repurposed engine model has been used for this investigation. Result from the investigation are presented in this section. The following assumptions have been adopted to validate this investigation.

- Engine operates 6000 hours annually.
- Engine power output is cycled 3 times a day over the duration of annual operation.
- Each cycling period respectively operates at 80%, 30% and 50% generating capacity (Table 25).

Table 25: Power Cycling Input Parameters

Operating Period	Generating Capacity (%)	Duration per year (hours)
Period A	80	2000
Period B	30	2000
Period C	50	2000

6.3.4.1 Effect of Engine Power Cycling on Present Worth and LCOE

Figure 149 and Figure 150 show that at baseline LCOE, power-cycling results in a 26% decrease in NPV, in both simple and combined cycle, over the engine's productive life. In order to match the NPV of the uncycled engine model, LCOE will have to increase by 26% in simple cycle and combined cycle applcations. This is so because in the power-cycled engine, the total power generated per year reduces and so does the amount of electricity sold based on generated power. Due to this decrease in generated power, the penalty incurred will, translate into a fall in benefits from power sold or a rise in the levelized cost of energy (LCOE) sold to consumers. The latter tends to push the burden of power cycling to consumers in form of increased cost while the former pushes the burden to operators as a fall in projected profit and an increase in maintenance cost.

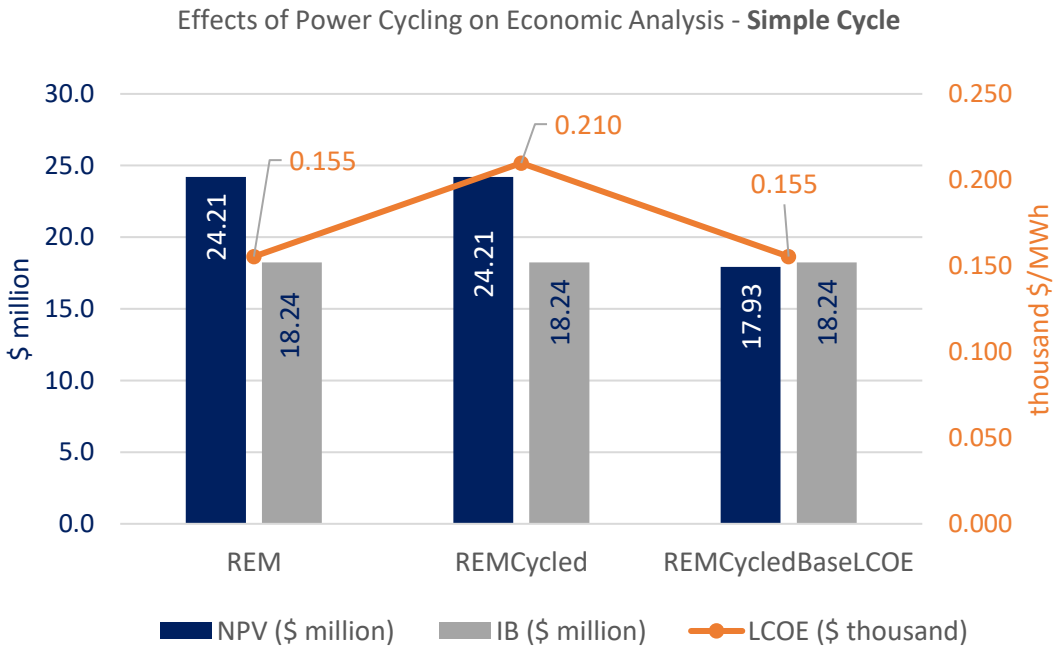

Figure 149: Effects of Power Cycling on Economic Analysis - Simple Cycle

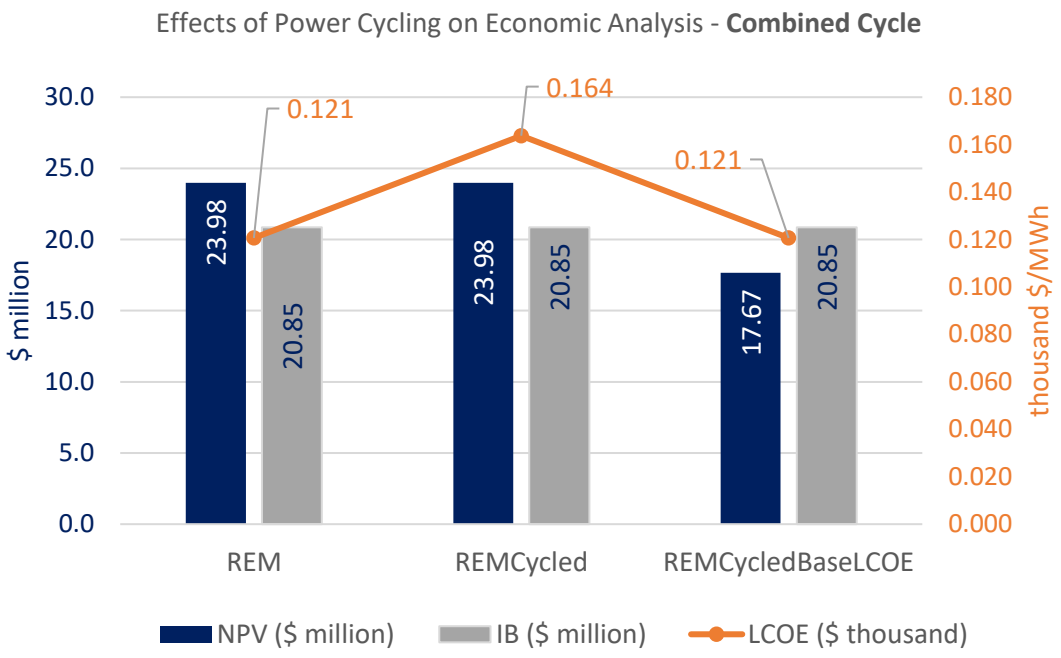

Figure 150: Effects of Power Cycling on Economic Analysis - Combined Cycle

6.3.4.2 *Effect of engine power cycling on Emissions*

Results in Figure 151 and Figure 152 reveal that greater amount of NOx is removed in the power-cycled engine in comparison to the uncycled engine. This is because in relation to the amount of NOx generated, the amount of NOx removed increases with power cycling. This is consistent for both simple and combined cycle investigations.

In Figure 152, the power-cycled engine has a lower cost effectiveness. This indicates that it costs less to control emissions in the power-cycled engine than in the uncycled engine. However, at baseline LCOE, the power-cycled engine has a greater impact on the cost of electricity.

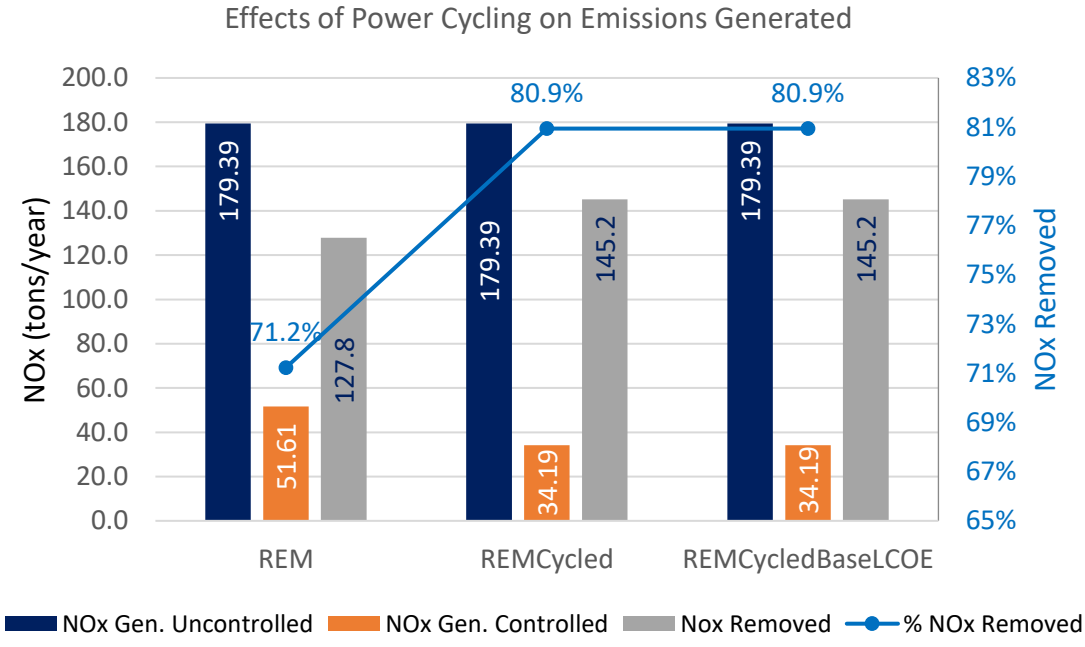

Figure 151: Effect of Engine Power Cycling on Emissions Generated

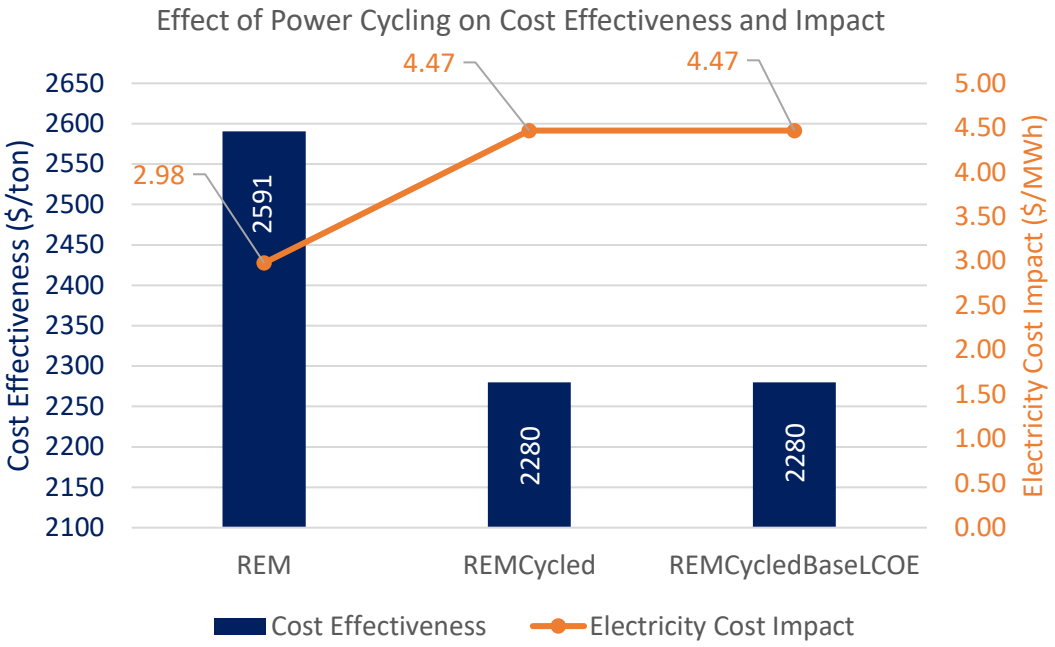

Figure 152: Effect of Engine Power Cycling on Cost Effectiveness and Electricity Cost Impact

6.3.4.3 *Effect of engine power cycling on Operating Costs*

Results shown in Figure 153 and Figure 154 reveal that power cycling of the repurposed engine model lowers the annual running cost and annual operation and maintenance cost. This is because at lower power setting the engine model burns less fuel to meet the required power demand. The amount of fuel consumed by a gas turbine is a major driving factor of cost. Thus, any reduction in the fuel consumed usually translates to a noticeable reduction in operation and maintenance cost. However, the magnitude of potential benefit attainable from a reduction in cost is to some degree, intercepted by a reduction in the power generated and sold with the power-cycled engine.

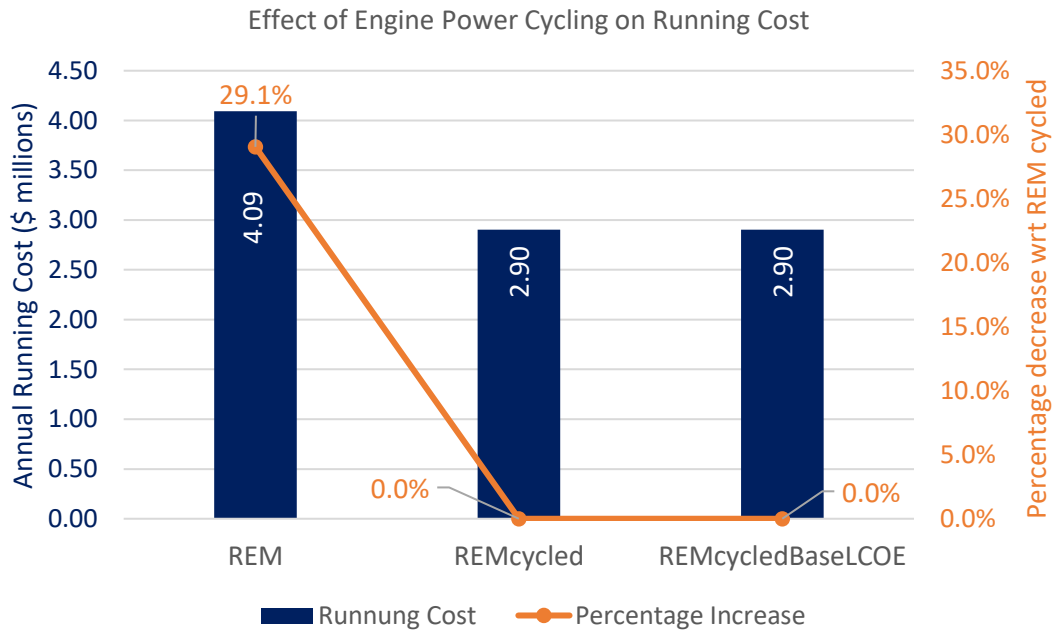

Figure 153: Effect of Engine Power Cycling on Running Cost

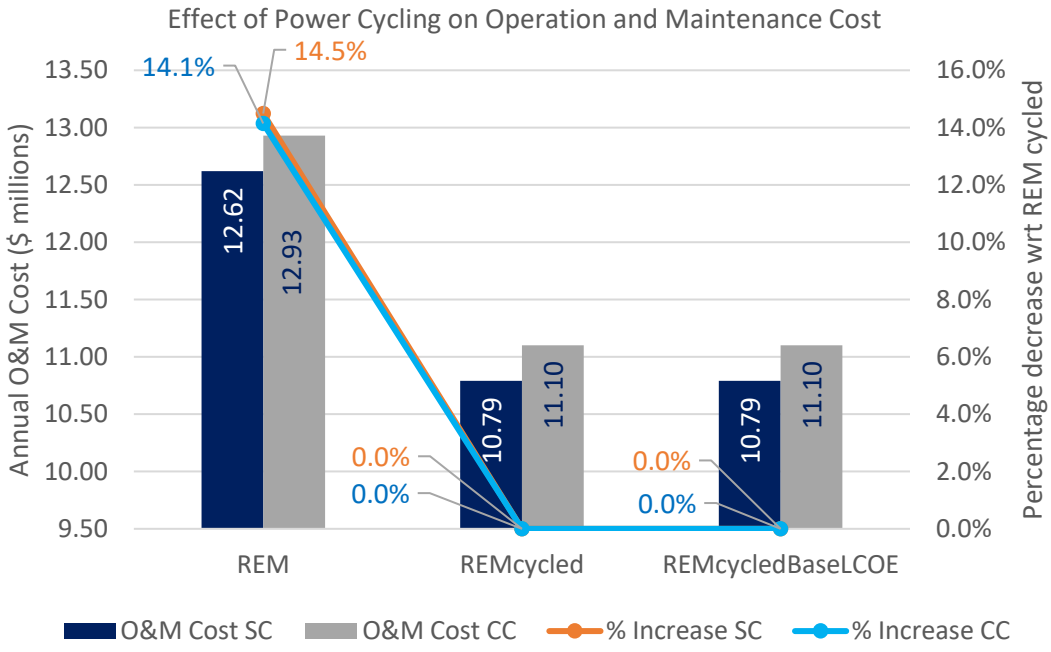

Figure 154: Effect of Power Cycling on Operation and Maintenance Cost

6.3.4.4 *Effect of engine power cycling on Return on Investment (ROI) and Break Even Point (BEP)*

In Figure 155 and Figure 156, at an increased LCOE, the power cycled engine model will break even at 5 years with an ROI of 22% at BEP and 232% at IPH. This is similar to the BEP and ROI for the uncycled engine. However, at baseline LCOE, the power-cycled engine will break even at 6.7years with lesser return on investment of 16% at BEP and 172% at IPH. Similar observations are identified in both simple and combined cycled investigations.

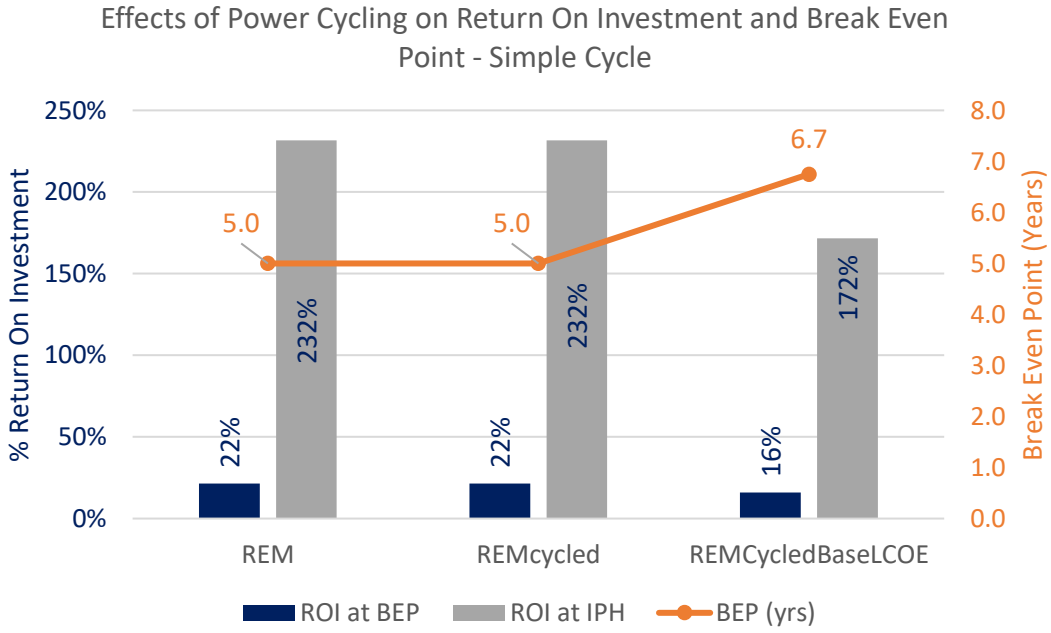

Figure 155: Effects of Power Cycling on Return on Investment and Break Even Point - Simple Cycle

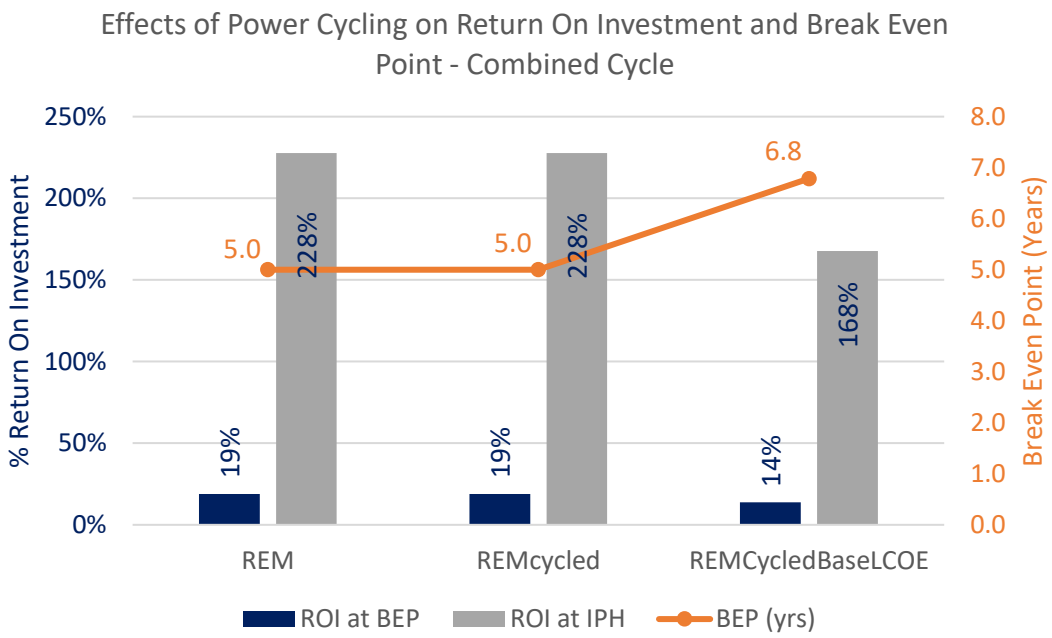

Figure 156: Effects of Power Cycling on Return on Investment and Break Even Point - Combined Cycle

In summary, based on the considered power-cycling scenario, power cycling of the repurposed engine model can result in an increased LCOE or a reduction in projected baseline profit over the investigated investment horizon. Furthermore, power cycling of the repurposed engine model fitted with the considered emissions control does not necessarily minimize the NOx emissions generated by the unit (Figure 151).

6.3.5 Techno-economic analysis results for REM operating in Tropical Environment.

Results and observations from an investigation into the effects of tropical environment on the economics of the repurposed engine model are presented in this section. Performance parameters used as input for this investigation are presented in Table 6.

Performance Input Parameters for Tropical Analysis

Operating Condition	Power Output (MW)	Fuel Flow (Kg/s)	TET (K)	Relative Humidity (%)	Altitude (m)	Exhaust Temperature (K)
ISA	18.51	1.1612	1310.15	60	0	770
TROPICAL	17.66	1.1729	1310.15	60	700	785

6.3.5.1 Effect of Tropical operation on Present worth and LCOE

Result in Figure 157 and Figure 158 reveal that operating the engine model in tropical region leads to a 3.3% decrease in NPV at an increased LCOE and a 6.4% decrease in NPV at baseline LCOE. With respect to operation in tropical region, LCOE increases by 3.1%. These results are consistent in both simple and combined cycle investigations.

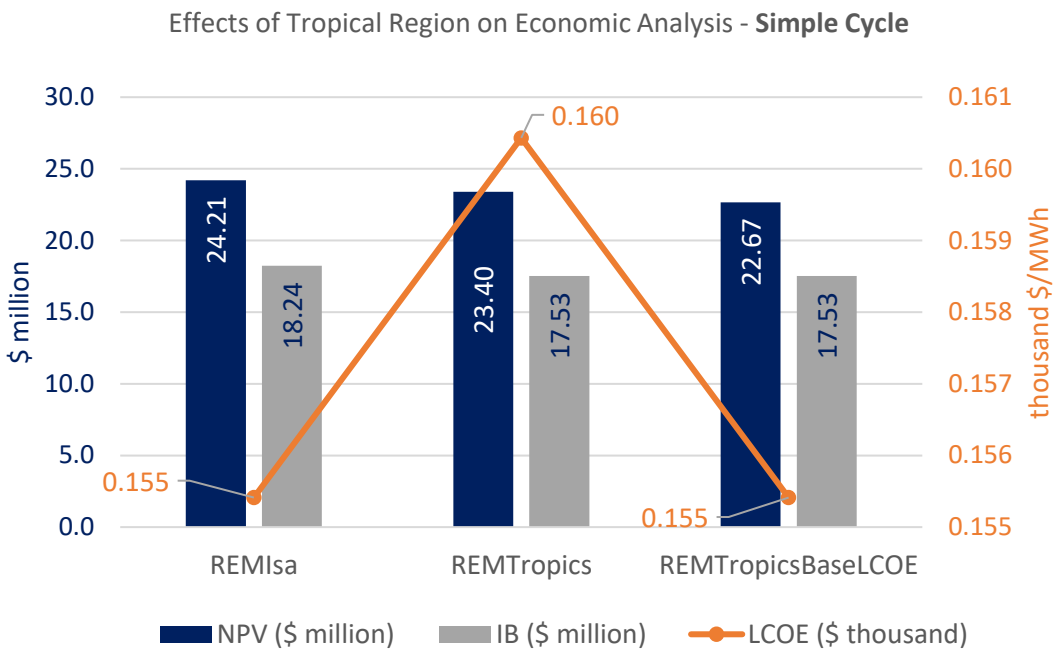

Figure 157: Effect of Tropical Region on Economic Analysis - Simple Cycle

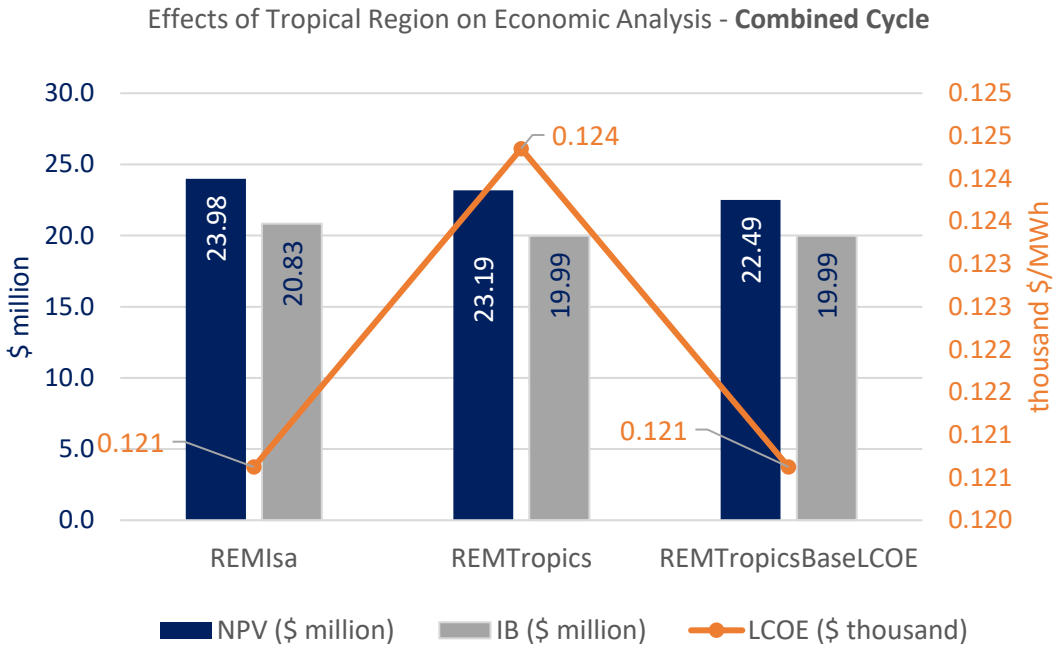

Figure 158: Effect of Tropical Region on Economic Analysis - Combined Cycle

6.3.5.2 Effect of Tropical operation on Emission

Figure 159 and Figure 160 present results for the repurposed engine model operating in tropical conditions at a fixed firing temperature. Results reveal that there is a 0.7% decrease in the quantity of NOx removed in relation to the quantity of NOx generated. This is attributable to an increase in the temperatures associated with the REM operating within the considered tropical scenario.

Performance simulation results for operation in tropical condition reveal an increase in engine fuel flow and exhaust temperature at constant firing temperature. This increase in exhaust temperature and fuel flow account for the increase in the quantity of NOx generated post emissions control and the decrease in the evaluated quantity of NOx removed.

In Figure 160, the REM operating in tropical conditions has a higher cost effectiveness in comparison to the REM operating at ISA conditions. This means that it will cost more to control emissions in tropical conditions than at ISA condition. Furthermore, engine model operation in tropical conditions will have a greater effect on the cost of electricity than operation at ISA condition.

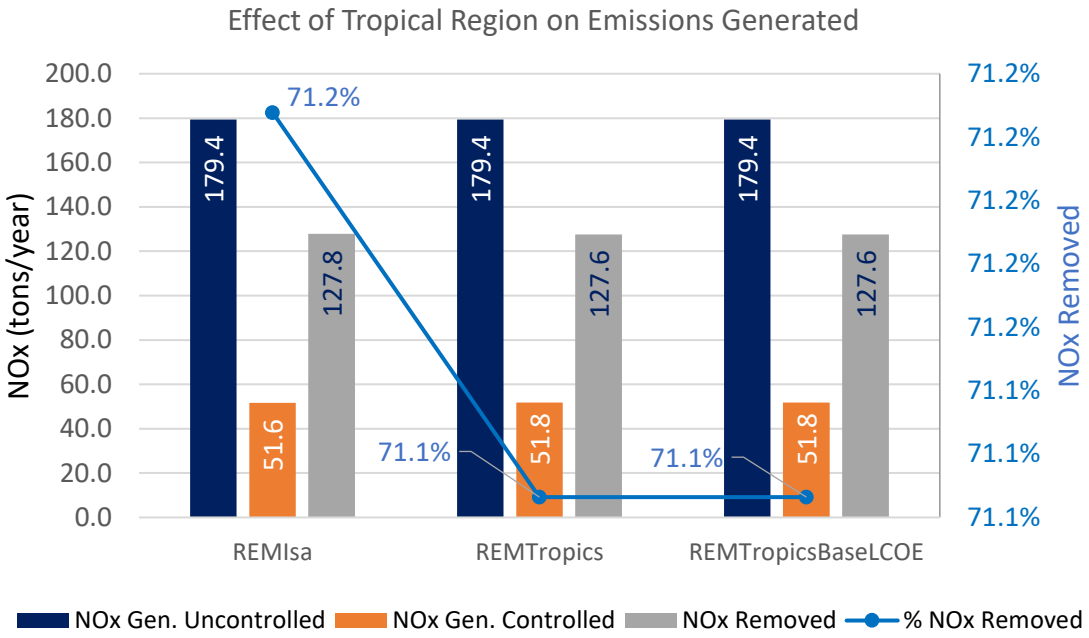

Figure 159: Effects of Tropical Region on Emissions Generation

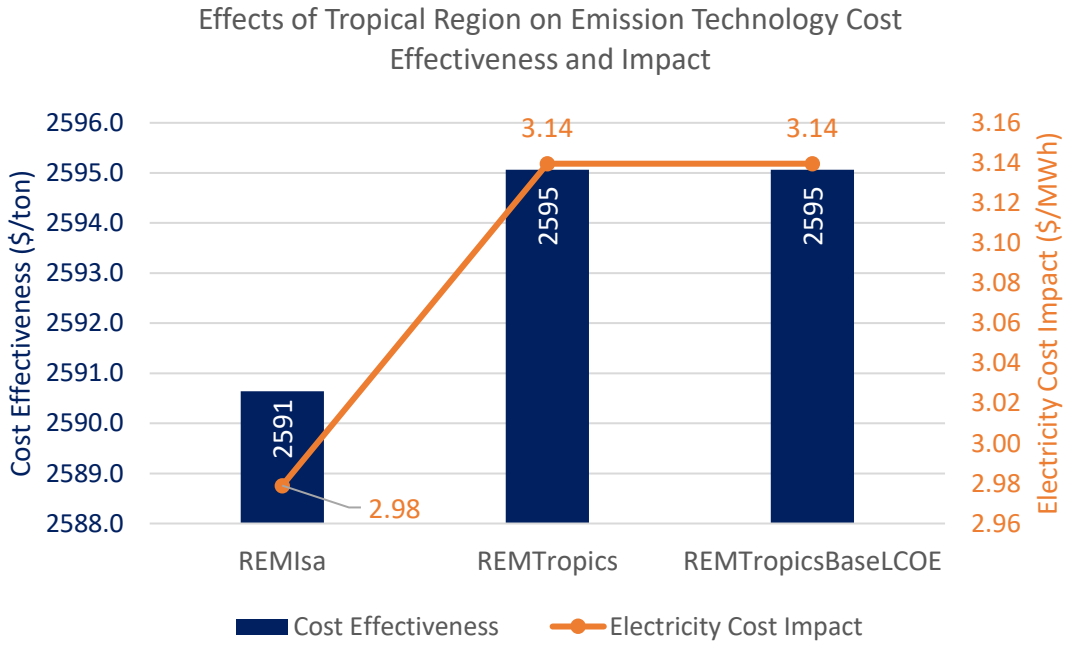

Figure 160: Effects of Tropical Region on Cost Effectiveness and Electricity Cost Impact

6.3.5.3 *Effect of Tropical operation on Costs*

Figure 161 and Figure 162 reveal that there is a 0.4% increase in annual running cost and annual operation and maintenance cost for the repurposed engine model operation within the considered tropical conditions.

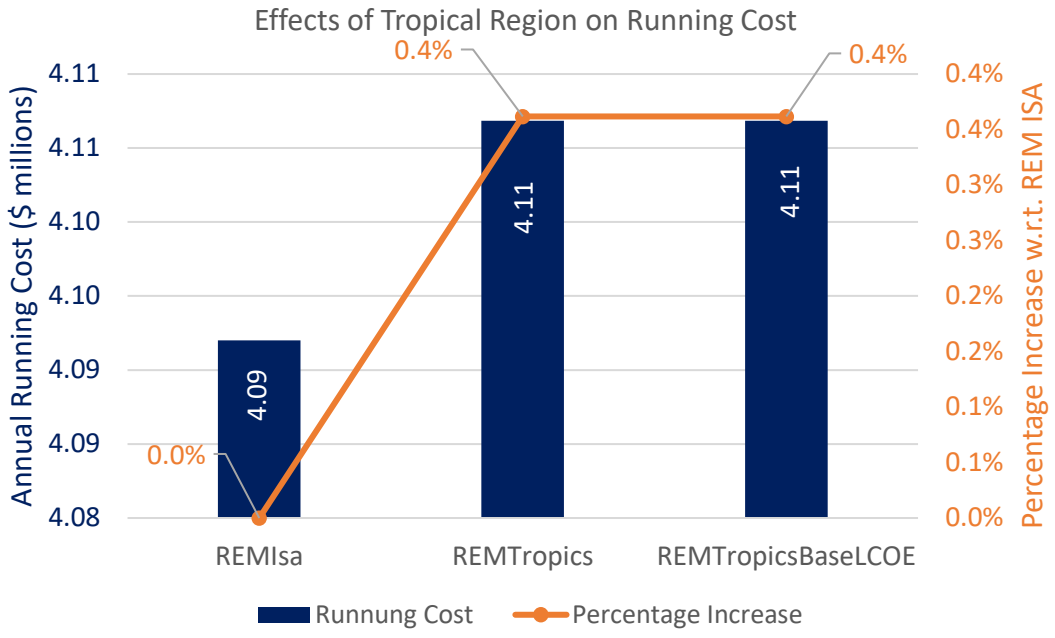

Figure 161: Effects of Tropical Region on Running Cost

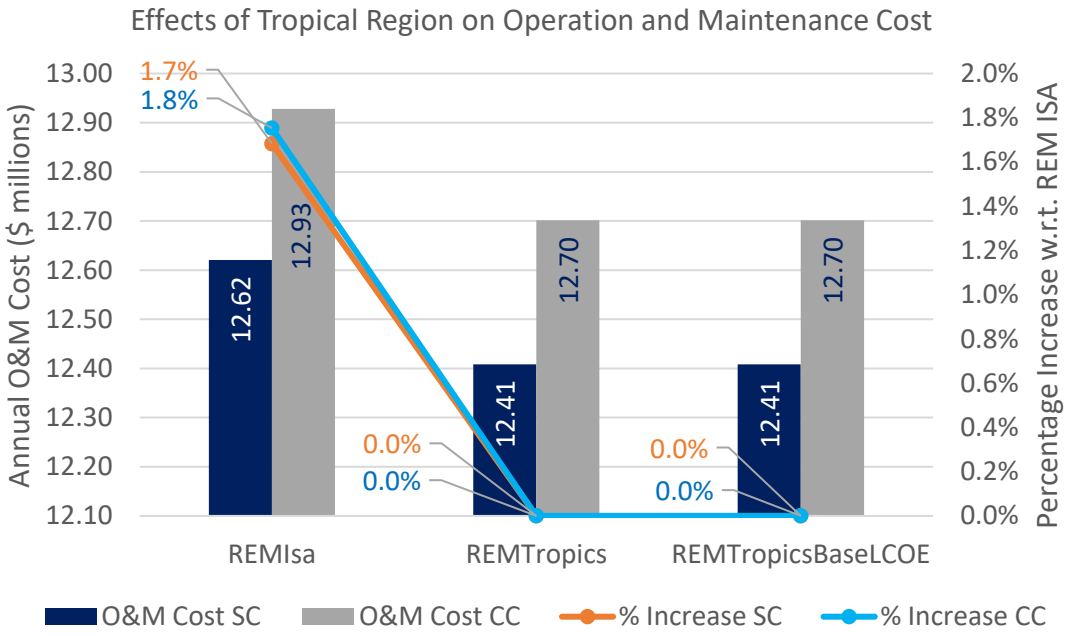

Figure 162: Effects of Tropical Region on Operation and Maintenance Cost

6.3.5.4 *Effect of Tropical operation on Return on Investment (ROI) and Break Even Point (BEP)*

Results in Figure 163 and Figure 164 show that operating the REM engine model within the considered tropical conditions will break even at 5years with a 22% ROI at BEP and a 233% ROI at IPH. For the engine model operating in similar conditions but at baseline LCOE, result indicate that the BEP will be around 5 year with 22% ROI at BEP and 226% ROI at IPH. Similar results are obtained for the engine model operating in combined cycle applications with a 13% decrease in ROI at break-even period and a 2% decrease in ROI over facility life.

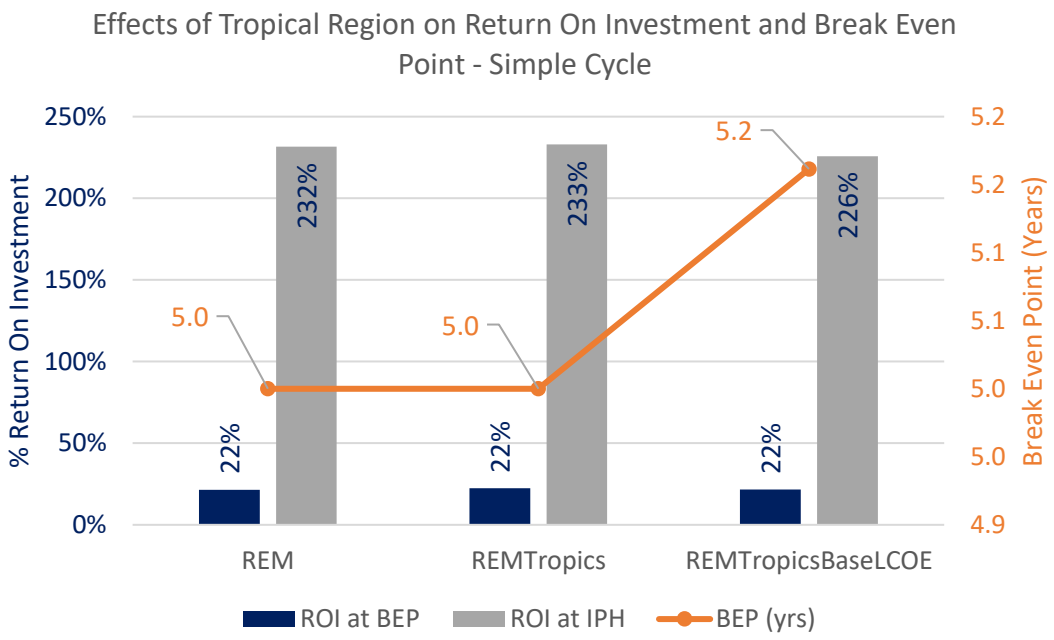

Figure 163: Effects of Tropical Region on Return on Investment and Break Even Point - Simple Cycle

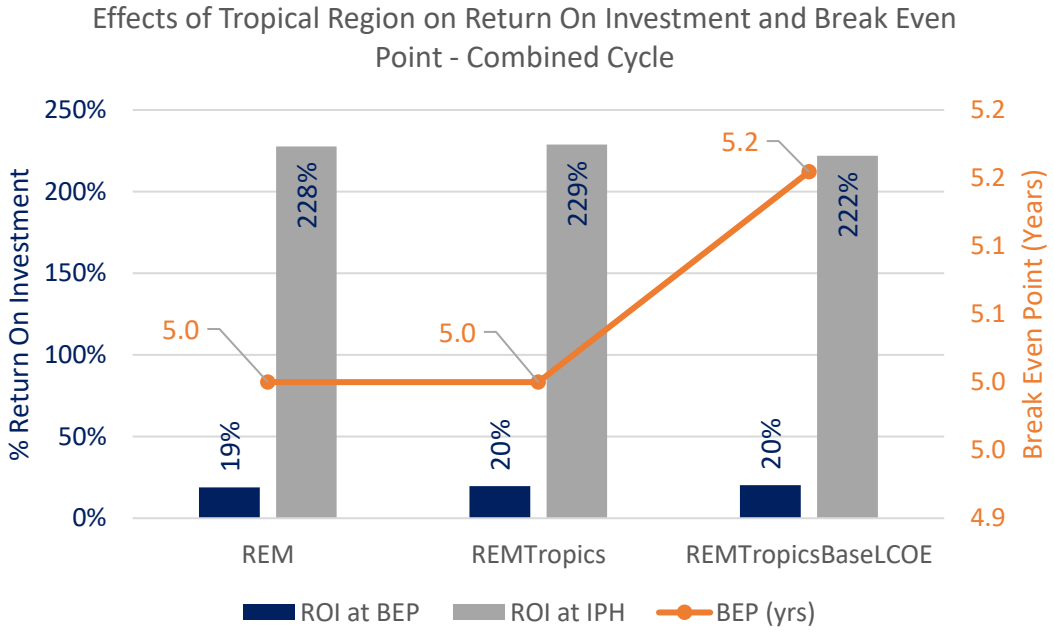

Figure 164: Effects of Tropical Region on Return on Investment and Break Even Point - Combined Cycle

In summary, the results reveal that it will cost more to operate the engine model in tropical environments than at ISA or close to ISA conditions. Furthermore, engine operation within the considered tropical conditions (Table 6) will result in less than 5% decrease in projected baseline benefits over the investigated horizon.

6.3.6 Effect of Emissions control technology on engine techno-economics

Investigation has been conducted into the techno-economic implications of adopting various emissions control technologies on the repurposed engine model. This investigation has been conducted to demonstrate one of the potential applications of the developed techno-economic analysis approach in the area of technology comparison.

To ensure investigation of the considered control technologies are valid and applicable, the following information as contained in Table 26 are supplied as part of the input data for the analysis. Values of emissions technology capital cost and emissions technology-owning cost

have been adapted from identical engines and adjusted for inflation to 2017 value (ONSITE SYCOM Energy Corporation , 1999).

All investigations in this section are with respect to the repurposed engine model REM.

Table 26: Emissions Technology Comparison Input data

Emissions Control Technology	Power Output (MW)	Max. Gen. Capacity (MW)	Fuel Flow (Kg/s)	Technology Capital Cost ($/kW)	Technology Owning Cost ($/kW)
UC	18.52	23	1.1612	0.00	0.00
DLN	18.52	23	1.1612	51.13	14.39
DLN+SCONOX	18.52	23	1.1612	269.37	71.39
DLN+SCR	18.52	23	1.1612	124.40	39.60
WS	18.73	23	1.1702	69.23	27.87
WS+SCONOX	18.73	23	1.1702	287.47	84.86
WS+SCR	18.73	23	1.1702	142.50	53.08

6.3.6.1 Effect of Emissions Control Technology on Present Worth and LCOE

Results obtained as shown in Figure 165 and Figure 166 reveal that the combination of water/steam injection with SCONOX technology delivers the highest NPV over the investigated horizon. How be it requires the largest investment base. The combination of water/steam injection technology with SCONOX results in the highest LCOE.

The implementation of DLN technology, alone, gives the lowest LCOE. Implementation of the DLN technology gives an LCOE 3% lower than the LCOE for water/steam injection. The DLN technology delivers a NPV 2% lower than NPV with water/steam injection. Furthermore, the implementation of DLN control technology requires an investment base 2% lower than the investment base required with water/steam injection. This result is consistent in both simple and combined cycle investigations.

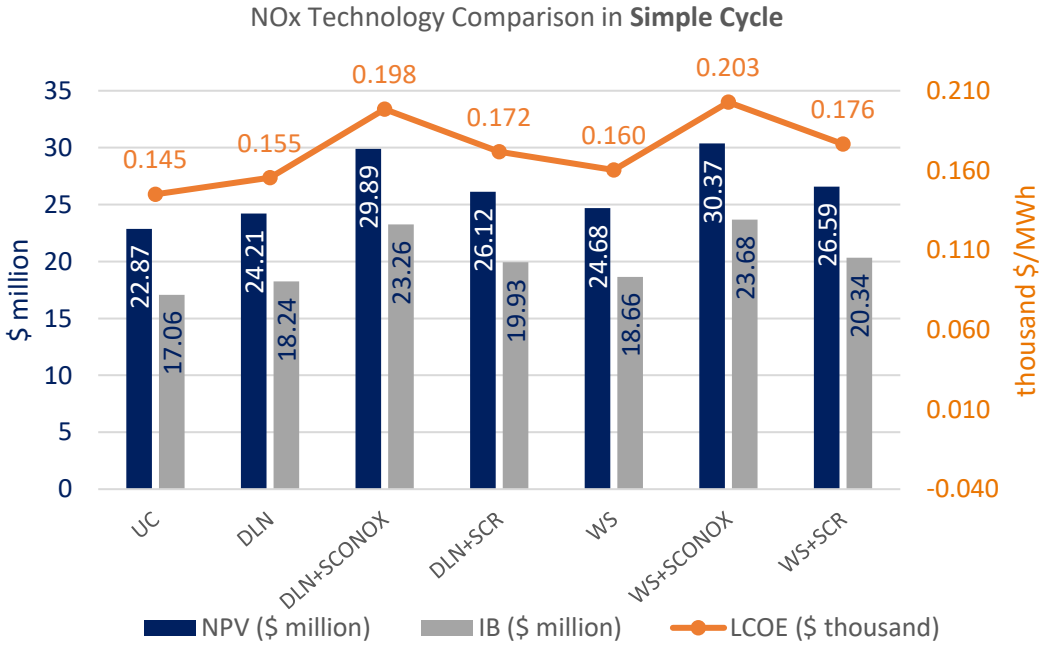

Figure 165: NOx Technology Comparison in Simple Cycle

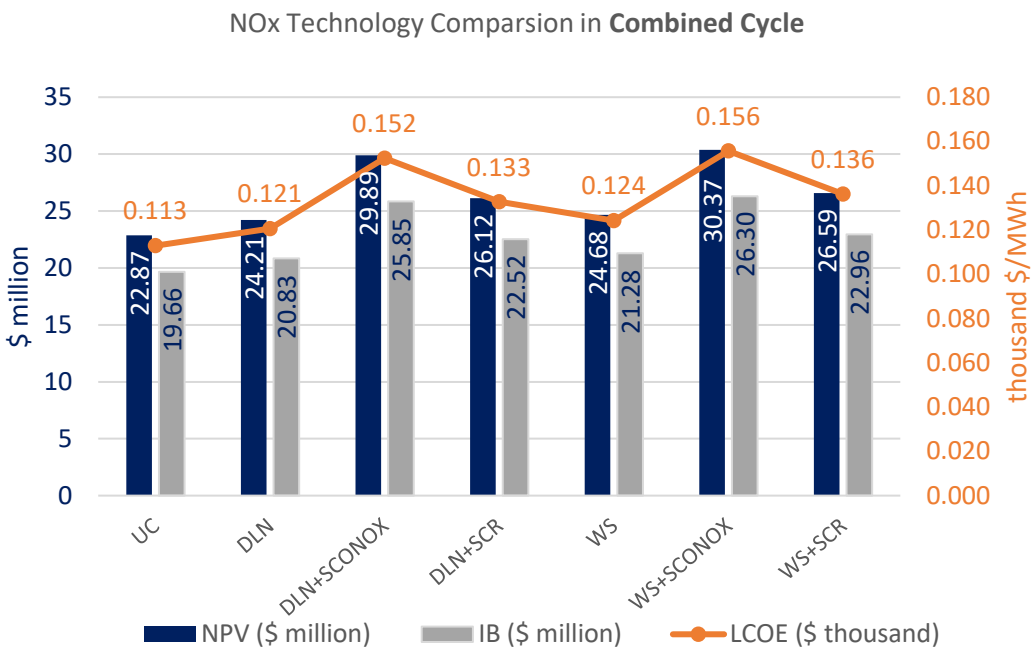

Figure 166: NOx Technology Comparison in Combined Cycle

6.3.6.2 *Effect of Emissions control technology on NOx Removed*

In Figure 167, results reveal that a combination of DLN technology with either SCONOX or SCR technology remove the largest quantity of NOx generated (up to 98%). Results also reveal that water/steam injection technology only remove about 50% of NOx emissions generated.

In Figure 168, the implementation of water/steam injection with SCONOX technology delivers the highest cost effectiveness and has the highest impact on the cost of electricity. This means that it will cost more to operate the repurposed engine model with WS+SCONOX technology. DLN control technology delivers the lowest cost effectiveness and has the least impact on the cost of electricity. This means that it will cost less to operate the engine model with DLN control technology implemented alone.

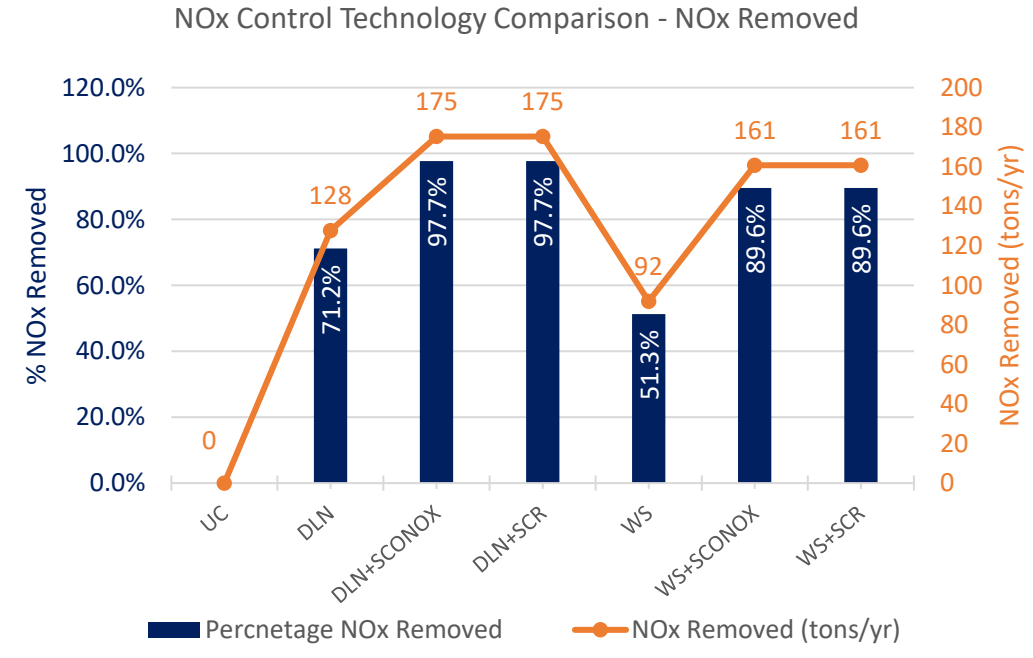

Figure 167: NOx Technology Comparison w.r.t. NOx Removed

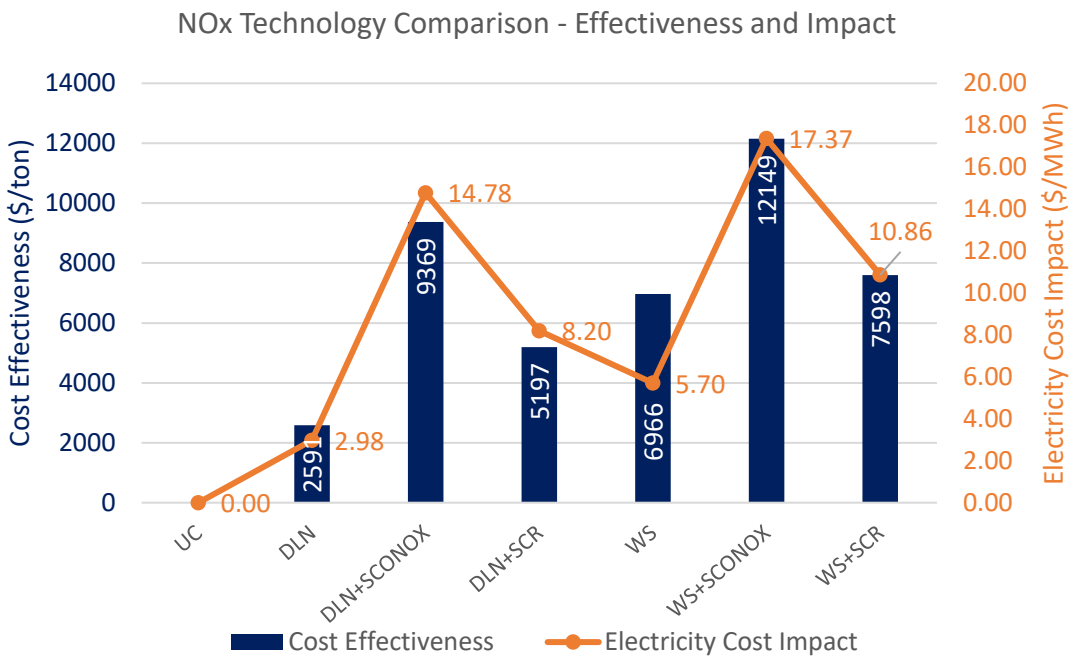

Figure 168: NOx Technology Comparison w.r.t. Effectiveness and Impact

6.3.6.3 *Effect of Emissions control technology on Costs*

Result in Figure 169 show that the implementation of a combination of water/steam injection with SCONOX technology has a greater impact on Annual running cost while the implementation of DLN technology has the least impact on running cost. With respect to the uncontrolled engine model, implementation of WS+SCONOX technology increases annual running cost by 34% while DLN technology increases annual running cost by 8%.

With respected to the uncontrolled engine model, results in Figure 170 reveals that WS+SCONOX technology increase annual operation and maintenance cost by 31% while DLN technology increase annual operation and maintenance cost by 7%.

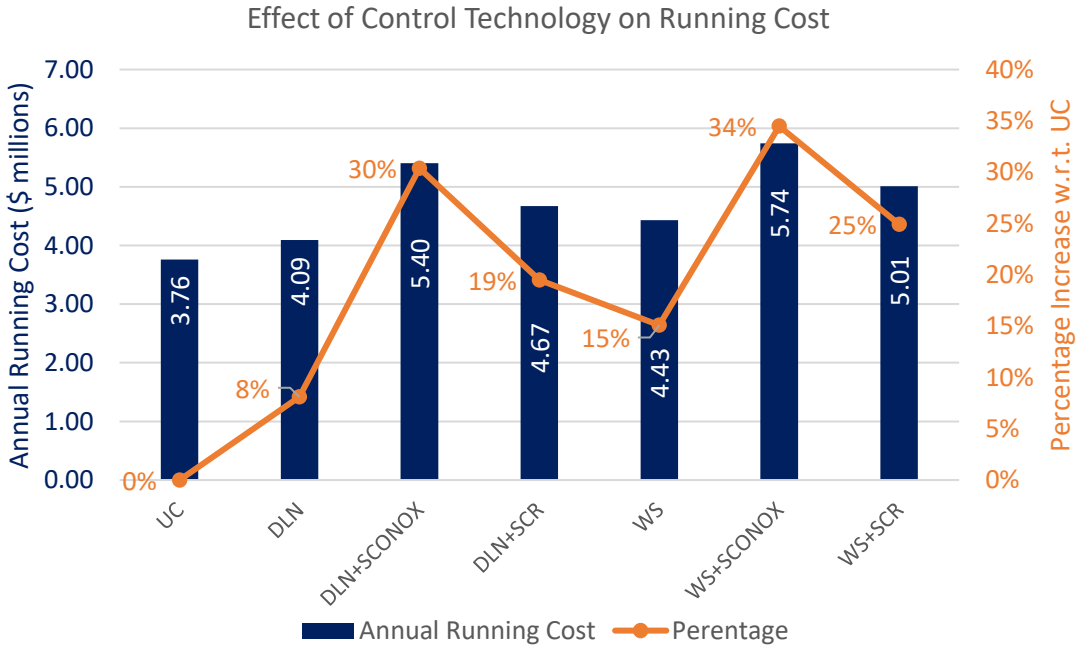

Figure 169: Effect of Emissions Control Technology on Running Cost

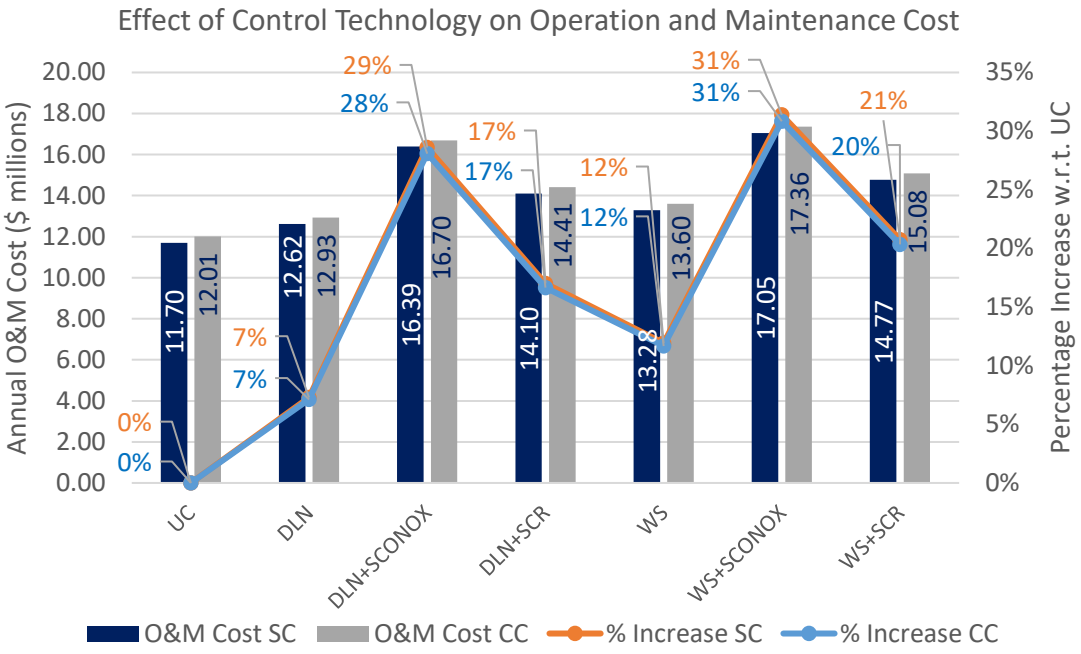

Figure 170: Effect of Emissions Control Technology on Operation and Maintenance Cost

6.3.6.4 *Effect of Emissions control technology on Return on Investment (ROI) and Break Even Point (BEP)*

Figure 171 and Figure 172 reveal that with respect to the considerations for this investigation, the repurposed engine model will break even at 5years. However, in relation to the return on investment, the DLN technology delivers the highest ROI at break-even period and delivers the highest ROI over the investigated horizon. WS+SCONOX technology delivers the lowest ROI at break-even period and delivers the lowest ROI over the investigated horizon. This observation is consistent in both simple and combined cycle investigations.

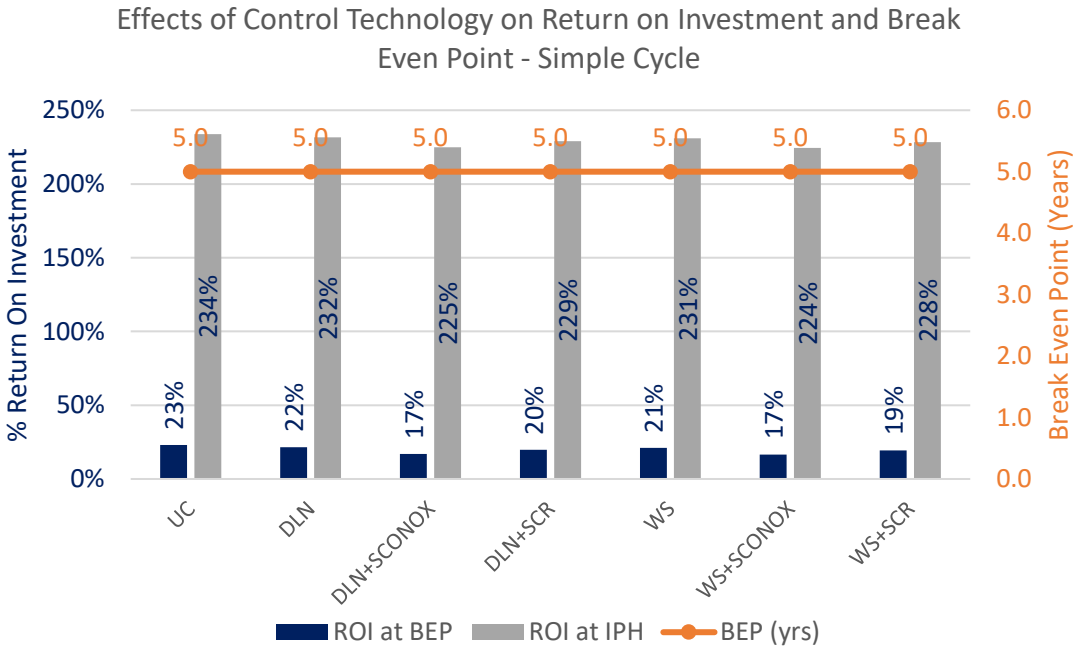

Figure 171: Effects of Control Technology on Return on Investment and Break Even Point - Simple Cycle

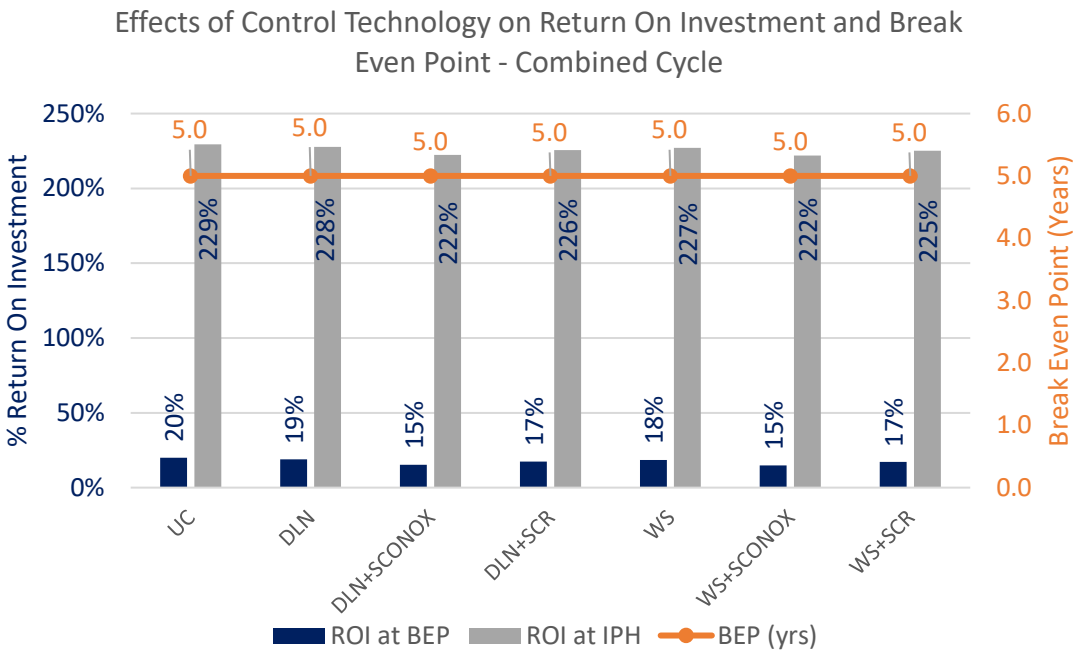

Figure 172: Effects of Control Technology on Return on Investment and Break Even Point - Combined Cycle

The choice of emissions control technology for any investment or project is often based on the efficiency and effectiveness of the technology, the effect of the technology on cost and benefits and the active policy on emissions in the proposed project environment. With respect to the considerations and requirements of this study, implementation of DLN technology for emissions control on the repurposed engine model favours the potential application of the engine for electrical power generation from a cost and emission policy perspective.

6.3.7 Effect of Acquisition Cost on engine techno-economics

The engine model investigated in this study is similar to the TUMANSKY-R-25-300 turbojet engine, repurposed, from a performance perspective, for electrical power generation. The TUMANSKY-R-25-300 power plant is used on the MiG-21 fighter jet and is one of the currently grounded aircraft fleet owned by the Nigerian Air force. Tech-economic analysis has been conducted to identify the potential for applying a model of the repurposed power plant for electrical power generation.

Economic analysis requires the application of acquisition cost for certain economic evaluations. However, there are two perspectives from which the economics for the repurposed engine model has been evaluated. The first perspective excludes engine acquisition cost in economic analysis based on the premise that the engines have previously been purchased along with the currently grounded aircraft fleet and no resource will be allocated for engine purchase in the proposed project. The second perspective includes engine acquisition cost in economic analysis based on the consideration that potential investors may be interested in accounting for engine acquisition cost in current economic evaluations even though no resource will be allocated for engine purchase in the currently proposed project. These two perspectives have led to the evaluation of the effect of acquisition cost on the economics of the repurposed engine.

In this investigation, 'REM' refers to the repurposed engine model economic evaluations with acquisition cost included and 'REMLessAcq' refers to the engine model economic evaluations with acquisition cost excluded (i.e. *acquisition cost = 0*).

6.3.7.1 Effect of Acquisition Cost on Present Worth and LCOE

Results in Figure 173 and Figure 174 reveal the following for economic evaluations ignoring acquisition cost.

- Very low values of LCOE (about 45% lower than with acquisition cost included)
- 68% lesser NPV over investigated horizon.
- 80% lesser investment base required.

The lower LCOE suggests that electricity can be sold at cheaper prices to consumers. The low NPV is attributable to the lesser investment base required and the lower LCOE realised from the economic evaluation. At baseline LCOE, the NPV for economic evaluations without acquisition cost increases by 45% at a fixed investment base. These results are consistent for evaluations in both simple and combined cycle application.

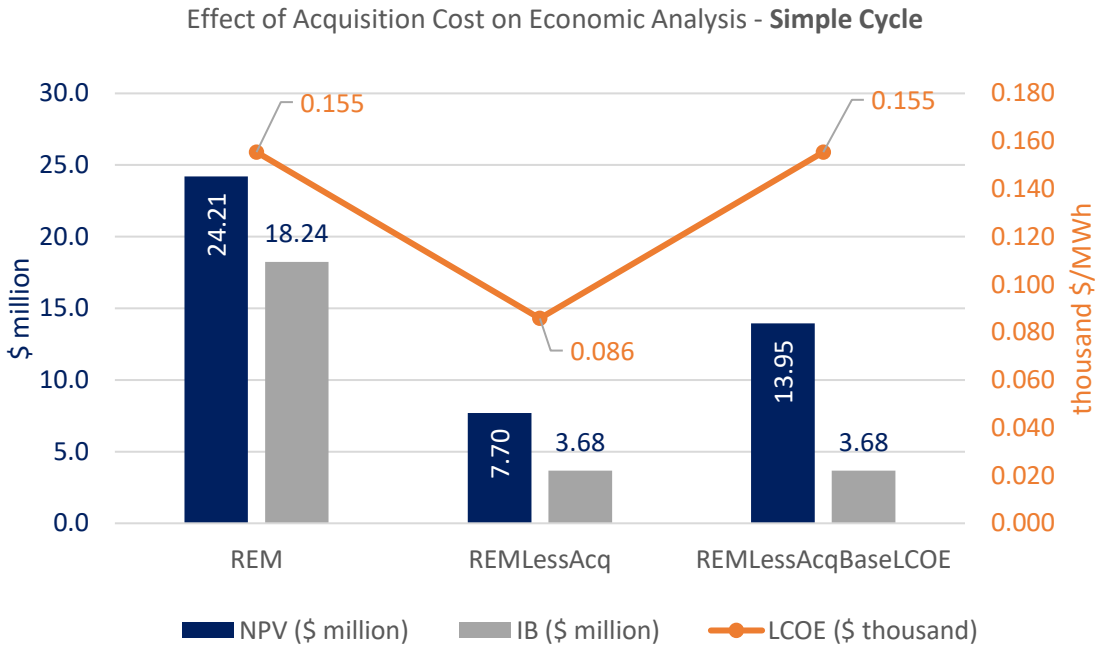

Figure 173: Effect of Acquisition Cost on Economic Analysis - Simple Cycle

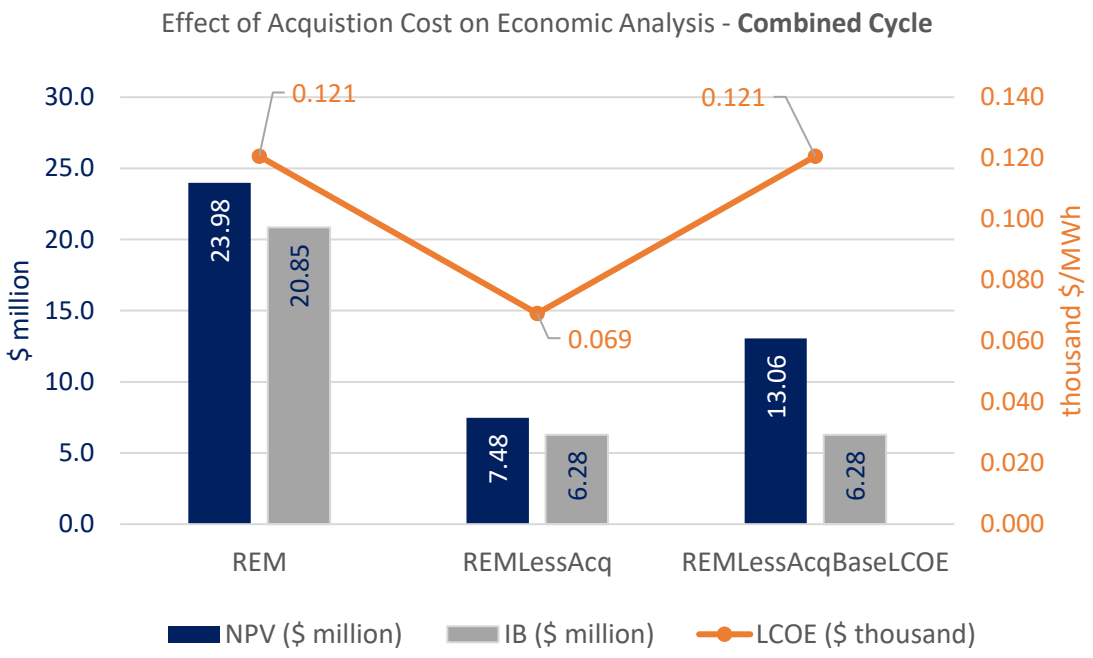

Figure 174: Effect of Acquisition Cost on Economic Analysis - Combined Cycle

6.3.7.2 *Effect of Acquisition Cost on NOx Removed*

Acquisition cost has no notable implication on the amount of NOx removed by the implemented emission control, the cost effectiveness of the emissions control technology or the electricity cost impact of the adopted technology. Results obtained as shown in Figure 175 and Figure 176 remain the same for all considerations.

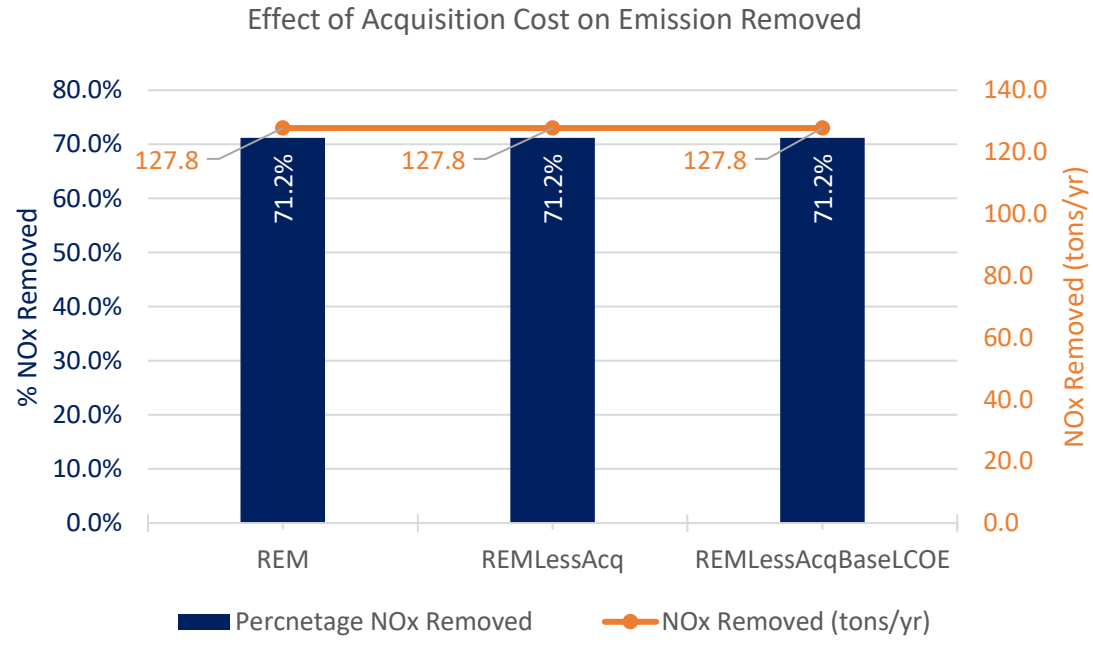

Figure 175: Effect of Acquisition Cost on NOx Emissions Removed

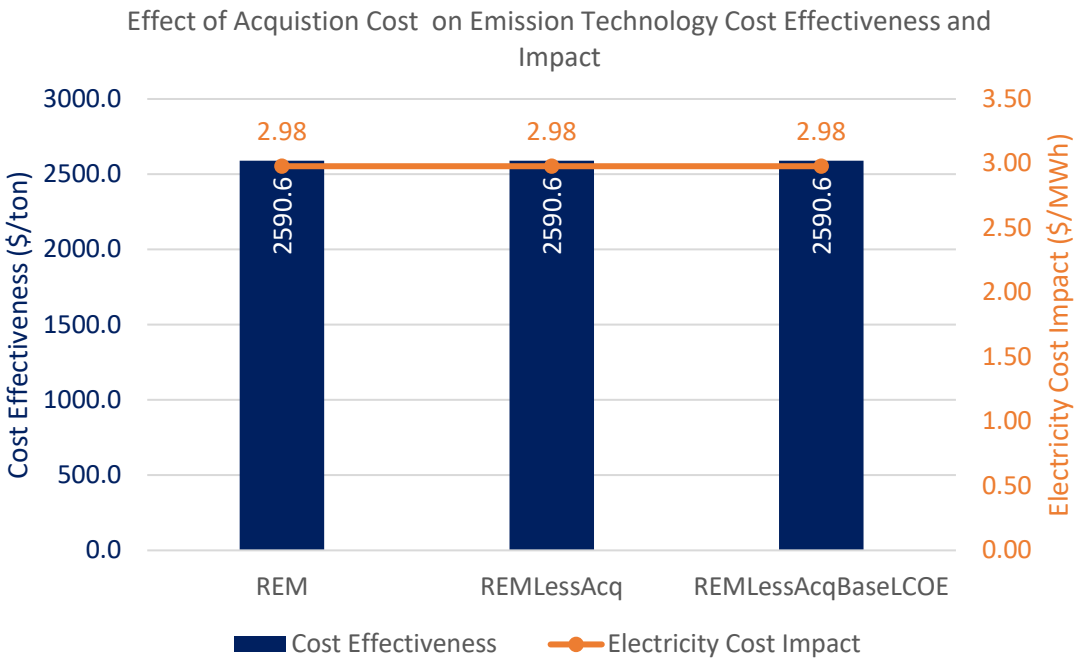

Figure 176: Effect of Acquisition Cost on Technology Cost effectiveness and impact

6.3.7.3 *Effect of Acquisition Cost on Running Costs*

Result in Figure 177 indicate that acquisition cost has not direct effect on the annual running cost of repurposed engine model. The results obtained remain the same across all considerations.

In Figure 178, it is evident that the inclusion of acquisition cost in the economic evaluations for the repurposed engine model results in an increase in annual operation and maintenance cost. This is because all overhead costs and standing charges associated with acquiring the repurposed engine model are accounted in the annual cost allocation. This leads to an increase in the annual overall cost associated with operating the unit. The Inclusion of acquisition cost in the economic evaluation of the repurposed engine model results in a 38% increase in operation and maintenance cost for both simple and combined cycle investigation.

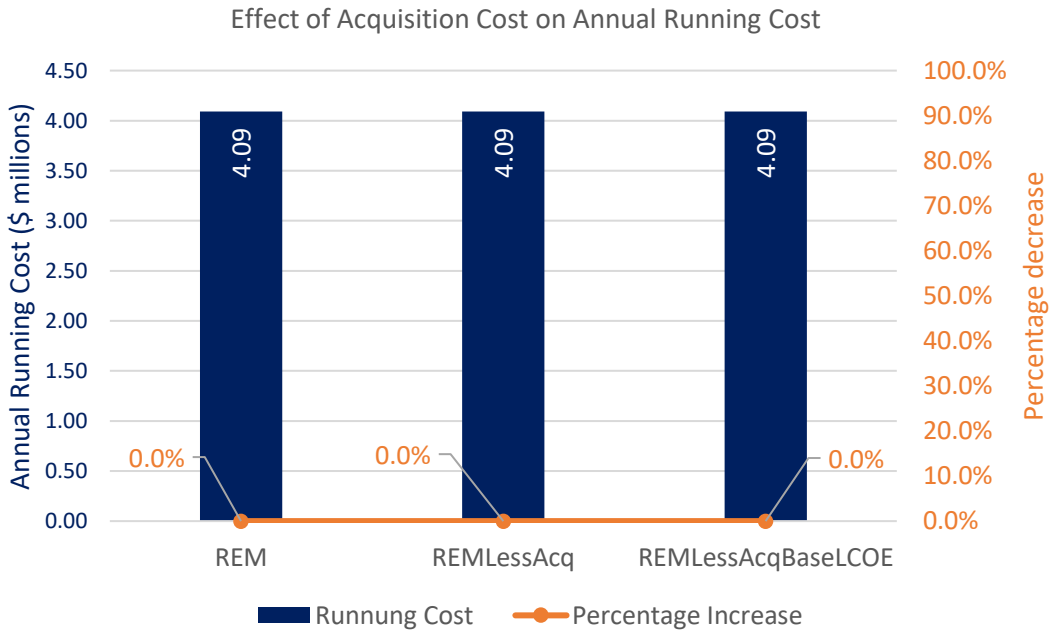

Figure 177: Effect of Acquisition Cost on Annual Running Cost

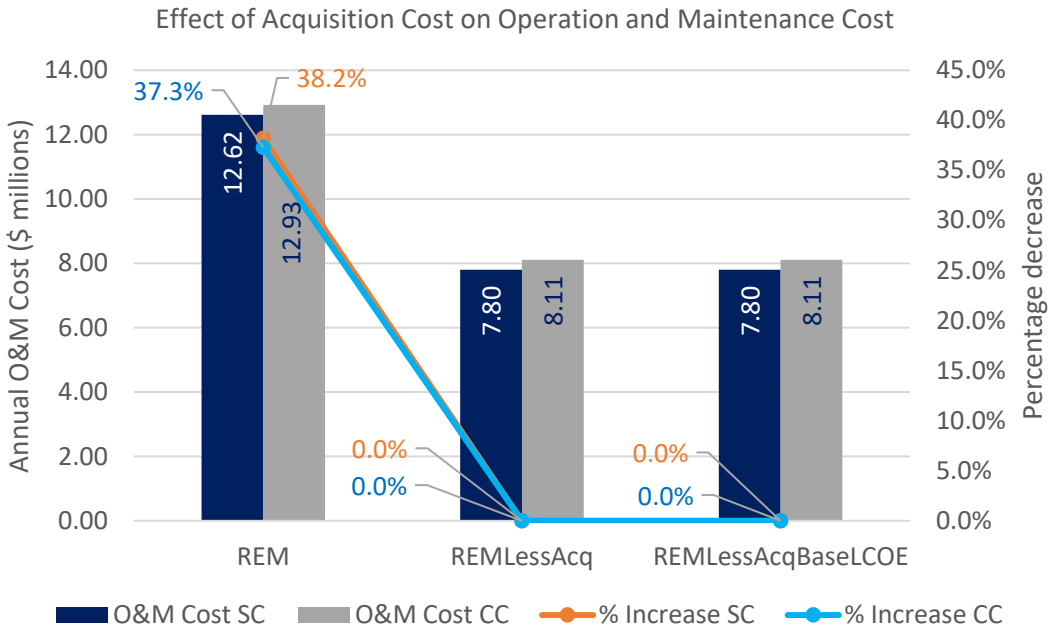

Figure 178: Effect of Acquisition Cost on Operation and Maintenance Cost

6.3.7.4 *Effect of Acquisition Cost on Return on Investment (ROI) and Break Even Point (BEP)*

Economic evaluations of the repurposed engine model ignoring acquisition cost, results in an earlier return on investment. Figure 179 and Figure 180 show that evaluations ignoring engine acquisition cost, break-even at 4years with higher return on investment of about 49% at break-even period and 357% over the investigated planning horizon. With respect to baseline LCOE, economic evaluations ignoring engine acquisition cost break-even at 2.2years with 27% ROI at break-even period and 197% ROI over the investigated planning horizon. Similar result are obtained for combined cycle investigation as shown in Figure 180.

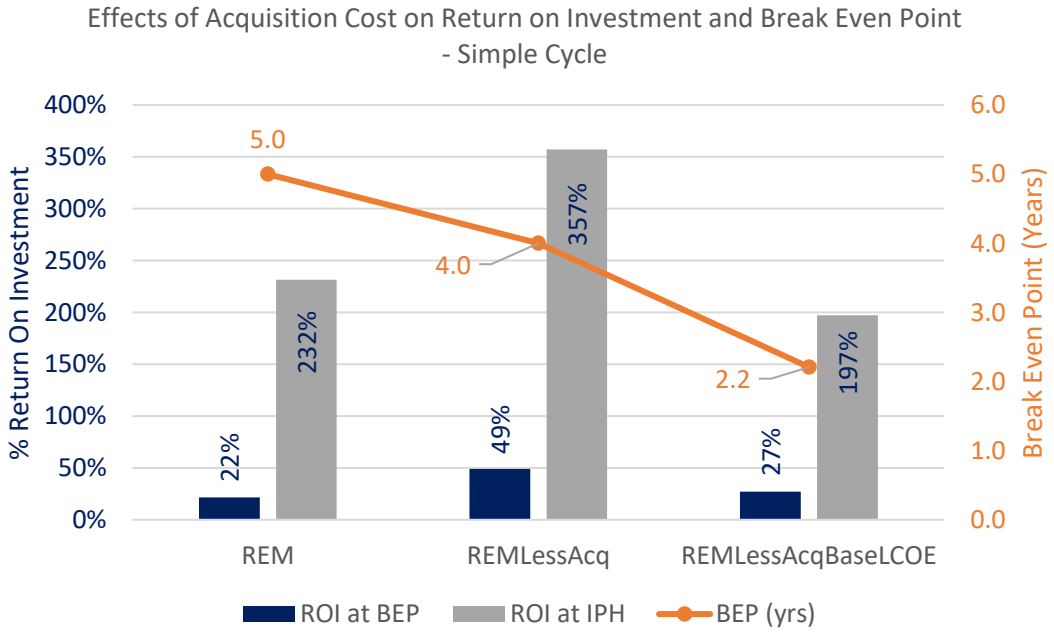

Figure 179: Effect of Acquisition Cost on Return on Investment and Break Even Point - Simple Cycle

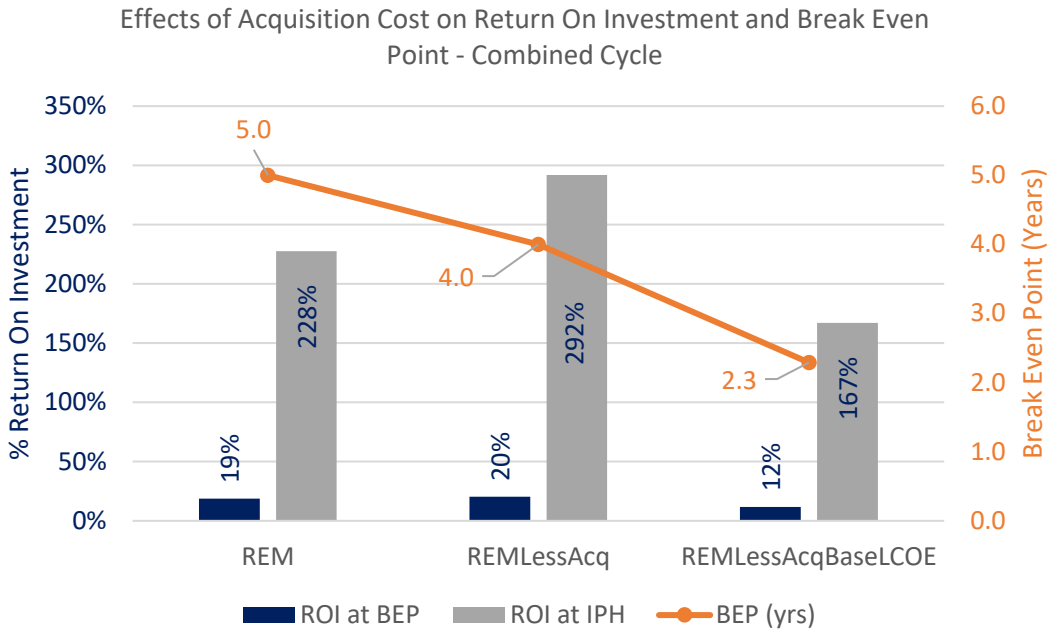

Figure 180: Effect of Acquisition Cost on Return on Investment and Break Even Point - Combined Cycle

Results obtained from this investigation reveal that acquisition cost significantly influences economic analysis. However, with respect to the considerations of this study, the choice of a perspective for economic evaluation is subjective. Potential investors will have to decide on an appropriate perspective, for economic evaluation, based on their policies, investment goals and objectives.

6.4 Optimization Analysis Results

Presented in this section are results from techno-economic optimization analysis conducted on the repurposed engine model. The optimization analysis involves both performance and economic optimization. Results are presented below.

6.4.1 Performance optimization

Performance optimization has been conducted from two perspectives. The first involves modifications to the basic thermodynamic cycle of the REM and the second implements an optimization algorithm to minimize a variable. The objective of performance optimization is to minimise fuel consumption and NOx emissions without loss of power output.

6.4.1.1 Modification to basic thermodynamic cycle

An intercooler has been implemented on the repurposed engine to optimise it performance. The implemented performance simulation model is presented is Appendix A. It is assumed that the cost of retrofitting an intercooler onto the repurposed engine model is 3% of acquisition cost. This has been include in the cost analysis. Presented below in Figure 181 - Figure 185 are the performance and economic implications of the intercooler on the REM.

Performance simulation conducted on the modified engine reveals a steady increase in power output between 10% - 14% and 13% - 19% decrease in compressor work with intercooler effectiveness ranging from 85% to 100%. Thermal efficiency increase is between 0.1% - 0.5% and exhaust gas temperatures fall is less than 1%.

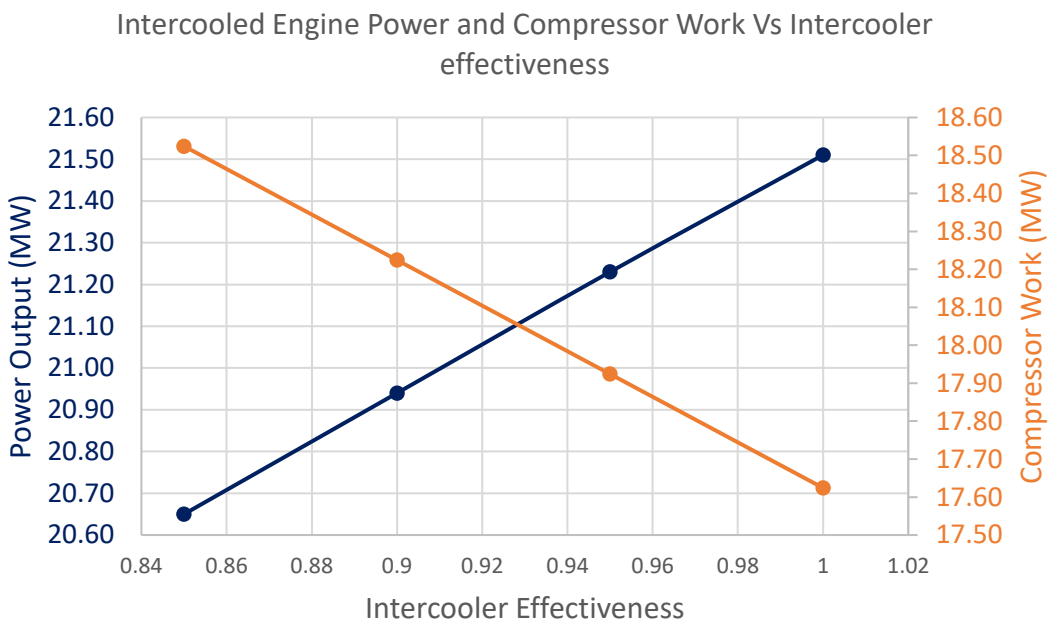

Figure 181: Intercooled Engine Power and Compressor Work Vs Intercooler effectiveness

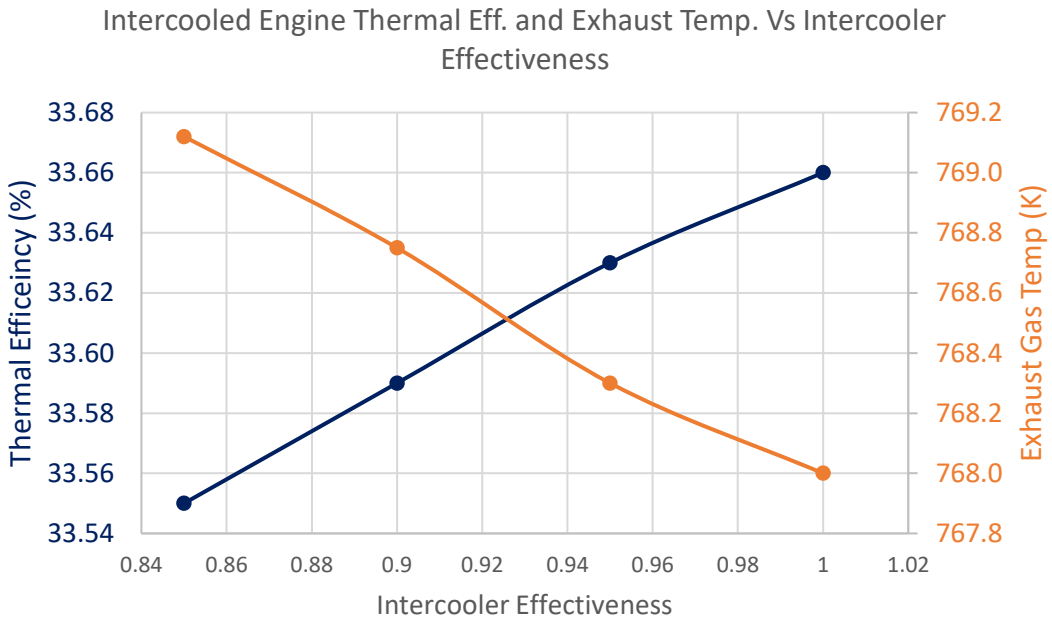

Figure 182: Intercooled Engine Thermal Eff. and Exhaust Temp. Vs Intercooler Effectiveness

Results in Figure 183 reveal a 1% drop in Specific fuel consumption with about 14% rise in fuel flow in comparison to the unmodified engine model. This increase in fuel flow results in a corresponding increase in NOx emissions generated and Annual running cost as shown in Figure 184 and Figure 185. However, there is a reduction in LCOE, between 21% and 25% observed in Figure 186, as intercooler effectiveness increases.

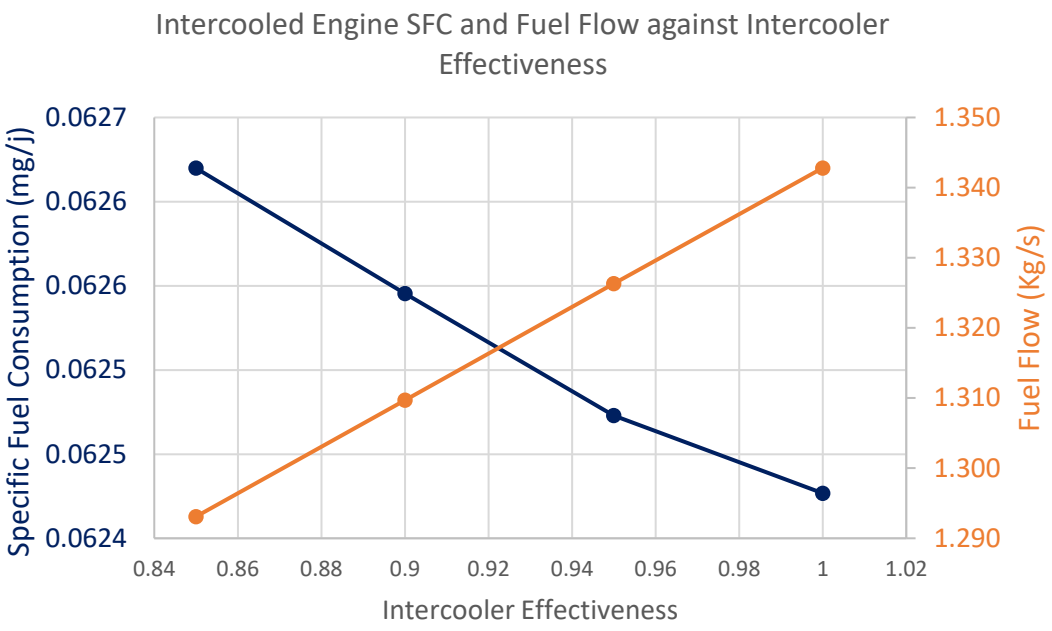

Figure 183: Intercooled Engine SFC and Fuel Flow against Intercooler Effectiveness

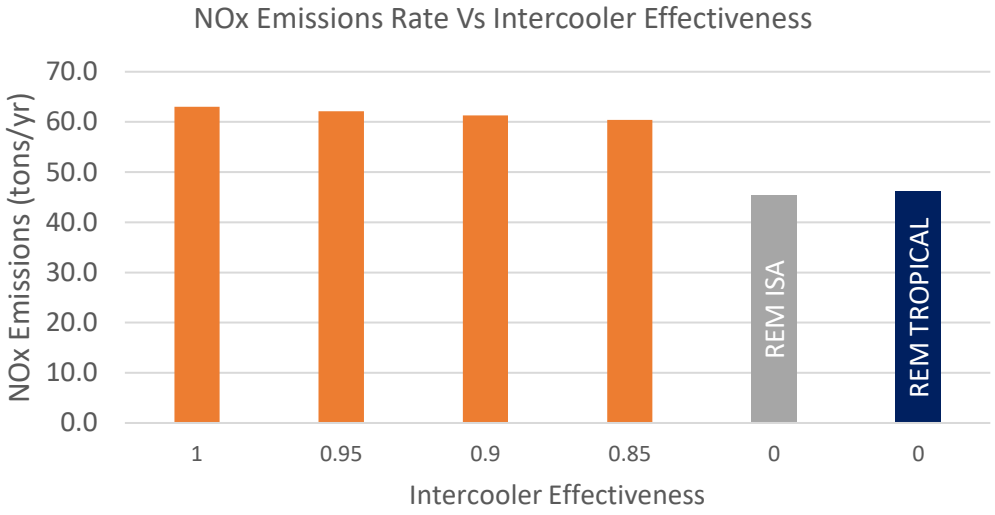

Figure 184: NOx Emissions Rate Vs Intercooler Effectiveness

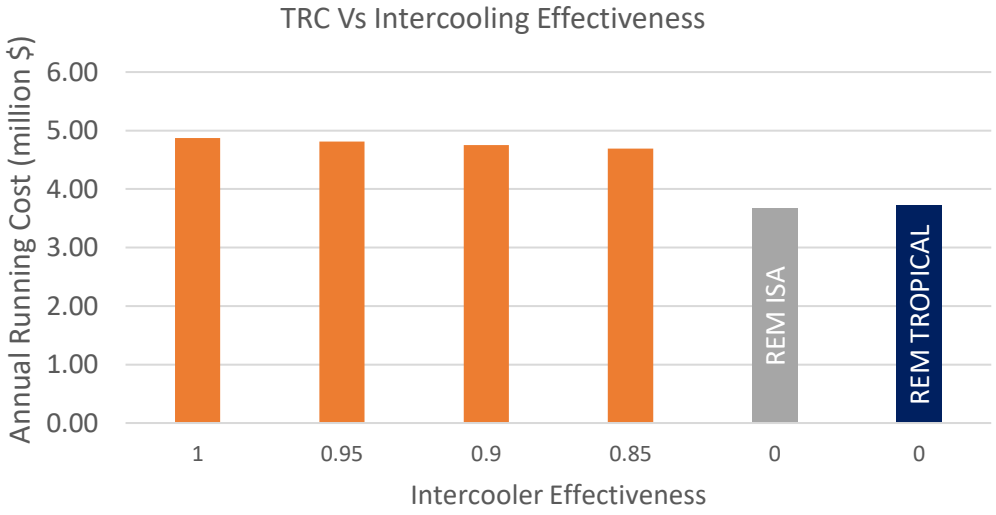

Figure 185: Annual Running Cost Vs Intercooler Effectiveness

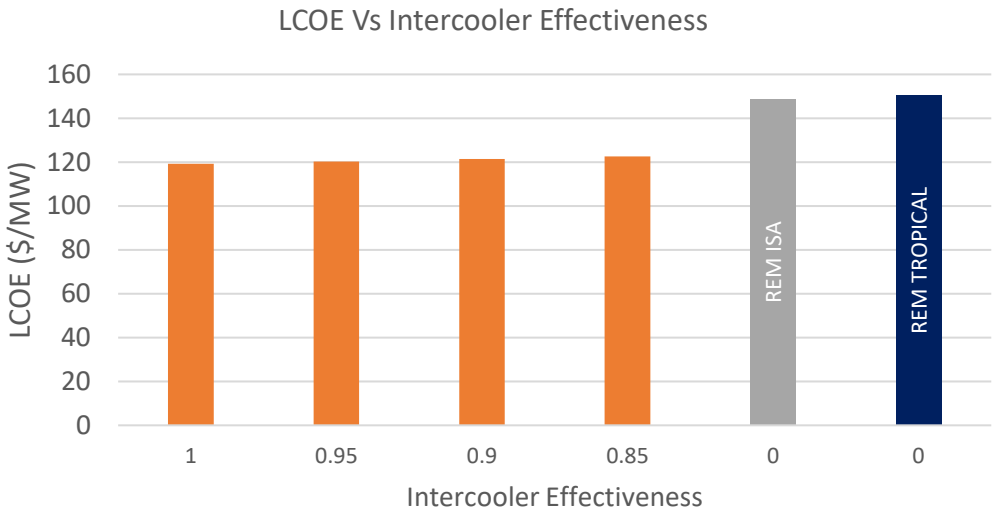

Figure 186: LCOE Vs Intercooler Effectiveness

Engine model modification with 85% intercooler effectiveness has been adopted as the baseline for further optimization analysis. This is because modification results at this condition tend towards achieving some of the outlined performance optimization objectives. Although there is a 14% increase in fuel flow and emissions generated, LCOE has been minimised by 21% with a 10% increase in power output. It is expected that further implementation of the optimization approach using optimization solver (results presented in 6.4.1.2) will deliver better results.

6.4.1.2 Optimization using optimization solver

Output from modifications made to the REM are supplied as input into the performance optimization solver described in section 5.6.2. Results are presented in Figure 187, Figure 188 and in Table 27.

The results for the optimized and un-optimized engine considerations are presented in the tables and charts shown below. The following representations describe each presented engine model considerations.

- $REM_{(Unoptimized)}$ refers to the non-intercooled and un-optimized engine model results.
- REMOptim refers to the non-intercooled but optimized engine model results.
- $REMINT_{(Unoptimized)}$ refers to the intercooled but un-optimized engine model results.
- REMOptimINT refers to the intercooled and optimized engine model results.

The optimized and non-intercooled engine model achieves a 45% reduction in fuel flow at a TET of 969.36K (26% decrease), EGT of 426K (45% decrease) and at fixed power output of 18.52MW.

The intercooled and optimized engine model achieves a 39% reduction in fuel flow at a TET of 970.44K (26% decrease), EGT of 425K (45% decrease) and a power output of 20.65MW which is the baseline power output of the intercooled engine model. The massive fall in EGT for the intercooled and optimized engine model does not support combined cycle application due to the low temperatures, except an external source of heating is supplied to achieve the required temperature for combined cycle application. This however, may increase operating cost and the levelized cost of electricity.

Table 27: Performance Optimization Results

	Fuel Flow Value (Kg/s)	Fuel Flow Reduction (%)	TET value (K)	EGT value (K)	POWER Value (MW)	EXIT Flag	Objective
REM (Unoptimized)	1.1612	0.0%	1310.15	770	18519635	Nan	Nan
REMOptim	0.6387	-45.0%	969.36	426	18519635	1	Minimize Fuel Flow
REMINT (Unoptimized)	1.2931	11.4%	1310.15	769	20654639	Nan	Nan
REMOptimINT	0.7112	-38.8%	970.44	425	20654639	1	Minimize Fuel Flow

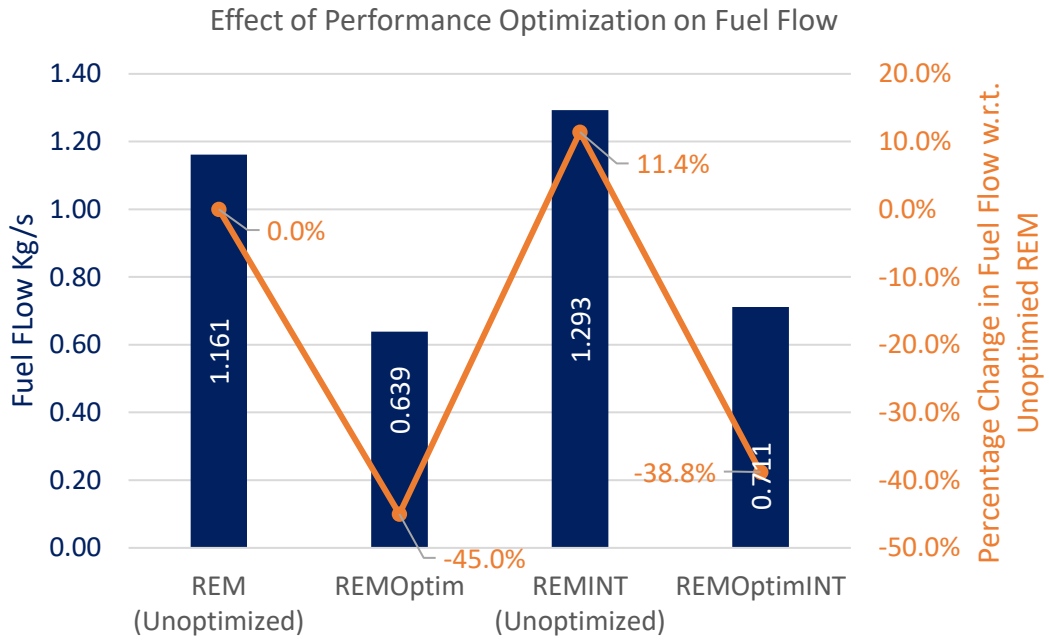

Figure 187: Effect of Performance Optimization on Fuel Flow

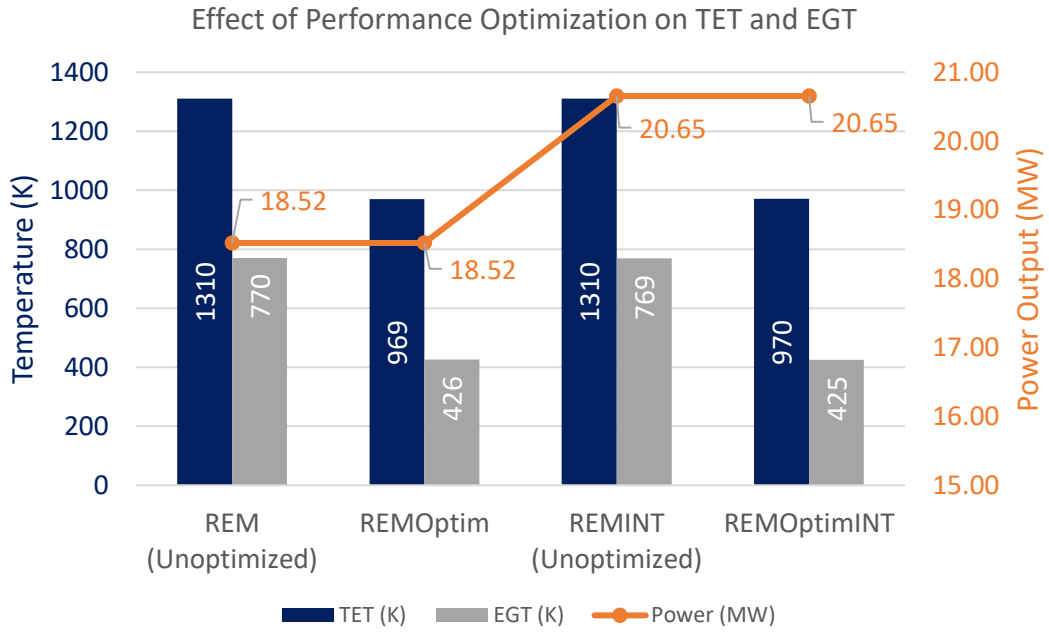

Figure 188: Effect of Performance Optimization on TET and EGT

6.4.2 Economic Optimization

Economic optimization is performed using the economic optimization solver, described in section 5.6.3, to minimise LCOE at maximum total annual benefits.

6.4.2.1 Optimization using optimization solver

Output from the baseline economic analysis of the REM are supplied as input into the economic optimization solver. Results are presented in Figure 189 - Figure 192 and in Table 28 and Table 29.

The optimized but non-intercooled engine model achieves a 25% reduction in LCOE with a 25% drop in total annual benefits at a minimum engine operating hours of 6000. The intercooled and optimized engine model achieves a 30% reduction in LCOE how be it at 22% drop in total annual benefits at minimum engine operating hours of 6000. This large drop in LCOE is attributable to the large drop in EGT during performance optimization, because of the engine model extracting more energy from the exhaust gas to maintain a fixed power output of 20.65MW. The fall in annual benefits is due to the lower cost at which electricity is sold in the optimized engine model. Similar results are obtained in combined cycle investigations.

Table 28: Economic Optimization Results - Simple Cycle

	EOH Value (hours)	LCOE Value ($/MW)	% LCOE Reduction	TA Benefits ($ millions)	TA Benefits Reduction (%)	EXIT Flag	Objective
REM (Unoptimized)	6000	155	0.0%	17.65	0.0%	Nan	Nan
REMOptim	6000	116	-25.2%	13.24	-25.0%	1	Minimize LCOE
REMINT (Unoptimized)	6000	146	-5.8%	18.49	4.8%	Nan	Nan
REMOptimINT	6000	108	-30.3%	13.78	-21.9%	1	Minimize LCOE

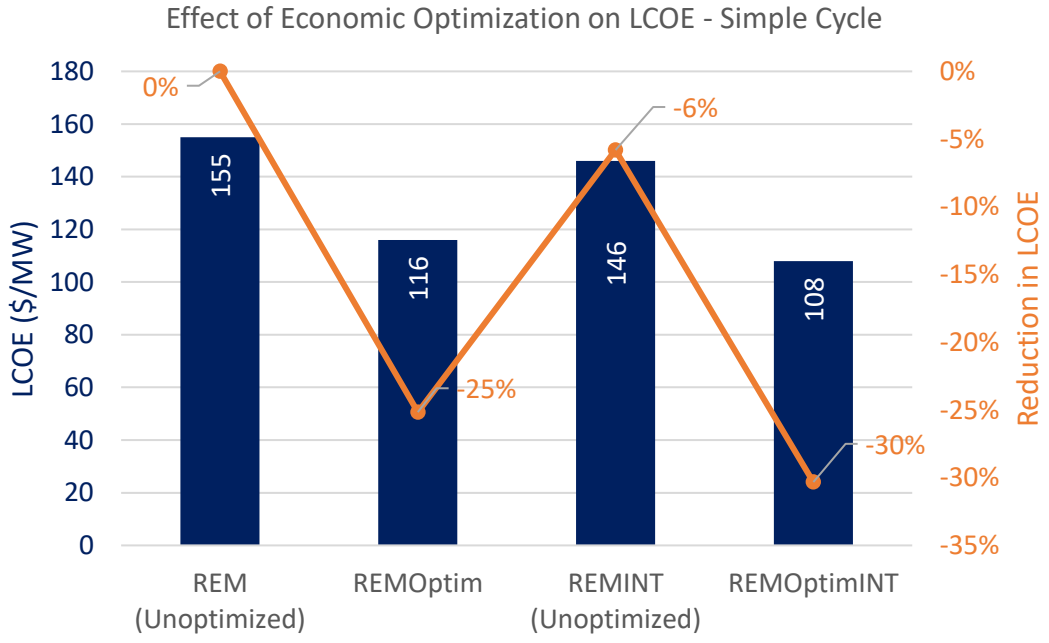

Figure 189: Effect of Economic Optimization on LCOE in Simple Cycle

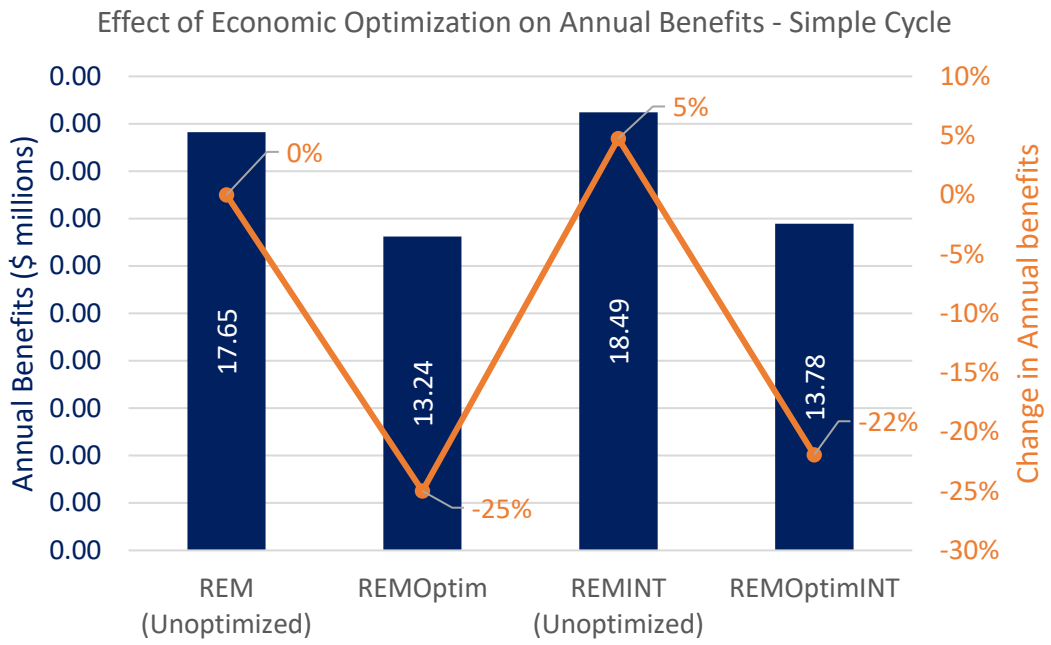

Figure 190: Effect of Economic Optimization on Annual Benefits - Simple Cycle

Table 29: Economic Optimization Results - Combined Cycle

	EOH Value (hours)	LCOE Value ($/MW)	% LCOE Reduction	TA Benefits ($ millions)	TA Benefits Reduction (%)	EXIT Flag	Objective
REM (Unoptimized)	6000	121	0.0%	18.48	0.0%	Nan	Nan
REMOptim	6000	90	-25.1%	13.93	-24.6%	1	Minimize LCOE
REMINT (Unoptimized)	6000	114	-5.7%	19.41	5.0%	Nan	Nan
REMOptimINT	6000	85	-29.8%	14.55	-21.3%	1	Minimize LCOE

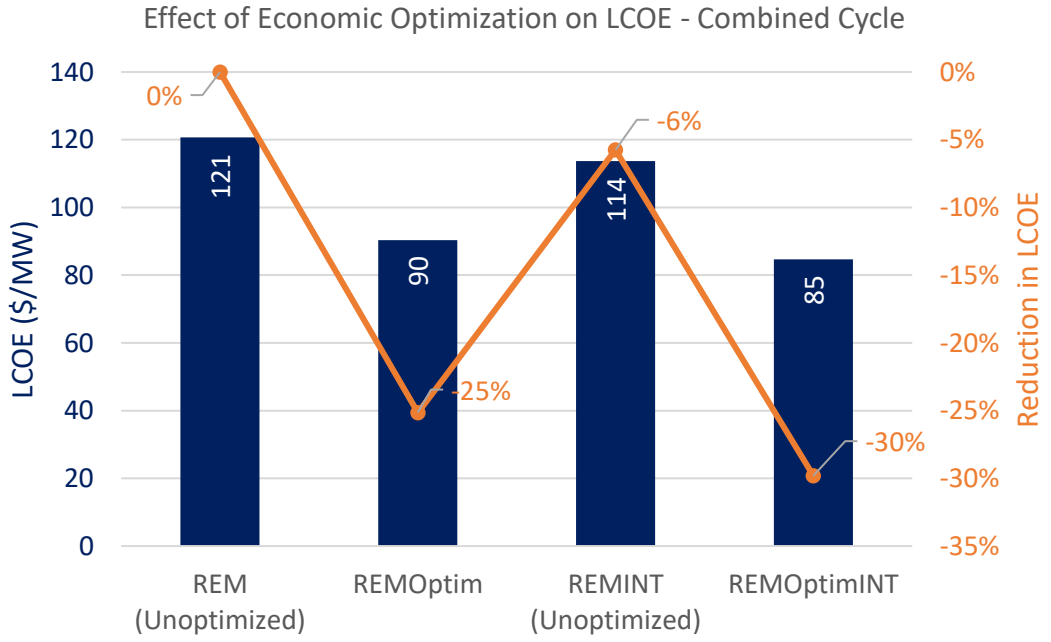

Figure 191: Effect of Economic Optimization on LCOE in Combined Cycle

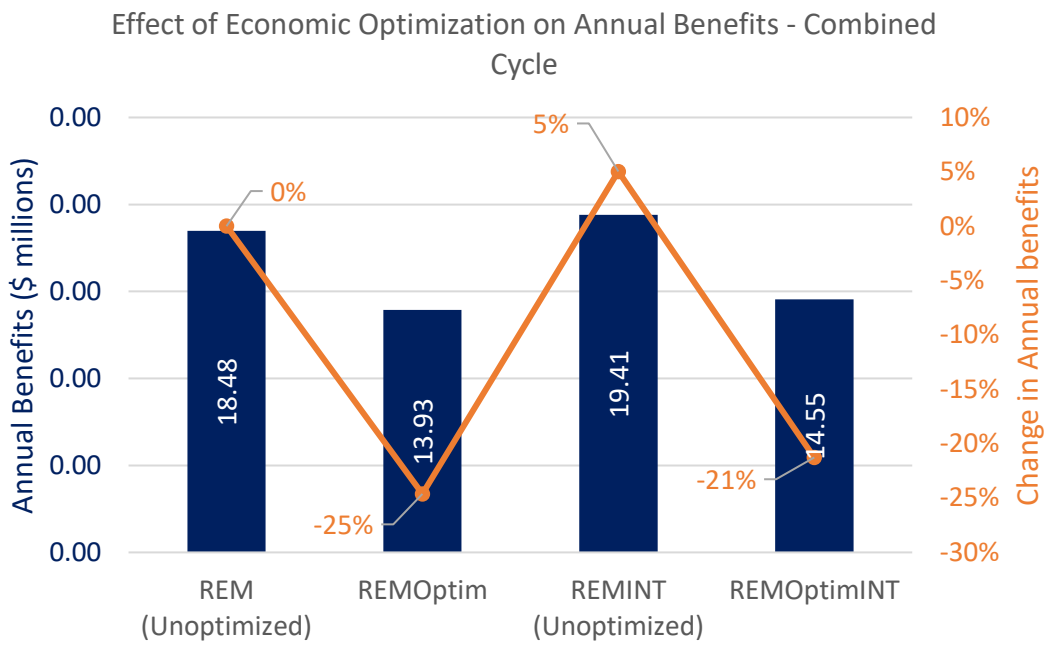

Figure 192: Effect of Economic Optimization on Annual Benefits in Combined Cycle

6.4.3 Techno-economic Analysis Results for the Optimized Engine model

Results from economic analysis conducted on the optimized and un-optimized repurposed engine model in simple and combined cycle application are presented in this section.

6.4.3.1 Effect of REM Optimization on Present worth Analysis Results

In simple cycle investigations, Figure 193 shows that optimization results in a 36% reduction in NPV for the non-intercooled engine model and a 34% reduction in NPV for the intercooled engine model. In relation to LCOE, Optimization delivers a 25% reduction in LCOE for the non-intercooled engine model and a 30% reduction in LCOE for the intercooled engine model. Introduction of an intercooler increases the investment base of the engine model by 2.2%.

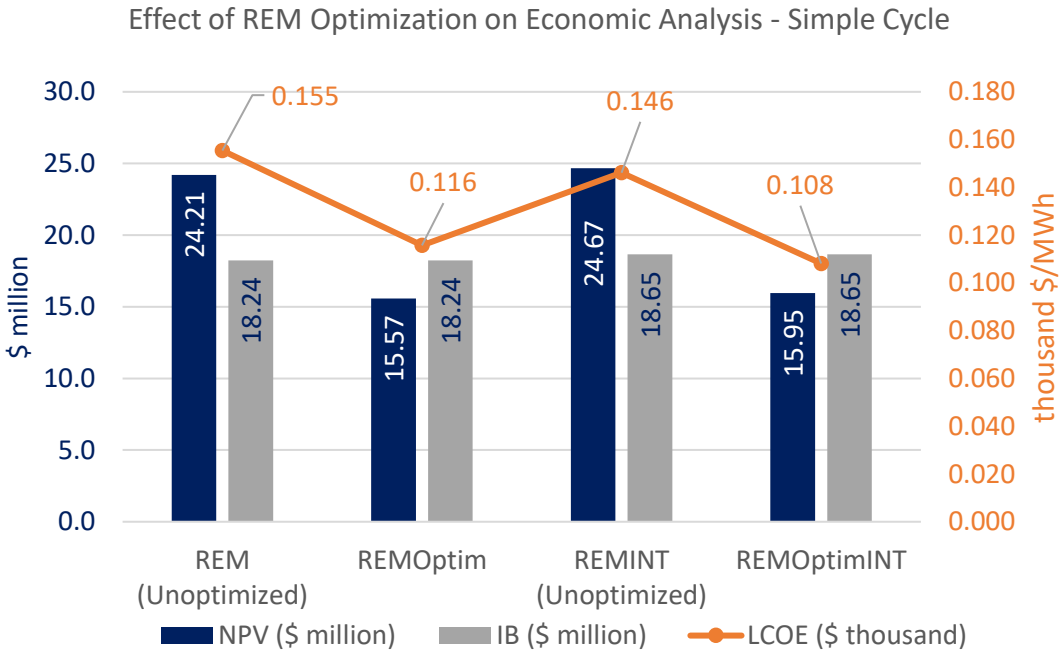

Figure 193: Effect of Optimization on Economic Analysis – Simple Cycle

In combined cycle investigations, Figure 194 shows that optimization results in a 38% reduction in NPV for the non-intercooled engine model and a 36% reduction in NPV for the intercooled engine model. In relation to LCOE, Optimization delivers a 25% reduction in LCOE for the non-intercooled engine model and a 30% reduction in LCOE for the intercooled engine model. Introduction of an intercooler increases the investment base of the engine model by 3.3%.

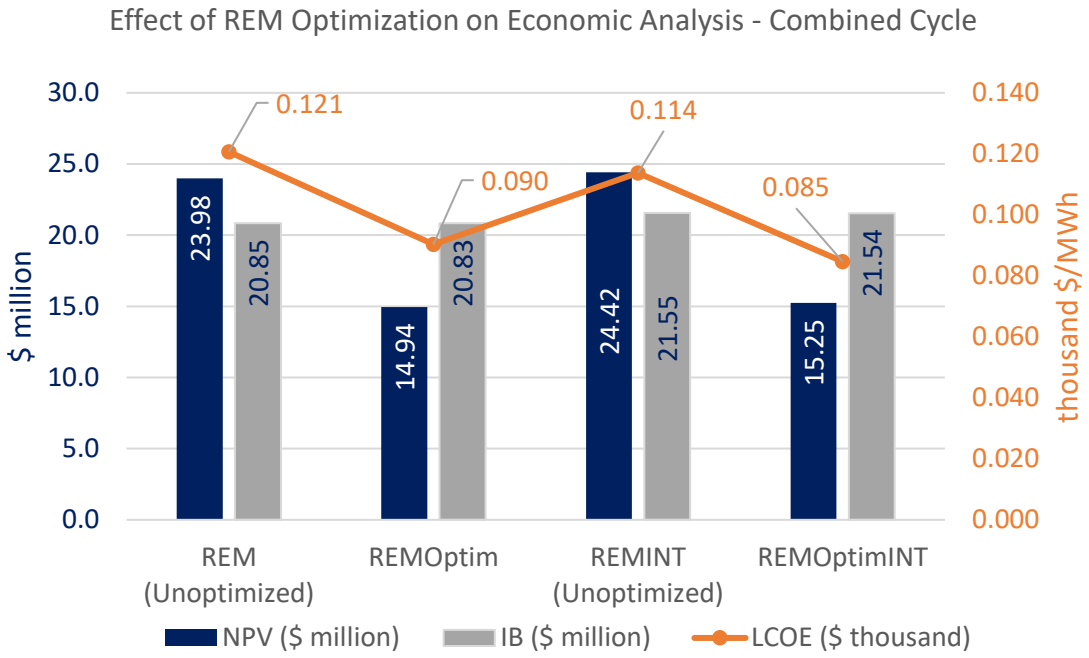

Figure 194: Effect of Optimization on Economic Analysis – Combined Cycle

6.4.3.2 *Effect of REM Optimization on Emission*

In Figure 195, optimization results in a 15% increase in the quantity of NOx removed for the non-intercooled engine model and a 14% increase in the quantity of NOx removed for the intercooled engine model with respect to quantity of NOx generated in the uncontrolled engine model. This result is consistent in both simple and combined cycle investigations.

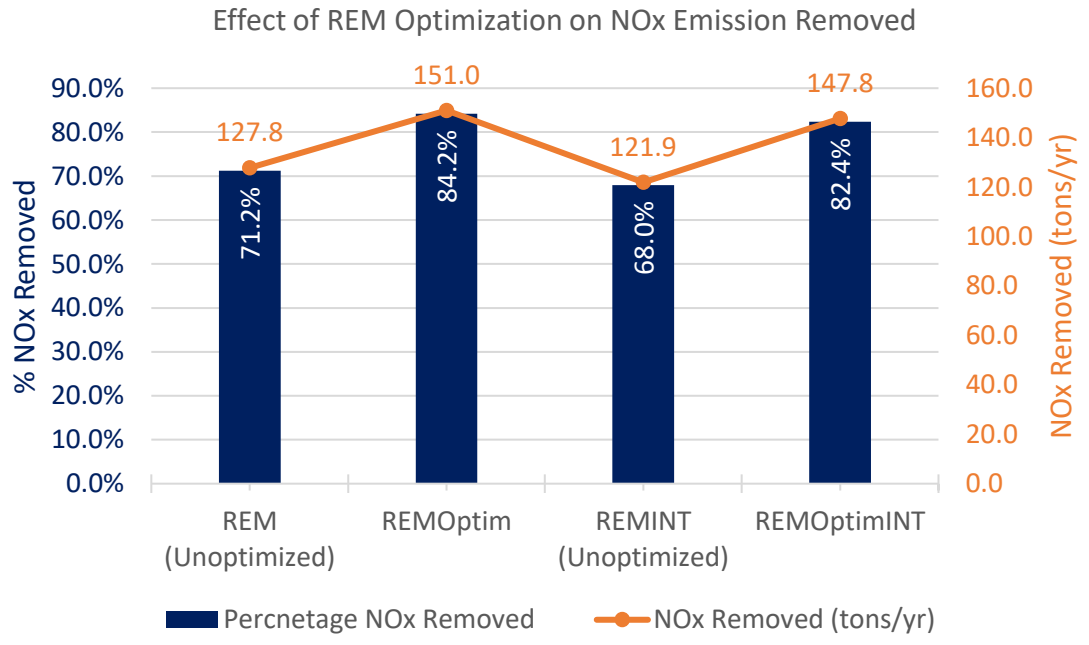

Figure 195: Effect of REM Optimization on NOx Emissions Removed

Figure 196 reveals that optimization results in an 18% reduction in emissions control cost effectiveness for the non-intercooled engine model and a 16% reduction for the intercooled engine model. This means it will cost less to remove NOx in the optimized engine model. Concerning electricity cost impact, the overall optimization analysis has no effect on the electricity cost impact of the emission control technology. However, the introduction of an intercooler results in a 10% decrease in electricity cost impact. This is because of the increase in power output associated with the implementation of an intercooler into the repurposed engine's thermodynamic cycle.

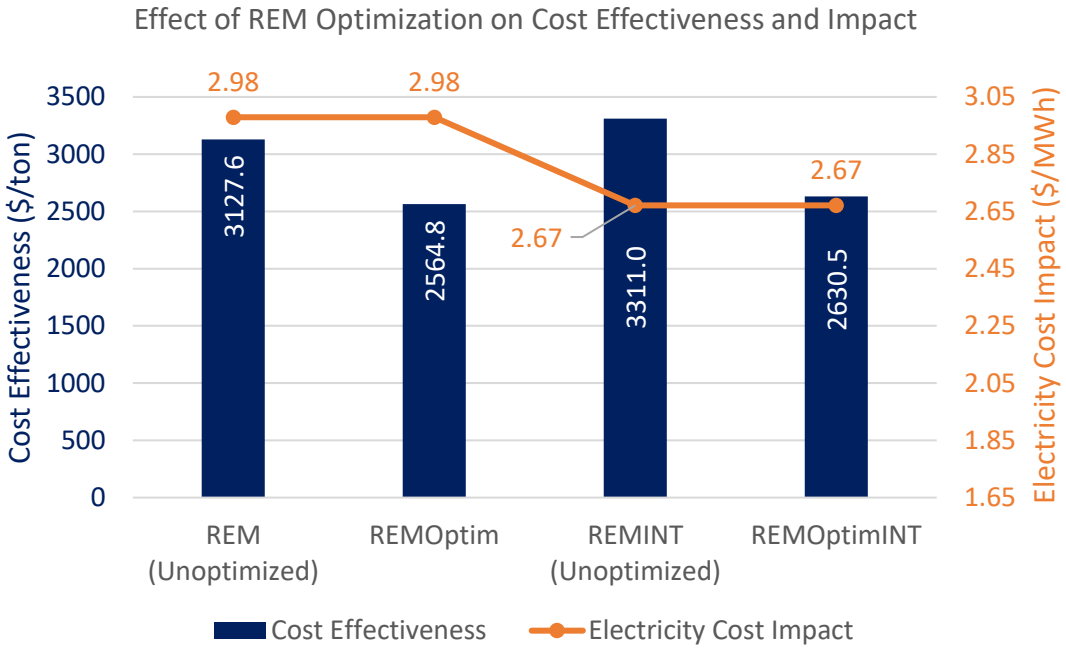

Figure 196: Effect of REM Optimization on Cost Effectiveness and Electricity Cost Impact

6.4.3.3 *Effect of REM Optimization on Cost*

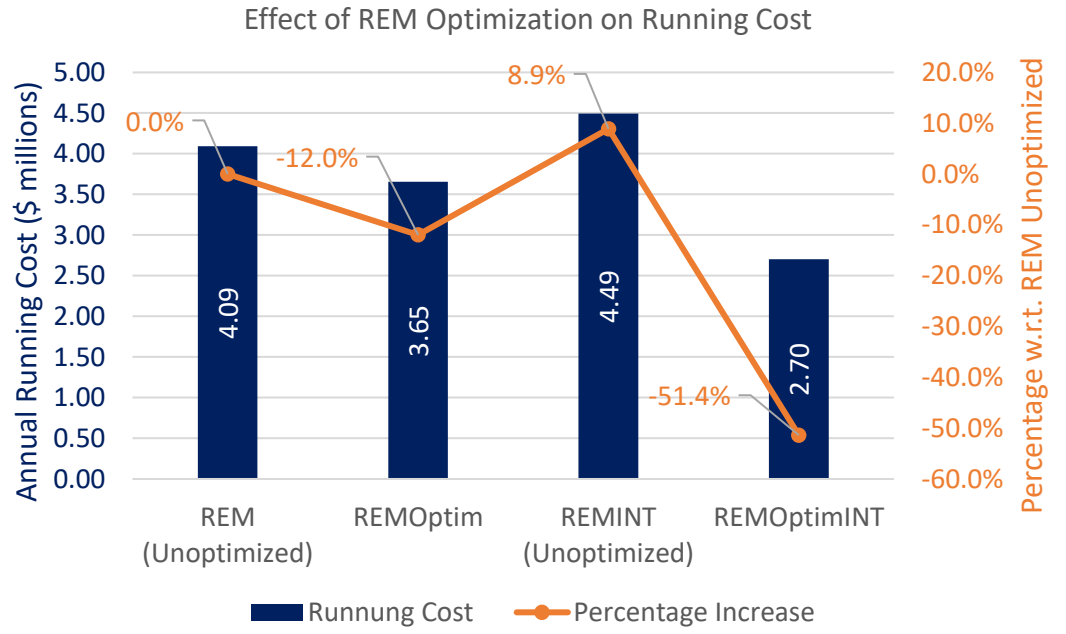

Figure 197: Effect of REM Optimization on Running Cost

Figure 197 reveals that optimization results in a 12% decrease in running cost with the non-intercooled engine model and a 51% decrease with the intercooled engine model. Furthermore, in Figure 198, optimization results in a 38% decrease in annual operation and maintenance cost in the non-intercooled engine model and a 31% decrease in the intercooled

engine model. The decrease in running and operating cost is attributable to the decrease in fuel flow achieved due to performance optimization.

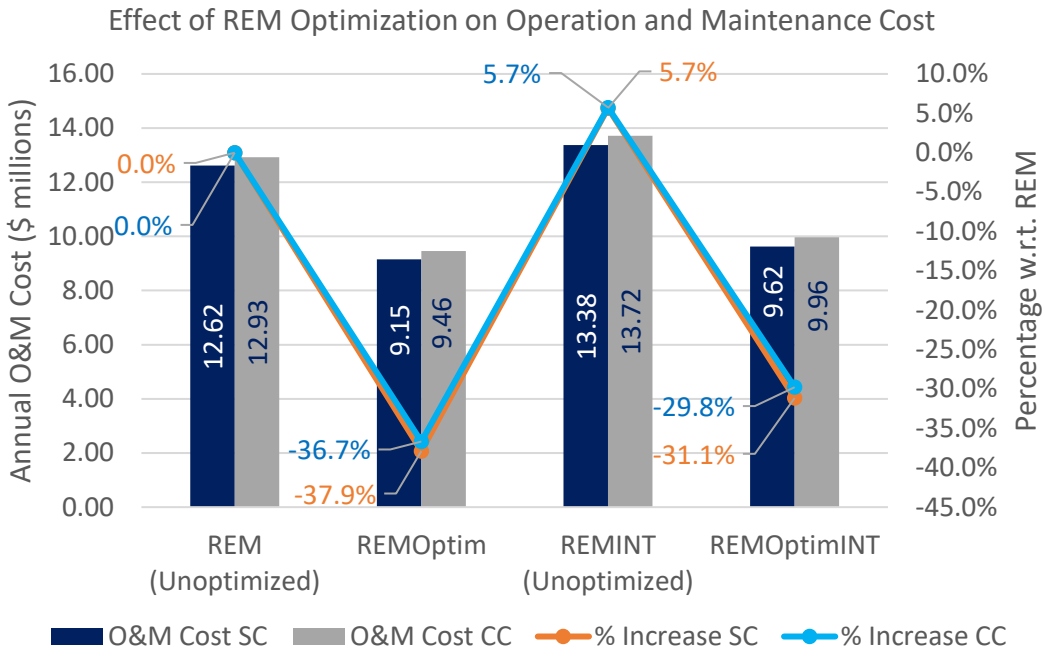

Figure 198: Effect of REM Optimization on Operation and Maintenance Cost

6.4.3.4 *Effect of REM Optimization on Return on Investment (ROI) and Break Even Point (BEP)*

Figure 199 and Figure 200 show that the optimized non-intercooled engine model will break even at 6 years with an ROI of 2% at break-even period and an ROI of 154% over the investigated horizon. The optimized and intercooled engine model will break even at 6years with an ROI of 2% at break-even period and an ROI of 154% over the investigated horizon. The decrease in ROI and increase in break-even period is attributable to the reduced LCOE realised post optimization.

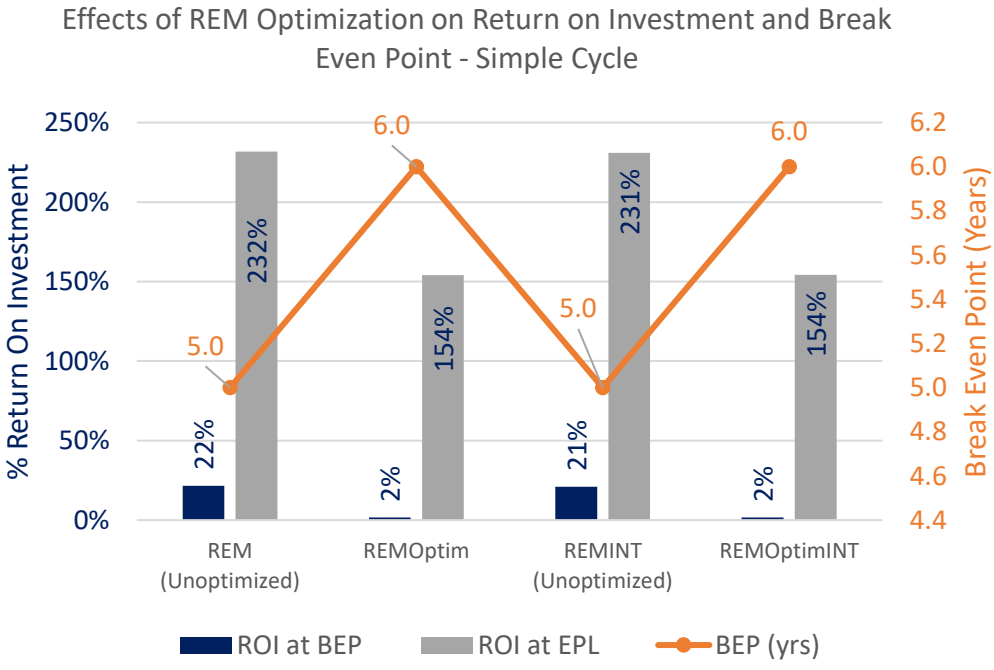

Figure 199: Effects of REM Optimization on Return on Investment and Break Even Point - Simple Cycle

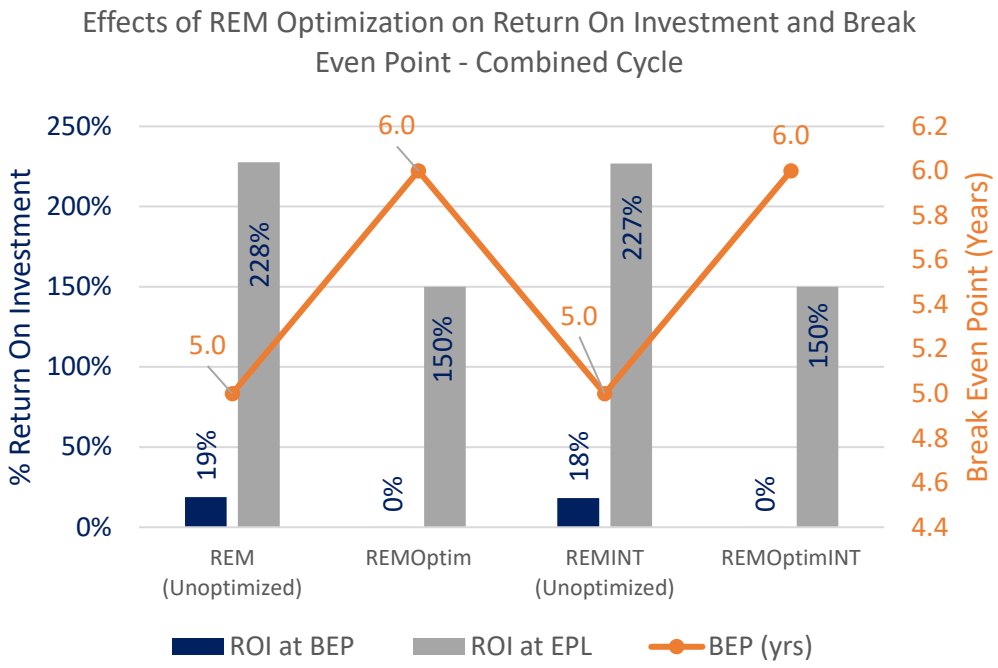

Figure 200: Effects of REM Optimization on Return on Investment and Break Even Point - Combined Cycle

In summary, performance optimization of the REM based on the considered optimization constraints, variables and boundaries results in an overall decrease in fuel flow, exit gas temperature and turbine entry temperature at fixed power output. The introduction of an intercooler increases the maximum power output generated. Economic optimization based on the considered optimization constraints, variables and boundaries results in an overall decrease in LCOE, NPV, running cost, operation and maintenance cost at minimum engine operating hours. The reduction in fuel flow and TET realised results in a decrease in the level of NOx emissions generated.

Optimization analysis conducted on the REM has satisfied the optimization goal and objectives defined in section 5.6.

7 DISCUSSION OF RESULTS

The techno-economic analysis conducted in this study implements element of performance modelling and simulation, cost and emissions modelling and estimation, present worth analysis and performance optimization analysis to evaluate the technical and economic implications of repurposing a turbojet engine model, similar to the Tumansky -R25-300, for electrical power generation.

7.1 Thermodynamic Performance Analysis Results

7.1.1 Performance Modelling and Simulation

To match the real engine performance, the performance simulation parameters of the engine model including cooling bypass, combustor pressure loss and duct pressure loss between the turbines and nozzle are varied. Comparison between the simulated and the actual turbojet engine performance at ISA revealed a less than 1% difference in maximum dry thrust. This suggests that the engine model simulation closely matches the real turbojet engine operation at ISA conditions.

A repurposed variant of the matched turbojet engine model (referred to as the repurposed engine model, REM) is created in TURBOMATCH. This is to simulate engine conversion from turbojet to aero-derivative engine. One major modification made to simulate the engine conversion is the replacement of the models exhaust nozzle and afterburner with a free power turbine. Convergence was achieved by varying duct pressure loss between the power turbines and exhaust. It is assumed that the combustor of the engine model is replaced with a DLN combustor burning natural gas. This gives the best performance output on the REM (about 3% increase in shaft power, 8.5% decrease in fuel flow and 1% increase in thermal efficiency) in comparison to other considered fuel types and is readily available in the case study region (Nigeria). The decreased fuel flow and increased thermal efficiency realised from replacing the combustor and fuel type favours emissions reduction. Application of a DLN combustor on the repurposed engine model removes 71% of NOx emissions generated in relation to the uncontrolled variant.

In comparison to operation at ISA conditions, operating the REM in tropical conditions results in a 5% decrease in power, 1% increase in fuel flow and a 6% decrease in thermal efficiency. This fall in performance output suggests that it will cost more to run the engine model in the considered tropical environment with higher levels of NOx emissions generated and lesser return on investment than at ISA conditions.

By comparison, the repurposed engine model delivers higher power to weight ratio than potential competitor engines like the LM2500 and GG4/FT4. However, its exhaust temperature is relatively lower (770K at ISA and 784K in tropical conditions) but can be used in combination with a condensate boiler to increase efficiency.

7.1.2 Performance Deterioration Analysis

Investigation into the effects of engine component degradation on the REM performance reveals the combined deterioration case to have the most severe effect on the engine models performance. Results show a 17% drop in power output, 7.8% drop in thermal efficiency, 8.4% increase in specific fuel consumption and a 3.4% increase in exhaust temperature at fixed firing temperature. The increase in exhaust temperature may seem to favour combined cycle

applications. However, the penalties incurred from the increased fuel flow, increased exhaust temperature, reduced output power and reduced thermal efficiency may have a notable effect on emissions generated and operating cost.

Additional results obtained indicate that with respect to the implanted deterioration rate and at constant firing temperature, after 24,000 hours of operation, power output for the washed model case drops by 6.7% to a value of 15.63 MW while that for the unwashed engine model case drops by 17% to 13.9MW. This indicates that engine washing on the REM minimises loss of power output by about 11% (based on the implanted deterioration) and will have a significant effect on the life, performance and economic output of the repurposed engine model. In actual operation, the REM may experience far less severe deterioration in component performance than is investigated in this study. Investigations conducted in this study have considered extreme circumstances to identify the engine model behaviour in a worst-case scenario based on knowledge of the potential engine-operating environment and culture.

Investigation conducted into the influence of component degradation on engine model transient performance reveals that engine model deterioration significantly influences the transient performance of the engine model during acceleration (Start-up) and deceleration (Shut down). Results indicate an average drop in power output of about 18% between the clean and deteriorated transient simulation case

7.2 Techno-economic Modelling and Analysis Results

7.2.1 Baseline Techno-economic analysis

The developed techno-economic analysis model is applied to perform baseline economic analysis on the repurposed engine model. This analysis is conducted to investigate the economic feasibility of operating the REM in simple or combined cycle applications. To ensure the validity of the analysis with respect to investigated scenarios, assumptions have been made.

Results reveal that investment in the REM over a 15-year planning horizon will break even at 5years with 22% return on investment (ROI) in simple cycle and 19% return on investment (ROI) in combined cycle. In simple cycle operation, the net present value (NPV) of the REM is $24.21 million at a levelized cost of energy (LCOE) of 0.155$/MWh and an investment base (IB) of $18.24 million. In combined cycle investigations, the REM delivers a NPV of $23.98 million at an LCOE of 0.121$/MWh and investment base of $20.85 million. Although the investment base require for combined cycle operation is 12.5% higher than for simple cycle, it delivers a high net present value, at the lowest cost (22% lower) to potential consumers, which is only 1% lower than the NPV obtained from simple cycle investigations. A 1% increase in the LCOE for the combined cycle investigation will deliver an NPV equivalent to that obtained in simple cycle operation while maintaining a cheaper cost of electricity to potential consumers.

Results retrieved from baseline investigation of the REM have been compared with those obtained from similar competitor units. A desirability grading system is applied to score each engine unit considered based on a set of desirable characteristics. The engine model consideration with the highest score tends to satisfy, reasonably, majority of the desired characteristics. From the results obtained in this study, the LM2500 engine model delivers the

highest desirability score with a value of 59%. The REM and GG4/FT4 model both have desirability scores of 52% and the LM1600 engine model emerged with a desirability score of 48%. Result from the desirability score may suggest that the most appropriate unit to invest in is the LM2500 engine model. However, considering that the potential investors already own the considered case study engine model, no resource will be allocated to acquire the engine model. The only resource allocation will be towards engine refurbishment and retrofitting needed to repurpose the engine model for electrical power generation.

With respect to the assumptions made in this study and results obtained from the baseline analysis, the repurposed engine model, REM, has a positive economic feasibility and from an economic perspective, can compete favourably with similar engines employed in electrical power generating applications. Provided there are no capital budgeting restrains, application of the repurposed engine model in combined cycle is recommended as opposed to simple cycle application. This is because, baseline investigation results reveal that operating the repurposed engine model in combined cycle will deliver reasonable profitability to the operator at the least cost to consumers.

7.2.2 Factors Influencing Baseline Techno-economic Analysis

7.2.2.1 Effect of engine deterioration on techno-economics

Analysis into the effects of engine deterioration on the REM economics reveals that in both simple and combined cycle investigations, engine degradation results in an increase in cost both to the operator in form of increased running cost and to the consumers as an increase in the cost of electricity. Thus, for the proposed investor to sustain and achieve the projected NPV, the levelized cost of electricity and productivity (in form of engine operating hours) may have to increase. In relation to emissions generation, deterioration of the REM results in an increase in the level of NOx generated which translates to higher cost of controlling emissions generated and greater impact of the emissions control technology on the cost of electricity.

7.2.2.2 Effect of transient operation on techno-economics

Investigation into the effect of transient operating regime on the techno-economics of the repurposed engine revealed no significant effect. This is due to the brief duration in which the repurposed engine model operates in the transient phase; as such, the evaluated effects of transient operations are too little to influence engine performance output and economics. Results from evaluations conducted at extreme transient operating conditions show only a 0.03% increase in running cost and a 0.02% increase in operation and maintenance cost. This observation is consistent in both simple and combined cycle investigations.

7.2.2.3 Effect of power cycling on techno-economics

Investigation into the effects of power cycling on the repurposed engine model reveals a 26% increase in the levelized cost of electricity (LCOE) in order to maintain Baseline net present value (NPV). Furthermore, power cycling the REM at baseline LCOE values, results in 26% decrease in NPV. This is so because in the power-cycled engine model, the total power output per year reduces and so does the amount of electricity sold based on the total power generated. Due to the decrease in electricity sold, it will take longer to break even. At baseline LCOE, investment in the power cycled repurposed engine model will break even at 7years (as opposed to 5years in the uncycled engine) with 16% return on investment.

7.2.2.4 *Effect of tropical operation on techno-economics*

Techno-economic analysis conducted for the repurposed engine model operating in tropical environment with conditions identical to those obtainable in the case study region, Nigeria; reveal a 0.4% increase in running and operating costs, with a 3.3% decrease in NPV and 3.1% increase in LCOE. This suggests that it will cost more to operate the engine model in identical conditions similar to the considered case study region than at ISA conditions. However, engine operation within the considered tropical conditions will result in less than 7% decrease in projected baseline benefits over the investigated horizon. The decrease in the economic output of the REM in tropical conditions is attributable to an overall decrease in the engine-model performance output.

7.2.2.5 *Effect of acquisition cost on techno-economics*

The effects of acquisition cost on the techno-economic analysis of the repurposed engine model has been investigated. Results reveal that at acquisition cost of zero (since power plant already exists and will not be purchased), LCOE reduces by 45% and the required investment base drops by 80%. NPV also drops by 68% from projected baseline values. This is because of the reduction in LCOE. To maintain projected baseline NPV, the levelized cost of energy (LCOE) will have to increase substantially. An acquisition cost of zero implemented in the techno-economic analysis of the repurposed engine model has no effect on operation and maintenance cost or the level of emissions generated and controlled.

7.3 Techno-economic optimization analysis Results

Performance and economic optimization analysis performed on the repurposed engine model with respect to the considered optimization constraints, variables and boundaries results in 51% decrease in running cost and 31% decrease in operation and maintenance cost. The introduction of an intercooler into the optimization analysis reduces the amount of NOx emissions generated at fixed minimum power output. This is because of a reduction in fuel flow and turbine entry temperature realised from reduced compressor work demanded by the REM, which will otherwise favour the generation of NOx emissions. An optimized and intercooled variant of the repurposed engine model delivers an LCOE 30% lower and a NPV 36% lower than the un-optimized engine model. To maintain baseline NPV, LCOE will have to increase.

In the optimized and intercooled engine model, performance optimization results in a 45% drop in exhaust gas temperature. This discourages the application of the optimized and intercooled REM variant for combined cycle applications except if the exhaust gas is reheated to a temperature sufficient to accommodate combined cycle applications. This will however incur additional running and operating costs and result in increased emission levels.

8 CONCLUSION

In line with the aim of this study, a techno-economic analysis model has been developed which takes into account technical, environmental and economic variables during analysis in order to arrive at reasonable solutions for gas turbine engine performance and system optimization from a technical and economic perspective, and in a viable and cost effective way. The following sections briefly describe the tasks performed to achieve the research aim.

8.1 Selection of Case Study Engine

In order to provide a baseline for the overall research analysis and investigation, a case study engine has been selected. The chosen engine is the Tumansky-R25-300 turbojet engine, which is the power plant, used on the MiG 21 fighter jet. This engine choice seeks to investigate an alternative but profitable use for the power plants of the grounded MIG 21 fighter jets owned by the Nigerian Air force. These aircrafts have been grounded due to lack of spare parts for maintenance.

8.2 Thermodynamic Performance Analysis

A performance model similar to the chosen case study engine is created and simulated using TURBOMATCH. To match the real engine performance at ISA conditions, identical performance and operating parameters are supplied into the engine model and simulation parameters including cooling bypass, combustor pressure loss and duct pressure loss between the turbines and nozzle are varied. Comparison between simulated and the actual turbojet engine performance at ISA conditions reveal a less than 1% difference in maximum dry thrust. This suggests that the engine model simulation closely matches the real turbojet engine operation at ISA conditions.

A repurposed variant of the turbojet engine (referred to as the repurposed engine model, REM) is created in TURBOMATCH. This is to simulate engine conversion from turbojet to aero derivative engine. Modifications made to simulate the engine model conversion involve the replacement of the models exhaust nozzle and afterburner with a free power turbine and the adoption of a DLN combustor burning natural gas a fuel. Model convergence was achieved by varying duct pressure loss between the power turbines and exhaust. Further performance analysis is conducted to investigate the effect of component deterioration, operating condition and transient operation on the repurposed engine model's performance.

8.3 Development of Cost and Economic analysis model

The developed techno-economic model incorporates several multidisciplinary methodologies, integrated as modular units and identified, in this study, as components of the overall techno-economic model. The model consist of a price estimating component, life approximating model component, emissions model component, performance modelling and simulation component, cost model component, optimization model component and a selection model component.

8.3.1 Price estimating model component

The Price estimating component applies artificial neural network (ANN) and regression analysis (RA) to estimate the acquisition cost for any gas turbine unit based on engine performance parameters of power output, heat rate and turbine rpm. Evaluations to validate the developed price-estimating model reveals higher accuracy (between 95-99%) for ANN

estimates in comparison to regression analysis estimates, which fall between 72%-98%. The dataset used for price estimation reveals a strong positive correlation between acquisition cost and engine power output, and a weak negative correlation between acquisition cost, turbine rpm and heat rate.

8.3.2 Life approximating model component

The life approximating model component utilises an approximation approach to estimate the remaining useful life of a gas turbine based on the effect of maximum operating temperatures on the engine's turbine blade.

8.3.3 Emissions model component

The emissions model component evaluates the amount of emissions generated by a gas turbine with respect to the gas turbine emissions activity, associated emissions factor (obtained from AP-42 data sheet) and the implemented engine emissions control system. The emissions model enables the evaluation of gas turbine engine emissions tax rate and quantity of emissions controlled by an implemented emission control technology. The considered emissions control technology include:

- Water/Steam injection
- dry low NOx (DLN) /Lean Premixed combustion
- Selective Catalytic Reduction (SCR) System
- SCONOx™ Catalytic Absorption System

As a validation to the developed emission-estimating approach, the emissions model is applied to predict emissions rate from investigations, conducted for the U.S. department of energy, by ONSITE SYCOM Energy Corporation in 1999 and investigations conducted by the California energy commission for the EL Segundo Power Redevelopment Project (ESPR) in 2007. Comparison of the emissions model estimates with those documented from investigations in past projects reveal a difference of less than 3%.

8.3.4 Performance-modelling and simulation component

The performance-modelling and simulation component permits modelling and simulation of steady state and transient gas turbines behaviour with the aid of computational models in TURBOMATCH. Integration of the performance component into the overall techno-economic model enables a wider and robust investigation of numerous techno-economic considerations and scenarios including, degradation, power cycling, transient and even novel Brayton cycle systems.

8.3.5 Cost model component

The cost model component is associated with cost analysis and utilizes input from other components to evaluate all direct and indirect operating costs and benefits associated with an investigated cycle or system.

8.3.6 Optimization model component

The optimization model component executes performance and economic optimization analysis to achieve optimum engine performance and economic benefits with respect to a set of defined objectives, constraints and variables. The optimization model has been applied in this study to minimise fuel consumption, emissions generated and the levelized cost of energy at fixed power output while maintaining profitability.

8.3.7 Selection model component

The selection model component executes present worth analysis to determine profitability and economic feasibility over an investigated horizon.

8.4 Baseline Techno-economic Analysis

The developed techno-economic modelling and analysis approach has been applied to investigate the feasibility from a performance and economic perspective of repurposing a turbojet engine model for electrical power generation. The case study engine model selected for this investigation is similar to the TUMANSKY-R25-300 turbojet engine, repurposed for electrical power generation. The techno-economic analysis conducted takes into account the steady state and transient engine performance of the repurposed engine model (REM).

8.4.1 Performance Analysis of repurposed engine model

At ISA conditions, burning natural gas (TOMZACK), the repurposed engine model, REM, delivers 18.52MW of power at 33.5% thermal efficiency and firing temperature of 1310.15K. With respect to the case, study environment (Tropical region), at an average altitude of 700m, the repurposed engine model delivers 17.66MW of Power at a thermal efficiency of 31.6% and turbine entry temperature of 1310.15K.

In comparison to operation at ISA, operating the REM in tropical conditions results in a 5% decrease in power, 1% increase in fuel flow and a 6% decrease in thermal efficiency. By comparison, the repurposed engine model delivers higher power to weight ratio than potential competitor engines like the LM2500 and GG4/FT4. However, its exhaust temperature is relatively low (770K at ISA and 784K in tropical conditions) but can be used in combination with a condensate boiler to increase efficiency.

Investigation into the effects of engine component degradation on the REM performance reveals the combined deterioration case to have the most severe effect on the engine models performance. Results show a 17% drop in power output, 7.8% drop in thermal efficiency and an 8.4% increase in specific fuel consumption at fixed firing temperature, due to combined engine deterioration effects. With respect to the implanted deterioration rate, engine washing minimises loss of power output by 11%.

Investigation conducted into the influence of component degradation on engine model transient performance revealed that, deterioration effects significantly influences the transient performance of the engine model during acceleration (Start-up) and deceleration (Shut down). Results indicate an average drop in power output of about 18% between the clean and deteriorated transient simulation case.

8.4.2 Economic Analysis of repurposed engine model

8.4.2.1 Baseline Economic Analysis

Using output obtained from the performance simulation and analysis, baseline economic analysis has been conducted on the repurposed engine model to investigate the economic feasibility of operating the unit in both simple and combined cycle applications. To ensure validity of the analysis to investigated scenarios, assumptions have been made.

Results reveal that investment in the REM over a 15years planning horizon will break even at 5years with 22% return on investment (ROI) in simple cycle and 19% ROI in combined cycle application. In simple cycle, the REM deliver a NPV of $24.21 million at a levelized cost of

energy, LCOE, of 0.155$/MWh and an investment base of $18.24 million. In combined cycle investigations, the REM delivers a NPV of $23.98 million at an LCOE of 0.121$/MWh and with an investment base of $20.85 million in combined cycle. The REM delivers a net present value, NPV, 1% higher, an LCOE 22% higher and an investment base 13% lower in simple cycle than in combined cycle investigations.

Results retrieved from baseline investigation of the REM have been compared with those obtained from similar competitor units. A desirability grading system has been developed and applied to score each engine unit considered based on a set of desirable criteria. The engine model consideration with the highest score tends to satisfy, reasonably, majority of the desired characteristics. From the results obtained in this study, the LM2500 engine model delivers the highest desirability score with a value of 59%. The REM and GG4/FT4 model both have desirability scores of 52% and the LM1600 engine model emerged with a desirability score of 48%.

With respect to the assumptions made in this study and results obtained from analysis, it can be concluded that the repurposed engine model, REM, has a positive economic feasibility and from an economic perspective, can compete favourably with units employed in similar electrical power generating applications.

8.4.2.2 Additional Economic Investigations

8.4.2.2.1 Degradation, Transient operation and Power cycling Effects

Analysis is into the effects of engine degradation and transient operation on the REM economics has been conducted. In both simple and combined cycle investigations, engine degradation results in an increase in cost to the operator in form of increased running cost and to the consumers as an increase in the cost of electricity.

Investigation into the effect of transient operating regime on the techno-economics of the repurposed engine revealed no significant effect. This is probably due to the brief duration in which the repurposed engine model operates in the transient phase; as such, the evaluated effects of transient operations are too little to influence engine performance output and economics. Results from evaluations conducted at extreme transient operating conditions show only a 0.03% increase in running cost and a 0.02% increase in operation and maintenance cost. This observation is consistent in both simple and combined cycle investigations.

Investigation into the effects of power cycling on the repurposed engine model reveals that at baseline LCOE, there is a 26% decrease in NPV realised. This is so because power cycling results in a reduction in annual power output. Thus, amount of electricity sold which is a function of the on amount of power generated will reduce. Due to the decrease in electricity sold, it will take longer to break even. At baseline LCOE, investment in the considered power cycled engine model will break even at 7years (as opposed to 5years in the uncycled engine) with 16% return on investment.

8.4.2.2.2 Tropical operation and Acquisition cost Effects

Techno-economic analysis conducted for the repurposed engine model operating in a tropical environment with conditions identical to those obtainable in the case study region, Nigeria reveal a 0.4% increase in running and operating costs, with a 3.3% decrease in NPV and 3.1%

increase in LCOE. The decrease in performance and increase in operating costs suggest that it will cost more to operate the engine model in the considered case study region than at ISA conditions.

The effects of acquisition cost on the techno-economic analysis of the repurposed engine model has been investigated. Results reveal that at acquisition cost of zero, LCOE reduces by 45% and the required investment base drops by 80%. NPV drops by 68% from projected baseline values. The consideration of zero acquisition costs is based on the knowledge that the Nigerian Air force (at purchase of the now grounded aircraft) has already acquired the power plant and thus will only be allocating resources towards refurbishment and retrofitting of a repurposed variant. The acquisition cost associated with the power plant at purchase in this regard is considered as sunk cost, which cannot be recovered. The consideration of sunk cost in the techno-economic analysis of the repurposed engine model has no effect on operation and maintenance cost or the level of emissions generated and controlled. Therefore, at baseline LCOE, with sunk cost consideration, investment in the repurposed engine model deliver an earlier return on investment at 2.2 years with 27% ROI.

8.5 Techno-economic Optimization Analysis

Performance and economic optimization analysis has been performed on the repurposed engine model to minimise fuel consumption, NOx emissions and LCOE while maintaining profitability in both simple and combined cycle applications. With respect to the considered optimization constraints, variables and boundaries, optimization analysis results in 51% decrease in running cost and a 31% decrease in operation and maintenance cost. The introduction of an intercooler into the optimization analysis reduces the amount of NOx emissions generated at fixed power output. The optimized and intercooled engine model variant delivers 30% lower LCOE and 36% lower NPV than the un-optimized engine model.

8.6 Techno-economic Cost Modelling and Analysis Tool

A techno-economic cost-modelling and analysis tool based on the developed techno-economic analysis methodology presented in this study, has been developed and applied to assess the potential, from a performance and economic perspective, of repurposing a turbojet engine for electrical power generation, optimized for minimum emissions and optimum economic benefit. This tool developed using MATLAB and Visual studios C sharp (C#) has been integrated with TURBOMATCH a performance modelling and simulation tool developed at Cranfield University. The integration of the tool with TURBOMATCH has extended its potential application scope to cover numerous areas including preliminary design investigation, technology comparison, power cycling analysis, project selection from alternatives, capital budgeting problems, novel cycle investigations, productive life cost analysis, life cycle cost analysis and sensitivity analysis e. t. c.

8.7 Summary

Based on the techno-economic analysis conducted, assumptions made and results obtained from this study, a method for assessing potentially significant solutions for gas turbine engine performance and system optimization from a technical and economic perspective and in a viable and cost effective way has been developed. The methodology has been applied to investigate the feasibility of repurposing a turbojet engine for electrical power generation.

Results obtained from the investigation suggest that, it is feasible to apply the repurposed engine model (REM) for electrical power generation from a performance and economic perspective, both within and outside the considered case study region with minimal loss in performance output and economic profitability. Furthermore, results reveal that the repurposed engine model (REM) can favourably compete, from an economic and performance perspective, with some of the competitor units considered in this study. An optimized variant of the REM can delivers up to 45% reduction in fuel flow, 45% reduction in NOx emission generated and up to 30% decrease in LCOE from baseline values while maintaining profitability. How be it at the detriment of a falling exhaust gas temperature, which discourages application of the REM in combined cycle.

In an un-optimized state and provided there are no capital budgeting constraints, application of the repurposed engine model in combined cycle is recommended as opposed to simple cycle application. This is because, baseline investigations reveal that operating the repurposed engine model in combined cycle will deliver reasonable profitability to the operator at higher thermal efficiency and at the least cost to consumers.

A techno-economic cost modelling and analysis tool based on the developed techno-economic analysis methodology has been developed and integrated with TURBOMATCH performance simulation software.

9 FUTURE WORK

- In this study, all investigation conducted are based on performance simulation models of a repurposed engine. Due to certain restrictions and limitations, a prototype is not available for detailed investigations. The outcome of this research may stir interests into the development of a working prototype necessary for detailed analysis, and investigation into the potential of repurposing the considered power plants.

- The implemented modification to the thermodynamic cycle of the repurposed engine model is an intercooler. Although this results in an increase in power out, there is a commensurate increase in fuel flow to achieve a specific firing temperature. Future efforts can investigate the potential of incorporating a heat exchanger between the high-pressure turbine and the combustor inlet to minimise the fuel flow required to achieve a specific firing temperature, this however may result in a drop in exhaust gas temperature and restrict the potential application of the repurposed engine model in combined cycle application.

- The price-estimating model implemented in this study, considers three independent variables, which are used to estimate engine acquisition costs. Increasing the number of independent variables considered can increase prediction accuracy, as there will be more independent variables describing the behaviour of the considered dependent variable.

- Because of the weak correlation observed between engine heat rate, turbine rpm and engine acquisition cost, only one independent variable is applied in the regression analysis model to estimate acquisition cost. Additional investigation can be conducted to compute a multiple correlation coefficient R, which will simultaneously take into account all information, provided in the compiled dataset to evaluate correlation between the dependent and independent variables. Evaluating the multiple correlation coefficient can enhance prediction accuracy of the dataset.

- This study incorporates a life approximation model, based on the outcome from an investigation conducted on the effect of deterioration on engine life. As such, life approximations may vary in some scenarios from those represented by the implemented approximation model. The development of a robust lifing model capable of computing or estimating the remaining useful life of any gas turbine will be a useful enhancement to the techno-economic methodology developed in this study.

10 BIBLIOGRAPHY

'Layi Fagbenle, R., 2014. *Exergy and Environmental Considerations in Gas Turbine Technology and Applications,* illinois, USA: 'Layi Fagbenle, Richard.

Advanced Animations UK, 2016. *Advanced Animations UK.* [Online]
Available at: http://www.advancedanimations.co.uk/portfolio/rolls-royce-avon-200-cutaway/
[Accessed 21 September 2016].

Akinyemi, O., 2008. *Gas Turbines Performance Prognostics,* Bedfordshire: Cranfield University.

Amaoge, U. D., 2011. *Industrial Gas Turbine Emission Assessment and Modelling for LNG Compression- A TERA Approach,* Cranfield, Bedfordshire: Cranfield University.

ASME Power & Energy Conference, 2018. *ASME's Resolving The Challenges Of Power Plant Cycling,* Orlando, Florida: ASME Power & Energy Conference.

Au, T., 1996. Depreciation and Corporate Taxes. In: *The Engineering Handbook.* Florida: CRC Press, Inc, pp. 1939-1946.

Baioni, C. A., 2009. *TERA for LNG - Risk Methodology for Gas Turbine Selection in LNG Application,* Bedfordshire: Cranfield University.

Banks, J., Carson, J., Nelson, B. & Nicol, D., 2001. Discrete-Event System Simulation. In: *Discrete-Event System Simulation.* Upper Saddle River, New Jersey, United States: Prentice Hall, pp. 3. ISBN 0-13-088702-1.

Beaves, R. G., 1996. Project Analysis Using Rate-of-Return Criteria. In: *The Engineering Handbook.* Florida: CRC Press, Inc, pp. 1926-1932.

Bender, R. W., 2006. Lean Pre-Mixed Combustion. In: *Gas Turbine Handbook.* Morgantown USA: U.S. Department of Energy's National Energy Technology Laboratory, pp. 217-227.

bpress, 2014. *bpress Website.* [Online]
Available at: http://www.bpress.cn/im/tag/GE-Gas-Turbines/
[Accessed 20 September 2016].

Brone, S. P. M., n.d. *Future NOx Taxation as an Incentive for Combustor Upgrades-A TERA Project,* Cranfield, Bedfordshire: Cranfield University.

Brooks, F. J., 2006. GE Gas Turbine Performance Characteristics. *GE Power Systems*.

Business Journals, Inc., 1975-1977. *Turbomachinery International.* Norwalk: Business Journals, Inc..

California Energy Commission, 2007. *El Segundo Power Redevelopment Project - Dry Cooling Amendment Proceeding.* [Online]
Available at:
https://www.energy.ca.gov/sitingcases/elsegundo_amendment/2007_amendment/owner/Appendices/3.1-A1_Air_Emission_Data.pdf
[Accessed 8 November 2018].

California Energy Commission, 2007. *El Segundo Power Redevelopment Project (ESPR) - Detailed Gas Turbine Emissions Calculations A1 Air Emission Data,* California USA: California Energy Commission.

Christina, C., 2011. *Ethanol-based Electricity Generation from Flex-Fuel Natural Gas Power Stations: A Techno-Economic Assessment and Case Study in Brazil,* London: Centre for Environmental Policy, Imperial College London.

Cranfield Department Of Power and Propulsion, 1999. *The TURBOMATCH Scheme.* Cranfield: Cranfield University Department of Power and Propulsion.

David, W. J., 2013. *Aero-derivative gas turbine engine with an advanced transition duct combustion assembly.* United States of America, Patent No. US 20130081407 A1.

Emad, S., 2013. *emadrlc.* [Online]
Available at: http://emadrlc.blogspot.co.uk/search?q=gas+turbine
[Accessed 21 September 2016].

Evangelos, T., 2008. *Technoeconomic Environmental and Risk Analysis of Marine Gas Turbine Power Plants,* Cranfield: Cranfield University.

Forecast International, 2018. *Industrial Trent 60 / MT30 Marine Engine,* Newtown, USA: PowerWeb - A Forecast International Inc. Subsidiary.

Gad-Briggs, A., Haslam, A. & Laskaridis, P., 2013. Effect of Change in Role of an Aircraft on Engine Life. *The Aeronautical Journal,* 117(1196), pp. 1053 - 1070.

Gas and Steam Turbines, 2012. *Gas and Steam Turbines - LM1800e Aeroderivative Gas Turbines.* [Online]
Available at: http://gasandsteamturbines.blogspot.com/2012/02/lm1800e-aeroderivative-gas-turbines.html
[Accessed 03 April 2019].

Gas Turbine International, 1977. Latest News - General Electric Sells. *Sawyer's Gas Turbine International,* 18(4), p. 56.

General Equipment, 2013. *Prattand Whitney FT4 Proposal.* North America: General Equipment.

Giampaolo, T., 2003. *Gas Turbine Handbook: Principle and Prcatices.* 2nd ed. Lilburn, GA: The Fairmont Press, Inc.

Glenn Research Center, 2015. *Nasa Website.* [Online]
Available at: https://www.grc.nasa.gov/www/k-12/airplane/brayton.html
[Accessed 21 September 2016].

GlobalSecurity, 2015. *GlobalSecurity Website.* [Online]
Available at: http://www.globalsecurity.org/military/world/nigeria/air-force-equipment-intro.htm
[Accessed 20 September 2016].

Gunston, B., 2001. Jane's Aero-engines. In: J. I. G. Bill Gunston, ed. *Jane's Aero-engines.* s.l.:Jane's Information Group, 1996, pp. 294 - 295.

Hans, D. R. & Douglas, G. F., 1999. The Application of Expert Systems and Neural Networks to Gas Turbine Prognostics and Diagnostics. *Journal of Engineering for Gas Turbines and Power,* Volume 121, pp. 607-612.

Hendrickson, C. & Sue, M., 1996. Project Selection from Alternatives. In: *The Engineering Handbook.* Florida: CRC Press, Inc, pp. 1933-1938.

Henssen, P., 2014. *Specialist Groundworks Contractors,* Cambridgeshire: Construction Group Association.

Higgins, J., 2005. *The Radical Statistician.* 5th ed. Carlifornia: The Management Advantage, Inc..

Hollmann, J. K. & Dysert, L. R., 2007. *Escalation Estimation: Working With Economics Consultants,* Morgantown, WV,: AACE International Transactions, AACE International,.

hyperphysics, 2016. *hyperphysics Website.* [Online]
Available at: http://hyperphysics.phy-astr.gsu.edu/hbase/mi.html
[Accessed 21 September 2016].

hyperphysics, 2016. *hyperphysics Website.* [Online]
Available at: http://hyperphysics.phy-astr.gsu.edu/hbase/rotq.html
[Accessed 22 September 2016].

Ilbas, M. & Mahmut, T., 2012. Estimation of Exhaust Gas Temperature Using Artificial Neural Network in Turbofan Engines. *Journal of Thermal Science and Technology,* 2(32), pp. 11-18.

Jayasinghe, D., n.d. *Towards the Development of A TERA Model To Assess The Potential of Bio SPKs For Civil Aviation,* Cranfield, Bedforshire: Cranfield University.

Jenkinson, L. R., Simpkin, P. & Rhodes, D., 1999. Aircraft Cost Estimation. In: *Civil Jet Aircraft Design.* London : Butterworth Heinemann, pp. 302-325.

Jiang, X., Lin, T. & Mendoza, E., 2016. *Enhancing Turbine Performance Degradation Prediction with Atmospheric Factors.* Atlanta, USA, Annual Conference of the Prognostic and Health Management Society 2016 .

Karsoliya, S., 2012. Approximating Number of Hidden layer neurons in Multiple Hidden Layer BPNN Architecture. *International Journal of Engineering Trends and Technology,* 3(6), pp. 714 - 717.

Khan, R. S., 2012. *TERA for Rotating Equipment Selection,* Cranfield: Cranfield University.

Kumar, K. S., 2013. *Towards the Development of A TERA Framework For Solarised Gas Turbines,* Cranfield, Bedfordshire: Cranfield University.

Kumar, N. et al., 2012. *Power Plant Cycling Costs,* Sunnyvale, California: National Renewable Energy Laboratory, NREL.

Kurz, R., Meher-Homji, C. & Brun, K., 2014. *Gas Trubine Degradation.* Houston, Texas, USA, Pump & Turbo 2014 Symposia.

Lagana, M. C., 2008. *TERA for LNG Applications,* Bedfordshire: Cranfield University.

Langmaak, S. et al., 2013. *An activity-based-parametric hybrid cost model to estimate the unit cost of a novel gas turbine component,* Derby, United kingdom: Rolls-Royce plc.

leatherneck, S., 2014. *DCS MIG-21 Bis - Flight manual.* s.l.:Simulations, leatherneck.

LeCun, Y. & Bottou, L. O. G. B. M. K.-R., 1998. *Efficient Back Prop,* New Jersey: Springer.

Li, Y. G., 2002. Performance Analysis Based Gas Turbine Diagnostics: A Review. *Journal of Power and Energy,* 216(5), pp. 363-377.

Li, Y. G. & Nilkitsaranont, P., 2009. Gas turbine performance prognostic for condition-based maintenace. *Journal of Applied Energy,* 86(10), pp. 2152-2161.

Lorenzo, G. D., 2012. *Advanced Low-Carbon Power Plants: The TERA Approach,* Cranfield: Cranfield University.

Marián, H., 2002. *leteckemotory Website.* [Online]
Available at: http://www.leteckemotory.cz/clanky/tumansky.php?en
[Accessed 28 September 2016].

MHPS Gas Turbine Generator Set , 2015. *Diy Trade Website.* [Online]
Available at:
http://www.diytrade.com/china/pd/13052460/MHPS_Gas_Turbine_Generator_Set.html#normal_img
[Accessed 21 September 2016].

Mikoyan Gurevich, 2011. *Aerospaceweb.org.* [Online]
Available at: http://www.aerospaceweb.org/aircraft/fighter/mig21/pics02.shtml
[Accessed 3 December 2018].

mm330046, 2007. *flickr Photostream mm330046.* [Online]
Available at: http://www.flickr.com/photos/8263353@N04/
[Accessed 3 December 2018].

Moothart, C., 2016. *Turning power plants of and on?,* Cincinnati, Ohio, USA: Squarespace.

NASA, 2015. NASA Cost Estimating Handbook Version 4.0. In: *NASA Cost Estimating Handbook Version 4.0.* s.l.:NASA, pp. C1-C7.

Naylor, P. H., 2004. *Gas turbine transient performance : heat soakage modelling,* Cranfield, United Kingdom: Cranfield University.

Ng, A., 2012. *Machine Learning,* San Francisco: Stanford University.

Ng, A. et al., 2013. *UFLDL Deep Learning Tutorial,* San Fransisco: Stanford University.

Nielsen, M. A., 2015. *Neural Networks and Deep Learning.* s.l.:Determination Press.

NIST/SEMATECH, 2013. *NIST/SEMATECH e-Handbook of Statistical Methods.* [Online]
Available at: http://www.itl.nist.gov/div898/handbook/eda/section3/eda3672.htm
[Accessed 13 June 2016].

N, S. A. et al., 2014. *Cost of New Entry Estimates for Combustion Turbine and Combined Cycle Plants in PJM,* s.l.: The Brattle Group, Inc..

Nye Thermodynamics Corporation, 2016. *Nye Thermodynamics Corporation.* [Online]
Available at: http://www.gas-turbines.com/trader/kwprice.htm
[Accessed 22 September 2016].

ONSITE SYCOM Energy Corporation , 1999. *Cost Analysis of NOx Control Alternatives for Stationary Gas Turbines,* Chicago: U.S. Department of Energy.

Orlando, I. J., Frank, G. L., Lars, K. J. & Tracy, R. J., 1994. *AN ARTIFICIAL NEURAL NETWORK SYSTEM FOR DIAGNOSING GAS TURBINE ENGINE FUEL FAULTS.* Wakefield, s.n.

Palm, T. & Qayum, A., 1985. *Private and Public Investment Analysis.* Cincinnati, Ohio: South-Western Publishing Co..

Paul, B., 2012. *Gas Turbines Applications, Failures and Root Cause Analysis,* s.l.: Braemar Adjusting.

Pavri, R. & Moore, G. D., 2001. *Gas Turbine Emissions and Control,* Atlanta, GA: GE Energy Systems.

Pequot Publishing Inc, 1973 - 2005. Competitive Bids and Orders. *Gas Turbine World,* January - Decemeber, 1-34(1-6), pp. 5-49.

Pequot Publishing Inc, 1973-2017. *Gas Turbine World Handbook.* Southport: Pequot Publishing Inc.

Rahman, M. M., Thamir, I. K. & Ahmed, A. N., 2011. Thermodynamic performance analysis of gas-turbine power-plant. *International Journal of the Physical Sciences ,* 6(14), pp. 3539-3550.

Rajkumar, R., 2016. *Principles of Cost Engineeering (Short Course),* Cranfield: Cranfield University.

Rajkumar, R. & Sackett, P., 2003. *Cost Engineering: The Practice and the Future.* Dearborn, Michigan: THE COMPUTER AND AUTOMATED SYSTEMS ASSOCIATION OF THE SOCIETY OF MANUFACTURING ENGINEERS.

Rooks, T., 2017. *Business - To prosper, poorest countries need avenues to electricity,* Berlin: Deutsche Welle.

Rowlands, D., 2017. *Gas Turbine Engine Price Estimation Using Regression Analysis,* Cranfield: Cranfield University.

Rowlands, D. O., 2014. *Application of Gas Turbine Performance Prognostics to Two Single Spool Gas Turbine Engines ,* Bedfordshire: Cranfield University.

Rowlands, D. O. & Savill, M., 2018. *Economic Modelling and Evaluation of a Repurposed Gas Turbine Engine.* Florida, USA, ASME 2018 Power Conference.

Rowlands, D. O. & Savill, M., 2018. *Gas Turbine Engine Price Estimation Using Artificial Neural Network.* Florida, USA, ASME 2018 Power Conference.

Saint-Germain, M. A., 2001. *Research methods-Simple Regression,* Long Beach, Carlifornia: Carlifornia State University.

Sambo, A. S., 2010. *Renewable Energy Development in Nigeria.* Accra, Ghana, A Paper Presented at the World Future Council/strategy Workshop on Renewable Energy.

Sani, A., 2014. Nigeria, 50 years behind stable power supply.. *Nigerian Tribune*, 6 September.

Saravanamuttoo, H., Cohen, H. & Rogers, G., 2001. Gas Turbine Theory. In: *Shaft Power Cycles - Reheat Cycles.* New Delhi: Published by Dorling Kindersley (India) Pvt. Ltd authorised by Pearson Education, Ltd, pp. 45-54.

Schorr, M. M. & Chalfin, J., 1999. *Gas Turbine NOx Emissions Approaching Zero – Is it Worth the Price?,* Schenectady, New York: General Electric Power Systems.

Senanayake, N. S., 2016. *Gas Turbine Cycles,* Sri Lanka: Dept of Mechanical Engineering, The Open University of Sri Lanka.

Shell Nigeria, 2018. *Unlocking Nigeria's Potential in Natural Gas.* [Online]
Available at: https://www.shell.com.ng/media/nigeria-reports-and-publications-briefing-notes/potential-in-natural-gas.html
[Accessed 17 December 2018].

Shiffman, D., 2012. The Nature of Code. In: *The Nature of Code.* California: Daniel Shiffman, p. 446.

Short, W. D., 1996. Present Worth Analysis. In: *The Engineering Handbook.* Florida: CRC Press, Inc, pp. 1919-1925.

Silva, V. V., Wael, K. & Fleming, P. J., 2005. Performance optimization of gas turbine engine. *Engineering Application of Artificial Intelligence,* Issue 18, pp. 575-583.

Smith, R. D., 2000. *Simulation Article,* New York: Model Blenders.

Sokolowski, J. A. & Banks, C. M., 2009. Principles of Modeling and Simulation. In: Hoboken, New Jerssey: Wiley, pp. 6. ISBN 978-0-470-28943-3..

Stephen, O. & Riti, S., 2006. Artificial Neural Networks in Fault Diagnosis: A Gas Turbine Scenario. In: *In: Palade V., Jain L., Bocaniala C.D. (eds) Computational Intelligence in Fault Diagnosis..* London: Springer, pp. 179-207.

Strategic Power Systems, Inc., 1997. *Operating Practices Guidebook:Combustion Turbine Operation and Maintenace Costs,* Albany, NY: Strategic Power Systems, Inc..

Techopedia, 2017. *Power Cycling.* [Online]
Available at: https://www.techopedia.com/definition/3726/power-cycling
[Accessed 9 October 2018].

The World Alliance for Decentralized Energy, 2006. *Steam Turbines,* Edinburgh: WADE.

The World Bank Group, 2019. *World Bank, Sustainable Energy for All (SE4ALL) database,* s.l.: The World Bank Group.

Thompson, G., 2009. *Statistical literacy guide 1- How to adjust for inflation ,* Westminster : House of Commons Library.

Torella, G., 1990. *Transient Performance and Behaviour of Gas Turbine Engines.* New York, The American Society of Mechanical Engineers, ASME.

Trembath, P., 2012. *Gas Turbine Performance Prognostics,* Cranfield Bedforshire: Cranfield University.

Turbosquid, 2015. *Tumasky Solid Engine Model.* [Art] (Turbosquid Website).

U. S. Energy Information Administration | Annual Energy Outlook, 2017. *AEO2017 Levelized Costs,* Washington DC: U. S. Energy Information Administration.

U.S. Bureau of Labor, 2017. *Statistics, U.S. Bureau of Labor Statistics- Databases, Tables & Calculators by Subject,* Washington, DC: U.S. Bureau of Labor.

U.S. Department of Energy | Office of Indian Energy, 2015. *Levelized Cost of Energy (LCOE),* Washington DC: U.S. Department of Energy .

United Nations, 2015. *Transforming Our World: The 2030 Agenda For Sustainable development,* United Nations: United nations.

United States Environmental Protection Agency, 1995. *AP 42, Fifth Edition Compilation of Air Pollutant Emissions Factors, Volume 1: Stationary Point and Area Sources, Chapter 3: Stationary Internal Combustion Sources.* 5th ed. North Carolina, USA: United States Environmental Protection Agency.

Walsh, P. & Fletcher, P., 2004. Gas Turbine Performance. In: *Gas Turbine Performance.* Oxford: Blackwell Science limited, p. 34.

Wanis, M., 2013. *Techno-Economic, Environmental and Risk Analysis (TERA) for Power Generation,* Cranfield: Cranfield University.

Welch, S. C., 2015. *Neural-Networks-Demystified,* Atlanta, Ga: GitHub, Inc.

WGPW, 2016. *Wood Group Pratt & Whitney Industrial Turbine Services L.L.C. Website.* [Online]
Available at: http://www.wgpwllc.com/index_files/Page830.htm
[Accessed 21 Septemeber 2016].

Zhang, N. & Lior, N., 2006. A novel near-zero CO2 emission thermal cycle with LNG cryogenic exergy utilization. *Energy,* Issue 31, p. 1666–1679.

APPENDIX A

TURBOMATCH ENGINE MODEL INPUT FILES

Aero-derivative Engine model design point at ISA - input file

Performance simulation modelling of AERODERIVATIVE ENGINE
SIMILAR TO TUMANSKY-R-25-300
BY
David Rowlands

!Turbomatch Programme:
Simulation of Design Point for AERODERIVATIVE ENGINE WITH FUEL TYPE NATURAL GAS (TOMZACK) - GT

////

DP SI GT VA FP
-1
-1

INTAKE	S1, 2	D1-6	R100	
COMPRE	S2, 3	D7-18	R102	V7 V8
COMPRE	S3, 4	D19-30	R103	V19 V20
PREMAS	S4, 5, 22	D31-34		
BURNER	S5, 6	D35-42	R104	
MIXEES	S6, 22, 7			
TURBIN	S7, 8	D43-57	V44	
TURBIN	S8, 9	D58-72	V59	
TURBIN	S9, 10	D73-87	V73	V74
DUCTER	S10, 11	D88-92	R105	
NOZCON	S11, 12, 1	D93-94	R110	
PERFOR	S1,0,0	D73,D96-98,110,100,104,0,0,0,0,0,0		

CODEND

DATA ITEMS ////

1 0.0 ! INTAKE: Altitude [m]
2 0.0 ! Deviation from ISA temperature [K]
3 0.0 ! Mach number
4 -1.0 ! Pressure recovery, according to USAF
5 0.0 ! Deviation from ISA pressure [atm]
6 60.0 ! Relative humidity [%]

7 -1.0 ! COMPRESSOR I: Z = (R-R[choke])/(R[surge]-R[choke]) (if -1 is given the default value of 0.85 is invoked)
8 -1.0 ! Relative rotational speed PCN (if -1 is given the default value of 1.0 is invoked)
9 2.131 ! DP Pressure ratio
10 0.8872 ! DP ETA
11 0.0 ! Error selection
12 5.0 ! Compressor map number
13 1.0 ! Shaft number

14 1.0 ! PR degradation scaling factor
15 1.0 ! NDMF degradation scaling factor
16 1.0 ! ETA degradation scaling factor
17 -1.0 ! Effective component volume [m^3] (only for transient)
18 0.0 ! Stator angle (VSV) relative to DP

19 -1.0 ! COMPRESSOR I: Z = (R-R[choke])/(R[surge]-R[choke]) (if -1 is given the default value of 0.85 is invoked)
20 -1.0 ! Relative rotational speed PCN (if -1 is given the default value of 1.0 is invoked)
21 4.480 ! DP Pressure ratio
22 0.8872 ! DP ETA
23 0.0 ! Error selection
24 5.0 ! Compressor map number
25 2.0 ! Shaft number
26 1.0 ! PR degradation scaling factor
27 1.0 ! NDMF degradation scaling factor
28 1.0 ! ETA degradation scaling factor
29 -1.0 ! Effective component volume [m^3] (only for transient)
30 0.0 ! Stator angle (VSV) relative to DP

31 0.9 ! PREMAS: LAMDA W Cooling bypass (Wout1/Win)
32 0.0 ! DELTA W
33 1.0 ! LAMBDA P
34 0.0 ! DELTA P

35 0.05 ! COMBUSTOR: Pressure loss (=DP/P inlet total)
36 0.99 ! Combustion efficiency
37 -1.0 ! Fuel flow (if -1.0, TET must be defined)
38 0.0 ! (>0) Water flow [kg s-1 or lb s-1] or (<0) WAR
39 288. ! Temperature of water stream [K]
40 0.0 ! Phase of water (0=liquid, 1=vapour)
41 1.0 ! ETA degradation scaling factor
42 0.08 ! Effective component volume [m^3] (only for transient)

43 0.0 ! HP TURBINE: Auxiliary or power output [W]
44 -1.0 ! Relative to max enthalpy drop to temperature ratio: ZT (if -1 is given the default value of 0.8 is invoked)
45 -1.0 ! Relative non-dim speed CN (if -1 is given the default value of 0.6 is invoked)
46 0.90 ! DP ETA
47 -1.0 ! Relative non-dim PCN (= -1 for compressor turbine)
48 2.0 ! Shaft Number (for power turbine, the value 0 is used)
49 5.0 ! Turbine map number
50 -1.0 ! Power law index "n" (POWER = PCN^n)
51 1.0 ! TF degradation scaling factor
52 1.0 ! DH degradation scaling factor

53 1.0 ! ETA degradation scaling factor
54 -1.0 ! Rotor rotational speed [RPS] (only for transient)
55 -1.0 ! Rotor moment of inertia [kg.m^2] (only for transient)
56 -1.0 ! Effective component volume [m^3] (only for transient)
57 0.0 ! NGV angle, relative to D.P.

58 0.0 ! HP TURBINE: Auxiliary or power output [W]
59 -1.0 ! Relative to max enthalpy drop to temperature ratio: ZT (if -1 is given the default value of 0.8 is invoked)
60 -1.0 ! Relative non-dim speed CN (if -1 is given the default value of 0.6 is invoked)
61 0.90 ! DP ETA
62 -1.0 ! Relative non-dim PCN (= -1 for compressor turbine)
63 1.0 ! Shaft Number (for power turbine, the value 0 is used)
64 5.0 ! Turbine map number
65 -1.0 ! Power law index "n" (POWER = PCN^n)
66 1.0 ! TF degradation scaling factor
67 1.0 ! DH degradation scaling factor
68 1.0 ! ETA degradation scaling factor
69 -1.0 ! Rotor rotational speed [RPS] (only for transient)
70 -1.0 ! Rotor moment of inertia [kg.m^2] (only for transient)
71 -1.0 ! Effective component volume [m^3] (only for transient)
72 0.0 ! NGV angle, relative to D.P.

73 -1.013 ! POWER TURBINE: Auxiliary or power output [W]
74 -1.0 ! Relative to max enthalpy drop to temperature ratio: ZT (if -1 is given the default value of 0.8 is invoked)
75 -1.0 ! Relative non-dim speed CN (if -1 is given the default value of 0.6 is invoked)
76 0.90 ! DP ETA (Isentropic efficiency)
77 1.0 ! Relative non-dim PCN (= -1 for compressor turbine)
78 0.0 ! Shaft Number (for power turbine, the value 0 is used)
79 5.0 ! Turbine map number
80 -1.0 ! Power law index "n" (POWER = PCN^n)
81 1.0 ! TF degradation scaling factor
82 1.0 ! DH degradation scaling factor
83 1.0 ! ETA degradation scaling factor
84 -1.0 ! Rotor rotational speed [RPS] (only for transient)
85 -1.0 ! Rotor moment of inertia [kg.m^2] (only for transient)
86 -1.0 ! Effective component volume [m^3] (only for transient)
87 0.0 ! NGV angle, relative to D.P.

88 0.0 ! DUCTER: Air Duct or Afterburner (0 if reheat/intercooler not needed, 1 if reheat/intercooler required later, 2 if reheat/intercooler required now)
89 0.01 ! Total Pressure Loss: DELTA (P)/Pin (Pressure loss = 1%)
90 0.0 ! Combustion Efficiency
91 0.0 ! Limiting Value of Fuel Flow (or 100000 if not needed)
92 -1.0 ! Effective Component Volume [m^3]

```
93 -1.0          ! CONVERGENT NOZZLE: = "-1" exit area is fixed)
94 1.0           ! Scaling factor

95 1.0           ! ENGINE RESULTS: Power output (= -1 for aero- engine)
96 1.0           ! Propeller efficiency (= -1 for turbojet/turbofan)
97 0.0           ! Scaling index ("1" = scaling, "0" = no scaling)
98 0.0           ! Only for scaling: Required DP net thrust/shaft power

-1
1 2 68.5         ! Item 2 at station 1 = Mass flow (kg/s)
6 6 1310.15      ! Item 6 at station 6 = Total temperature (K)
-1               ! End of DP data
-3
```

Aero-derivative Engine model Tropical Condition - input file

Performance simulation modelling of AERODERIVATIVE ENGINE
SIMILAR TO TUMANSKY-R-25-300
BY
David Rowlands

!Turbomatch Programme:
Simulation of Tropical Operation of AERODERIVATIVE ENGINE WITH FUEL TYPE NATURAL GAS (TOMZACK) - GT

```
////

DP SI GT VA FP
-1
-1
INTAKE      S1, 2          D1-6          R100
COMPRE      S2, 3          D7-18         R102    V7 V8
COMPRE      S3, 4          D19-30        R103    V19 V20
PREMAS      S4, 5, 22      D31-34
BURNER      S5, 6          D35-42        R104
MIXEES      S6, 22, 7
TURBIN      S7, 8          D43-57        V44
TURBIN      S8, 9          D58-72        V59
TURBIN      S9, 10         D73-87        V73     V74
DUCTER      S10, 11        D88-92        R105
NOZCON      S11, 12, 1     D93-94        R110
PERFOR      S1,0,0         D73,D96-98,110,100,104,0,0,0,0,0,0
CODEND

DATA ITEMS ////

1 700.0          ! INTAKE: Altitude [m]
```

2 0.0 ! Deviation from ISA temperature [K]
3 0.0 ! Mach number
4 -1.0 ! Pressure recovery, according to USAF
5 0.0 ! Deviation from ISA pressure [atm]
6 60.0 ! Relative humidity [%]

7 -1.0 ! COMPRESSOR I: Z = (R-R[choke])/(R[surge]-R[choke]) (if -1 is given the default value of 0.85 is invoked)
8 -1.0 ! Relative rotational speed PCN (if -1 is given the default value of 1.0 is invoked)
9 2.131 ! DP Pressure ratio
10 0.8872 ! DP ETA
11 0.0 ! Error selection
12 5.0 ! Compressor map number
13 1.0 ! Shaft number
14 1.0 ! PR degradation scaling factor
15 1.0 ! NDMF degradation scaling factor
16 1.0 ! ETA degradation scaling factor
17 -1.0 ! Effective component volume [m^3] (only for transient)
18 0.0 ! Stator angle (VSV) relative to DP

19 -1.0 ! COMPRESSOR I: Z = (R-R[choke])/(R[surge]-R[choke]) (if -1 is given the default value of 0.85 is invoked)
20 -1.0 ! Relative rotational speed PCN (if -1 is given the default value of 1.0 is invoked)
21 4.480 ! DP Pressure ratio
22 0.8872 ! DP ETA
23 0.0 ! Error selection
24 5.0 ! Compressor map number
25 2.0 ! Shaft number
26 1.0 ! PR degradation scaling factor
27 1.0 ! NDMF degradation scaling factor
28 1.0 ! ETA degradation scaling factor
29 -1.0 ! Effective component volume [m^3] (only for transient)
30 0.0 ! Stator angle (VSV) relative to DP

31 0.9 ! PREMAS: LAMDA W Cooling bypass (Wout1/Win)
32 0.0 ! DELTA W
33 1.0 ! LAMBDA P
34 0.0 ! DELTA P

35 0.05 ! COMBUSTOR: Pressure loss (=DP/P inlet total)
36 0.99 ! Combustion efficiency
37 -1.0 ! Fuel flow (if -1.0, TET must be defined)
38 0.0 ! (>0) Water flow [kg s-1 or lb s-1] or (<0) WAR
39 288. ! Temperature of water stream [K]

40 0.0 ! Phase of water (0=liquid, 1=vapour)
41 1.0 ! ETA degradation scaling factor
42 0.08 ! Effective component volume [m^3] (only for transient)

43 0.0 ! HP TURBINE: Auxiliary or power output [W]
44 -1.0 ! Relative to max enthalpy drop to temperature ratio: ZT (if -1 is given the default value of 0.8 is invoked)
45 -1.0 ! Relative non-dim speed CN (if -1 is given the default value of 0.6 is invoked)
46 0.90 ! DP ETA
47 -1.0 ! Relative non-dim PCN (= -1 for compressor turbine)
48 2.0 ! Shaft Number (for power turbine, the value 0 is used)
49 5.0 ! Turbine map number
50 -1.0 ! Power law index "n" (POWER = PCN^n)
51 1.0 ! TF degradation scaling factor
52 1.0 ! DH degradation scaling factor
53 1.0 ! ETA degradation scaling factor
54 -1.0 ! Rotor rotational speed [RPS] (only for transient)
55 -1.0 ! Rotor moment of inertia [kg.m^2] (only for transient)
56 -1.0 ! Effective component volume [m^3] (only for transient)
57 0.0 ! NGV angle, relative to D.P.

58 0.0 ! HP TURBINE: Auxiliary or power output [W]
59 -1.0 ! Relative to max enthalpy drop to temperature ratio: ZT (if -1 is given the default value of 0.8 is invoked)
60 -1.0 ! Relative non-dim speed CN (if -1 is given the default value of 0.6 is invoked)
61 0.90 ! DP ETA
62 -1.0 ! Relative non-dim PCN (= -1 for compressor turbine)
63 1.0 ! Shaft Number (for power turbine, the value 0 is used)
64 5.0 ! Turbine map number
65 -1.0 ! Power law index "n" (POWER = PCN^n)
66 1.0 ! TF degradation scaling factor
67 1.0 ! DH degradation scaling factor
68 1.0 ! ETA degradation scaling factor
69 -1.0 ! Rotor rotational speed [RPS] (only for transient)
70 -1.0 ! Rotor moment of inertia [kg.m^2] (only for transient)
71 -1.0 ! Effective component volume [m^3] (only for transient)
72 0.0 ! NGV angle, relative to D.P.

73 -1.013 ! POWER TURBINE: Auxiliary or power output [W]
74 -1.0 ! Relative to max enthalpy drop to temperature ratio: ZT (if -1 is given the default value of 0.8 is invoked)
75 -1.0 ! Relative non-dim speed CN (if -1 is given the default value of 0.6 is invoked)
76 0.90 ! DP ETA (Isentropic efficiency)
77 1.0 ! Relative non-dim PCN (= -1 for compressor turbine)
78 0.0 ! Shaft Number (for power turbine, the value 0 is used)
79 5.0 ! Turbine map number

```
80 -1.0          ! Power law index "n" (POWER = PCN^n)
81 1.0           ! TF degradation scaling factor
82 1.0           ! DH degradation scaling factor
83 1.0           ! ETA degradation scaling factor
84 -1.0          ! Rotor rotational speed [RPS] (only for transient)
85 -1.0          ! Rotor moment of inertia [kg.m^2] (only for transient)
86 -1.0          ! Effective component volume [m^3] (only for transient)
87 0.0           ! NGV angle, relative to D.P.

88 0.0           ! DUCTER: Air Duct or Afterburner (0 if reheat/intercooler not needed, 1 if
reheat/intercooler required later, 2 if reheat/intercooler required now)
89 0.01          ! Total Pressure Loss: DELTA(P)/Pin (Pressure loss = 1%)
90 0.0           ! Combustion Efficiency
91 0.0           ! Limiting Value of Fuel Flow (or 100000 if not needed)
92 -1.0          ! Effective Component Volume [m^3]

93 -1.0          ! CONVERGENT NOZZLE: = "-1" exit area is fixed)
94 1.0           ! Scaling factor

95 1.0           ! ENGINE RESULTS: Power output (= -1 for aer- engine)
96 1.0           ! Propeller efficiency (= -1 for turbojet/turbofan)
97 0.0           ! Scaling index ("1" = scaling, "0" = no scaling)
98 0.0           ! Only for scaling: Required DP net thrust/shaft power

-1
1 2 68.5         ! Item 2 at station 1 = Mass flow (kg/s)
6 6 1310.15      ! Item 6 at station 6 = Total temperature (K)
-1               ! End of DP data
-3
```

Deteriorated Aero-derivative Engine model - input file

Performance simulation modelling of AERODERIVATIVE ENGINE
SIMILAR TO TUMANSKY-R-25-300
BY
David Rowlands

!Turbomatch Programme:
DETERIORATED ENGINE SIMULATION - FUEL TYPE NATURAL (TOMZACK) - GT

```
////

OD SI GT VA FP
-1
-1
INTAKE      S1, 2       D1-6        R100
COMPRE      S2, 3       D7-18       R102    V7 V8
```

COMPRE	S3, 4	D19-30	R103	V19 V20
PREMAS	S4, 5, 22	D31-34		
BURNER	S5, 6	D35-42	R104	
MIXEES	S6, 22, 7			
TURBIN	S7, 8	D43-57	V44	
TURBIN	S8, 9	D58-72	V59	
TURBIN	S9, 10	D73-87	V73	V74
DUCTER	S10, 11	D88-92	R105	
NOZCON	S11, 12, 1	D93-94	R110	
PERFOR	S1,0,0	D73,D96-98,110,100,104,0,0,0,0,0,0		

CODEND

DATA ITEMS ////

1 0.0 ! INTAKE: Altitude [m]
2 0.0 ! Deviation from ISA temperature [K]
3 0.0 ! Mach number
4 -1.0 ! Pressure recovery, according to USAF
5 0.0 ! Deviation from ISA pressure [atm]
6 60.0 ! Relative humidity [%]

7 -1.0 ! COMPRESSOR I: Z = (R-R[choke])/(R[surge]-R[choke]) (if -1 is given the default value of 0.85 is invoked)
8 -1.0 ! Relative rotational speed PCN (if -1 is given the default value of 1.0 is invoked)
9 2.131 ! DP Pressure ratio
10 0.8872 ! DP ETA
11 0.0 ! Error selection
12 5.0 ! Compressor map number
13 1.0 ! Shaft number
14 1.0 ! PR degradation scaling factor
15 1.0 ! NDMF degradation scaling factor
16 1.0 ! ETA degradation scaling factor
17 -1.0 ! Effective component volume [m^3] (only for transient)
18 0.0 ! Stator angle (VSV) relative to DP

19 -1.0 ! COMPRESSOR I: Z = (R-R[choke])/(R[surge]-R[choke]) (if -1 is given the default value of 0.85 is invoked)
20 -1.0 ! Relative rotational speed PCN (if -1 is given the default value of 1.0 is invoked)
21 4.480 ! DP Pressure ratio
22 0.8872 ! DP ETA
23 0.0 ! Error selection
24 5.0 ! Compressor map number
25 2.0 ! Shaft number
26 1.0 ! PR degradation scaling factor
27 1.0 ! NDMF degradation scaling factor

28 1.0 ! ETA degradation scaling factor
29 -1.0 ! Effective component volume [m^3] (only for transient)
30 0.0 ! Stator angle (VSV) relative to DP

31 0.9 ! PREMAS: LAMDA W Cooling bypass (Wout1/Win)
32 0.0 ! DELTA W
33 1.0 ! LAMBDA P
34 0.0 ! DELTA P

35 0.05 ! COMBUSTOR: Pressure loss (=DP/P inlet total)
36 0.99 ! Combustion efficiency
37 -1.0 ! Fuel flow (if -1.0, TET must be defined)
38 0.0 ! (>0) Water flow [kg s-1 or lb s-1] or (<0) WAR
39 288. ! Temperature of water stream [K]
40 0.0 ! Phase of water (0=liquid, 1=vapour)
41 1.0 ! ETA degradation scaling factor
42 0.08 ! Effective component volume [m^3] (only for transient)

43 0.0 ! HP TURBINE: Auxiliary or power output [W]
44 -1.0 ! Relative to max enthalpy drop to temperature ratio: ZT (if -1 is given the default value of 0.8 is invoked)
45 -1.0 ! Relative non-dim speed CN (if -1 is given the default value of 0.6 is invoked)
46 0.90 ! DP ETA
47 -1.0 ! Relative non-dim PCN (= -1 for compressor turbine)
48 2.0 ! Shaft Number (for power turbine, the value 0 is used)
49 5.0 ! Turbine map number
50 -1.0 ! Power law index "n" (POWER = PCN^n)
51 1.0 ! TF degradation scaling factor
52 1.0 ! DH degradation scaling factor
53 1.0 ! ETA degradation scaling factor
54 -1.0 ! Rotor rotational speed [RPS] (only for transient)
55 -1.0 ! Rotor moment of inertia [kg.m^2] (only for transient)
56 -1.0 ! Effective component volume [m^3] (only for transient)
57 0.0 ! NGV angle, relative to D.P.

58 0.0 ! HP TURBINE: Auxiliary or power output [W]
59 -1.0 ! Relative to max enthalpy drop to temperature ratio: ZT (if -1 is given the default value of 0.8 is invoked)
60 -1.0 ! Relative non-dim speed CN (if -1 is given the default value of 0.6 is invoked)
61 0.90 ! DP ETA
62 -1.0 ! Relative non-dim PCN (= -1 for compressor turbine)
63 1.0 ! Shaft Number (for power turbine, the value 0 is used)
64 5.0 ! Turbine map number
65 -1.0 ! Power law index "n" (POWER = PCN^n)
66 1.0 ! TF degradation scaling factor
67 1.0 ! DH degradation scaling factor

```
68 1.0          ! ETA degradation scaling factor
69 -1.0         ! Rotor rotational speed [RPS] (only for transient)
70 -1.0         ! Rotor moment of inertia [kg.m^2] (only for transient)
71 -1.0         ! Effective component volume [m^3] (only for transient)
72 0.0          ! NGV angle, relative to D.P.

73 -1.013       ! POWER TURBINE: Auxiliary or power output [W]
74 -1.0         ! Relative to max enthalpy drop to temperature ratio: ZT (if -1 is given the default value
of 0.8 is invoked)
75 -1.0         ! Relative non-dim speed CN (if -1 is given the default value of 0.6 is invoked)
76 0.90         ! DP ETA (Isentropic efficiency)
77 1.0          ! Relative non-dim PCN (= -1 for compressor turbine)
78 0.0          ! Shaft Number (for power turbine, the value 0 is used)
79 5.0          ! Turbine map number
80 -1.0         ! Power law index "n" (POWER = PCN^n)
81 1.0          ! TF degradation scaling factor
82 1.0          ! DH degradation scaling factor
83 1.0          ! ETA degradation scaling factor
84 -1.0         ! Rotor rotational speed [RPS] (only for transient)
85 -1.0         ! Rotor moment of inertia [kg.m^2] (only for transient)
86 -1.0         ! Effective component volume [m^3] (only for transient)
87 0.0          ! NGV angle, relative to D.P.

88 0.0          ! DUCTER: Air Duct or Afterburner
89 0.01         ! Total Pressure Loss: DELTA (P)/Pin (Pressure loss = 1%)
90 0.0          ! Combustion Efficiency
91 0.0          ! Limiting Value of Fuel Flow (or 100000 if not needed)
92 -1.0         ! Effective Component Volume [m^3]

93 -1.0         ! CONVERGENT NOZZLE: = "-1" exit area is fixed)
94 1.0          ! Scaling factor

95 1.0          ! ENGINE RESULTS: Power output (= -1 for aero- engine)
96 1.0          ! Propeller efficiency (= -1 for turbojet/turbofan)
97 0.0          ! Scaling index ("1" = scaling, "0" = no scaling)
98 0.0          ! Only for scaling: Required DP net thrust/shaft power

-1
1 2 68.5        ! Item 2 at station 1 = Mass flow (kg/s)
6 6 1310.15     ! Item 6 at station 6 = Total temperature (K)
-1              ! End of DP data
-3
            ! Introducing deterioration! AT 4800 hours
14 0.988    ! COMPRE#1 DETERIORATION OF 1.2% IN PRESSURE RATIO
15 0.992    ! COMPRE#1 DETERIORATION OF 0.8% IN EFFICIENCY
16 0.996    ! COMPRE#1 DETERIORATION OF 0.4% IN NON-DIMENSIONAL MASS FLOW//////
```

```
26 0.988   ! COMPRE#2 DETERIORATION OF 1.2% IN PRESSURE RATIO
27 0.992   ! COMPRE#2 DETERIORATION OF 0.8% IN EFFICIENCY
28 0.996   ! COMPRE#2 DETERIORATION OF 0.4% IN NON-DIMENSIONAL MASS FLOW//////
41 0.992   ! BURNER   DETERIORATION OF 0.8% IN COMBUSTION EFFICIENCY
51 0.996   ! TURBIN#1 DETERIORATION OF 0.4% IN NON-DIMENSIONAL MASS FLOW
52 0.995   ! TURBIN#1 DETERIORATION OF 0.5% IN EFFICIENCY
53 0.997   ! TURBIN#1 DETERIORATION OF 0.3% IN DH/T (ENTHALPY DROP)/////////
66 0.996   ! TURBIN#2 DETERIORATION OF 0.4% IN NON-DIMENSIONAL MASS FLOW
67 0.995   ! TURBIN#2 DETERIORATION OF 0.5% IN EFFICIENCY
68 0.997   ! TURBIN#2 DETERIORATION OF 0.3% IN DH/T (ENTHALPY DROP)/////////
81 0.996   ! TURBIN#3 DETERIORATION OF 0.4% IN NON-DIMENSIONAL MASS FLOW
82 0.995   ! TURBIN#3 DETERIORATION OF 0.5% IN EFFICIENCY
83 0.997   ! TURBIN#3 DETERIORATION OF 0.3% IN DH/T (ENTHALPY DROP)/////////
-1
-1         ! RUN at DP TET
           ! AT 9600 hours
14 0.976   ! COMPRE#1 DETERIORATION OF 2.4% IN PRESSURE RATIO
15 0.984   ! COMPRE#1 DETERIORATION OF 1.6% IN EFFICIENCY
16 0.992   ! COMPRE#1 DETERIORATION OF 0.8% IN NON-DIMENSIONAL MASS FLOW//////
26 0.976   ! COMPRE#2 DETERIORATION OF 2.4% IN PRESSURE RATIO
27 0.984   ! COMPRE#2 DETERIORATION OF 1.6% IN EFFICIENCY
28 0.992   ! COMPRE#2 DETERIORATION OF 0.8% IN NON-DIMENSIONAL MASS FLOW//////
41 0.984   ! BURNER   DETERIORATION OF 1.6% IN COMBUSTION EFFICIENCY
51 0.992   ! TURBIN#1 DETERIORATION OF 0.8% IN NON-DIMENSIONAL MASS FLOW
52 0.99    ! TURBIN#1 DETERIORATION OF 1.0% IN EFFICIENCY
53 0.994   ! TURBIN#1 DETERIORATION OF 0.6% IN DH/T (ENTHALPY DROP)/////////
66 0.992   ! TURBIN#2 DETERIORATION OF 0.8% IN NON-DIMENSIONAL MASS FLOW
67 0.99    ! TURBIN#2 DETERIORATION OF 1.0% IN EFFICIENCY
68 0.994   ! TURBIN#2 DETERIORATION OF 0.6% IN DH/T (ENTHALPY DROP)/////////
81 0.992   ! TURBIN#3 DETERIORATION OF 0.8% IN NON-DIMENSIONAL MASS FLOW
82 0.99    ! TURBIN#3 DETERIORATION OF 1.0% IN EFFICIENCY
83 0.994   ! TURBIN#3 DETERIORATION OF 0.6% IN DH/T (ENTHALPY DROP)/////////
-1
-1         ! RUN at DP TET
           ! AT 14400 hours
14 0.964   ! COMPRE#1 DETERIORATION OF 3.6% IN PRESSURE RATIO
15 0.976   ! COMPRE#1 DETERIORATION OF 2.4% IN EFFICIENCY
16 0.988   ! COMPRE#1 DETERIORATION OF 1.2% IN NON-DIMENSIONAL MASS FLOW//////
26 0.964   ! COMPRE#2 DETERIORATION OF 3.6% IN PRESSURE RATIO
27 0.976   ! COMPRE#2 DETERIORATION OF 2.4% IN EFFICIENCY
28 0.988   ! COMPRE#2 DETERIORATION OF 1.2% IN NON-DIMENSIONAL MASS FLOW//////
41 0.976   ! BURNER   DETERIORATION OF 2.4% IN COMBUSTION EFFICIENCY
51 0.988   ! TURBIN#1 DETERIORATION OF 1.2% IN NON-DIMENSIONAL MASS FLOW
52 0.985   ! TURBIN#1 DETERIORATION OF 1.5% IN EFFICIENCY
53 0.991   ! TURBIN#1 DETERIORATION OF 0.9% IN DH/T (ENTHALPY DROP)/////////
66 0.988   ! TURBIN#2 DETERIORATION OF 1.2% IN NON-DIMENSIONAL MASS FLOW
```

```
67 0.985   ! TURBIN#2 DETERIORATION OF 1.5% IN EFFICIENCY
68 0.991   ! TURBIN#2 DETERIORATION OF 0.9% IN DH/T (ENTHALPY DROP)/////////
81 0.988   ! TURBIN#3 DETERIORATION OF 1.2% IN NON-DIMENSIONAL MASS FLOW
82 0.985   ! TURBIN#3 DETERIORATION OF 1.5% IN EFFICIENCY
83 0.991   ! TURBIN#3 DETERIORATION OF 0.9% IN DH/T (ENTHALPY DROP)/////////
-1
-1          ! RUN at DP TET
            ! AT 19200 hours
14 0.952   ! COMPRE#1 DETERIORATION OF 4.8% IN PRESSURE RATIO
15 0.968   ! COMPRE#1 DETERIORATION OF 3.2% IN EFFICIENCY
16 0.984   ! COMPRE#1 DETERIORATION OF 1.6% IN NON-DIMENSIONAL MASS FLOW//////
26 0.952   ! COMPRE#2 DETERIORATION OF 4.8% IN PRESSURE RATIO
27 0.968   ! COMPRE#2 DETERIORATION OF 3.2% IN EFFICIENCY
28 0.984   ! COMPRE#2 DETERIORATION OF 1.6% IN NON-DIMENSIONAL MASS FLOW//////
41 0.968   ! BURNER   DETERIORATION OF 3.2% IN COMBUSTION EFFICIENCY
51 0.984   ! TURBIN#1 DETERIORATION OF 1.6% IN NON-DIMENSIONAL MASS FLOW
52 0.98    ! TURBIN#1 DETERIORATION OF 2.0% IN EFFICIENCY
53 0.988   ! TURBIN#1 DETERIORATION OF 1.2% IN DH/T (ENTHALPY DROP)/////////
66 0.984   ! TURBIN#2 DETERIORATION OF 1.6% IN NON-DIMENSIONAL MASS FLOW
67 0.98    ! TURBIN#2 DETERIORATION OF 2.0% IN EFFICIENCY
68 0.988   ! TURBIN#2 DETERIORATION OF 1.2% IN DH/T (ENTHALPY DROP)/////////
81 0.984   ! TURBIN#3 DETERIORATION OF 1.6% IN NON-DIMENSIONAL MASS FLOW
82 0.98    ! TURBIN#3 DETERIORATION OF 2.0% IN EFFICIENCY
83 0.988   ! TURBIN#3 DETERIORATION OF 1.2% IN DH/T (ENTHALPY DROP)/////////
-1
-1          ! RUN at DP TET
            ! AT 24000 hours
14 0.94    ! COMPRE#1 DETERIORATION OF 6.0% IN PRESSURE RATIO
15 0.96    ! COMPRE#1 DETERIORATION OF 4.0% IN EFFICIENCY
16 0.98    ! COMPRE#1 DETERIORATION OF 2.0% IN NON-DIMENSIONAL MASS FLOW//////
26 0.94    ! COMPRE#2 DETERIORATION OF 6.0% IN PRESSURE RATIO
27 0.96    ! COMPRE#2 DETERIORATION OF 4.0% IN EFFICIENCY
28 0.98    ! COMPRE#2 DETERIORATION OF 2.0% IN NON-DIMENSIONAL MASS FLOW//////
41 0.96    ! BURNER   DETERIORATION OF 4.0% IN COMBUSTION EFFICIENCY
51 0.98    ! TURBIN#1 DETERIORATION OF 2.0% IN NON-DIMENSIONAL MASS FLOW
52 0.975   ! TURBIN#1 DETERIORATION OF 2.5% IN EFFICIENCY
53 0.985   ! TURBIN#1 DETERIORATION OF 1.5% IN DH/T (ENTHALPY DROP)/////////
66 0.98    ! TURBIN#2 DETERIORATION OF 2.0% IN NON-DIMENSIONAL MASS FLOW
67 0.975   ! TURBIN#2 DETERIORATION OF 2.5% IN EFFICIENCY
68 0.985   ! TURBIN#2 DETERIORATION OF 1.5% IN DH/T (ENTHALPY DROP)/////////
81 0.98    ! TURBIN#3 DETERIORATION OF 2.0% IN NON-DIMENSIONAL MASS FLOW
82 0.975   ! TURBIN#3 DETERIORATION OF 2.5% IN EFFICIENCY
83 0.985   ! TURBIN#3 DETERIORATION OF 1.5% IN DH/T (ENTHALPY DROP)/////////
-1
-1        ! RUN at DP TET
-3
```

Aero-derivative Engine model With Intercooler - input file

Performance simulation modelling of AERODERIVATIVE ENGINE
SIMILAR TO TUMANSKY-R-25-300
BY
David Rowlands

!Turbomatch Programme:
Simulation of AERODERIVATIVE ENGINE (WITH INTERCOOLER) - FUEL TYPE NATURAL GAS (TOMZACK) - GT

```
////
DP SI GT VA FP
-1
-1
INTAKE      S1, 2          D1-6        R104
COMPRE      S2, 3          D7-18       R106    V7 V8
DUCTER      S3, 4          D19-23      R107
COMPRE      S4, 5          D24-35      R108    V24 V25
PREMAS      S5, 6, 22      D36-39
BURNER      S6, 7          D40-47      R109
MIXEES      S7, 22, 8
TURBIN      S8, 9          D48-62      V49
TURBIN      S9, 10         D63-77      V64
TURBIN      S10, 11        D78-92      V78 V79
DUCTER      S11, 12        D93-97      R110
NOZCON      S12, 13, 1     D98-99      R111
PERFOR      S1,0,0         D78,D101-103,111,104,109,0,0,0,0,0,0
CODEND

DATA ITEMS ////
1 0.0          ! INTAKE: Altitude [m]
2 0.0          ! Deviation from ISA temperature [K]
3 0.0          ! Mach number
4 -1.0         ! Pressure recovery, according to USAF
5 0.0          ! Deviation from ISA pressure [atm]
6 60.0         ! Relative humidity [%]

7 -1.0         ! COMPRESSOR I: Z = (R-R[choke])/(R[surge]-R[choke])(if -1 is given the
default value of 0.85 is invoked)
8 -1.0         ! Relative rotational speed PCN (if -1 is given the default value of 1.0 is
invoked)
9 2.131        ! DP Pressure ratio
10 0.8872      ! DP ETA
11 0.0         ! Error selection
12 5.0         ! Compressor map number
13 1.0         ! Shaft number
```

14 1.0 ! PR degradation scaling factor
15 1.0 ! NDMF degradation scaling factor
16 1.0 ! ETA degradation scaling factor
17 -1.0 ! Effective component volume [m^3] (only for transient)
18 0.0 ! Stator angle (VSV) relative to DP

19 2.0 ! DUCTER: Air Duct or Afterburner (0 if reheat/intercooler not needed, 1 if reheat/intercooler required later, 2 if reheat/intercooler required now)
20 0.01 ! Total Pressure Loss: DELTA (P)/Pin (Pressure loss = 1%)
21 0.0 ! Combustion Efficiency
22 0.0 ! Limiting Value of Fuel Flow (or 100000 if not needed)
23 -1.0 ! Effective Component Volume [m^3]

24 -1.0 ! COMPRESSOR I: Z = (R-R[choke])/(R[surge]-R[choke])(if -1 is given the default value of 0.85 is invoked)
25 -1.0 ! Relative rotational speed PCN (if -1 is given the default value of 1.0 is invoked)
26 4.480 ! DP Pressure ratio
27 0.8872 ! DP ETA
28 0.0 ! Error selection
29 5.0 ! Compressor map number
30 2.0 ! Shaft number
31 1.0 ! PR degradation scaling factor
32 1.0 ! NDMF degradation scaling factor
33 1.0 ! ETA degradation scaling factor
34 -1.0 ! Effective component volume [m^3] (only for transient)
35 0.0 ! Stator angle (VSV) relative to DP

36 0.9 ! PREMAS: LAMDA W Cooling bypass (Wout1/Win)
37 0.0 ! DELTA W
38 1.0 ! LAMBDA P
39 0.0 ! DELTA P

40 0.05 ! COMBUSTOR: Pressure loss (=DP/P inlet total)
41 0.99 ! Combustion efficiency
42 -1.0 ! Fuel flow (if -1.0, TET must be defined)
43 0.0 ! (>0) Water flow [kg s-1 or lb s-1] or (<0) WAR
44 288. ! Temperature of water stream [K]
45 0.0 ! Phase of water (0=liquid, 1=vapour)
46 1.0 ! ETA degradation scaling factor
47 0.08 ! Effective component volume [m^3] (only for transient)

48 0.0 ! HP TURBINE: Auxiliary or power output [W]
49 -1.0 ! Relative to max enthalpy drop to temperature ratio:ZT (if -1 is given the default value of 0.8 is invoked)
50 -1.0 ! Relative non-dim speed CN (if -1 is given the default value of 0.6 is invoked)

51 0.90 ! DP ETA
52 -1.0 ! Relative non-dim PCN (= -1 for compressor turbine)
53 2.0 ! Shaft Number (for power turbine, the value 0 is used)
54 5.0 ! Turbine map number
55 -1.0 ! Power law index "n" (POWER = PCN^n)
56 1.0 ! TF degradation scaling factor
57 1.0 ! DH degradation scaling factor
58 1.0 ! ETA degradation scaling factor
59 -1.0 ! Rotor rotational speed [RPS] (only for transient)
60 -1.0 ! Rotor moment of inertia [kg.m^2] (only for transient)
61 -1.0 ! Effective component volume [m^3] (only for transient)
62 0.0 ! NGV angle, relative to D.P.

63 0.0 ! LP TURBINE: Auxiliary or power output [W]
64 -1.0 ! Relative to max enthalpy drop to temperature ratio:ZT (if -1 is given the default value of 0.8 is invoked)
65 -1.0 ! Relative non-dim speed CN (if -1 is given the default value of 0.6 is invoked)
66 0.90 ! DP ETA
67 -1.0 ! Relative non-dim PCN (= -1 for compressor turbine)
68 1.0 ! Shaft Number (for power turbine, the value 0 is used)
69 5.0 ! Turbine map number
70 -1.0 ! Power law index "n" (POWER = PCN^n)
71 1.0 ! TF degradation scaling factor
72 1.0 ! DH degradation scaling factor
73 1.0 ! ETA degradation scaling factor
74 -1.0 ! Rotor rotational speed [RPS] (only for transient)
75 -1.0 ! Rotor moment of inertia [kg.m^2] (only for transient)
76 -1.0 ! Effective component volume [m^3] (only for transient)
77 0.0 ! NGV angle, relative to D.P.

78 -1.013 ! POWER TURBINE: Auxiliary or power output [W]
79 -1.0 ! Relative to max enthalpy drop to temperature ratio:ZT (if -1 is given the default value of 0.8 is invoked)
80 -1.0 ! Relative non-dim speed CN (if -1 is given the default value of 0.6 is invoked)
81 0.90 ! DP ETA (Isentropic efficiency)
82 1.0 ! Relative non-dim PCN (= -1 for compressor turbine)
83 0.0 ! Shaft Number (for power turbine, the value 0 is used)
84 5.0 ! Turbine map number
85 -1.0 ! Power law index "n" (POWER = PCN^n)
86 1.0 ! TF degradation scaling factor
87 1.0 ! DH degradation scaling factor
88 1.0 ! ETA degradation scaling factor
89 -1.0 ! Rotor rotational speed [RPS] (only for transient)
90 -1.0 ! Rotor moment of inertia [kg.m^2] (only for transient)
91 -1.0 ! Effective component volume [m^3] (only for transient)
92 0.0 ! NGV angle, relative to D.P.

```
93 0.0          ! DUCTER: Air Duct or Afterburner (0 if reheat/intercooler not needed, 1 if
reheat/intercooler required later, 2 if reheat/intercooler required now)
94 0.01         ! Total Pressure Loss: DELTA (P)/Pin (Pressure loss = 1%)
95 0.0          ! Combustion Efficiency
96 0.0          ! Limiting Value of Fuel Flow (or 100000 if not needed)
97 -1.0         ! Effective Component Volume [m^3]

98 -1.0         ! CONVERGENT NOZZLE: = "-1" exit area is fixed)
99 1.0          ! Scaling factor

100 1.0         ! ENGINE RESULTS: Power output (= -1 for aero engine)
101 1.0         ! Propeller efficiency (= -1 for turbojet/turbofan)
102 0.0         ! Scaling index ("1" = scaling, "0" = no scaling)
103 0.0         ! Only for scaling: Required DP net thrust/shaft power
-1
1 2 68.5        ! Item 2 at station 1 = Mass flow (kg/s) 367.06
4 6 288.15      ! Item 6 at station 4 = Total temperature (K) FOR INTERCOOLER (-1.0)
7 6 1310.15     ! Item 6 at station 7 = Total temperature (K) FOR COMBUSTOR
-1
-1
4 6 295.32      ! Item 6 at station 4 = Total temperature (K) FOR INTERCOOLER (-0.95)
-1
-1
4 6 302.50      ! Item 6 at station 4 = Total temperature (K) FOR INTERCOOLER (-0.90)
-1
-1
4 6 309.67      ! Item 6 at station 4 = Total temperature (K) FOR INTERCOOLER (-0.85)
-1
-1
4 6 316.85      ! Item 6 at station 4 = Total temperature (K) FOR INTERCOOLER (-0.80)
-1
-1
4 6 324.02      ! Item 6 at station 4 = Total temperature (K) FOR INTERCOOLER (-0.75)
-1
-1
4 6 331.19      ! Item 6 at station 4 = Total temperature (K) FOR INTERCOOLER (-0.70)
-1
-1
4 6 338.37      ! Item 6 at station 4 = Total temperature (K) FOR INTERCOOLER (-0.65)
-1              ! End of DP data
-3
```

Aero-derivative Engine model transient simulation - input file

TRANSIENT Performance simulation modelling of AERODERIVATIVE ENGINE
SIMILAR TO TUMANSKY-R-25-300
BY
David Rowlands

!Turbomatch Programme:
Transient Performance Simulation for AERODERIVATIVE ENGINE
(FUEL INCREMENT WITH TIME) FUEL TYPE KEROSENE - KE

////

```
TR SI KE VA FP
-1
-1
INTAKE      S1, 2          D1-6          R100
COMPRE      S2, 3          D7-18         R102    V7 V8
COMPRE      S3, 4          D19-30        R103    V19 V20
PREMAS      S4, 5, 22      D31-34
BURNER      S5, 6          D35-42        R104
MIXEES      S6, 22, 7
TURBIN      S7, 8          D43-57        V44
TURBIN      S8, 9          D58-72        V59
TURBIN      S9, 10         D73-87        V73     V74
DUCTER      S10, 11        D88-92        R105
NOZCON      S11, 12, 1     D93-94        R110
PERFOR      S1,0,0         D73,D96-98,110,100,104,0,0,0,0,0,0
CODEND
DATA ITEMS ////

1 0.0          ! INTAKE: Altitude [m]
2 0.0          ! Deviation from ISA temperature [K]
3 0.0          ! Mach number
4 -1.0         ! Pressure recovery, according to USAF
5 0.0          ! Deviation from ISA pressure [atm]
6 60.0         ! Relative humidity [%]

7 -1.0         ! COMPRESSOR I: Z = (R-R[choke])/(R[surge]-R[choke])(if -1 is given the
default value of 0.85 is invoked)
8 -1.0         ! Relative rotational speed PCN (if -1 is given the default value of 1.0 is
invoked)
9 2.131        ! DP Pressure ratio
10 0.8872      ! DP ETA
11 0.0         ! Error selection
12 5.0         ! Compressor map number
13 1.0         ! Shaft number
```

14 1.0 ! PR degradation scaling factor
15 1.0 ! NDMF degradation scaling factor
16 1.0 ! ETA degradation scaling factor
17 0.355 ! Effective component volume [m^3] (only for transient)
18 0.0 ! Stator angle (VSV) relative to DP

19 -1.0 ! COMPRESSOR I: Z = (R-R[choke])/(R[surge]-R[choke])(if -1 is given the default value of 0.85 is invoked)
20 -1.0 ! Relative rotational speed PCN (if -1 is given the default value of 1.0 is invoked)
21 4.480 ! DP Pressure ratio
22 0.8872 ! DP ETA
23 0.0 ! Error selection
24 5.0 ! Compressor map number
25 2.0 ! Shaft number
26 1.0 ! PR degradation scaling factor
27 1.0 ! NDMF degradation scaling factor
28 1.0 ! ETA degradation scaling factor
29 0.160 ! Effective component volume [m^3] (only for transient)
30 0.0 ! Stator angle (VSV) relative to DP

31 0.9 ! PREMAS: LAMDA W Cooling bypass (Wout1/Win)
32 0.0 ! DELTA W
33 1.0 ! LAMBDA P
34 0.0 ! DELTA P

35 0.05 ! COMBUSTOR: Pressure loss (=DP/P inlet total)
36 0.99 ! Combustion efficiency
37 -1.0 ! Fuel flow (if -1.0, TET must be defined)
38 0.0 ! (>0) Water flow [kg s-1 or lb s-1] or (<0) WAR
39 288. ! Temperature of water stream [K]
40 0.0 ! Phase of water (0=liquid, 1=vapour)
41 1.0 ! ETA degradation scaling factor
42 0.716 ! Effective component volume [m^3] (only for transient) (0.08 Previous value)

43 0.0 ! HP TURBINE: Auxiliary or power output [W]
44 -1.0 ! Relative to max enthalpy drop to temperature ratio:ZT (if -1 is given the default value of 0.8 is invoked)
45 -1.0 ! Relative non-dim speed CN (if -1 is given the default value of 0.6 is invoked)
46 0.90 ! DP ETA
47 -1.0 ! Relative non-dim PCN (= -1 for compressor turbine)
48 2.0 ! Shaft Number (for power turbine, the value 0 is used)
49 5.0 ! Turbine map number
50 -1.0 ! Power law index "n" (POWER = PCN^n)
51 1.0 ! TF degradation scaling factor
52 1.0 ! DH degradation scaling factor

53 1.0 ! ETA degradation scaling factor
54 185.83 ! Rotor rotational speed [RPS] (only for transient)
55 16.5 ! Rotor moment of inertia [kg.m^2] (only for transient)
56 0.120 ! Effective component volume [m^3] (only for transient)
57 0.0 ! NGV angle, relative to D.P.

58 0.0 ! LP TURBINE: Auxiliary or power output [W]
59 -1.0 ! Relative to max enthalpy drop to temperature ratio:ZT (if -1 is given the default value of 0.8 is invoked)
60 -1.0 ! Relative non-dim speed CN (if -1 is given the default value of 0.6 is invoked)
61 0.90 ! DP ETA
62 -1.0 ! Relative non-dim PCN (= -1 for compressor turbine)
63 1.0 ! Shaft Number (for power turbine, the value 0 is used)
64 5.0 ! Turbine map number
65 -1.0 ! Power law index "n" (POWER = PCN^n)
66 1.0 ! TF degradation scaling factor
67 1.0 ! DH degradation scaling factor
68 1.0 ! ETA degradation scaling factor
69 185.83 ! Rotor rotational speed [RPS] (only for transient)
70 7.4 ! Rotor moment of inertia [kg.m^2] (only for transient)
71 0.136 ! Effective component volume [m^3] (only for transient)
72 0.0 ! NGV angle, relative to D.P.

73 -1.013 ! POWER TURBINE: Auxiliary or power output [W]
74 -1.0 ! Relative to max enthalpy drop to temperature ratio: ZT (if -1 is given the default value of 0.8 is invoked)
75 -1.0 ! Relative non-dim speed CN (if -1 is given the default value of 0.6 is invoked)
76 0.90 ! DP ETA (Isentropic efficiency)
77 1.0 ! Relative non-dim PCN (= -1 for compressor turbine)
78 0.0 ! Shaft Number (for power turbine, the value 0 is used)
79 5.0 ! Turbine map number
80 -1.0 ! Power law index "n" (POWER = PCN^n)
81 1.0 ! TF degradation scaling factor
82 1.0 ! DH degradation scaling factor
83 1.0 ! ETA degradation scaling factor
84 50.0 ! Rotor rotational speed [RPS] (only for transient)
85 45.7 ! Rotor moment of inertia [kg.m^2] (only for transient)
86 0.136 ! Effective component volume [m^3] (only for transient)
87 0.0 ! NGV angle, relative to D.P.

88 0.0 ! DUCTER: Air Duct or Afterburner (0 if reheat/intercooler not needed, 1 if reheat/intercooler required later, 2 if reheat/intercooler required now)
89 0.01 ! Total Pressure Loss: DELTA(P)/Pin (Pressure loss = 1%)
90 0.0 ! Combustion Efficiency
91 0.0 ! Limiting Value of Fuel Flow (or 100000 if not needed)
92 -1.0 ! Effective Component Volume [m^3]

```
93 -1.0          ! CONVERGENT NOZZLE: = "-1" exit area is fixed)
94 1.0           ! Scaling factor

95 1.0           ! ENGINE RESULTS: Power output (= -1 for aero-engine)
96 1.0           ! Propeller efficiency (= -1 for turbojet/turbofan)
97 0.0           ! Scaling index ("1" = scaling, "0" = no scaling)
98 0.0           ! Only for scaling: Required DP net thrust/shaft power

-1
1 2 68.5         ! Item 2 at station 1 = Mass flow (kg/s)
6 6 1310.15      ! Item 6 at station 6 = Total temperature (K)
-1               ! End of DP data
-1
6 6 750.0        ! Item 6 at station 6 = Total temperature (K)
-1
-1
6 6 800.0        ! Item 6 at station 6 = Total temperature (K)
-1
-1
6 6 850.0        ! Item 6 at station 6 = Total temperature (K)
-1
-1
6 6 900.0        ! Item 6 at station 6 = Total temperature (K)
-1
-1
6 6 950          ! Item 6 at station 6 = Total temperature (K)
-1
-1
6 6 1000.0       ! Item 6 at station 6 = Total temperature (K)
-1
-1
6 6 1050.0       ! Item 6 at station 6 = Total temperature (K)
-1
-1
6 6 1100.0       ! Item 6 at station 6 = Total temperature (K)
-1
-1
6 6 1150.0       ! Item 6 at station 6 = Total temperature (K)
-1
-1
6 6 1200.0       ! Item 6 at station 6 = Total temperature (K)
-1
-1
6 6 1250.0       ! Item 6 at station 6 = Total temperature (K)
-1
```

-1
6 6 1300.0 ! Item 6 at station 6 = Total temperature (K)
-1
-1
6 6 1310.15 ! Item 6 at station 6 = Total temperature (K)
-1
-1
6 6 1350.0 ! Item 6 at station 6 = Total temperature (K)
-1 ! End of ODP data
-3

Aero-derivative Engine model fuel Schedule – input file

TRANSIENT Performance simulation modelling of AERODERIVATIVE ENGINE
SIMILAR TO TUMANSKY-R-25-300
BY
David Rowlands

!Turbomatch Programme:
Transient Performance Simulation for AERODERIVATIVE ENGINE
(FUEL SCHEDULE CREATED)

CODEIN
PRECED 15. ! No. of preceding DP and OD simulation (initial DP calc. including)
INITIM 0. ! Initial time [sec]
TRANGE 60. ! Transient performance simulation duration [sec]
STEPLN 0.001 ! Length of one transient step [sec]
FSCHED 2.0 ! Type of the fuel schedule 1 - Fuel schedule with time, 2– Fuel schedule calculated from referred fuel flow against rotational speed (from table)
FSTBLE 19.0 ! No. of records in fuel schedule table
PRINTS 1, 50, 20 ! 1st number - 1 = Printed time points are specified by following two numbers, 2 = Printed time points are specified in the table delimited with commands PLOTIN and PLOTEND ;2nd number - Number of first transient time steps printed; 3rd number - Every next print takes place after this number of time steps
BDTRAN D1, 3 ! Brick data, which are being changed during transient simulation
SVTRAN ! Station vectors which are being changed during transient simulation
CODEND

FUELSCHEDULEIN
FS 1
159.495597 0.05019611! Ref. rotational speed N_shaft/sqrt (Tt26/T[ISA SLS]), Referred fuel flow Wff/(P3/P[ISA SLS]*sqrt(T3/T[ISA SLS]))
158.701018 0.048826012
157.6988954 0.04742885
156.2125896 0.04599492
154.7250061 0.04451951

153.2234464 0.043007712
151.8353080 0.041778821
151.4675081 0.041457361
149.3603679 0.039868139
146.3583700 0.038222717
143.2823917 0.036533443
141.5490743 0.034826819
140.1073006 0.033185826
138.7814584 0.031599257
137.4550318 0.030137572
136.5058822 0.029191928
133.8892706 0.030395500
131.5674253 0.028339918
125.2263040 0.028265097

0.00 ! Time to initiate transient
188.528 ! Final N [rps]
1.2038 ! Final Wff [kg/s] not from calculated ref.fuelflow but from off design simulations
1350.0 ! Maximum Permissible COT [K]
FS 2
159.495597 0.027028674! Ref. rotational speed N_shaft/sqrt (Tt26/T[ISA SLS]), Referred fuel flow Wff/(P3/P[ISA SLS]*sqrt(T3/T[ISA SLS]))
158.701018 0.026290929
157.6988954 0.025538611
156.2125896 0.024766496
154.7250061 0.023972044
153.2234464 0.023157999
151.8353080 0.022496288
151.4675081 0.022323195
149.3603679 0.021467459
146.3583700 0.020581463
143.2823917 0.019671854
141.5490743 0.018752903
140.1073006 0.017869291
138.7814584 0.017014984
137.4550318 0.016227923
136.5058822 0.015718730
133.8892706 0.016366808
131.5674253 0.015259956
125.2263040 0.015219668

30.0 ! Time to initiate transient
131.514 ! Final N [rps]
0.1331 ! Final Wff [kg/s] not from calculated ref.fuelflow but from off design simulations

```
750.0           ! Limiting COT [K]
FUELSCHEDULEND

DATAIN
TIME   D1   D3
0.0     0.0  0.0
DATAEND
```

Aero-derivative Engine model with Water/Steam Injection input file

Performance simulation modelling of AERODERIVATIVE ENGINE
SIMILAR TO TUMANSKY-R-25-300
BY
David Rowlands

!Turbomatch Programme:
Simulation of AERODERIVATIVE ENGINE WITH WATER/ STEAM INJECTION - FUEL TYPE NATURAL GAS (TOMZACK) - GT

```
////

OD SI GT VA FP
-1
-1
INTAKE          S1, 2           D1-6            R100
COMPRE          S2, 3           D7-18           R102    V7 V8
COMPRE          S3, 4           D19-30          R103    V19 V20
PREMAS          S4, 5, 22       D31-34
BURNER          S5, 6           D35-42          R104
MIXEES          S6, 22, 7
TURBIN          S7, 8           D43-57          V44
TURBIN          S8, 9           D58-72          V59
TURBIN          S9, 10          D73-87          V73     V74
DUCTER          S10, 11         D88-92          R105
NOZCON          S11, 12, 1      D93-94          R110
PERFOR          S1,0,0          D73,D96-98,110,100,104,0,0,0,0,0,0
CODEND

DATA ITEMS ////

1 0.0           ! INTAKE: Altitude [m]
2 0.0           ! Deviation from ISA temperature [K]
3 0.0           ! Mach number
4 -1.0          ! Pressure recovery, according to USAF
5 0.0           ! Deviation from ISA pressure [atm]
6 60.0          ! Relative humidity [%]

7 -1.0          ! COMPRESSOR I: Z = (R-R[choke])/(R[surge]-R[choke])
8 -1.0          ! Relative rotational speed PCN
```

```
9 2.131         ! DP Pressure ratio
10 0.8872       ! DP ETA
11 0.0          ! Error selection
12 5.0          ! Compressor map number
13 1.0          ! Shaft number
14 1.0          ! PR degradation scaling factor
15 1.0          ! NDMF degradation scaling factor
16 1.0          ! ETA degradation scaling factor
17 -1.0         ! Effective component volume [m^3] (only for transient)
18 0.0          ! Stator angle (VSV) relative to DP

19 -1.0         ! COMPRESSOR I: Z = (R-R[choke])/(R[surge]-R[choke])
20 -1.0         ! Relative rotational speed PCN
21 4.480        ! DP Pressure ratio
22 0.8872       ! DP ETA
23 0.0          ! Error selection
24 5.0          ! Compressor map number
25 2.0          ! Shaft number
26 1.0          ! PR degradation scaling factor
27 1.0          ! NDMF degradation scaling factor
28 1.0          ! ETA degradation scaling factor
29 -1.0         ! Effective component volume [m^3] (only for transient)
30 0.0          ! Stator angle (VSV) relative to DP

31 0.9          ! PREMAS: LAMDA W Cooling bypass (Wout1/Win)
32 0.0          ! DELTA W
33 1.0          ! LAMBDA P
34 0.0          ! DELTA P

35 0.05         ! COMBUSTOR: Pressure loss (=DP/P inlet total)
36 0.99         ! Combustion efficiency
37 -1.0         ! Fuel flow (if -1.0, TET must be defined)
38 0.0          ! (>0) Water flow [kg s-1 or lb s-1] or (<0) WAR
39 288.         ! Temperature of water stream [K]
40 0.0          ! Phase of water (0=liquid, 1=vapour)
41 1.0          ! ETA degradation scaling factor
42 0.08         ! Effective component volume [m^3] (only for transient)

43 0.0          ! HP TURBINE: Auxiliary or power output [W]
44 -1.0         ! Relative to max enthalpy drop to temperature ratio: ZT
45 -1.0         ! Relative non-dim speed CN (if -1 is given the default value of 0.6 is invoked)
46 0.90         ! DP ETA
47 -1.0         ! Relative non-dim PCN (= -1 for compressor turbine)
48 2.0          ! Shaft Number (for power turbine, the value 0 is used)
49 5.0          ! Turbine map number
50 -1.0         ! Power law index "n" (POWER = PCN^n)
```

```
51 1.0          ! TF degradation scaling factor
52 1.0          ! DH degradation scaling factor
53 1.0          ! ETA degradation scaling factor
54 -1.0         ! Rotor rotational speed [RPS] (only for transient)
55 -1.0         ! Rotor moment of inertia [kg.m^2] (only for transient)
56 -1.0         ! Effective component volume [m^3] (only for transient)
57 0.0          ! NGV angle, relative to D.P.

58 0.0          ! HP TURBINE: Auxiliary or power output [W]
59 -1.0         ! Relative to max enthalpy drop to temperature ratio: ZT
60 -1.0         ! Relative non-dim speed CN (if -1 is given the default value of 0.6 is invoked)
61 0.90         ! DP ETA
62 -1.0         ! Relative non-dim PCN (= -1 for compressor turbine)
63 1.0          ! Shaft Number (for power turbine, the value 0 is used)
64 5.0          ! Turbine map number
65 -1.0         ! Power law index "n" (POWER = PCN^n)
66 1.0          ! TF degradation scaling factor
67 1.0          ! DH degradation scaling factor
68 1.0          ! ETA degradation scaling factor
69 -1.0         ! Rotor rotational speed [RPS] (only for transient)
70 -1.0         ! Rotor moment of inertia [kg.m^2] (only for transient)
71 -1.0         ! Effective component volume [m^3] (only for transient)
72 0.0          ! NGV angle, relative to D.P.

73 -1.013       ! POWER TURBINE: Auxiliary or power output [W]
74 -1.0         ! Relative to max enthalpy drop to temperature ratio: ZT
75 -1.0         ! Relative non-dim speed CN (if -1 is given the default value of 0.6 is invoked)
76 0.90         ! DP ETA (Isentropic efficiency)
77 1.0          ! Relative non-dim PCN (= -1 for compressor turbine)
78 0.0          ! Shaft Number (for power turbine, the value 0 is used)
79 5.0          ! Turbine map number
80 -1.0         ! Power law index "n" (POWER = PCN^n)
81 1.0          ! TF degradation scaling factor
82 1.0          ! DH degradation scaling factor
83 1.0          ! ETA degradation scaling factor
84 -1.0         ! Rotor rotational speed [RPS] (only for transient)
85 -1.0         ! Rotor moment of inertia [kg.m^2] (only for transient)
86 -1.0         ! Effective component volume [m^3] (only for transient)
87 0.0          ! NGV angle, relative to D.P.

88 0.0          ! DUCTER: Air Duct or Afterburner
89 0.01         ! Total Pressure Loss: DELTA (P)/Pin (Pressure loss = 1%)
90 0.0          ! Combustion Efficiency
91 0.0          ! Limiting Value of Fuel Flow (or 100000 if not needed)
92 -1.0         ! Effective Component Volume [m^3]
```

```
93 -1.0          ! CONVERGENT NOZZLE: = "-1" exit area is fixed)
94 1.0           ! Scaling factor

95 1.0           ! ENGINE RESULTS: Power output (= -1 for aero- engine)
96 1.0           ! Propeller efficiency (= -1 for turbojet/turbofan)
97 0.0           ! Scaling index ("1" = scaling, "0" = no scaling)
98 0.0           ! Only for scaling: Required DP net thrust/shaft power
-1
1 2 68.5         ! Item 2 at station 1 = Mass flow (kg/s)
6 6 1310.15      ! Item 6 at station 6 = Total temperature (K)
-1               ! End of DP data
38 0.2          ! WAR
-1
-1
38 0.4          ! WAR
-1
-1
38 0.6          ! WAR
-1
-1
38 0.8          ! WAR
-1
-1
38 1.0          ! WAR
-1
-1
38 1.2          ! WAR
-1
-1
38 1.4          ! WAR
-1
-1
38 1.6          ! WAR
-1
-1
38 1.8          ! WAR
-1
-1
38 2.0          ! WAR
-1
-1
-3
```

APPENDIX B

WATER/STEAM INJECTION ANALYSIS RESULTS

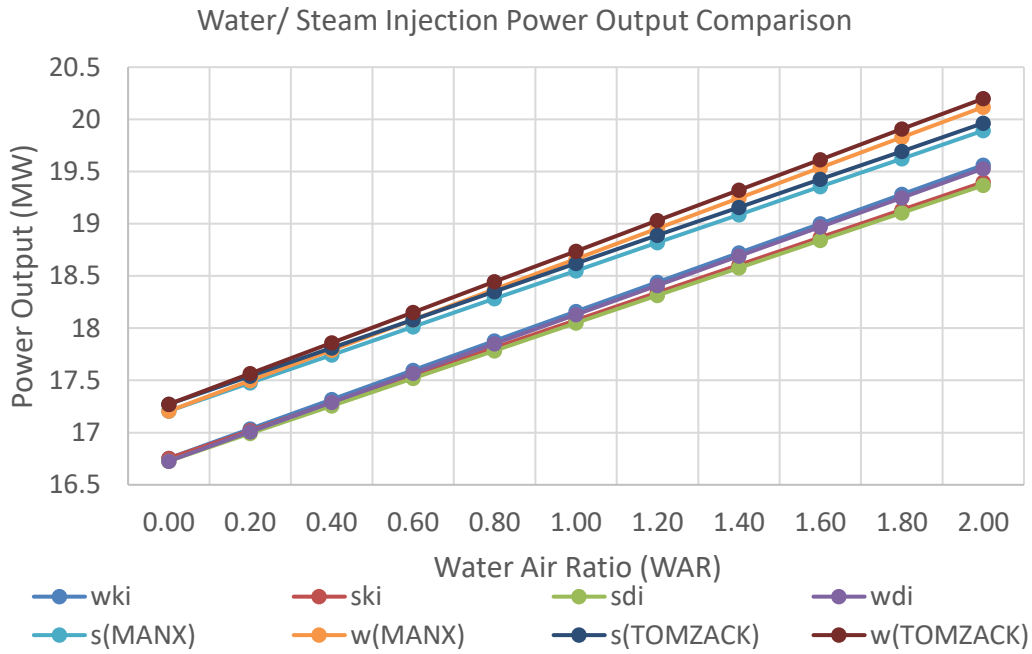

Figure 201: Water/ Steam Injection Power Output Comparison

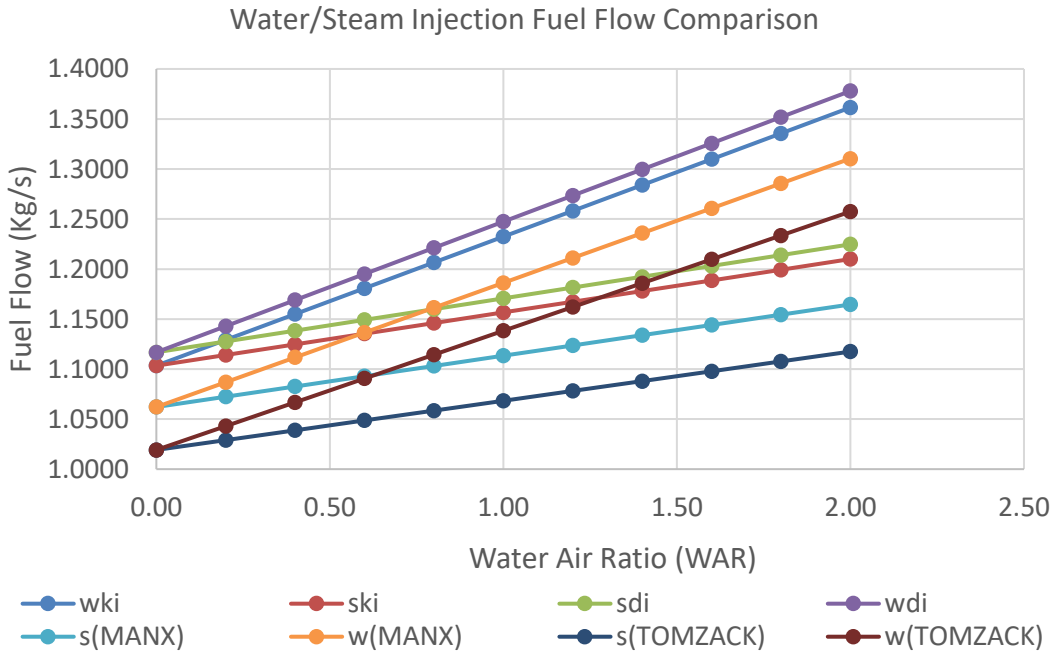

Figure 202: Water/Steam Injection Fuel Flow Comparison

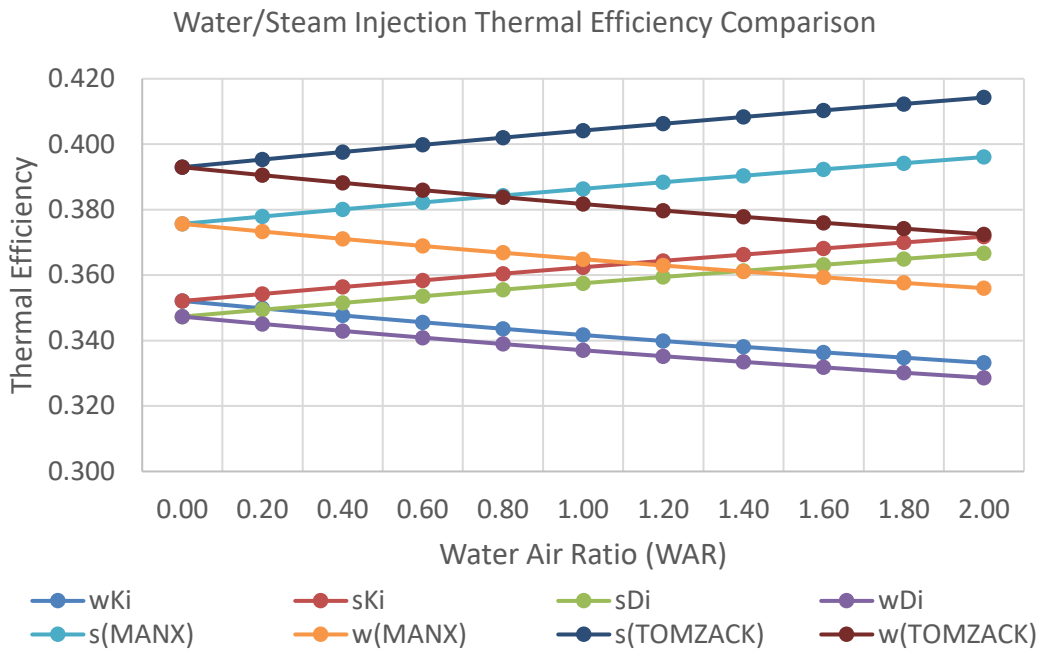

Figure 203: Water/Steam Injection Thermal Efficiency Comparison

APPENDIX C

ECONOMIC COST MODELLING TOOL

*** Actual Source Codes written in MATLAB and C# are provided as electronic source ***

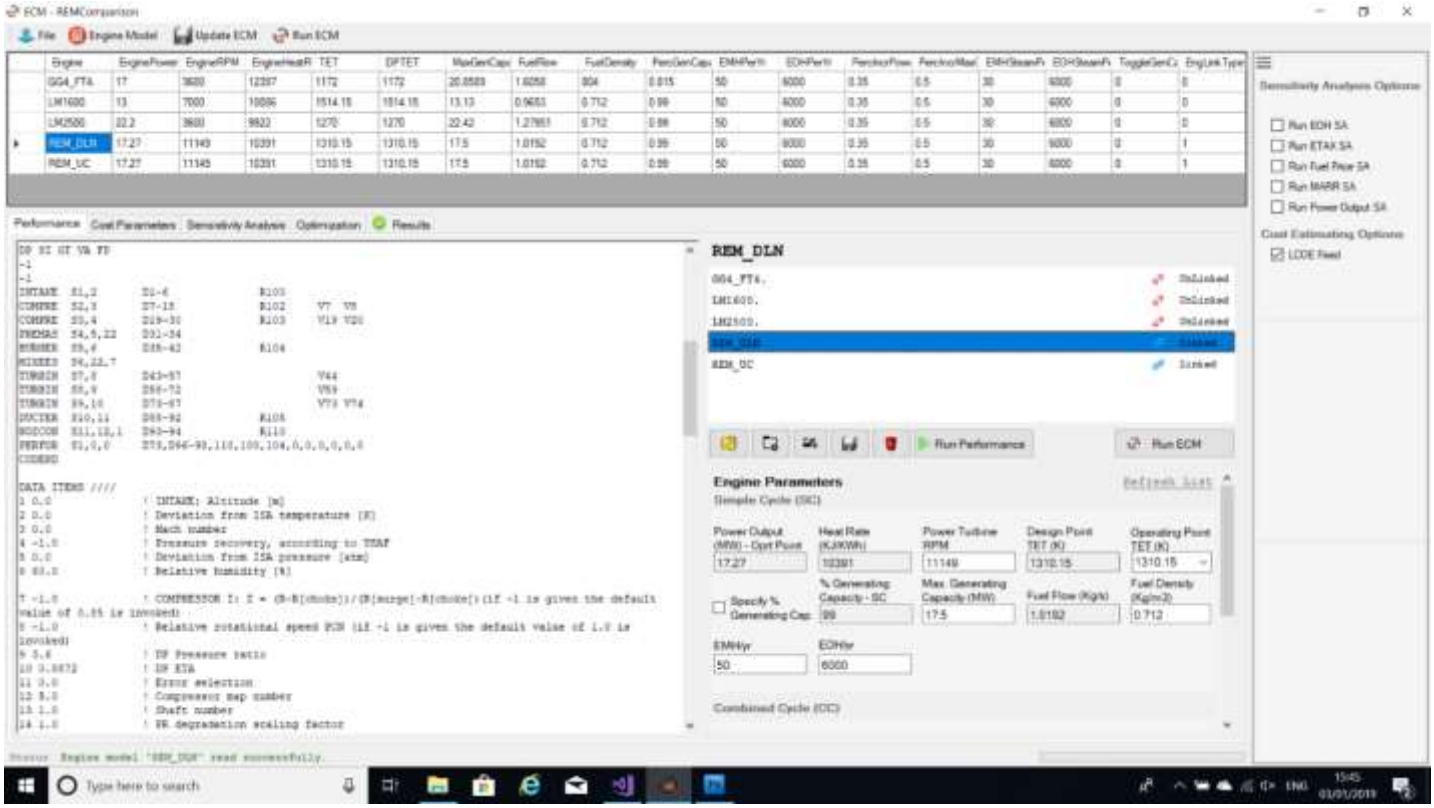

ECM Performance Tab

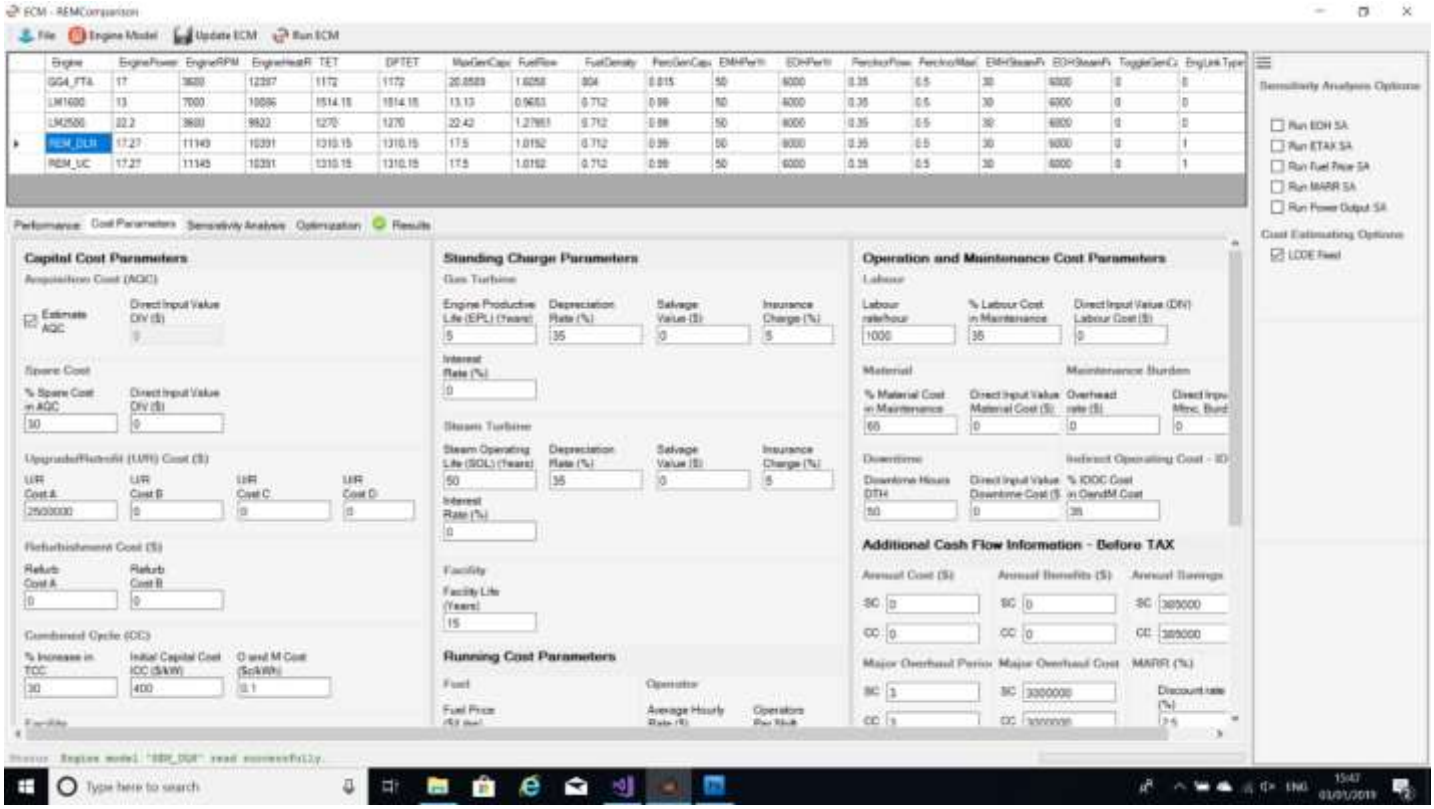

ECM Cost Parameters Tab

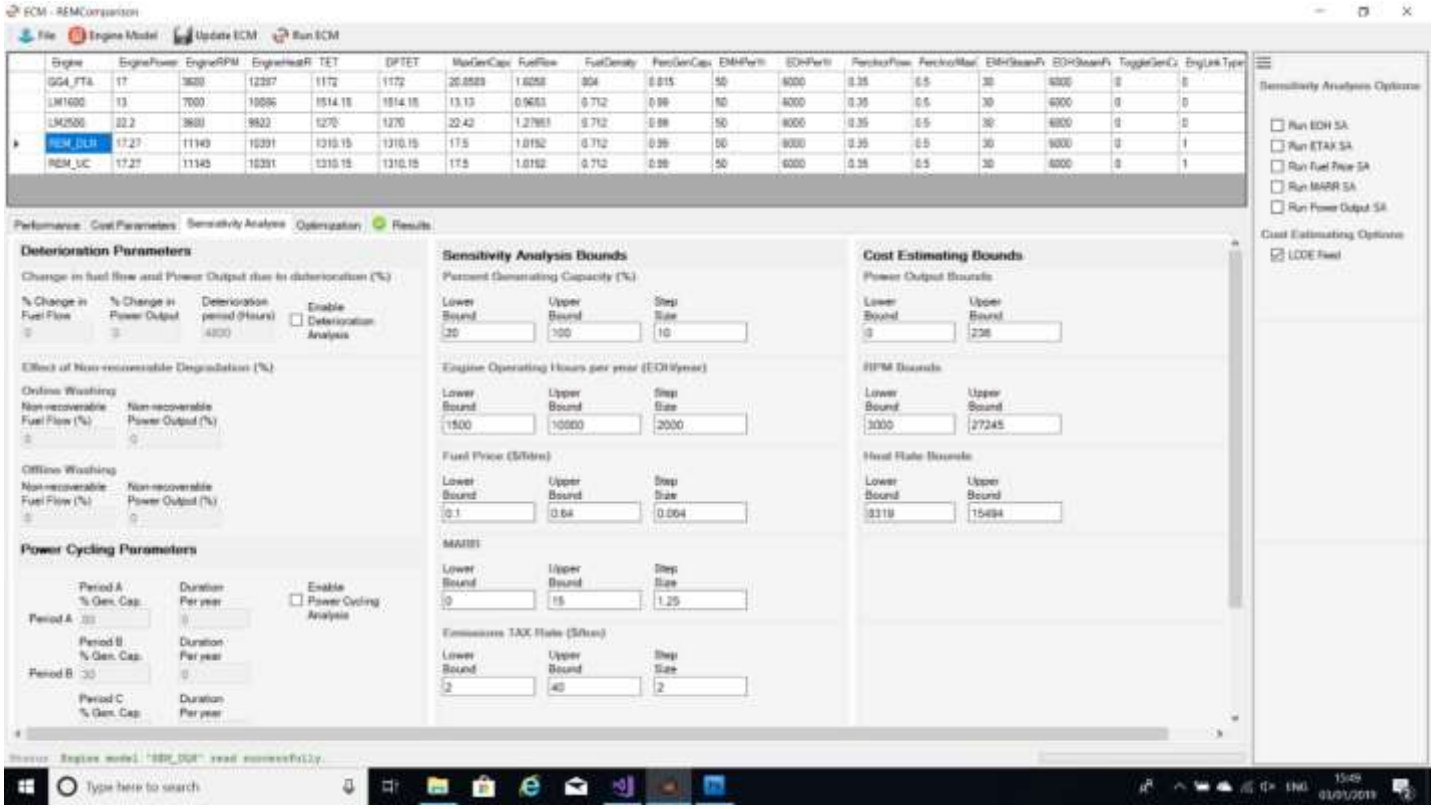

ECM Sensitivity Analysis Tab

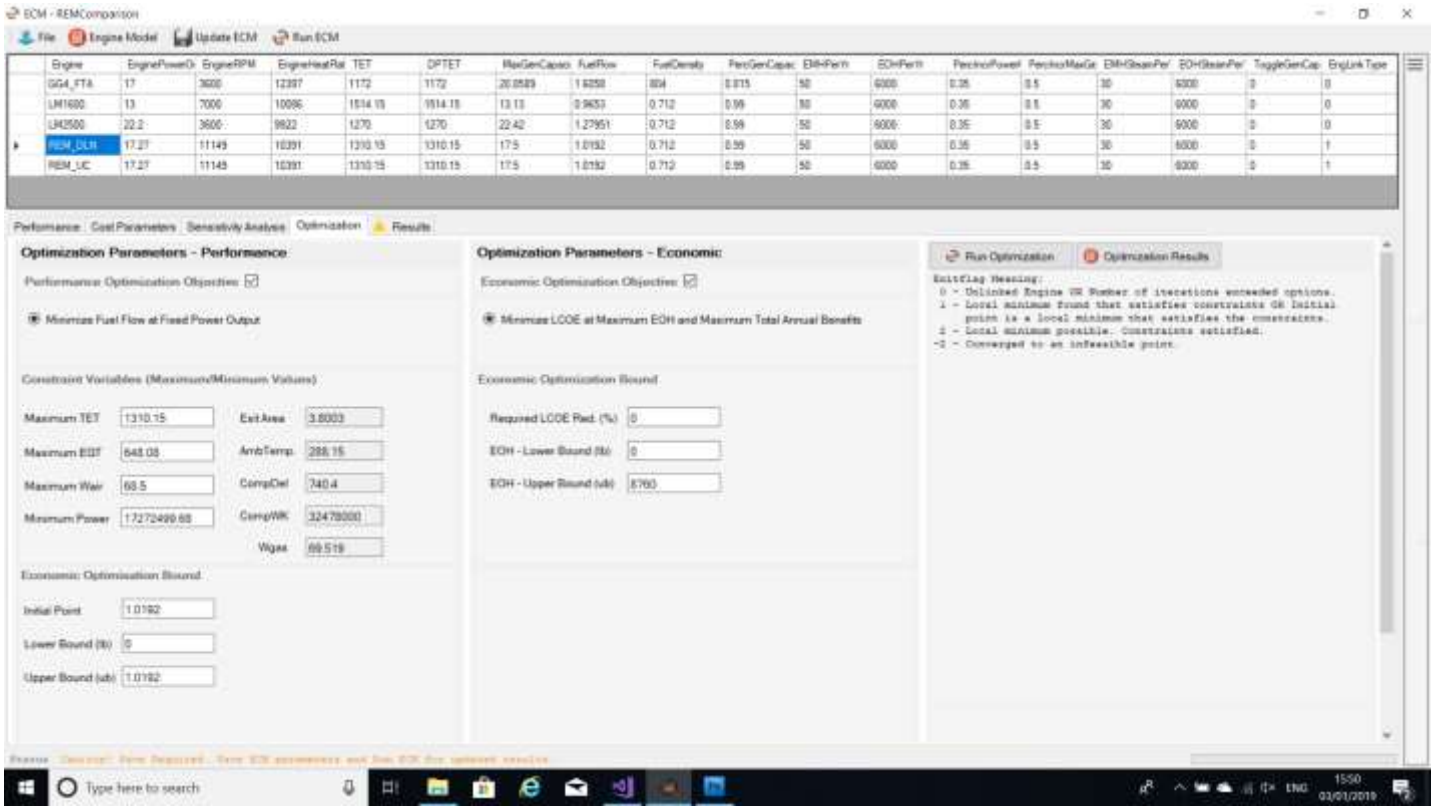

ECM Optimization Tab

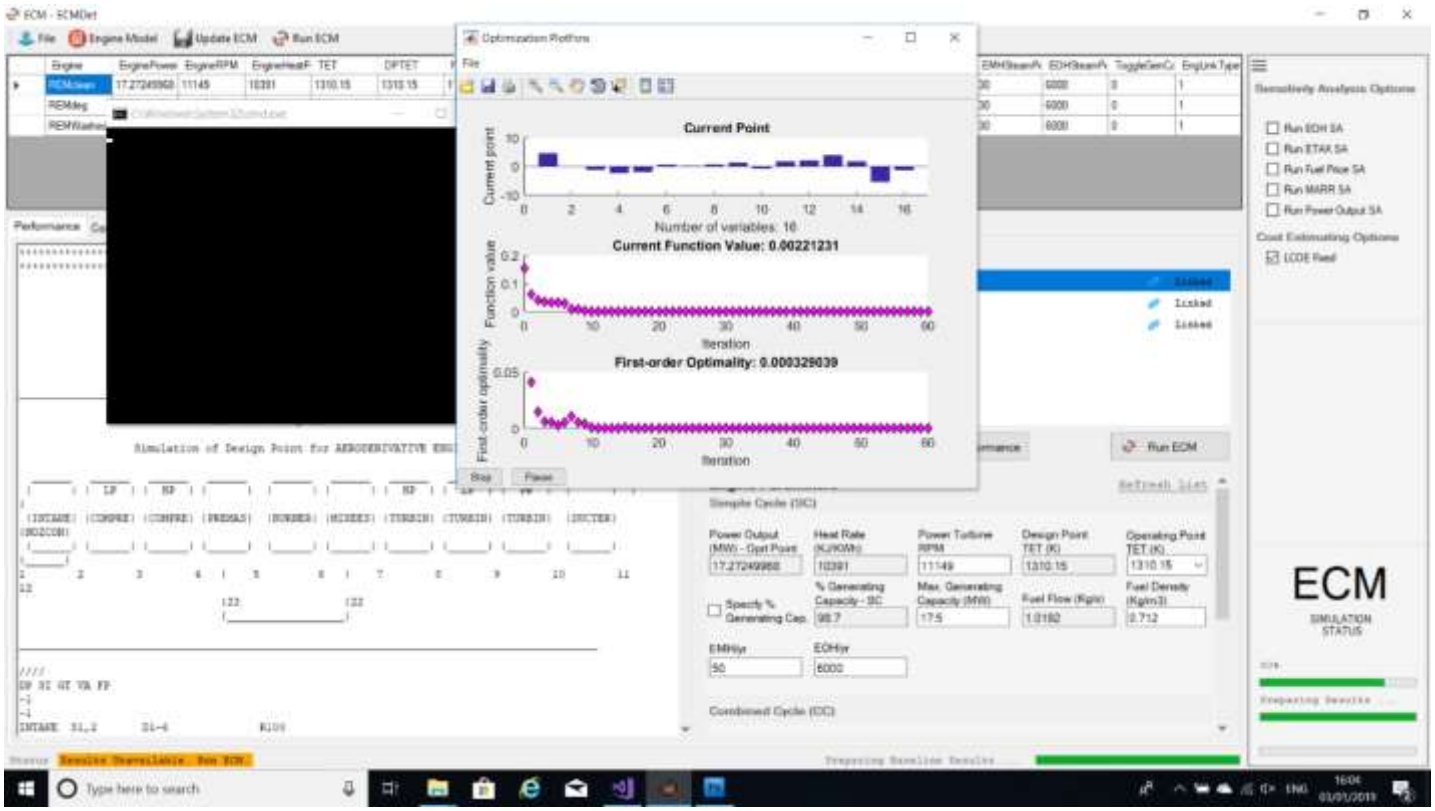

ECM Simulation Running

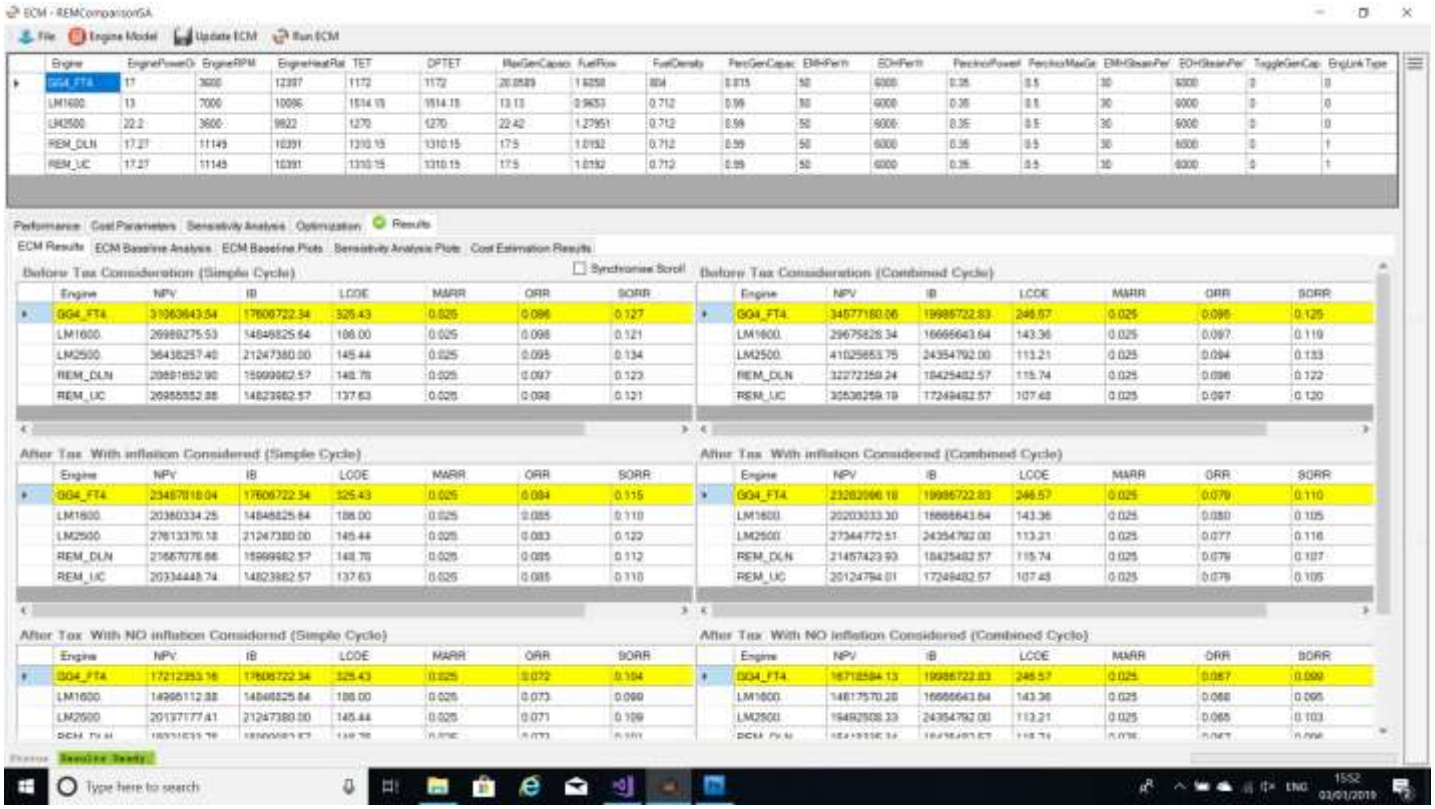

ECM Baseline Present Worth Analysis Results Tab

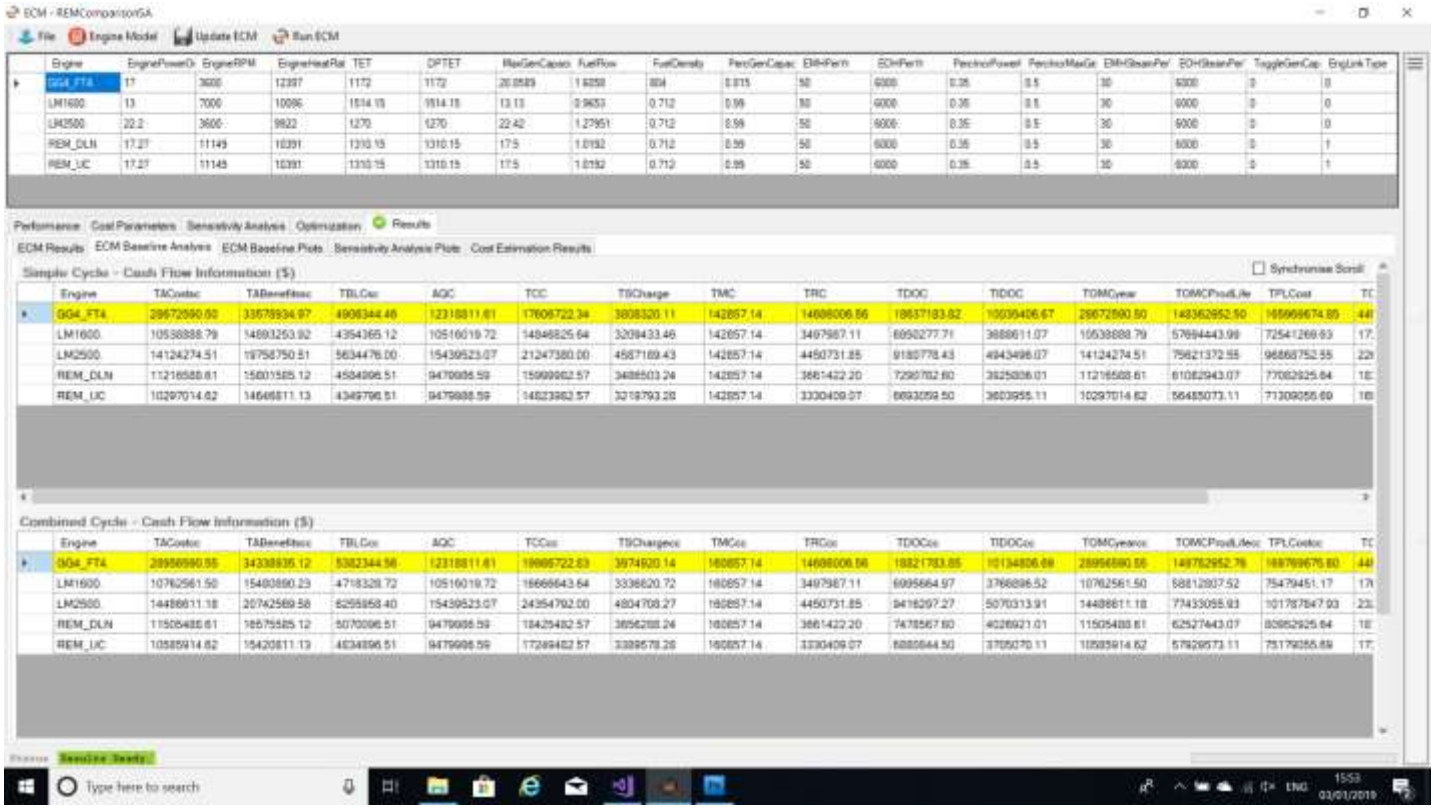

ECM Baseline Cost and Benefits Results Tab

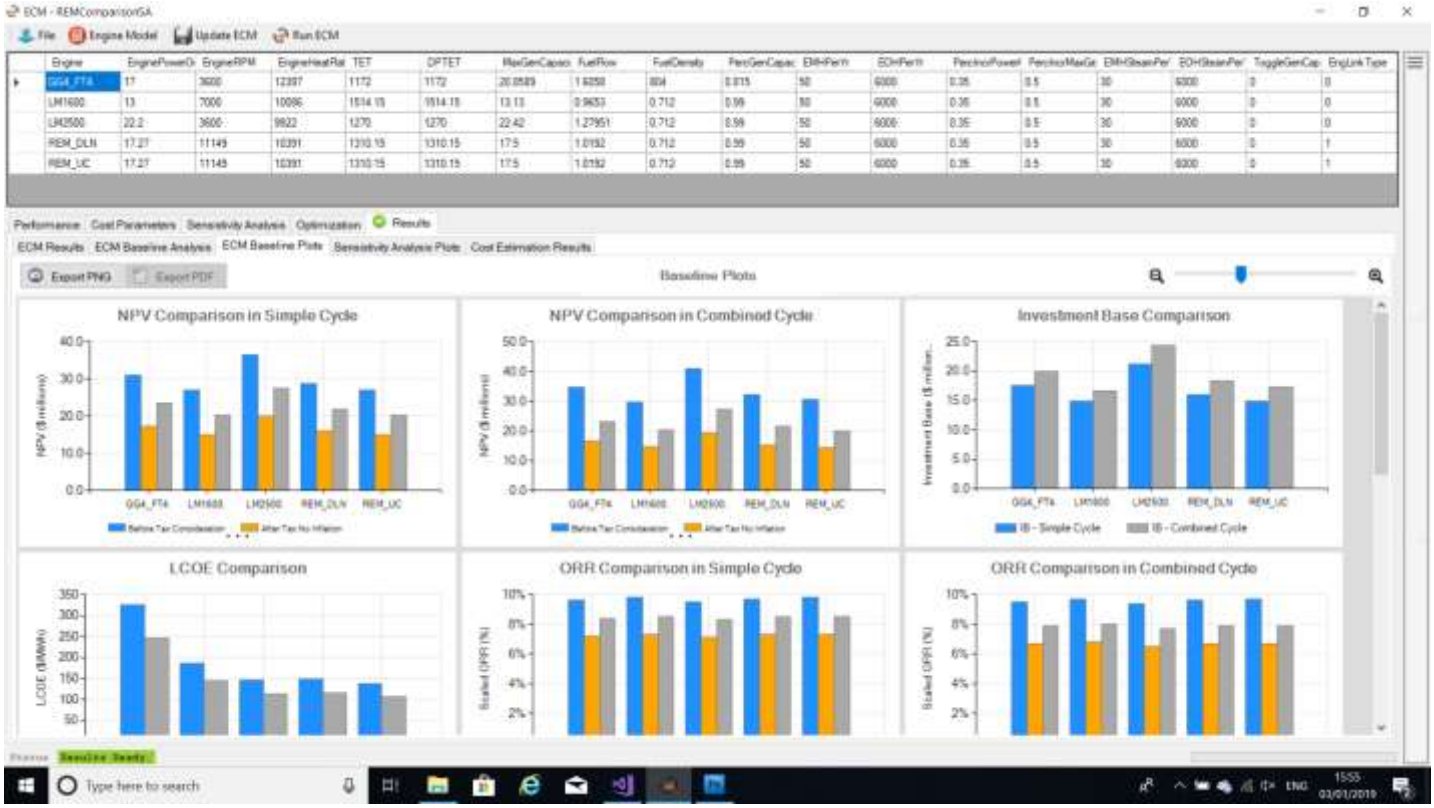

ECM Baseline Plots Tab

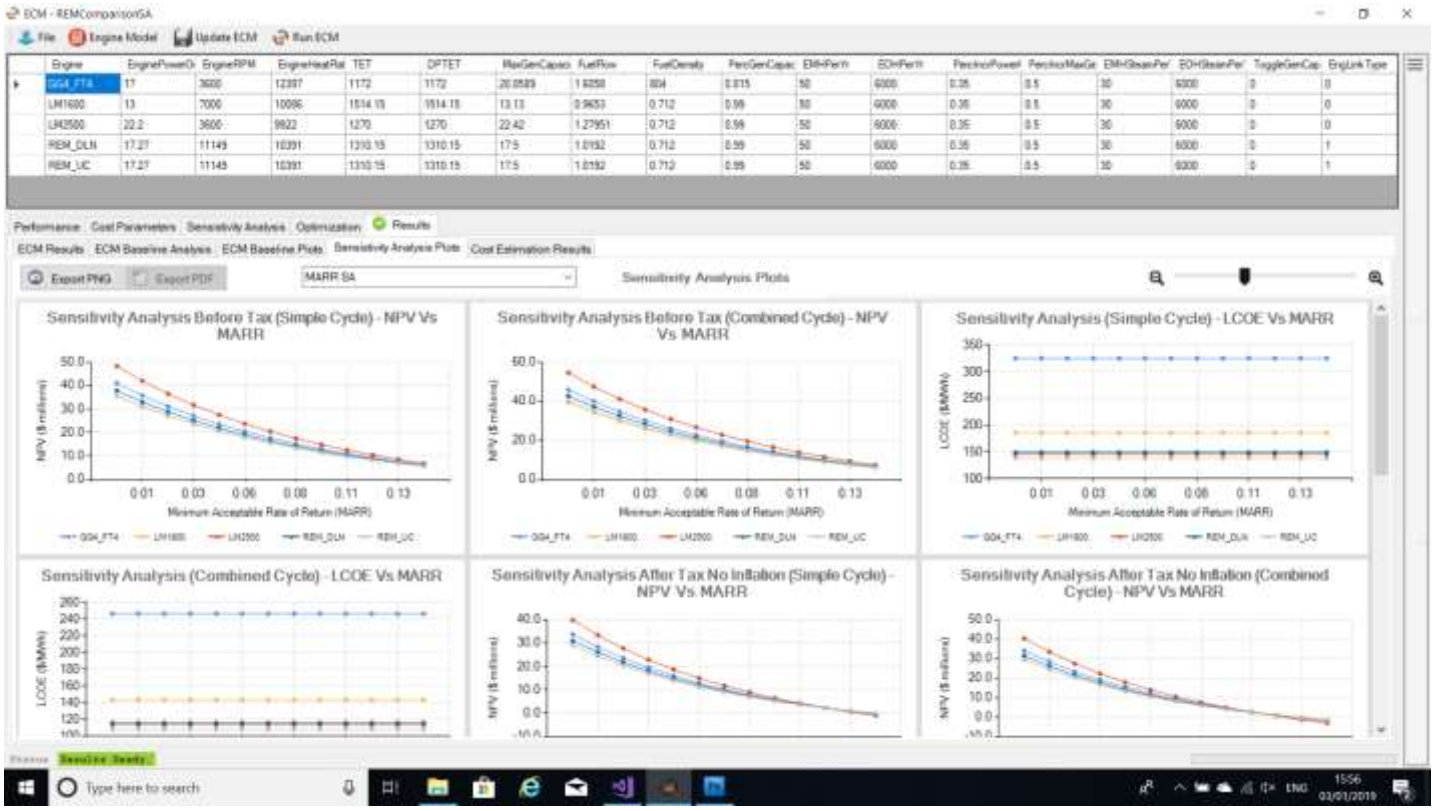

ECM Sensitivity Analysis Plot Tab

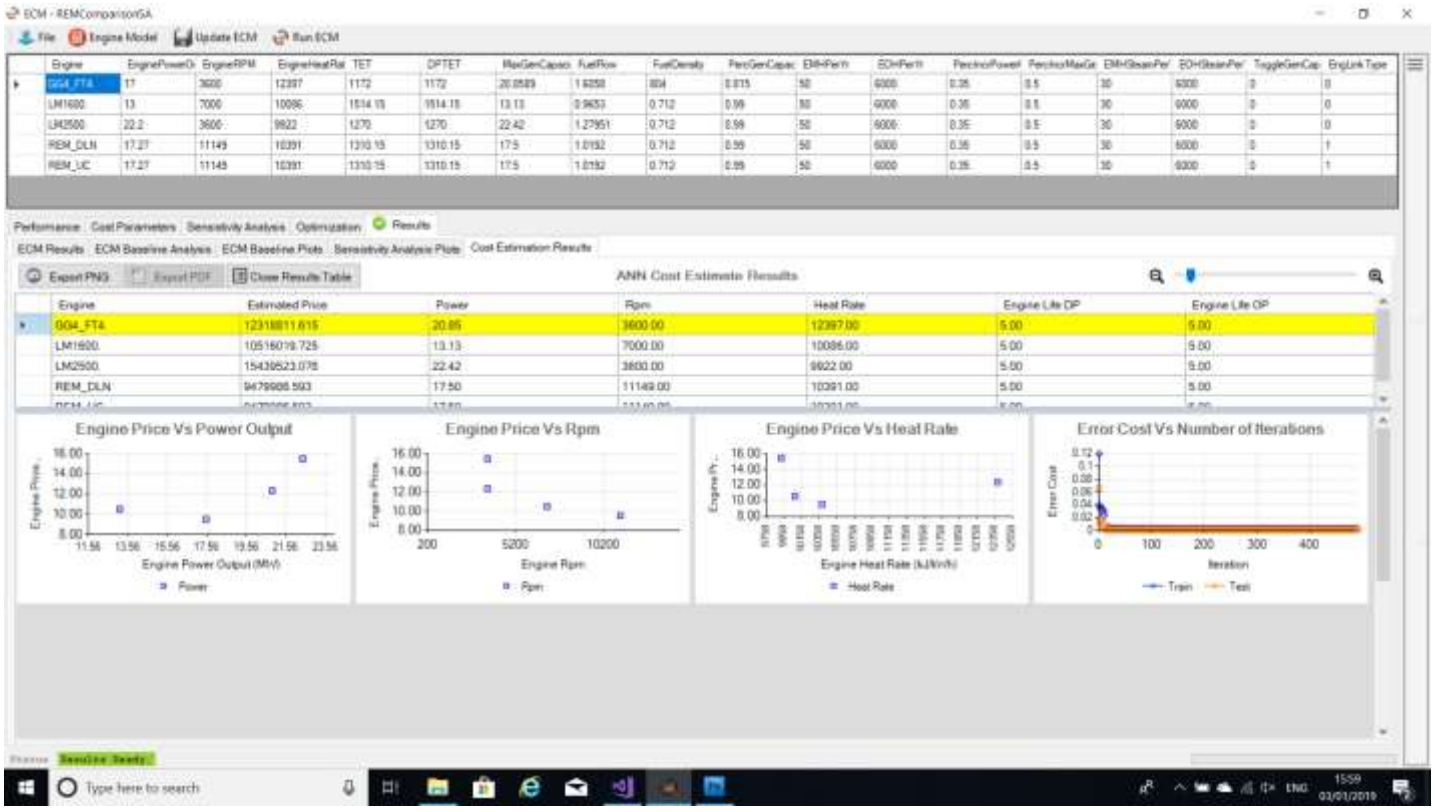

ECM Price Estimating Plots Tab

*** Actual Source Codes written in MATLAB and C# are provided as electronic source ***

APPENDIX D

ENGINE ACQUSITION COST DATASET

Acquistion Cost Dataset (Corrected for Inflation, 2017 $)

S/N	Manufacturer	Model	Output (MW)	Turbine RPM	Heat Rate (KJ/KWh)	Acquisition Cost ($ millions)
1	ABB	GT35	17.0	3600	11252.215	15.96
2	ABB	GT10	21.8	7700	10977.899	15.01
3	ABB	GT10	24.6	7700	10513.673	15.96
4	ABB	GT8	48.5	6300	11341.895	24.65
5	ABB	GT8C	52.6	6200	10529.499	25.28
6	ABB	GT11N	81.6	3600	11289.142	40.56
7	ABB	GT11N	83.9	3600	10940.972	40.56
8	ABB	GT11N2	109.2	3600	10582.252	48.47
9	ABB	GT13D2	100.5	3000	11183.636	48.71
10	ABB	GT13E	148.0	3000	10397.616	67.11
11	ABB	GT13E2	164.3	3000	10086.374	77.94
12	ALLISON	501KB5	3.7	14250	12995.174	3.90
13	ALLISON	501KH	3.7	14600	13043.707	4.55
14	ALLISON	570KA	4.6	11500	12898.109	5.63
15	ALLISON	571KA	5.6	11500	11236.389	6.06
16	DRESSER	DC990	4.2	7200	12470.809	4.09
17	GE	5271RA	20.3	5100	13504.768	11.28
18	GE	5371PA	26.8	5100	12375.854	14.84
19	GE	M5382C	28.3	4670	12309.385	15.23
20	GE	6541B	39.3	5100	11141.434	22.73
21	GE	6101FA	71.8	5100	10276.284	40.05
22	GE	7111EA	84.9	3600	10774.273	29.02
23	GE	7171EF	126.2	3600	10540.049	43.31
24	GE	7191F	151.3	3600	10154.953	45.71
25	GE	7221FA	161.7	3600	9751.9196	51.13
26	GE	9161E	119.4	3000	10661.381	37.03
27	GE	9171E	125.9	3000	11204.737	38.11
28	GE	9231EC	173.7	3000	9954.4911	50.09
29	GE	9281F	217.9	3000	10154.953	62.07
30	GE	9301F	214.0	3000	10234.082	65.34
31	GE	9311FA	228.2	3000	9875.3616	70.01
32	GE	LM500	3.9	7000	12059.336	2.85
33	GE	LM1600	13.4	7000	10086.374	10.36
34	GE	LM2500	22.2	3600	9921.7842	14.27
35	GE	LM2500PH	19.7	3600	10160.228	15.47
36	GE	LM5000PD	33.4	3600	9907.0134	20.42
37	GE	LM5ST80	46.3	3600	8619.8402	22.08
38	GE	LM5ST120	51.5	3600	8319.1481	22.98
39	GE	LM5000PC	33.7	3600	9864.811	20.72
40	GE	LM6000PA	41.0	3600	9200.1232	18.17

41	GE	LM6 50HZ	40.4	3600	9337.281	18.92
42	KWU	V64.3	60.7	5400	10239.357	30.39
43	KWU	V84.2	103.2	3600	10782.713	35.34
44	KWU	V84.2	106.2	3600	10681.427	35.04
45	KWU	V84.3	139.0	3600	10086.374	49.62
46	KWU	V84.3	152.7	3600	9970.317	51.88
47	KWU	V94.2	148.8	3000	10772.163	44.98
48	KWU	V94.2	154.0	3000	10619.179	44.98
49	KWU	V94.3	200.4	3000	10075.823	61.07
50	KWU	V94.3	219.0	3000	9970.317	67.03
51	MITSUBISHI	MF111A	12.8	9660	11790.296	8.71
52	MITSUBISHI	MF111B	14.8	9660	11494.879	9.31
53	MITSUI	SB60	12.7	5680	12090.988	8.86
54	NUOVO PIGNONE	PGT10	10.0	7900	11078.13	7.81
55	RR	SPEY SK15	11.6	5220	11088.681	8.56
56	RR	AVON	14.6	5500	12539.388	7.21
57	RR	RB211	25.3	4800	10075.823	16.67
58	RR	RB211	27.2	4800	10102.2	17.27
59	RUSTON	TB5000	3.8	7950	14190.557	2.64
60	RUSTON	TORNADO	6.2	11085	11964.38	6.28
61	RUSTON	TYPHOON	3.9	16570	11985.482	3.59
62	RUSTON	TYPHOON	4.6	17380	11974.931	3.77
63	RUSTON	HURRICANE	1.6	27245	14580.929	1.65
64	SOLAR	SATURN	1.1	22120	15493.556	1.20
65	SOLAR	CENTAUR	3.9	14950	12924.485	2.55
66	SOLAR	TAURUS	4.4	14950	12924.485	2.85
67	SOLAR	MARS	8.8	8568	11579.284	6.46
68	SOLAR	MARS	10.0	9000	11130.883	6.91
69	TURBOMECA	M	1.1	22000	13847.663	1.40
70	TP&M	FT4C3F	29.8	3600	11473.778	12.34
71	TP&M	FT8	25.6	3600	9363.6575	23.81
72	WESTINGHOUSE	251 B10A	42.3	5420	11183.636	16.52
73	WESTINGHOUSE	251 B12	47.7	5400	10993.725	19.52
74	WESTINGHOUSE	251 B12A	49.2	5400	11014.826	21.02
75	WESTINGHOUSE	501 D5	106.8	3600	10656.106	33.19
76	WESTINGHOUSE	501 D5	109.4	3600	10561.151	34.54
77	WESTINGHOUSE	501 D5	121.3	3600	10434.543	37.54
78	WESTINGHOUSE	501F	163.5	3600	9991.4182	51.81
79	WESTINGHOUSE	701D5	133.8	3000	10508.398	39.80
80	WESTINGHOUSE	701DA	138.5	3000	10592.802	41.30
81	WESTINGHOUSE	701F	235.7	3000	9790.9568	70.58
82	SIEMENS	SGT400	12.9	9500	10925.146	10.17
83	WESTINGHOUSE	W-501D	90.0	3600	11526.531	25.98
84	PRATT & WHITNEY	FT4C-3F	25.0	3000	12396.955	15.14

85	GENERAL ELECTRIC	Fr9FA	220.0	3600	11806.121	14.46
86	SOLAR MARS	100	10.6	11170	10935.697	5.39

APPENDIX E

LIST OF PUBLICATIONS

Rowlands, D. O. & Savill, M., 2018. Economic Modelling and Evaluation of a Repurposed Gas Turbine Engine. Florida, USA, ASME 2018 Power Conference.

Rowlands, D. O. & Savill, M., 2018. Gas Turbine Engine Price Estimation Using Artificial Neural Network. Florida, USA, ASME 2018 Power Conference.